

**Inhibitors of Cdc25 Phosphatases;  
Potential Anti-Cancer Drugs and Tools for  
Chemical Genetics**

**James Charles Collins**

Thesis submitted in partial fulfilment of the  
requirements for the degree of Doctor of Philosophy

Supervisors:

Prof Alan Armstrong

Dr David Mann

Chemistry Department  
Imperial College London

## Abstract

Cdc25 phosphatases play a crucial role in the regulation of the cell cycle, and overexpression of the three known isoforms has been directly correlated with poor cancer prognosis. Inhibition of this enzyme could prove to be an effective therapeutic strategy, but the most potent reported inhibitors lack specificity and an appropriate mechanism of action. Furthermore, more basic research is needed into the structure and precise cellular function of the different cdc25 isoforms.

Following a literature survey, panels of novel inhibitors modelled on the natural product dysidiolide and reported quinonoid compounds were synthesised. Initial phosphatase assay results with cdc25A discouraged any further synthesis of related inhibitors.

The untagged catalytic domain of each isoform was prepared, expressed and purified to carry out NMR structural studies. However, preliminary spectra showed a high degree of conformational flexibility that made further analysis prohibitively difficult. Extensive screening of crystallisation conditions also did not prove successful.

As an alternative strategy, a ligand-based virtual screening approach using an optimised selection of reported inhibitors resulted in discovery of diarylthiazoles as novel, potent and drug-like inhibitors of cdc25 and the related phosphatase VHR. Some of these compounds also demonstrated potent anti-proliferative activity against a panel of cell lines.

Parallel synthesis of a wide range of diarylthiazole analogues using a regioselective, sequential Pd-coupling approach proved moderately successful, identifying promising novel inhibitors for further development, although without significantly increasing the binding affinity. Screening of a wide range of commercially-available compounds chosen by a substructure analysis identified further promising inhibitors, which compare favourably with the best literature compounds. Attempts to develop novel methodology for the rapid and divergent synthesis of aminothiazoles ultimately proved unsuccessful with respect to various approaches to the difficult C-N bond formation, but simple conditions were found for the synthesis and Suzuki coupling of a highly electron-rich aminothiazole C4-triflate.

## **Acknowledgements**

I would like to thank Prof Alan Armstrong and Dr David Mann for giving me the opportunity to work on this project, and for their guidance and advice. In addition, I would like to acknowledge:

- the members of the Armstrong and Mann groups for help and advice.
- Prof Steve Matthews and Dr Pete Simpson for their assistance with the NMR studies.
- Prof Paul Freemont, Ciaran McKeown and Dr Pascale Hazel for assistance with protein crystallisation.
- Dr Caroline Low for performing the virtual screening and, with Dr Albert Jaxa-Chamiec, for subsequent advice and assistance.
- Dr Nat Monck and Dr Tony Raynham for organising my placement at Cancer Research Technology and providing assistance and advice, access to equipment and compounds from the CRT library for testing.
- Dr Cathy Tralau-Stewart, Dr Hayley Cordingley and Dr Katie Chapman of Imperial's Drug Discovery Centre labs for providing assistance with (and recently taking over) the biological assays.

Finally, I would like to thank Karen McCague for proof-reading and for her useful suggestions.

## **Declaration of Originality**

All unattributed research and discussion contained in this thesis can be considered the work of the author, with appropriate credit and references given where the work of others is reported or discussed, and bearing in mind the recognised help and assistance of co-workers outlined in the acknowledgements section above.

# Contents

<b>1</b>	<b>Background and Project Aims</b>	<b>10</b>
1.1	<i>Cdc25 as an Anti-Cancer Target for Medicinal Chemistry</i>	13
1.1.1	Known Inhibitors of Cdc25	15
1.2	<i>Structural Aspects of Cdc25 Catalytic Domains</i>	18
1.3	<i>Protein-Ligand Engineering for Chemical Genetics</i>	21
<b>2</b>	<b>Analogue Synthesis – Dysidiolide Analogues</b>	<b>23</b>
<b>3</b>	<b>Assay Development</b>	<b>29</b>
<b>4</b>	<b>Analogue Synthesis – Quinone Analogues</b>	<b>32</b>
4.1	<i>Phthalazinediones</i>	32
4.2	<i>Diketopiperazines</i>	35
<b>5</b>	<b>Structural Biology</b>	<b>42</b>
5.1	<i>NMR Studies</i>	42
5.1.1	Protein Preparation	42
5.1.2	1D <sup>1</sup> H-NMR: Buffer Optimisation and Confirmation of Protein Folding	45
5.1.3	2D NMR: Isotopic Labelling and HSQC Results	49
5.2	<i>Crystallisation Studies</i>	51
<b>6</b>	<b>Ligand-Based Virtual Screening</b>	<b>54</b>
6.1	<i>Template Selection and Screening Results</i>	54
6.2	<i>Assay Results</i>	57
6.2.1	Initial Cdc25 Activity Assays	57
6.2.2	Phosphatase Selectivity Assays	60
6.2.3	Cell-Based Assays: MTS Assays, Flow Cytometry and Phosphorylation Status	65
<b>7</b>	<b>Analogue Synthesis Part 3 – Analogues of Screening Hits</b>	<b>69</b>
7.1	<i>Parallel Synthesis by a Divergent Coupling Approach</i>	69
7.1.1	Optimisation of Regioselective Suzuki Coupling	70
7.1.2	Library 1 – Suzuki Coupling	72
7.1.3	Library 2 – Aminocarbonylation	74
7.1.4	Library 3 – Amide, Sulfonamide and Urea Analogues of Furanamide	84
7.1.5	Library 4 – Buchwald-Hartwig Coupling	76
7.1.6	Library 5 – Consecutive One-pot Suzuki Coupling for Variation of Thiazole 2-Position	77

7.1.7	Assay Results	78
<b>7.2</b>	<b><i>Screening of CRT Compounds</i></b>	<b>87</b>
7.2.1	Compound Selection	87
7.2.2	Assay Results	88
<b>7.3</b>	<b><i>Target-Oriented Synthesis</i></b>	<b>91</b>
7.3.1	Analogues of C7264901 (335) with Decreased Toxicological Liability	101
<b>8</b>	<b>Development of a Divergent Synthesis of 2-(Hetero)aryl Aminothiazoles</b>	<b>105</b>
<b>8.1</b>	<b><i>Initial Approaches to the Synthesis of Diarylaminothiazole 87</i></b>	<b>105</b>
<b>8.2</b>	<b><i>Oxidative C-H Amination of 4-Substituted Thiazoles</i></b>	<b>107</b>
<b>8.3</b>	<b><i>Regioselective Buchwald-Hartwig Amination of Dibromothiazole</i></b>	<b>109</b>
<b>8.4</b>	<b><i>Consecutive Suzuki and Buchwald-Hartwig Coupling Approach</i></b>	<b>110</b>
8.4.1	Synthesis of 4-Halo-2-aminothiazole Linchpin	110
8.4.2	Buchwald-Hartwig Coupling of 4-Aryl-2-aminothiazoles	112
8.4.3	Suzuki Coupling of 4-Triflyl-2-aminothiazoles	114
<b>9</b>	<b>Reassessment of Assay Results</b>	<b>121</b>
<b>10</b>	<b>Generation of Cdc25 Active Site Mutants</b>	<b>125</b>
<b>11</b>	<b>Summary and Future Work</b>	<b>128</b>
<b>12</b>	<b>Experimental</b>	<b>130</b>
<b>13</b>	<b>Biochemistry – Materials and Methods</b>	<b>248</b>
13.1	<i>Preparation of Constructs</i>	252
<b>14</b>	<b>Appendix</b>	<b>267</b>
14.1	<i>Solution Constitutions</i>	267
14.2	<i>Parallel Synthesis – Attempted Reactions</i>	269
14.3	<i>Full In Vitro Phosphatase Assay Results for Synthesised Compounds</i>	274
<b>15</b>	<b>References</b>	<b>254</b>

## Abbreviations

A	alanine
A549	an epithelial cell line
Ac	acetyl
Ala	alanine
Am	amyl
AP	alkaline phosphatase
aq.	aqueous
Ar	aryl
Arg	arginine
Asp	aspartic acid
ATP	adenosine triphosphate
A.U.	arbitrary units
BINAP	2,2'-bis(diphenylphosphino)-1,1'-binaphthyl
bipy	2,2'-bipyridine
BME	$\beta$ -mercaptoethanol
Boc	<i>tert</i> -butoxycarbonyl
BPV(pic)	dipotassium bisperoxo (picolinate) oxovanadate (V)
br	broad
BSA	bovine serum albumin
Bu	butyl
C	cysteine
C33A	a cervical carcinoma cell line
Cdc	cell division cycle
CDI	1,1'-carbonyldiimidazole
CDK	cyclin-dependent kinase
CI	chemical ionisation MS
CHAPS	(3-[(3-cholamidopropyl)dimethylammonio]-1-propanesulfonate)
cLogP	calculated logP, where P is the partition coefficient
cm	centimetre(s)
Cyc	cyclin
Cys	cysteine
d	doublet/day(s)
D	aspartic acid
dba	dibenzylideneacetone
DBU	1,8-diazabicyclo[5.4.0]undec-7-ene
DDC	Imperial College's Drug Discovery Centre
dH <sub>2</sub> O	distilled water
DIAD	diisopropyl azodicarboxylate
DIBAL	diisobutylaluminium hydride
DIPEA	<i>N,N</i> -diisopropylethylamine
DMAP	dimethylaminopyridine
DME	dimethoxyethane
DMEDA	<i>N,N'</i> -dimethylethylenediamine
DMF	<i>N,N</i> -dimethylformamide
DMSO	dimethyl sulfoxide
DNA	deoxyribonucleic acid
dNTP	deoxyribonucleotide triphosphate
dppf	1,1'-bis(diphenylphosphino)ferrocene

DTT	dithiothreitol
DUSP	dual-specificity phosphatase
<i>E. Coli</i>	<i>Escherichia Coli</i>
EDTA	ethylenediaminetetraacetic acid
eq.	equivalents
ERK	extracellular-signal-regulated kinase
Et	ethyl
F	phenylalanine
FemX	a melanoma cell line
g	gram(s)
GST	glutathione S-transferase
h	hour(s)
H	histidine
HATU	2-(7-aza-1H-benzotriazole-1-yl)-1,1,3,3-tetramethyluronium hexafluorophosphate
Hep3B	hepatoma 3B, a liver cancer cell line
HPLC	high-performance liquid chromatography
HSQC	Heteronuclear Single Quantum Coherence
HT29	heterotransplantable – 29, a colon cancer cell line
HWE	Horner-Wadsworth-Emmons
Hz	Hertz
IC <sub>50</sub>	half maximal inhibitory concentration
IMes	1,3-bis(mesityl)imidazolium
IPTG	isopropyl β-D-thiogalactopyranoside
IR	infra-red
kbp	kilobase pair(s)
kDa	kilo-Daltons
KOD	<i>Thermococcus kodakaraensis</i>
krpm	kilo-revolutions per minute
kV	kilovolt(s)
LAR	leucocyanidin reductase, an oxidoreductase enzyme
LB	Luria Broth
LHMDS	lithium bis(trimethylsilyl)amide
LE	ligand efficiency
LLE	lipophilic ligand efficiency
LNCaP	lymph node carcinoma of the prostate, a prostate cancer cell line
μg	microgram(s)
μL	microlitre(s)
μm	micrometre(s)
μM	micromolar
m	multiplet
M	molar
mA	milliamp(s)
MAPK	mitogen-activated protein (MAP) kinase
MCF-7	Michigan Cancer Foundation – 7, a breast cancer cell line
MDA-MB	M.D. Anderson – metastatic breast, a breast cancer cell line
Me	methyl
mg	milligram(s)
MHz	megaHertz
min	minute(s)

MKP	MAPK phosphatase
mL	millilitre(s)
mM	millimolar
mmol	millimole(s)
mp	melting point
mRNA	messenger RNA
Ms	mesyl
MS	mass spectrum/mass spectrometry
MTS	3-(4,5-dimethylthiazol-2-yl)-5-(3-carboxymethoxyphenyl)-2-(4-sulfophenyl)-2H-tetrazolium
MVK	methylvinylketone
MW	molecular weight
Myc	myelocytomatosis gene product, a transcription factor
NBS	<i>N</i> -bromosuccinimide
NCI	National Cancer Institute
N.D.	not determined
NETN	NP40, EDTA, Tris-HCl, NaCl (see Appendix)
NHC	<i>N</i> -heterocyclic carbene
NIH-3T3	National Institute of Health – 3T3, a fibroblast cell line
nm	nanometre
NMR	nuclear magnetic resonance
NP40	octylphenolpoly(ethyleneglycolether)
OMFP	3- <i>O</i> -methylfluorescein phosphate
PCR	polymerase chain reaction
petrol	petroleum ether (40-60 °C)
Ph	phenyl
Phe	phenylalanine
pin	pinacolate
ppm	parts per million
PNPP	<i>para</i> -nitrophenyl phosphate
PTP	protein tyrosine phosphatase
R	arginine
Raf	rapidly accelerated fibrosarcoma, a family of kinases
Ras	rat sarcoma, a family of GTPase proteins
R <sub>f</sub>	retention factor
RNA	ribonucleic acid
ROS	reactive oxygen species
r.t.	room temperature
s	second(s), singlet
SAR	structure-activity relationship(s)
SDS	sodium dodecylsulfate
SDS-PAGE	SDS-polyacrylamide gel electrophoresis
SEM	standard error of the mean
t	triplet
TAE	tris/acetate/EDTA (see Appendix)
Taq	<i>Thermus aquaticus</i>
TBAB	tetra- <i>n</i> -butylammonium bromide
TCDI	1,1'-thiocarbonyldiimidazole
Tf	triflyl
TFA	trifluoroacetic acid



THF	tetrahydrofuran
Thr	threonine
TLC	thin layer chromatography
TMEDA	tetramethylethylenediamine
TMS	trimethylsilyl, tetramethylsilane
$t_R$	retention time
Tris	tris(hydroxymethyl)aminomethane
Tween	polysorbate 20
Tyr	tyrosine
UV	ultra-violet
VHR	vaccinia H1-related phosphatase
W	Watt(s)

# 1 Background and Project Aims

The eukaryotic cell cycle can be divided into four phases. In the S (synthesis) phase the nuclear DNA is replicated, and in the M (mitotic) phase the cell undergoes first nuclear then cytoplasmic division. Dividing these key stages are the G<sub>1</sub> and G<sub>2</sub> (gap) phases, when decisions are made about whether to commit to the next stage of division.

The essential processes of the cell cycle are primarily regulated by two key classes of interacting protein; cyclins and cyclin-dependent kinases (CDKs). These molecules operate at the transitions between the cycle phases, and as such allow environmental signals to regulate progression of the cell cycle. Cyclins bind to CDKs and control their ability to phosphorylate certain target proteins. This occurs in a cyclical fashion, involving the synthesis and degradation of different cyclins at different stages of the cell cycle.<sup>1</sup>

Cell division cycle 25 (cdc25) family proteins are highly conserved dual specificity phosphatases that regulate CDK activation by removal of inhibitory phosphate groups from both threonine and tyrosine residues.<sup>2,3</sup> Specifically, dephosphorylation of two CDK residues (Thr14 and Tyr15 for CDK1) in the loop involved in positioning the  $\gamma$ -phosphate of ATP relieves inhibition of the CDK-cyclin complex, reversing the effect of CDK-inhibitory kinase Wee1 and ultimately ensuring irreversible transition to the next stage of the cell cycle (Figure 1).<sup>4,5,6</sup>

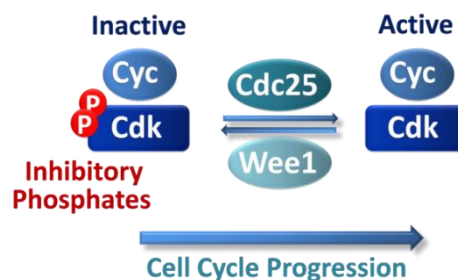


**Figure 1** – Cdc25 removes inhibitory phosphates from CDK/cyclin complexes

There are three isoforms of cdc25 (A, B and C), which share a highly conserved C-terminal catalytic domain that contains the active site and substrate recognition regions. The N-terminal domain is highly divergent, and this is amplified by alternative splicing that

generates at least 12 splice variants.<sup>2</sup> The N-domain is thought to play a purely regulatory role, and it contains common features that serve this purpose; nuclear import-export signals control the cellular localisation and phosphorylation, and ubiquitination sites control protein activity, degradation and regulatory association.<sup>2</sup> The catalytic domain contains the key nucleophilic cysteine residue that the majority of phosphatases use to displace the phosphate group from their substrates, with subsequent hydrolysis of the phospho-cysteine intermediate.

The specific functions of the three *cdc25* isoforms are not yet fully understood.<sup>7</sup> The initial models were conceptually simple, with each isoform acting on specific CDK/cyclin substrates at well-defined points in the cell cycle (Figure 2).<sup>2</sup> For example, the role of *cdc25A* was thought to promote transfer to the S phase by dephosphorylation of both the CDK2-cyclin E and CDK2-cyclin A complexes,<sup>8,9</sup> and *cdc25B* and *C* were thought to individually play key roles in the activation of CDK1-cyclin B at the G<sub>2</sub>-M transition, irreversibly driving the cell into mitosis.

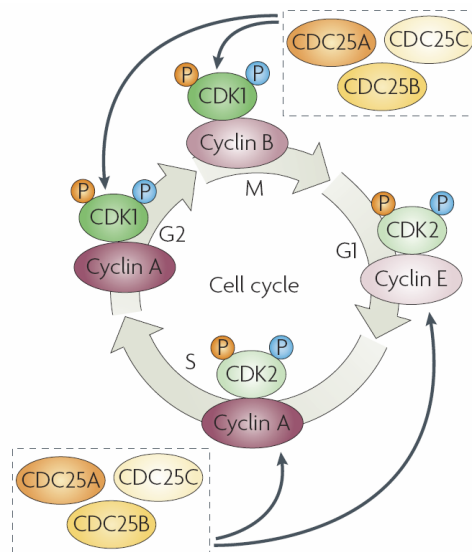


**Figure 2** – Roles of *cdc25* in the cell cycle <sup>2</sup>

This relatively simple picture has been significantly complicated by recent studies which have revealed conflicting data regarding the roles of the three *cdc25* isoforms. Using the RNA interference method of targeted inhibition, first *cdc25B* and then *cdc25C* were found to affect the rate of progression into the S phase, despite the presence of functional *cdc25A*.<sup>10,11</sup> Similar results have been obtained for entry into M phase, with evidence for a key role for *cdc25C* in certain feedback loops for *cdc25A* activation, demonstrating the cooperative nature

of these phosphatases.<sup>12</sup> Further data were provided by studies in which *cdc25B*- and *C*-knockout mice develop normally in terms of the cell cycle, response to DNA damage and regulation of *cdc25A*.<sup>13</sup> However, not only has the applicability of this study to human cells has been questioned,<sup>14</sup> other recent studies have also found that *cdc25B* is essential for recovery of cell cycle function following a period of arrest caused by DNA damage.<sup>15</sup> It is likely therefore that the web of interactions is more complex and cooperative than previously thought, and that there are subtle functional differences between the isoforms. This evidence suggests an overall picture of the *cdc25* phosphatases being largely functionally-interchangeable, with the differing activity observed with different substrates perhaps suggesting evolution in progress towards a more narrow range of specialised activity. This is supported by the comparison with lower eukaryotic systems that possess a single *cdc25* protein to carry out all the required phosphatase activity, different from the human isoforms yet exhibiting structural characteristics of all three.<sup>7</sup>

The role of *cdc25* phosphatases in the cellular response to DNA damage is also the subject of investigation, as these enzymes are key components in the pathway that leads to cell cycle arrest at the G2/M checkpoint. Multiple stress-activated kinases, involved in the response to events such as DNA strand breaks, converge to phosphorylate *cdc25* and promote its nuclear export, thereby separating *cdc25* from its nuclear CDK substrates and restraining proliferation whilst repair is effected.<sup>14</sup>

This project comprises three strands of interlinked research:

1. the synthesis and testing of novel (and potent) inhibitors of *cdc25*
2. the elucidation of novel structural and ligand-binding information
3. the identification of the precise cellular role of *cdc25* isoforms *via* protein-ligand engineering

In the following sections, the background to each of these aspects will be discussed in detail and in context with the proposed goals of the project.

## 1.1 *Cdc25 as an Anti-Cancer Target for Medicinal Chemistry*

Given the key role of the *cdc25* phosphatases in determining whether a cell passes through the checkpoints in the cell cycle, it is not surprising that *cdc25* has been implicated in tumour formation, and there is an extensive body of research to support this hypothesis. Hemizygous disruption of *cdc25A* has been shown to inhibit both cellular transformation and mammary tumourigenesis in mice;<sup>16</sup> this evidence points to the activity of *cdc25A* alone being a key rate-determining factor in some cancers. A wide variety of other studies have classified *cdc25* as a proto-oncogene, exerting a synergistic effect with known oncogenes *Myc*,<sup>17,18</sup> *Ras*<sup>19</sup> and *Raf*,<sup>17</sup> and being down-regulated by the tumour suppressor *p53*.<sup>19</sup>

Studies of various human cancers have revealed that *cdc25* is overexpressed in the majority of cases, in a manner often specific to the individual isoform (Figure 3).<sup>2,20</sup> Importantly, it has been observed that there is usually a correlation between this overexpression and certain clinicopathological features that result in a poor prognosis. The results of these studies are clouded by contradictory data regarding mRNA and protein levels, between which there is a well-recognised disparity,<sup>21</sup> and it is clear that factors including the low cellular abundance and the many splice variants of *cdc25* make this kind of analysis unreliable.<sup>2</sup>

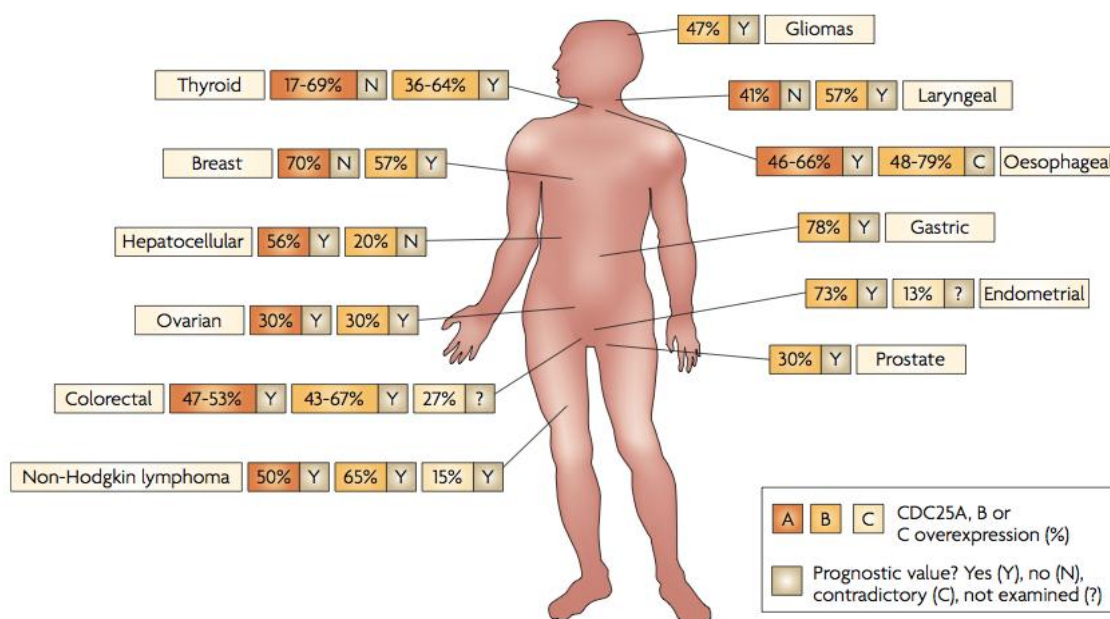


**Figure 3** – Overexpression of *cdc25* in primary tumour samples from patients<sup>2</sup>

However, it is not even necessary to conclusively prove that deregulation of the cdc25 phosphatases plays a direct and well-defined role in tumour progression when their substrates, the CDKs, have generated extensive and long-running research programmes to find antiproliferative cancer drugs *via* direct inhibition of these kinases. The high specificity and well-defined mechanism of cdc25 makes its inhibition an obvious candidate for an indirect route to the same objective, but this phosphatase has only more recently attracted interest as a drug target.<sup>2,20,22</sup>

The key milestone of proof-of-principle use of a selective cdc25 inhibitor to prevent or reverse tumour growth had yet to be reached at the outset of this project. Despite the evidence above, it was unclear whether the inhibition of cdc25 would only suffice to cause a temporary cytostatic effect, although it has been postulated that a consequence of any inhibitor-mediated cell-cycle arrest in unstable tumour cells might be the activation of apoptotic pathways.<sup>2</sup> The increasing reports of the effects of selective cdc25 inhibitors in the subsequent years have somewhat allayed these concerns (see section 1.1.1), and in any case it has been demonstrated that positive cooperative effects are possible using a combination therapy with known drugs, such as paclitaxel.<sup>23</sup>

Given their close homology, the issue of isoform selectivity has been considered another potential complication of cdc25 as a medicinal chemistry target. This resolves to two potential pharmacological strategies. A pan-cdc25 inhibitor should prove most effective in terms of an antiproliferative effect, circumventing any loss of efficacy from the putative partial functional redundancy of the three isoforms described above. Alternatively a selective inhibitor might exploit the observed differences in cdc25 isoform overexpression in specific human tumours (Figure 3), selectively causing tumour cell cycle arrest with little effect on normal cells.

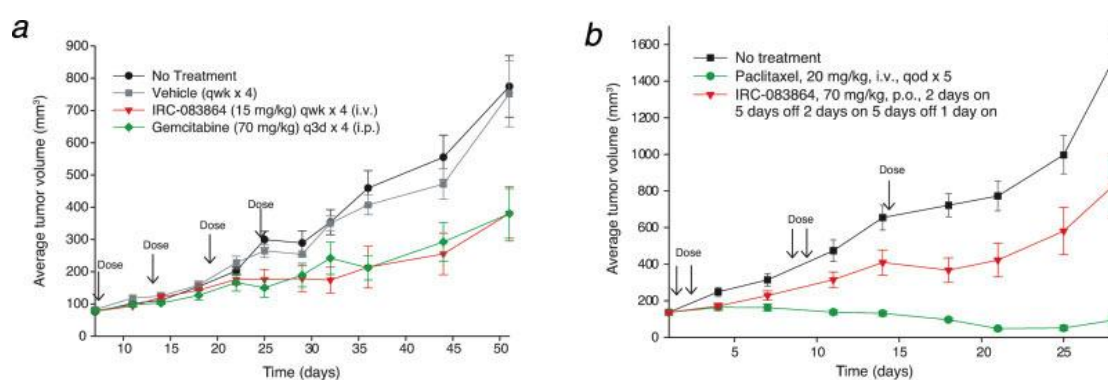
Importantly, developing a cell cycle inhibitor targeted at a phosphatase will mitigate the usual kinase inhibitor issues of problematic selectivity profiles and relatively poor cellular activity due to competition with high intracellular concentrations of ATP.<sup>17</sup> Even at lower ATP concentrations, where an ATP-competitive kinase inhibitor might be more active, inhibition of phosphatases is likely more influential than that of kinases from the same signal transduction pathway. This is due to the inherent kinetic advantage of a first-order dephosphorylation reaction over the competing second-order phosphorylation, potentially making phosphatases a much more biochemically-powerful target for inhibition.<sup>24</sup> The

weakness in this argument is the difficulty in finding phosphatase inhibitors with drug-like properties due to the inherently charged and hydrophilic active site pockets that have evolved to bind phosphate di-anions.<sup>25</sup>

It is worth considering that the best pharmacological approach might prove to be the *activation* of cdc25 phosphatases in combination with the current range of DNA-damaging chemo- or radiotherapies, the theory being that this will force the cell past the key repair checkpoints and on to apoptosis.<sup>2</sup> However, in the absence of any known generally-applicable strategy for enzyme activation with small molecules, this approach cannot be currently investigated.

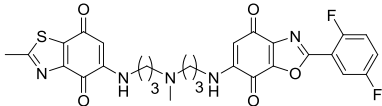
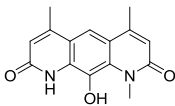
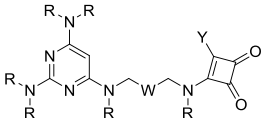
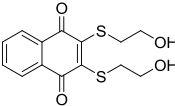
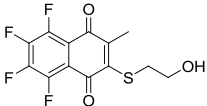
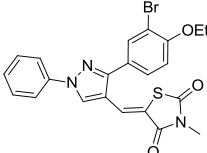
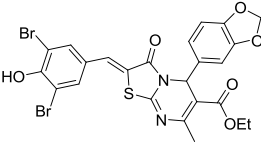
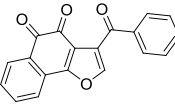
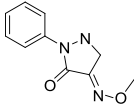
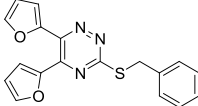
### 1.1.1 Known Inhibitors of Cdc25

As stated previously, the relatively recent addition of cdc25 to the list of recognised targets for medicinal chemistry translates to a relative scarcity of small-molecule inhibitors, particularly those with any cell activity (a selection shown in Table 1). The most successful class of cdc25 inhibitors are quinonoid compounds, with a range of reported structures displaying nanomolar potency, including many with correspondingly good cell activity.<sup>26-42</sup> The most advanced cdc25 drug candidate by some margin is Ipsen's bis-quinone IRC-08364 (**1**), recently licensed by Debiopharm although yet to enter clinical trials. IRC-08364 exerts low-nanomolar inhibition of all three cdc25 isoforms and a variety of cell lines, and has also shown moderate activity against mice bearing human tumour xenografts (Figure 4).<sup>43</sup>



**Figure 4** – Growth inhibition of xenografted tumours by IRC-083864 (**1**)<sup>43</sup>

**Table 1** – Selected *cdc25* inhibitors possessing cell activity

Cmpd No.	Structure	<i>In vitro</i> IC <sub>50</sub> ( <i>cdc25</i> isoform)	Cell IC <sub>50</sub> (cell line)	Phosphatase Selectivity	Reversibility
1 <sup>43</sup>		23-53 nM (A, B, C)	7-587 nM (panel of cell lines)	8 fold vs. VHR, PTP1B	Irreversible
2 <sup>44</sup>		150-230 nM (A, B, C)	0.1 μM (3 cell lines)	13-fold vs. PTP1B; 100-fold vs. LAR	N.D.
3 <sup>45</sup>		<1 μM (C)	<2 μM (MiaPaca2, DU-145)	N.D.	N.D.
4 <sup>26</sup>		32-96 nM (A, B, C)	1 μM average (NCI 60 tumour cell panel)	20-fold vs. VHR, PTP1B	Irreversible
5 <sup>46</sup>		0.8-1.0 μM (A, B)	1 μM (Hep3B, PLC, FemX)	Selective vs. MKP-1, PTP1B	Irreversible
6 <sup>47</sup>		2.3 μM (B)	10 μM (HT-29) <sup>a</sup>	N.D.	Reversible
7 <sup>48</sup>		4.5 μM (B)	3.4 μM (LNCaP)	N.D.	Reversible
8 <sup>31</sup>		5-10 μM (A, B, C)	1.2 μM (MDA-MB-435); 6.5 μM (PC-3)	Selective vs. VHR, PTP1B, PP2	Reversible
9 <sup>49</sup>		6.4 μM (B)	7-8 μM (MCF-7, HT-29, A549)	4-fold vs. PTP1B; >20-fold vs. VHR	Irreversible
10 <sup>50</sup>		13.8 μM (B)	20-25 μM (PC-3, MDA-MB-435)	Selective vs. MKP1,3	Reversible

<sup>a</sup> – also reported to show “comparable activity to cisplatin in C33A xenograft”



Although the data shown in Figure 4 are amongst the first *in vivo* evidence to support the hypothesis of small-molecule cdc25 inhibition for cancer therapy, the use of these simple quinone structures for cysteine phosphatase inhibition is likely to cause concern throughout the later stages of drug development for the simple reason that this functionality acts as a reactive *irreversible* inhibitor, and the mechanism of inhibition has been shown in nearly all cases to be *via* their oxidative or electrophilic properties. The cdc25 phosphatases are extremely sensitive to irreversible modification of the highly nucleophilic active-site cysteine by oxidation or covalent attachment, and this susceptibility provides an explanation for the high potency and observed selectivity of quinonoid compounds. The concerns over the safety of these compounds arise from the likely oxidation or covalent modification of a wide variety of other cellular components, the generation of reactive oxygen species (ROS), and the effect of the resulting cell damage.<sup>51</sup> It is clear that in the context of certain chemotherapy, the high toxicity of quinone-based drugs is a tolerable side-effect given the lethality of the disease itself, as evidenced by the widespread use of the anthracyclines such as daunorubicin. However, in these examples the complexity of the surrounding molecular architecture might be expected to confer higher selectivity, and in any case a key aim of future cancer medicinal chemistry is to find alternatives to reduce the undesirable side-effects that are virtually synonymous with current chemotherapy.

This project will therefore focus on reversible cdc25 inhibitors, in which there is growing interest but still few reported cell-active compounds (Table 1, compounds **6-8**, **10**), and none with the required potency and pharmacokinetic parameters to be considered a good drug candidate. Many of the compounds shown in Table 1 are single screening hits, for which no further biological investigations or SAR studies have been attempted. In addition to these cell-active compounds, there is also a range of natural products and screening hits reported as cdc25 inhibitors that fit the conventional model of phosphatase inhibitors, with a vague pharmacophore comprising an anionic phosphate mimic and a large hydrophobic region (Figure 5).<sup>52-69</sup> Although this class of compounds likely violates many of the common rules that govern desirable pharmacokinetic properties, the relative success of Wyeth's related PTP1B inhibitor Ertiprotafib (**18**) in reaching phase II clinical trials for the treatment of diabetes should allow the similar compounds in Figure 5 to be considered for further inhibitor development.<sup>70</sup>

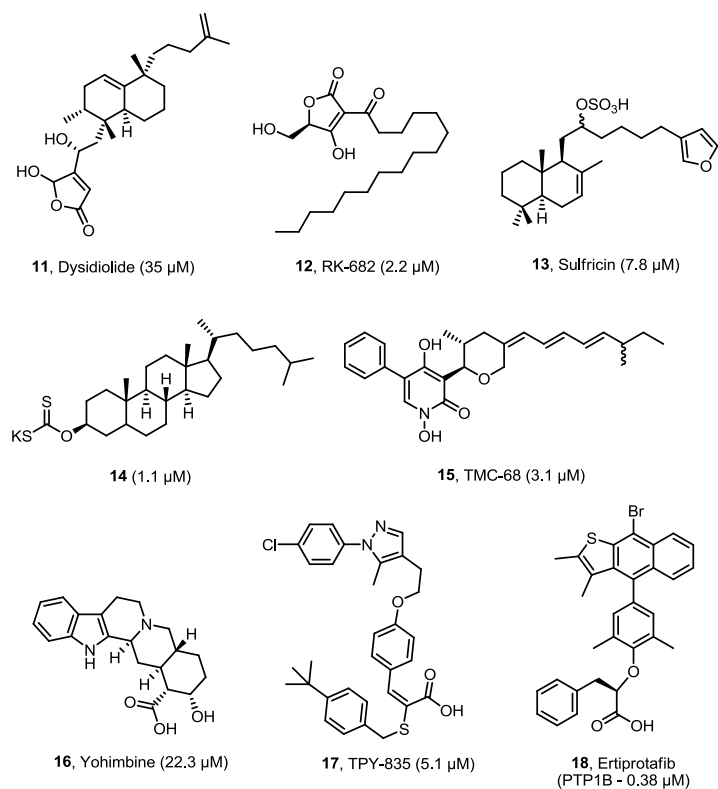


**Figure 5** – Selected *cdc25* inhibitors containing a conventional anionic phosphate-mimic ( $\text{IC}_{50}$  against *cdc25A* or *B* shown in brackets)

Despite the growing consensus placing it amongst the most interesting and relevant anti-cancer targets, the lack of success in development of inhibitors of *cdc25* is not solely attributable to the general issues of targeting phosphatases discussed previously, but also to the relative paucity of structural information that might guide rational design or modelling studies. This project aimed to try to address this problem, which is discussed in detail in the next section.

## 1.2 Structural Aspects of *Cdc25* Catalytic Domains

The catalytic domains of each *cdc25* isoform have identical phosphatase activity towards their appropriate physiological substrate compared to the full-length proteins.<sup>71</sup> This has allowed efforts to understand the structural and mechanistic basis for the activity and selectivity of these enzymes to focus purely on the C-terminal catalytic domain.

The crystal structures of the catalytic domains of cdc25A and B (Figure 6) revealed an unusual topology that is radically different to all other protein tyrosine phosphatases (PTPs), the only similarity being the active site loop containing the key sequence of eight residues that catalyse dephosphorylation, the HCX<sub>5</sub>R motif.<sup>72,73</sup> As in other PTPs, this loop is located at the top of a long alpha-helix, the dipole of which lowers the pK<sub>a</sub> of the active site cysteine from *ca.* 8.0 to *ca.* 5.9. The effect is to favour the deprotonated thiolate form and thereby increase the nucleophilicity of this residue towards the phosphate substrates. A side effect of the dramatic increase in acidity of the active site cysteine is the corresponding increase in the rate of its oxidation, calculated to be 400-fold faster than that for glutathione, the major cellular anti-oxidant.<sup>74</sup> Under normal circumstances, oxidation of a cysteine residue cannot be used for regulatory purposes since any oxidation beyond the initial sulfenic acid is considered essentially irreversible. However, the presence of a nearby second cysteine behind the active site loop allows the reversible formation under mild oxidative conditions of a disulfide bond, which has been resolved in crystal structures. This has led to the proposal that the cdc25 phosphatases are at least partly regulated by this mechanism.<sup>27,74,75</sup>

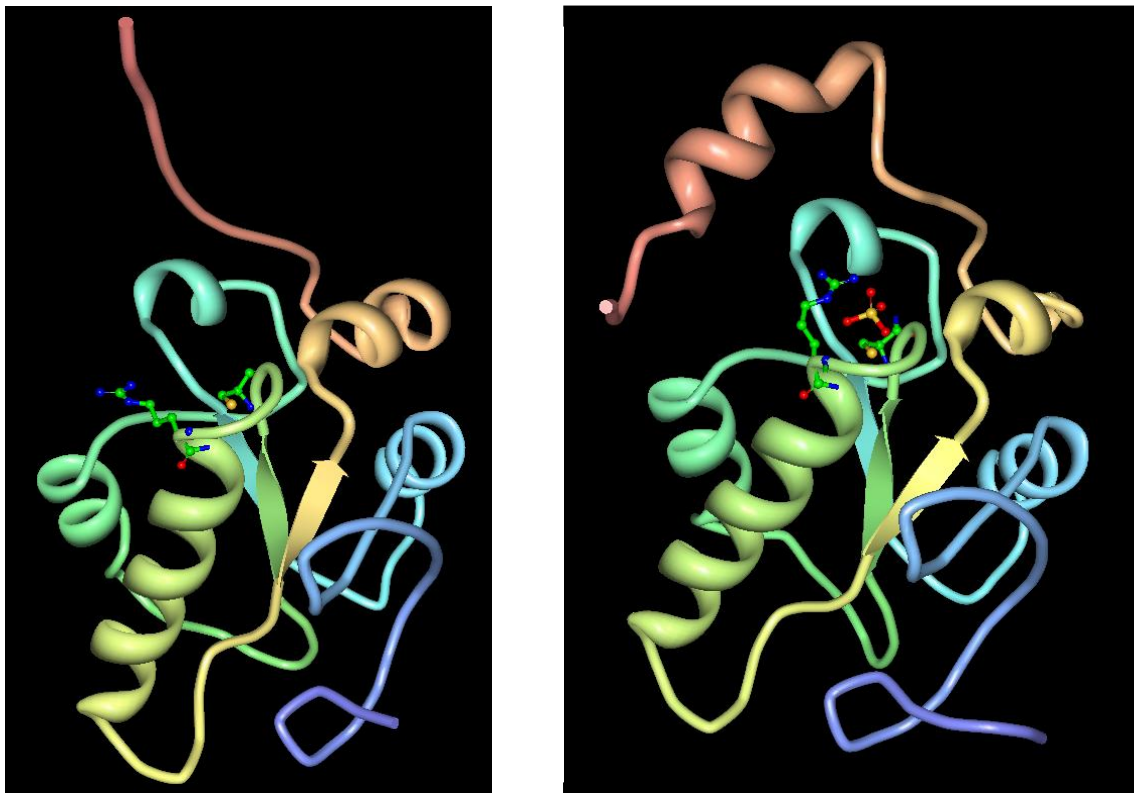


**Figure 6** – Crystal structures of catalytic domains of cdc25A (left) and cdc25B (right)

A very rare feature of the *cdc25* crystal structures compared to other phosphatases is the absence of a residue that could serve as the catalytic acid in the dephosphorylation, normally found on an overhanging loop that is absent in the *cdc25* active site. This observation prompted extensive investigations that identified an ideally placed aspartic acid residue on the CDK2 substrate. This catalytic model perhaps explains the high specificity achieved by these phosphatases and represents a novel and extremely elegant example of a distinct evolutionary solution.<sup>76-79</sup> This is supported by the absence of any significant substrate recognition pockets around the shallow, solvent-exposed active site that would differentiate between phosphorylated substrates, which would be insufficient to explain the observed six order of magnitude difference in rates between the dephosphorylation of the protein substrate and the complementary short peptide sequences.<sup>77</sup> An additional theory is that of key “hot-spot” residues in regions of the large, relatively featureless *cdc25*-CDK2 interface that are distant from the active site yet critical for docking and phosphatase activity. A number of these hot-spot residues have since been identified by virtual docking and point mutation studies.<sup>6,79-82</sup>

The major differences in the crystal structures of the catalytic domains of *cdc25A* and *B* suggest that the *cdc25A* crystal structure does not display the protein in its correctly folded, physiologically relevant conformation. Evidence for this conclusion is initially found by close comparison of the active site; whereas the conserved HCX<sub>5</sub>R loop in *cdc25B* displays an almost identical molecular architecture to the vast majority of other phosphatases, the active site of *cdc25A* contains a number of differences.<sup>72</sup> The most serious consequence of this altered folding is that the arginine residue involved in the dephosphorylation mechanism is orientated away from the active site. Furthermore, all attempts to crystallise an anionic substrate mimic into the active site of *cdc25A* have been unsuccessful, including with phosphate, tungstate and vanadate,<sup>22</sup> and there are no reports of any difficulty achieving this for *cdc25B*. The most obvious difference between the two crystal structures is the conformation and resolution of the C-terminal residues. In *cdc25B*, an additional  $\alpha$ -helix is formed adjacent to the active site, with a key H-bond between a glutamic acid in the HCX<sub>5</sub>R loop and a conserved methionine.<sup>73</sup> This creates a more structured cleft for substrate binding compared to the relatively flat surface of the *cdc25A* crystal structure, in which the C-terminus extends as a long, unstructured random coil away from the core and is almost completely unresolved. Given the similarity between these two isoforms of C-terminal primary sequence, substrate specificity and inhibitor potency, it is reasonable to find such a significant structural difference as potential evidence that at least one of these crystal

structures is not biologically relevant. Although in theory the structure of either isoform could be the anomaly, the additional fundamental active site differences explained above point to the problem being with cdc25A. This is corroborated by the fact that, whilst cdc25B has been crystallised many times in a number of different studies (including as various mutants and in different oxidation states), there has only been the one reported crystal of cdc25A. Tellingly, the crystal structure of a truncated form of cdc25B, lacking the C-terminal helix, demonstrates an arrangement of the active site that appears closer to that of the crystal structure of cdc25A. The importance of the extreme C-terminal sequence to substrate binding has been confirmed by a variety of deletion and isoform-hybridisation studies.<sup>83</sup> The additional pocket in cdc25B adjacent to the active site, created by the C-terminal helix, has also been proposed as a possible small-molecule binding site for a wide range of published inhibitors (see Figure 31). This secondary pocket has been dubbed the “swimming pool” due to the large number of water molecules found there in the crystal structure.<sup>84</sup>

To summarise, the available structural data for cdc25 are poor, with only cdc25B having been reproducibly crystallised. In addition, the active-site features of this protein – specifically the lack of many significant structural features – further increases the difficulty of a modelling-based approach to new cdc25 inhibitors. The final missing piece of data is the lack of any crystal structures with bound small molecule inhibitors; this is generally considered a prerequisite for both rational design of better inhibitors in the same class and also the validation of any docking technique prior to virtual screening for novel inhibitor classes. Section 5 further discusses these issues and details attempts to provide some of this missing information.

### ***1.3 Protein-Ligand Engineering for Chemical Genetics***

The third aim of this project is to attempt to elucidate the precise function of each cdc25; this is a challenging goal that would undoubtedly further the understanding of cell cycle regulation and may ultimately lead to novel therapeutic targets or the discovery of new biochemical pathways. The highly conserved nature of the active sites of the cdc25 isoforms will likely necessitate an approach to their differentiation that transcends the conceptually simple search for a specific chemical inhibitor. Protein-ligand engineering involves site-specific mutation of the target enzyme, usually creating an enlarged active site pocket (or “hole”). The inhibitor is then chemically modified, usually by addition of a sterically

demanding group (or “bump”), in an attempt to exploit the additional binding region now available (Figure 7A).<sup>85</sup> The modified inhibitor should exhibit a larger binding affinity for the mutant enzyme than for all three wild-type *cdc25* isoforms, allowing specific inhibition of the target enzyme. Alternative methods of protein-ligand engineering involve interfering with the inhibitor binding interactions by altering the direction of H-bonding and ion pairs (Figure 7B).

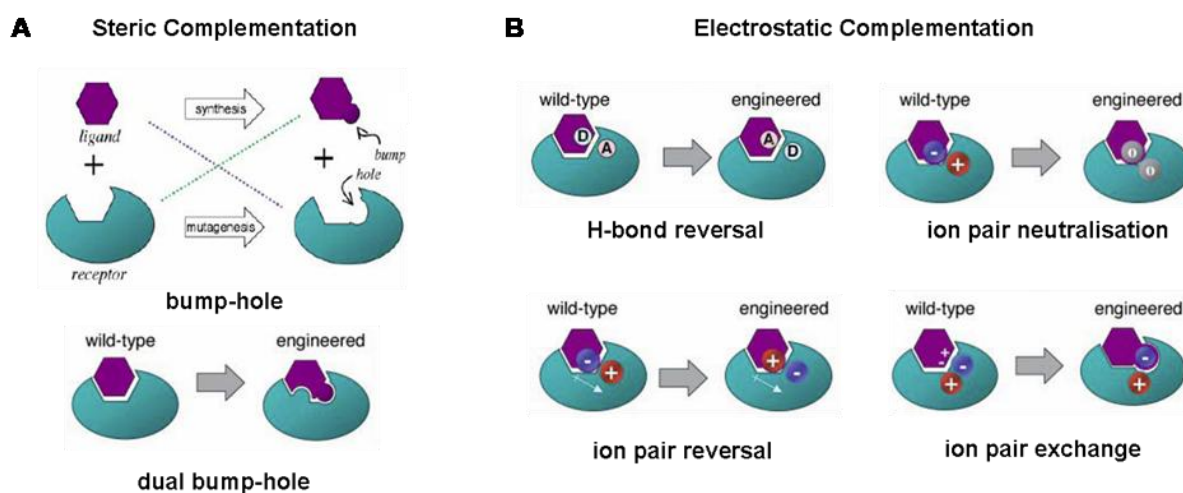


**Figure 7** – Approaches for chemical genetics<sup>85</sup>

There are numerous benefits of the selective inhibitor approach to altering the function of *cdc25* (chemical genetics) over using directed genetic mutations (classical genetics).<sup>86,87</sup> The most obvious is the conditional nature of the inhibition, which not only allows study of the effect of removing the target enzyme activity at different stages of the cell life-cycle (especially vital in this case), but during *in vivo* studies also allows selection of a target enzyme (such as *cdc25A*) that is required for foetal development. Chemical genetics also allows careful tuning of the experiment by using different inhibitor concentrations, as opposed to the all-or-nothing result of a classical genetic mutation.

Success in this approach will likely require the crystal structure of a bound small-molecule inhibitor to allow selection of the appropriate positions for the respective bump and hole modifications, which is the combined goal of the first two aims of this research discussed above. This technique has found most success in the kinase field, where highly conserved ATP-binding sites make protein-ligand-engineering both important and widely applicable,<sup>88</sup> but has been extended to phosphatases in a recent study on the prototypical members of the protein tyrosine phosphatase (PTP) family.<sup>89</sup>

## 2 Analogue Synthesis – Dysidiolide Analogues

At the outset of the project, very few of the more drug-like inhibitors shown in Table 1 had been reported. Additionally, it was thought that choosing approaches less likely to be pursued in the pharmaceutical industry might result in a greater overall contribution to the field. The structurally complex phosphate mimic dysidiolide (Figure 5) was chosen with the aim of synthesising structural analogues to probe the SAR and ultimately find more potent inhibitors. Dysidiolide (**11**) was isolated in 1996 from a marine sponge and was the first reported natural product inhibitor of cdc25, with low micromolar activity against both the purified enzyme and two cell lines, and good selectivity against a small panel of related phosphatases.<sup>90</sup>

A survey of the literature had revealed that the vitamin D<sub>3</sub> steroid rings provide an alternative hydrophobic region to the complex decalin core of dysidiolide (Figure 8).<sup>61,91</sup> Given the undoubtedly imprecise binding mode for the large alkyl sections of this class of inhibitors, it was thought

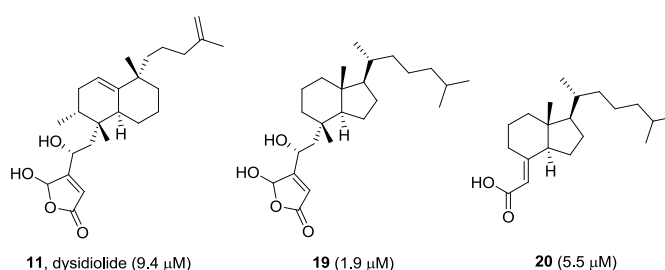


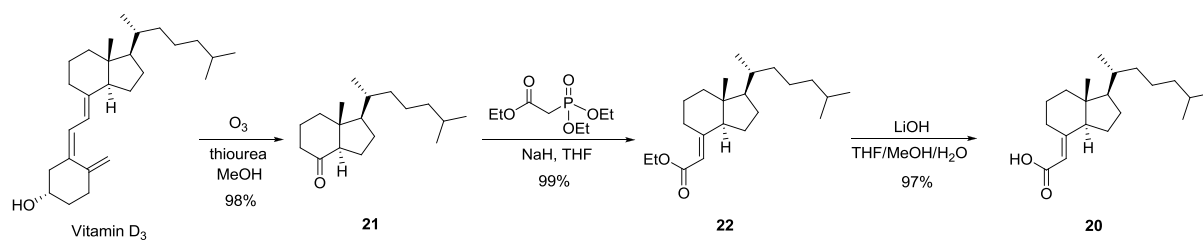
**Figure 8** – Comparison of dysidiolide (**11**) with simpler analogues **19** and **20**<sup>61,91</sup>

(IC<sub>50</sub> against cdc25A shown in brackets)

possible in this research to investigate the effect of various phosphate mimic functionalities without significant alteration of the binding position or orientation. This would allow sequential optimisation of the hydrophilic and hydrophobic regions, with the obvious need in the second stage to considerably reduce the size and lipophilicity of the latter region. The few reported studies of dysidiolide SAR made no attempt to survey the activity of common phosphate bioisosteres, and synthetic efforts to investigate the hydrophobic region have largely focussed on the possible diastereomers of the key butenolide side chain.<sup>56,59</sup>

Synthesis of carboxylic acid **20** from vitamin D<sub>3</sub> began with ozonolysis using a modified reduction with thiourea in order to simplify purification of ketone **21** (Scheme 1). The subsequent Horner-Wadsworth-Emmons olefination was extremely slow under standard conditions, and also resulted in considerable epimerisation of the ring-junction proton to give the more stable *cis*-fused 6,5-system. However, it was found that using a large excess of the phosphonate reagent gave virtually quantitative conversion to the desired ethyl ester **22**, with

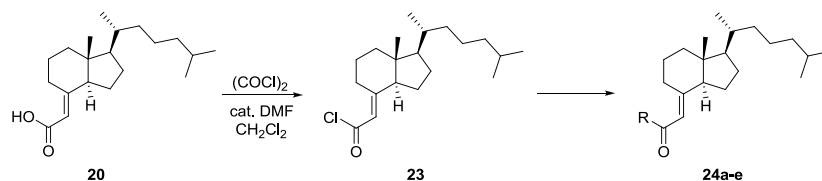
92:8 *E:Z* selectivity and no observed epimerisation. Hydrolysis of this ester gave carboxylic acid **20**, a known potent *cdc25A* inhibitor used as a reference in the initial assay development.



**Scheme 1** – Synthesis of carboxylic acid **20**

Conversion to the acid chloride under standard conditions allowed acylation of a variety of amines, amides and sulfides to give a range of conventional carboxylic acid bioisosteres **24a-e** (Table 2).<sup>92</sup> The *N*-acetyl and *N*-trifluoroacetyl amides were also prepared but were found to be unstable to hydrolysis and could not be isolated.

**Table 2** – Synthesis of carboxylic acid bioisosteres **24a-e**

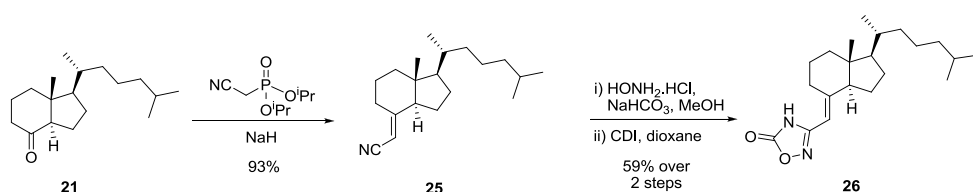


Product	R	Conditions	Yield from <b>20</b> (%)
<b>24a</b>	-NHSO <sub>2</sub> Me	H <sub>2</sub> NSO <sub>2</sub> Me, DMAP, Et <sub>3</sub> N, CH <sub>2</sub> Cl <sub>2</sub> , r.t.	73
<b>24b</b>	-NHCN	NaNHCN, THF, r.t.	84
<b>24c</b>	-SH	NaSH, EtOH, -10 °C	81
<b>24d</b>	-NHOH	NH <sub>2</sub> OH, THF/H <sub>2</sub> O, 5 °C	85
<b>24e</b>	-NHCO <sub>2</sub> Me	H <sub>2</sub> NCO <sub>2</sub> Me, PhMe, 80 °C	53

Attempted synthesis of the corresponding vinyl tetrazole, a widely-used bioisostere for the carboxylate group,<sup>92</sup> (Scheme 2) began with HWE-olefination of ketone **21** to give unsaturated nitrile **25** in moderate yield using stoichiometric phosphonate. This reaction proceeded much more rapidly than for the phosphonoacetate, presumably due to the higher

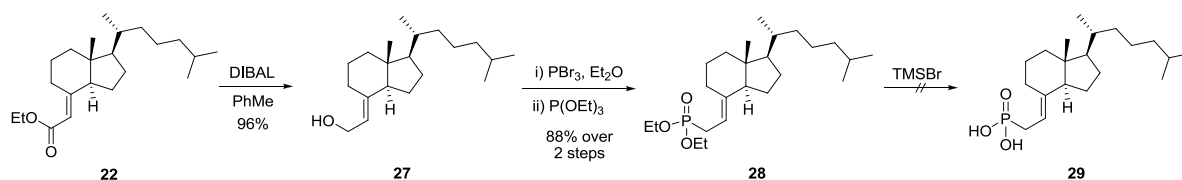


nucleophilicity and smaller size of the  $\alpha$ -nitrile anion. The yield could however be increased by using an excess of the cyanomethylphosphonate. The subsequent tetrazole synthesis proved unsuccessful, as even under forcing conditions the azide cycloaddition proved to be extremely slow and only very low conversion was observed after seven days. An alternative acidic heterocycle, oxadiazolone **26**, was successfully synthesised by hydroxylamine addition and acylation using CDI. Attempted acylation of the amidoxime intermediate using TCDI also gave **26** after work-up, indicating hydrolytic instability of the thiocarbonyl group.



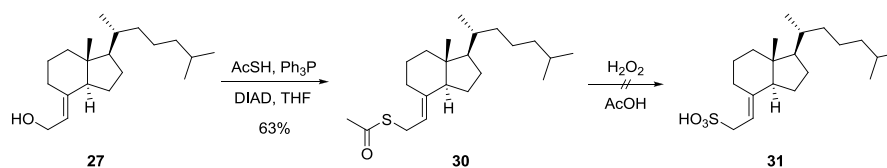
**Scheme 2** – Synthesis of oxadiazolone **26**

Attempts to utilise a diphosphonate HWE reagent in the synthesis of the corresponding vinylphosphonic acid were unsuccessful, reflecting the hindered, stabilised nature of the diphosphonate anion. An alternative allylphosphonate, **28**, was prepared in good yield by DIBAL reduction, bromination and Arbusov reaction (Scheme 3). It was found that using shorter reaction times with higher temperatures resulted in less decomposition of the reactive allyl bromide than prolonged heating at lower temperatures. Acid hydrolysis using TMSBr to give the free phosphonic acid **29** was successful, but isolation and purification of this highly amphiphilic compound proved extremely difficult. This became a recurring problem for synthesis of other highly acidic dysidiolide analogues, and was not resolved prior to the initial assay results which prompted us to halt any further efforts (see Section 4). The use of the allyl phosphonate had allowed the possibility of electrophilic fluorination to give the  $\alpha$ -mono- and di-fluorophosphonic acids, which possesses very similar  $pK_a$  values to the phosphate group of the *cdc25* substrates.<sup>93,94</sup> However, preliminary investigations into this transformation using standard conditions found it to require extensive optimisation, and this was also not achieved prior to the initial negative assay results.



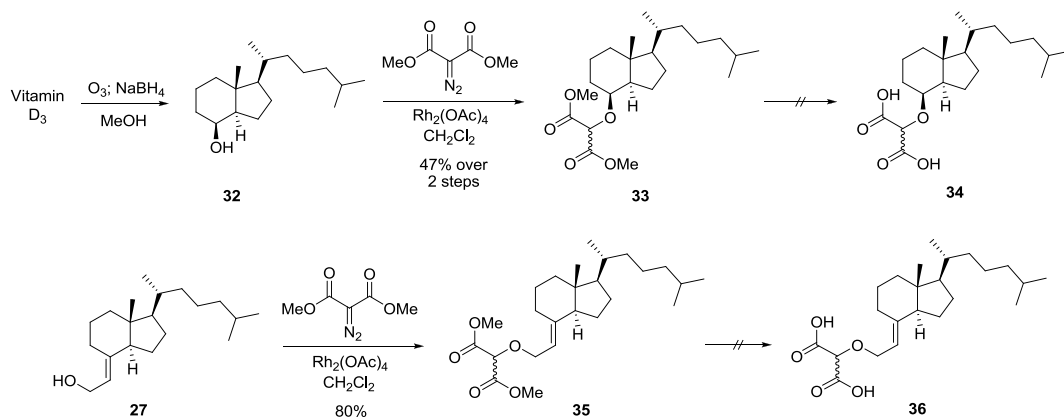
**Scheme 3** – Attempted synthesis of phosphonic acid **29**

The direct synthesis of sulfonic acid analogue **31** from the allylic bromide intermediate previously prepared was unsuccessful due to the instability of the bromide to various standard nucleophilic sulfonation conditions. An alternative route from allylic alcohol **27** involved successful Mitsunobu displacement by thioacetic acid and subsequent hydrolysis-oxidation of thioacetate **30** (Scheme 4). Various oxidation conditions were attempted to give clean conversion to sulfonic acid **31**, but as with the phosphonic acid it did not prove possible to fully purify the highly amphiphilic product prior to the initial assays.



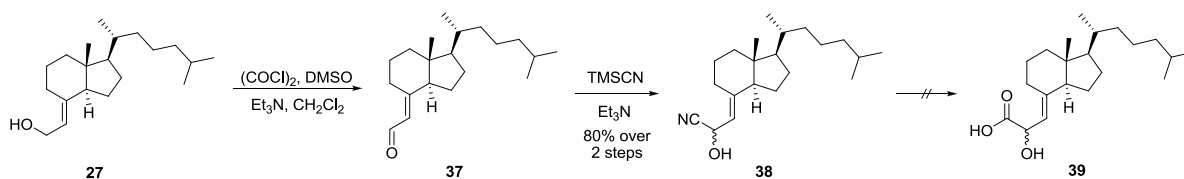
**Scheme 4** – Attempted synthesis of sulfonic acid **31**

Attempted synthesis of malonic acid derivative **34** (Scheme 5) began with reductive ozonolysis of vitamin D<sub>3</sub>, to give only one diastereomer of alcohol **32** in accordance with the literature precedent.<sup>60</sup> Carbenoid insertion into alcohols **27** and **32** using dimethyl diazomalonate proceeded in good yield to give diesters **33** and **35**. Predictably, the malonic acid derivatives resulting from the subsequent hydrolysis caused similar difficulties in purification to the phosphonic and sulfonic acids, and once again these compounds were not satisfactorily purified prior to the initial assays.



**Scheme 5** – Attempted synthesis of dicarboxylic acids **34** and **36**

Synthesis of  $\alpha$ -hydroxy carboxylic acid **39** was attempted *via* hydrolysis of cyanohydrin **38**, prepared from alcohol **27** in 2 steps (Scheme 6). It was found that immediate reaction of the crude aldehyde gave higher yields, and rapid reaction under solvent-free conditions proved most successful.<sup>95</sup> However, attempted acid hydrolysis of nitrile **38** resulted in rapid decomposition under a variety of conditions.



**Scheme 6** – Attempted synthesis of  $\alpha$ -hydroxy carboxylic acid **39**

A simple route to the synthesis of a variety of alternative inhibitors can be clearly envisaged by acylation reactions of carboxylic acid **20** or alcohol **27**. Coupling of acid **20** with various alcohols and amines under common coupling conditions proved to be unexpectedly difficult, particularly with heterocyclic and aromatic amines. As a result, only the esters of maltol (**40**) and mandelic acid (**41**) were successfully synthesised in good yield and tested in the phosphatase assay (Figure 9). These compounds were designed to hopefully mimic the binding modes of known quinone and  $\alpha$ -aryl carboxylate inhibitors respectively (see Figure 5).<sup>5</sup> Alternative aryl carboxylic acid **42** was also prepared from alcohol **27** using phthalic anhydride.

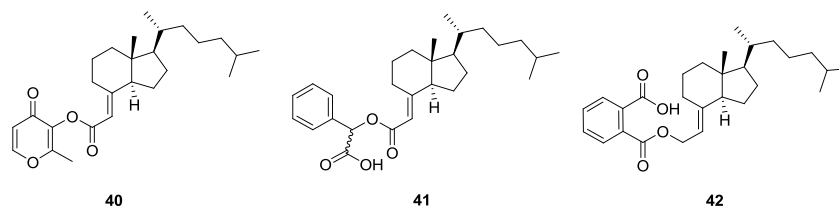
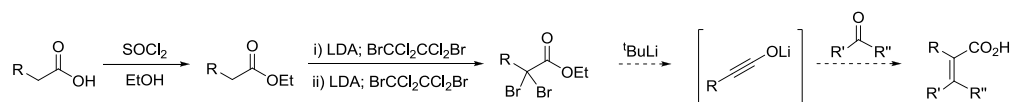


**Figure 9** – Other inhibitors synthesised by acylation reactions

A further strategy considered for analogue synthesis was the introduction of various  $\alpha$ -substituents to carboxylic acid inhibitor **20**. Ynolate chemistry was chosen as the best method for olefination of the unreactive ketone **21** to give tetra-substituted alkenes (Scheme 7).<sup>96</sup> A selection of dibromoester substrates were prepared from the corresponding acids by a three step esterification and bromination sequence, with optimisation required to overcome the significant purification problems that resulted from incomplete conversion in the bromination reactions. However, optimisation of the ynolate olefination reaction was also not completed before the results of the initial assays terminated this line of investigation. A further proposed strategy that could not be completed was the synthesis of tetric acid phosphate mimics based on the potent *cdc25* inhibitors inspired by natural product RK-682 (**12**, see Figure 5).<sup>57</sup>



**Scheme 7** – Proposed synthesis of  $\alpha$ -substituted analogues of carboxylic acid inhibitor **20** by ynolate olefination of ketone **21**

To summarise, the first library of novel compounds was based on known inhibitor **20**, focussing on alternative phosphate mimics. Low reactivity and difficult purification were found to be common problems with this class of compound, and the original goal of a two-stage optimisation of dysidiolide analogues towards more drug-like compounds was at this stage considered too ambitious to warrant further investigation. The next sections detail the development of the *cdc25* phosphatase assay used above and subsequent attempts to use the literature quinonoid inhibitors as starting points for the development of novel, reversible inhibitors.

### 3 Assay Development

A validated *cdc25* phosphatase activity assay was required for the testing of the synthesised compounds. In order to obtain significant quantities of purified *cdc25A*, a construct had previously been prepared by co-workers for bacterial expression of GST-fused *cdc25A* using a pGEX vector. This fusion to GST (glutathione *S*-transferase), a high-affinity glutathione-binding enzyme, allows simple purification by selective immobilisation on glutathione-functionalised beads. pGEX vectors place expression of the gene of interest under control of the powerful *tac* promoter; this is then activated by the addition of IPTG (a non-hydrolysable mimic of a lactose metabolite), triggering high levels of transcription of the associated gene.

Initial expression and purification using standard conditions gave moderate levels of both yield and purity (assessed by SDS-PAGE analysis). The yield of protein expression is dependent on the length of time and the temperature following induction with IPTG, and is affected by unknown factors such as protein solubility, toxicity and degradation. The expression of GST-fused *cdc25A* was therefore optimised for incubation temperatures and time; SDS-PAGE analysis of the cell lysates suggested that lower temperatures and longer induction times resulted in optimal yields of GST-*cdc25A*.

In accordance with many of the published protocols, the phosphatase activity assay development initially used *para*-nitrophenyl phosphate (PNPP, Figure 10A) as a small molecule substrate. PNPP assays measure the absorbance of the *para*-nitrophenol product using a photometer, and are commonly chosen due to the simplicity and low cost. The assay was designed to confirm the linear dependence of the end-point absorbance measurement on the concentration of solid-supported GST-*cdc25A*, using a standard buffer composition and assay conditions. Addition of NaOH stops the reaction and ensures that all the phenol product is in the deprotonated, chromogenic form prior to measurement of the absorbance. An approximate linear correlation between enzyme concentration and absorbance was observed, but these assays suffered from a very low signal to noise ratio and were also poorly reproducible. Attempts to intensify the measured absorbance signal by increasing reaction times and PNPP concentration did not achieve a significant improvement.

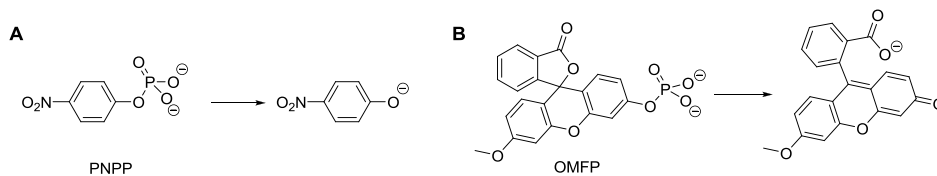


**Figure 10** – Artificial substrates for phosphatases

It has been reported that an alternative artificial substrate, 3-*O*-methylfluorescein phosphate (OMFP, Figure 10B) is a much better substrate for *cdc25*, with a thousand-fold improvement in the reaction rate.<sup>97</sup> Furthermore, the dephosphorylated product is fluorescent, inherently increasing the sensitivity of the measurements. A further practical advantage of using a continuous (as opposed to end-point) assay was the ability to obtain a full kinetic profile for each individual assay well, eliminating the error caused by reliance on a single end-point reading. Linear regression of the obtained data points thus allows direct measurement of the reaction rate. A potential disadvantage with this alternative assay was the reportedly high background rate of OMFP hydrolysis at the alkaline pH required for the assay, with a half-life of one hour.<sup>97</sup> Originally, it was hoped that the use of a very short reaction time would circumvent this issue, but fortunately it became clear that the rate of background hydrolysis in the buffer used was negligible.

The initial OMFP assay results demonstrated a much improved signal to noise ratio over the colourimetric method. Screening of conditions around those reported for literature inhibitor assays found suitable conditions using the minimum quantities of the solid-supported protein and OMFP that still produced a strong fluorescence signal.<sup>52</sup> The recorded fluorescence was linear throughout the assay and independent of minor changes in the substrate concentration. It was next confirmed that relatively high concentrations of DMSO (10-20%) had little effect on the phosphatase activity or OMFP hydrolysis.

The accuracy and reliability of the optimised assay was confirmed by measurement of the IC<sub>50</sub> value of a reference inhibitor, dysidiolide analogue **20**. Inhibitor assays were performed in triplicate, with 8-10 concentrations for a full IC<sub>50</sub> measurement, the reaction rates then data-fitted to a standard sigmoid curve using SigmaPlot.<sup>98</sup> It was discovered during these initial attempts that the reproducibility of the data was much lower than anticipated, a possible result of the inherent difficulties in using small amounts of solid-supported enzyme in a reaction setup that did not allow for mixing during the experiment. It was not known whether

the variation in results was due to unpredictable settling of the beads in the assay wells or a result of inconsistent transfer of the stock enzyme suspension leading to differences in the number of beads in each well. To address this issue, the enzyme was eluted from the beads using reduced glutathione to interfere with the binding interactions, this free glutathione then being removed from the GST-cdc25A stock solution by dialysis.

The subsequent assays proved to be much more reproducible, and the literature  $IC_{50}$  value for reference inhibitor **20** was reproducibly achieved within experimental error. This result validated the accuracy and reliability of the OMFP assay, and allowed testing of the novel inhibitors synthesised previously. Unfortunately, the results obtained for the initial compounds tested were disappointing. Many of the less-polar compounds showed no inhibition at all, possibly suggesting problems of solubility or the likely absolute requirement for this class of compounds to have an anionic phosphate mimic in order to bind to the active site. The remainder of the compounds exhibited poor inhibition, with projected  $IC_{50}$  values  $> 50 \mu\text{M}$ . The only exception was ketosulfonamide **24a** (cdc25A  $IC_{50}$   $9.3 \mu\text{M}$ ), with potency comparable to the reference carboxylic acid. It was clear, therefore, that no conclusions could be drawn from the results regarding the phosphate-mimic preference of cdc25A and, as discussed in the previous section, the synthetic efforts towards similar compounds that had yet to be completed were halted.

The successful development and validation of the cdc25A fluorimetric phosphatase assay provided a good basis for the synthesis of the next class of literature inhibitor analogues, discussed in Section 4.

## 4 Analogue Synthesis – Quinone Analogues

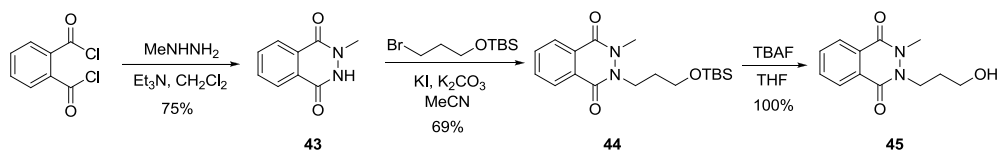
Having been unsuccessful in our attempts to find novel dysidiolide analogues with improved potency (and ultimately improved pharmacokinetic properties), we next reconsidered the reported quinonoid *cdc25* inhibitors as a possible starting point for further development. Whilst the reasons outlined above for the initial rejection of this class remained valid, chiefly their irreversible mechanism of inhibition, an alternative strategy was proposed based on consideration of the proposed binding affinity of these structures for the *cdc25* active site *prior* to the alkylation/oxidation event, with conventional binding models put forward in the literature based on molecular modelling for a range of quinone inhibitors.<sup>26,30,42,99,100</sup> Our concept was to mimic these proposed binding interactions of the quinone carbonyl oxygens by synthesising analogues of similar molecular shape and size, containing the requisite carbonyl groups but lacking the ability to irreversibly alkylate or oxidise the key *cdc25* active-site cysteine. Two classes of simple heterocycle matching these criteria were investigated; phthalazinediones and diketopiperazines.

It was noted at this stage that the proposed modifications of the existing literature inhibitors were of a highly speculative nature, and that the long-term success of the project likely resided with the implementation of a more rational approach to inhibitor design. Contemporaneously with the synthesis of quinone analogues described in this section, it was therefore decided to attempt to obtain novel structural and ligand-binding information for *cdc25* (see Section 5).

### 4.1 *Phthalazinediones*

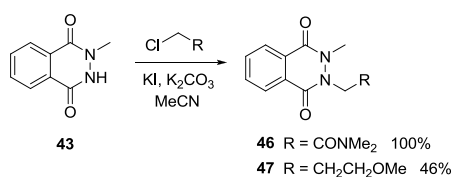
Direct isosteric replacement of two adjacent carbon atoms from the literature naphthoquinone core results in the cyclic hydrazide phthalazinedione. This was identified as the simplest and most direct modification that would result in rapidly synthetically-accessible non-quinonoid analogues. An isostere of a potent literature quinone (an analogue of **4**) was therefore synthesised in 3 steps by reaction of phthaloyl dichloride with methylhydrazine to give the intermediate mono-alkyl phthalazinedione **43**, alkylation with TBS-protected 3-bromopropanol and deprotection, giving target alcohol **45** in good overall yield (Scheme 8).





**Scheme 8** – Synthesis of phthalazinedione **45**

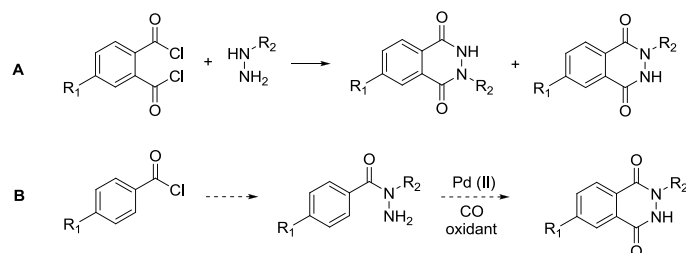
Two further analogues were prepared from the corresponding alkyl chlorides, including the methyl ether analogue of alcohol **45** (Scheme 9).



**Scheme 9** – Synthesis of phthalazinedione analogues **46** and **47**

These three phthalazinediones were subsequently assayed against *cdc25A*, and were found to show no inhibition up to 100  $\mu$ M. The most likely reason for the failure of this approach is that the reported specific initial binding of the quinone inhibitors is very weak, with the reported  $IC_{50}$  value deriving almost exclusively from the effect of the ensuing covalent attachment, despite the various literature docking studies and SAR interpretation. Alternatively, the isosteric replacement in the phthalazinedione series may have a larger effect on the binding than originally considered.

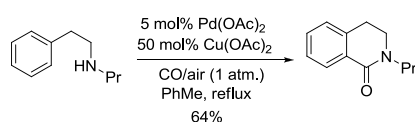
Despite the inapplicability to the *cdc25* project, in order for phthalazinediones to be integrated into the array of heterocycles that are routinely explored in the course of other medicinal chemistry investigations it is necessary that they can be synthesised in a regioselective manner with respect to the substituents on the phenyl ring and the amide nitrogens. Current methods of phthalazinedione synthesis almost invariably proceed (as above) from a benzoic di-acid precursor and a hydrazine, with one of the components symmetrically substituted to avoid the inevitable and likely inseparable mixture of regioisomers that would result (Scheme 10, Route A). An alternative method was proposed that would allow for simple and flexible synthesis of any regioisomer by directed C-H activation and carbonylative cyclisation of a benzoic hydrazide under Pd catalysis (Scheme 10, Route B).



**Scheme 10** – Conventional and proposed syntheses of substituted phthalazinediones

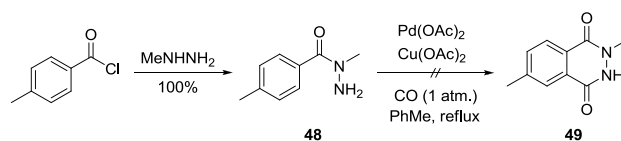
The regiochemical outcome would be controlled by the simple choice of either *ortho*- or *para*-substituted benzoyl chlorides, and by using orthogonal strategies for regioselective synthesis of mono-substituted hydrazides; acylation of a substituted hydrazine under mild conditions usually results in selective reaction of the secondary amine, whereas alkylation or reductive amination of an unsubstituted hydrazide will likely occur on the terminal amine-like nitrogen.

The proposed synthesis has strong precedent in Orito's synthesis of benzolactams by a similar mechanism (Scheme 11).<sup>101</sup> It was noted, however, that the increased electron-deficiency of the aryl ring of the benzoic hydrazides would likely result in a greatly reduced rate of reaction.



**Scheme 11** – Orito's benzolactam synthesis by directed C-H carbonylation

Slow addition of *p*-toluoyl chloride to a large excess of methylhydrazine resulted in quantitative, regioselective mono-acylation, but the hydrazide product **48** did not undergo the desired carbonylative ring-closure under Orito's conditions, using a full equivalent of the Cu(OAc)<sub>2</sub> oxidant at this stage (Scheme 12). Repeat attempts were unsuccessful and the methodology was not pursued further due to the lack of inhibition observed for this class of compound in the enzyme assays.



**Scheme 12** – Attempted phthalazinedione synthesis by directed C-H carbonylation

## 4.2 Diketopiperazines

The diketopiperazine (DKP) strategy, the more speculative of the two approaches, was based on the convergence of two observations; the comparatively flat conformation of the DKP ring should place the amide carbonyl groups in similar orientations to that in quinones,<sup>102</sup> and alkenyl DKPs might display a qualitatively similar binding mode to the analogous thiazolidinedione cdc25 inhibitors reported by Kim<sup>47</sup> (Figure 11).

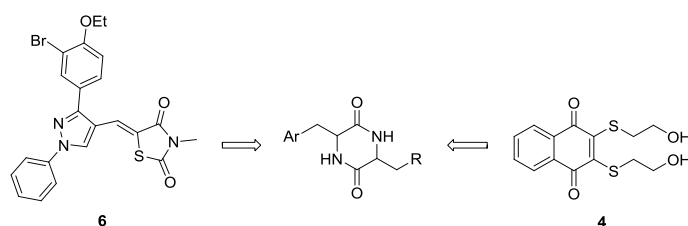
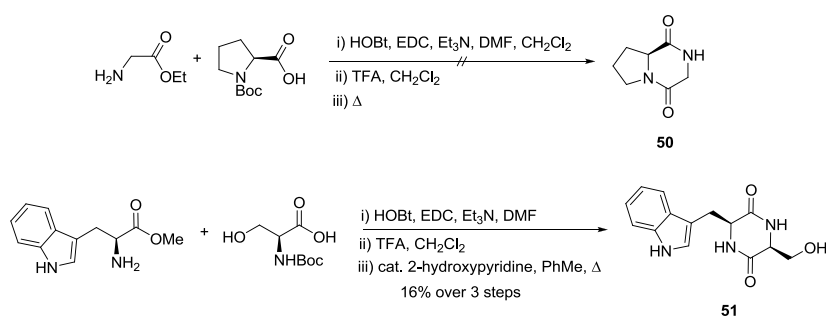


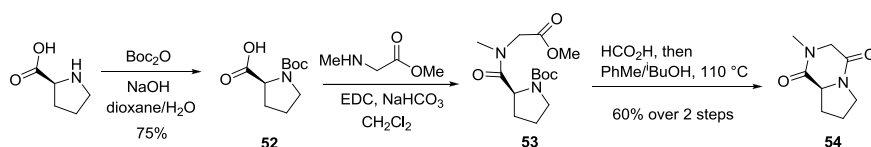
**Figure 11** – Comparison of proposed DKP structures with literature inhibitors

An initial test of a direct DKP synthesis was attempted by a reported amino acid dimerisation with no purification of the intermediates, but gave a very low overall yield (Scheme 13). A similar 3-step DKP synthesis was attempted using alternative, more-functionalised amino acid derivatives, with characterisation of crude intermediates to identify the problematic step. Once again a very low yield of crude DKP product **51** was obtained, with the final cyclisation proving most difficult (Scheme 13).



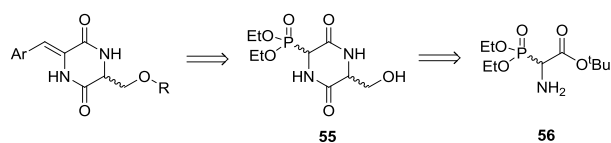
**Scheme 13** – Attempted rapid synthesis of DKPs by amino acid dimerisation

Modified conditions for the DKP ring closure reaction allowed efficient synthesis of non-aromatic naphthoquinone mimic **54** from proline and sarcosine in good overall yield (Scheme 14).



**Scheme 14** – Synthesis of DKP **54** by amino acid dimerisation

These initial attempts prompted the proposal of a novel strategy to access a library of 3-alkenyl, 6-alkyl DKPs by derivatisation of an appropriately functionalised common intermediate (Scheme 15). This would circumvent carrying out the problematic ring-closure reaction for each target compound. DKP **55**, formed from the coupling and cyclisation of serine and  $\alpha$ -phosphonoglycine ester **56**, was identified as an appropriate core molecule, allowing olefination and O-alkylation as the last steps in the synthesis of a potentially diverse library of compounds. The use of a phosphonate intermediate for the synthesis of alkenyl DKPs has been shown to be an efficient strategy,<sup>103,104</sup> with the considerable advantage of avoiding the coupling of unreactive dehydro amino acids.<sup>105</sup>

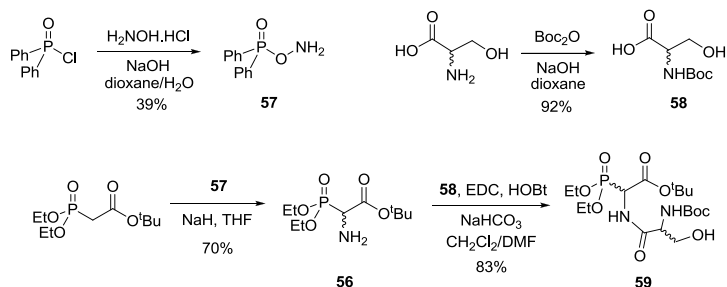


**Scheme 15** – Proposed synthesis of a DKP library *via* phosphonate intermediate **55**

This choice of substitution pattern for the proposed DKP library was based on a qualitative comparison with the literature quinone inhibitors and Kim's thiazolidinedione **6** (Figure 11). Introducing conjugated aryl groups to one position of the DKP would mimic both the diarylpyrazole of **6** and the benzene ring of the naphthoquinone inhibitors. This would also have the effect of increasing the planarity of the DKP ring. The introduction of small alkyl groups to the remaining unsubstituted position would mimic the range of known quinone inhibitor substituents, such as the thioethanol chains in quinone **4**.

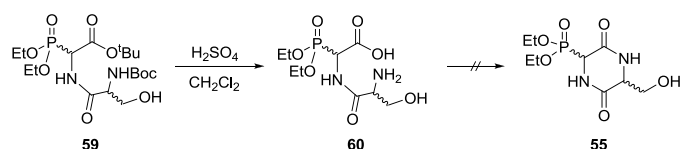
The shortest route to racemic phosphonoglycine **56** was proposed to be *via* direct amination of a phosphonoacetate anion, and the required aminating reagent DPPONH<sub>2</sub> (**57**) was synthesised according to the literature procedure in moderate yield (Scheme 16). In order to increase the efficiency of the synthetic route, the simultaneous deprotection of both the carboxylic acid and the amine required for the final cyclisation was made possible by the use of *tert*-butyl phosphonoacetate in conjunction with *N*-Boc serine. Amination of *tert*-butyl

diethylphosphonoacetate was carried out in good yield, and the product (**56**) coupled with *N*-Boc serine **58** under standard conditions to give phosphono-dipeptide **59**, although this compound was not fully purified prior to the attempted cyclisation reactions.



**Scheme 16** – Synthesis of protected dipeptide **59**

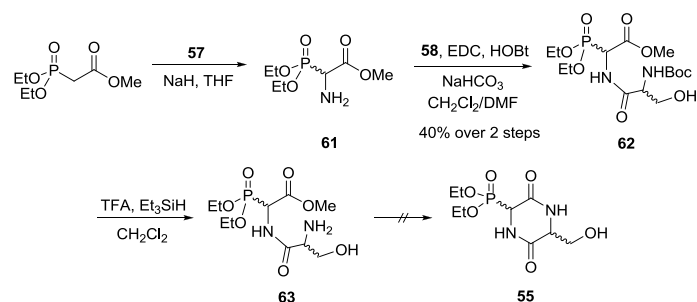
Attempted removal of both the Boc group and the *tert*-butyl ester under standard TFA conditions proved to be a very slow reaction, with long reaction times leading to decomposition. Addition of triethylsilane as a cation scavenger appeared to prevent the side-reactions, but did not improve the low conversion. Full deprotection was finally achieved using sulfuric acid in  $\text{CH}_2\text{Cl}_2$  (Scheme 17). However, cyclisation of resulting crude amino acid **60** proved equally problematic. A variety of reported conditions for DKP synthesis were attempted, including both carbodiimide and HCl activation of the carboxylic acid. In all cases, very low conversion was observed, even when using more forcing conditions.



**Scheme 17** – Attempted synthesis of phosphono-diketopiperazine **55**

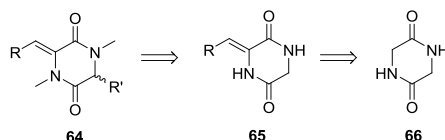
Although cyclisation conditions for DKPs in the literature are quite varied and substrate-dependent, the most general method is microwave heating of the methyl amino-ester in water. Cyclisation precursor **63** was synthesised in three steps and in comparable yields to the *tert*-butyl series, although coupling product **62** proved similarly difficult to fully purify (Scheme 18). However, the cyclisation reaction was again unsuccessful and resulted in a large number of products by  $^{31}\text{P}$ -NMR and TLC analysis of the crude reaction mixture. The difficulties encountered in ring-closure of these phosphono-dipeptides appear to be specific to these

substrates, and could stem from issues with steric hindrance, conformational preferences or problems of chemoselectivity around this highly-functionalised core.



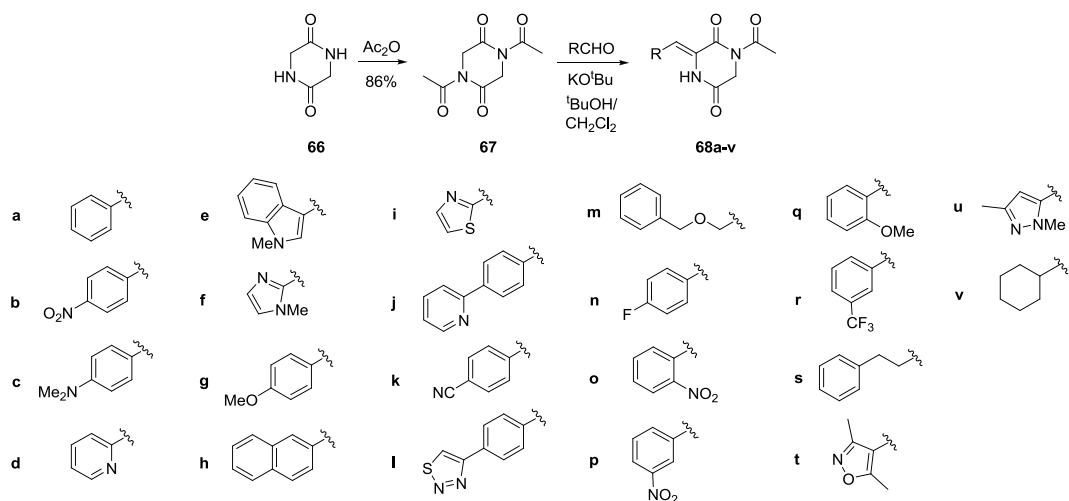
**Scheme 18** – Attempted synthesis of phosphono-diketopiperazine **55** via amino-ester **63**

A proposed alternative route to these structures was based on a known aldol condensation that has not yet been fully explored in the synthesis of a diverse library of DKPs (Scheme 19).<sup>106</sup> This route has the obvious advantage of avoiding the cyclisation step that had previously proved difficult. Other additional changes of strategy were introduced at this stage; N-methylation of the intermediate alkenyl DKPs should increase solubility of the products and also allows direct electrophilic alkylation of the unsubstituted DKP ring carbon in the final step.



**Scheme 19** – Proposed synthesis of diketopiperazines from glycine anhydride (**66**)

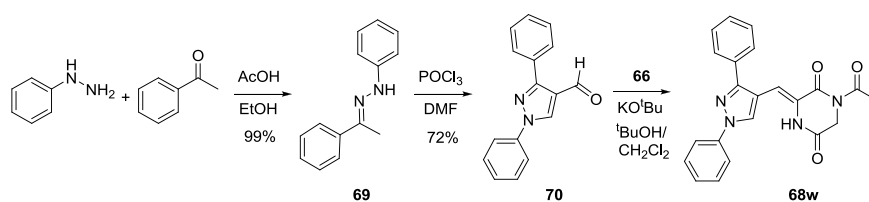
The initial acetylation step proceeded smoothly to give diimide **67**, and the subsequent aldol condensation was carried out in  $\text{CH}_2\text{Cl}_2$  rather than the more common DMF solvent in order to allow precipitation of the product, greatly increasing the yield of the desired mono-alkenylated DKP product **68** (Scheme 20).<sup>107</sup> A range of aromatic and heteroaromatic aldehydes were used successfully in this reaction, and although unbranched aliphatic aldehydes were predicted to be too susceptible to self-condensation, good yields of the desired aldol product were obtained in two examples (**68m** and **68s**).



**Scheme 20** – Synthesis of a DKP library by aldol condensation

The regioselective deacetylation has been proposed to occur *via* intramolecular acyl transfer to the alkoxide intermediate formed following the initial aldol reaction.<sup>106</sup> The resulting acetate then undergoes elimination in a stereoselective manner to give the *Z*-alkene with high selectivity, purportedly resulting from the minimisation of the steric interaction between the aryl group and the DKP carbonyl.<sup>106</sup>

In order to directly compare the alkenyl DKPs with analogous literature alkenyl thiazolidinedione inhibitor **6**, diarylpyrazole aldehyde **70** was prepared from hydrazone **69** in good yield using the Vilsmeier-Haack reagent (Scheme 21).

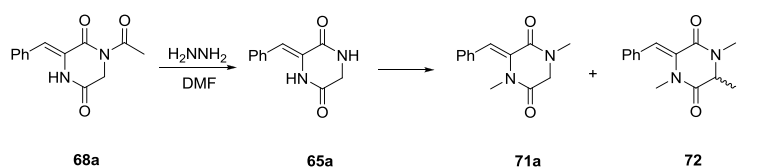


**Scheme 21** – Synthesis of diarylpyrazole DKP **68w**

Following minor modifications to the literature procedure, the subsequent deacetylation gave the highly insoluble alkenyl DKPs with good overall mass recovery, although general recrystallisation conditions proved elusive. Under standard conditions of sodium hydride and iodomethane, the attempted di-methylation of the parent benzylidene DKP proved problematic, resulting in a mixture of desired di-methylated product **71a** and tri-methylated compound **72**, which were inseparable by column chromatography (Table 3, Entry 1).

Variation of temperature, equivalents of MeI and order of addition did not improve the ratio of products (Entry 2). A screen of weaker bases incapable of generating significant concentrations of the amide enolates gave better results; Ba(OH)<sub>2</sub> initially gave only a trace of tri-methylated compound **72** but this ratio worsened on scale-up, whilst K<sub>2</sub>CO<sub>3</sub> was found to give complete selectivity regardless of scale (Entries 3-5).

**Table 3** – Optimisation of dimethylation of alkenyl-DKP **65a**



Entry	Base (eq.)	Eq. MeI	Conditions	Result
1	NaH (2.1)	5	DMF, r.t.	<b>71a</b> and <b>72</b>
2	NaH (2)	5	DMF, 0 °C	<b>71a</b> and <b>72</b>
3	Ag <sub>2</sub> O (3)	4	DMF, r.t.	Complex mixture
4	Ba(OH) <sub>2</sub> (10)	10	3:1 DMF/H <sub>2</sub> O, r.t.	<b>71a</b> and <b>72</b> (trace)
5	K <sub>2</sub> CO <sub>3</sub> (10)	10	DMF, r.t.	<b>71a</b>

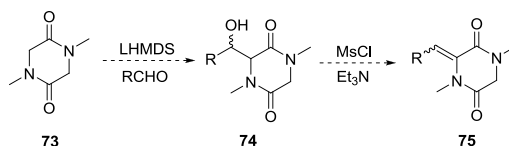
Despite this success, purification of the target compounds at this final stage proved particularly lengthy. Furthermore, the optimised conditions for methylation were deemed incompatible with any nucleophilic functionality on the aryl and heteroaryl groups, such as pyridines. At this stage, the first 7 final compounds were screened against cdc25A, B and C (Table 4), and only the analogue of thiazolidinedione **6**, diarylpyrazole **71w**, showed any activity (IC<sub>50</sub> *ca.* 100 μM). These disappointing initial results, combined with the speculative nature of the approach, led us to terminate this line of investigation without completion of the synthesis of the remaining dimethyl alkenyl DKPs, and we next investigated possible methods of virtual screening for discovery of novel inhibitor classes (see Section 6).



**Table 4** – DKPs tested in initial assay

	Structure	Overall Yield (%)		Structure	Overall Yield (%)
71a		52	71q		28
71g		29	71v		24
71h		54	71w		40

The considered advantages of the above synthetic route to the DKP targets, in particular the mild thermodynamic aldol condensation using the di-imide, were eventually largely outweighed by the difficulties in subsequently switching the groups on the amide nitrogens. A possible alternative would be a direct 2-step aldol condensation approach using sarcosine anhydride, **73** (Scheme 22).

**Scheme 22** – Proposed synthesis of alkenyl DKPs from sarcosine anhydride, **73**

In summary, small libraries of phthalazinediones and DKPs were prepared as possible naphthoquinone analogues with a reversible mode of cdc25 inhibition. These compounds were not found to show any significant inhibition in *in vitro* assays, and this approach was halted in favour of ligand-based virtual screening as discussed in Section 6.

## 5 Structural Biology

### 5.1 NMR Studies

#### 5.1.1 Protein Preparation

It had been recognised, following the failure of the optimisation of dysidiolide-analogue **20**, that an approach containing a larger rational design element arising from molecular modelling techniques would likely prove more effective. However, as discussed previously, the crystal structure of cdc25A is unsuitable for this purpose, there is no reported structure for cdc25C, and there is no validated ligand binding information for any of the isoforms. Efforts were therefore made to obtain detailed, physiologically relevant structures of the cdc25 isoforms with associated ligand binding information. This information would be of great value to the field, and would lay a strong foundation from which to achieve the aims of the project, in terms of finding novel inhibitors and also the chemical genetics approach to dissect the precise cellular roles of the isoforms.

Protein structure determination by NMR is a technique that has been rapidly growing in scope and influence due to the ongoing development and implementation of new methods and technologies, allied with the exponential increase in available computing power.<sup>108</sup> It is now almost considered straightforward to determine the structure of small proteins (<25 kDa). One of the chief advantages of protein NMR over X-ray crystallography is obtaining the solution conformation, which could be especially relevant for this project given the uncertainty discussed previously about the validity of the crystal structure of cdc25A.

Collaboration with Imperial College's Cross-Faculty NMR Centre allowed access to an 800 MHz cryoprobe NMR machine, sufficient to provide high resolution protein structures. The untagged catalytic domains of the cdc25 isoforms are within the size limit of 25 kDa, and therefore should be suitable for NMR structure determination. The start of the catalytic domain is defined as the highly conserved LIGD sequence, highlighted in blue in Figure 12. The HCX<sub>5</sub>R active site loop is highlighted in yellow. This sequence alignment demonstrates the difference in the levels of conservation in the two domains between the isoforms.

```

cdc25a  MELG-PEPPHRRRLFFA--C--SPPPASQP----VVKALFGASA-AGGLSPVTNLTVMQDLQGLGSDYEQP---
cdc25b  MEVVPQPEPAPGSALSPAGVCGGAQRPGHLPGLLLGSHGLLGSVRAAASSPVTTLTQTMHDLAAGLGSRSRLTHLS
cdc25c  MSTELFSSSTREEGSSSGSPFRSNQRKMLN-LLLERDTSFTVCPDVPRTPVGKFLGDSANLSILSGGTPKRCLD

cdc25a  LEVKNNNSNLQRMGSSESTDGFCGLDSPGLD---SKENLEN-----PMRRIHSLPQKLLGCSPALK
cdc25b  LSRRASESSLSESSSESSDAGLCMDSPSPMDPHMAEQTFEQAIQAASRIIRNEQFAIRRFQSMPVRLLGHPVLR
cdc25c  LSNLSSGEITATQLTTSAD----LDETGHLDSGLQEVHLAG-----MNHQHLMKCSPAQL

cdc25a  R-SHSDSLDHDIFQLIDP-----DENKENEAFEFKKPVRPVSFGCLHSHGLQEKGDLFTQRQNSAPARMLSSNE
cdc25b  NITNSQAPDGRKRKSEAGSGAASSSGEDKENDGFVFKMPWKPHPSSTHALAEWASRREAFAPRSPSSAPDLMCLSP
cdc25c  LCSTPNGLDR-----GHRKRD-----AMCSSSA

cdc25a  RDSSEPGNFIFLFTPQSPVTATLSD--EDDGFVDLLDGENLKNEEETPSCMASLWTAPLVMRTTN-----LDN
cdc25b  DRKMEVEELSPLALGRFSLTPAEGDTEEDDGFVDILES-DLKDDDAVPPGMESLISAPLVKTKLEKEEEKDLVMYS
cdc25c  NKENDNGNLVDSSEMKYLGSPITTT-----VPKLDKNPNLGEDQAEIISDELMEFSLKQDEAK-----VS

cdc25a  RCK-LFDSPSLCSSSTRSVLKRPERSQEESPPGSTKRRKSMGASPKESTNPEKAHETLHQSLSLASSPKGTIEN
cdc25b  KCQRLRFPSPMPCSVIRPILKRLERPDRDTPVQNKRRRSVT--PPEEQQEAEPEKARVLRKSKSLCHD---EIEEN
cdc25c  RSG-LYRSPMPENLNRPLKQVEKFKDNTIPDKVKKKYFSGQGKLRKG-----LCLKKTVSLCDI---TITQ

cdc25a  ILDNDPRD--LIGDFSKGYLFHTVAGKHQDLKYISPEIMASVLNGKFANLIKEFVIIDCRYPYEYEGGHKGAVN
cdc25b  LLDSDHRE--LIGDYSKAFLLQTVDGKHQDLKYISPETMVALLTGKFSNIVDKFVIDCRYPYEYEGGHKTAVN
cdc25c  MLEEDSNQGHLLIGDFSKVFCALPTVSGKHQDLKYVNPETVAALLSGKFGGLIEKFYVIDCRYPYEYLGHHIQGALN

cdc25a  LHMEEEVEDFLLKKPIVPTD-GKRVIIVFHCEFSSEGGPRMCRYVREDRLGNEYPKLHYPELYVLKGGYKEFFM
cdc25b  LPLERDAESFLLKSPIAPCSLDKRVILIFHCEFSSEGGPRMCRFIRERDRAVNDYPSLYPEMYILKGGYKEFFP
cdc25c  LYSQEELFNFFLLKKPIVPLDTQKRIIIVFHCEFSSEGGPRMCRCLREEDRSLNQYPALYYPELYILKGGYRDFFP

cdc25a  KCQSYCEPPSYRPMHHEDFKEDLKKFRTKSRTWAGEKSKREMYSLKKL---
cdc25b  QHPNFCPEQDYRPMNHEAFKDELKTFRLKTRSWAGERSRRELCSRLQDQ---
cdc25c  EYMELCEFPQSYCPMHHQDHKTELLRCRSQSKVQEGERQLREQIALLVKDMSP

```

**Figure 12** – Amino acid sequence alignment of cdc25 isoforms

**Blue**– start of the catalytic domain; **Yellow**– conserved active site loop;  
**Red** – hydrophobic; **Blue** – acidic; **Pink** – basic; **Green** – other hydrophilic

A construct containing the catalytic domain of cdc25A was available and the initial strategy necessitated the addition of a GST-tag in order to allow simple purification of large quantities of protein. This was achieved by sub-cloning the insert coding for cdc25A(cat.) into the pGEX-KG vector used previously for the full-length cdc25A. The resulting construct also contained a thrombin cleavage site between the GST tag and the cdc25A domain, which would subsequently allow the large GST tag to be removed, leaving the purified, untagged catalytic domain for use in the NMR studies. However, only very low expression of GST-cdc25A(cat.) was observed, and attempts to optimise the induction conditions for time and temperature had little effect.

As an alternative strategy, the cdc25A(cat.) insert was sub-cloned into the pET21a vector to parallel the literature crystallisation attempts. This vector places the transcription under the

control of the T7 promoter, adding an additional amplification step to the induction of protein expression. Specifically, IPTG now induces the compatible host cell line (BL21) to express the T7 RNA polymerase, which then proceeds to start rapid and extensive transcription of the desired gene in the pET21a plasmid. The disadvantage of using this vector is the absence of the GST fusion system, necessitating an alternative purification strategy, but during the initial expression experiments it became apparent that the pET21a/BL21 expression system was generating extremely high levels of cdc25A(cat.), with yields of up to 25 mg/L.

In accordance with literature protocols, the untagged cdc25A(cat.) was purified by an ion-exchange strategy, starting with extraction from the cell lysate using negatively-charged sulfopropyl-sepharose beads. The protein was eluted from the beads using a linear gradient of NaCl to disrupt the electrostatic interactions.<sup>72</sup> Fractions found to contain high levels of cdc25A(cat.) by OMFP fluorescence assay were concentrated using a 10 kDa centrifugal filter and the retentate then passed through a gel filtration column. This technique retains molecules smaller than the bead pore sizes (chosen to be *ca.* 20 kDa) by effectively presenting a much larger column volume than for the larger protein molecules, which elute very quickly. Analysis of the fractions and concentration as before resulted in overall high yields of cdc25A(cat.) with acceptable purity by SDS-PAGE analysis.

The catalytic domains of cdc25B and C were prepared from the full length versions using polymerase chain reaction (PCR). A primer was designed such that the polymerase activity started at the LIGD site, amplifying only the C-terminal domain. The polynucleotide products were then purified and ligated into the pGEM-T vector, and the insert genes were then each sub-cloned into the pET21a vector to give good expression as for cdc25A(cat.). Purification by the optimised conditions gave the expected high-concentration solution of active phosphatase.

Initial 1D <sup>1</sup>H-NMR experiments indicated that the recombinant cdc25A(cat.) contained an encouraging level of secondary structure, as evidenced by the complexity of the spectrum and the appearance of peaks at higher and lower chemical shift values than those expected for amino acids in solution. However, in order to obtain data of the quality necessary for protein structure determination, millimolar sample concentrations of isotopically labelled protein were required, that furthermore were stable and soluble at around 30 °C for long periods, the increased temperature an important part of achieving a good signal-to-noise ratio. Finding

buffer conditions that fulfil these requirements is considered the most laborious and difficult part of the protein NMR process, and is often the limiting factor. As these initial NMR experiments had resulted in extensive precipitation at the moderate protein concentrations used, various buffers were screened to give better solubility and stability.

### 5.1.2 $1D^1H$ -NMR: Buffer Optimisation and Confirmation of Protein Folding

Screening for optimal buffer conditions for cdc25A began with the variation of pH and the salt composition of the buffer: Adjusting the pH away from the protein pI (estimated to be 6.3 for cdc25A) usually increases the solubility due to the additional net charge. It is also preferable to use as low a pH as the protein can tolerate due to the subsequent reduction in base-catalysed amide proton exchange in the NMR spectrum. The nature and concentration of the buffer salt can also play an important role. Chaotropic salts (*e.g.* LiCl, KSCN) prevent aggregation by interfering with protein-protein interactions, but can destabilise the protein. Kosmotropic salts (*e.g.* Na<sub>2</sub>SO<sub>4</sub>) provide structure to the bulk solvent, raising the energetic cost of hydrating partially unfolded protein and thus providing stability.<sup>109</sup> The Hofmeister series ranks ions according to these properties, allowing the choice of a small sample of salts that should be representative of the entire range.<sup>110,111</sup> Various additives can also be included to provide extra stability and solubility, the most common class being non-denaturing detergents.

In order to maximise the number of different buffer conditions included in the screen, 30  $\mu$ L protein samples were added to a 96-well plate, humidified and subsequently sealed to prevent evaporation. The initial screen covered 7 pH values in the range 4.5-7.5, three salts (KSCN, NaCl and Na<sub>2</sub>SO<sub>4</sub>) and three salt concentrations (0 mM, 50 mM and 150 mM), each with 10 mg/mL cdc25A(cat.). Incubation of the plate at 37 °C for 24 h was followed by visual inspection of the level of precipitation. All wells contained some precipitate, with ten of the buffers giving noticeably less precipitation. Small aliquots of each of these ten solutions were tested in the OMFP assay, the assumption being that if the remaining soluble protein were correctly folded then significant phosphatase activity (and thus fluorescence) would be observed (Table 5). The results displayed clear trends; the chaotropic salt KSCN was detrimental to solubility, cdc25A(cat.) is less soluble in the pH range 5.5-6.5 (although it cannot be ruled out that this is an unexplained effect of the citrate buffer rather than the pH),

and soluble protein at pH < 5.5 is essentially inactive. The best conditions used either NaCl or Na<sub>2</sub>SO<sub>4</sub> at variable concentration in higher pH buffer, but significant precipitation was observed in all cases.

pH	Salt (mM)	Fluorescence (A.U.)
4.5	-	0.7
4.5	NaCl (50)	1.6
5.0	-	1.1
5.0	NaCl (50)	1.6
7.0	NaCl (150)	33.9
7.0	Na <sub>2</sub> SO <sub>4</sub> (150)	33.1
7.5	NaCl (50)	37.7
7.5	NaCl (150)	31.4
7.5	Na <sub>2</sub> SO <sub>4</sub> (50)	34.2
7.5	Na <sub>2</sub> SO <sub>4</sub> (150)	33.0

**Table 5** – Buffer optimisation assay results for selected wells

A selection of the buffer conditions that contained active soluble protein were then used for a small set of 1D <sup>1</sup>H-NMR experiments. An observation from the initial scan was that the peak corresponding to methyl group protons at their standard chemical shift (*i.e.* not shifted by secondary structure effects) was larger than expected for a fully folded protein. It was thought that a possible reason for an increased level of disorder could be the lack of regular structure in the cdc25A C-terminal region as demonstrated by the unresolved nature of this region in the literature crystal structure, although it had been hoped that the solution structure of cdc25A(cat.) would display the additional helical fold found in cdc25B. Only full NMR structure determination would reveal whether this helix does exist in solution for cdc25A, but at this stage it was hypothesised that the binding of an anionic substrate mimic might assist in the correct folding of the positively charged C-terminal region. If this were the case, comparison of the disorder (*i.e.* the relative size of the unstructured methyl group peak) in the presence and absence of substrate mimics might reveal a change that would provide evidence for this hypothesis. A 1D <sup>1</sup>H-NMR spectrum was therefore run on four samples, all at pH 7.5, with the following buffer salts: Na<sub>2</sub>SO<sub>4</sub>, Na<sub>3</sub>PO<sub>4</sub> and reported potent vanadate inhibitor BPV(Pic) (dipotassium bisperoxo (picolinato) oxovanadate (V))<sup>112</sup> with NaCl. It was predicted that sulfate and phosphate anions might mimic the active site interactions of the substrate phosphate group, with BPV(Pic) likely to have a similar mode of action. Unfortunately, whilst various significant peak shifts suggested some kind of binding event,

the spectra obtained did not show any significant reduction in the relative size of the unstructured peak.

A second round of solubility screening was therefore attempted using commonly-used additives with a NaCl buffer: glycerol, various detergents (CHAPS, Triton X-100 and octylglucoside) and a combination of arginine and glutamic acid (Arg+Glu), based on a report suggesting that these amino acids provide stability and prevent aggregation for a variety of unrelated proteins.<sup>113</sup> Additionally, the concentration of *cdc25A*(cat.) was varied to investigate the solubility limit. After 24 h incubation, precipitation was again observed in all the wells and the remaining solutions were sampled for the OMFP activity assay (Figure 13).

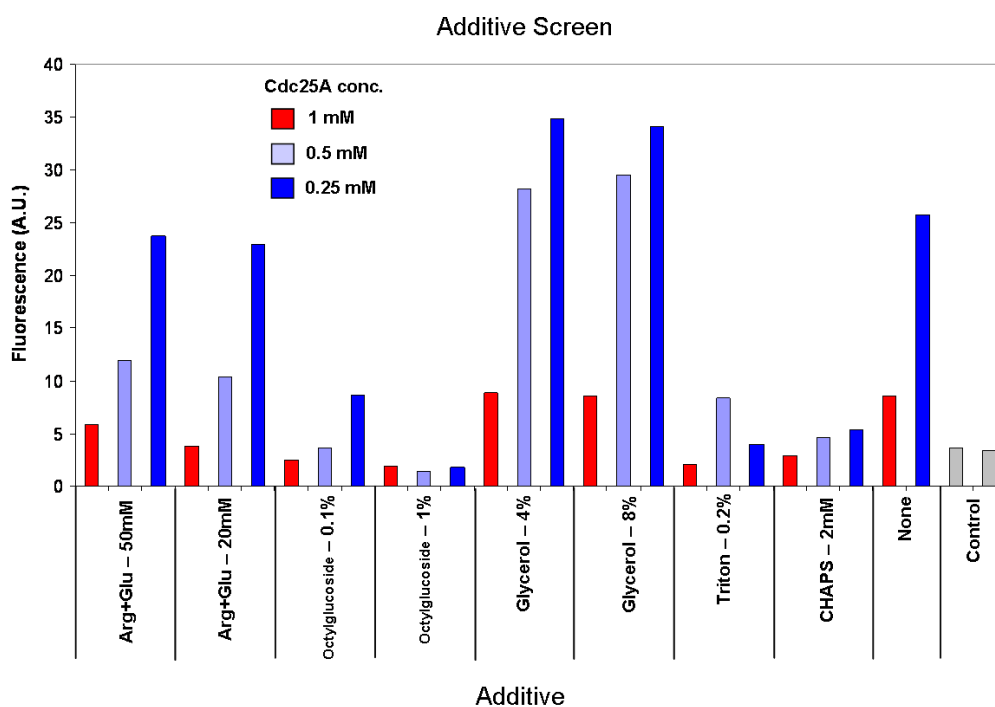


**Figure 13** – Assay results for additive screen

It was immediately clear that all the wells containing the detergents contained either completely precipitated or inactivated enzyme. Whilst the amino-acid combination proved no better than the control buffer containing no additive, glycerol notably improved both solubility and activity. However, this additive was subsequently excluded on the basis that any increased viscosity of the solution cannot be tolerated when trying to determine the structure of a relatively large protein, due to the increased tumbling times and hence lower resolution. The higher activity of the wells with lower enzyme concentrations also suggested

that the effect of aggregation and precipitation was greater than just to return the levels of soluble active protein to a threshold concentration. A follow-up screen investigated the reported beneficial effect of introducing the Arg+Glu additive prior to the concentration of the protein solution, preventing aggregation during this process and significantly helping subsequent stability,<sup>113</sup> but no difference was observed for a variety of *cdc25A* concentrations.

The effect of using glycine instead of ionic buffer salts was also investigated. Although this additive was not expected to assist the solubility, it is known to have a significant positive effect on the thermal stability of protein solutions.<sup>114</sup> Furthermore, the use of a neutral zwitterionic species does not contribute to the conductance of the solution. Electrically conductive samples have increased resistance and thus thermal noise,<sup>115</sup> which can have a significant detrimental effect on the sensitivity, especially for cryogenic NMR probes. The replacement of buffer salt with 0.5 M glycine was demonstrated not to affect the solubility, and this was identified as a possible solution to any later issues with signal sensitivity.

As none of the buffer or additive screens had discovered conditions that improved the solubility beyond that of the final storage buffer following the gel filtration column (Tris-HCl, 200 mM NaCl, 1 mM DTT, 1 mM EDTA, pH 7.5), a screen of *cdc25A* concentrations was carried out to identify the maximum concentration at which precipitation did not occur in this buffer. Samples with concentrations ranging from 100-450  $\mu$ M (in 50  $\mu$ M increments) were incubated at either 20 °C or 30 °C for three days. The lower temperature appeared to be much more suitable, with all samples below 300  $\mu$ M containing no visible precipitate; for the 30 °C samples, the limit was 150  $\mu$ M. Surprisingly, <sup>1</sup>H-NMR scans showed that the partially-precipitated samples that had high initial concentrations had a higher *final* solution concentration of correctly folded protein than the non-precipitated samples, in almost the ratio that would be predicted from the starting concentrations (this was subsequently verified by Bradford assay). This result contradicted the previous findings regarding the lower final enzymatic activity of highly concentrated samples. Importantly, the higher concentration samples were found to be stable at 30 °C following the removal of the precipitate, also contradicting earlier observations. The reason for this unexpected attainment of sample stability was unclear and was attributed to continual small improvements to the experimental procedure, which ultimately produced purer, less-aggregated protein.



A subsequent screen looking at higher concentrations (300-1000  $\mu\text{M}$  in 50  $\mu\text{M}$  increments) under the same buffer conditions with incubation at 30  $^{\circ}\text{C}$  found that the maximum correctly-folded protein solution concentration by  $^1\text{H}$ -NMR stabilised at roughly 450  $\mu\text{M}$ , with a corresponding increase in signal intensity (example shown in Figure 14). This screen also directly compared the effect of exchanging NaCl for glycine for each sample. The results confirmed earlier observations that high concentrations of glycine provide comparable solubility and stability to moderate salt concentrations.

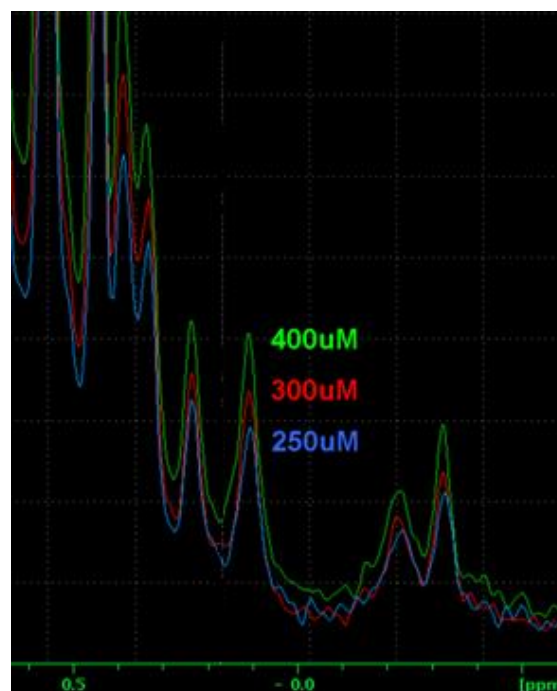


**Figure 14** – Concentration dependence of  $^1\text{H}$ -NMR peak intensity

The solubility screens therefore identified the optimal pH, ruled out the use of common additives, established the maximum solution concentration and confirmed the suitability of glycine as a salt equivalent. Overall, the optimal buffer conditions allowed the generation of stable, saturated protein solutions that maintained correct folding even when incubated at 30  $^{\circ}\text{C}$  for up to 1 week.

### 5.1.3 2D NMR: Isotopic Labelling and HSQC Results

Advanced protein NMR techniques require isotopic labelling in order to resolve structural data. For preliminary studies,  $^{15}\text{N}$ -labelled proteins are used to generate simple HSQC spectra that provide information using the amide N-H coupling. Further experiments require  $^{13}\text{C}$ - and occasionally  $^2\text{H}$ -labelling. This isotopic labelling is achieved by growing the bacteria in a medium that contains these specific elements only as the desired isotope. A common additional strategy to assist with the peak assignment is the use of specific labelled amino acids in an unlabelled medium.

The most common method of generating isotopically labelled protein in *E. coli* is using M9 minimal growth media, which has been designed to allow the bacteria to grow in a solution containing a small number of specified ingredients with a single source of carbon and nitrogen (glucose and ammonium chloride respectively) that can be easily obtained in the desired isotopically pure form.<sup>116</sup> For the expression of *cdc25A*, this method produced very poor yields of active protein. Attempted optimisation of the expression conditions did not improve the yield, and therefore this method was not considered practical or economical. It was clear that the low protein yield was primarily due to very poor bacterial growth, and the minimal medium was therefore modified by the addition of vitamin and micronutrient solutions. However, as before the resulting yield of protein was low, even following attempted optimisation.

As an alternative approach, “rich” media contain the cell lysate of algae grown in minimal media, and thus contain isotopically-labelled cell components such as amino acids. Bacteria generally grow much more efficiently in these media, and the increase in yield can justify the significantly increased cost. However, although the expression levels using the Spectra-9 rich medium were relatively high, the first <sup>15</sup>N-NMR scan of isotopically-enriched protein unexpectedly showed a high ratio of unfolded protein. Since it is known that bacteria can need time to adapt to new media before induction of protein expression,<sup>117</sup> it was theorised that the abrupt switch from the normal LB medium to the rich medium during the final scale-up may have been the cause. The expression was repeated using the rich medium for the smaller initial cultures, but the same poor folding was observed. An alternative theory was considered, where Spectra-9 is deficient in a nutrient or cell component that the bacteria require to successfully produce high levels of folded protein. This theory was supported by the observation that using a final culture medium containing 10% LB / 90% Spectra-9 produced high yields of correctly folded protein by <sup>15</sup>N-NMR, although the corresponding 10% drop in NMR signal would negatively impact on the quality of structural information obtainable from later studies.

The <sup>15</sup>N-<sup>1</sup>H HSQC scans using the labelled, correctly-folded protein produced another unexpected result, with a significant proportion of the peaks (corresponding to each amino-acid) being unresolved, likely resulting from the effect of conformational lability on the NMR timescale, perhaps due to the unstructured C-terminal domain. This continual change in chemical environment for the affected N-Hs averages the (already weak) observed signals

until they can no longer be resolved from the background noise. No improvement was observed on binding of the vanadate inhibitor BPV(pic). Although a number of possible NMR studies might allow confirmation of this theory, such as synthesis of a truncated form of cdc25A, or selective labelling of certain methyl groups to study solution dynamics, the priority was to obtain alternative structural data to aid the medicinal chemistry investigations.

A preliminary 1D  $^1\text{H}$ -NMR scan of cdc25B promisingly showed a high degree of folding (more so than for cdc25A).  $^{15}\text{N}$  labelled cdc25B was therefore prepared, but the  $^{15}\text{N}$ - $^1\text{H}$  HSQC spectrum was again found to lack a large number of amino acid peaks, suggesting that on the NMR timescale cdc25B displays analogous conformational flexibility to cdc25A. For cdc25C, preliminary  $^1\text{H}$ -NMR scans showed a greater degree of disorder than for cdc25B, and the labelling studies were therefore not attempted.

A recent literature computational study of the molecular dynamics of cdc25A and B supports these conclusions regarding the conformational flexibility of the C-terminus, which in solution is predicted to be either unfolded or in an equilibrium between a partially-folded and disordered state.<sup>100</sup> The same result is found for large sections of the N-terminal domain, providing an explanation for the difficulty in obtaining crystals of the full-length cdc25 proteins. Additionally, this study strongly advises against structure-based virtual screening using even the fully-folded published crystal structure of cdc25B, as the exposed nature and high flexibility of the active site region result in a large diversity of possible binding modes for reported inhibitors under dynamic conformational conditions, with transient exposure of hydrophobic cavities and clefts that might provide the majority of any real binding interaction.

## 5.2 *Crystallisation Studies*

Following our failure to obtain novel NMR-derived structures for the cdc25 isoforms, it was considered that switching to X-ray crystallography might prove more successful. As stated previously, there are effectively no reported viable structures for cdc25A or cdc25C, presumably despite considerable effort following the initial discovery and characterisation of these important enzymes, yet it was hoped that a fresh approach to this challenge might prove more successful. This reasoning was predominantly based on the rapid improvement of crystallisation technologies in recent years, with the advent of large libraries of commercial

crystallisation buffers that have made the technique almost routine. Furthermore, the optimisation of the buffer conditions already carried out to obtain high solution concentrations of large quantities of pure protein for  $^1\text{H-NMR}$  was directly applicable to the preparation of samples for crystallisation.

Collaboration with Prof Paul Freemont and Imperial College's Centre for Structural Biology crystallisation facility allowed access to high throughput crystallisation screen technology,<sup>118</sup> using the sitting-drop crystallisation technique. Specifically, the protein of interest is added using a Mosquito liquid dispensing robot to a range of commercially available pre-dispensed 96-well plate crystallisation screens (*i.e.* with a wide variety of buffers and additives) and incubated. A sub- $\mu\text{L}$  droplet of the buffer is placed by the robot into a small, shallow sub-well adjacent to the larger well of the buffer reservoir. A sub- $\mu\text{L}$  droplet of the high-concentration protein solution is precisely added to the same location and the plate incubated for several weeks. Once the plate is sealed, the headspace above each sub-well is shared with that of the adjacent large buffer reservoir, ensuring no changes in solution constitution by evaporation processes.

Large cultures of all three *cdc25* isoforms were prepared and purified by the standard method, before a further automated gel filtration step in order to achieve the rigorous purity required to grow high-quality crystals, as analysed by SDS-PAGE. The samples were then concentrated to high levels (15-20 mg/mL) and immediately added to nine commercially available crystallisation screen plates (a total of 864 buffer conditions per isoform). The plates were incubated at 22 °C and each well was visually inspected by microscope at intervals rising from approximately one day to one week over a several week period.

Despite the breadth of the initial screen, no definitively positive results were observed. For each isoform, a repeat screen was therefore performed. Due to protein degradation, a new large batch of each protein was required to be expressed and purified by both ion exchange and gel filtration for each new screen. The plates were again monitored for several weeks, and at this stage it was decided that a different approach should be taken for each of the three isoforms:

- For *cdc25A*, due to the lack of any positive results in the screen, combined with the known difficulties in producing a relevant crystal for this isoform, further efforts towards crystallisation were discontinued.

- Since similarly-negative results were observed for *cdc25B*, a larger-scale screen comprising three 24-well plates was carried out based on the published literature crystallisation conditions.<sup>73</sup> Unfortunately, no positive results were obtained at two *cdc25B* concentrations tested.
- The second 9 × 96-well plate buffer screen carried out with *cdc25C* also varied the buffer:protein ratio, using 1:1 and 1:2 for each buffer condition. This screen showed some positive results for the precipitant MPD (2-methyl-2,4-pentanediol) and the co-solvent PEG (various sizes from 200 to 3350). A follow-up screen was carried out with four 24-well plates at the 2 µL scale (rather than 100 nL), varying precipitant concentrations and pH. This screen was monitored for two weeks, at which point a smaller subset of conditions was identified as potentially promising. A further two plate follow-up screen was similarly performed but proved ultimately inconclusive.

At this stage, the failure of the two structural biology approaches had focussed our attention instead on using *ligand*-based virtual screening, thus circumventing the need for any additional structural information for the generation of new inhibitor classes for *cdc25* (See Section 6). An alternative strategy towards crystallisation was implemented by co-workers, focussed on generating the reported crystal of *cdc25B*(cat.) by exact replication of the literature conditions; this time generating and using an identical construct.<sup>119</sup> Success was eventually achieved using a specially-created construct missing the short sequence of C-terminal residues that are not resolved in the literature structure. The crystals obtained are currently being used by co-workers in the Mann and Freemont groups for soaking and co-crystallisation experiments with the best novel inhibitors discussed in later sections. Further cloning efforts are also underway by these co-workers to increase the protein stability.

## 6 Ligand-Based Virtual Screening

As discussed previously, the lack of structural information for cdc25 (particularly in the form of a bound small molecule crystal structure), combined with the relatively featureless active site surface, makes the discovery of new classes of inhibitor extremely difficult. Despite this, during the course of this project two studies were reported that described the structure-based virtual screening of the reported cdc25B(cat.) crystal structure to identify novel, reversible cdc25 inhibitors with micromolar potency.<sup>120,121</sup> It was still felt, however, that this approach could not be sufficiently validated to ensure that the docking scores would translate into real inhibition.

The disappointing results of our attempts to both synthesise analogues of literature compounds and obtain new structural information led to collaboration with Dr Caroline Low of Imperial College's Drug Discovery Centre to carry out ligand-based virtual screening. This technique involves the computational analysis of literature inhibitors to provide a pharmacophore template which can be compared against libraries of commercial compounds in order to find new inhibitor structural classes. The software of choice, FieldScreen,<sup>122</sup> uses molecular field-based similarity<sup>123</sup> as the basis for these structural comparisons, and has proven successful in finding novel inhibitors of p38 MAP kinase,<sup>124</sup> the corticotrophin releasing factor 1 receptor,<sup>125</sup> as well as a highly ligand-efficient antagonist of the oxytocin receptor.<sup>126</sup> In this technique, the key electrostatic and van der Waals properties that control the binding interactions of molecules are calculated and considered in terms of four types of 3D molecular field descriptors, or "field points". Compounds with similar field point patterns are assumed to bind in similar manners, regardless of their underlying structure.

### 6.1 Template Selection and Screening Results

Selection of the correct training set for the creation of the template is critical, and this immediately proved a problem for our application of this technique to cdc25. The reported potencies of all irreversible inhibitors (when reported as a binding constant *e.g.* IC<sub>50</sub>) are essentially meaningless as descriptors of the strength of the binding interactions, since in theory only a stoichiometric quantity of the inhibitor could completely inactivate the enzyme, given sufficient time. The scarcity of the remaining reported reversible inhibitors, particularly

at this stage of the project, meant that even fairly large, weakly-binding structures had to be considered. A further concern was that the lack of structural information or kinetic data for these reported inhibitors meant that it could not be assumed these compounds were necessarily all binding at the active site, a factor which could seriously interfere with the creation of a relevant template.

Given these factors, the inclusion in one of the contemporaneously-published structure-based virtual screening studies of a crystal structure of cdc25B containing a bound synthetic peptide in the active site prompted us to investigate the potential use of this structure as the basis for the template.<sup>121</sup> In particular, knowing the precise 3D conformation of an active inhibitor removes a large part of the uncertainty in ligand-based screening. The peptide structure and surrounding protein surface were reconstructed from the coordinate tables in the original BASF patent,<sup>127</sup> and analysis showed that although a number of atoms were unresolved, they were not in direct contact with the protein (Figure 15).

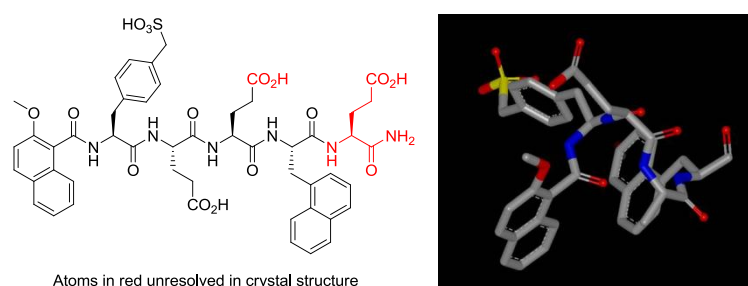


**Figure 15** – Crystal structure of BASF synthetic peptide

Unfortunately, no useful information could be gained from further analysis of the bound structure, as the only functionality fully in contact with the protein surface proved to be the benzyloxysulfonate anion and parts of the two naphthyl groups. This peptide clearly therefore exhibits a binding mode that had been predicted for a large class of cdc25 inhibitors; an anionic phosphate mimic bound in the catalytic loop and a large hydrophobic region bound in an adjacent cleft.

After surveying a range of combinations of literature inhibitors, the training set that proved optimal with respect to finding a common pharmacophore consisted of pyrazole **6**<sup>47</sup>, thiazolopyrimidine **7**<sup>121</sup> and naphthofurandione **8**<sup>31</sup> (Figure 16 and Table 1). Despite its *ortho*-quinone motif, naphthofurandione **8** is reported to be a reversible inhibitor. No similar studies

had been performed for thiazolopyrimidine **7**, and it was recognised that there was potential for irreversible cdc25 cysteine alkylation by conjugate addition to the  $\alpha,\beta$ -unsaturated amide functionality, which therefore prompted investigation using a reversibility assay. Prolonged incubation of cdc25A(cat.) with thiazolopyrimidine **7**, followed by subsequent dilution to a concentration at which the inhibitor is inactive, resulted in similar phosphatase activity to control experiments, proving this compound does not irreversibly inactivate cdc25. Further evidence is provided by the published observation of a reversible kinetic profile for the inhibition of the closely related PTP1B by analogous thioxothiazolidinone inhibitors.<sup>128</sup>

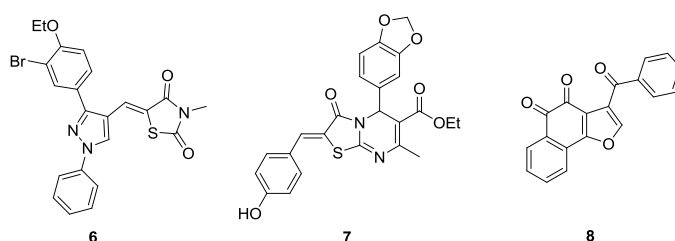


**Figure 16** – Optimal training set for preparation of field point template

The templates were created using the FieldTemplater software package,<sup>129</sup> which was used to determine a consensus view of the most similar conformations of each set of three compounds. A set of conformations was generated for each molecule, using an upper threshold of 6 kcal/mol above the calculated global energy minimum, which covers all conformations likely to be readily accessible at 37 °C. In the optimal set, this gave 200 conformations of pyrazole **6**, 111 conformations of thiazolopyrimidine **7** and 18 conformations of naphthofurandione **8**. The field point pattern surrounding each conformation was then calculated and exhaustive cross-correlation of the overlay score for every single pair of field point patterns resulted in the highest-scoring pattern of fields common to all three molecules. Three templates were identified, all containing the same conformation of pyrazole **6** (Table 6). These results strongly suggested that conformation 81 (Figure 17) was the bioactive conformation of **6**, and on this basis the field point pattern associated with this structure was used as the input for the virtual screen of commercial compounds.



**Table 6** – Conformations of the training set with a high overlap score

Template	Conformation identified <sup>a</sup>		
	6	7	8
A	81	5	2
B	81	8	4
C	81	8	16

*a* – Conformations numbered from lowest to highest calculated energy

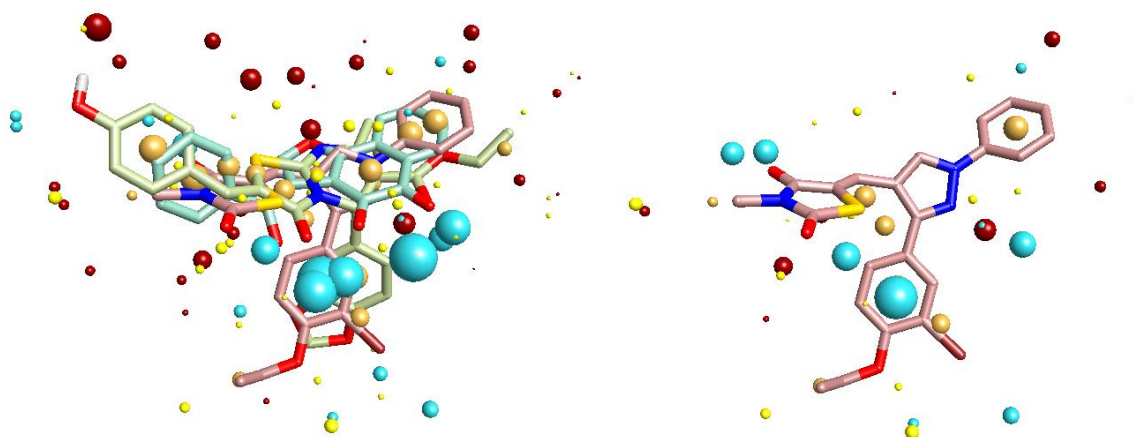


**Figure 17** – Field point template B (left) and conformation 81 of diarylpyrazole **6** (right)

Negatively charged field points shown in cyan, positively charged fields in red, surface hydrophobic points in yellow and centres of hydrophobic mass in orange. Underlying structures are coloured as follows; **6** is pink, **7** is green and **8** is cyan.

A library of two million commercial compounds was screened using FieldScreen<sup>122,130</sup> and a list was compiled of 200 compounds found to have the highest overlay score with the field point pattern of conformation 81 of pyrazole **6**. The vast majority (95%) of these compounds were found to contain the same diarylpyrazole motif as the input structure. Resubmission of the screen filtering out this structural class resulted in a second list of 200 non-diarylpyrazole compounds from which candidates were selected for testing.

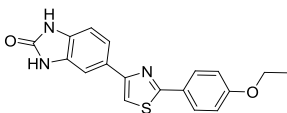
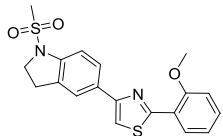
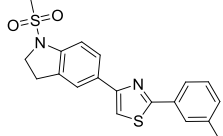
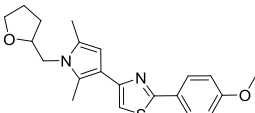
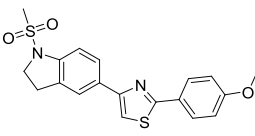
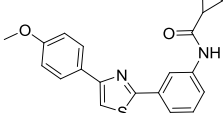
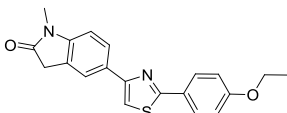
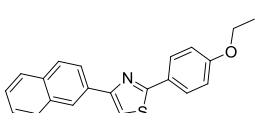
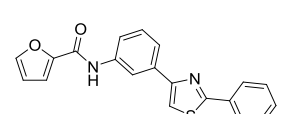
## 6.2 Assay Results

### 6.2.1 Initial Cdc25 Activity Assays

Fluorimetric *in vitro* cdc25 activity assays were carried out as described in Section 4, and further validated by the repetition of the literature IC<sub>50</sub> measurement for template

thiazolopyrimidine **7** (14.4  $\mu\text{M}$  against *cdc25B*(cat.), lit.<sup>121</sup> 13.0  $\mu\text{M}$ ). An initial screen of six commercial compounds from the FieldScreen list identified simple diarylthiazole T5308252 (**83**) as a micromolar inhibitor of all three *cdc25* isoforms. Testing of an additional 28 commercially-sourced thiazoles identified eight further good hits (Table 7).

**Table 7** – Virtual screen hits active in Cdc25 activity assay

Cmpd No.	Cmpd Name	Structure	IC <sub>50</sub> $\pm$ SEM ( $\mu\text{M}$ )		
			Cdc25A	Cdc25B	Cdc25C
76	T5896241		2.36 $\pm$ 0.27	8.93 $\pm$ 0.54	10.2 $\pm$ 0.3
77	T5959818		4.02 $\pm$ 0.46	10.1 $\pm$ 1.2	14.2 $\pm$ 1.8
78	T5982914		5.62 $\pm$ 0.99	19.0 $\pm$ 2.9	24.3 $\pm$ 3.4
79	T5765678		6.36 $\pm$ 1.02	12.1 $\pm$ 2.2	24.7 $\pm$ 8.2
80	T5846763		6.49 $\pm$ 1.15	17.5 $\pm$ 3.2	18.0 $\pm$ 2.0
81	T5705971		10.2 $\pm$ 1.2	14.9 $\pm$ 2.5	16.8 $\pm$ 3.1
82	T5871826		9.54 $\pm$ 1.91	22.7 $\pm$ 1.5	> 100
83	T5308252		13.0 $\pm$ 4.0	13.6 $\pm$ 2.3	31.5 $\pm$ 12.6
84	C7991374		17.8 $\pm$ 6.9	> 50 <sup>a</sup>	> 50 <sup>b</sup>

*a* – 78% inhibition at 100  $\mu\text{M}$ . *b* – 82% inhibition at 100  $\mu\text{M}$ .

This represents a hit rate for the virtual screening of 26%, obtained from testing a very small number of compounds. For this and all subsequent inhibitor data, IC<sub>50</sub> values shown represent

the mean of at least 3 experiments using 6-10 compound concentrations. The IC<sub>50</sub> and SEM values were calculated using SigmaPlot data-fitting software.

These compounds all share a common 2,4-diarylthiazole core apart from thiazole **79**, which has a 3-pyrrole attached at the thiazole 4-position. Many of the aryl rings attached at this 4-position share a similar feature; benzo-fused 5-membered nitrogen-containing heterocycles attached *via* the 5-position (5-benzimidazolone for compound **76**, 5-dihydroindole for compounds **77**, **78** and **80**, 5-oxindole for compound **82**). Compounds **81** and **84** both contain simple amides of a 3-aniline, but attached to different positions of the thiazole ring. The possibility that the 2- and 4-substituents of the thiazole are interchangeable suggested that position of the heteroatoms in the thiazole core might not significantly affect the binding interaction.

At this stage, the compounds identified were amongst the most potent reversible cdc25 inhibitors reported. Crucially, they also fulfilled the majority of the criteria used to select promising hit compounds for further development: they are relatively small, stable, easily synthesised, sufficiently water-soluble and have an appropriately “drug-like” structure. Additionally, no diarylthiazoles have been previously reported to inhibit any dual-specificity phosphatase. In order to confirm these inhibitors as acting by reversible binding to the active site, a reversibility assay was carried out on a selection of these compounds as described for thiazolopyrimidine **7**, with no inhibition of cdc25A observed following the dilution step.

The original intention was then to compare the field points of those compounds that were active with those that were inactive, to try to gain additional SAR information. Unfortunately, it became clear that the active compounds were not predicted to bind in a consistent orientation due to the inherent symmetry of their field point patterns (and structures). When the conformations and field points of four of the top five inhibitors are displayed as aligned to the template (not shown), the first and last compounds bind in one orientation with the sulfonamide/urea functionality at the top, and the middle two compounds bind in the other orientation with the sulfonamide functionality at the bottom (Figure 18). The existence of two similar low-energy conformations makes any computational analysis of SAR difficult. This finding further supports the suggestion that the positioning of the heteroatoms in the thiazole core may have little overall effect on the binding.

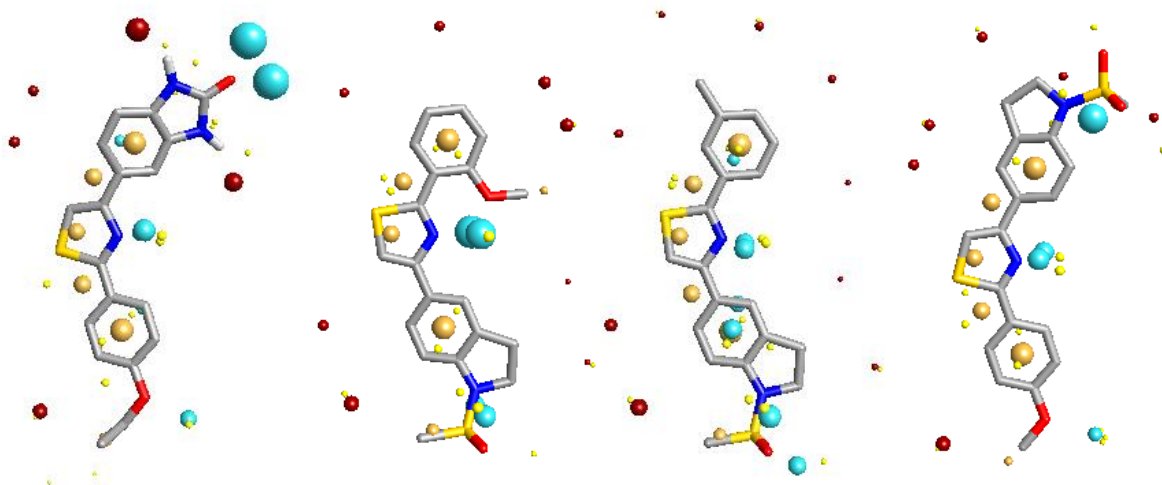


**Figure 18** – Conformations and Field Points of diarylthiazoles **76**, **77**, **78** and **80** oriented as aligned to template pyrazole **6** (not shown)

### 6.2.2 Phosphatase Selectivity Assays

The choice of phosphatases for a relevant selectivity panel was determined by consideration of two factors: structural relationship to *cdc25* and relevance as a therapeutic target. For the former criterion, it is necessary to balance the use of highly related phosphatases as a stringent test of inhibitor selectivity with the sampling of phosphatases from a wide range of structural classes to give confidence in the breadth and range of any observed selectivity. It was further hoped that the use of phosphatases whose inhibition may result in a potential clinical benefit would provide the advantage of serendipitous discovery of inhibitors with interesting biological activity against pathways and diseases not directly the focus of this project.

Alkaline phosphatase (AP) was selected as a ubiquitous, generic phosphatase with little substrate specificity.<sup>131</sup> The remaining phosphatases were all chosen from the large protein tyrosine phosphatase super-family, containing the majority of phosphatases critical to signal transduction.<sup>24</sup> Based on structure and substrate preference, this family can be further divided as shown in Figure 19. Protein tyrosine phosphatase 1B (PTP1B) is commonly used as a control for conventional PTPs and is a comparatively well-validated and investigated drug target for the treatment of a range of diseases such as diabetes.<sup>132</sup>

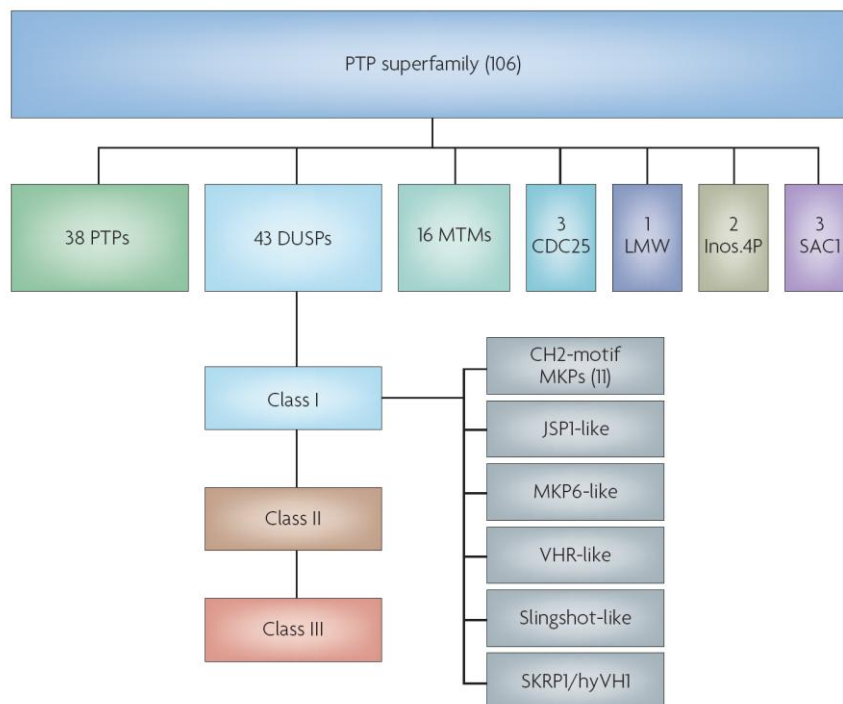


**Figure 19** – Sub-classification of the PTP superfamily of phosphatases<sup>24</sup>

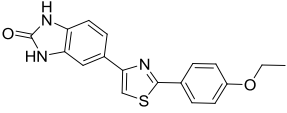
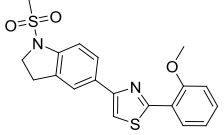
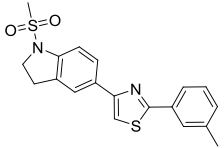
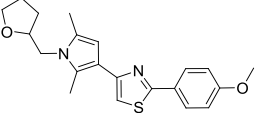
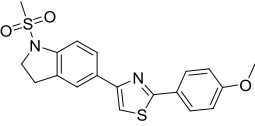
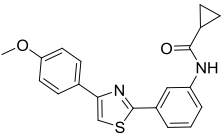
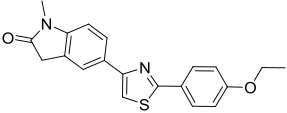
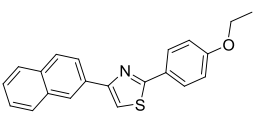
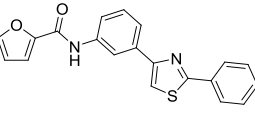
The selectivity panel was completed by 3 dual-specificity phosphatases (DUSPs) from the MAPK-phosphatase (MKP) class that, alongside *cdc25*, are also emerging drug targets with close links to human cancers and chronic inflammatory diseases.<sup>24</sup> MKP-1 and MKP-3 are typical members of this family that have well-characterised influences over the activities of the MAP kinases (yet quite different substrate preferences) and are overexpressed in various human tumour types.<sup>24,133</sup> VHR (vaccinia virus phosphatase VH1-related) is a poorly-studied DUSP that is believed to be involved in regulation of the MAP kinases, although data regarding its cellular substrates are conflicting.<sup>24,25,134</sup> Cells lacking VHR undergo cell cycle arrest, suggesting that VHR inhibition may work synergistically with *cdc25* inhibition.<sup>135</sup> Although evidence for VHR as a valid drug discovery target is comparatively weak, recent reports have strongly linked VHR up-regulation to cancer progression.<sup>136,137</sup> The overall medicinal chemistry profiles for the MKPs and VHR were similar at this stage of the project, with few reported reversible inhibitors of moderate potency (MKP-1<sup>138-141</sup>, VHR<sup>57,142-145</sup>) and no crystallographic inhibitor-binding information on which to base a rational design approach. A more-recent reported crystal structure of VHR bound to a small-molecule inhibitor provides very little useful information for rational design, with only the interactions of an anionic phosphate mimic and non-specific hydrophobic regions in a similar manner to that of the BASF peptide discussed previously bound to *cdc25B* (see Figure 15).<sup>146</sup>

Optimisation of enzyme concentration and buffer pH was performed for AP, PTP1B and VHR, establishing validated and reproducible fluorescence assay conditions using the OMFP artificial substrate, with sodium orthovanadate as a positive control for inhibition. Following poor results obtained with commercial MKP-1 and -3, discussion with Prof Steve Keyse (Dundee) highlighted the requirement for the use of both large quantities of enzyme and complexation to the appropriate MAPK to result in a level of phosphatase activity suitable for *in vitro* assays.

Expression of significant quantities of His-tagged MKP-3 from a donated construct was found to be problematic; His-purification was successful following the prescribed denaturing conditions (8 M urea), but the subsequent renaturing by dialysis proved sensitive and capricious. A donated sample of purified MKP-3 and its associated kinase ERK-1 was found to show reproducible activity in the colourimetric PNPP assay initially tried for cdc25. The expression and *in vitro* assay of MKP-1 was expected to be similarly difficult, and MKP-5 was chosen as an alternative. This phosphatase is uniquely characterised by high activity that is independent of substrate binding, and has been linked to demyelinating diseases such as multiple sclerosis.<sup>147</sup> Optimisation of the OMFP assay conditions as above proved successful. After the completion of these assays, it was noted that the University of Pittsburgh groups responsible for most of the medicinal chemistry investigations into MKP-1 and MKP-3 had reported reservations over the biological relevancy of their *in vitro* assays, and as such had developed a complex cell-based assay for MKP-3.<sup>148</sup>

The nine thiazole inhibitors found by the virtual screening were assayed against the phosphatase selectivity panel, showing no inhibition of AP, PTP1B, MKP-3 or MKP-5, but uniformly strong inhibition of VHR, with IC<sub>50</sub> values comparable to that for cdc25A and no significant selectivity (Table 8).

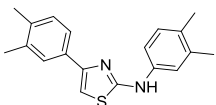
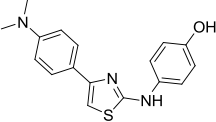
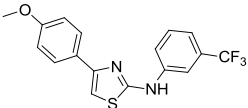
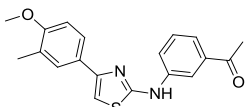
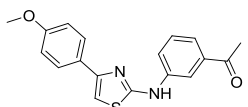
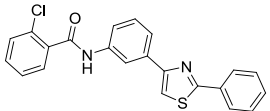
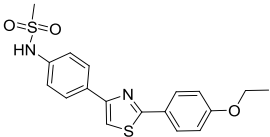
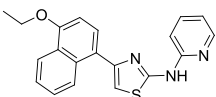
**Table 8** – Phosphatase selectivity screen of cdc25-active compounds from Table 7

Cmpd No.	Cmpd Name	Structure	IC <sub>50</sub> ± SEM (μM)				
			VHR	PTP1B	MKP-3	MKP-5	AP
76	T589-6241		1.92 ± 0.30	>100	>100	>100	>100
77	T595-9818		2.68 ± 0.78	>100	>100	>100	>100
78	T598-2914		8.04 ± 0.65	>100	>100	>100	>100
79	T576-5678		8.29 ± 1.39	>100	>100	>100	>100
80	T584-6763		8.10 ± 0.57	>100	>100	>100	>100
81	T570-5971		8.89 ± 1.26	>100	>100	>100	>100
82	T587-1826		10.6 ± 1.2	>100	>100	>100	>100
83	T530-8252		4.44 ± 0.57	>100	>100	>100	>100
84	C799-1374		26.1 ± 4.6	>100	>100	>100	>100

Following this discovery that the diarylthiazoles active against cdc25 were also similarly active against VHR, we next tested against VHR the compounds in the initial set that were inactive against cdc25, and found four VHR-selective inhibitors (Table 9, compounds **89-92**). Two of the four VHR-selective inhibitors found in this screen were diarylaminothiazoles. Based on a simple hypothesis that this alternative core structure might show a general selectivity for VHR against cdc25, 19 further aminothiazoles from the virtual screening results were purchased and assayed, resulting in four further VHR-selective diarylaminothiazole inhibitors (compounds **85-88**), supporting this structural hypothesis for

selectivity. The VHR selectivity ranged from >15-fold for aminothiazole **85** to approximately 3-fold against *cdc25B* for aminothiazole **92**. Whilst the diarylaminothiazole compounds identified mostly contain simple aryl substituents, there are no general structural features or SAR trends observed, excluding compounds **87** and **88** that are differentiated by a single methyl group. The selectivity of diarylthiazoles **90** and **91** for VHR over *cdc25* provides interesting SAR data; for **90**, replacement of the 2-chlorobenzene with furan (compound **84**) results in increased *cdc25* inhibition, and for **91** the analogous dihydroindole sulfonamide **80** exhibits potent *cdc25* inhibition.

**Table 9** – VHR-selective inhibitors

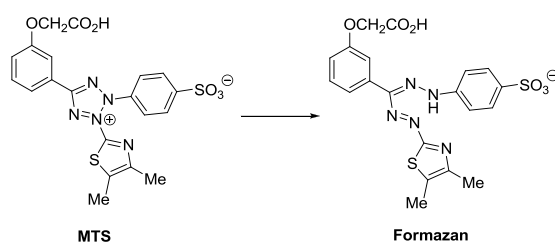
Cmpd No.	Cmpd Name	Structure	IC <sub>50</sub> ± SEM (μM)				PTP1B/MKP-3/MKP-5/AP
			Cdc25A	Cdc25B	Cdc25C	VHR	
<b>85</b>	C565 -3548		>100	>100	>100	6.72 ± 1.67	>100
<b>86</b>	C785 -3655		>100	>100	>100	8.15 ± 2.17	>100
<b>87</b>	C609 -9253		>100	>100	>100	8.41 ± 1.11	>100
<b>88</b>	C718 -8297		>50 <sup>a</sup>	>50 <sup>b</sup>	>100	11.5 ± 2.9	>100
<b>89</b>	C593 -5510		>100	>50 <sup>c</sup>	>100	20.7 ± 2.9	>100
<b>90</b>	C616 -2452		>100	>100	>100	23.8 ± 8.3	>100
<b>91</b>	T559 -8472		>100	>100	>100	24.3 ± 3.0	>100
<b>92</b>	T0511 -8034		>100	>50 <sup>d</sup>	>100	31.9 ± 5.9	>100

Compounds with IC<sub>50</sub> > 50 μM: inhibition at 100 μM: a – 67%, b – 67%, c – 60%, d – 52%.



### 6.2.3 Cell-Based Assays: MTS Assays, Flow Cytometry and Phosphorylation Status

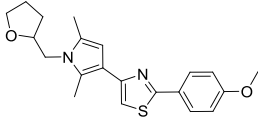
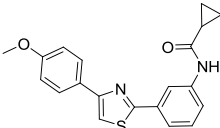
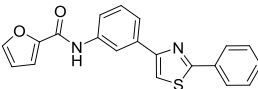
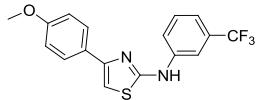
In order to test the potential cellular effects of these *cdc25*/VHR inhibitors, the MTS assay was chosen to provide quantitative data about growth inhibition (the expected phenotype of the enzyme inhibition). This assay quantitatively measures mitochondrial activity *via* bio-reduction of an arylated tetrazole derivative to give a coloured formazan product (Figure 20), and can be performed in a high-throughput 96-well format.



**Figure 20** – Molecular mechanism of colourimetric MTS assay

The assay, carried out by co-workers in the Mann group, was optimised for cell number and incubation time.<sup>119</sup> The compounds active in the *in vitro* enzyme assays were then screened against various cell lines, with IC<sub>50</sub> values subsequently measured for active compounds. Four compounds were found to have a concentration-dependent anti-proliferative effect at concentrations below 40  $\mu$ M against at least one cell line, with IC<sub>50</sub> values comparable to the *in vitro* inhibition of *cdc25A* and/or VHR (Table 10). Furanamide **84** was found to inhibit proliferation in all cell lines tested with IC<sub>50</sub> values at or slightly below those found *in vitro* against *cdc25*/VHR. At this stage, the poor solubility of this class of compounds proved a persistent problem, limiting testing at any higher concentrations.

**Table 10** – MTS assay results for cell-active compounds

Cmpd No.	Cmpd Name	Structure	MTS Cell Assay IC <sub>50</sub> ± SEM (μM)			
			293T	MCF7	HeLa	3T3
79	T576-5678		6.92 ± 3.46	41% inhibition at 40 μM	>40	N.D.
81	T570-5971		5.76 ± 0.88	49% inhibition at 40 μM	55% inhibition at 40 μM	N.D.
84	C799-1374		7.95 ± 0.95	5.28 ± 1.76	9.64 ± 1.33	14.89 ± 3.07
87	C609-9253		8.96 ± 2.25	50% inhibition at 40 μM	23.61 ± 1.79	27% inhibition at 40 μM

This growth inhibition was further investigated by biochemistry collaborators using flow cytometry.<sup>119</sup> Selected active compounds were added at 40 μM to cultures of NIH-3T3 cells (mouse fibroblasts) that were chosen as a representative example of cells with a normal cell cycle, and following incubation the cells were harvested and analysed by quantification of DNA synthesis. Although no difference in cell cycle profile was observed between the control and treated cells, it was proposed that non-specific cell cycle checkpoint inhibition would not cause accumulation of cell population in any particular phase. Encouragingly, the cells showed no sign of increased apoptosis (sub-G<sub>1</sub> population), demonstrating that these compounds are not inherently toxic.

NIH-3T3 cells were therefore synchronised, starting with an initial quiescence by removal of the growth serum so that all entered the G<sub>0</sub> phase. Addition of growth serum then re-started cell growth, synchronised at the G<sub>1</sub> phase. Flow cytometry indicated that a selection of the compounds inhibited S phase entry to some degree by their action at the G<sub>1</sub>/S phase transition following the release from quiescence (Figure 21), although the effect was not pronounced for compounds **76**, **77** and **84**.

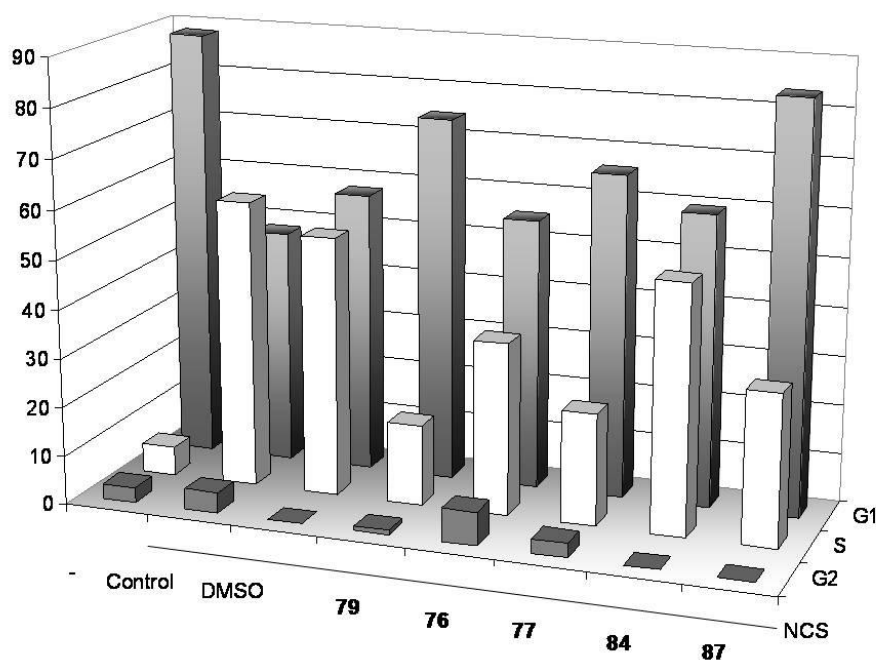


**Figure 21** – Quantification of DNA synthesis in NIH-3T3 cells

Quiescent cells (-) were stimulated with 10% serum (NCS) without addition (control), vector control only (DMSO) or in the presence of *cdc25*/VHR inhibitors (40  $\mu$ M). Inhibitors were added concurrently with the serum and incubated for 17 h before harvesting and staining with propidium iodide. Data is expressed as the % of the given population in G1 (quiescence), S (synthesis) or G2 (mitotic) phase of the cell cycle.

To test more directly the cellular targets of these active compounds, collaborators in the Mann group then assessed the phosphorylation status of CDK2 and MAPK, the reported targets of *cdc25* and VHR respectively.<sup>119</sup> NIH-3T3 cells were synchronized *via* quiescence as before, and treated with the compounds following resumption of the cell cycle. Immunoblotting of the treated cells revealed that for compound **79**, an increase in the level of phosphorylated CDK2 was observed, consistent with *cdc25* inhibition (Figure 22). However, no similar results were obtained in this initial study for the other cell-active compounds. No increase in phosphorylated MAPK was observed with any of the compounds tested, suggesting that none of these compounds acts as an inhibitor of a MAPK phosphatase *in vivo*. These phosphorylation status results suggest that furanamide inhibitor **84** might produce its cellular anti-proliferative effect by inhibition of a target not tested in this study. This is supported by the observation that some of the MTS assay  $IC_{50}$  values for furanamide **84** were slightly lower than those from the *in vitro* enzyme assays. Furthermore, the absence of any effect on the phosphorylation status of a physiologically relevant MAPK by VHR inhibitor **87** suggests that either this compound also exerts an anti-proliferative effect *via* inhibition of an unknown target, or inhibition of VHR causes G1 arrest by an undiscovered pathway that does not include MAPK.

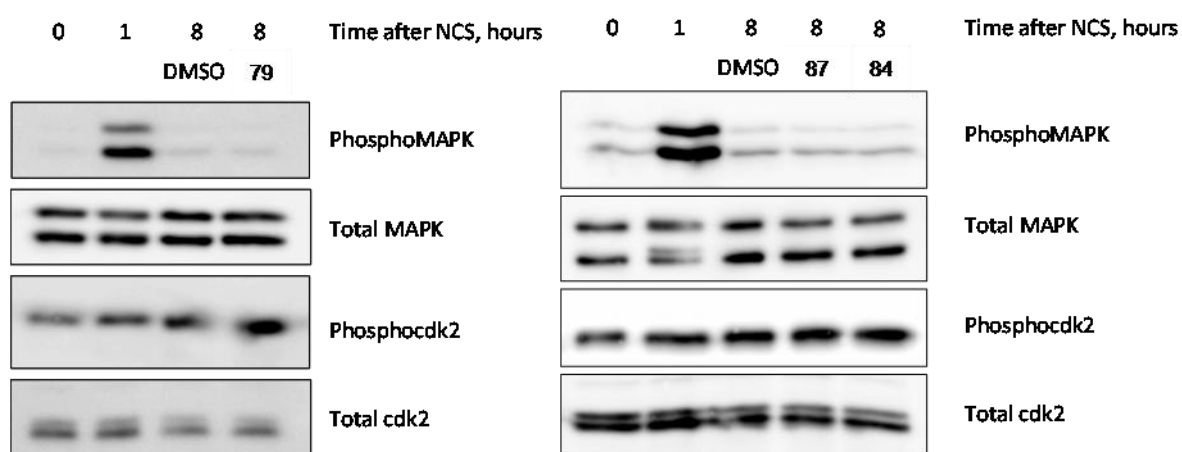


**Figure 22** – Analysis of CDK2 and MAPK phosphorylation status in treated cells

NIH 3T3 cells were rendered quiescent by culture in 0.5% serum for 72 h. Cells were then stimulated with 10% normal calf serum for 1 h. Compounds (40  $\mu$ M) or vehicle (DMSO) were then added and the cells incubated for a further 7 h followed by immunoblotting for the indicated form of each protein. Samples were also harvested immediately prior to serum addition (0) and immediately prior to compound/DMSO addition (1).

To summarise, nine diarylthiazoles were discovered to have good potency against the cdc25 isoforms and VHR, and a further eight compounds were identified with selectivity for VHR. Four compounds were then shown to exert an anti-proliferative effect against various cell lines with low micromolar potency comparable to the measured *in vitro* values, suggesting good cell membrane permeability. These compounds showed no cytotoxicity, demonstrating only the expected cell cycle arrest, and showed selectivity against related targets. The next section describes the synthesis and testing of compound libraries based around these hits.

## 7 Analogue Synthesis Part 3 – Analogues of Screening Hits

### 7.1 Parallel Synthesis by a Divergent Coupling Approach

Following the successful virtual screening, it was decided that an appropriate medicinal chemistry strategy would be not to immediately begin the process of systematically optimising the most potent compounds, but to instead attempt to further explore the broader SAR in the hope of perhaps discovering novel and more potent structural classes not likely to be accessible by an optimisation strategy. The rationalisation for this diversity-oriented approach was based on the relatively wide range of structural classes found in the virtual screen that exhibited similar inhibitory potency, suggesting potential tolerance of a variety of functionality, specifically at the C4-position (Figure 23).

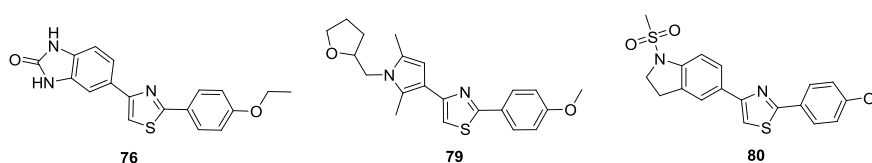
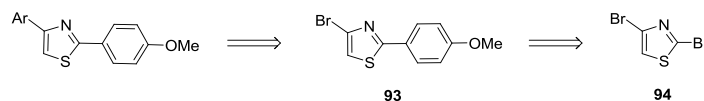


**Figure 23** – Selected inhibitors with diverse C4 substituents, yet similar potency

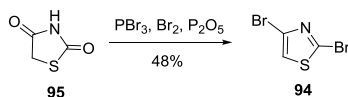
In order to prepare diverse libraries of analogues in a rapid and divergent manner, the conventional Hantzsch approach to diarylthiazoles was rejected in favour of a more modern approach based on Pd-catalysed cross-coupling of bromide **93**, itself potentially derived from a regioselective Suzuki coupling of 2,4-dibromothiazole **94** (Scheme 23). This regioselective coupling had little precedent at this stage of the project, although a comprehensive investigation into this reaction and that of similar heterocycles has subsequently been reported.<sup>149</sup>



**Scheme 23** – Proposed synthesis of diarylthiazoles by regioselective Suzuki coupling

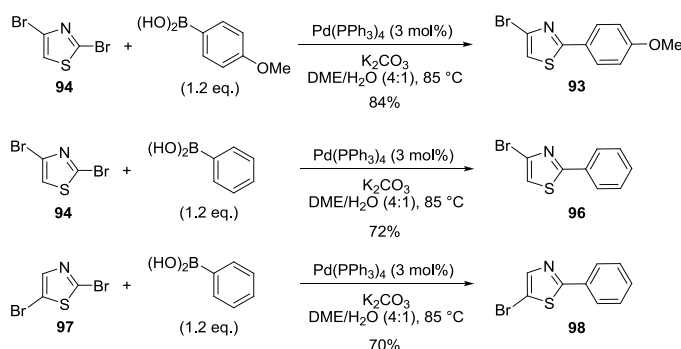
### 7.1.1 Optimisation of Regioselective Suzuki Coupling

Although 2,4-dibromothiazole is commercially available, we anticipated requiring a significant quantity of this key core unit for the synthesis of inhibitor libraries, and therefore attempted synthesis *via* bromination of 2,4-thiazolidinedione (**95**). Literature conditions using  $\text{POBr}_3$  proved highly variable, and the high cost of the bromination reagent made it unsuitable for gram-scale reactions when used in the large excess required. A small set of reaction conditions and work-up procedures were explored in order to optimise this reaction, and *in situ* preparation of  $\text{POBr}_3$ <sup>150</sup> allowed reproducible isolation of large quantities of 2,4-dibromothiazole (> 15 g) in good purity and moderate yield (Scheme 24).



**Scheme 24** – Synthesis of 2,4-dibromothiazole, **94**

Following a brief screen of conditions, successful regioselective Suzuki coupling of 2,4-dibromothiazole was achieved using a small excess of the boronic acid to achieve full conversion (Scheme 25). Similarly good yields were obtained with the less-reactive phenylboronic acid, and an identical result was observed for the analogous coupling of the corresponding 2.5-dibromothiazole (**97**), allowing the exploration of the influence of the thiazole substitution pattern.

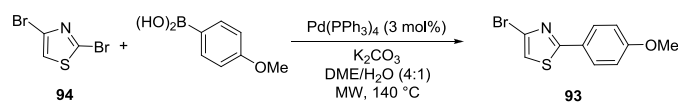


**Scheme 25** – Synthesis of bromothiazoles **93**, **96** and **98** by regioselective Suzuki coupling

Collaboration with Cancer Research Technology (CRT) allowed access to a range of parallel synthesis equipment, including a semi-automated microwave reactor. The conditions for the regioselective Suzuki coupling were therefore adapted for microwave heating to allow rapid

synthesis of compound libraries. The initial conditions chosen for the model reaction of the dibromide with *p*-methoxyphenylboronic acid were successful, with mono-coupled product isolated in 68% yield (Table 11, Entry 1). Lowering the excess of boronic acid to 1.05 eq. led to incomplete conversion (Entries 2 and 3). Intermediate levels of boronic acid excess gave correspondingly intermediate conversion values (Entries 4 and 5), suggesting that 1.2 eq. is the optimal value. On scaling up, the reaction time had to be extended from 20 to 30 minutes to achieve full conversion (Entries 6 and 7). Further scale up again caused lower conversion and similarly lower yield (Entry 8). At this stage, various non-chromatographic methods were attempted to remove the excess boronic acid that proved the major impurity in the crude reaction mixture, including using a basic carbonate resin and a PhMe/NaHCO<sub>3</sub>(aq.) work-up. Although these were moderately successful, further purification was still necessary, so for later reactions only column chromatography was used.

**Table 11** – Optimisation of regioselective Suzuki coupling under microwave heating



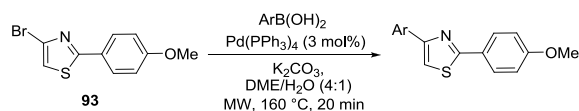
Entry	Scale / mmol	Time / min	Eq. boronic acid	Conversion (Yield) / % <sup>a</sup>
1	0.5	20	1.2	100 (68)
2	0.2	20	1.05	66
3	0.2	20	1.05	61 <sup>b</sup>
4	0.2	20	1.1	84
5	0.2	20	1.15	97
6	2.0	20	1.2	89 (81)
7	2.0	30	1.2	100 (74)
8	4.0	30	1.2	83 (54)

*a* – Conversion calculated from HPLC UV trace. *b* – Using *p*-cyanophenylboronic acid

Following the success of the initial regioselective Suzuki coupling and large scale synthesis of bromide **93** as a common intermediate, attempts were made to optimise the second coupling under microwave conditions as before. Four boronic acids with varying electronic character and sensitivity to protodeboronation were then used, with a slightly higher reaction temperature of 160 °C. Whilst 4-pyridyl and 4-acetamidophenyl boronic acids (Entries 1 and

2) gave full conversion, 2-thiophene boronic acid was unreactive under these conditions (Entry 3) and 4-(1H)-pyrazole boronic acid gave a low conversion (Entry 4). A second coupling was attempted on the crude mixture of this latter reaction, increasing the SM/product ratio to 1:1. The moderate success of these test coupling reactions was considered sufficient to proceed with the library synthesis.

**Table 12** – Optimisation of Suzuki coupling of 4-bromothiazole **93** under microwave heating

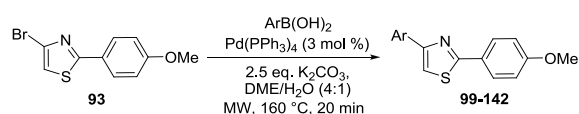


Entry	Boronic acid (1.2 eq.)	Conversion / % <sup>a</sup>
1	4-pyridine	100
2	4-AcNHPH	100
3	2-thiophene	19
4	4-(1H)-pyrazole	29, 50 <sup>b</sup>

*a* – Conversion calculated from HPLC UV trace. *b* – Initial conversion of 29%; further reaction with additional 1.2 eq. boronic acid and 3 mol% catalyst gave 50% conversion.

### 7.1.2 Library 1 – Suzuki Coupling

Choice of a subset of boronic acids and esters for the Suzuki coupling from the full range of 245 available for use<sup>151</sup> began by generation of a virtual library of all possible Suzuki products and calculation of the properties of these compounds using StarDrop software.<sup>152</sup> Compounds with high lipophilicity (cLogP > 6) or high MW (> 500) were discarded, along with those derived from simple alkylboronic acids. The remaining 188 compounds were subjected to an optimisation algorithm to determine a selection of 75 that would be both maximally diverse (based on Tanimoto coefficients<sup>153</sup>) and give products compliant with the Lipinski rules,<sup>154</sup> with a weighting of 90:10 in favour of diversity.

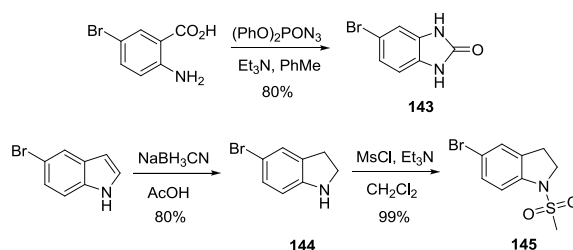


**Scheme 26** – Suzuki coupling of 4-bromothiazole **93**



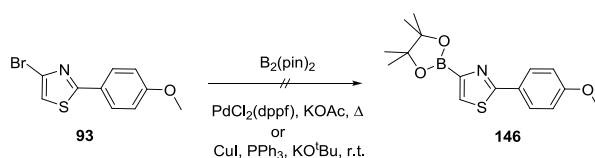
Of the 77 library reactions, 44 proved successful (**99-142**), with pyridyl, indolyl and amine-containing boronic acids disproportionately represented amongst those that failed. This high level of attrition was not unexpected given the known difficulties in the unoptimised coupling of heterocyclic boronic acids, particularly those with coordinating functionality that can deactivate the catalyst. As for all subsequent libraries, a sample of each product was purified by preparative mass-directed reverse-phase HPLC. For each library, a list of all the reactions attempted is included in the appendix.

At this stage, the resynthesis of potent inhibitors **76** and **80** (Table 7) and their analogues was attempted by an alternative Suzuki coupling strategy using the thiazole boronate ester. Optimisation of this route would greatly expand the range of potential substituents that could be introduced at the C4 position. Bromides **143** and **145** were prepared by Curtius rearrangement and reduction/mesylation respectively, with both obtained in high yield (Scheme 27).



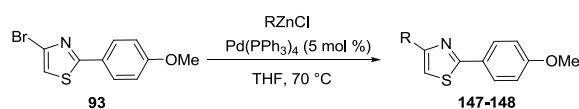
**Scheme 27** –Synthesis of aryl bromide coupling partners **143** and **145**

Attempted Miyaura borylation of 4-bromothiazole **93** resulted in decomposition under both standard Pd-<sup>155</sup> and recently-reported Cu-catalysis<sup>156</sup> (Scheme 28). No further attempt was made to optimise this reaction at this stage, but a subsequent literature study has successfully developed conditions for the preparation of thiazole boronate esters and the difficult subsequent Suzuki coupling.<sup>157</sup>



**Scheme 28** – Attempted borylation of bromothiazole **93**

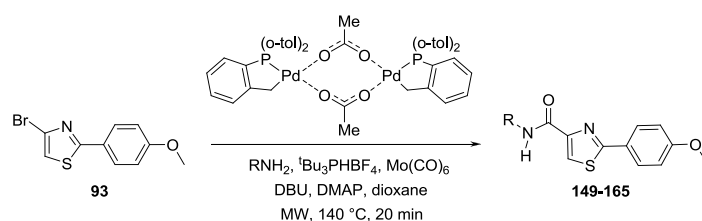
An analogous synthesis of C4-alkyl substituted thiazoles was investigated using the Negishi coupling of alkyl zinc halides (Scheme 29), but under standard conditions<sup>158</sup> low conversions were obtained. Given the limited selection of alkyl zinc reagents available in the CRT compound collection and the high calculated lipophilicity of the resulting products, this reaction was not optimised further. An alternative regioselective Negishi coupling of 2,4-dibromothiazole was however subsequently optimised (see Section 7.3).



**Scheme 29** – Negishi coupling of 4-bromothiazole **93**

### 7.1.3 Library 2 – Aminocarbonylation

An alternative method for rapidly achieving high structural diversity at the thiazole 4-position was by aminocarbonylation of bromothiazole **93** with a library of amines. The ability to simply switch between the synthesis of C4-aryl compounds and C4-amide compounds from a common intermediate demonstrates the power of the Pd-coupling approach to synthesis of diverse analogue libraries. The reported microwave conditions for a similar transformation used *trans*-di( $\mu$ -acetato)bis[*o*-(di-*o*-tolyl-phosphino)benzyl] dipalladium(II) as the preferred catalyst due to its high thermal stability, acting to slowly release active Pd species and prevent any aggregation<sup>159</sup>. A range of amines of varying reactivity was tested under literature conditions (Scheme 30),<sup>160</sup> with high to moderate conversions following the trend of amine nucleophilicity as expected.



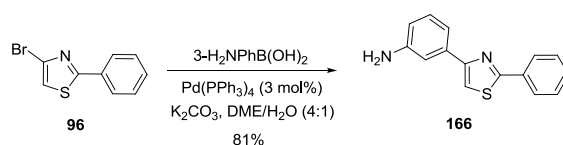
**Scheme 30** – Aminocarbonylation of bromothiazole **93**

In the preparation of a library of aminocarbonylation reactions, the choice of amines was computationally optimised as above based on size and diversity. Of the 33 reactions attempted, 17 resulted in isolation of the desired product (**149-165**). The unsuccessful reactions used

almost exclusively the least reactive (usually electron-deficient heteroaromatic) amines, suggesting that, under these conditions, the aminocarbonylation reaction requires a certain level of amine nucleophilicity to overcome competing pathways.

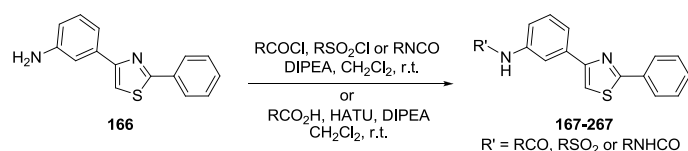
#### 7.1.4 Library 3 – Amide, Sulfonamide and Urea Analogues of Furanamide **84**

Given the relative prevalence of 3-aminophenyl amides in the virtual screening hits, and the broad antiproliferative activity of furanamide **84** (Table 7), a library of amides and amide analogues was considered as a simple and efficient way to explore SAR in this region. Aniline precursor **166** was prepared by Suzuki coupling under the standard microwave conditions in good yield and the reaction could be scaled up successfully (Scheme 31), despite the concern that the unprotected amine might cause problems by coordination to the simple catalyst.



**Scheme 31** – Synthesis of library precursor **166**

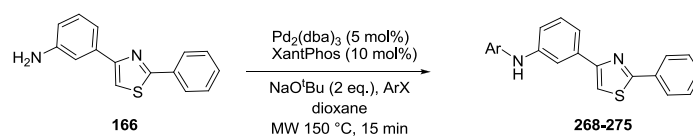
A selection of acid chlorides ( $\times 32$ ), sulfonyl chlorides ( $\times 23$ ) and isocyanates ( $\times 13$ ) were reacted in parallel with aniline **166** at room temperature under standard conditions, following computational selection of an optimal set according to size and diversity (Scheme 32). Eleven reactions were unsuccessful, in this case most likely reflecting the quality of the starting material, leaving 27 amides (**167-193**), 18 sulfonamides (**194-211**) and 12 ureas (**212-223**). In order to further probe the SAR in this region, a further library of 60 amides selected by the same criteria was prepared from a selection of carboxylic acids using the coupling reagent HATU under standard conditions, with 44 reactions successful (**224-267**).



**Scheme 32** – Synthesis of amide, sulfonamide and urea libraries from aniline **166**

### 7.1.5 Library 4 – Buchwald-Hartwig Coupling

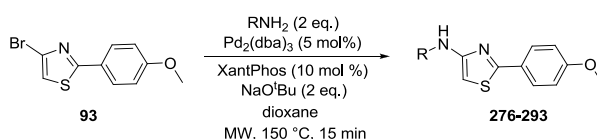
A further strategy for investigation of the SAR around the furoyl aniline of cell-active inhibitor **84** was the attachment of various aromatic and heteroaromatic groups directly to the aniline intermediate **166** in place of the furoyl group. A small screen of standard conditions for Buchwald-Hartwig coupling found XantPhos<sup>161</sup> to be the best ligand for this transformation (Scheme 33). This reaction possesses a higher degree of difficulty than many standard aminations due to the preferred use of stoichiometric aniline rather than the usual excess of amine nucleophile.



**Scheme 33** – Buchwald-Hartwig coupling of aniline **166**

These conditions were used in the synthesis of a small library of arylated anilines, with only 8 of the 17 reactions successful (**268-275**). Coupling partners bearing the most activated halides (such as 2-pyridyl and 2-pyrimidyl) gave the best results; this seemed to be a bigger factor than whether the halide in question was bromide or chloride.

The same screen of standard Buchwald-Hartwig conditions was then used for the amination of bromothiazole **93**, with XantPhos again proving slightly superior (Scheme 34). These compounds would be, in effect, “reverse” aminothiazoles which may have very similar properties to the conventional 2-aminothiazoles, but are much less common on account of the inapplicability of the Hantzsch condensation approach to this substitution pattern. This strategy was conceived as a method to prepare regioisomeric analogues of the cell-active 2-aminothiazole **87** (see Table 9), which contains a *p*-methoxyphenyl group at the C4-position, since the 2-aminothiazole core structure is both extensively covered in the patent literature and also has been identified as a potent toxicological liability (see Section 7.3.1).

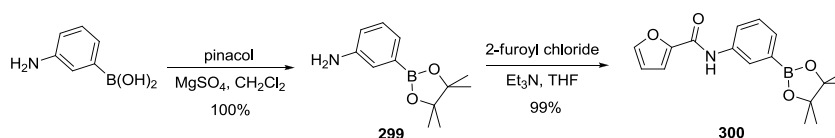


**Scheme 34** – Buchwald-Hartwig coupling of 4-bromothiazole **93**

A selection of amines was introduced at this position, attempting to achieve both diversity (using StarDrop optimisation) and also the introduction of groups similar to those found in the identified aminothiazole inhibitors. As with the aminocarbonylation reactions, the most nucleophilic amines gave superior results, with 18 out of 39 reactions successful (**276-293**). For more direct SAR, and in order to discover novel 2-aminothiazole inhibitors for a patent application, a small panel of five 2-aminothiazoles were prepared by Hantzsch synthesis (**294-298**), the products closely related to the cell-active inhibitor **87**.

#### 7.1.6 Library 5 – Consecutive One-pot Suzuki Coupling for Variation of Thiazole 2-Position

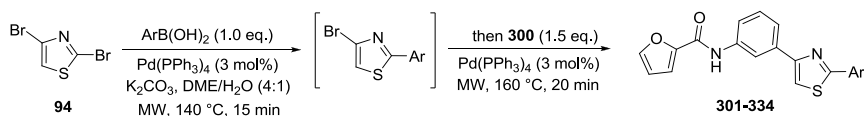
In order to vary the simple phenyl substituent of cell-active furanamide **84** (Table 7), a one-pot consecutive Suzuki coupling procedure was envisaged to allow quick access to a library of diarylthiazoles with a common 4-substituent and a diverse range of aryl and heteroaryl groups at the 2-position. The required boronic acid for the installation of the furanamide group was initially prepared by simple acylation of 3-aminobenzeneboronic acid. However, the difficulties encountered during the purification of this compound led to a change in strategy, with protection as the pinacol ester and subsequent acylation in quantitative yield to give boronate **300** (Scheme 35).



**Scheme 35** –Synthesis of boronate ester **300**

Initial attempts at a one-pot two-step reaction sequence using the standard microwave Suzuki coupling conditions optimised previously with three heteroaryl boronic acids resulted in a successful reaction but a large number of by-products, making purification difficult. A silica pad filtration between the two couplings did not improve the results, nor did switching to conventional heating at a lower temperature. Three alternative aryl boronic acids were chosen, and these gave good results for the double coupling sequence (Scheme 36), likely due to the greater stability and lower propensity for side reactions of aryl boronic acids compared to their heteroaryl analogues. Concurrent exploration of room temperature Suzuki reactions

based on reports by Fu<sup>162</sup> and Buchwald<sup>163</sup> ultimately proved unnecessary, but in any case did not result in the clean primary coupling that this one-pot procedure requires.



**Scheme 36** – Consecutive one-pot Suzuki couplings of 2,4-dibromothiazole

A library of compounds was synthesised by this route, investigating simple alterations to the phenyl ring in a comprehensive approach, as well as attempting to introduce some diversity of size and functionality at this position (using StarDrop optimisation). Overall, 34 out of 46 reactions were successful (**301-334**), although often with poor purity. As expected, the difficulties observed during the reaction optimisation when using heteroaryl boronic acids were also found during the library synthesis, and even for the aryl boronic acids the purity of the final compound was not high enough in many cases. A better approach would have been to clarify the importance of the thiazole core orientation prior to this library synthesis, potentially allowing the use of a common mono-coupled intermediate as for Library 1.

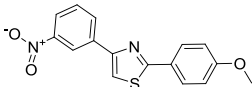
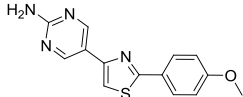
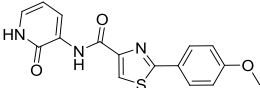
### 7.1.7 Assay Results

All the compounds successfully synthesised and purified from the above small libraries were then tested in the OMFP phosphatase assay against *cdc25A* and VHR. It was considered that the greater potency observed for this class of inhibitor against *cdc25A* in the virtual screening results would likely translate to these analogues, thus allowing testing against *cdc25B* and *C* of only those compounds found to be potent against *cdc25A*. The screening results for all synthesised compounds are given in an abbreviated form in the appendix.

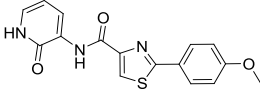
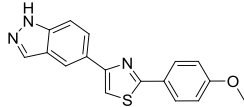
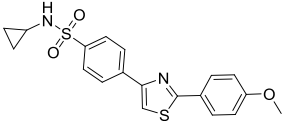
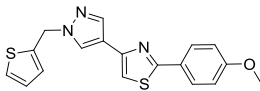
The results of the C4-variation from libraries 1 and 2 (Suzuki coupling and aminocarbonylation) proved disappointing, and largely contradicted the hypothesis from the virtual screening results that a wide exploration of structural diversity at this position would result in potentially much more potent inhibitors (see Figure 23). Inhibition of *cdc25A* was particularly poor, with all of the synthesised compounds at least 5-fold worse than the best compounds from the virtual screen (Table 13). The two most potent compounds (**134** and **118**)

are however promising hits, being both small and less lipophilic, but give contradictory SAR information regarding the preferred electronic character at this position. Amide-linked pyridone **157**, synthesised by aminocarbonylation, definitively justified this speculative synthetic effort by demonstrating the possibility of removing a lipophilic aryl unit whilst maintaining good potency. This pyridone was the most potent of the compounds from libraries 1 and 2 against VHR (Table 14). A greater number of inhibitors were discovered against VHR than for cdc25A, although again without much interpretable SAR. Overall, these libraries were not successful at improving the potency of the virtual screening hits.

**Table 13** – Libraries 1 and 2: selected cdc25A-active compounds

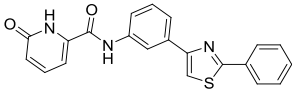
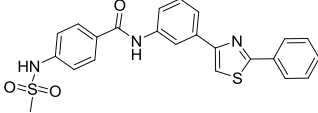
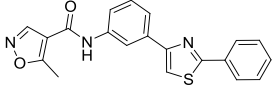
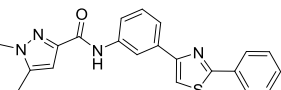
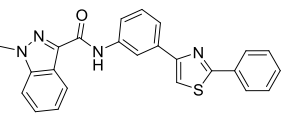
Cmpd No.	Cmpd Name	Structure	IC <sub>50</sub> ± SEM (µM)	
			Cdc25A	VHR
134	CRT-99		14.5 ± 0.9	>50
118	CRT-59		16.7 ± 1.5	>50
157	CRT-129		18.1 ± 2.0	5.29 ± 0.63

**Table 14** – Libraries 1 and 2: selected VHR-active compounds

Cmpd No.	Cmpd Name	Structure	IC <sub>50</sub> ± SEM (µM)	
			Cdc25A	VHR
157	CRT-129		18.1 ± 2.0	5.29 ± 0.63
141	CRT-113		48.0 ± 8.9	8.85 ± 1.47
117	CRT-57		54% inhibition at 50 µM	9.65 ± 1.46
139	CRT-106		54% inhibition at 50 µM	10.7 ± 2.0

More success was found in the variation of the amide region of cell-active furoyl aniline **84**, with pyridone **238** exhibiting very low micromolar activity against cdc25A (Table 15). Unfortunately, there again were not any simple SAR trends that could be elucidated from the data, but in general alternative small heterocycles gave similar potency to the furan of **84**.

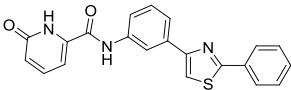
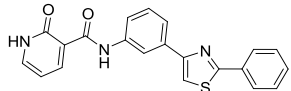
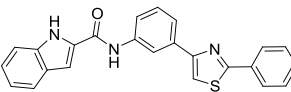
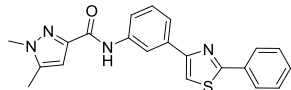
**Table 15** – Library 3 amides: selected cdc25A-active compounds

Cmpd No.	Cmpd Name	Structure	IC <sub>50</sub> ± SEM (μM)	
			Cdc25A	VHR
238	CRT-284		1.17 ± 0.40	2.60 ± 0.20
254	CRT-280		9.44 ± 1.08	>50
173	CRT-180		10.8 ± 3.0	16.2 ± 1.1
169	CRT-167		11.0 ± 2.0	10.5 ± 1.2
237	CRT-260		12.4 ± 1.4	16.1 ± 3.5

Similar results were found for VHR, although for this enzyme a further pyridone, **240**, proved potent and selective (Table 16). This compound is both an isomer of **238** and a direct analogue of aminocarbonylation product **157**, which has the alternatively-oriented amide linker and is missing the central phenyl ring. The similarity in potency of these compounds suggested a possible SAR trend that was supported by further data, specifically that the phenyl-thiazole-phenyl motif of these inhibitors likely represents a non-specific hydrophobic interaction. In this example, removal of the central phenyl group could theoretically shift the placement of the remaining thiazole-phenyl motif such that the pyridones of **157** and **240** overlay. The virtually-identical VHR potency for these two pyridones further suggests that the additional size and lipophilicity of the extra phenyl ring contributes little to the binding interaction, allowing a possible switch to a more lead-like core structure – see Figure 26 for a computational assessment of this theory.

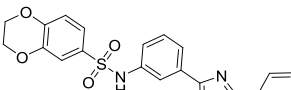
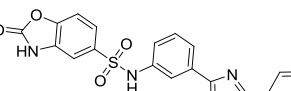
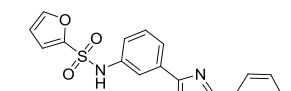
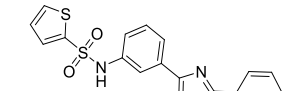


**Table 16** – Library 3 amides: selected VHR-active compounds

Cmpd No.	Cmpd Name	Structure	IC <sub>50</sub> ± SEM (μM)	
			Cdc25A	VHR
238	CRT-284		1.17 ± 0.40	2.60 ± 0.20
240	CRT-233		>50	5.26 ± 0.41
257	CRT-248		30.3 ± 7.2	10.3 ± 0.8
169	CRT-167		11.0 ± 2.0	10.5 ± 1.2

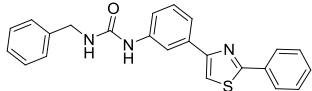
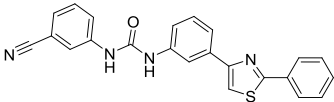
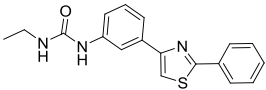
The sulfonamide analogues showed similar levels of mid-micromolar activity to many of the amides, again providing no clear SAR (Table 17). Direct comparison of cell-active furanamide **84** with its sulfonamide analogue **204** found a two-fold increase in potency for VHR with the sulfonamide, and a two-fold drop in potency for cdc25. Benzoxazolone **201** was found as a promising low micromolar cdc25 hit perhaps comparable to the benzimidazolone virtual screening hit **76**, with no similar compounds tested.

**Table 17** – Library 3 sulfonamides: selected compounds ranked by VHR activity

Cmpd No.	Cmpd Name	Structure	IC <sub>50</sub> ± SEM (μM)	
			Cdc25A	VHR
198	CRT-193		>50	9.29 ± 0.85
201	CRT-197		3.21 ± 0.30	11.7 ± 1.6
204	CRT-201		>50	13.1 ± 0.8
200	CRT-195		47.2 ± 5.4	13.3 ± 1.1

The compounds in the small urea library all proved broadly active with moderate potency (Table 18), pointing to a concerning lack of structure-dependency in the binding of these compounds. The high lipophilicity and low solubility of these ureas additionally discouraged any further investigation into this class of compounds.

**Table 18** – Library 3 ureas: selected compounds ranked by cdc25A activity

Cmpd No.	Cmpd Name	Structure	IC <sub>50</sub> ± SEM (μM)	
			Cdc25A	VHR
214	CRT-208		14.9 ± 1.0	8.50 ± 0.34
222	CRT-218		18.2 ± 1.9	5.59 ± 0.56
213	CRT-207		20.0 ± 2.8	12.6 ± 0.8

As expected, some of the 4-aminothiazoles showed similar levels of VHR selectivity to the 2-aminothiazoles found in the virtual screening, with aminopyridine 277 having promisingly good potency for its size and lipophilicity (Table 19). However, the direct 4-aminothiazole analogue of cell-active 2-aminothiazole screening hit **87** proved inactive, suggesting that the binding may not be as insensitive to the thiazole orientation as predicted. The library of N-arylated derivatives of aniline **166** also prepared by Buchwald-Hartwig coupling proved mostly inactive.

**Table 19** – Library 4: selected compounds ranked by VHR activity

Cmpd No.	Cmpd Name	Structure	IC <sub>50</sub> ± SEM (μM)	
			Cdc25A	VHR
277	CRT-351		33.4 ± 3.4	7.13 ± 0.50
283	CRT-370		>50	13.3 ± 1.0
271	CRT-334		29.7 ± 4.1	20.6 ± 1.5
268	CRT-324		>50	25.8 ± 1.7

Although it had been hoped that the variation of the 2-phenyl group of furanamide **84** would provide broad scope for optimisation, almost every compound tested proved inactive against cdc25A (Table 20). By contrast, a wide variety of functionality was tolerated by VHR, with a maximum two-fold increase in potency over the parent phenyl compound. This data displays perhaps the only clear SAR trend found across the parallel synthesis libraries, and might be applicable as method of introducing VHR selectivity and some additional potency to many of the successful compounds from the other small libraries above.

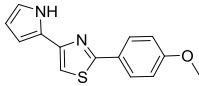
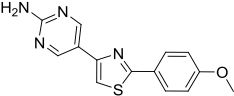
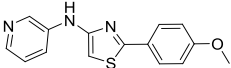
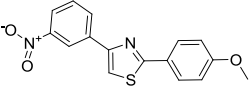
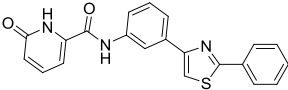
**Table 20** – Library 5: selected compounds ranked by VHR activity

Cmpd No.	Cmpd Name	Structure	IC <sub>50</sub> ± SEM (μM)	
			Cdc25A	VHR
307	CRT-408		>50	12.6 ± 1.2
319	CRT-430		>50	13.8 ± 1.8
305	CRT-406		>50	16.2 ± 1.0

As discussed previously, identification of the most-promising lead compounds from these diverse libraries required consideration not only of overall potency and selectivity, but also compound size and lipophilicity. This analysis was based on two observations: during the lead optimisation, process compounds become larger and more lipophilic, and also drug candidates that are lipophilic tend to have poor pharmacokinetic parameters and increased binding promiscuity.<sup>164,165</sup> In order for this to be a quantitative analysis, applicable across any structural class, various binding efficiency metrics have recently been developed. Ligand efficiency (LE) determines which compounds make the most effective use of their size, calculating the average free-energy change of binding attributed to each heavy atom in the molecule.<sup>164</sup> Lipophilic ligand efficiency (LLE) determines the relationship between the potency and lipophilicity (as the calculated partition coefficient cLogP),<sup>165</sup> in theory identifying compounds that deliver a high contribution of their affinity from the specific electronic interactions of polar hydrophilic functionality, as opposed to the non-specific hydrophobic interactions of lipophilic compounds.

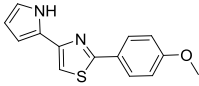
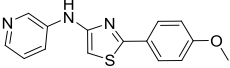
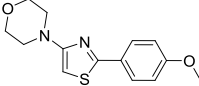
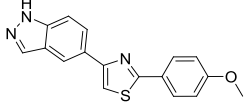
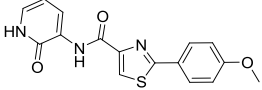
In this project, the narrow spread of observed potencies limits the utility of the ligand efficiency metric, as the value is predominantly determined by the much-greater spread of compound size, ultimately resulting largely in the elevation of the smallest compounds to the highest rankings. As such, pyrrole **105** ranks highest for both cdc25A (Table 21) and VHR (Table 22). The Suzuki coupling products **118** and **134** also score highly for cdc25A, ahead of the potent pyridone **238**. For VHR, this latter compound ranks lower than the smaller amide-linked pyridone **157**.

**Table 21** – Top compounds ranked by cdc25A LE

Cmpd No.	Cmpd Name	Structure	Cdc25A IC <sub>50</sub> (μM)	LE <sup>a</sup>
105	CRT-24		25.6 ± 1.7	0.35
118	CRT-59		16.7 ± 1.5	0.33
277	CRT-351		33.4 ± 3.4	0.31
134	CRT-99		14.5 ± 0.9	0.30
238	CRT-284		1.17 ± 0.40	0.30

*a* – LE = ΔG / no. of heavy atoms

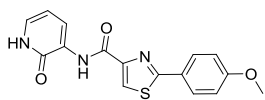
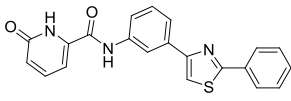
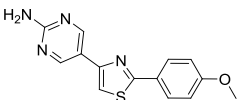
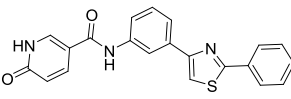
**Table 22** – Top compounds ranked by VHR LE

Cmpd No.	Cmpd Name	Structure	VHR IC <sub>50</sub> (μM)	LE <sup>a</sup>
105	CRT-24		12.6 ± 1.7	0.37
277	CRT-351		7.13 ± 0.50	0.35
276	CRT-346		26.8 ± 3.5	0.33
141	CRT-113		8.85 ± 1.47	0.31
157	CRT-129		5.29 ± 0.63	0.31

*a* – LE = ΔG / no. of heavy atoms

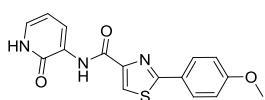
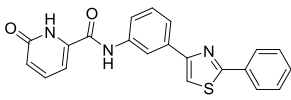
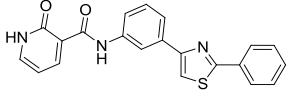
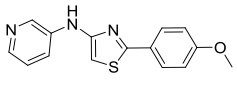
In contrast to the LE tables, the LLE measurement provides more novel insight into which compounds qualify as good leads, with the inclusion of the previously-unconsidered cLogP values. For both cdc25A (Table 23) and VHR (Table 24), the highly polar pyridones compounds rank highly, with aminocarbonylation product **157** generating particularly high efficiency scores for both enzymes.

**Table 23** – Top compounds ranked by cdc25A LLE

Cmpd No.	Cmpd Name	Structure	Cdc25A IC <sub>50</sub> (μM)	cLogP	LLE <sup>a</sup>
157	CRT-129		18.1 ± 2.0	1.0	3.8
238	CRT-284		1.17 ± 0.40	3.0	2.9
118	CRT-59		16.7 ± 1.5	2.1	2.6
227	CRT-235		21.0 ± 1.6	2.7	1.9

$$a - LLE = pIC_{50} - cLogP$$

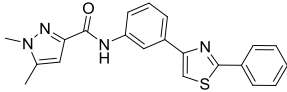
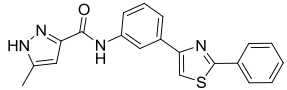
**Table 24** – Top compounds ranked by VHR LLE

Cmpd No.	Cmpd Name	Structure	VHR IC <sub>50</sub> (μM)	cLogP	LLE <sup>a</sup>
157	CRT-129		5.29 ± 0.63	1.0	4.3
238	CRT-284		2.60 ± 0.20	3.0	2.6
240	CRT-233		5.26 ± 0.41	2.8	2.5
277	CRT-351		7.13 ± 0.50	3.1	2.0

$$a - LLE = pIC_{50} - cLogP$$

In order to rapidly confirm that the cell-activity from the virtual screening hits had been maintained in the synthesis of these compound libraries, and also to identify novel cell-active compounds for a patent application, several close analogues of furanamide **84** found to be cdc25A inhibitors were tested against a panel of cell lines by co-workers in the Mann group. Pyrazoles **169** and **232** proved active at similar low micromolar concentrations to their *in vitro* IC<sub>50</sub> values (Table 25).

**Table 25** – MTS assay results; proof of retention of cell-activity

Cmpd No.	Cmpd Name	Structure	MTS Cell Assay IC <sub>50</sub> ± SEM (μM)		
			293T	HeLa	3T3
<b>169</b>	CRT-167		6.64 ± 1.00	17.2 ± 2.0	16.5 ± 1.8
<b>232</b>	CRT-251		7.39 ± 0.37	10.4 ± 0.4	9.51 ± 0.48

In summary, parallel synthesis, purification and testing of a wide range of compound structures based around the virtual screening hits was only moderately successful; although no significant increase in potency was observed, many of the synthesised compounds possessed better physical properties as quantified by binding efficiency metrics. During the parallel synthesis effort carried out on placement at CRT, we were also granted access to small samples of any commercial compounds contained in the company library, and the next section describes the subsequent compound selection and phosphatase assays.

## 7.2 Screening of CRT Compounds

### 7.2.1 Compound Selection

In order to rapidly expand the SAR of the virtual screening hits, three substructure-based searches were performed on the CRT database of 90,000 compounds. As before, all the compound properties were calculated using StarDrop and compounds with undesired features or properties were discarded (including high complexity, similarity to compounds in active CRT research programs and compounds where the desired substructure formed only part of the side-chain of a large alternative core structure). As in the virtual screening,

diarylpyrazoles were also excluded to attempt to move further from the initial literature template inhibitor. The chosen compounds comprised:

- 399 commercially available 2,4-disubstituted thiazoles
- 979 commercially available N-,C4-disubstituted 2-aminothiazoles
- 564 commercially available 5-membered aromatic heterocycles (containing at least one nitrogen atom) with a 1,3-substitution pattern containing at least one (hetero)aromatic ring

Of this selection, a subset of 983 compounds was retrieved (based on a minimum number per CRT storage plate to reduce robot usage). Each compound was tested in triplicate at 20  $\mu\text{M}$  against *cdc25A* and VHR using the fluorescence assays developed previously. Those showing >50% inhibition were purchased (if available) and full 10-concentration  $\text{IC}_{50}$  values were measured.

Prior to these assays, a pET21a construct expressing untagged VHR (previously obtained commercially) had been prepared by co-workers in the Mann group, but this was found to not express efficiently, perhaps due to poor solubility of the resulting protein.<sup>119</sup> A construct for GST-tagged VHR was prepared by co-workers as an alternative, and in our hands this gave high yields of protein, readily purified using the GST tag.

### 7.2.2 Assay Results

The assay results for selected compounds from the CRT library are shown in Table 26 and Table 27. The data showed that this screen was successful in finding a variety of low-micromolar hit compounds for both *cdc25A* and VHR. Pyrazinoyl aminothiazole **335** represented the most promising of a range of acylaminothiazoles identified as good *cdc25A* hits, with quinazolinone **341** highly potent and VHR selective. Various non-thiazole core structures were identified including oxadiazoles **353-356** that represented a novel alternative series with likely lower lipophilicity than the corresponding thiazoles. Compounds **363-368** possess one alkyl substituent on the arylthiazole core, and as such were thought likely to deviate from the highly planar conformation and poor solubility of the virtual screening hits.



**Table 26** – Selected active compounds from CRT library grouped by structural class, ranked by cdc25A activity

Cmpd No.	Cmpd Name	Structure	Cdc25A IC <sub>50</sub> (μM)	VHR IC <sub>50</sub> (μM)	Cmpd No.	Cmpd Name	Structure	Cdc25A IC <sub>50</sub> (μM)	VHR IC <sub>50</sub> (μM)
335	C726-4901		3.3 ± 0.3	3.1 ± 0.1	344	C742-6778		5.3 ± 0.5	2.07 ± 0.34
336	CD 0663-0359		5.1 ± 1.1	21.2 ± 2.7	345	C741-1786		7.9 ± 0.7	9.1 ± 0.5
337	C727-0205		6.7 ± 0.7	3.1 ± 0.4	346	C593-5313		20.3 ± 4.0	28.8 ± 11.3
338	C728-2381		9.5 ± 1.2	14.1 ± 2.2	347	ASN 0488-0636		N.D.	13.9 ± 0.9
339	C725-5305		13.4 ± 2.4	12.5 ± 1.8	348	CD 8009-2477		4% inhibition at 20 μM	21.4 ± 2.7
340	C593-2609		14.5 ± 13.5	24.2 ± 2.6	349	ASN 1214-3136		27% inhibition at 20 μM	17.8 ± 6.6
341	C749-5697		7% inhibition at 20 μM	1.64 ± 0.55	350	C785-7802		20.5 ± 5.3	8.3 ± 1.0
342	C728-9542		1% inhibition at 20 μM	11.0 ± 0.9	351	C785-1425		~75	17.2 ± 4.4
343	ASN 0658-8123		0% inhibition at 20 μM	41.1 ± 9.0	352	C656-9389		~100	31.2 ± 10.6

**Table 27** – Selected active compounds from CRT library grouped by structural class, ranked by cdc25A activity

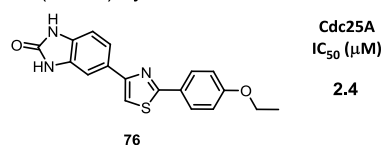
Cmpd No.	Cmpd Name	Structure	Cdc25A IC <sub>50</sub> (μM)	VHR IC <sub>50</sub> (μM)	Cmpd No.	Cmpd Name	Structure	Cdc25A IC <sub>50</sub> (μM)	VHR IC <sub>50</sub> (μM)
353	C888-5549		12.2 ± 1.4	9.4 ± 1.2	362	SP-00521		~50	25.6 ± 7.3
354	SEW-03756		18% inhibition at 20 μM	19.8 ± 2.7	363	CD G569-0282		7.2 ± 0.4	10.6 ± 1.1
355	CD E595-0578		7.1 ± 1.4	14.5 ± 1.0	364	CD G856-2968		11.4 ± 0.8	11.2 ± 1.1
356	CD E595-0205		7.8 ± 1.6	18.1 ± 1.6	365	CD G571-0233		18.6 ± 1.4	33.6 ± 8.8
357	KO 3T-0868		20.5 ± 4.8	~50	366	CD G571-0231		20.5 ± 1.7	18.4 ± 1.4
358	KO 5F-909		14.9 ± 3.3	36.2 ± 5.7	367	CD G856-2962		31.6 ± 4.2	~50
359	SP-00519		6.3 ± 0.8	3.3 ± 0.4	368	KM-03222		4.0 ± 0.6	2.47 ± 0.33
360	SP-00707		14.8 ± 2.2	34.0 ± 5.4	369	SP-00559		26.4 ± 3.6	~50
361	SPB-05833		32.5 ± 4.8	20.4 ± 1.7					

### 7.3 Target-Oriented Synthesis

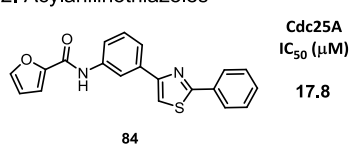
At this stage of the project, a variety of structural classes had been discovered as new and promising leads for *cdc25* inhibition, but with no outstanding candidate for further development; Figure 24 illustrates some of the different groups of substructures obtained. In order to maximise the value of the single analogues synthesised and purified by non-parallel methods, it was decided to attempt to delineate the key structural classes further by the preparation of hybrid structures in order to challenge specific hypotheses.

#### Initial Hits from Virtual Screen

##### 1. Di(hetero)arylthiazoles

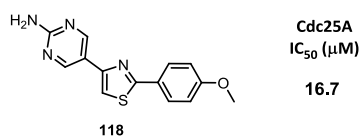


##### 2. Acylanilinothiazoles

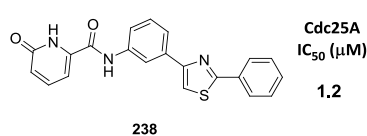


#### Synthesised Compounds

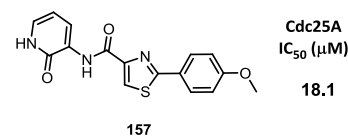
##### 1. Di(hetero)arylthiazoles



##### 2. Acylanilinothiazoles

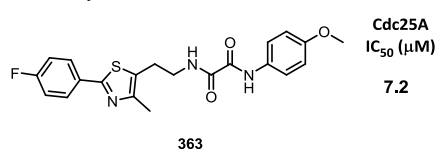


##### 3. 4-Amidothiazoles

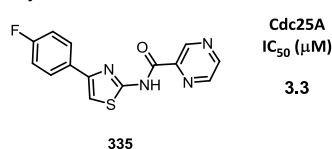


#### Hits from Structural Analogue Screen

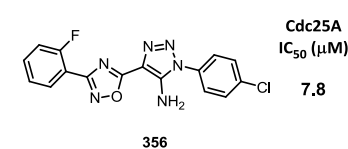
##### 4. Alkyl-linked amides



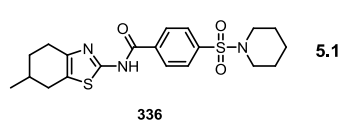
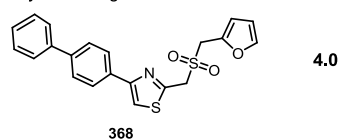
##### 5. Acyl-2-aminothiazoles



##### 6. Oxadiazole-aminothiazoles



Possibly including



Possibly including

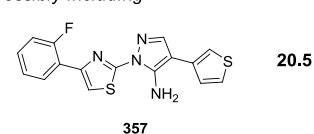


**Figure 24** – Summary of key compound classes

A computational analysis of the potential binding modes of a selection of the novel inhibitors was attempted using the FieldTemplater and FieldAlign software. Although various combinations of compounds were tested, very little consensus was obtained with respect to a possible binding conformation, both in terms of the ranked overlap scores within a sample of compounds and especially in terms of comparing the results of templating the same compound against different sets of similar inhibitors. Similarly, the broadest and most

information-rich template, generated from templating all the low energy conformations (approximately 100) of each of the 7 compounds with potencies of less than 5  $\mu\text{M}$  against every conformation of the other 6 compounds, was only able to find a common overlay for 5 of the 7 compounds, this overlay also suffering from the same inconsistencies as described above. Attempted analysis of inactive compounds also gave no viable information, probably due to the relatively small difference between nominally active and inactive compounds in the current data.

A necessary alternative was therefore to adopt a more qualitative approach in assessing the potential similarities between inhibitor binding modes, using the modelling software to assess the feasibility of any hypotheses. The first hypothesis derived from the possible similar binding modes for pyridones **157** (Table 14) and **240** (Table 16) discussed previously, which pointed towards groups 2 and 3 (Figure 24) potentially overlaying the key functionality. It was proposed that the group 5 acylaminothiazoles such as **335**, to some extent isomeric with the group 3 amidothiazoles, might also bind in a similar fashion; in each case the additional non-amide-containing thiazole substituent is usually a small, relatively lipophilic aryl group (Figure 25).

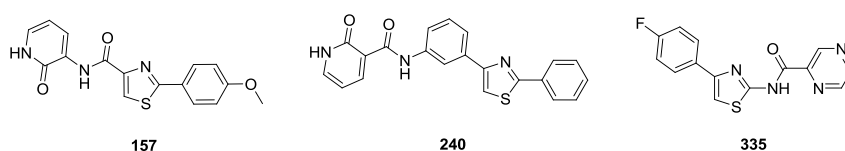


**Figure 25** – Inhibitors proposed to share a similar binding mode

The optimal overlaid conformations of pyridones **157** and **240** (generated from the larger template containing 7 compounds with diverse structures) appeared to support the above hypothesis (Figure 26), with the pyridone amides superimposed at the expense of the lipophilic thiazole rings, each of which is instead aligned with an aryl group. However, the validity of this overlay is questioned by the preference for the orientation of the pyridones; in one example, the carbonyl groups are placed on the same side of the planar molecule, and in the other the amide and pyridone N-Hs are similarly aligned. This has the effect of enhancing the field point pattern for the central linking amide in both cases, with these presumably high energy conformations scoring much higher with respect to field point overlap due to this exaggerated electronic character. On the other hand, all the conformations used are accessible

at room-temperature energy, so perhaps the perceived repulsion in these displayed conformations is not as high as it might seem.

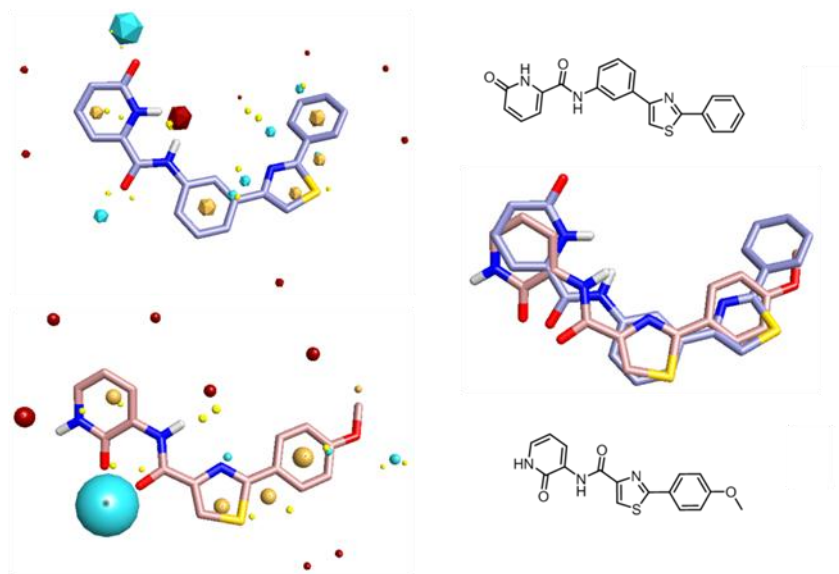


**Figure 26** – FieldTemplater overlay of pyridones **240** and **157**

A similar overlay between groups 3 and 5 identified the same conformation of 4-amidothiazole pyridone **157**, this time aligning well with acylaminothiazole **335** despite the reversal of both the amide orientation and that of the thiazole ring (Figure 27). As before, the highly-convincing overlay of steric and electronic fields are put in doubt by the questionable conformations, with acylpyrimidine **335** aligning the lone pairs of the carbonyl and azine nitrogen to match the large negative field point found in the matching conformation of pyridone **157**.

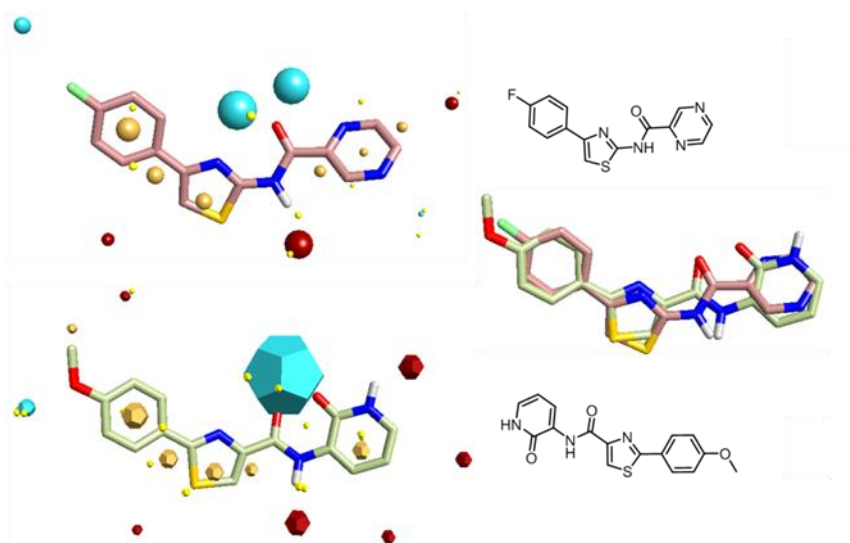


**Figure 27** – FieldTemplater overlay of pyridone **157** and pyrazinoyl aminothiazole **335**

It was also theorised that the alkyl-linked amides of group 4 might represent more flexible versions of the acylanilinothiazoles of group 2, with the central phenyl ring of the latter replaced by the alkyl linker. FieldTemplater analysis demonstrated that the flexible ethyl-linked oxamide compounds such as **365** can adopt very similar conformations to the more rigid pyridone aniline **238** (Figure 28).

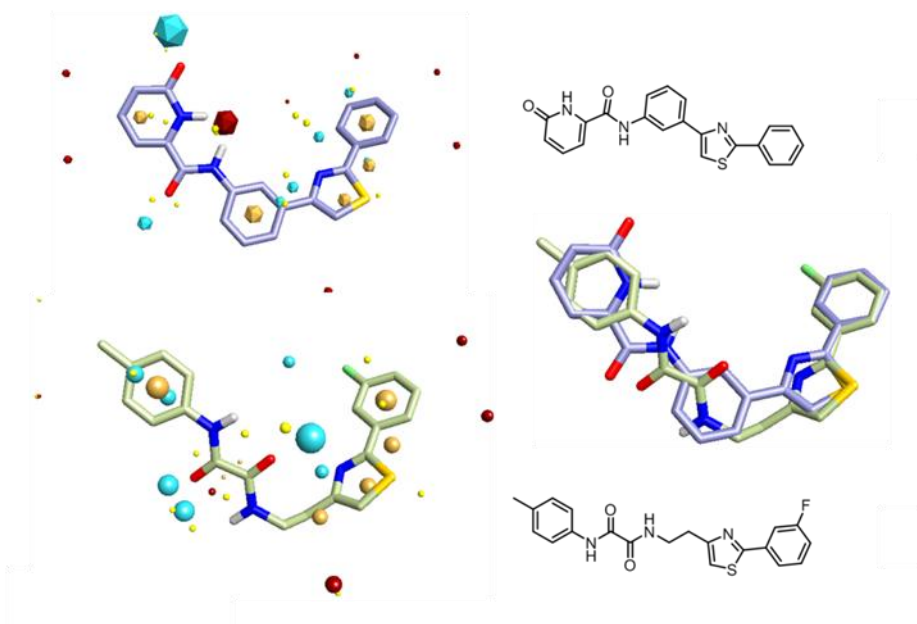
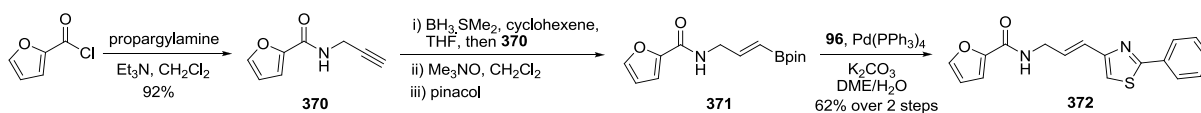


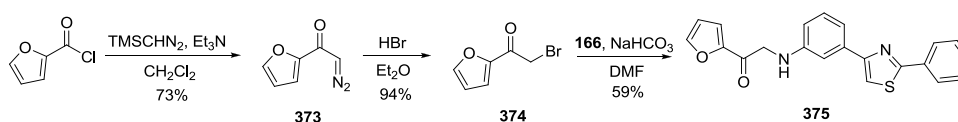
**Figure 28** – FieldTemplater overlay of pyridone **238** and bis-oxamide **365**

It was therefore proposed that replacement of the central phenyl ring of furanamide **84** (Table 7) with an allyl analogue should provide a smaller, more flexible and less lipophilic variant (cLogP 3.65 vs. 4.58), and prove a test of the necessity of an aromatic group at this position. Synthesis of required vinylboronate coupling partner **371** was achieved by acylation of propargylamine with 2-furoyl chloride in high yield and use of the resulting propargyl amide (**370**) in the standard hydroboration/oxidation/esterification sequence (Scheme 37), although purification of boronate product **371** proved difficult. At this stage, the choice was made to attempt the subsequent coupling reaction with bromothiazole **96** under the standard Suzuki conditions used previously, and this reaction was successful, giving vinylthiazole **372** in a good overall yield. Further problems with complete purification were to be addressed pending the outcome of an initial enzyme assay. Many of the purification issues with this reaction sequence might have been avoided by diverting the boronate ester synthesis to give the corresponding trifluoroborate, which in addition to other practical advantages are generally readily recrystallised to high purity.



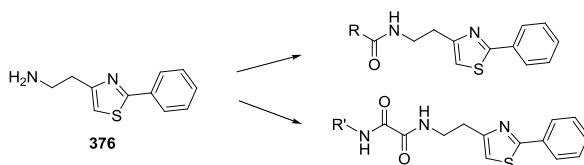
**Scheme 37** – Synthesis of allyl furanamide **372**

A further test of the influence of both the amide functionality and the conformational rigidity of furanamide **84** was envisaged by the synthesis of the corresponding  $\alpha$ -aminoketone **375**, with the inclusion of a methylene spacer (Scheme 38). Complete conversion of 2-furoyl chloride to diazoketone **373** using TMSCHN<sub>2</sub> required minor optimisation of the literature conditions; additional equivalents of the diazomethane reagent did not increase the rate enough to prevent the competing decomposition of the product, and it was found that inclusion of a base (Et<sub>3</sub>N) and a change in solvent (Et<sub>2</sub>O to CH<sub>2</sub>Cl<sub>2</sub>) gave complete conversion and a good isolated yield of the desired product. Rhodium-catalysed insertion of this diazoketone into the N-H bond of aniline **166** was attempted as a direct route to target  $\alpha$ -aminoketone **375**, but this reaction was unsuccessful, producing a complex mixture of products. An alternative route to  $\alpha$ -aminoketone **375** was successfully carried out *via* synthesis of the intermediate  $\alpha$ -bromoketone (**374**) in high yield, and standard nucleophilic substitution.



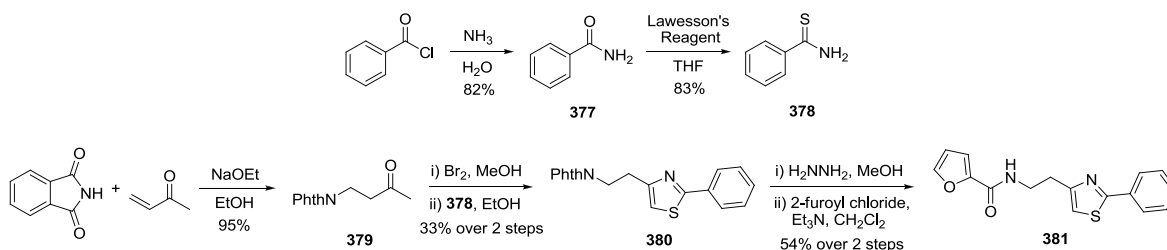
**Scheme 38** – Synthesis of  $\alpha$ -anilino ketone **375**

A further test of the potential similarity between groups 2 and 4 shown in Figure 28 was proposed as the synthesis of 2-aminoethyl-substituted thiazole **376** that would allow for both the generation of flexible and smaller analogues of the active furan and pyridone amides **84** and **238**, and also synthesis of a small library of bis-oxamide inhibitors (Scheme 39).



**Scheme 39** – Proposed synthesis of amide and bis-oxamide libraries from amine **376**

The synthetic strategy involved synthesis of 4-(2-aminoethyl)-thiazole precursor **376** by a literature condensation route<sup>166</sup> in order to straightforwardly generate a large quantity of this common intermediate (Scheme 40). Thiobenzamide (**378**) was prepared in two steps in good yield by benzylation of ammonia and subsequent thionation using Lawesson's reagent. Required  $\beta$ -amino ketone **379** was prepared in protected form and high yield by the conjugate addition of phthalimide to MVK with catalytic ethoxide base. Regioselective bromination of the less-hindered  $\alpha$ -position of ketone **379** was carried out as described in the literature,<sup>166</sup> but the <sup>1</sup>H-NMR data for the major product of the mixture obtained from this reaction did not match that reported. However, use of this crude bromide in the subsequent condensation with thiobenzamide gave the expected 4-(2-aminoethyl)-thiazole **380** in moderate yield over the two steps. None of the thiazole product that would have resulted from bromination on the more-substituted position of ketone **379** was detected, but it is possible that the fairly mild condensation reaction conditions were selective for thioamide S-alkylation with only the primary bromide. Removal of the phthalimide group and subsequent amine acylation gave target furanamide **381** in good yield over the two steps. The initial plan to optimise and scale-up this route in preparation for bis-oxamide library synthesis was not completed due to the reassessment of the assay results (see Section 9).

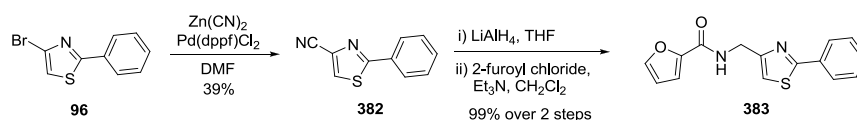


**Scheme 40** – Synthesis of ethylene-linked thiazole furanamide **381**

To complete the investigation of smaller, alkyl-linked furanamide thiazoles, methylene-linked analogue **383** was prepared from bromothiazole **96** (Scheme 41). The initial test of Pd-

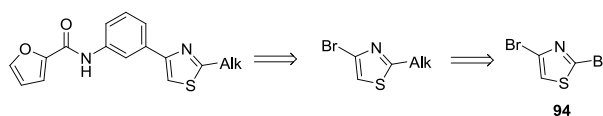


catalysed cyanation under microwave conditions was successful, albeit giving nitrile **382** in low yield. It was considered that lower temperature might have provided a cleaner reaction and higher yield, as much decomposition was observed. Nitrile **382** was then reduced and acylated in quantitative yield to give target furanamide **383**.



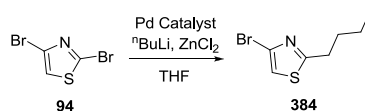
**Scheme 41** – Synthesis of methylene-linked thiazole furanamide **383**

As part of the exploration of chemistry likely to be relevant for future inhibitor synthesis, the SAR for the thiazole 2-position of analogues of furanamide **84** discussed previously had suggested that small alkyl substituents might prove optimal. In keeping with the divergent coupling-based strategy employed in this research, a regioselective Negishi coupling of 2,4-dibromothiazole was used employing readily-accessible alkylzinc chlorides (Scheme 42).



**Scheme 42** – Proposed synthesis of 2-alkyl analogues of furanamide **84**

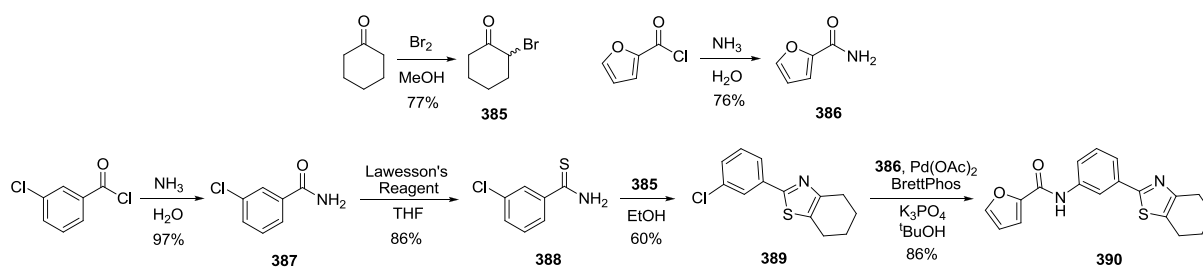
The literature conditions reported<sup>167</sup> for this reaction were reproducibly found to give a low conversion (Table 28, Entry 1), with the product inseparable from the starting dibromide. A parallel series of small-scale test reactions were carried out to determine the cause of the poor conversion (Entries 2-7). The initial theory of poor catalyst activation was challenged by the similarly-poor conversion obtained from Pd(dppf) prepared from alternative precursors, and also when using PPh<sub>3</sub> or S-Phos as ligands. The highest conversions obtained in these test reactions resulted from increasing the reaction temperature (Entry 4) and using alternative bidentate phosphine bis(2-diphenylphosphinophenyl)ether (DPE-Phos) (Entry 7). A combination of these improved conditions on a larger scale (Entry 8) gave almost complete conversion of the starting dibromide, with a small quantity of the di-coupled product observed by <sup>1</sup>H-NMR.

**Table 28** – Optimisation of regioselective Negishi coupling of dibromothiazole **94**

Entry	Catalyst	Conditions	Scale (mmol)	Conversion (%) <sup>a</sup>
1	Pd <sub>2</sub> (dba) <sub>3</sub> , dppf	r.t., 16 h	1.0	21
2	Pd(MeCN) <sub>2</sub> Cl <sub>2</sub> , dppf	r.t., 16 h	0.2	4
3	Pd(dppf)Cl <sub>2</sub>	r.t., 16 h	0.2	6
4	Pd <sub>2</sub> (dba) <sub>3</sub> , dppf	70 °C, 16 h	0.2	15
5	Pd(PPh <sub>3</sub> ) <sub>2</sub> Cl <sub>2</sub>	r.t., 16 h	0.2	1
6	Pd(MeCN) <sub>2</sub> Cl <sub>2</sub> , S-Phos	r.t., 16 h	0.2	2
7	Pd(MeCN) <sub>2</sub> Cl <sub>2</sub> , DPE-Phos	r.t., 16 h	0.2	29
8	Pd(MeCN) <sub>2</sub> Cl <sub>2</sub> , DPE-Phos	70 °C, 60 h	1.0	97

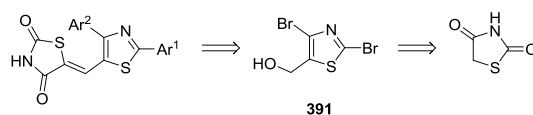
*a* – Conversion calculated by ratio of integrals of thiazole 5-H peaks in <sup>1</sup>H-NMR

The somewhat unusual 4,5,6,7-tetrahydrobenzothiazole structure found in screening hit **336** (see Section 7.2.2) was considered as a possible alternative to 2-alkylthiazoles for design of a small hydrophobic region. The positioning of the thiazole substituents (alternatively construed as the position of the sulfur atom in the ring) has been proposed to be potentially insignificant, allowing the small hydrophobic region to be installed at the C4- and C5-positions instead. According to this strategy, a fused cycloalkyl analogue of furanamide **84** was synthesised (Scheme 43). The route required the synthesis of chloride **389** as an intermediate for a final-step Buchwald amidation that could be used for simple late-stage diversification. Monobromination of cyclohexanone was initially attempted using two sets of conditions recently reported as being especially suited to this transformation; NBS in DMSO (purported to weaken the N-Br bond by coordination) gave rapid conversion but a complex mixture, and NBS in Et<sub>2</sub>O catalysed by NH<sub>4</sub>OAc gave a low conversion. Using the more conventional conditions of Br<sub>2</sub> in MeOH gave a good yield of desired bromide **385**. 3-Chlorobenzamide (**387**) was prepared and thionated in high yield, and condensed with bromide **385** to give key intermediate chloride **389**. Amidation with furanamide **386** using a recently-reported Buchwald ligand<sup>168</sup> proceeded in excellent yield to give target compound **390**.



**Scheme 43** – Synthesis of 4,5-fused cycloalkyl thiazole **390**

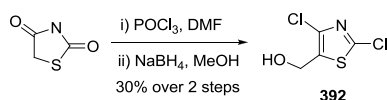
As further exploration of thiazole coupling chemistry, a key experiment proposed following the virtual screening was to directly compare the novel diarylthiazole hits to diarylpyrazole template **6** (see Figure 16) by the addition of the extra C-5 substituent removed in the screening process, the thiazolidine-2,4-dione. A direct and divergent synthesis was planned *via* dibromothiazole **391**, which contained an additional hydroxymethyl substituent that could be transformed into a variety of 5-substituents (Scheme 44). This in turn could be prepared from a known double bromination/formylation of thiazolidine-2,4-dione,<sup>169</sup> similar to the conditions used for the synthesis of 2,4-dibromothiazole but including an equivalent of DMF to perform a further Vilsmeier-Haack formylation at the free C5-position.



**Scheme 44** – Retrosynthetic analysis for divergent coupling-based approach to 5-substituted 2,4-diarylthiazoles

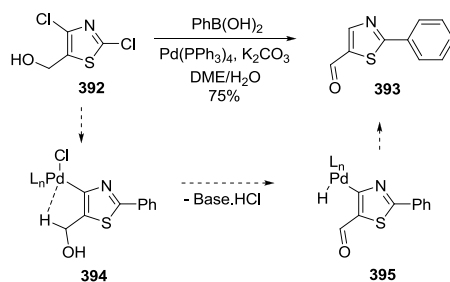
Unfortunately, initial attempts at this literature transformation with  $\text{POBr}_3/\text{DMF}$  gave a low mass recovery. Previous experience with  $\text{POBr}_3$  suggested this reagent can give inconsistent results, and an alternative strategy was to substitute bromine for chlorine using  $\text{POCl}_3$ , likely giving a cleaner halogenation reaction in addition to the lower cost and easier handling of the reagent. A further advantage would be the exploration of the Suzuki coupling of the 2,4-dichlorothiazole for possible use in place of the dibromothiazole for other syntheses. The desired alcohol was obtained in moderate yield over 2 steps following  $\text{NaBH}_4$  reduction (Scheme 45). This reduction gave several advantages: the aldehyde intermediate proved difficult to purify and somewhat unstable to long-term storage. Furthermore, use of this aldehyde in the key Suzuki coupling as a more direct synthetic strategy was likely to give

poorer regioselectivity due to the additional conjugative electron-withdrawal from the 4-chloride.



**Scheme 45** – Synthesis of 5-substituted 2,4-dichlorothiazole **392**

At this stage of the project, no examples of regioselective Suzuki coupling of a 2,4-dichlorothiazole without a conjugated electron-withdrawing substituent at the 5-position had been reported. An initial test reaction using the unsubstituted 2,4-dichlorothiazole under the optimised microwave Suzuki conditions gave an encouraging 81% conversion to the 2-phenyl-4-chlorothiazole. However, attempted regioselective Suzuki coupling of the 5-hydroxymethyl dichlorothiazole instead gave 5-formylthiazole **393** in good yield (Scheme 46), possibly by intramolecular transfer of a hydride to the adjacent Pd centre in oxidative adduct **394**, simultaneously oxidising the alcohol and reducing the C4-position. Further experiments are necessary to investigate the generality of this reaction, and to test the proposed reaction sequence and intramolecular hydride delivery. Interception of the initially-formed 2-phenyl intermediate and resubmission to the reaction conditions would confirm the order of events, and synthesis of the deuterated hydroxymethyl analogue would test the proposed intramolecular nature of the reduction.



**Scheme 46** – Synthesis of 5-formyl-2-phenylthiazole **393** and proposed mechanism

### 7.3.1 Analogues of C7264901 (**335**) with Decreased Toxicological Liability

Although the combination of high potency, small size and low cLogP seemed to make pyrazinoyl aminothiazole **335** an attractive target for future development, 2-aminothiazoles are not generally considered as viable hit structures by medicinal chemists due to concerns about a metabolically-induced toxic effect *in vivo*. This has been discovered to result from ring-opening of the thiazole ring following epoxidation of the C4 and C5 positions, and depends critically on the 5-position being both electron-rich and unsubstituted.<sup>170</sup> Consequently, simple aminothiazole analogues with an additional methyl or fluoro substituent, or with the C5 carbon replaced by a nitrogen, have been found to exhibit greatly-reduced toxicity.<sup>170,171</sup> The synthesis of similar analogues of aminothiazole **335** that retained good potency would therefore allow this compound to be considered for further development (Figure 29).

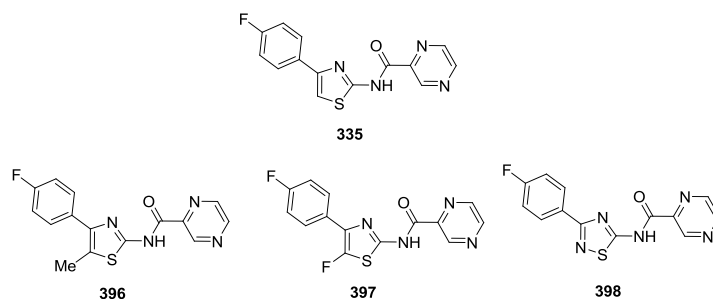
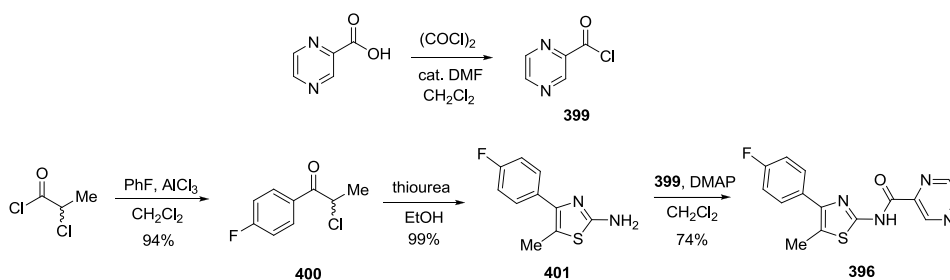


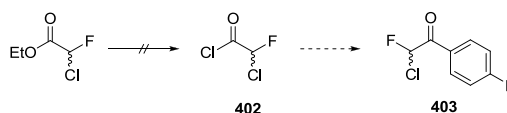
**Figure 29** – Pyrazinoyl aminothiazole **335** and proposed reduced-toxicity analogues **396-398**

The 5-methyl analogue **396** was prepared using a classic heterocyclic synthesis route, with Friedel-Crafts acylation of fluorobenzene, subsequent condensation with thiourea to give the aminothiazole, and acylation to give the desired amide (Scheme 47). Whilst the initial two steps proceeded in excellent yield, the amide bond formation proved much more challenging. Pyrazinoyl chloride **399** was found to be difficult to prepare with good purity, susceptible to decomposition, and poorly soluble. A variety of conditions were used for the acylation of aminothiazole **401** with different batches of the acid chloride prepared and purified by different methods, and the best conditions were found to be the use of oxalyl chloride for the initial chlorination, and immediate reaction with the aminothiazole using a full equivalent of DMAP.



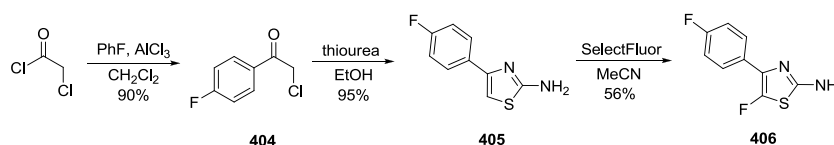
**Scheme 47** – Synthesis of 5-methyl aminothiazole analogue **396**

The synthesis of the 5-fluoro analogue was initially planned by this successful route used for the 5-methyl analogue, which required the synthesis of chlorofluoroacetyl chloride **402** (Scheme 48). Hydrolysis of the commercially available ester and standard work-up gave the carboxylic acid, but this was found to be both highly volatile and water-soluble. As an alternative, the sodium salt was prepared in good yield, but attempts at chlorination of this compound were stopped due to the extremely high volatility of the acid chloride product.



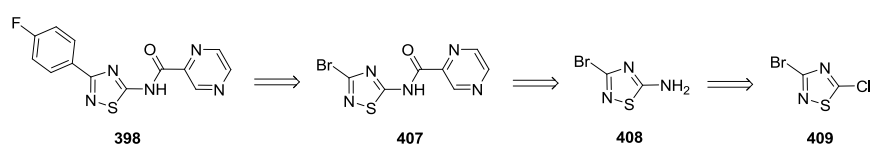
**Scheme 48** – Attempted synthesis of chlorofluoroketone **403**

An alternative strategy was carried out using electrophilic fluorination of the unsubstituted aminothiazole ring (Scheme 49). The Friedel-Crafts acylation and thiourea condensation again proceeded in excellent yield to give unsubstituted aminothiazole **405**. The fluorination reaction gave good conversion to the product by  $^1\text{H-NMR}$ , but no separation of starting aminothiazole and product was observed by TLC analysis. Although increasing the equivalents of SelectFluor<sup>®</sup> gave a mixture of products, the use of a new batch of the fluorination reagent gave full conversion and a moderate yield of the 5-fluoro target compound **406**. Unfortunately, at this stage all attempts at acylation with the pyrazinoyl chloride were unsuccessful.



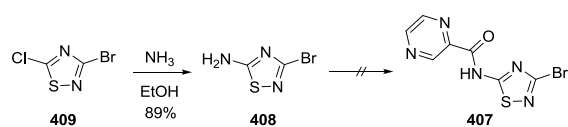
**Scheme 49** – Synthesis of 5-fluoro aminothiazole analogue **406**

Thiadiazole analogue **398** was envisaged to be prepared according to an adapted literature route from 3-bromo-5-chloro-1,2,4-thiadiazole (**409**) by regioselective amination, acylation with pyrazinoyl chloride and Suzuki coupling to install the 3-aryl group (Scheme 50).<sup>172</sup> Whereas the literature synthesis of similar compounds requires intermediate Boc-protection for the 5-amino group in order to obtain good yields in the Suzuki coupling, it was hoped that in this case a more efficient synthesis would be to first introduce the desired pyrazinoyl group in order to deactivate this amine.



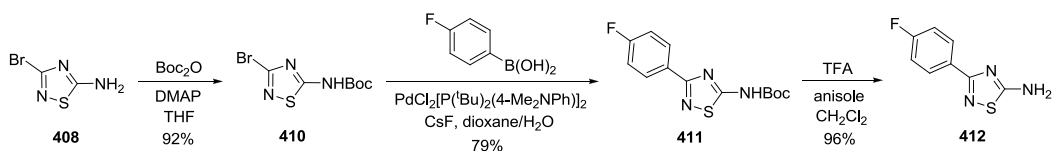
**Scheme 50** – Proposed synthesis of thiadiazole analogue **398**

The initial chloride displacement was successful, and the yield of amine **408** was improved by changing the work-up procedure (Scheme 51). However, as for the 5-methyl aminothiazole, the initial acylation attempts with the pyrazinoyl chloride were unsuccessful. As observed with the 5-fluoro analogue, the conditions that eventually proved reactive with the 5-methyl compound gave a very low conversion with the more electron-poor thiadiazole amine, and more forcing conditions resulted in decomposition (it had been noted by the group developing the subsequent Suzuki coupling that bromide **408** was unstable to basic conditions and elevated temperatures).



**Scheme 51** – Unsuccessful synthesis of pyrazinoyl aminothiadiazole **407**

It was hoped that the corresponding 3-aryl-5-aminothiadiazole might prove a more stable coupling partner for the unreactive pyrazinoyl chloride, and the literature route to this compound proved successful, giving the desired amine **412** in high yield (Scheme 52).



**Scheme 52** – Synthesis of 3-aryl-5-aminothiadiazole **412**

All further attempts to acylate the amine of both the 5-fluoro and the thiadiazole analogues, including HATU coupling, were unsuccessful, and the reassessment of the original assay results (see Section 9) lowered the priority of this strand of research.

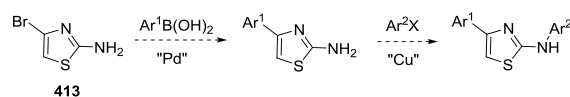
In summary, a range of chemistry was explored towards the synthesis of individual target compounds that attempted to provide information about binding modes or structural alternatives, rather than simply to further increase the potency of the best inhibitors. At this stage of the project, it became clear that much of the original assay data on which these hypotheses were based was not reliable, and a full reassessment was carried out (see Section 9). During this period, novel and relevant methodology towards aminothiazole synthesis was investigated which could be performed independently of the results of the original assays, and this research is discussed in the next section.



## 8 Development of a Divergent Synthesis of 2-(Hetero)aryl Aminothiazoles

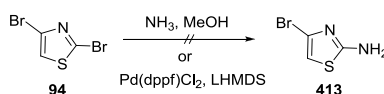
### 8.1 Initial Approaches to the Synthesis of Diarylaminothiazole 87

Immediately following the successful virtual screening, the synthesis of a further quantity of aminothiazole **87** (see Table 9) was required for biological testing. However, the divergent Suzuki coupling strategy used above for the synthesis of diarylthiazoles was not immediately applicable to this class of compound, as it had been reported that 2-halothiazoles are poor substrates for Pd-catalysed aminations with aniline nucleophiles (see Section 8.3 for further discussion).<sup>173</sup> Simple direct nucleophilic substitutions also do not work well for these substrates. It was proposed that the recently reported copper-catalysed arylation of 2-aminothiazoles<sup>174</sup> could be used in combination with a Suzuki coupling of 4-bromo-2-aminothiazole in a divergent coupling strategy that mirrors that proposed for the diarylthiazoles (Scheme 53).



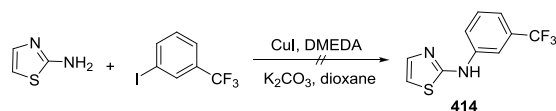
**Scheme 53** – Proposed synthesis of diarylaminothiazoles by a sequential coupling strategy

Synthesis of aminothiazole **413** has not been reported, and attempts to access this compound from 2,4-dibromothiazole were unsuccessful; direct amination with ammonia in a sealed tube gave very low conversion, as did Pd-catalysed coupling with LHMDS<sup>175</sup> (Scheme 54).



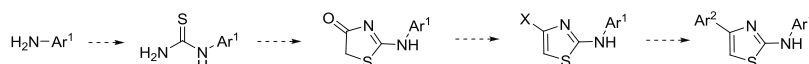
**Scheme 54** – Attempted synthesis of 4-bromo-2-aminothiazole, **413**

Prior to any further attempts at the synthesis of this bromide coupling precursor, the aminothiazole N-arylation step was tested using 2-aminothiazole and the trifluoromethyl iodobenzene necessary for the synthesis of VHR inhibitor **87** (see Table 9). Unfortunately, a complex mixture of products was repeatedly obtained using the standard literature conditions (Scheme 55),<sup>174</sup> and it was decided that the low yields and difficult purifications resulting from this chemistry were not appropriate for parallel synthesis of compound libraries.



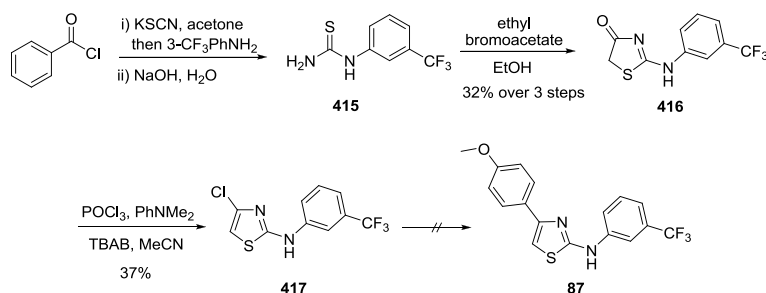
**Scheme 55** – Attempted copper-catalysed N-arylation of 2-aminothiazole

At this stage, in order to prepare target diarylaminothiazole **87**, a compromise strategy was devised, incorporating a final coupling step on a halo-aminothiazole synthesised *via* a conventional condensation/halogenation route (Scheme 56).



**Scheme 56** – Proposed synthesis of diarylaminothiazoles by a divergent coupling strategy

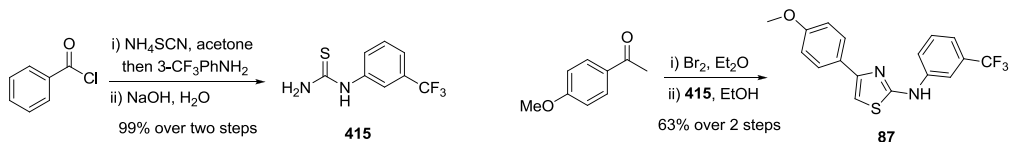
The synthesis of thiourea **415** was achieved by a reported two-step procedure involving formation of benzoyl thiocyanate, immediate reaction with the trifluoromethyl aniline, isolation of the benzoyl thiourea and then subsequent hydrolysis (Scheme 57).<sup>176</sup> The crude thiourea obtained was condensed with ethyl bromoacetate to give aminothiazolone **416** in moderate yield over the three steps. The subsequent chlorination was carried out using unusual conditions reported in the literature to give a low (but comparative) yield of 4-chloro-2-aminothiazole **417**.<sup>177</sup> Unfortunately, attempted Suzuki coupling under a variety of standard conditions with Pd(PPh<sub>3</sub>)<sub>4</sub> repeatedly gave low conversion, and it is likely that a more electron-rich catalyst would have proved more successful for the difficult oxidative addition into the very electron-rich heteroaryl chloride.



**Scheme 57** – Attempted synthesis of diarylaminothiazole **87** by Suzuki coupling

At this stage, attempts at developing novel coupling routes towards diarylaminothiazoles were postponed due to the immediate requirement for preparation of VHR inhibitor **87** for biological testing, but this Suzuki coupling approach was subsequently further investigated

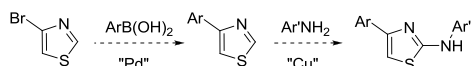
(see Section 8.4.3). Hantzsch synthesis of aminothiazole **87** was successfully carried out by condensation of thiourea **415** and the appropriate bromoketone in good overall yield (Scheme 58).



**Scheme 58** – Hantzsch synthesis of diarylaminothiazole **87**

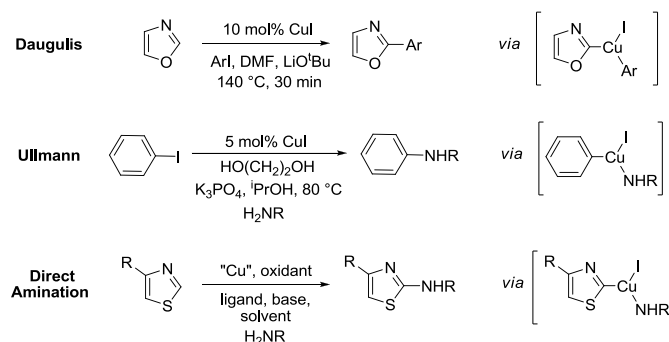
## 8.2 Oxidative C-H Amination of 4-Substituted Thiazoles

Prior to any further investigations into the Suzuki coupling of chlorothiazole **417**, a direct C-H amination of thiazole was reported by Mori using various amine nucleophiles under oxidative Cu catalysis, although with a fairly narrow substrate scope.<sup>178</sup> This suggested an alternative rapid and flexible route to diarylthiazoles by Suzuki coupling of commercially available 4-bromothiazole prior to direct amination at the 2-position (Scheme 59). These reactions could also potentially be performed sequentially in a one-pot process.



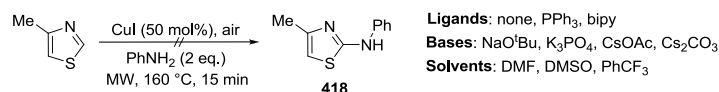
**Scheme 59** – Proposed synthesis of aminothiazoles by sequential Pd- and Cu-catalysis

A screen of ten solvents was performed using Mori's conditions to try to find an alternative to the microwave-inert xylene, in preparation for application to rapid library synthesis. However, this reaction proved highly sensitive to small variations in substrate and conditions, with only trace amounts of product obtained in all cases, and thus was not suitable to analogue synthesis. Instead, we sought to find new, more broadly applicable conditions for this transformation by analogy with existing Cu-catalysed reactions. In theory, the proposed reaction is a mechanistic combination of the direct arylation of acidic heterocyclic protons pioneered by Daugulis<sup>179</sup> (which is purported to proceed *via* copper-assisted deprotonation) and Ullmann coupling<sup>180</sup> (which aminates aryl-copper intermediates).



**Scheme 60** – Proposed synthesis of aminothiazoles by direct amination

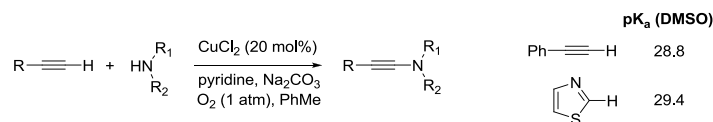
A screen of conditions common to these two coupling reactions was performed using 4-methylthiazole and aniline, with all combinations of selected ligands, bases and solvents (Scheme 61).



**Scheme 61** – Attempted direct amination of 4-methylthiazole

No definitively positive results were obtained by LCMS analysis, and a wider screen of conditions was explored that alternately varied the base, ligand, solvent, temperature and copper source from Daugulis' optimised conditions. As before, no successful conditions were observed, with widespread decomposition presumably resulting from oxidation of the aniline.

An even closer literature analogy was made to Stahl's recently-reported direct amidation of alkynes,<sup>181</sup> which similarly involves the desired copper-assisted deprotonation and oxidative amination of a relatively acidic position (Scheme 62). The similarity in  $pK_a$  between terminal alkyne protons (29)<sup>182</sup> and the acidic C-2 position of 5-membered azoles (25-29)<sup>183</sup> provides a firm mechanistic basis for the desired thiazole amination. Further support is given by recent development of the analogous direct thiolation of benzoxazole under CuI catalysis, which proceeds *via* a similar mechanism.<sup>184</sup> Two further screens of conditions were carried out to broadly cover and merge the reaction conditions used by Mori and Stahl, but as before only small amounts of the desired products were obtained.

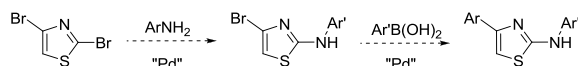


**Scheme 62** – Stahl’s direct amidation of terminal alkynes

At this stage, the lack of success achieved in the optimisation of a general oxidative Cu-catalysed approach led to reconsideration of the Pd-catalysed amination of 2,4-dibromothiazole.

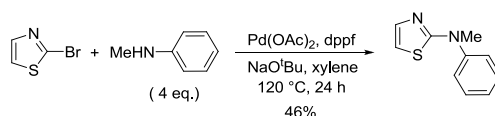
### 8.3 Regioselective Buchwald-Hartwig Amination of Dibromothiazole

As an alternative strategy, it was proposed that a regioselective Buchwald-Hartwig amination of 2,4-dibromothiazole could be followed by a Suzuki coupling at the 4-position to access diarylaminothiazoles in a rapid and divergent manner (Scheme 63).



**Scheme 63** – Proposed synthesis of aminothiazoles from 2,4-dibromothiazole by sequential Pd-catalysis

For this reaction pathway, an excess of amine cannot be used in the Buchwald-Hartwig coupling in order to prevent a second amination occurring. However, Hartwig has shown that the thiazole 2-position is a very difficult substrate for amination, with a low yield being obtained for the amination of 2-bromothiazole with a 4-fold excess of methylaniline under highly-optimised conditions that differed from the general conditions used for other substrates (Scheme 64).<sup>173</sup>



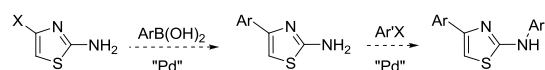
**Scheme 64** – Hartwig’s Pd-catalysed amination of 2-bromothiazole

It was hoped that the recent advances in phosphine ligand design, including the availability of the competing Buchwald ligands, would allow us to improve on Hartwig’s results and also to demonstrate the first regioselective amination of thiazoles. A 26-member ligand set was tested

with 2,4-dibromothiazole and *p*-anisidine (1 eq.) on small scale under high-temperature microwave conditions. Follow up screens using conventional heating on those reactions found to give traces of product by LCMS analysis gave very low conversion, as expected from Hartwig's result above. Following this initial failure of the more advanced ligands to provide any greater success in this reaction, the Pd-catalysed approach was not further investigated. At this stage, the difficulties encountered with the various thiazole amination reactions in the previous two sections prompted reconsideration of the aminothiazole arylation strategy found to give poor results using recently-reported Cu-catalysis (see Scheme 55).

#### 8.4 Consecutive Suzuki and Buchwald-Hartwig Coupling Approach

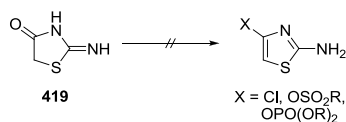
The latest generation of Buchwald's biarylphosphine catalysts have been shown to rapidly arylate hindered and poorly-nucleophilic amides with aryl chlorides under mild conditions,<sup>168</sup> and it was proposed that this reaction might be applicable to the analogous arylation of 2-aminothiazoles. Reported methods for Pd-catalysed aminothiazole arylation require the use of highly-activated halides<sup>185</sup> or strong bases incompatible with a range of functional groups.<sup>186</sup> The sequential coupling approach would therefore require an initial Suzuki reaction at the C4-position of a 4-halo-2-aminothiazole precursor (Scheme 65).



**Scheme 65** – Proposed synthesis of diarylaminothiazoles from functionalised 2-aminothiazoles by sequential Pd-catalysis

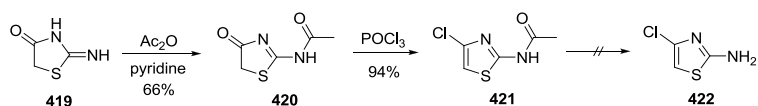
##### 8.4.1 Synthesis of Diarylaminothiazole Precursor 4-Halo-2-aminothiazole

The most direct method for the synthesis of 4-halo-2-aminothiazole was proposed to be the functional group interconversion of the carbonyl moiety of pseudothiohydantoin (**419**) (Scheme 66). Deprotonation and reaction with electrophiles was however found to occur preferentially on the 2-amino group. A reported literature preparation of 4-chloro-2-aminothiazole from pseudothiohydantoin (without yield or experimental) suggested simple treatment with POCl<sub>3</sub> would work,<sup>187</sup> but multiple attempts resulted in a complex mixture and very poor mass recovery.



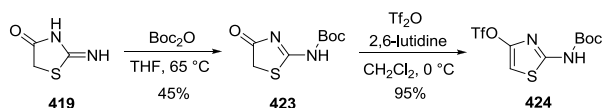
**Scheme 66** – Attempted activation of the 4-position of pseudothiohydantoin for cross-coupling

An alternative three-step route was then attempted, the first two steps having been previously reported (Scheme 67).<sup>188</sup> Pseudothiohydantoin was acetylated and then chlorinated in good overall yield and purity. However, deacetylation proved more difficult than anticipated as the acidic conditions commonly used for close analogues repeatedly resulted in comprehensive decomposition. Attempts under basic conditions or with amine nucleophiles (such as ammonia and hydrazine) gave very low conversion, and ultimately this route was not further pursued.



**Scheme 67** – Attempted synthesis of 4-chloro-2-aminothiazole (**422**)

As an alternative, *N*-Boc aminothiazolone **423** was prepared (Scheme 68). Although only a moderate yield was obtained using reported conditions,<sup>189</sup> logical adaptations such as addition of catalytic DMAP or switching to DMF solvent (pseudothiohydantoin is poorly soluble in THF) resulted in a mixture of products that proved difficult to separate. *N*-Boc aminothiazolone **423** did not prove stable to the POCl<sub>3</sub> chlorination conditions, so a sulfonation was used as a mild alternative. The nonaflate derivative was initially targeted due to its greater stability,<sup>190</sup> but the nonafllyl fluoride electrophile proved highly unreactive, a finding mirrored in an analogous literature sulfonation of a pyrazolidone, where the nonafllyl anhydride was used instead.<sup>191</sup> Triflate **424** was instead prepared according to a literature method in excellent yield, which dropped slightly on scale-up.



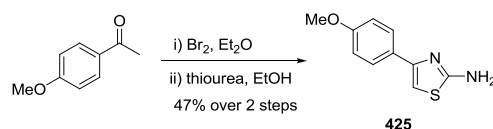
**Scheme 68** – Synthesis of *N*-protected triflate **424**

Removal of the Boc group using standard TFA conditions gave a clean reaction but poor yield of 30%. Optimisation of reagents and work-up procedures gave an maximum yield of 72% of

the crude 4-triflyl-2-aminothiazole, but it became clear that this compound suffered from poor stability (in a seemingly analogous fashion to the 4-chloro analogue that proved difficult to isolate) and it was therefore decided that the deprotected triflate did not represent a viable common intermediate for a divergent coupling strategy. Although deprotection following the coupling reaction was thought likely to result in improved yield and ease of synthesis, this alternative strategy somewhat compromised the initial ideal of a rapid, divergent approach.

#### 8.4.2 Buchwald-Hartwig Coupling of 4-Aryl-2-aminothiazoles

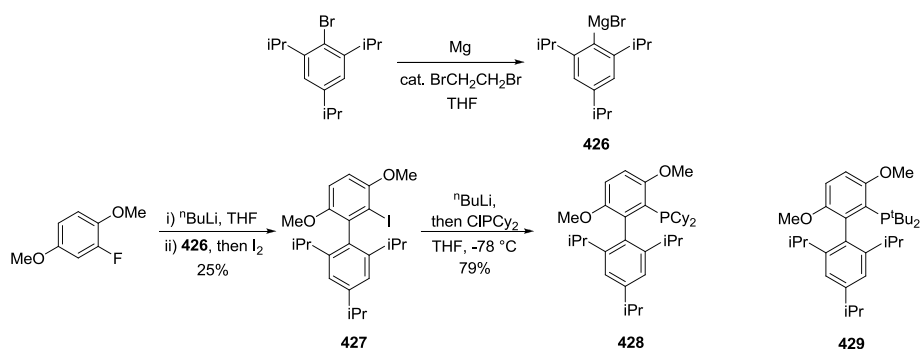
The key novel reaction of the proposed new strategy towards aminothiazoles was the N-(hetero)arylation of the free 2-amino group using Buchwald's conditions for Pd-catalysed arylation of amides.<sup>168</sup> This approach is valuable and highly relevant as a method for final-stage diversification from 4-substituted 2-aminothiazoles, which can be synthesised on large scale by conventional condensation chemistry. 4-Aryl-2-aminothiazole **425** was prepared by Hantzsch condensation from the acetophenone in moderate yield on large scale (Scheme 69). The attempted synthesis of the  $\alpha$ -halo-acetophenone by the Friedel-Crafts route previously successful for fluorobenzene derivatives gave a poor yield using the more reactive anisole.



**Scheme 69** –Synthesis of 4-aryl-2-aminothiazole **425**

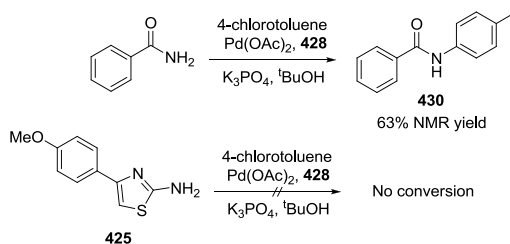
The key biarylphosphine ligand used for Buchwald's arylation of primary amides is <sup>t</sup>BuBrettPhos (**429**). Using the published route,<sup>192</sup> biaryl iodide precursor **427** was obtained on gram-scale in comparable yield by addition of hindered aryl Grignard **426** across an *in situ*-prepared benzyne intermediate (Scheme 70). Attempted reaction of iodide **427** with di-*tert*-butyl chlorophosphine under the reported conditions gave a very low conversion, and as an alternative the analogous dicyclohexylphosphine, BrettPhos (**428**), shown to be similarly competent in the amidation reactions, was prepared in good yield.





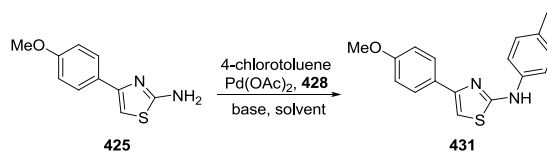
**Scheme 70** – Synthesis of Buchwald ligand BrettPhos, **428**

In the initial test reaction, a solution of Pd catalyst and ligand was pre-activated<sup>193</sup> and added to two reactions: amination of 4-chlorotoluene with benzamide and with 4-aryl aminothiazole **425** (Scheme 71). A good <sup>1</sup>H-NMR yield of tolylamide **430** was obtained, in line with Buchwald's results,<sup>168</sup> but no conversion of aminothiazole **425** was observed.



**Scheme 71** – Attempted Buchwald arylation of benzamide and aminothiazole **425**

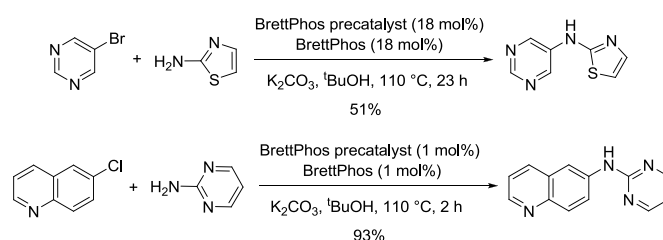
A screen of stronger bases was carried out, giving only moderate conversion even under harsh conditions (Table 29). With the proposed advantage of mild conditions and wide substrate scope now not applicable, no advantage could be foreseen in further optimisation of this methodology. Additionally, the low purity of these reactions proffered no practical advantage. Although N-arylation of aminothiazoles with aryl chlorides has yet to be demonstrated, it was felt that if successful this would only represent an incremental increase over the known methods.

**Table 29** – Attempted *N*-arylation of aminothiazole **425** using stronger bases

Entry	Base (eq.)	Solvent	Conditions	Conversion <sup>a</sup> (%)
1	K <sub>2</sub> CO <sub>3</sub> (2.4)	<sup>t</sup> BuOH	100 °C, 15 h	0
2	NaO <sup>t</sup> Bu (2.4)	dioxane	110 °C, 15 h	13
3	NaO <sup>t</sup> Bu (2.4)	PhMe	110 °C, 15 h	51
4	LHMDS (2.4)	THF	100 °C, 15 h	42

*a* – Conversion calculated by ratio of integrals in <sup>1</sup>H-NMR

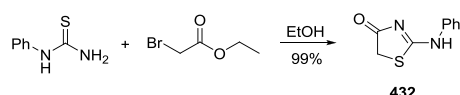
In an extensive study published immediately following these results, Buchwald also demonstrated that 2-aminothiazoles are abnormally poor nucleophiles for *N*-arylation reactions (Scheme 72).<sup>194</sup> In attempting to exemplify virtually every conceivable class of amine arylation reaction, with particular emphasis on the use of heterocycles, the sole use of 2-aminothiazole in coupling with a bromopyrimidine gave only a moderate yield, despite an extended reaction time and extremely high catalyst loading. Although this result attracted no special comment, comparison of the arylation of the similarly electron-deficient 2-aminopyrimidine suggests that the poor results found for 2-aminothiazoles may stem from an effect specific to this compound class, with unexpectedly strong catalyst chelation from the sulfur and exocyclic nitrogen perhaps the most likely possibility.

**Scheme 72** – Selected examples of amino-heterocycle arylation reported by Buchwald<sup>194</sup>

#### 8.4.3 Suzuki Coupling of 4-Triflyl-2-aminothiazoles

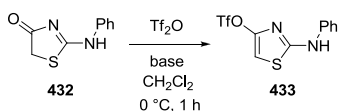
A Suzuki coupling approach to the divergent synthesis of 4-aryl-2-aminothiazoles from a 4-halo precursor, as briefly explored previously (Scheme 57), would still represent valuable

methodology for analogue synthesis. Practically, the most efficient route would be large-scale synthesis of a thiazolone using a classical condensation approach, followed by activation of the C-4 position towards Pd-insertion. This general strategy has been reported once in the literature,<sup>177</sup> using unusual optimised chlorination conditions to give generally poor to moderate yields of the 4-chloro-2-aminothiazole, although these were then used in nucleophilic substitution reactions rather than Pd coupling. For our initial investigations, the known *N*-phenyl aminothiazolone **432** was prepared in high yield (Scheme 73).



**Scheme 73** – Synthesis of *N*-phenyl-2-aminothiazolone, **432**

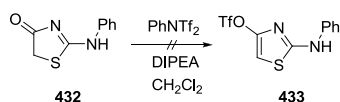
*N*-Phenyl aminothiazolone **432** was then subjected to the triflation conditions previously successful for *N*-Boc analogue **424** (Table 30, Entry 1). The initial attempt used a reduced number of equivalents of Tf<sub>2</sub>O compared to the *N*-Boc example due to concerns about possible N-triflation, and gave a 44% isolated yield of the product **433** without full conversion of the starting material. Increasing the equivalents of Tf<sub>2</sub>O gave only a small increase in the observed <sup>1</sup>H-NMR yield (Entries 2-3), and lowering the temperature showed no improvement (Entry 4). At this stage, the thiazolone starting material was further purified by recrystallisation as a precaution against any residual impurities not visible by NMR analysis. The conditions for Entry 3 were repeated, without any improvement in yield (Entry 5). Increasing the equivalents of Tf<sub>2</sub>O (Entry 6) decreased the yield, as did conducting the reaction at a higher temperature for less time (Entry 7). Changing the Tf<sub>2</sub>O addition protocol worked well when a 30 minute gap was introduced (Entry 8). Slow addition was less effective (Entry 9), but the small volumes being used limit any differences in addition speed. A further increase in yield was seen when switching to Et<sub>3</sub>N (Entry 10), and combining this base with the modified addition led to a <sup>1</sup>H-NMR yield of 72% (Entry 11). Alternative addition protocols did not improve this result (Entries 12-13). A scaled-up repeat of Entry 11, where the slow addition of the Tf<sub>2</sub>O was clearly more effective at keeping the concentration low, gave an isolated yield of 85%, double that of the initial attempt (Entry 14).

**Table 30** – Optimisation of triflation of 2-aminothiazolone **432**

Entry	Eq. Tf <sub>2</sub> O	Changes to procedure	Base (eq.)	NMR yield <sup>a</sup> (Isolated yield) / %
1	1.2	-	2,6-lutidine (2)	N.D. (44)
2	1.5	-	2,6-lutidine (3)	33
3	2.0	-	2,6-lutidine (3)	54
4	2.0	-78 °C, 1.5 h	2,6-lutidine (3)	38
5	2.0	-	2,6-lutidine (3)	48
6	3.0	-	2,6-lutidine (3)	41
7	3.0	0 °C to r.t., 15 min	2,6-lutidine (3)	40
8	2.5	1.5 eq. added, stirred 30 min, 1.0 eq. added	2,6-lutidine (3)	64
9	2.0	Slower addition	2,6-lutidine (3)	48
10	2.0	-	Et <sub>3</sub> N (3)	60
11	2.5	1.5 eq. added, stirred 30 min, 1.0 eq. added	Et <sub>3</sub> N (3)	72
12	2.0	1.0 eq. added, stirred 30 min, 1.0 eq. added	Et <sub>3</sub> N (3)	68
13	2.0	4 aliquots of 0.5 eq. added in 10 min intervals	Et <sub>3</sub> N (3)	63
14 <sup>b</sup>	2.0	1.5 eq. added, stirred 30 min, 0.5 eq. added	Et <sub>3</sub> N (3)	N.D. (85)

*a* – Yield determined by ratio of integrals in <sup>1</sup>H-NMR compared to internal standard (1,3,5-trimethoxybenzene). *b* – 10 mmol scale (all other reactions performed at 1 mmol scale)

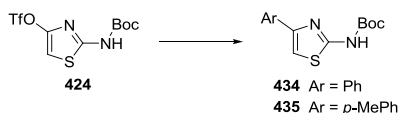
Literature precedent for the conversion of a pyrazolone to the corresponding pyrazole triflate suggested that using the more mild PhNTf<sub>2</sub> triflating agent might give better yields than Tf<sub>2</sub>O,<sup>195</sup> but this reagent gave no conversion with aminothiazolone **432** (Scheme 74).



**Scheme 74** – Attempted triflation of aminothiazolone **432** with PhNTf<sub>2</sub>

Following the successful synthesis of aminothiazole triflates **424** and **433**, the Suzuki coupling reactions were then investigated. *N*-Boc triflate **424** was chosen for the initial reactions due to its simpler synthesis and purification. The Suzuki coupling conditions first attempted were a range of common literature conditions, which uniformly gave fairly clean reactions but incomplete conversion by <sup>1</sup>H-NMR (Table 31, Entries 1-6). After switching to the *p*-tolyl boronic acid to aid crude NMR interpretation, microwave heating conditions were found to result in decomposition of the starting material (Entries 7-8).

**Table 31** – Optimisation of Suzuki coupling of triflate **424**

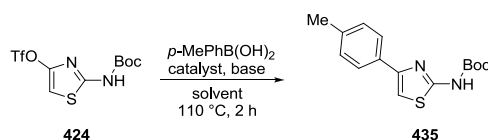


Entry	ArB(OH) <sub>2</sub> (eq.)	Catalyst (mol%)	Base (eq.)	Solvent	Conditions	Conversion <sup>a</sup> (%)
1	Ph (1.5)	Pd(PPh <sub>3</sub> ) <sub>4</sub> (2)	K <sub>2</sub> CO <sub>3</sub> (2)	PhMe	85 °C, 16 h	46
2	Ph (1.5)	Pd(PPh <sub>3</sub> ) <sub>4</sub> (2)	K <sub>2</sub> CO <sub>3</sub> (2)	DME/H <sub>2</sub> O (4:1)	85 °C, 16 h	65
3	Ph (1.5)	Pd(PPh <sub>3</sub> ) <sub>4</sub> (2)	KF (2)	DME/H <sub>2</sub> O (4:1)	85 °C, 16 h	50
4	Ph (1.5)	Pd(PPh <sub>3</sub> ) <sub>4</sub> (2)	LiOH (2)	DME/H <sub>2</sub> O (4:1)	85 °C, 16 h	83
5	Ph (1.5)	Pd(dppf)Cl <sub>2</sub> (2)	K <sub>3</sub> PO <sub>4</sub> (2)	dioxane	85 °C, 16 h	84
6	Ph (1.5)	Pd(dppf)Cl <sub>2</sub> (2)	K <sub>2</sub> CO <sub>3</sub> (2)	dioxane/H <sub>2</sub> O (4:1)	85 °C, 16 h	85
7	<i>p</i> -Tolyl (1.5)	Pd(dppf)Cl <sub>2</sub> (5)	K <sub>2</sub> CO <sub>3</sub> (3)	dioxane/H <sub>2</sub> O (4:1)	150 °C, 15 min	decomposition
8	<i>p</i> -Tolyl (1.5)	Pd(PPh <sub>3</sub> ) <sub>2</sub> Cl <sub>2</sub> (5)	K <sub>2</sub> CO <sub>3</sub> (3)	dioxane/H <sub>2</sub> O (4:1)	150 °C, 15 min	decomposition

<sup>a</sup> – Conversion determined by ratio of integrals in <sup>1</sup>H-NMR compared to internal standard (1,3,5-trimethoxybenzene)

In order to improve the conversion, a screen of more-active catalysts was carried out, using four different Buchwald biaryl ligands, a Nolan NHC complex<sup>196</sup> and an air-stable electron-rich catalyst reported by Amgen (PdCl<sub>2</sub>[P(<sup>t</sup>Bu)<sub>2</sub>(4-Me<sub>2</sub>NPh)]<sub>2</sub>)<sup>197</sup> (Table 32, Entries 1-6). All gave complete conversion, but the <sup>1</sup>H-NMR yield was fairly low in every case.

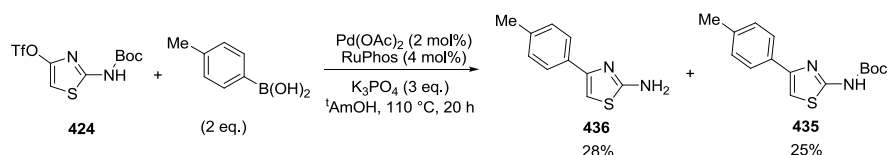
**Table 32** – Optimisation of Suzuki coupling of triflate **424**



Entry	Catalyst (mol%)	Base (3 eq.)	Solvent	NMR Yield <sup>a</sup> (%)
1	Pd(OAc) <sub>2</sub> (4), S-Phos (8)	K <sub>3</sub> PO <sub>4</sub>	<sup>t</sup> AmOH	21
2	Pd(OAc) <sub>2</sub> (4), RuPhos (8)	K <sub>3</sub> PO <sub>4</sub>	<sup>t</sup> AmOH	35
3	Pd(OAc) <sub>2</sub> (4), X-Phos (8)	K <sub>3</sub> PO <sub>4</sub>	<sup>t</sup> AmOH	23
4	Pd(OAc) <sub>2</sub> (4), (2-Ph)PhPCy <sub>2</sub> (8)	K <sub>3</sub> PO <sub>4</sub>	<sup>t</sup> AmOH	14
5	Pd(OAc) <sub>2</sub> (4), IMes (8)	Cs <sub>2</sub> CO <sub>3</sub>	dioxane	15
6	PdCl <sub>2</sub> [P( <sup>t</sup> Bu) <sub>2</sub> (4-Me <sub>2</sub> NPh)] <sub>2</sub> (4)	K <sub>2</sub> CO <sub>3</sub>	/H <sub>2</sub> O (10:1)	N.D.
7 <sup>b</sup>	Pd(OAc) <sub>2</sub> (4), RuPhos (8)	K <sub>3</sub> PO <sub>4</sub>	<sup>t</sup> AmOH	87 <sup>c</sup>

*a* – Yield determined by ratio of integrals in <sup>1</sup>H-NMR compared to internal standard (1,3,5-trimethoxybenzene). *b* – 20 h, 0.5 mmol scale. *c* – Deprotected 4-arylaminothiazole product obtained.

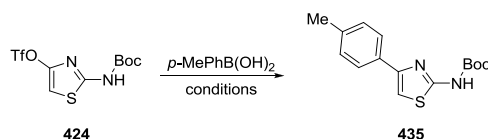
Repeating the best of these conditions on a larger scale gave a good yield of the coupled, but also deprotected, aminothiazole (Entry 7), which was encouraging given that the envisaged next step in this methodology would be this deprotection. However, all attempts to repeat this result were unsuccessful, with mixtures of protected and deprotected aminothiazoles being obtained in moderate yields. Two screens of conditions slightly varying the coupling conditions and the catalyst loadings gave similar results (example shown in Scheme 75).



**Scheme 75** – Attempted one-pot Suzuki coupling/deprotection of triflate **424**

It was hoped that milder conditions could be found that would give reproducible yields of the protected compound, and a screen around some of the more successful conditions from the first screen was carried out (Table 33). The best result (Entry 1) gave a clean, full conversion to a good <sup>1</sup>H-NMR yield of the coupled, protected aminothiazole **435** using Suzuki and Miyaura's originally-reported conditions.<sup>198</sup> The use of KBr to stabilise the Pd catalyst was not successful (Entry 2),<sup>199</sup> and alternative catalyst systems gave lower yields (Entry 3) or low conversion (Entry 4).

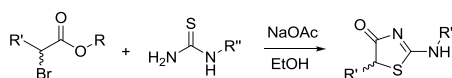
**Table 33** – Optimisation of Suzuki coupling of triflate **424**



Entry	Catalyst (mol%)	Base (eq.)	Solvent	Conditions	NMR Yield <sup>a</sup> / %
1	Pd(PPh <sub>3</sub> ) <sub>4</sub> (3)	K <sub>3</sub> PO <sub>4</sub> (1.5)	dioxane	85 °C, 15 h	79
2	Pd(PPh <sub>3</sub> ) <sub>4</sub> (3), KBr (1.5 eq.)	K <sub>3</sub> PO <sub>4</sub> (1.5)	dioxane	85 °C, 15 h	36
3	Pd(dppf)Cl <sub>2</sub> (3)	K <sub>3</sub> PO <sub>4</sub> (1.5)	THF	60 °C, 15 h	58
4	Pd <sub>2</sub> (dba) <sub>3</sub> (3), <sup>t</sup> Bu <sub>3</sub> PHBF <sub>4</sub> (6)	KF (3.3)	THF	60 °C, 15 h	N.D.

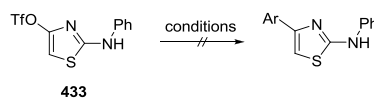
*a* – Yield determined by ratio of integrals in <sup>1</sup>H-NMR compared to internal standard (1,3,5-trimethoxybenzene)

With optimised conditions for coupling of *N*-Boc triflate **424**, a range of aminothiazolones were synthesised with the aim of exploring the scope of the substituents that could be used (Table 34). In addition to *N*-phenyl thiazolone **432** prepared previously, three 5-substituted *N*-phenyl thiazolones were also prepared (**437–440**). The methyl and fluoro analogues (Entries 2 and 4) would ultimately generate 2-aminothiazole analogues with small substituents at the C5-position to block *in vivo* metabolism, as discussed in Section 7.3.1. The use of ethyl chloroacetate was unsuccessful for the fluoro compound, so the corresponding bromide was used instead. Synthesis of a 2-allyl aminothiazolone was also successful (Entry 5).

**Table 34** – Synthesis of 2-aminothiazolones

Entry	Cmpd No.	R'	R''	Yield (%)
1	<b>432</b>	H	Ph	99
2	<b>437</b>	Me	Ph	88
3	<b>438</b>	Ph	Ph	85
4	<b>439</b>	F	Ph	52
5	<b>440</b>	H	Allyl	60

Suzuki coupling of *N*-phenyl triflate **433** was initially attempted using the Pd(OAc)<sub>2</sub>/RuPhos system since there was no longer an issue of Boc deprotection, but triflate hydrolysis was the major reaction in the <sup>t</sup>AmOH solvent used (Scheme 76). A small screen of electron-rich catalysts under anhydrous conditions (dioxane) resulted in a complex mixture, again with some hydrolysis observed. The conditions successful for the *N*-Boc triflate **424** resulted in low conversion. The rate of reaction was increased substantially using CsOAc,<sup>200</sup> but the major product was again from triflate hydrolysis. A screen of very mild conditions was carried out, using common catalysts and Fu's Pd(OAc)<sub>2</sub>/PCy<sub>3</sub> system<sup>162</sup> in THF at r.t. and 60 °C. Low conversions were obtained for the room temperature reactions, and again mostly hydrolysis was observed at 60 °C, confirmed by repeat reactions. No further optimisation was attempted, and it is likely that for the *N*-phenyl series the triflate is too unstable, suggesting the use of a halide or perhaps a nonaflate alternative.

**Scheme 76** – Attempted Suzuki coupling of triflate **433**

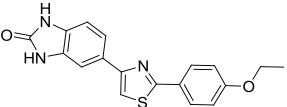
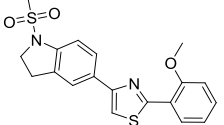
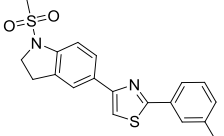
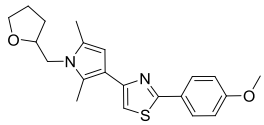
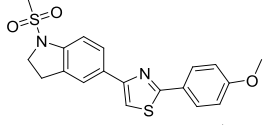
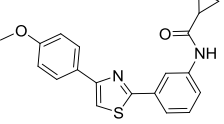
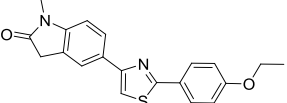
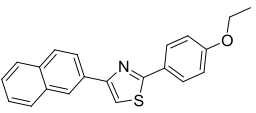
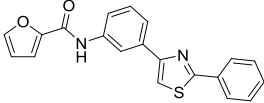
To summarise, attempted development of novel methodology towards the divergent synthesis of aminothiazoles proved ultimately unsuccessful. However, simple conditions were found for the synthesis and Suzuki coupling of a highly electron-rich aminothiazole C4-triflate.



## 9 Reassessment of Assay Results

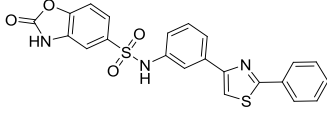
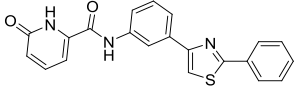
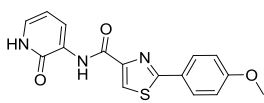
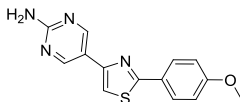
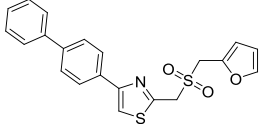
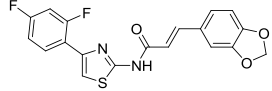
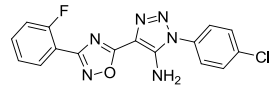
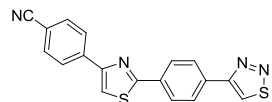
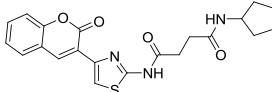
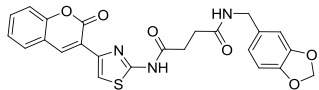
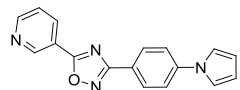
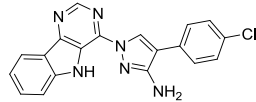
Collaboration with Imperial's Drug Discovery Centre (DDC) led to the biochemical assays being re-established at this late stage in the DDC labs to provide continuity following completion of this project and greater assay throughput. The resulting assay optimisation by DDC co-workers found a high detergent dependence for many of the novel inhibitors reported above, with a corresponding drop in potency in a detergent-controlled assay (Table 35).

**Table 35** – Comparison of cdc25-active virtual screening hits: detergent effect

Cmpd No.	Cmpd Name	Structure	IC <sub>50</sub> (μM) - no detergent		IC <sub>50</sub> (μM) - with detergent	
			Cdc25A	VHR	Cdc25A	VHR
76	T5896241		2.36	1.92	23.4	20.0
77	T5959818		4.02	2.68	41.7	39.8
78	T5982914		5.62	8.04	31.6	39.8
79	T5765678		6.36	8.29	30.9	33.1
80	T5846763		6.49	8.10	42.7	45.7
81	T5705971		10.2	8.89	> 100	> 100
82	T5871826		9.54	10.6	33.9	64.6
83	T5308252		13.0	4.44	30.2	60.3
84	C7991374		17.8	26.1	> 100	> 100

Testing of a further selection of active compounds gave more mixed results, with many of the more polar compounds retaining their original potency (Table 36).

**Table 36** – Selected active detergent-insensitive inhibitors

Cmpd No.	Cmpd Name	Structure	IC <sub>50</sub> (μM) - no detergent		IC <sub>50</sub> (μM) - with detergent			
			Cdc25A	VHR	Cdc25A	Cdc25B	Cdc25C	VHR
201	CRT-197		3.21	11.7	2.14	3.55	44.7	34.7
238	CRT-284		1.17	2.60	6.92	4.17	8.51	>100
157	CRT-129		18.1	5.29	17.4	6.76	N.D.	> 100
118	CRT-59		16.7	>50	25.1	19.5	>100	>100
368	KM-03222		4.00	2.47	2.75	1.70	9.55	25.7
338	C728-2381		9.5	14.1	7.41	2.69	11.0	66.1
356	CD E595-0205		7.8	18.1	8.71	5.62	4.47	21.9
359	SP-00519		6.3	3.3	12.3	3.02	8.91	> 100
345	C741-1786		7.9	9.1	12.3	5.89	9.33	25.1
344	C742-6778		5.3	2.07	20.0	0.89	8.32	17.0
353	C888-5549		12.2	9.4	24.0	5.37	4.79	95.5
358	KO 5F-909		14.9	36.2	27.5	6.46	5.50	44.7

This detergent-dependency of some of these inhibitors is a result of compound aggregation under the assay conditions. The phenomenon of aggregation has only been relatively recently investigated, and displays many counter-intuitive properties.<sup>201</sup> There is a specific, reproducible and reversible Critical Aggregation Concentration (CAC) above which large particles suddenly form, often in the mid-micromolar range. These particles strongly bind the enzymes to their surface, reducing the solution concentration and hence enzyme activity to near zero. A complicating factor for identifying aggregation behaviour is that this CAC results in a characteristically steep hill-slope on an IC<sub>50</sub> curve; the resulting curve looks very similar to that seen under optimal conditions for non-aggregation inhibitors. It has also been reported that the aggregation effect can be optimised by conventional medicinal chemistry approaches, displaying clear, interpretable SAR within a series.<sup>202</sup>

The original non-detergent assay conditions have been widely used in literature studies of cdc25 inhibitors, and the IC<sub>50</sub> values for multiple reported inhibitors were successfully repeated over the course of this project. Despite these misleading results, the use of detergent controls in enzyme assays was known at this early stage to be important for the confirmation of the expected mechanism of inhibition. However, these experiments were de-prioritised following the initial cell assay results which demonstrated inhibition of proliferation at similar IC<sub>50</sub> values to the *in vitro* assays, and the subsequent confirmation of cdc25 as the likely target protein. These results cannot be caused by aggregation, which would not occur in the highly-concentrated intracellular environment, and as such this was taken as fairly conclusive evidence that the discovered class of inhibitors worked by a standard stoichiometric binding mode of inhibition. Upon the realisation of the detergent dependency, the obtained cell results and their interpretation must be called into question, and further studies are underway. The possibility of cell inhibition by an alternative pathway does provide an explanation to the incongruities in the original cell data observed at the time, namely why the more potent *in vitro* inhibitors were not cell active, and why the anti-proliferation activity did not correlate well with the flow cytometry data.

There are several key conclusions from analysis of the new assay data in Tables 35 and 36:

- Whilst the compounds identified in the virtual screen are only weak cdc25 and VHR inhibitors, the subsequent synthesis and screening efforts have found significantly-improved hits.

- The cell-active furanamide **84**, the compound around which much of the parallel synthesis and subsequent target-oriented synthesis is based, does not inhibit cdc25 or VHR to any significant extent below 100  $\mu$ M.
- Of the compounds in Table 36 found to be detergent-insensitive inhibitors for cdc25, the majority show greatly reduced VHR inhibition, and no VHR-specific compounds have so far been identified under the new assay conditions. There are now a wide range of compounds exhibiting moderate to good selectivity for cdc25 over VHR, and these results suggest the inhibitory effect of aggregation is proportionally much greater for VHR.
- The majority of the most potent compounds appear to be detergent-insensitive, with the converse observation that many compounds thought to be moderate to low potency inhibitors have now been excluded. This has the overall effect of dramatically sharpening the SAR across the various compound series, making future interpretation for lead optimisation much simpler.
- Due to the inclusion of cdc25B and cdc25C in the re-assaying of compounds in Table 36, it is now clear that the original assumption from the virtual screening (and the majority of the reported literature) that inhibitors would likely show low selectivity is incorrect. Various compounds actually show moderate to high selectivity for cdc25B (and often C) against cdc25A; for example, bis-amide **344** is the first nM-potency hit identified, with 10-fold selectivity over cdc25C and >20-fold over cdc25A and VHR. One conclusion from this additional data is that missed active compounds are quite probable, and all compounds should be re-screened against cdc25B and C.
- A higher proportion of non-diarylthiazole analogues proved to be detergent-independent, perhaps suggesting a particular aggregation problem with the core substructures identified in the virtual screen.

Further testing is currently ongoing by DDC co-workers to complete the re-testing of the various compound sets against all the required phosphatases, and also to investigate the anti-proliferative activity against various cell lines in the context of the new IC<sub>50</sub> values. Analysis of the kinetics of inhibitor binding for selected compounds is also underway.

## 10 Generation of Cdc25 Active Site Mutants

Despite the lack of a reliable crystal structure for *cdc25A*, or any ligand binding information, the homology with the *cdc25B* active site allows prediction of residues that might be suitable for the point mutation necessary for the bump-hole approach to substrate determination. Various reports have docked published inhibitors into the active site, and although there are often differences in conformation and orientation, there is a general consensus regarding which residues are important for the binding interactions (Figure 30).<sup>26,31,42,99</sup> The generation of a panel of active site point mutants would also provide immediate information as to the likely binding site for novel inhibitors, prior to any attempted steric complementation.

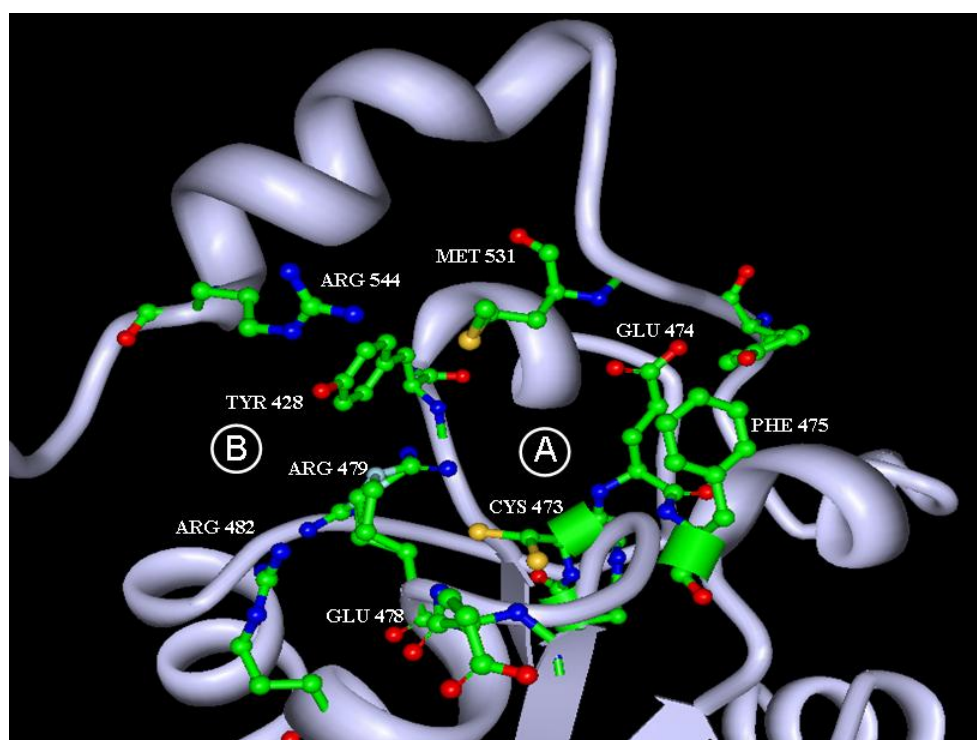


**Figure 30** – Selected active site amino acids of *cdc25B*

The additional binding pocket created by the C-terminal helix (the space denoted as **B** in Figure 30) has been proposed to be similarly important for inhibitor binding to the active site loop, and contains two crucial arginine residues, R482 and R544. The latter arginine is located at the C-terminal end of this extra helix and thus is not found in this position in the crystal structure of *cdc25A*. These arginine residues are considered by some reports to be ideally placed to anchor the carbonyl groups of quinone derivatives *via* H-bonds (Figure 31i),<sup>26</sup> although in other cases it is predicted that small aromatic systems stack between the



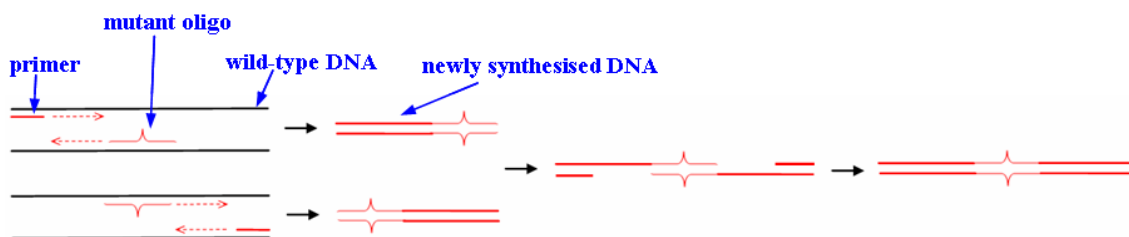


**Figure 32** – Schematic of PCR technique used to generate mutants

For *cdc25A*, the F432A, R439A and R439D mutants were synthesised by this method and ligated into the pET21a vector. The first two correspond to steric alterations of the active site by changing to a smaller alanine residue, whereas the latter change of an arginine residue for an aspartic acid can be considered a reversal of the electrostatic properties. This allows two different methods of inhibitor-mutant complementation to be pursued.

The strategy for further experiments to find a mutant-selective inhibitor will likely be determined by the success in ligand-binding experiments following the successful crystallisation of *cdc25B* and the ongoing assay results which have started to uncover isoform-selective inhibitors (see Section 9), although the selectivity achievable with a bump-hole approach is likely to be much greater.

## 11 Summary and Future Work

The initial aims of this project encompassed a range of challenging areas regarding the discovery of *cdc25* inhibitors and the elucidation of novel structural information. The early research focussed on analogues of the structurally complex literature inhibitor dysidiolide, specifically attempting at this stage to optimise the butenolide phosphate mimic. However, these analogues proved difficult to prepare and purify, and the initial *cdc25* phosphatase assays did not uncover any promising novel inhibitors. A further series of literature analogues were subsequently prepared based on the large class of literature quinonoid *cdc25* inhibitors, with a strategy designed to mimic the reported non-covalent binding interactions of the quinone carbonyl groups whilst removing the oxidative and electrophilic properties. This approach was also unsuccessful, emphasising the likely dominant influence of the chemical modification of the *cdc25* active-site cysteine on the observed inhibitor potency.

Attempted structural studies of the *cdc25* catalytic domains began with the successful optimisation of buffer conditions to give a thermally stable sample with the strongest possible NMR signal. However, preliminary structural studies showed a high degree of conformational flexibility, suggesting future work in this area may require selective isotopic labelling techniques to further understand the solution dynamics of this partially-disordered enzyme. Similarly, although extensive screening of crystallisation conditions did not prove successful in this project, ongoing work by co-workers is focussed on the expression and crystallisation of specially-designed truncated forms of *cdc25B* with greater stability that might lead to the first inhibitor-bound crystal structure for this phosphatase class. Ultimately, isoform-selective inhibitors derived from either medicinal chemistry or protein-ligand engineering would allow biochemistry collaborators to investigate the precise cellular roles of the *cdc25* isoforms.

A ligand-based virtual screening approach was successful in finding diarylthiazoles as novel, potent and drug-like inhibitors of *cdc25* and the related phosphatase VHR, although it was later discovered that a substantial component of the potency of these compounds derived from detergent-sensitive aggregation. However, parallel synthesis of a wide range of diarylthiazole analogues, and subsequent substructure-based screening of commercial compounds has identified a range of extremely promising, detergent-insensitive novel inhibitors. Many of these compounds have affinities and physical properties that classify them as excellent leads



for further development, and a medicinal chemistry lead optimisation programme will hopefully result in potent, reversible and cell-active cdc25 inhibitors for *in vivo* anti-cancer studies. Support from a range of biochemical assays and structural studies has been established in this project, and should increase the potential for rapid optimisation of the chosen inhibitor class. The selection of a lead structure will depend on the results of ongoing phosphatase and cell proliferation assays.

Various approaches to C-N bond formation for the rapid and divergent synthesis of 2-aminothiazoles proved unsuccessful, although the Suzuki coupling of a highly electron-rich aminothiazole C4-triflate was optimised. Further work in this area is likely to re-examine the recently-developed oxidative C-H amination reaction, as further publications in this emerging area are clarifying important mechanistic aspects and slowly expanding the substrate scope. Any further attempts to achieve the N-arylation of 2-aminothiazoles by Pd-catalysis will likely need an alternative strategy to prevent the catalyst deactivation that has been proposed to impede this reaction.

## 12 Experimental

**General methods:** All reactions were carried out under an argon atmosphere at r.t. using oven-dried glassware, unless otherwise specified.

**Solvents:** Petrol refers to the fraction of light petroleum-ether boiling between 40-60 °C. THF, PhMe, CH<sub>2</sub>Cl<sub>2</sub>, MeOH and Et<sub>2</sub>O were purified by Innovative Technology Inc. PureSolv™ Solvent Purification System. Other solvents were used as purchased from Sigma-Aldrich or BDH, with DME, EtOH, MeCN, dioxane and DMF obtained in Sure-Seal™ bottles.

**Reagents:** Chemicals were purchased from Acros Organics, Aldrich Chemical Co., Alfa Aesar, Apollo Scientific, Avocado Chemical Co., Fisher Scientific, Fluka, Fluorochem, Lancaster Synthesis, Maybridge and Sigma Chemical Co. and handled in accordance with COSHH regulations. <sup>n</sup>BuLi was titrated against diphenylacetic acid.

**Chromatography:** Flash chromatography was performed on silica gel (Merck Kieselgel 60 F<sub>254</sub> 230-400 mesh). TLC was performed on glass-backed plates pre-coated with silica (0.2 mm, 60 F<sub>254</sub>), which were developed using standard visualising agents: UV fluorescence (254 and 366 nm) and KMnO<sub>4</sub> with appropriate heating.

**<sup>1</sup>H-NMR spectroscopy:** These were recorded on Bruker AV-400 instruments at 400 MHz; chemical shifts ( $\delta_{\text{H}}$ ) are quoted in ppm (to the nearest 0.01 ppm) downfield from TMS by referencing to the appropriate residual solvent peak (CHCl<sub>3</sub>,  $\delta$  = 7.24 ppm, DMSO-d<sub>5</sub>,  $\delta$  = 2.50 ppm, CD<sub>3</sub>OD,  $\delta$  = 3.31 ppm), with coupling constants ( $J$ ) reported to the nearest 0.1 Hz.

**<sup>13</sup>C-NMR spectroscopy:** These were recorded on Bruker AV-400 instruments at 101 MHz; chemical shifts ( $\delta_{\text{C}}$ ) are quoted in ppm (to the nearest 0.1 ppm) downfield from TMS by referencing to the appropriate solvent peak (CDCl<sub>3</sub>,  $\delta$  = 77.0 ppm, DMSO-d<sub>6</sub>,  $\delta$  = 39.4 ppm, CD<sub>3</sub>OD,  $\delta$  = 49.2 ppm).

**<sup>31</sup>P-NMR spectroscopy:** These were recorded on Bruker AV-400 instruments at 162 MHz; chemical shifts ( $\delta_{\text{P}}$ ) are quoted in ppm (to the nearest 0.01 ppm) downfield from 85% H<sub>3</sub>PO<sub>4</sub>.

**<sup>19</sup>F-NMR spectroscopy:** These were recorded on Bruker AV-400 instruments at 376 MHz; chemical shifts ( $\delta_{\text{F}}$ ) are quoted in ppm (to the nearest 0.01 ppm) downfield from CFC<sub>3</sub>.

**MS:** These were recorded on either VG Platform II or VG AutoSpec spectrometers, with only selected major peaks being reported, with intensities quoted as percentages of the base peak.

**IR spectroscopy:** These were recorded as thin films on a Perkin Elmer Spectrum 100 FT-IR Spectrometer. Only selected absorbances ( $\nu_{\max}$ ) are reported, to the nearest  $1\text{ cm}^{-1}$ .

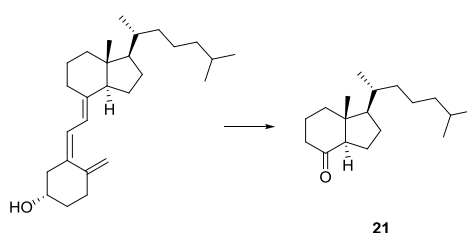
**Melting Points:** Melting points were determined on a Reichert microscope melting point apparatus.

**Nomenclature:** Compounds were named using IUPAC nomenclature.

**Compounds prepared by parallel synthesis and HPLC purification:**

All parallel microwave reactions were performed using a Biotage Initiator Sixty microwave. All compounds were purified by mass-directed preparative HPLC, with the MS of the isolated product in every case giving a strong peak for the correct molecular ion. Preparative HPLC-MS was performed using one of two separate Waters systems and a  $50 \times 19\text{ mm}$  C18 reverse-phase column from either SunFire or XBridge. In each case the injection volume was  $500\ \mu\text{L}$  and the flow rate was  $25\text{ mL/min}$ . The mobile phases of water and methanol contained either 0.1% formic acid (acidic conditions) or 0.03% ammonium hydroxide (basic conditions). For the acidic conditions, the elution gradient was water/methanol (75:25  $\rightarrow$  15:85), total run time 5.8 min. For the basic conditions, the elution gradient was water/methanol (85:15  $\rightarrow$  15:85), total run time 7 min.

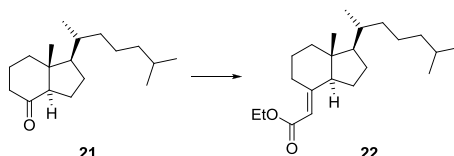
**(1R,3aR,7aR)-1-((R)-1,5-Dimethyl-hexyl)-7a-methyl-octahydro-inden-4-one, 21** <sup>203</sup>



$\text{O}_2$  was bubbled through a stirred solution of vitamin  $\text{D}_3$  (5.00 g, 13.0 mmol) in MeOH (150 mL) at  $-78\text{ }^\circ\text{C}$  for 10 min.  $\text{O}_3$  was then bubbled through the solution until a blue colour was observed, and for a further 15 min (1.5 h in total), before  $\text{O}_2$  was bubbled through for 10 min to give a colourless solution. Thiourea (6.93 g, 91.2 mmol) was added and the solution stirred at  $-78\text{ }^\circ\text{C}$  for 1 h, followed by 17 h at r.t. The solvent was removed *in vacuo* and the residue partitioned between  $\text{H}_2\text{O}$  (50 mL) and pentane (50 mL). The aqueous layer was extracted with pentane ( $3 \times 30\text{ mL}$ ) and the combined organic layers were dried ( $\text{MgSO}_4$ ) and the solvent removed *in vacuo*. Column chromatography eluting with  $\text{Et}_2\text{O}$ /petrol (0:1  $\rightarrow$  1:3) afforded the

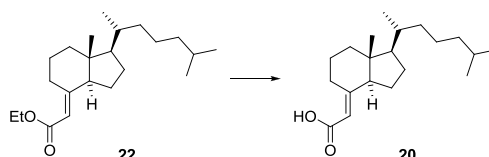
title compound as a colourless oil (3.37 g, 98%),  $R_f$  0.45 (Et<sub>2</sub>O/petrol 1:19);  $\delta_H$  (400 MHz, CDCl<sub>3</sub>) (identifiable peaks) 2.44 (1H, dd,  $J$  11.7, 7.5, COCH), 0.94 (3H, d,  $J$  6.2, CH<sub>3</sub>), 0.86 (3H, d,  $J$  6.5, CH<sub>3</sub>), 0.85 (3H, d,  $J$  6.6, CH<sub>3</sub>), 0.63 (3H, s, CH<sub>3</sub>);  $m/z$  (CI) 282 (MNH<sub>4</sub><sup>+</sup>, 100%), 265 (MH<sup>+</sup>, 12). Data is in agreement with the literature.<sup>203</sup>

**[(1R,3aS,7aR)-1-((R)-1,5-Dimethyl-hexyl)-7a-methyl-octahydro-inden-(4E)-ylidene]-acetic acid ethyl ester, **22****<sup>204</sup>



Triethyl phosphonoacetate (12.6 mL, 63.8 mmol) was added dropwise to a slurry of NaH (2.23 g, 60% dispersion in mineral oil, 55.8 mmol) in THF (35 mL) at 0 °C. The mixture was stirred at r.t. for 1 h to give a colourless solution. A solution of ketone **21** (2.09 g, 7.89 mmol) in THF (5 mL) was added dropwise at 0 °C and the reaction mixture stirred at r.t. for 20 h. The resulting yellow solution was poured into sat. aq. NH<sub>4</sub>Cl and extracted with Et<sub>2</sub>O (3 × 60 mL). The combined organic layers were dried (MgSO<sub>4</sub>) and the solvent removed *in vacuo*. Column chromatography eluting with Et<sub>2</sub>O/petrol (0:1 → 1:9) afforded the title compound as a colourless oil (2.65 g, 99%),  $R_f$  0.80 (Et<sub>2</sub>O/petrol 1:3);  $\nu_{max}$  (CDCl<sub>3</sub>)/cm<sup>-1</sup> 1712, 1644;  $\delta_H$  (400 MHz, CDCl<sub>3</sub>) (identifiable peaks) 5.45 (1H, s, C=CH), 4.19-4.10 (2H, m, OCH<sub>2</sub>), 3.90-3.81 (1H, m, C=CCH), 0.92 (3H, d,  $J$  6.1, CH<sub>3</sub>), 0.87 (3H, d,  $J$  6.6, CH<sub>3</sub>), 0.86 (3H, d,  $J$  6.7, CH<sub>3</sub>), 0.58 (3H, s, CH<sub>3</sub>);  $\delta_C$  (101 MHz, CDCl<sub>3</sub>) 167.0, 163.5, 111.9, 59.5, 56.9, 56.8, 47.1, 40.2, 39.5, 36.1, 36.0, 29.7, 28.0, 27.4, 23.8, 22.8, 22.6, 22.2, 18.8, 15.3, 14.3, 12.1;  $m/z$  (CI) 352 (MNH<sub>4</sub><sup>+</sup>, 100%), 335 (MH<sup>+</sup>, 86), 289 (13), 221 (12). Found: MH<sup>+</sup>, 335.2948. C<sub>22</sub>H<sub>39</sub>O<sub>2</sub> requires MH<sup>+</sup>, 335.2950. Data is in agreement with the literature.<sup>204</sup>

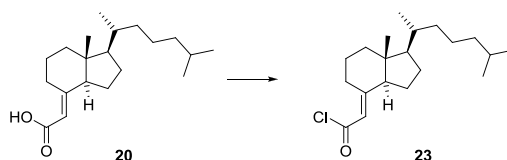
**[(1R,3aS,7aR)-1-((R)-1,5-Dimethyl-hexyl)-7a-methyl-octahydro-inden-(4E)-ylidene]-acetic acid, **20****<sup>91</sup>



A solution of ester **22** (519 mg, 1.55 mmol) and LiOH.H<sub>2</sub>O (652 mg, 15.5 mmol) in THF/MeOH/H<sub>2</sub>O (3:1:1) (10 mL) was stirred at reflux for 4.5 h. The reaction mixture was then added to aq. NaHCO<sub>3</sub> and extracted with petrol (3 × 20 mL). The combined organic

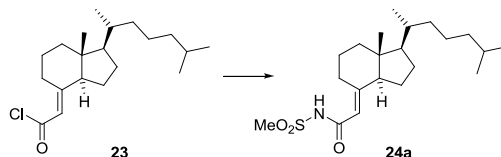
layers were washed with brine, and the combined aqueous layers acidified with 1 M HCl and extracted with Et<sub>2</sub>O (3 × 30 mL). The combined organic layers were dried (MgSO<sub>4</sub>) and the solvent removed *in vacuo* to afford the title compound as a white solid (456 mg, 97%), mp 117-119 °C; R<sub>f</sub> 0.26 (Et<sub>2</sub>O/petrol 1:3); [α]<sub>D</sub><sup>20</sup> +129.3 (c. 3.00 in CH<sub>2</sub>Cl<sub>2</sub>); ν<sub>max</sub> (CDCl<sub>3</sub>)/cm<sup>-1</sup> 3431, 1687, 1638; δ<sub>H</sub> (400 MHz, CDCl<sub>3</sub>) (identifiable peaks) 5.49 (1H, s, C=CH), 3.90-3.80 (1H, m, C=CCH), 2.13 (1H, t, *J* 9.1, C=CCH<sub>2</sub>), 2.02 (1H, d, *J* 12.6, C=CCH<sub>2</sub>), 0.93 (3H, d, *J* 5.8, CH<sub>3</sub>), 0.87 (3H, d, *J* 6.6, CH<sub>3</sub>), 0.86 (3H, d, *J* 6.5, CH<sub>3</sub>), 0.58 (3H, s, CH<sub>3</sub>); *m/z* (CI) 324 (MNH<sub>4</sub><sup>+</sup>, 22%), 263 (18), 120 (57), 61 (100). Found: MNH<sub>4</sub><sup>+</sup>, 324.2905. C<sub>20</sub>H<sub>38</sub>NO<sub>2</sub> requires MNH<sub>4</sub><sup>+</sup>, 324.2903. Data is in agreement with the literature.<sup>91</sup>

**[(1R,3aS,7aR)-1-((R)-1,5-Dimethyl-hexyl)-7a-methyl-octahydro-inden-(4E)-ylidene]-acetyl chloride, **23****



Oxalyl chloride (65 μL, 0.75 mmol) was added dropwise to a stirred solution of carboxylic acid **20** (207 mg, 0.68 mmol) in CH<sub>2</sub>Cl<sub>2</sub> (5 mL) at 0 °C. Following addition of DMF (1 drop), the reaction mixture was stirred at 0 °C for 10 min and then at r.t. for 2.5 h. The solvent and excess oxalyl chloride were removed *in vacuo* to give the title compound as a yellow solid, which was used without purification in the subsequent reactions.

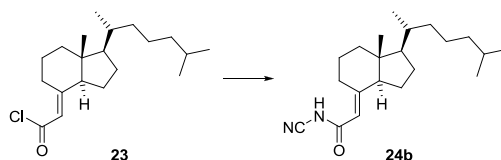
***N*-[2-[(1R,3aS,7aR)-1-((R)-1,5-Dimethyl-hexyl)-7a-methyl-octahydro-inden-(4E)-ylidene]-acetyl]-methanesulfonamide, **24a****



A solution of acid chloride **23** (110 mg, 0.34 mmol) in CH<sub>2</sub>Cl<sub>2</sub> (2 mL) was added dropwise to a solution of MeSO<sub>2</sub>NH<sub>2</sub> (162 mg, 1.70 mmol), DMAP (4 mg, 0.03 mmol) and Et<sub>3</sub>N (60 μL, 0.44 mmol) in CH<sub>2</sub>Cl<sub>2</sub> (1 mL) to give an orange solution. The reaction mixture was stirred at r.t. for 18 h before being poured into aq. NH<sub>4</sub>Cl and extracted with Et<sub>2</sub>O (3 × 10 mL). The combined organic layers were dried (MgSO<sub>4</sub>) and the solvent removed *in vacuo*. Column chromatography eluting with Et<sub>2</sub>O/petrol (1:3 → 1:0) afforded the title compound as a white

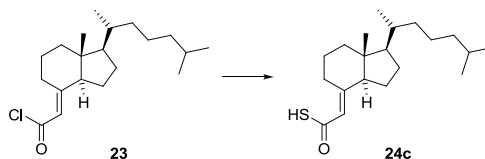
solid (95 mg, 73% over 2 steps), mp 125-128 °C;  $R_f$  0.22 (Et<sub>2</sub>O/petrol 1:1);  $[\alpha]_D^{20} +65.5$  (c. 3.85 in CH<sub>2</sub>Cl<sub>2</sub>);  $\nu_{\max}$  (CHCl<sub>3</sub>)/cm<sup>-1</sup> 3183, 1667, 1635, 1335, 1131;  $\delta_H$  (400 MHz, CDCl<sub>3</sub>) (identifiable peaks) 8.34 (1H, s, NH), 5.38 (1H, s, C=CH), 3.92-3.84 (1H, m, C=CCH), 3.33 (3H, s, SO<sub>2</sub>CH<sub>3</sub>), 2.13 (1H, t,  $J$  9.0, C=CCH<sub>2</sub>), 2.02 (1H, d,  $J$  12.7, C=CCH<sub>2</sub>), 0.92 (3H, d,  $J$  5.7, CH<sub>3</sub>), 0.86 (3H, d,  $J$  6.7, CH<sub>3</sub>), 0.86 (3H, d,  $J$  6.7, CH<sub>3</sub>), 0.57 (3H, s, CH<sub>3</sub>);  $\delta_C$  (101 MHz, CDCl<sub>3</sub>) 168.4, 164.4, 111.4, 57.2, 56.8, 47.7, 41.8, 39.9, 39.5, 36.0, 35.9, 29.8, 28.0, 27.4, 24.0, 23.8, 22.8, 22.6, 22.1, 18.8, 12.2;  $m/z$  (CI) 401 (MNH<sub>4</sub><sup>+</sup>, 86%), 323 (66), 306 (67), 91 (100). Found: MNH<sub>4</sub><sup>+</sup>, 401.2843. C<sub>21</sub>H<sub>41</sub>N<sub>2</sub>O<sub>3</sub>S requires MNH<sub>4</sub><sup>+</sup>, 401.2838.

**[(1R,3aS,7aR)-1-((R)-1,5-Dimethyl-hexyl)-7a-methyl-octahydro-inden-(4E)-ylidene]-N-cyano-acetamide, 24b**



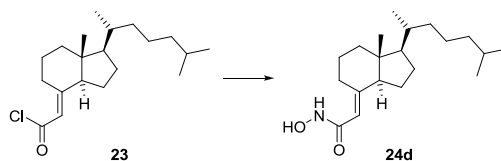
A solution of acid chloride **23** (111 mg, 0.34 mmol) in THF (1 mL) was added dropwise to a solution of NaNHCN (66 mg, 1.03 mmol) in THF (5 mL) and stirred for 18 h. The reaction mixture was added to aq. NaHCO<sub>3</sub> and extracted with petrol (3 × 20 mL). The combined organic layers were washed with brine, and the combined aqueous layers acidified with 1 M HCl and extracted with Et<sub>2</sub>O (3 × 30 mL). The combined organic layers were dried (MgSO<sub>4</sub>) and removed *in vacuo*. Column chromatography eluting with Et<sub>2</sub>O/petrol (1:1 → 1:0) afforded the title compound as a white gum (24 mg, 24% over two steps, 84% based on recovered carboxylic acid **20**),  $R_f$  0.56 (Et<sub>2</sub>O);  $[\alpha]_D^{20} +106.7$  (c. 1.20 in CH<sub>2</sub>Cl<sub>2</sub>);  $\nu_{\max}$  (CHCl<sub>3</sub>)/cm<sup>-1</sup> 3335, 3191, 2162, 1694, 1634;  $\delta_H$  (400 MHz, CDCl<sub>3</sub>) (identifiable peaks) 5.61 (1H, br s, C=CH), 4.04 (1H, br s, NH), 3.87-3.78 (1H, m, C=CCH), 2.21-2.15 (1H, m, C=CCH<sub>2</sub>), 2.04 (1H, d,  $J$  12.9, C=CCH<sub>2</sub>), 0.93 (3H, d,  $J$  5.7, CH<sub>3</sub>), 0.87 (3H, d,  $J$  6.6, CH<sub>3</sub>), 0.86 (3H, d,  $J$  6.6, CH<sub>3</sub>), 0.58 (3H, s, CH<sub>3</sub>);  $\delta_C$  (101 MHz, CDCl<sub>3</sub>) 183.6, 169.9, 165.0, 108.0, 57.3, 56.7, 47.9, 39.8, 39.4, 35.9, 30.1, 28.0, 27.3, 24.0, 23.8, 22.8, 22.5, 22.0, 18.7, 12.2;  $m/z$  (CI) 348 (MNH<sub>4</sub><sup>+</sup>, 100%), 306 (48), 289 (67). Found MNH<sub>4</sub><sup>+</sup>, 348.3015. C<sub>21</sub>H<sub>38</sub>N<sub>3</sub>O requires MNH<sub>4</sub><sup>+</sup>, 348.3015.

**[(1R,3aS,7aR)-1-((R)-1,5-Dimethyl-hexyl)-7a-methyl-octahydro-inden-(4E)-ylidene]-thioacetic acid, 24c**



A solution of acid chloride **23** (111 mg, 0.34 mmol) in THF (1 mL) was added dropwise to a solution of NaSH (58 mg, 1.03 mmol) in EtOH (5 mL) at -10 °C and stirred for 4 h. The reaction mixture was poured into aq. NaHCO<sub>3</sub> and extracted with petrol (3 × 20 mL). The combined organic layers were washed with brine, and the combined aqueous layers acidified with 1 M HCl and extracted with Et<sub>2</sub>O (3 × 30 mL). The combined organic layers were dried (MgSO<sub>4</sub>) and the solvent removed *in vacuo*. Column chromatography eluting with Et<sub>2</sub>O/petrol (1:1 → 1:0) afforded the title compound as a white solid (71 mg, 81% over two steps), mp 105-110 °C;  $[\alpha]_{\text{D}}^{20} +208.4$  (c. 0.95 in CH<sub>2</sub>Cl<sub>2</sub>);  $\nu_{\text{max}}$  (CHCl<sub>3</sub>)/cm<sup>-1</sup> 2360, 1698, 1612, 1265, 1032;  $\delta_{\text{H}}$  (400 MHz, CDCl<sub>3</sub>) (identifiable peaks) 5.96 (1H, s, C=CH), 3.70 (1H, d, *J* 13.0, C=CCH), 2.15 (1H, m, C=CCH<sub>2</sub>), 2.01 (1H, d, *J* 12.3, C=CCH<sub>2</sub>), 0.87 (6H, d, *J* 6.1, 2 × CH<sub>3</sub>), 0.59 (3H, s, CH<sub>3</sub>);  $\delta_{\text{C}}$  (101 MHz, CDCl<sub>3</sub>) 165.6, 159.2, 116.3, 57.1, 56.8, 48.0, 41.3, 39.9, 39.4, 36.0, 31.0, 28.0, 27.4, 24.0, 23.8, 22.8, 22.6, 22.1, 18.7, 12.3; *m/z* (CI) 340 (MNH<sub>4</sub><sup>+</sup>, 50%), 322 (MH<sup>+</sup>, 18), 289 (100), 261 (26). Found: MNH<sub>4</sub><sup>+</sup>, 340.2672. C<sub>20</sub>H<sub>38</sub>NOS requires MNH<sub>4</sub><sup>+</sup>, 340.2674.

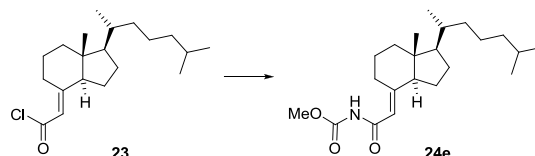
**2-[(1R,3aS,7aR)-1-((R)-1,5-Dimethyl-hexyl)-7a-methyl-octahydro-inden-(4E)-ylidene]-N-hydroxy-acetamide, 24d**



A solution of acid chloride **23** (115 mg, 0.35 mmol) in THF (1 mL) was added dropwise to a solution of NH<sub>2</sub>OH (50% aq., 140 μL, 2.10 mmol) in THF (1.5 mL) at -15 °C. The reaction was slowly warmed to 5 °C and stirred for 1 h. The reaction mixture was added to 1 M HCl and extracted with CHCl<sub>3</sub> (3 × 25 mL). The combined organic layers were dried (MgSO<sub>4</sub>) and the solvent removed *in vacuo*. Column chromatography eluting with AcOH/Et<sub>2</sub>O/petrol (0:1:1 → 1:49:0) afforded the title compound as a pale orange oil (96 mg, 85% over two steps), *R<sub>f</sub>* 0.50 (Et<sub>2</sub>O);  $[\alpha]_{\text{D}}^{20} +105.8$  (c. 4.80 in CH<sub>2</sub>Cl<sub>2</sub>);  $\nu_{\text{max}}$  (CHCl<sub>3</sub>)/cm<sup>-1</sup> 3216, 1655, 1265;  $\delta_{\text{H}}$  (400 MHz, CDCl<sub>3</sub>) (identifiable peaks) 5.27 (1H, br s, C=CH), 3.71 (1H, br s, C=CCH), 0.93 (3H,

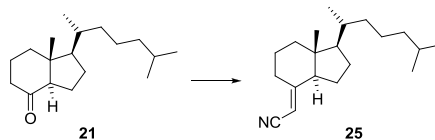
d,  $J$  5.8, CH<sub>3</sub>), 0.86 (3H, d,  $J$  6.6, CH<sub>3</sub>), 0.86 (3H, d,  $J$  6.6, CH<sub>3</sub>), 0.56 (3H, s, CH<sub>3</sub>);  $\delta_C$  (101 MHz, CDCl<sub>3</sub>) 166.7, 160.6, 109.4, 56.7, 54.4, 46.9, 40.0, 39.4, 36.0, 35.9, 28.0, 27.4, 24.0, 23.8, 22.8, 22.5, 22.2, 18.8, 12.0;  $m/z$  (CI) 339 (MNH<sub>4</sub><sup>+</sup>, 87%), 322 (MH<sup>+</sup>, 100), 289 (12). Found MH<sup>+</sup>, 322.2756. C<sub>20</sub>H<sub>36</sub>NO<sub>2</sub> requires MH<sup>+</sup>, 322.2746.

**[2-[(1R,3aS,7aR)-1-((R)-1,5-Dimethyl-hexyl)-7a-methyl-octahydro-inden-(4E)-ylidene]-acetyl]-carbamic acid methyl ester, 24e**



To a solution of acid chloride **23** (115 mg, 0.35 mmol) in PhMe (1 mL) was added methyl carbamate (79 mg, 1.05 mmol) and the resulting solution was stirred at 80 °C for 2 h. The reaction mixture was cooled and purification by column chromatography eluting with Et<sub>2</sub>O/petrol (1:3 → 1:1) afforded the title compound as a colourless oil (69 mg, 53% over two steps),  $R_f$  0.30 (Et<sub>2</sub>O/petrol 1:1);  $[\alpha]_D^{20}$  120.0 (*c.* 2.45 in CHCl<sub>3</sub>);  $\nu_{max}$  (CHCl<sub>3</sub>)/cm<sup>-1</sup> 3216, 1655, 1265;  $\delta_H$  (400 MHz, CDCl<sub>3</sub>) (identifiable peaks) 7.80 (1H, br s, NH), 6.24 (1H, s, C=CH), 3.76 (3H, s, OCH<sub>3</sub>), 3.28-3.07 (1H, m, C=CCH), 0.86 (3H, d,  $J$  6.6, CH<sub>3</sub>), 0.85 (3H, d,  $J$  6.6, CH<sub>3</sub>), 0.58 (3H, s, CH<sub>3</sub>);  $\delta_C$  (101 MHz, CDCl<sub>3</sub>) 166.2, 165.7, 152.5, 112.7, 65.8, 57.2, 56.8, 52.8, 47.4, 40.1, 39.4, 36.0, 30.3, 28.0, 27.4, 23.8, 22.8, 22.5, 22.2, 18.7, 12.1;  $m/z$  (CI) 381 (MNH<sub>4</sub><sup>+</sup>, 100%), 364 (MH<sup>+</sup>, 82), 324 (10). Found MH<sup>+</sup>, 364.2859. C<sub>22</sub>H<sub>38</sub>NO<sub>3</sub> requires MH<sup>+</sup>, 364.2852.

**[(1R,3aS,7aR)-1-((R)-1,5-Dimethyl-hexyl)-7a-methyl-octahydro-inden-(4E)-ylidene]-acetonitrile, 25**

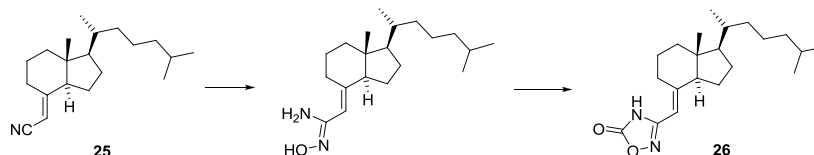


Diisopropyl cyanomethylphosphonate (3.44 mL, 17.0 mmol) was added dropwise to a slurry of NaH (610 mg, 60% dispersion in mineral oil, 14.9 mmol) in THF (20 mL) at 0 °C. The mixture was stirred at r.t. for 1 h to give a colourless solution. A solution of ketone **21** (1.12 g, 4.26 mmol) in THF (5 mL) was added dropwise at 0 °C and the reaction mixture stirred at r.t. for 15 h. The resulting orange solution was poured into sat. aq. NH<sub>4</sub>Cl and extracted with Et<sub>2</sub>O (3 × 30 mL). The combined organic layers were dried (MgSO<sub>4</sub>) and the solvent removed



*in vacuo*. Column chromatography eluting with Et<sub>2</sub>O/petrol (0:1 → 1:9) afforded the title compound as a colourless oil (1.14 g, 93%), R<sub>f</sub> 0.74 (Et<sub>2</sub>O/petrol 1:3); [α]<sub>D</sub><sup>20</sup> +112.0 (c. 2.25 in CH<sub>2</sub>Cl<sub>2</sub>); ν<sub>max</sub> (CHCl<sub>3</sub>)/cm<sup>-1</sup> 2218, 1628; δ<sub>H</sub> (400 MHz, CDCl<sub>3</sub>) (identifiable peaks) 4.89 (1H, s, C=CH), 2.92 (1H, dd, *J* 14.0, 4.3, C=CCH), 0.92 (3H, d, *J* 5.9, CH<sub>3</sub>), 0.86 (3H, d, *J* 6.6, CH<sub>3</sub>), 0.86 (3H, d, *J* 6.5, CH<sub>3</sub>), 0.55 (3H, s, CH<sub>3</sub>); δ<sub>C</sub> (101 MHz, CDCl<sub>3</sub>) 168.9, 117.4, 90.7, 56.5, 56.1, 47.3, 39.5, 39.4, 36.0, 35.9, 33.0, 27.8, 26.9, 24.9, 22.8, 22.6, 21.8, 18.7, 11.9; *m/z* (CI) 305 (MNH<sub>4</sub><sup>+</sup>, 100%). Found: MNH<sub>4</sub><sup>+</sup>, 305.2962. C<sub>20</sub>H<sub>37</sub>N<sub>2</sub> requires MNH<sub>4</sub><sup>+</sup>, 305.2957.

**3-[(1R,3aS,7aR)-1-((R)-1,5-Dimethyl-hexyl)-7a-methyl-octahydro-inden-(4E)-ylidenemethyl]-4H-[1,2,4]oxadiazol-5-one, 26**

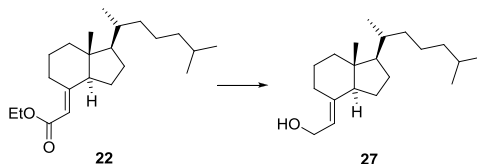


According to the method of Sangshetti,<sup>205</sup> to a solution of nitrile **25** (515 mg, 1.79 mmol) in MeOH (12 mL) was added NH<sub>2</sub>OH.HCl (249 mg, 3.59 mmol) and NaHCO<sub>3</sub> (603 mg, 7.18 mmol). The reaction mixture was stirred at reflux for 8 h before being cooled to r.t. and filtered. The filtrate was concentrated *in vacuo*, a further 5 mL of MeOH was added and the resulting suspension was filtered again. The filtrate was concentrated *in vacuo* to give the intermediate amidoxime as a white semi-solid which was used without further purification in the subsequent reaction.

To a solution of the intermediate amidoxime (144 mg, 0.45 mmol) in dioxane (3 mL) was added CDI (91 mg, 0.56 mmol). The reaction mixture was stirred at reflux for 45 min to give a yellow solution, which was cooled to r.t. The solvent was removed *in vacuo*, water (5 mL) and 2 M HCl (5 mL) were added before extraction with CHCl<sub>3</sub> (3 × 15 mL). The organic layers were combined, washed with brine, dried (MgSO<sub>4</sub>) and concentrated *in vacuo*. Column chromatography eluting with Et<sub>2</sub>O/petrol (0:1 → 1:9) gave the title compound as a yellow oil (91 mg, 59% over 2 steps), R<sub>f</sub> 0.69 (Et<sub>2</sub>O/petrol 1:3); [α]<sub>D</sub><sup>20</sup> +125.7 (c. 4.25 in CH<sub>2</sub>Cl<sub>2</sub>); ν<sub>max</sub>/cm<sup>-1</sup> 3369, 1628, 819; δ<sub>H</sub> (400 MHz, CDCl<sub>3</sub>) (identifiable peaks) 4.88 (1H, s, C=CH), 2.91 (1H, dd *J* 14.0, 4.5, C=CCH), 0.92 (3H, d, *J* 6.0, CH<sub>3</sub>), 0.86 (3H, d, *J* 6.7, CH<sub>3</sub>), 0.86 (3H, d, *J* 6.6, CH<sub>3</sub>), 0.55 (3H, s, CH<sub>3</sub>); δ<sub>C</sub> (101 MHz, CDCl<sub>3</sub>) 168.8, 165.4, 117.3, 91.6, 90.7, 56.4,

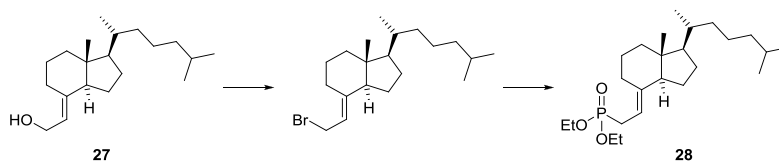
56.0, 47.2, 39.5, 39.4, 36.0, 35.8, 33.0, 28.0, 27.3, 23.6, 22.8, 22.5, 21.7, 18.7, 11.9;  $m/z$  (CI) 305 (decarboxylation product, 100%).

**2-[(1R,3aS,7aR)-1-((R)-1,5-Dimethyl-hexyl)-7a-methyl-octahydro-inden-(4E)-ylidene]-ethanol, **27****



DIBAL (1.0 M in hexanes, 11.8 mL, 11.8 mmol) was added to a solution of ester **22** (1.60 g, 3.77 mmol) in PhMe (8 mL) at  $-78\text{ }^{\circ}\text{C}$ . The reaction mixture was stirred for 1.5 h at this temperature before being poured into aq.  $\text{Na}_2\text{SO}_4$ , filtered through Celite<sup>®</sup> and extracted with  $\text{Et}_2\text{O}$  ( $3 \times 25\text{ mL}$ ). The combined organic layers were dried ( $\text{MgSO}_4$ ) and the solvent removed *in vacuo*. Column chromatography eluting with  $\text{Et}_2\text{O}$ /petrol (0:1  $\rightarrow$  1:1) afforded the title compound as a colourless oil (1.35 g, 96%),  $R_f$  0.23 ( $\text{Et}_2\text{O}$ /petrol 1:3);  $[\alpha]_{\text{D}}^{20} +51.9$  (*c.* 4.20 in  $\text{CH}_2\text{Cl}_2$ );  $\nu_{\text{max}}$  ( $\text{CHCl}_3$ )/ $\text{cm}^{-1}$  3366, 1667, 2165, 996;  $\delta_{\text{H}}$  (400 MHz,  $\text{CDCl}_3$ ) (identifiable peaks) 5.20 (1H, t,  $J$  7.0, C=CH), 4.19 (2H, d,  $J$  7.0,  $\text{CH}_2\text{O}$ ), 2.62-2.58 (1H, m, C=CCH), 0.91 (3H, d,  $J$  6.4,  $\text{CH}_3$ ), 0.86 (3H, d,  $J$  6.6,  $\text{CH}_3$ ), 0.85 (3H, d,  $J$  6.7,  $\text{CH}_3$ ), 0.54 (3H, s,  $\text{CH}_3$ );  $\delta_{\text{C}}$  (101 MHz,  $\text{CDCl}_3$ ) 143.7, 119.2, 58.6, 56.6, 55.6, 45.3, 40.3, 39.5, 36.1, 28.7, 28.0, 27.6, 23.8, 23.5, 22.8, 22.5, 22.1, 18.8, 11.8;  $m/z$  (CI) 310 ( $\text{MNH}_4^+$ , 8%), 292 ( $\text{MH}^+$ , 47%), 275 (100%). Found  $\text{MNH}_4^+$ , 310.3120.  $\text{C}_{21}\text{H}_{38}\text{N}_3\text{O}$  requires  $\text{MNH}_4^+$ , 310.3110.

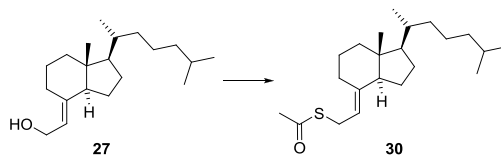
**[2-[(1R,3aS,7aR)-1-((R)-1,5-Dimethyl-hexyl)-7a-methyl-octahydro-inden-(4E)-ylidene]-ethyl]-phosphonic acid diethyl ester, **28****



$\text{PBr}_3$  (147  $\mu\text{L}$ , 1.56 mmol) was added to a stirred solution of alcohol **27** (912 mg, 3.12 mmol) in  $\text{Et}_2\text{O}$  (20 mL) at  $0\text{ }^{\circ}\text{C}$ . The reaction mixture was stirred for 4 h before being poured into ice-water and extracted with  $\text{Et}_2\text{O}$  ( $3 \times 25\text{ mL}$ ). The combined organic layers were dried ( $\text{MgSO}_4$ ) and the solvent removed *in vacuo* to give the crude intermediate bromide, which was used without purification in the next reaction.

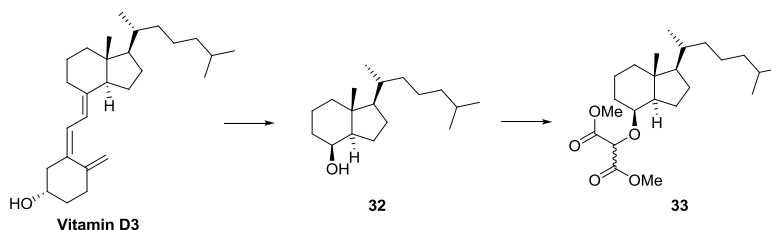
The intermediate bromide was added to P(OEt)<sub>3</sub> (5 mL) and heated to reflux at 170 °C for 5 h. The reaction mixture was cooled, poured into ice-water, acidified with 1 M HCl and extracted with Et<sub>2</sub>O (3 × 20 mL). The combined organic layers were dried (MgSO<sub>4</sub>) and the solvent removed *in vacuo*. Column chromatography eluting with Et<sub>2</sub>O/petrol (1:3 → 1:0) afforded the title compound as a colourless oil (1.13 g, 88%), R<sub>f</sub> 0.27 (Et<sub>2</sub>O); [α]<sub>D</sub><sup>20</sup> + 88.0 (*c.* 0.75 in CH<sub>2</sub>Cl<sub>2</sub>); ν<sub>max</sub> (CHCl<sub>3</sub>)/cm<sup>-1</sup> 1668, 1254, 1054, 1030; δ<sub>H</sub> (400 MHz, CDCl<sub>3</sub>) (identifiable peaks) 4.90 (1H, m, C=CH), 4.11-3.99 (4H, m OCH<sub>2</sub>), 2.64-2.48 (3H, m PCH<sub>2</sub>, C=CCH), 0.87 (3H, d, *J* 6.4, CH<sub>3</sub>), 0.82 (3H, d, *J* 6.6, CH<sub>3</sub>), 0.82 (3H, d, *J* 6.5, CH<sub>3</sub>), 0.51 (3H, s, CH<sub>3</sub>); δ<sub>C</sub> (101 MHz, CDCl<sub>3</sub>) 143.8, 107.9, 65.8, 63.6, 61.5, 56.4, 55.7, 45.3, 40.3, 39.4, 36.0, 28.6, 27.9, 27.5, 23.7, 23.1, 22.7, 22.4, 22.1, 18.7, 11.7; *m/z* (CI) 430 (48%), 413 (MH<sup>+</sup>, 100). Found MH<sup>+</sup>, 413.3196. C<sub>24</sub>H<sub>46</sub>O<sub>3</sub>P requires MH<sup>+</sup>, 413.3185.

**Thioacetic acid S-[2-[(1R,3aS,7aR)-1-((R)-1,5-dimethyl-hexyl)-7a-methyl-octahydro-inden-(4E)-ylidene]-ethyl] ester, 30**



Diisopropyl azodicarboxylate (480 μL, 2.42 mmol) was added to a solution of PPh<sub>3</sub> (635 mg, 2.42 mmol) in THF (4 mL) at 0 °C. The resulting white slurry was stirred at this temperature for 30 min before a solution of alcohol **27** (353 mg, 1.21 mmol) in THF (1 mL) was added. The reaction mixture was stirred for 5 min before the addition of thiolacetic acid (170 μL, 2.42 mmol) and then for 1 h at 0 °C, followed by a further 1 h at r.t. The reaction mixture was then washed with sat. aq. NaHCO<sub>3</sub> (4 × 25 mL) and the solvent removed *in vacuo*. Hexane (25 mL) was added and the solution was filtered through Celite<sup>®</sup> and then silica. The solvent was removed *in vacuo* to give a yellow oil and purification by column chromatography eluting with Et<sub>2</sub>O/petrol (0:1 → 1:3) afforded the title compound as a pale yellow oil (268 mg, 63%), R<sub>f</sub> 0.68 (Et<sub>2</sub>O/petrol 1:3); [α]<sub>D</sub><sup>20</sup> +70.2 (*c.* 2.45 in CH<sub>2</sub>Cl<sub>2</sub>); ν<sub>max</sub> (CHCl<sub>3</sub>)/cm<sup>-1</sup> 1693, 1665, 1135, 1111, 630; δ<sub>H</sub> (400 MHz, CDCl<sub>3</sub>) (identifiable peaks) 5.00 (1H, t, *J* 8.0, C=CH), 3.65-3.49 (2H, m, CH<sub>2</sub>S), 2.67-2.59 (1H, m, C=CCH), 2.31 (3H, s, COCH<sub>3</sub>), 0.90 (3H, d, *J* 6.5, CH<sub>3</sub>), 0.86 (3H, d, *J* 6.7, CH<sub>3</sub>), 0.85 (3H, d, *J* 6.7, CH<sub>3</sub>), 0.51 (3H, s, CH<sub>3</sub>); δ<sub>C</sub> (101 MHz, CDCl<sub>3</sub>) 169.1, 144.1, 116.8, 109.4, 56.5, 55.6, 45.4, 40.3, 39.5, 36.1, 30.4, 28.6, 28.0, 27.6, 26.7, 23.8, 23.4, 22.8, 22.5, 22.1, 18.8, 11.7; *m/z* (CI) 368 (92%), 351 (MH<sup>+</sup>, 100), 309 (27), 274 (35). Found MH<sup>+</sup>, 351.2724. C<sub>22</sub>H<sub>39</sub>SO requires MH<sup>+</sup>, 351.2722.

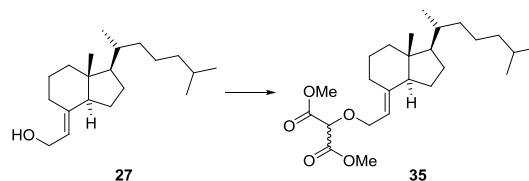
**2-[(1R,3aR,4S,7aR)-1-((R)-1,5-Dimethyl-hexyl)-7a-methyl-octahydro-inden-4-yloxy]-malonic acid dimethyl ester, **33****



O<sub>2</sub> was bubbled through a stirred solution of vitamin D<sub>3</sub> (5.00 g, 13.0 mmol) in MeOH (150 mL) at -78 °C for 10 min. O<sub>3</sub> was then bubbled through the solution until a blue colour was observed, and for a further 15 min (1.5 h in total), before O<sub>2</sub> was bubbled through for 10 min to give a colourless solution. NaBH<sub>4</sub> (4.43 g, 117 mmol) was added and the solution stirred at -78 °C for 1 h, followed by 1.5 h at r.t. 1 M HCl (50 mL) was added and the MeOH removed *in vacuo*. The aqueous solution was extracted with Et<sub>2</sub>O (3 × 200 mL) and the combined organic layers dried (MgSO<sub>4</sub>) and the solvent removed *in vacuo*. Partial purification by column chromatography eluting with Et<sub>2</sub>O/petrol (1:3 → 1:1) afforded alcohol **32** as a colourless oil (2.01 g), which was used directly in subsequent reactions.

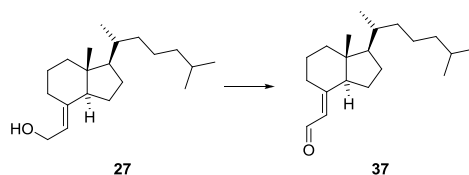
According to the method of Cox,<sup>206</sup> Rh<sub>2</sub>(OAc)<sub>4</sub> (5 mg, 0.01 mmol) was added to a stirred solution of alcohol **32** (259 mg, 0.97 mmol) and dimethyl diazomalonate (153 mg, 0.97 mmol) in CH<sub>2</sub>Cl<sub>2</sub> (3 mL) at r.t. to give a green solution. After stirring for 2.5 h, the solvent was removed *in vacuo* and purification by column chromatography eluting with Et<sub>2</sub>O/petrol (5:95 → 15:85), affording the title compound as a colourless oil (303 mg, 47% over 2 steps), R<sub>f</sub> 0.56 (Et<sub>2</sub>O/petrol 1:1); [α]<sub>D</sub><sup>20</sup> +71.3 (*c.* 1.15 in CH<sub>2</sub>Cl<sub>2</sub>); ν<sub>max</sub> (CHCl<sub>3</sub>)/cm<sup>-1</sup> 1771, 1749, 1163, 1128; δ<sub>H</sub> (400 MHz, CDCl<sub>3</sub>) (identifiable peaks) 4.47 (1H, s, OCH(CO<sub>2</sub>Me)<sub>2</sub>), 3.78 (3H, s, OCH<sub>3</sub>), 3.77 (3H, s, OCH<sub>3</sub>), 3.73 (1H, m, OCH), 2.02-1.95 (1H, m, OCHCH), 0.92 (3H, s, CH<sub>3</sub>), 0.88 (3H, d, *J* 6.5, CH<sub>3</sub>), 0.86 (3H, d, *J* 6.5, CH<sub>3</sub>), 0.85 (3H, d, *J* 6.3, CH<sub>3</sub>); δ<sub>C</sub> (101 MHz, CDCl<sub>3</sub>) 167.9, 167.7, 79.0, 78.3, 56.7, 52.7, 52.6, 52.3, 42.0, 40.4, 39.5, 36.0, 35.3, 29.7, 28.0, 27.2, 23.8, 22.8, 22.5, 22.4, 18.6, 17.7, 13.2; *m/z* (CI) 414 (MNH<sub>4</sub><sup>+</sup>, 100%), 282 (5). Found MNH<sub>4</sub><sup>+</sup>, 414.3226. C<sub>23</sub>H<sub>44</sub>NO<sub>5</sub> requires MNH<sub>4</sub><sup>+</sup>, 414.3219.

**2-[2-[(1R,3aS,7aR)-1-((R)-1,5-Dimethyl-hexyl)-7a-methyl-octahydro-inden-(4E)-ylidene]-ethoxy]-malonic acid dimethyl ester, **35****



According to the method of Cox,<sup>206</sup> Rh<sub>2</sub>(OAc)<sub>4</sub> (4 mg, 0.007 mmol) was added to a stirred solution of alcohol **27** (213 mg, 0.73 mmol) and dimethyl diazomalonate (124 mg, 0.78 mmol) in CH<sub>2</sub>Cl<sub>2</sub> (2 mL) at r.t. to give a green solution. After stirring for 3 h, the solvent was removed *in vacuo* and purification by column chromatography eluting with Et<sub>2</sub>O/petrol (1:3 → 1:1) afforded the title compound as a colourless oil (245 mg, 80%), R<sub>f</sub> 0.50 (Et<sub>2</sub>O/petrol 1:1); [α]<sub>D</sub><sup>20</sup> +59.1 (c. 1.05 in CH<sub>2</sub>Cl<sub>2</sub>); ν<sub>max</sub> (CHCl<sub>3</sub>)/cm<sup>-1</sup> 1748, 1667, 1266, 1238, 1166, 1026; δ<sub>H</sub> (400 MHz, CDCl<sub>3</sub>) (identifiable peaks) 5.12 (1H, t, *J* 7.3, C=CH), 4.57 (1H, s, OCH), 4.30-4.18 (2H, m, OCH<sub>2</sub>), 3.79 (6H, s, 2 × OCH<sub>3</sub>), 2.56-2.50 (1H, m, C=CCH), 0.90 (3H, d, *J* 6.4, CH<sub>3</sub>), 0.85 (3H, d, *J* 6.6, CH<sub>3</sub>), 0.85 (3H, d, *J* 6.6, CH<sub>3</sub>), 0.53 (3H, s, CH<sub>3</sub>); δ<sub>C</sub> (101 MHz, CDCl<sub>3</sub>) 167.3, 167.2, 147.3, 114.6, 66.4, 65.8, 56.5, 55.8, 52.8, 45.4, 40.2, 39.4, 36.0, 28.8, 28.0, 27.5, 23.8, 23.4, 22.8, 22.5, 22.1, 18.8, 11.9; *m/z* (CI) 454 (4%), 440 (MH<sup>+</sup>, 100), 275 (29) Found MH<sup>+</sup>, 440.3377. C<sub>25</sub>H<sub>46</sub>NO<sub>5</sub> requires MH<sup>+</sup>, 440.3376.

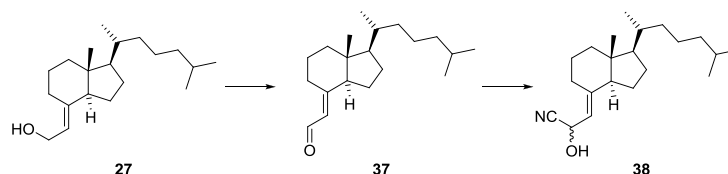
**[(1R,3aS,7aR)-1-((R)-1,5-Dimethyl-hexyl)-7a-methyl-octahydro-inden-(4E)-ylidene]-acetaldehyde, **37****<sup>204</sup>



To a solution of oxalyl chloride (2 M in CH<sub>2</sub>Cl<sub>2</sub>, 990 μL, 1.98 mmol) in CH<sub>2</sub>Cl<sub>2</sub> at -60 °C was added DMSO (0.28 mL, 3.98 mmol). The reaction mixture was stirred for 5 min before dropwise addition of alcohol **27** (482 mg, 1.66 mmol) in CH<sub>2</sub>Cl<sub>2</sub> (3 mL) and further stirring for 15 min. Et<sub>3</sub>N (1.11 mL, 7.97 mmol) was then added dropwise before the reaction mixture was stirred for 5 min and then allowed to warm to r.t. The solvent was removed *in vacuo* and purification by column chromatography eluting with Et<sub>2</sub>O/petrol (1:4) gave the title compound as a colourless oil (349 mg, 73%), R<sub>f</sub> 0.40 (Et<sub>2</sub>O/petrol 1:3); δ<sub>H</sub> (400 MHz, CDCl<sub>3</sub>) (identifiable peaks) 10.10 (1H, d, *J* 8.2, CHO), 5.73 (1H, d, *J* 8.2, C=CH), 3.39-3.33 (1H, m, C=CCH), 0.93 (3H, d, *J* 5.9, CH<sub>3</sub>), 0.86 (3H, d, *J* 6.6, CH<sub>3</sub>), 0.86 (3H, d, *J* 6.5, CH<sub>3</sub>), 0.60

(3H, s, CH<sub>3</sub>); *m/z* (CI) 308 (100%), 291 (MH<sup>+</sup>, 74), 273 (42). Found MH<sup>+</sup>, 291.2694. C<sub>20</sub>H<sub>35</sub>O requires MH<sup>+</sup>, 291.2688. Data is in agreement with the literature.<sup>204</sup>

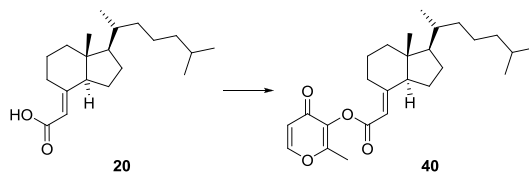
### 3-[(1R,3aS,7aR)-1-((R)-1,5-Dimethyl-hexyl)-7a-methyl-octahydro-inden-(4E)-ylidene]-2-hydroxy-propionitrile, **38**



To a solution of oxalyl chloride (2 M in CH<sub>2</sub>Cl<sub>2</sub>, 0.71 mL, 1.41 mmol) in CH<sub>2</sub>Cl<sub>2</sub> (3 mL) at -60 °C was added DMSO (0.20 mL, 2.81 mmol). The reaction mixture was stirred for 5 min before dropwise addition of alcohol **27** (342 mg, 1.17 mmol) in CH<sub>2</sub>Cl<sub>2</sub> (1 mL) and further stirring for 15 min. Et<sub>3</sub>N (0.79 mL, 5.62 mmol) was then added dropwise before the reaction mixture was stirred for 5 min and then allowed to warm to r.t. The solvent was removed *in vacuo* to give crude aldehyde **37**, which was used in the next reaction without purification.

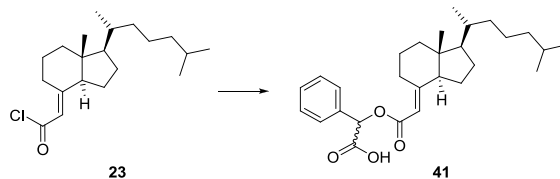
According to the method of Baeza,<sup>207</sup> to a mixture of aldehyde **37** (339 mg, 1.17 mmol) and Et<sub>3</sub>N (33 μL, 0.24 mmol) at r.t. was added TMSCN (172 μL, 1.29 mmol) and the reaction mixture was stirred for 2 h. The volatile materials were removed *in vacuo* to give an orange oil and purification by column chromatography eluting with Et<sub>2</sub>O/petrol (1:3) gave the title compound as a colourless oil (297 mg, 80% over 2 steps), R<sub>f</sub> 0.11 (Et<sub>2</sub>O/petrol 1:3); [α]<sub>D</sub><sup>20</sup> +54.4 (*c.* 1.25 in CH<sub>2</sub>Cl<sub>2</sub>); ν<sub>max</sub> (CHCl<sub>3</sub>)/cm<sup>-1</sup> 3420, 2254, 1662, 1028, 909; δ<sub>H</sub> (400 MHz, CDCl<sub>3</sub>) (identifiable peaks) 5.27-5.17 (2H, m, C=CH, CHOH), 2.56 (1H, m, C=CCH), 0.92 (3H, d, *J* 6.3, CH<sub>3</sub>), 0.87 (3H, d, *J* 6.6, CH<sub>3</sub>), 0.86 (3H, d, *J* 6.7, CH<sub>3</sub>), 0.56 (3H, s, CH<sub>3</sub>); δ<sub>C</sub> (101 MHz, CDCl<sub>3</sub>) 149.5, 119.7, 115.2, 57.3, 56.5, 55.4, 46.2, 45.8, 39.9, 39.4, 36.0, 29.3, 28.0, 27.5, 23.8, 23.3, 22.8, 22.5, 21.9, 18.8, 11.8; *m/z* (CI) 308 (100%), 291 (40), 273 (18). Found MH<sup>+</sup>, 317.2720. C<sub>20</sub>H<sub>35</sub>O requires MH<sup>+</sup>, 317.2719.

**[(1R,3aS,7aR)-1-((R)-1,5-Dimethyl-hexyl)-7a-methyl-octahydro-inden-(4E)-ylidene]-acetic acid 2-methyl-4-oxo-4H-pyran-3-yl ester, 40**



To a stirred solution of carboxylic acid **20** (42 mg, 0.14 mmol) in CH<sub>2</sub>Cl<sub>2</sub> (3 mL) at r.t. was added DCC (31 mg, 0.15 mmol), 3-hydroxy-2-methylpyrone (19 mg, 0.15 mmol) and DMAP (2 mg, 0.02 mmol). The reaction mixture was stirred for 3 d before being filtered to remove the white urea precipitate, which was washed with CH<sub>2</sub>Cl<sub>2</sub>. Brine (10 mL) was added to the filtrate, and the organic layer separated. The aqueous layer was extracted with CH<sub>2</sub>Cl<sub>2</sub> (2 × 10 mL). The combined organic layers were dried (Na<sub>2</sub>SO<sub>4</sub>) and the solvent removed *in vacuo*. Column chromatography eluting with Et<sub>2</sub>O/petrol (1:3 → 1:0) afforded the title compound as a colourless oil (40 mg, 70%), R<sub>f</sub> 0.40 (Et<sub>2</sub>O); [α]<sub>D</sub><sup>20</sup> +35.0 (c. 0.40 in CH<sub>2</sub>Cl<sub>2</sub>); ν<sub>max</sub> (CHCl<sub>3</sub>)/cm<sup>-1</sup> 1766, 1664, 1171; δ<sub>H</sub> (400 MHz, CDCl<sub>3</sub>) (identifiable peaks) 7.65 (1H, d, *J* 5.8, pyrone 6-H), 6.39 (1H, d, *J* 5.8, pyrone 5-H), 5.72 (1H, br s, O<sub>2</sub>CCH=C), 2.23 (3H, s, pyrone CH<sub>3</sub>), 0.86 (3H, d, *J* 6.7, CH<sub>3</sub>), 0.86 (3H, d, *J* 6.5, CH<sub>3</sub>); δ<sub>C</sub> (101 MHz, CDCl<sub>3</sub>) 172.0, 168.8, 158.9, 154.0, 138.7, 133.2, 125.6, 116.9, 54.3, 51.5, 41.2, 40.9, 39.5, 35.4, 34.8, 33.6, 29.7, 29.0, 28.0, 24.4, 22.8, 22.5, 21.4, 19.8, 14.9; *m/z* (CI) 415 (MH<sup>+</sup>, 98%), 225 (100), 127 (20). Found: MH<sup>+</sup>, 415.2853. C<sub>26</sub>H<sub>39</sub>O<sub>4</sub> requires MH<sup>+</sup>, 415.2848.

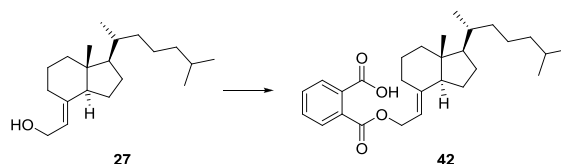
**(2-[(1R,7aR)-1-((R)-1,5-Dimethyl-hexyl)-7a-methyl-octahydro-inden-(4E)-ylidene]-acetoxy)-phenyl-acetic acid, 41**



To a stirred solution of (+/-)-mandelic acid (96 mg, 0.63 mmol) and DMAP (7 mg, 0.063 mmol) in CH<sub>2</sub>Cl<sub>2</sub> (0.5 mL) at r.t. was added acid chloride **23** (41 mg, 0.13 mmol) and Et<sub>3</sub>N (90 μL, 0.63 mmol). The reaction mixture was stirred for 14 h before sat. aq. NaHCO<sub>3</sub> (10 mL) was added. The aqueous layer was extracted with CH<sub>2</sub>Cl<sub>2</sub> (3 × 20 mL) and then acidified with 1 M HCl before being extracted with CH<sub>2</sub>Cl<sub>2</sub> (3 × 20 mL). The combined organic layers were dried (MgSO<sub>4</sub>) and the solvent removed *in vacuo*. Column chromatography eluting with AcOH/Et<sub>2</sub>O/petrol (2:25:75 → 2:33:67) afforded the title compound as a colourless oil (48

mg, 87%),  $R_f$  0.50 (Et<sub>2</sub>O/petrol 1:5:5);  $[\alpha]_D^{20}$  +24.2 (c. 1.73 in CH<sub>2</sub>Cl<sub>2</sub>);  $\nu_{\max}$  (CHCl<sub>3</sub>)/cm<sup>-1</sup> 1731, 1643, 1143;  $\delta_H$  (400 MHz, CDCl<sub>3</sub>) (identifiable peaks) 7.52-7.45 (2H, m, Ar-H), 7.40-7.35 (3H, m, Ar-H), 5.91 (1H, s, OCHCO<sub>2</sub>H), 5.60 (1H, br s, CH=C), 0.91 (3H, d,  $J$  6.5, CH<sub>3</sub>), 0.87 (6H, d,  $J$  6.4, 2 × CH<sub>3</sub>), 0.86 (3H, s, CH<sub>3</sub>);  $\delta_C$  (101 MHz, CDCl<sub>3</sub>) 174.1, 171.6, 133.3, 133.2, 129.4, 128.8, 127.6, 125.4, 74.0, 54.3, 51.4, 41.4, 40.8, 39.5, 35.4, 34.8, 33.6, 29.6, 29.0, 28.0, 24.4, 22.8, 22.6, 21.3, 19.8;  $m/z$  (CI) 458 (95%), 441 (MH<sup>+</sup>, 29), 289 (30), 272 (100), 97 (22). Found: MH<sup>+</sup>, 441.3004. C<sub>28</sub>H<sub>41</sub>O<sub>4</sub> requires MH<sup>+</sup>, 441.3005.

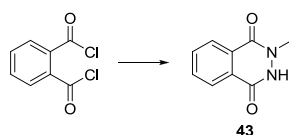
**Phthalic acid mono-(2-[(1R,3aS,7aR)-1-((R)-1,5-dimethyl-hexyl)-7a-methyl-octahydro-inden-(4E)-ylidene]-ethyl) ester, **42****



To a stirred solution of phthalic anhydride (51 mg, 0.34 mmol) in THF (2 mL) at r.t. was added alcohol **27** (95 mg, 0.33 mmol) and Et<sub>3</sub>N (142  $\mu$ L, 1.02 mmol). The reaction mixture was stirred for 14 h before sat. aq. NaHCO<sub>3</sub> (10 mL) was added. The aqueous layer was extracted with Et<sub>2</sub>O (3 × 15 mL) and then acidified with 1 M HCl before being extracted with Et<sub>2</sub>O (3 × 40 mL). The combined organic layers were dried (MgSO<sub>4</sub>) and the solvent removed *in vacuo*. Column chromatography eluting with Et<sub>2</sub>O/petrol (1:1 → 3:1) afforded the title compound as a white semi-solid (143 mg, 100%),  $R_f$  0.70 (Et<sub>2</sub>O);  $[\alpha]_D^{20}$  +42.0 (c. 1.33 in CH<sub>2</sub>Cl<sub>2</sub>);  $\nu_{\max}$  (CHCl<sub>3</sub>)/cm<sup>-1</sup> 1726, 1702, 1285, 1124, 1072;  $\delta_H$  (400 MHz, CDCl<sub>3</sub>) (identifiable peaks) 7.93 (1H, dd,  $J$  7.5, 1.3, Ar-H), 7.70 (1H, dd,  $J$  7.4, 1.3, Ar-H), 7.58 (2H, m, Ar-H), 5.23 (1H, t,  $J$  7.3, OCH<sub>2</sub>CH=C), 4.91 (2H, d,  $J$  7.4, OCH<sub>2</sub>CH=C), 2.70 (1H, m, C=CCH), 0.91 (3H, d,  $J$  6.4, CH<sub>3</sub>), 0.87 (3H, d,  $J$  6.7, CH<sub>3</sub>), 0.86 (3H, d,  $J$  6.5, CH<sub>3</sub>), 0.54 (3H, s, CH<sub>3</sub>);  $\delta_C$  (101 MHz, CDCl<sub>3</sub>) 171.7, 168.3, 147.2, 133.6, 132.2, 130.7, 130.1, 128.8, 113.3, 62.3, 56.5, 55.7, 45.5, 40.3, 39.5, 36.0, 28.9, 28.0, 27.5, 23.8, 23.5, 22.8, 22.5, 22.1, 18.8, 11.8;  $m/z$  (CI) 441 (MH<sup>+</sup>, 1%), 292 (24), 275 (100), 184 (45). Found: MH<sup>+</sup>, 441.3009. C<sub>28</sub>H<sub>41</sub>O<sub>4</sub> requires MH<sup>+</sup>, 441.3005.

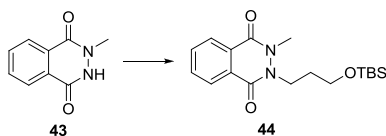


## 2-Methyl-2,3-dihydro-phthalazine-1,4-dione, **43**<sup>208</sup>



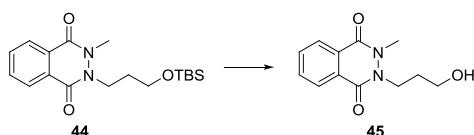
To a stirred solution of phthaloyl dichloride (5.00 mL, 34.7 mmol) and Et<sub>3</sub>N (14.5 mL, 104 mmol) in CH<sub>2</sub>Cl<sub>2</sub> (200 mL) at 0 °C was added methylhydrazine (1.85 mL, 34.7 mmol) dropwise. The reaction mixture was allowed to warm to r.t. and stirred for 14 h. The solvent was removed *in vacuo* and the residue suspended in Et<sub>2</sub>O and filtered. Recrystallisation from EtOH afforded the title compound as white amorphous crystals (4.55 g, 75%), mp > 250 °C;  $\delta_{\text{H}}$  (400 MHz, CDCl<sub>3</sub>) 11.63 (1H, s, NH), 8.23-8.19 (1H, m, Ar-H), 7.98-7.94 (1H, m, Ar-H), 7.92-7.84 (2H, m, Ar-H), 3.56 (3H, s, CH<sub>3</sub>);  $m/z$  (ES) 294 (26%), 253 (17), 251 (100), 210 (27), 144 (18). Found: MH<sup>+</sup>, 177.0669. C<sub>9</sub>H<sub>9</sub>N<sub>2</sub>O<sub>2</sub> requires MH<sup>+</sup>, 177.0664. Data is in agreement with the literature.<sup>208</sup>

## 2-[3-(*tert*-Butyl-dimethyl-silyloxy)-propyl]-3-methyl-2,3-dihydro-phthalazine-1,4-dione, **44**



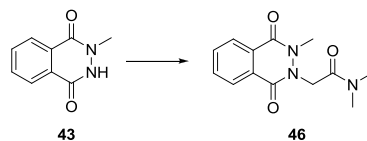
A suspension of phthalazine dione **43** (50 mg, 0.28 mmol), (3-bromo-propoxy)-*tert*-butyl-dimethyl-silane (79  $\mu$ L, 0.34 mmol), K<sub>2</sub>CO<sub>3</sub> (59 mg, 0.43 mmol) and KI (24 mg, 0.14 mmol) in MeCN (4 mL) was stirred at reflux for 24 h. The reaction mixture was cooled, filtered and the solvent removed *in vacuo*. Column chromatography eluting with Et<sub>2</sub>O/petrol (1:3  $\rightarrow$  1:1) afforded the title compound as a colourless oil (68 mg, 69%), R<sub>f</sub> 0.66 (Et<sub>2</sub>O/petrol 1:1);  $\nu_{\text{max}}$  (CHCl<sub>3</sub>)/cm<sup>-1</sup> 1649, 1590, 1328, 1258, 1097;  $\delta_{\text{H}}$  (400 MHz, CDCl<sub>3</sub>) 8.40-8.34 (1H, m, Ar-H), 7.95-7.90 (1H, m, Ar-H), 7.77-7.70 (2H, m, Ar-H), 4.37 (2H, t,  $J$  6.2, CH<sub>2</sub>O), 3.81 (2H, t,  $J$  6.2, CH<sub>2</sub>N), 3.70 (3H, s, NCH<sub>3</sub>), 2.03 (2H, quin,  $J$  6.2, CH<sub>2</sub>CH<sub>2</sub>O), 0.87 (9H, s, C(CH<sub>3</sub>)<sub>3</sub>), 0.03 (6H, s, 2  $\times$  SiCH<sub>3</sub>);  $\delta_{\text{C}}$  (101 MHz, CDCl<sub>3</sub>) 158.8, 149.8, 132.5, 131.7, 129.0, 126.9, 124.9, 123.3, 63.6, 59.7, 38.8, 32.0, 25.9, 18.3, -5.4;  $m/z$  (ES) 515 (7%), 351 (4), 350 (26), 349 (MH<sup>+</sup>, 100), 297 (7). Found: MH<sup>+</sup>, 349.1947. C<sub>18</sub>H<sub>29</sub>N<sub>2</sub>O<sub>3</sub>Si requires MH<sup>+</sup>, 349.1947.

## 2-(3-Hydroxy-propyl)-3-methyl-2,3-dihydro-phthalazine-1,4-dione, 45



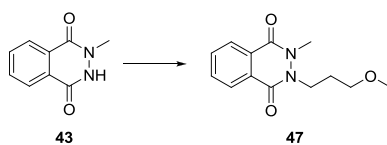
To a stirred solution of TBS-protected alcohol **44** (33 mg, 0.095 mmol) in THF (0.1 mL) at 0 °C was added TBAF (1 M in THF, 114  $\mu$ L, 0.11 mmol) dropwise. The reaction mixture was stirred for 2 h, the solvent removed *in vacuo*. Column chromatography eluting with MeOH/Et<sub>2</sub>O (0:1  $\rightarrow$  1:9) afforded the title compound as a white semi-solid (22 mg, 100%),  $R_f$  0.21 (Et<sub>2</sub>O);  $\nu_{\max}$  (CHCl<sub>3</sub>)/cm<sup>-1</sup> 1641, 1579, 1332, 1266, 1102;  $\delta_H$  (400 MHz, CDCl<sub>3</sub>) 8.34-8.28 (1H, m, Ar-H), 7.87-7.82 (1H, m, Ar-H), 7.73-7.65 (2H, m, Ar-H), 4.39 (2H, t,  $J$  6.0, CH<sub>2</sub>O), 3.86 (2H, t,  $J$  6.0, CH<sub>2</sub>N), 3.64 (3H, s, NCH<sub>3</sub>), 2.50 (1H, br s, OH), 2.07 (2H, quin,  $J$  6.0, CH<sub>2</sub>CH<sub>2</sub>O);  $\delta_C$  (101 MHz, CDCl<sub>3</sub>) 158.7, 149.9, 132.5, 131.8, 128.8, 126.9, 124.6, 123.3, 63.9, 59.4, 38.8, 31.9;  $m/z$  (ES) 401 (18%), 236 (13), 235 (MH<sup>+</sup>, 100), 211 (4), 177 (4). Found: MH<sup>+</sup>, 235.1094. C<sub>12</sub>H<sub>15</sub>N<sub>2</sub>O<sub>3</sub> requires MH<sup>+</sup>, 235.1083.

## *N,N*-Dimethyl-2-(3-methyl-1,4-dioxo-3,4-dihydro-1*H*-phthalazin-2-yl)-acetamide, 46



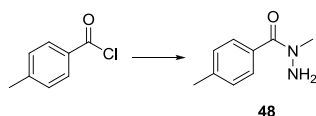
A suspension of phthalazine dione **43** (75 mg, 0.43 mmol), *N,N*-dimethyl-2-chloroacetamide (53  $\mu$ L, 0.51 mmol), K<sub>2</sub>CO<sub>3</sub> (147 mg, 1.07 mmol) and KI (71 mg, 0.43 mmol) in MeCN (4 mL) was stirred at reflux for 40 h. The reaction mixture was cooled, filtered and the solvent removed *in vacuo*. Column chromatography eluting with MeOH/EtOAc (2:98) afforded the title compound as a white solid (111 mg, 100%), mp 118-119 °C;  $R_f$  0.56 (EtOAc);  $\nu_{\max}$  (neat)/cm<sup>-1</sup> 2943, 1648, 1621, 1586, 1492, 1328;  $\delta_H$  (400 MHz, CDCl<sub>3</sub>) 8.35-8.28 (1H, m, Ar-H), 8.04-7.98 (1H, m, Ar-H), 7.74-7.67 (2H, m, Ar-H), 4.94 (2H, s, CH<sub>2</sub>N), 3.63 (3H, s, NNCH<sub>3</sub>), 3.03 (3H, s, NCH<sub>3</sub>), 2.95 (3H, s, NCH<sub>3</sub>);  $\delta_C$  (101 MHz, CDCl<sub>3</sub>) 167.1, 158.9, 148.9, 132.8, 132.1, 129.1, 126.9, 124.4, 123.7, 63.8, 38.9, 36.3, 35.7;  $m/z$  (ES) 325 (11%), 263 (15), 262 (MH<sup>+</sup>, 100). Found: MH<sup>+</sup>, 262.1198. C<sub>13</sub>H<sub>16</sub>N<sub>3</sub>O<sub>3</sub> requires MH<sup>+</sup>, 262.1192.

## 2-(3-Methoxy-propyl)-3-methyl-2,3-dihydro-phthalazine-1,4-dione, 47

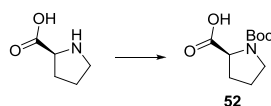


A suspension of phthalazine dione **43** (75 mg, 0.43 mmol), 1-chloro-3-methoxy-propane (55 mg, 0.51 mmol),  $K_2CO_3$  (147 mg, 1.07 mmol) and KI (71 mg, 0.43 mmol) in MeCN (4 mL) was stirred at reflux for 40 h. The reaction mixture was cooled, filtered and the solvent removed *in vacuo*. Column chromatography eluting with EtOAc/petrol (1:1  $\rightarrow$  4:1) afforded the title compound as a white solid (49 mg, 46%), mp 100-102 °C;  $R_f$  0.80 (EtOAc);  $\nu_{max}$  (neat)/ $cm^{-1}$  1649, 1621, 1590, 1328;  $\delta_H$  (400 MHz,  $CDCl_3$ ) 8.38-8.29 (1H, m, Ar-H), 7.95-7.87 (1H, m, Ar-H), 7.75-7.66 (2H, m, Ar-H), 4.33 (2H, t,  $J$  6.3,  $CH_2O$ ), 3.68 (3H, s,  $OCH_3$ ), 3.55 (2H, t,  $J$  6.3,  $CH_2N$ ), 3.33 (3H, s,  $NCH_3$ ), 2.08 (2H, quin,  $J$  6.3,  $CH_2CH_2O$ );  $\delta_C$  (101 MHz,  $CDCl_3$ ) 158.9, 149.8, 132.6, 131.9, 129.1, 127.0, 124.9, 123.5, 69.5, 64.0, 58.9, 38.9, 29.2;  $m/z$  (ES) 415 (4%), 250 (14), 249 ( $MH^+$ , 100). Found:  $MH^+$ , 249.123.4  $C_{13}H_{17}N_2O_3$  requires  $MH^+$ , 249.1239.

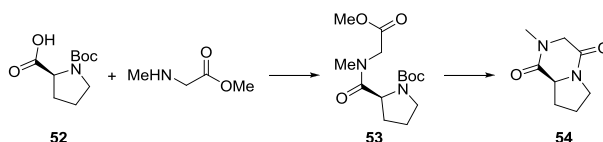
## 4-Methyl-benzoic acid *N*-methyl-hydrazide, 48<sup>209</sup>



A solution of *p*-toluoyl chloride (661  $\mu$ L, 5.0 mmol) in  $CH_2Cl_2$  (33 mL) was added to a solution of methylhydrazine (2.66 mL, 50 mmol) in  $CH_2Cl_2$  (33 mL) at 0 °C over 1.5 h, and the resulting solution stirred at 0 °C for 30 min and at r.t. for a further 1.5 h. The reaction mixture was poured into sat. aq.  $NaHCO_3$  (50 mL), and the aqueous layer extracted with  $CH_2Cl_2$  (3  $\times$  50 mL). The combined organic layers were dried ( $Na_2SO_4$ ) and the solvent removed *in vacuo*. Column chromatography eluting with MeOH:EtOAc (0:1  $\rightarrow$  5:95) afforded the title compound as a colourless oil which solidified on storage at -20 °C (824 mg, 100%),  $R_f$  0.60 (EtOAc);  $\delta_H$  (400 MHz,  $CDCl_3$ ) 7.33 (2H, d,  $J$  6.6, Ar 2-H, 6-H), 7.16 (2H, d, 7.9, Ar 3-H, 5-H), 4.34 (2H, br s,  $NH_2$ ), 3.18 (3H, s,  $NCH_3$ ), 2.33 (3H, s,  $ArCH_3$ );  $m/z$  (ES) 331 (4%), 228 (4), 166 (6), 165 ( $MH^+$ , 100). Found:  $MH^+$ , 165.1020.  $C_9H_{13}N_2O$  requires  $MH^+$ , 165.1028. Data is in agreement with the literature.<sup>209</sup>

**(S)-Pyrrolidine-1,2-dicarboxylic acid 1-*tert*-butyl ester, 52**<sup>210</sup>

To a stirred solution of L-proline (10.0 g, 86.9 mmol) in a mixture of 1 M NaOH (85 mL), dioxane (80 mL) and H<sub>2</sub>O (40 mL) at 0 °C was added di-*tert*-butyl dicarbonate (19.0 g, 86.9 mmol). The reaction mixture was stirred for 30 min at 0 °C and 2 h at r.t. before the dioxane was removed *in vacuo*. The remaining aqueous solution was washed with CH<sub>2</sub>Cl<sub>2</sub> (2 × 50 mL), acidified to pH 3 with citric acid, and extracted with EtOAc (3 × 100 mL). The combined organic layers were dried (MgSO<sub>4</sub>) and the solvent removed *in vacuo* to give a white crystalline powder. Recrystallised from EtOAc/petrol afforded the title compound as white crystals (14.0 g, 75%), mp 129-130 °C;  $\delta_{\text{H}}$  (400 MHz, CDCl<sub>3</sub>) (mixture of rotamers) 8.70 (1H, br s, OH), 4.36-4.16 (1H, m, CHCO), 3.69-3.18 (2H, m, CH<sub>2</sub>N), 2.37-1.74 (4H, m, CH<sub>2</sub>CH<sub>2</sub>CH), 1.44 (4.7H, s, C(CH<sub>3</sub>)<sub>3</sub>), 1.39 (4.3H, s, C(CH<sub>3</sub>)<sub>3</sub>); *m/z* (ES) 510 (85%), 341 (38), 336 (100), 279 (68), 238 (MNa<sup>+</sup>, 39). Found: MNa<sup>+</sup>, 238.1067. C<sub>10</sub>H<sub>17</sub>N<sub>2</sub>O<sub>4</sub>Na requires MNa<sup>+</sup>, 238.1055. Data is in agreement with the literature.<sup>210</sup>

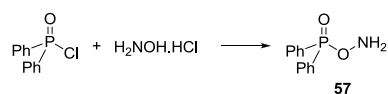
**(S)-2-Methyl-hexahydro-pyrrolo[1,2-*a*]pyrazine-1,4-dione, 54**<sup>211</sup>

To a stirred suspension of *N*-Boc L-proline **52** (5.00 g, 23.3 mmol), sarcosine methyl ester hydrochloride (3.25 g, 23.3 mmol), and NaHCO<sub>3</sub> (5.86 g, 69.8 mmol) in CH<sub>2</sub>Cl<sub>2</sub> (60 mL) at 0 °C was added EDC (4.68 g, 24.4 mmol). The reaction mixture was stirred for 18 h at r.t. before the addition of 1 M HCl (30 mL). The aqueous layer was then extracted with 30 mL CH<sub>2</sub>Cl<sub>2</sub> before being basified with 30 mL 20% aq. NaHCO<sub>3</sub> and extracted with CH<sub>2</sub>Cl<sub>2</sub> (3 × 30 mL). The combined organic layers were dried (MgSO<sub>4</sub>) and the solvent removed *in vacuo*. Partial purification by column chromatography eluting with EtOAc afforded crude dipeptide **53** (4.53 g), which was used directly in the subsequent ring-closure.

According to the method of Nitecki,<sup>212</sup> dipeptide **53** (4.12 g, 13.8 mmol) was dissolved in formic acid (100 mL) and stirred for 4 h at r.t. The solvent was removed *in vacuo* and the residue dissolved in a mixture of isobutanol (75 mL) and PhMe (25 mL). The solution was heated to 110 °C in an open flask for 3 h, removing any remaining formic acid and effecting cyclisation. The solvent was removed *in vacuo* and purification by column chromatography

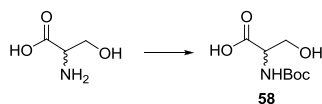
eluting with MeOH/EtOAc (0:1 → 1:9) afforded the title compound as a white gum (2.15 g, 60% over 2 steps),  $R_f$  0.14 (EtOAc);  $\delta_H$  (400 MHz,  $CDCl_3$ ) 4.08 (1H, d,  $J$  16.7,  $CH_3NCH_2$ ), 4.04-3.94 (1H, m, NCH), 3.69 (1H, d,  $J$  16.7,  $CH_3NCH_2$ ), 3.58-3.47 (1H, m,  $CH_2CH_2N$ ), 3.47-3.38 (1H, m,  $CH_2CH_2N$ ), 2.89 (3H, s,  $CH_3$ ), 2.34-2.25 (1H, m, proline 3-H or 4-H), 1.99-1.89 (2H, m, proline 3-H or 4-H), 1.86-1.77 (1H, m, proline 3-H or 4-H);  $m/z$  (ES) 335 (54%), 319 (21), 251 (100), 206 (22), 169 ( $MH^+$ , 57). Found:  $MH^+$ , 169.0973.  $C_8H_{13}N_2O_2$  requires  $MH^+$ , 169.0977. Data is in agreement with the literature.<sup>211</sup>

### ***O*-Diphenylphosphinyl hydroxylamine, 57**<sup>213</sup>



According to the method of Armstrong,<sup>213</sup> 7.1 M NaOH (7.0 mL) was added to a stirred solution of hydroxylamine hydrochloride (3.96 g, 57.0 mmol) in  $H_2O$  (8.5 mL). Dioxane (30 mL) was added and the solution cooled to 0 °C. Diphenylphosphinyl chloride (5.00 g, 21.1 mmol) in dioxane (25 mL) was added with vigorous stirring to give a white precipitate. After 4 min,  $H_2O$  (30 mL) was added and the slurry was filtered under vacuum, washing with cold  $H_2O$  (30 mL). The white solid was dried *in vacuo* for 3 h, then purified by stirring as a slurry with 0.25 M NaOH (50 mL) at 0 °C for 30 min. The product was filtered under vacuum, washing with cold  $H_2O$  (30 mL), then dried *in vacuo* for 7 d to give the title compound as a white powdery solid (1.90 g, 39%, *ca.* 90% purity), mp >150 (decomp.);  $\delta_H$  (400 MHz,  $CDCl_3$ ) 7.88-7.81 (4H, m, Ar-H), 7.57-7.53 (2H, m, Ar-H), 7.50-7.44 (4H, m, Ar-H), 1.74 (2H, br s,  $NH_2$ ). Data is in agreement with the literature.<sup>213</sup>

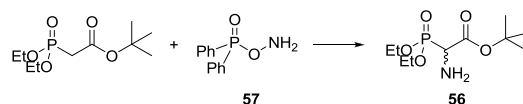
### ***N*-Boc DL-serine, 58**<sup>214</sup>



$Boc_2O$  (2.49 g, 11.4 mmol) was added to a stirred solution of DL-serine (1.00 g, 9.50 mmol) in 2:1 1 M NaOH/dioxane (30 mL) at 0 °C and stirred at r.t. overnight. The dioxane was removed *in vacuo* and the resulting aqueous solution was washed with  $Et_2O$  (2 × 40 mL). EtOAc (40 mL) was added followed by acidification with 1 M HCl to pH 2 whilst stirring. NaCl was added to the aqueous layer, which was then extracted with EtOAc (3 × 40 mL), dried ( $MgSO_4$ ), filtered and the solvent removed *in vacuo* to give the title compound as a colourless viscous oil (1.80 g, 92%, *ca.* 75% purity),  $\delta_H$  (400 MHz,  $CDCl_3$ ) 5.86 (1H, br d,  $J$

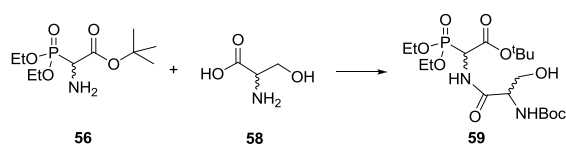
7.5, NH), 4.36 (1H, br s, CHNH), 4.09-4.00 (1H, m, CHHOH), 3.90-3.81 (1H, m, CHHOH), 1.44 (9H, s, C(CH<sub>3</sub>)<sub>3</sub>); *m/z* (ES<sup>-</sup>) 272 (100%), 204 (M<sup>-</sup>, 94), 174 (20), 130 (38). Found: M<sup>-</sup>, 204.0865. C<sub>8</sub>H<sub>14</sub>NO<sub>5</sub> requires M<sup>-</sup>, 204.0872. Data is in agreement with the literature.<sup>214</sup>

***tert*-Butyl  $\alpha$ -amino(diethylphosphono)acetate, **56**<sup>215</sup>**



*tert*-Butyl diethylphosphonoacetate (260  $\mu$ L, 1.12 mmol) was added dropwise to a stirred suspension of NaH (48 mg, 60% dispersion in mineral oil, 1.24 mmol) in THF (5 mL) at 0 °C and stirred for 30 min to give a clear solution. The solution was transferred by cannula to a stirred suspension of DPPONH<sub>2</sub> (**57**) (220 mg, 90% purity, 0.85 mmol) in THF (5 mL) at -78 °C. The reaction mixture was stirred for 2 h at -78 °C and 16 h at r.t. CH<sub>2</sub>Cl<sub>2</sub> (25 mL) was added and the solution was extracted with 20% aq. *p*-TsOH (3  $\times$  20 mL). The combined aqueous extracts were basified with NaHCO<sub>3</sub>, extracted with CH<sub>2</sub>Cl<sub>2</sub> (3  $\times$  50 mL), dried (MgSO<sub>4</sub>) and the solvent removed *in vacuo* to give the title compound as a colourless oil (160 mg, 70%),  $\delta_{\text{H}}$  (400 MHz, CDCl<sub>3</sub>) 4.21-4.12 (4H, m, 2  $\times$  OCH<sub>2</sub>), 3.81 (1H, d, *J* 19.9, CHNH<sub>2</sub>), 1.84 (2H, br s, NH<sub>2</sub>), 1.48 (9H, s, C(CH<sub>3</sub>)<sub>3</sub>), 1.36-1.30 (6H, m, CH<sub>2</sub>CH<sub>3</sub>);  $\delta_{\text{P}}$ [<sup>1</sup>H] (162 MHz, CDCl<sub>3</sub>) 20.48; *m/z* (ES) 557 (100%), 268 (MH<sup>+</sup>, 27). Found: MH<sup>+</sup>, 268.1325. C<sub>10</sub>H<sub>23</sub>NO<sub>5</sub>P requires MH<sup>+</sup>, 268.1314. Data is in agreement with the literature.<sup>215</sup>

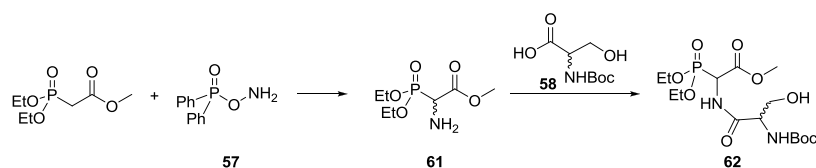
***tert*-Butyl (2-*tert*-butoxycarbonylamino-3-hydroxy-propionylamino)-(diethoxyphosphoryl)-acetate, **59****



To a solution of amine **56** (64 mg, 0.24 mmol) and carboxylic acid **58** (60 mg, 0.29 mmol) in 3:1 CH<sub>2</sub>Cl<sub>2</sub>/DMF (4 mL) at 0 °C was added NaHCO<sub>3</sub> (24 mg, 0.29 mmol), HOBt (46 mg, 0.34 mmol) and EDC (65 mg, 0.34 mmol). The reaction mixture was stirred for 16 h at r.t., whereupon H<sub>2</sub>O (5 mL) was added. The aqueous layer was extracted with EtOAc (3  $\times$  10 mL). The organic extracts were extracted with H<sub>2</sub>O (20 mL) and brine (20 mL), dried (Na<sub>2</sub>SO<sub>4</sub>) and the solvent removed *in vacuo* to give a colourless oil. Partial purification by column chromatography eluting with MeOH/EtOAc (0:1  $\rightarrow$  5:95) afforded the title compound as a colourless oil (90 mg, 83%, *ca.* 90% purity), *R<sub>f</sub>* 0.35 (EtOAc);  $\delta_{\text{H}}$  (400 MHz, CDCl<sub>3</sub>) 7.22-

7.03 (1H, m, NH), 5.61-5.47 (1H, m, NH), 5.05 (1H, dd,  $J$  21.1, 9.0, PCH), 4.30-3.98 (6H, m,  $2 \times \text{CH}_2\text{O}$ ,  $\text{CH}_2\text{OH}$ ), 3.70-3.62 (1H, m,  $\text{CHCH}_2\text{OH}$ ), 1.49 (9H, s,  $\text{C}(\text{CH}_3)_3$ ), 1.45 (9H, d,  $J$  4.7,  $\text{C}(\text{CH}_3)_3$ ), 1.38-1.30 (6H, m,  $2 \times \text{CH}_2\text{CH}_3$ );  $\delta_{\text{P}}$  (162 MHz,  $\text{CDCl}_3$ ) 17.2;  $m/z$  (ES) 539 (9%), 477 ( $\text{MNa}^+$ , 100), 455 ( $\text{MH}^+$ , 8), 343 (9). Found:  $\text{MH}^+$ , 455.2152.  $\text{C}_{18}\text{H}_{36}\text{N}_2\text{O}_9\text{P}$  requires  $\text{MH}^+$ , 455.2158.

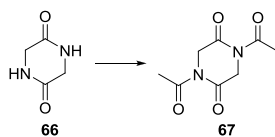
**Methyl (2-*tert*-butoxycarbonylamino-3-hydroxy-propionylamino)-(diethoxyphosphoryl)-acetate, 62**



Methyl diethylphosphonoacetate (220  $\mu\text{L}$ , 1.20 mmol) was added dropwise to a stirred suspension of NaH (52 mg, 60% dispersion in mineral oil, 1.30 mmol) in THF (5 mL) at 0 °C and stirred for 30 min to give a clear solution. The solution was transferred by cannula to a stirred suspension of DPPONH<sub>2</sub> (230 mg, 90% purity, 0.90 mmol) in THF (5 mL) at -78 °C. The reaction mixture was stirred for 2 h at -78 °C and 16 h at r.t.  $\text{CH}_2\text{Cl}_2$  (25 mL) was added and the solution was extracted with sat. aq. *p*-TsOH (3  $\times$  20 mL). The combined aqueous extracts were basified with  $\text{NaHCO}_3$ , extracted with  $\text{CH}_2\text{Cl}_2$  (3  $\times$  50 mL), dried ( $\text{MgSO}_4$ ) and the solvent removed *in vacuo* to give amine **61** which was used directly without further purification.

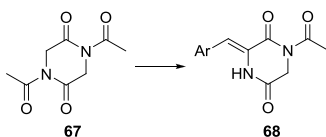
To a solution of amine **61** (130 mg, 0.59 mmol) and carboxylic acid **58** (150 mg, 0.71 mmol) in 3:1  $\text{CH}_2\text{Cl}_2/\text{DMF}$  (9 mL) at 0 °C was added  $\text{NaHCO}_3$  (70 mg, 0.83 mmol), HOBT (0.11 g, 0.83 mmol) and EDC (160 mg, 0.83 mmol). The reaction mixture was stirred for 16 h at r.t., whereupon  $\text{H}_2\text{O}$  (15 mL) was added. The aqueous layer was extracted with EtOAc (3  $\times$  20 mL), the organic extracts were extracted with  $\text{H}_2\text{O}$  (40 mL) and brine (40 mL), dried ( $\text{Na}_2\text{SO}_4$ ) and the solvent removed *in vacuo* to give a colourless oil. Partial purification by column chromatography eluting with MeOH/EtOAc (0:1 to 5:95) afforded the title compound as a colourless oil (150 mg, *ca.* 95% purity, 40% over 2 steps),  $R_f$  0.20 (EtOAc);  $\delta_{\text{H}}$  (400 MHz,  $\text{CDCl}_3$ ) 7.34 (1H, br s, NH), 5.57 (1H, br s, NH), 5.16 (1H, dd,  $J$  21.7, 8.9, PCH), 4.30-4.00 (6H, m,  $2 \times \text{CH}_2\text{O}$ ,  $\text{CH}_2\text{OH}$ ), 3.81 (3H, s,  $\text{OCH}_3$ ), 3.71-3.65 (1H, m,  $\text{CHCH}_2\text{OH}$ ), 1.46 (4.5H, s,  $\text{C}(\text{CH}_3)_3$ ), 1.45 (4.5H, s,  $\text{C}(\text{CH}_3)_3$ ), 1.38-1.29 (6H, m,  $2 \times \text{CH}_2\text{CH}_3$ ).

### 1,4-Diacetyl-piperazine-2,5-dione, **67** <sup>216</sup>



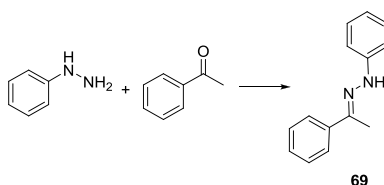
According to the method of Shawe,<sup>216</sup> a stirred suspension of glycine anhydride (25.0 g, 0.22 mol) in Ac<sub>2</sub>O (130 mL) was heated to reflux for 7 h. The solvent from the resulting brown solution was removed *in vacuo* and recrystallisation twice from EtOAc/hexane afforded the title compound as off-white amorphous crystals (37.5 g, 86%), mp 100-102 °C;  $\delta_{\text{H}}$  (400 MHz, CDCl<sub>3</sub>) 4.61 (4H, s, 2 × NCH<sub>2</sub>), 2.60 (6H, s, 2 × CH<sub>3</sub>);  $\delta_{\text{C}}$  (101 MHz, CDCl<sub>3</sub>) 170.8, 165.9, 47.2, 26.8; *m/z* (CI) 217 (12%), 216 (MNH<sub>4</sub><sup>+</sup>, 100), 174 (5), 77 (4), 52 (96). Found: MNH<sub>4</sub><sup>+</sup>, 216.0988. C<sub>8</sub>H<sub>14</sub>N<sub>3</sub>O<sub>4</sub> requires MNH<sub>4</sub><sup>+</sup>, 216.0984. Data is in agreement with the literature.<sup>216</sup>

### General procedure for synthesis of 1-acetyl-3-arylidene-piperazine-2,5-diones



According to the method of Gallina,<sup>106</sup> to a stirred solution of diacetyl-piperazine-2,5-dione **67** (1 eq.) and aldehyde (2 eq.) in CH<sub>2</sub>Cl<sub>2</sub> at 0 °C was added a solution of KO<sup>t</sup>Bu (1 eq.) in <sup>t</sup>BuOH. The reaction mixture was stirred at r.t. for 16 h and the resulting precipitate was isolated by filtration and washed with cold EtOAc.

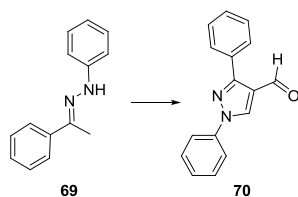
### *N*-Phenyl-*N'*-[1-phenyl-eth-(*E*)-ylidene]-hydrazine, **69** <sup>217</sup>



According to the method of Rathelot,<sup>217</sup> a solution of phenylhydrazine (550  $\mu$ L, 5.59 mmol), acetophenone (711  $\mu$ L, 6.10 mmol) and glacial acetic acid (0.25 mL) in EtOH (25 mL) was stirred at reflux for 6 h. The solvent was removed *in vacuo* and the resulting residue was triturated with petrol to give the title compound as a white powder (1.17 g, 99%), mp 102-103 °C;  $\delta_{\text{H}}$  (400 MHz, CDCl<sub>3</sub>) 7.93-7.86 (2H, m, Ar-H), 7.52-7.44 (2H, m, Ar-H), 7.44-7.36 (3H, m, Ar-H), 7.32-7.26 (2H, m, Ar-H), 7.03-6.95 (1H, m, Ar-H), 2.27 (3H, s, CH<sub>3</sub>); *m/z* (ES) 313 (5%), 212 (16), 211 (MH<sup>+</sup>, 100), 209 (3), 133 (2). Found: MH<sup>+</sup>, 211.1241. C<sub>14</sub>H<sub>15</sub>N<sub>2</sub> requires MH<sup>+</sup>, 211.1235. Data is in agreement with the literature.<sup>217</sup>

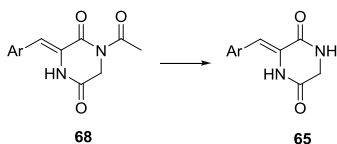


### 1,3-Diphenyl-1*H*-pyrazole-4-carbaldehyde, **70** <sup>218</sup>



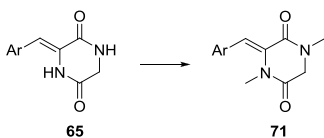
According to the method of Rathelot,<sup>217</sup> POCl<sub>3</sub> (666 μL, 7.14 mmol) was added dropwise to DMF (553 μL, 7.14 mmol) at 0 °C. The reaction mixture was stirred for 20 min to give a white solid. A solution of hydrazone **69** (500 mg, 2.38 mmol) in DMF (3 mL) was added dropwise at 0 °C and the reaction mixture was stirred at r.t. for 30 min to give a clear solution. The reaction was then heated to reflux for 5 h before being cooled to r.t. Sat. aq. K<sub>2</sub>CO<sub>3</sub> (8 mL) was added to give a suspension which was isolated by filtration, washing with cold H<sub>2</sub>O. The crude product was then dissolved in CH<sub>2</sub>Cl<sub>2</sub>, filtered to remove impurities and the solvent was removed *in vacuo*. Recrystallisation of the resulting solid from EtOH afforded the title compound as off-white amorphous crystals (427 mg, 72%), mp 146-147 °C; δ<sub>H</sub> (400 MHz, CDCl<sub>3</sub>) 10.07 (1H, s, CHO), 8.58 (1H, s, pyrazole-H), 7.90-7.80 (4H, m, Ar-H), 7.59-7.50 (5H, m, Ar-H), 7.46-7.40 (1H, m, Ar-H); *m/z* (ES) 250 (16%), 249 (MH<sup>+</sup>, 100), 227 (4), 218 (4), 206 (3). Found: MH<sup>+</sup>, 249.1031. C<sub>16</sub>H<sub>13</sub>N<sub>2</sub>O requires MH<sup>+</sup>, 249.1028. Data is in agreement with the literature.<sup>218</sup>

### General procedure for synthesis of 3-arylidene-piperazine-2,5-diones



To a stirred suspension of 1-acetyl-3-arylidene-piperazine-2,5-dione **68** in DMF (*ca.* 0.5 M) at r.t. was added dropwise hydrazine hydrate (4 eq.). The reaction mixture was stirred for 2.5 h before being poured onto an amount of ice approximately twice the volume of the reaction solvent. The precipitate was isolated by filtration and washed with cold H<sub>2</sub>O and EtOAc.

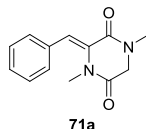
### General procedure for synthesis of 1,4-dimethyl 3-arylidene piperazine-2,5-diones



To a stirred suspension of 3-arylidene-piperazine-2,5-dione (1 eq.) and K<sub>2</sub>CO<sub>3</sub> (4 eq.) in DMF (*ca.* 0.1 M) at r.t. was added dropwise MeI (4 eq.). The reaction mixture was stirred for 16 h

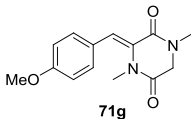
before being partitioned between EtOAc and 20% brine/H<sub>2</sub>O. The organic layer was extensively extracted with 20% brine/H<sub>2</sub>O to remove the DMF. The combined aqueous layers were then re-extracted with a small volume of EtOAc. The combined organic layers were dried (MgSO<sub>4</sub>) and the solvent removed *in vacuo*. The crude product was purified by column chromatography.

### 1,4-Dimethyl-3-[1-phenyl-meth-(Z)-ylidene]-piperazine-2,5-dione, 71a <sup>219</sup>



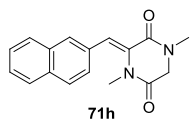
Colourless oil (500 mg, 52% over 3 steps),  $R_f$  0.56 (EtOAc);  $\delta_H$  (400 MHz, CDCl<sub>3</sub>) 7.45-7.18 (6H, m, 5 × Ar-H, C=CH), 4.12 (2H, s, CH<sub>2</sub>CO), 3.10 (3H, s, CH<sub>3</sub>), 2.89 (3H, s, CH<sub>3</sub>);  $m/z$  (ES) 308 (52%), 231 (MH<sup>+</sup>, 100), 217 (30), 208 (18), 197 (20). Found: MH<sup>+</sup>, 231.1138. C<sub>13</sub>H<sub>15</sub>N<sub>2</sub>O<sub>2</sub> requires MH<sup>+</sup>, 231.1134. Data is in agreement with the literature.<sup>219</sup>

### 3-[1-(4-Methoxy-phenyl)-meth-(Z)-ylidene]-1,4-dimethyl-piperazine-2,5-dione, 71g



White semi-solid (190 mg, 29% over 3 steps),  $R_f$  0.25 (CH<sub>2</sub>Cl<sub>2</sub>);  $\nu_{max}$  (CHCl<sub>3</sub>)/cm<sup>-1</sup> 1680, 1624, 1607, 1513, 1370, 1248, 1165, 911, 723;  $\delta_H$  (400 MHz, CDCl<sub>3</sub>) 7.16 (2H, d,  $J$  8.6, Ar-H), 7.10 (1H, s, C=CH), 6.85-6.80 (2H, d,  $J$  8.6, Ar-H), 4.02 (2H, s, CH<sub>2</sub>CO), 3.75 (3H, s, OCH<sub>3</sub>), 2.99 (3H, s, NCH<sub>3</sub>), 2.84 (3H, s, NCH<sub>3</sub>);  $\delta_C$  (101 MHz, CDCl<sub>3</sub>) 165.0, 162.8, 159.8, 131.0, 130.2, 125.8, 121.7, 113.8, 55.3, 52.4, 34.8, 34.0;  $m/z$  (ES) 427 (35%), 262 (15), 261 (MH<sup>+</sup>, 100), 232 (35), 211 (19). Found: MH<sup>+</sup>, 261.1248. C<sub>14</sub>H<sub>17</sub>N<sub>2</sub>O<sub>3</sub> requires MH<sup>+</sup>, 261.1239.

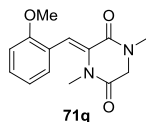
### 1,4-Dimethyl-3-[1-naphthalen-2-yl-meth-(Z)-ylidene]-piperazine-2,5-dione, 71h



Pale orange gum (282 mg, 54% over 3 steps),  $R_f$  0.42 (MeOH/CH<sub>2</sub>Cl<sub>2</sub> 5:95);  $\nu_{max}$  (CHCl<sub>3</sub>)/cm<sup>-1</sup> 1683, 1621, 1370, 1339, 1266, 733;  $\delta_H$  (400 MHz, CDCl<sub>3</sub>) 7.78-7.73 (3H, m, Ar-H), 7.67 (1H, s, C=CH), 7.47-7.40 (2H, m, Ar-H), 7.37 (2H, m, Ar-H), 4.07 (2H, s, CH<sub>2</sub>CO), 3.03 (3H, s, CH<sub>3</sub>), 2.84 (3H, s, CH<sub>3</sub>);  $\delta_C$  (101 MHz, CDCl<sub>3</sub>) 164.8, 162.4, 133.0, 132.9, 131.8, 131.2, 129.1, 128.1, 128.1, 127.7, 126.9, 126.8, 126.6, 121.8, 52.4, 35.2, 34.2;

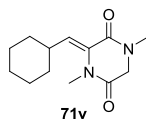
$m/z$  (ES) 447 (22%), 282 (20), 281 ( $\text{MH}^+$ , 100), 242 (33), 222 (21). Found:  $\text{MH}^+$ , 281.1298.  $\text{C}_{17}\text{H}_{17}\text{N}_2\text{O}_2$  requires  $\text{MH}^+$ , 281.1290.

### 3-[1-(2-Methoxy-phenyl)-meth-(Z)-ylidene]-1,4-dimethyl-piperazine-2,5-dione, 71q



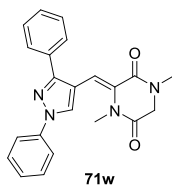
Colourless oil (187 mg, 28% over 3 steps),  $R_f$  0.53 (MeOH/EtOAc 5:95);  $\nu_{\text{max}}$  ( $\text{CHCl}_3$ )/ $\text{cm}^{-1}$  1680, 1624, 1596, 1485, 1426, 1370, 1245, 1026, 727;  $\delta_{\text{H}}$  (400 MHz,  $\text{CDCl}_3$ ) 7.34-7.28 (2H, m, Ar-H), 7.16 (1H, d,  $J$  7.8, C=CH), 6.97-6.87 (2H, m, Ar-H), 4.10 (2H, s,  $\text{CH}_2\text{CO}$ ), 3.84 (3H, s,  $\text{OCH}_3$ ), 3.08 (3H, s,  $\text{NCH}_3$ ), 2.82 (3H, s,  $\text{NCH}_3$ );  $\delta_{\text{C}}$  (101 MHz,  $\text{CDCl}_3$ ) 164.5, 162.4, 157.3, 131.9, 130.4, 130.1, 122.9, 120.2, 117.7, 110.5, 55.5, 52.3, 34.2, 34.0;  $m/z$  (ES) 386 (50%), 262 (8), 261 ( $\text{MH}^+$ , 100), 247 (24), 232 (42). Found:  $\text{MH}^+$ , 261.1237.  $\text{C}_{14}\text{H}_{17}\text{N}_2\text{O}_3$  requires  $\text{MH}^+$ , 261.1239.

### 3-[1-Cyclohexyl-meth-(Z)-ylidene]-1,4-dimethyl-piperazine-2,5-dione, 71v



White gum (141 mg, 24% over 3 steps),  $R_f$  0.53 (EtOAc);  $\nu_{\text{max}}$  ( $\text{CHCl}_3$ )/ $\text{cm}^{-1}$  2929, 2852, 1687, 1631, 1426, 1384, 1314, 991;  $\delta_{\text{H}}$  (400 MHz,  $\text{CDCl}_3$ ) 6.04 (1H, d,  $J$  6.0, C=CH), 3.95 (2H, s,  $\text{CH}_2\text{CO}$ ), 3.25 (3H, s,  $\text{NCH}_3$ ), 2.99 (3H, s,  $\text{NCH}_3$ ), 2.46-2.34 (1H, m, C=CCH), 1.80-1.73 (2H, m, Cy-H), 1.73-1.65 (3H, m, Cy-H), 1.34-1.16 (5H, m, Cy-H);  $\delta_{\text{C}}$  (101 MHz,  $\text{CDCl}_3$ ) 164.5, 163.0, 131.1, 130.5, 52.3, 37.0, 35.0, 33.9, 32.8, 25.7, 25.5;  $m/z$  (ES) 403 (50%), 314 (72), 240 (42), 237 ( $\text{MH}^+$ , 100), 220 (51). Found:  $\text{MH}^+$ , 237.1611.  $\text{C}_{13}\text{H}_{21}\text{N}_2\text{O}_2$  requires  $\text{MH}^+$ , 237.1603.

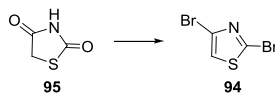
### 3-[1-(1,3-Diphenyl-1H-pyrazol-4-yl)-meth-(Z)-ylidene]-1,4-dimethyl-piperazine-2,5-dione, 71w



White gum (120 mg, 40% over 3 steps),  $R_f$  0.33 (MeOH/ $\text{CH}_2\text{Cl}_2$  2:98);  $\nu_{\text{max}}$  ( $\text{CHCl}_3$ )/ $\text{cm}^{-1}$  1684, 1632, 1598, 1502, 1370, 1268, 758, 695;  $\delta_{\text{H}}$  (400 MHz,  $\text{CDCl}_3$ ) 7.90 (1H, s, pyrazole-

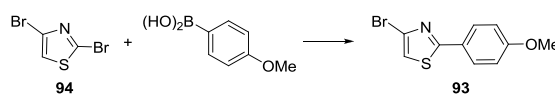
H), 7.76-7.71 (4H, m, Ar-H), 7.49-7.37 (5H, m, Ar-H), 7.31 (1H, t, *J* 7.4, Ar-H), 7.20 (1H, s, C=CH), 3.96 (2H, s, CH<sub>2</sub>CO), 3.03 (3H, s, NCH<sub>3</sub>), 2.95 (3H, s, CH<sub>3</sub>N);  $\delta_C$  (101 MHz, CDCl<sub>3</sub>) 164.5, 162.4, 152.6, 139.4, 132.3, 131.7, 129.6, 128.7, 128.6, 127.9, 127.8, 127.1, 119.1, 114.4, 112.7, 52.3, 34.2, 34.0; *m/z* (ES) 498 (6%), 389 (5), 374 (22), 373 (MH<sup>+</sup>, 100), 309 (6). Found: MH<sup>+</sup>, 373.1668. C<sub>22</sub>H<sub>21</sub>N<sub>4</sub>O<sub>2</sub> requires MH<sup>+</sup>, 373.1665.

### 2,4-Dibromo-thiazole, **94**<sup>220</sup>



Adapted from the method of Amb,<sup>150</sup> bromine (18.9 mL, 369 mmol) was added slowly to stirred PBr<sub>3</sub> (34.7 mL, 369 mmol) cooled in a water bath to give a yellow solid. P<sub>2</sub>O<sub>5</sub> (17.5 g, 123 mmol) was added and the solids thoroughly mixed with a spatula under N<sub>2</sub>. The reaction was then heated to 100 °C for 3 h to give a black oil, before being cooled to r.t. to give a black solid. Thiazolidine-2,4-dione (17.9 g, 154 mmol) was added, and the solids mixed thoroughly with a spatula under N<sub>2</sub>. The reaction mixture was then heated to 170 °C for 2.5 h before being cooled to r.t. and placed in a water bath. MeOH (200 mL) was then added very slowly down the condenser, resulting in a large volume of HBr gas, which was piped through a Dreschel bottle into a large container of sat. aq. Na<sub>2</sub>CO<sub>3</sub>. After 15 min stirring, the suspension was decanted into a large conical flask and neutralised by the addition of solid Na<sub>2</sub>CO<sub>3</sub>. The resulting suspension was partitioned between H<sub>2</sub>O (200 mL) and Et<sub>2</sub>O (200 mL), and the aqueous layer extracted with Et<sub>2</sub>O (4 × 200 mL). The combined organic layers were dried (MgSO<sub>4</sub>) and the solvent removed *in vacuo*. Recrystallisation from hexane afforded the title compound as pale brown crystals (11.3 g). The remaining oil was purified by column chromatography eluting with Et<sub>2</sub>O/petrol (0:1 → 5:95) to give the title compound as white rods (6.57 g, total yield 17.9 g, 48%), mp 78-81 °C; R<sub>f</sub> 0.30 (Et<sub>2</sub>O/petrol 5:95);  $\delta_H$  (400 MHz, CDCl<sub>3</sub>) 7.19 (1H, s, thiazole-H);  $\delta_C$  (101 MHz, CDCl<sub>3</sub>) 136.5, 124.4, 121.0; *m/z* (CI) 407 (15%), 405 (14), 246 (MH<sup>+</sup>, 51), 244 (MH<sup>+</sup>, 100), 242 (MH<sup>+</sup>, 49). Found MH<sup>+</sup>, 241.8276. C<sub>3</sub>H<sub>2</sub>NBr<sub>2</sub>S requires 241.8275. Data is in agreement with the literature.<sup>220</sup>

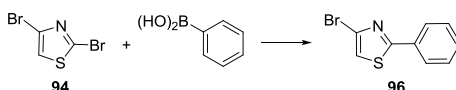
### 4-Bromo-2-(4-methoxy-phenyl)-thiazole, **93**<sup>221</sup>



A suspension of dibromothiazole **94** (122 mg, 0.50 mmol), 4-methoxyphenylboronic acid (91 mg, 0.60 mmol), K<sub>2</sub>CO<sub>3</sub> (173 mg, 1.25 mmol) and Pd(PPh<sub>3</sub>)<sub>4</sub> (17 mg, 0.015 mmol) in

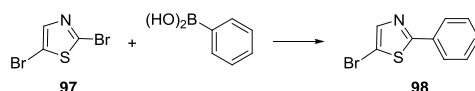
DME/H<sub>2</sub>O (4:1, 3 mL) was stirred at reflux for 72 h. The reaction was then partitioned between H<sub>2</sub>O (20 mL) and EtOAc (20 mL), the aqueous layer was extracted with EtOAc (3 × 20 mL) and the combined organic layers washed with brine (50 mL) and dried (Na<sub>2</sub>SO<sub>4</sub>). The solvent was removed *in vacuo* and purification by column chromatography eluting with Et<sub>2</sub>O/petrol (1:9 → 1:3) afforded the title compound as off-white rods (114 mg, 84%), mp 70-73 °C; R<sub>f</sub> 0.68 (Et<sub>2</sub>O/petrol 1:1); ν<sub>max</sub> (neat)/cm<sup>-1</sup> 3116, 1600, 1520, 1464, 1259; δ<sub>H</sub> (400 MHz, CDCl<sub>3</sub>) 7.87-7.80 (2H, m, Ar-H), 7.10 (1H, s, thiazole-H), 6.94-9.88 (2H, m, Ar-H), 3.82 (3H, s, CH<sub>3</sub>); δ<sub>C</sub> (101 MHz, CDCl<sub>3</sub>) 169.1, 161.8, 128.1, 125.8, 125.6, 115.6, 114.5, 55.6; *m/z* (CI) 295 (49%), 272 (MH<sup>+</sup>, 98), 271 (35), 270 (MH<sup>+</sup>, 100), 192 (26). Found MH<sup>+</sup>, 269.9588. C<sub>10</sub>H<sub>9</sub>NOBrS requires 269.9588. Data is in agreement with the literature.<sup>221</sup>

#### 4-Bromo-2-phenyl-thiazole, **96**<sup>149</sup>



A suspension of dibromothiazole **94** (500 mg, 2.1 mmol), phenylboronic acid (276 mg, 2.3 mmol), K<sub>2</sub>CO<sub>3</sub> (710 mg, 5.1 mmol) and Pd(PPh<sub>3</sub>)<sub>4</sub> (71 mg, 0.06 mmol) in DME/H<sub>2</sub>O (4:1, 15 mL) was stirred at reflux for 15 h. The reaction was then partitioned between H<sub>2</sub>O (30 mL) and EtOAc (30 mL). The aqueous layer was extracted with EtOAc (3 × 30 mL) and the combined organic layers washed with brine (60 mL) and dried (Na<sub>2</sub>SO<sub>4</sub>). The solvent was removed *in vacuo* and purification by column chromatography eluting with Et<sub>2</sub>O/petrol (1:4) afforded the title compound as an off-white solid (355 mg, 72%), mp 73-75 °C; R<sub>f</sub> 0.63 (EtOAc/petrol 1:4); δ<sub>H</sub> (400 MHz, CDCl<sub>3</sub>) 7.99-7.95 (2H, m, Ar-H), 7.50-7.46 (3H, m, Ar-H), 7.25 (1H, s, thiazole-H); *m/z* (CI) 243 (22%), 242 (MH<sup>+</sup>, 100), 241 (34), 240 (MH<sup>+</sup>, 98). Found MH<sup>+</sup>, 239.9477. C<sub>9</sub>H<sub>7</sub>NBrS requires 239.9483. Data is in agreement with the literature.<sup>149</sup>

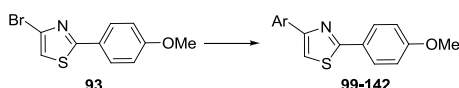
#### 5-Bromo-2-phenyl-thiazole, **98**<sup>149</sup>



A suspension of 2,5-dibromothiazole (485 mg, 1.9 mmol), phenylboronic acid (276 mg, 2.3 mmol), K<sub>2</sub>CO<sub>3</sub> (710 mg, 5.1 mmol) and Pd(PPh<sub>3</sub>)<sub>4</sub> (71 mg, 0.06 mmol) in DME/H<sub>2</sub>O (4:1, 15 mL) was stirred at reflux for 15 h. The reaction was then partitioned between H<sub>2</sub>O (30 mL) and EtOAc (30 mL). The aqueous layer was extracted with EtOAc (3 × 30 mL) and the combined organic layers washed with brine (60 mL) and dried (Na<sub>2</sub>SO<sub>4</sub>). The solvent was

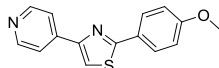
removed *in vacuo* and purification by column chromatography eluting with Et<sub>2</sub>O/petrol (1:6) afforded the title compound as a white solid (347 mg, 70%), mp 79-81 °C; R<sub>f</sub> 0.67 (EtOAc/petrol 1:4); δ<sub>H</sub> (400 MHz, CDCl<sub>3</sub>) 7.87-7.82 (2H, m, Ar-H), 7.72 (1H, s, thiazole-H), 7.45-7.40 (3H, m, Ar-H); *m/z* (CI) 244 (51%), 242 (MH<sup>+</sup>, 100), 241 (32), 240 (MH<sup>+</sup>, 96). Found MH<sup>+</sup>, 239.9479. C<sub>9</sub>H<sub>7</sub>NBrS requires 239.9483. Data is in agreement with the literature.<sup>149</sup>

#### Parallel Synthesis: General Procedure for Suzuki Couplings



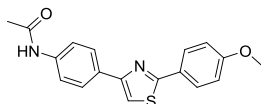
A solution of bromide **93** (27 mg, 100 μmol), boronic acid (120 μmol), K<sub>2</sub>CO<sub>3</sub> (35 mg, 250 μmol) and Pd(PPh<sub>3</sub>)<sub>4</sub> (3.5 mg, 3 μmol) in DME/H<sub>2</sub>O (4:1, 0.5 mL) was heated (MW, 160 °C, 20 min). Upon cooling, the reaction mixture was partitioned between H<sub>2</sub>O (5 mL) and CH<sub>2</sub>Cl<sub>2</sub> (10 mL), the organic layer separated, the solvent removed *in vacuo* and the product purified by HPLC under acidic conditions.

#### 4-[2-(4-Methoxy-phenyl)-thiazol-4-yl]-pyridine, **99** (JCC-CRT-10)



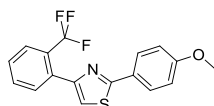
Light brown powder (2.0 mg, 7% yield, *ca.* 60% purity by <sup>1</sup>H-NMR), δ<sub>H</sub> (400 MHz, DMSO-d<sub>6</sub>) 8.68-8.65 (2H, m, pyridine 2-H, 6-H), 8.45 (1H, s, thiazole-H), 8.02-7.97 (4H, m, pyridine 3-H, 5-H, Ar 3-H, 5-H), 7.12-7.08 (2H, m, Ar 2-H, 6-H), 3.84 (3H, s, CH<sub>3</sub>). t<sub>R</sub> (HPLC) 2.60 min.

#### *N*-(4-[2-(4-Methoxy-phenyl)-thiazol-4-yl]-phenyl)-acetamide, **100**<sup>222</sup> (JCC-CRT-13)



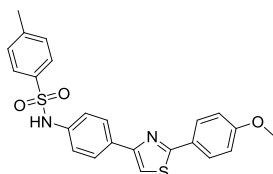
Light brown powder (2.0 mg, 6% yield, *ca.* 60% purity by <sup>1</sup>H-NMR), δ<sub>H</sub> (400 MHz, DMSO-d<sub>6</sub>) 10.07 (1H, s, NH), 7.98-7.93 (5H, m, Ar-H, thiazole-H), 7.67 (2H, d, *J* 8.8, Ar-H), 7.08 (2H, d, *J* 8.8, Ar-H), 3.84 (3H, s, OCH<sub>3</sub>), 2.06 (3H, s, COCH<sub>3</sub>). t<sub>R</sub> (HPLC) 3.65 min.

**2-(4-Methoxy-phenyl)-4-(2-trifluoromethyl-phenyl)-thiazole, 101** (JCC-CRT-16)



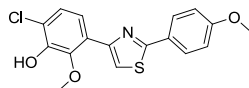
Orange gum (1.2 mg, 34% yield, *ca.* 98% purity by  $^1\text{H-NMR}$ ),  $\delta_{\text{H}}$  (400 MHz, DMSO- $\text{d}_6$ ) 7.95-7.84 (3H, m, 2  $\times$  Ar-H, thiazole-H), 7.82-7.71 (3H, m, Ar-H), 7.66 (1H, br. t,  $J$  7.4, Ar-H), 7.10-7.04 (2H, m, Ar-H), 3.83 (3H, s,  $\text{CH}_3$ ).  $t_{\text{R}}$  (HPLC) 4.13 min.

***N*-(4-[2-(4-Methoxy-phenyl)-thiazol-4-yl]-phenyl)-4-methyl-benzenesulfonamide, 102** <sup>222</sup>  
(JCC-CRT-17)



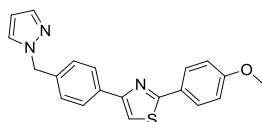
Light brown gum (0.9 mg, 22% yield, *ca.* 90% purity by  $^1\text{H-NMR}$ ),  $\delta_{\text{H}}$  (400 MHz, DMSO- $\text{d}_6$ ) 10.36 (1H, s, NH), 7.95-7.90 (3H, m, Ar-H, thiazole-H), 7.87 (2H, d,  $J$  8.6, Ar-H), 7.67 (2H, d,  $J$  8.3, Ar-H), 7.34 (2H, d,  $J$  8.3, Ar-H), 7.17 (2H, d,  $J$  8.6, Ar-H), 7.09-7.04 (2H, m, Ar-H), 3.83 (3H, s,  $\text{OCH}_3$ ), 2.32 (3H, s,  $\text{ArCH}_3$ ).  $t_{\text{R}}$  (HPLC) 4.05 min.

**6-Chloro-2-methoxy-3-[2-(4-methoxy-phenyl)-thiazol-4-yl]-phenol, 103** (JCC-CRT-22)



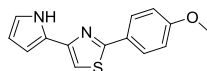
Dark brown solid (1.0 mg, 29% yield, *ca.* 80% purity by  $^1\text{H-NMR}$ ),  $\delta_{\text{H}}$  (400 MHz, DMSO- $\text{d}_6$ ) 9.65 (1H, s, OH), 8.04 (1H, s, thiazole-H), 8.01-7.92 (2H, m, Ar-H), 7.65 (1H, d,  $J$  1.9, Ar-H), 7.57 (1H, d,  $J$  1.9, Ar-H), 7.11-7.03 (2H, m, Ar-H), 3.93 (3H, s,  $\text{CH}_3$ ), 3.83 (3H, s,  $\text{CH}_3$ ).  $t_{\text{R}}$  (HPLC) 4.05 min.

**2-(4-Methoxy-phenyl)-4-(4-pyrazol-1-ylmethyl-phenyl)-thiazole, 104** (JCC-CRT-23)



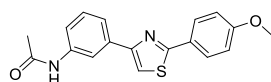
Light brown gum (0.6 mg, 18% yield, *ca.* 95% purity by  $^1\text{H-NMR}$ ),  $\delta_{\text{H}}$  (400 MHz, DMSO- $\text{d}_6$ ) 8.29 (1H, s, pyrazole-H), 7.95 (1H, s, thiazole-H), 7.93-7.89 (2H, m, Ar-H), 7.66 (1H, s, pyrazole-H), 7.39-7.25 (5H, m, pyrazole-H, 4  $\times$  Ar-H), 7.09-7.03 (2H, m, Ar-H), 5.38 (2H, s,  $\text{CH}_2$ ), 3.82 (3H, s,  $\text{CH}_3$ ).  $t_{\text{R}}$  (HPLC) 3.85 min.

**2-[2-(4-Methoxy-phenyl)-thiazol-4-yl]-pyrrole-1-carboxylic acid *tert*-butyl ester, 105** (JCC-CRT-24)



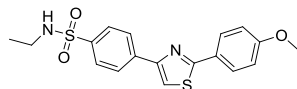
Brown solid (1.4 mg, 5% yield, *ca.* 80% purity by  $^1\text{H-NMR}$ ),  $\delta_{\text{H}}$  (400 MHz, DMSO- $d_6$ ) 11.33 (1H, s, NH), 7.98-7.91 (2H, m, Ar-H), 7.54 (1H, s, thiazole-H), 7.10-7.05 (2H, m, Ar-H), 6.83 (1H, d,  $J$  1.9, pyrrole-H), 6.56 (1H, m, pyrrole-H), 6.11 (1H, dd,  $J$  5.7, 1.9, pyrrole-H), 3.83 (3H, s,  $\text{CH}_3$ ).  $t_{\text{R}}$  (HPLC) 4.14 min.

***N*-(3-[2-(4-Methoxy-phenyl)-thiazol-4-yl]-phenyl)-acetamide, 106** (JCC-CRT-27)



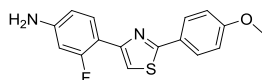
Light brown gum (2.7 mg, 8% yield, *ca.* 90% purity by  $^1\text{H-NMR}$ ),  $\delta_{\text{H}}$  (400 MHz, DMSO- $d_6$ ) 10.08 (1H, s, NH), 8.21 (1H, s, thiazole-H), 7.99 (1H, s, Ar-H), 7.98-7.94 (2H, m, Ar-H), 7.66 (2H, dd,  $J$  8.0, 1.8, Ar-H), 7.37 (1H, t,  $J$  7.9, Ar-H), 7.10 (2H, d,  $J$  8.9, Ar-H), 3.84 (3H, s,  $\text{OCH}_3$ ), 2.07 (3H, s,  $\text{COCH}_3$ ).  $t_{\text{R}}$  (HPLC) 3.64 min.

***N*-Ethyl-4-[2-(4-methoxy-phenyl)-thiazol-4-yl]-benzenesulfonamide, 107** (JCC-CRT-29)



Off-white powder (6.0 mg, 16% yield, *ca.* 98% purity by  $^1\text{H-NMR}$ ),  $\delta_{\text{H}}$  (400 MHz, DMSO- $d_6$ ) 8.30 (1H, s, thiazole-H), 8.24 (2H, d,  $J$  8.5, Ar-H), 7.99 (2H, d,  $J$  8.5, Ar-H), 7.87 (2H, d,  $J$  8.5, Ar-H), 7.61 (1H, t,  $J$  5.7, NH), 7.10 (2H, d,  $J$  8.5, Ar-H), 3.84 (3H, s,  $\text{OCH}_3$ ), 2.86-2.76 (2H, m,  $\text{CH}_2$ ), 0.98 (3H, t,  $J$  7.3,  $\text{CH}_2\text{CH}_3$ ).  $t_{\text{R}}$  (HPLC) 3.69 min.

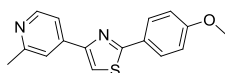
**3-Fluoro-4-[2-(4-methoxy-phenyl)-thiazol-4-yl]-phenylamine, 108** (JCC-CRT-30)



Light brown powder (9.9 mg, 33% yield, *ca.* 85% purity by  $^1\text{H-NMR}$ ),  $\delta_{\text{H}}$  (400 MHz, DMSO- $d_6$ ) 7.96-7.91 (2H, m, Ar-H), 7.79 (1H, d,  $J$  2.4, thiazole-H), 7.65 (1H, dd,  $J$  12.9, 1.7, Ar-H), 7.58 (1H, dd,  $J$  8.3, 1.8, Ar-H), 7.09-7.03 (2H, m, Ar-H), 6.82 (1H, dd,  $J$  9.2, 8.5, Ar-H), 5.38 (2H, s,  $\text{NH}_2$ ), 3.83 (3H, s,  $\text{CH}_3$ ).  $t_{\text{R}}$  (HPLC) 3.72 min.

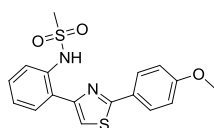


**4-[2-(4-Methoxy-phenyl)-thiazol-4-yl]-2-methyl-pyridine, 109** (JCC-CRT-31)



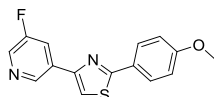
Off-white solid (2.3 mg, 8% yield, *ca.* 98% purity by  $^1\text{H-NMR}$ ),  $\delta_{\text{H}}$  (400 MHz, DMSO- $d_6$ ) 8.52 (1H, d, *J* 5.2, pyridine-H), 8.40 (1H, s, thiazole-H), 8.02-7.95 (2H, m, Ar-H), 7.88 (1H, s, pyridine-H), 7.78 (1H, d, *J* 5.2, pyridine-H), 7.12-7.06 (2H, m, Ar-H), 3.84 (3H, s, OCH<sub>3</sub>), 2.55 (3H, s, ArCH<sub>3</sub>).  $t_{\text{R}}$  (HPLC) 4.05 min.

***N*-(2-[2-(4-Methoxy-phenyl)-thiazol-4-yl]-phenyl)-methanesulfonamide, 110** (JCC-CRT-32)



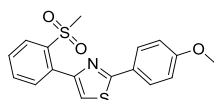
Light brown solid (1.6 mg, 4% yield, *ca.* 85% purity by  $^1\text{H-NMR}$ ),  $\delta_{\text{H}}$  (400 MHz, DMSO- $d_6$ ) 8.29 (1H, s, NH), 8.00-7.94 (3H, m, thiazole-H, 2  $\times$  Ar-H), 7.56 (2H, d, *J* 7.5, Ar-H), 7.42 (1H, t, *J* 7.1, Ar-H), 7.23 (1H, t, *J* 7.5, Ar-H), 7.12 (2H, d, *J* 8.8, Ar-H), 3.85 (3H, s, OCH<sub>3</sub>), 3.06 (3H, s, SO<sub>2</sub>CH<sub>3</sub>).  $t_{\text{R}}$  (HPLC) 3.74 min.

**3-Fluoro-5-[2-(4-methoxy-phenyl)-thiazol-4-yl]-pyridine, 111** (JCC-CRT-34)



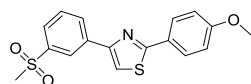
Light brown powder (0.9 mg, 3% yield, *ca.* 85% purity by  $^1\text{H-NMR}$ ),  $\delta_{\text{H}}$  (400 MHz, DMSO- $d_6$ ) 9.15 (1H, s, pyridine-H), 8.58 (1H, d, *J* 2.7, pyridine-H), 8.38 (1H, s, thiazole-H), 8.33-8.28 (1H, m, pyridine-H), 8.04-7.98 (2H, m, Ar-H), 7.10 (2H, d, *J* 8.9, Ar-H), 3.84 (3H, s, CH<sub>3</sub>).  $t_{\text{R}}$  (HPLC) 3.87 min.

**4-(2-Methanesulfonyl-phenyl)-2-(4-methoxy-phenyl)-thiazole, 112** (JCC-CRT-35)



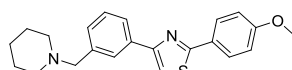
Light brown powder (2.1 mg, 6% yield, *ca.* 60% purity by  $^1\text{H-NMR}$ ),  $\delta_{\text{H}}$  (400 MHz, DMSO- $d_6$ ) 8.11 (1H, d, *J* 6.8, Ar-H), 7.89 (2H, d, *J* 8.8, Ar-H), 7.76-7.72 (1H, m, Ar-H), 7.70 (1H, d, *J* 7.4, Ar-H), 7.11-7.06 (2H, m, Ar-H), 3.83 (3H, s, OCH<sub>3</sub>), 3.52 (3H, s, SO<sub>2</sub>CH<sub>3</sub>).  $t_{\text{R}}$  (HPLC) 3.30 min.

**4-(3-Methanesulfonyl-phenyl)-2-(4-methoxy-phenyl)-thiazole, 113 (JCC-CRT-51)**



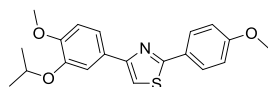
Off-white powder (14.4 mg, 42% yield, *ca.* 98% purity by  $^1\text{H-NMR}$ ),  $\delta_{\text{H}}$  (400 MHz,  $\text{DMSO-d}_6$ ) 8.55 (1H, t,  $J$  1.6, Ar-H), 8.38 (1H, dt,  $J$  8.1, 1.1, Ar-H), 8.34 (1H, s, thiazole-H), 7.99 (2H, d,  $J$  8.8, Ar-H), 7.92 (1H, dt,  $J$  8.0, 1.1, Ar-H), 7.76 (1H, t,  $J$  7.8, Ar-H), 7.10 (2H, d,  $J$  8.8, Ar-H), 3.84 (3H, d,  $J$  3.3,  $\text{OCH}_3$ ), 3.30 (3H, s,  $\text{SO}_2\text{CH}_3$ ).  $t_{\text{R}}$  (HPLC) 3.59 min.

**1-(3-[2-(4-Methoxy-phenyl)-thiazol-4-yl]-benzyl)-piperidine, 114 (JCC-CRT-54)**



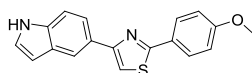
Light brown gum (16.0 mg, 44% yield, *ca.* 95% purity by  $^1\text{H-NMR}$ ),  $\delta_{\text{H}}$  (400 MHz,  $\text{DMSO-d}_6$ ) 8.19 (1H, s, thiazole-H), 8.06 (1H, s, Ar-H), 7.98-7.95 (2H, m, Ar-H), 7.91 (1H, d,  $J$  7.8, Ar-H), 7.42 (1H, t,  $J$  7.6, Ar-H), 7.30 (1H, d,  $J$  7.6, Ar-H), 7.12-7.05 (2H, m, Ar-H), 3.84 (3H, s,  $\text{CH}_3$ ), 3.55 (2H, s,  $\text{NCH}_2\text{Ar}$ ), 2.45-2.37 (4H, m,  $2 \times \text{NCH}_2\text{CH}_2$ ), 1.57-1.48 (4H, m,  $2 \times \text{NCH}_2\text{CH}_2$ ), 1.44-1.36 (2H, m,  $\text{NCH}_2\text{CH}_2\text{CH}_2$ ).  $t_{\text{R}}$  (HPLC) 2.25 min.

**4-(3-Isopropoxy-4-methoxy-phenyl)-2-(4-methoxy-phenyl)-thiazole, 115 (JCC-CRT-55)**



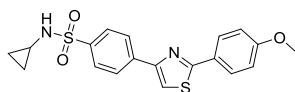
Brown oil (8.0 mg, 22% yield, *ca.* 95% purity by  $^1\text{H-NMR}$ ),  $\delta_{\text{H}}$  (400 MHz,  $\text{DMSO-d}_6$ ) 7.97-7.92 (3H, m, thiazole-H, Ar-H), 7.62-7.57 (2H, m, Ar-H), 7.10-7.02 (3H, m, Ar-H), 4.66 (1H, hept,  $J$  6.0,  $\text{CH}(\text{CH}_3)_2$ ), 3.83 (3H, s,  $\text{OCH}_3$ ), 3.80 (3H, s,  $\text{OCH}_3$ ), 1.29 (6H, d,  $J$  6.1,  $\text{CH}(\text{CH}_3)_2$ ).  $t_{\text{R}}$  (HPLC) 4.51 min.

**5-[2-(4-Methoxy-phenyl)-thiazol-4-yl]-1H-indole, 116 (JCC-CRT-56)**



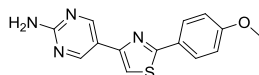
Light brown powder (14.7 mg, 48% yield, *ca.* 90% purity by  $^1\text{H-NMR}$ ),  $\delta_{\text{H}}$  (400 MHz,  $\text{DMSO-d}_6$ ) 11.18 (1H, s, NH), 8.26 (1H, s, thiazole-H), 8.01-7.95 (2H, m, Ar-H), 7.87 (1H, s, Ar-H), 7.78 (1H, dd,  $J$  8.5, 1.6, Ar-H), 7.46 (1H, d,  $J$  8.4, Ar-H), 7.40-7.36 (1H, m, Ar-H), 7.12-7.06 (2H, m, Ar-H), 6.51 (1H, d,  $J$  2.0, Ar-H), 3.84 (3H, s,  $\text{CH}_3$ ).  $t_{\text{R}}$  (HPLC) 3.99 min.

***N*-Cyclopropyl-4-[2-(4-methoxy-phenyl)-thiazol-4-yl]-benzenesulfonamide, 117** (JCC-CRT-57)



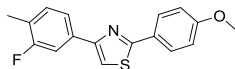
Light brown powder (15.2 mg, 39% yield, *ca.* 95% purity by  $^1\text{H-NMR}$ ),  $\delta_{\text{H}}$  (400 MHz, DMSO- $\text{d}_6$ ) 8.30 (1H, s, thiazole-H), 8.29-8.24 (2H, m, Ar-H), 8.01-7.96 (2H, m, Ar-H), 7.94 (1H, d, *J* 2.7, NH), 7.92-7.87 (2H, m, Ar-H), 7.12-7.07 (2H, m, Ar-H), 3.84 (3H, s,  $\text{CH}_3$ ), 2.19-2.11 (1H, m, NCH), 0.52-0.46 (2H, m,  $\text{CH}_2$ ), 0.42-0.36 (2H, m,  $\text{CH}_2$ ).  $t_{\text{R}}$  (HPLC) 3.82 min.

**5-[2-(4-Methoxy-phenyl)-thiazol-4-yl]-pyrimidin-2-ylamine, 118** (JCC-CRT-59)



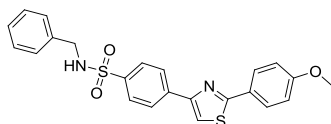
White powder (7.1 mg, 25% yield, *ca.* 80% purity by  $^1\text{H-NMR}$ ),  $\delta_{\text{H}}$  (400 MHz, DMSO- $\text{d}_6$ ) 8.86 (2H, s,  $\text{NH}_2$ ), 7.97-7.93 (2H, m, Ar-H), 7.92 (1H, s, thiazole-H), 7.10-7.04 (2H, m, Ar-H), 6.89 (2H, s, pyrimidine-H), 3.83 (3H, s,  $\text{CH}_3$ ).  $t_{\text{R}}$  (HPLC) 3.30 min.

**4-(3-Fluoro-4-methyl-phenyl)-2-(4-methoxy-phenyl)-thiazole, 119** (JCC-CRT-60)



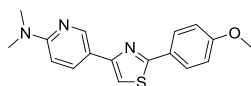
Light brown powder (3.2 mg, 11% yield, *ca.* 95% purity by  $^1\text{H-NMR}$ ),  $\delta_{\text{H}}$  (400 MHz, DMSO- $\text{d}_6$ ) 8.13 (1H, s, thiazole-H), 8.01-7.94 (2H, m, Ar-H), 7.80 (1H, d, *J* 1.3, Ar-H), 7.78 (1H, s, Ar-H), 7.38 (1H, t, *J* 8.0, Ar-H), 7.11-7.05 (2H, m, Ar-H), 3.84 (3H, s,  $\text{OCH}_3$ ), 2.28 (3H, d, *J* 1.3,  $\text{ArCH}_3$ ).  $t_{\text{R}}$  (HPLC) 5.23 min.

***N*-Benzyl-4-[2-(4-methoxy-phenyl)-thiazol-4-yl]-benzenesulfonamide, 120** (JCC-CRT-62)



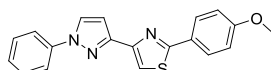
Off-white powder (6.8 mg, 16% yield, *ca.* 95% purity by  $^1\text{H-NMR}$ ),  $\delta_{\text{H}}$  (400 MHz, DMSO- $\text{d}_6$ ) 8.30 (1H, s, thiazole-H), 8.25-8.17 (3H, m, NH, 2  $\times$  Ar-H), 8.02-7.97 (2H, m, Ar-H), 7.92-7.87 (2H, m, Ar-H), 7.32-7.18 (5H, m, Ar-H), 7.14-7.06 (2H, m, Ar-H), 4.02 (2H, d, *J* 5.8,  $\text{CH}_2$ ), 3.85 (3H, s,  $\text{CH}_3$ ).  $t_{\text{R}}$  (HPLC) 4.10 min.

**(5-[2-(4-Methoxy-phenyl)-thiazol-4-yl]-pyridin-2-yl)-dimethyl-amine, 121 (JCC-CRT-63)**



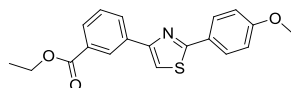
Yellow powder (6.5 mg, 21% yield, *ca.* 98% purity by  $^1\text{H-NMR}$ ),  $\delta_{\text{H}}$  (400 MHz, DMSO- $d_6$ ) 8.76 (1H, d, *J* 2.4, pyridine-H), 8.09 (1H, dd, *J* 8.9, 2.4, pyridine-H), 7.98-7.92 (2H, m, Ar-H), 7.83 (1H, s, thiazole-H), 7.12-7.04 (2H, m, Ar-H), 6.72 (1H, d, *J* 8.9, pyridine-H), 3.83 (3H, s, OCH<sub>3</sub>), 3.08 (6H, s, N(CH<sub>3</sub>)<sub>2</sub>).  $t_{\text{R}}$  (HPLC) 2.44 min.

**2-(4-Methoxy-phenyl)-4-(1-phenyl-1H-pyrazol-3-yl)-thiazole, 122 (JCC-CRT-65)**



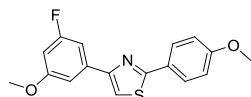
Light brown powder (12.0 mg, 36% yield, *ca.* 98% purity by  $^1\text{H-NMR}$ ),  $\delta_{\text{H}}$  (400 MHz, DMSO- $d_6$ ) 8.62 (1H, d, *J* 2.4, pyrazole-H), 8.49 (1H, t, *J* 1.8, ArH), 8.24 (1H, s, thiazole-H), 8.04-7.94 (3H, m, Ar-H), 7.88-7.81 (1H, m, Ar-H), 7.80 (1H, d, *J* 1.6, Ar-H), 7.59 (1H, t, *J* 7.9, Ar-H), 7.14-7.06 (2H, m, Ar-H), 6.59 (1H, dd, *J* 2.4, 1.7, pyrazole-H), 3.84 (3H, s, CH<sub>3</sub>).  $t_{\text{R}}$  (HPLC) 4.23 min.

**3-[2-(4-Methoxy-phenyl)-thiazol-4-yl]-benzoic acid ethyl ester, 123 (JCC-CRT-67)**



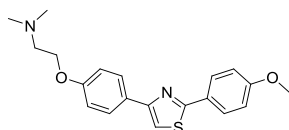
Off-white powder (5.8 mg, 17% yield, *ca.* 98% purity by  $^1\text{H-NMR}$ ),  $\delta_{\text{H}}$  (400 MHz, DMSO- $d_6$ ) 8.60 (1H, t, *J* 1.6, Ar-H), 8.32-8.27 (1H, m, Ar-H), 8.24 (1H, s, thiazole-H), 8.02-7.93 (3H, m, Ar-H), 7.63 (1H, t, *J* 7.8, Ar-H), 7.15-7.05 (2H, m, Ar-H), 4.37 (2H, q, *J* 7.2, CH<sub>2</sub>), 3.84 (3H, s, OCH<sub>3</sub>), 1.36 (3H, t, *J* 7.1, CH<sub>2</sub>CH<sub>3</sub>).  $t_{\text{R}}$  (HPLC) 4.86 min.

**4-(3-Fluoro-5-methoxy-phenyl)-2-(4-methoxy-phenyl)-thiazole, 124 (JCC-CRT-68)**



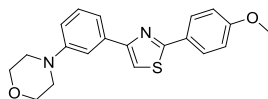
Off-white powder (8.7 mg, 28% yield, *ca.* 95% purity by  $^1\text{H-NMR}$ ),  $\delta_{\text{H}}$  (400 MHz, DMSO- $d_6$ ) 8.22 (1H, s, thiazole-H), 8.01-7.94 (2H, m, Ar-H), 7.48-7.42 (2H, m, Ar-H), 7.12-7.04 (2H, m, Ar-H), 6.84 (1H, dt, *J* 10.8, 2.3, Ar-H), 3.85 (3H, s, CH<sub>3</sub>), 3.84 (3H, s, CH<sub>3</sub>).  $t_{\text{R}}$  (HPLC) 4.83 min.

**(2-(4-[2-(4-Methoxy-phenyl)-thiazol-4-yl]-phenoxy)-ethyl)-dimethyl-amine, 125** (JCC-CRT-71)



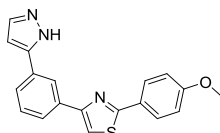
Off-white solid (7.4 mg, 21% yield, *ca.* 90% purity by  $^1\text{H-NMR}$ ),  $\delta_{\text{H}}$  (400 MHz, DMSO- $d_6$ ) 8.18 (1H, s, thiazole-H), 7.99-7.92 (4H, m, Ar-H), 7.11-7.00 (4H, m, Ar-H), 4.12 (2H, t,  $J$  5.7, OCH $_2$ ), 3.83 (3H, s, OCH $_3$ ), 2.71 (2H, t,  $J$  5.8, NCH $_2$ ), 2.28 (6H, s, N(CH $_3$ ) $_2$ ).  $t_{\text{R}}$  (HPLC) 2.21 min.

**4-(3-[2-(4-Methoxy-phenyl)-thiazol-4-yl]-phenyl)-morpholine, 126** (JCC-CRT-72)



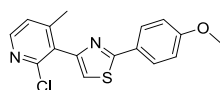
Light brown powder (11.4 mg, 32% yield, *ca.* 98% purity by  $^1\text{H-NMR}$ ),  $\delta_{\text{H}}$  (400 MHz, DMSO- $d_6$ ) 8.07 (1H, s, thiazole-H), 8.01-7.93 (2H, m, Ar-H), 7.63-7.57 (1H, m, Ar-H), 7.48 (1H, d,  $J$  7.8, Ar-H), 7.31 (1H, t,  $J$  8.0, Ar-H), 7.11-7.05 (2H, m, Ar-H), 6.95 (1H, dd,  $J$  8.1, 2.1, Ar-H), 3.83 (3H, s, CH $_3$ ), 3.81-3.73 (4H, m, 2  $\times$  OCH $_2$ ), 3.22-3.16 (4H, m, 2  $\times$  NCH $_2$ ).  $t_{\text{R}}$  (HPLC) 4.27 min.

**2-(4-Methoxy-phenyl)-4-[3-(2H-pyrazol-3-yl)-phenyl]-thiazole, 127** (JCC-CRT-73)



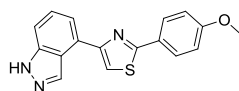
Brown gum (11.3 mg, 34% yield, *ca.* 80% purity by  $^1\text{H-NMR}$ ),  $\delta_{\text{H}}$  (400 MHz, DMSO- $d_6$ ) 8.47 (1H, s, Ar-H), 8.16 (1H, s, thiazole-H), 8.04-7.93 (3H, m, Ar-H), 7.80 (2H, m, Ar-H), 7.51 (1H, t,  $J$  7.7, Ar-H), 7.16-7.07 (2H, m, Ar-H), 6.82 (1H, d,  $J$  2.1, Ar-H), 3.84 (3H, s, CH $_3$ ).  $t_{\text{R}}$  (HPLC) 4.04 min.

**2-Chloro-3-[2-(4-methoxy-phenyl)-thiazol-4-yl]-4-methyl-pyridine, 128** (JCC-CRT-74)



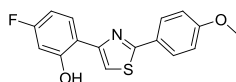
Off-white solid (14.1 mg, 44%, *ca.* 3:1 starting material/product),  $\delta_{\text{H}}$  (400 MHz, DMSO- $d_6$ ) 8.34 (1H, d,  $J$  5.0, pyridine-H), 7.91 (2H, d,  $J$  8.8, Ar-H), 7.79 (1H, s, thiazole-H), 7.43 (1H, d,  $J$  4.9, pyridine-H), 7.06 (2H, d,  $J$  8.8, Ar-H), 3.83 (3H, s, OCH $_3$ ), 2.20 (3H, s, ArCH $_3$ ).

**4-[2-(4-Methoxy-phenyl)-thiazol-4-yl]-1H-indazole, 129** (JCC-CRT-75)



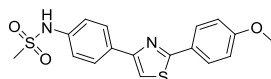
Off-white solid (12.8 mg, 42% yield, *ca.* 98% purity by  $^1\text{H-NMR}$ ),  $\delta_{\text{H}}$  (400 MHz, DMSO- $\text{d}_6$ ) 13.25 (1H, s, NH), 8.71 (1H, s, indazole 3-H), 8.27 (1H, s, thiazole-H), 8.08-8.00 (2H, m, Ar-H), 7.80 (1H, d, *J* 6.8, Ar-H), 7.57 (1H, d, *J* 8.3, Ar-H), 7.48-7.41 (1H, m, Ar-H), 7.16-7.09 (2H, m, Ar-H), 3.85 (3H, s,  $\text{CH}_3$ ).  $t_{\text{R}}$  (HPLC) 3.88 min.

**5-Fluoro-2-[2-(4-methoxy-phenyl)-thiazol-4-yl]-phenol, 130** (JCC-CRT-77)



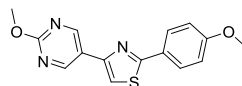
Light brown solid (11.2 mg, 37% yield, *ca.* 98% purity by  $^1\text{H-NMR}$ ),  $\delta_{\text{H}}$  (400 MHz, DMSO- $\text{d}_6$ ) 11.27 (1H, s, OH), 8.20-8.12 (1H, m, Ar-H), 8.10 (1H, s, thiazole-H), 7.98-7.90 (2H, m, Ar-H), 7.13-7.05 (2H, m, Ar-H), 6.81-6.73 (2H, m, Ar-H), 3.84 (3H, s,  $\text{CH}_3$ ).  $t_{\text{R}}$  (HPLC) 4.85 min.

***N*-(4-[2-(4-Methoxy-phenyl)-thiazol-4-yl]-phenyl)-methanesulfonamide, 131** (JCC-CRT-92)



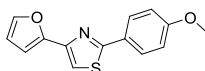
Very light brown powder (13.9 mg, 39% yield, *ca.* 90% purity by  $^1\text{H-NMR}$ ),  $\delta_{\text{H}}$  (400 MHz, DMSO- $\text{d}_6$ ) 9.93 (1H, s, NH), 8.04-7.93 (5H, m, 4  $\times$  Ar-H, thiazole-H), 7.29 (2H, d, *J* 8.6, Ar-H), 7.08 (2H, d, *J* 8.6, Ar-H), 3.83 (3H, s,  $\text{OCH}_3$ ), 3.03 (3H, s,  $\text{SO}_2\text{CH}_3$ ).  $t_{\text{R}}$  (HPLC) 3.61 min.

**2-Methoxy-5-[2-(4-methoxy-phenyl)-thiazol-4-yl]-pyrimidine, 132** (JCC-CRT-95)



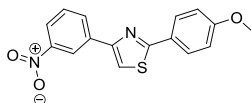
Light brown solid (5.6 mg, 19%, *ca.* 1.25:1 starting material/product),  $\delta_{\text{H}}$  (400 MHz, DMSO- $\text{d}_6$ ) 9.21 (2H, s, pyrimidine-H), 8.20 (1H, s, thiazole-H), 8.02-7.96 (2H, m, Ar-H), 7.09 (2H, m, Ar-H), 3.98 (3H, s,  $\text{CH}_3$ ), 3.84 (3H, s,  $\text{CH}_3$ ).

**4-Furan-2-yl-2-(4-methoxy-phenyl)-thiazole, 133<sup>223</sup>** (JCC-CRT-97)



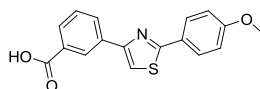
Off-white powder (3.0 mg, 12% yield, *ca.* 95% purity by <sup>1</sup>H-NMR),  $\delta_{\text{H}}$  (400 MHz, DMSO-*d*<sub>6</sub>) 7.97-7.91 (2H, m, Ar-H), 7.78-7.76 (2H, m, thiazole-H, furan-H), 7.10-7.06 (2H, m, Ar-H), 6.88 (1H, d, *J* 3.2, furan-H), 6.63 (1H, dd, *J* 3.3, 1.8, furan-H), 3.83 (3H, s, CH<sub>3</sub>). *t*<sub>R</sub> (HPLC) 3.97 min.

**2-(4-Methoxy-phenyl)-4-(3-nitro-phenyl)-thiazole, 134** (JCC-CRT-99)



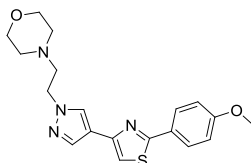
Light brown solid (3.6 mg, 12% yield, *ca.* 90% purity by <sup>1</sup>H-NMR),  $\delta_{\text{H}}$  (400 MHz, DMSO-*d*<sub>6</sub>) 8.85-8.81 (1H, m, Ar-H), 8.51-8.46 (1H, m, Ar-H), 8.42 (1H, s, thiazole-H), 8.26-8.19 (1H, m, Ar-H), 8.04-7.95 (2H, m, Ar-H), 7.78 (1H, t, *J* 8.0, Ar-H), 7.15-7.06 (2H, m, Ar-H), 3.84 (3H, s, CH<sub>3</sub>). *t*<sub>R</sub> (HPLC) 4.73 min.

**3-[2-(4-Methoxy-phenyl)-thiazol-4-yl]-benzoic acid, 135** (JCC-CRT-100)



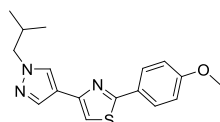
Light brown solid (6.1 mg, 20% yield, *ca.* 80% purity by <sup>1</sup>H-NMR),  $\delta_{\text{H}}$  (400 MHz, DMSO-*d*<sub>6</sub>) 13.17 (1H, br s, OH), 8.60 (1H, s, Ar-H), 8.27 (1H, d, *J* 7.8, Ar-H), 8.23 (1H, s, thiazole-H), 7.98 (2H, d, *J* 8.8, Ar-H), 7.94 (1H, d, *J* 7.7, Ar-H), 7.60 (1H, t, *J* 7.7, Ar-H), 7.10 (2H, d, *J* 8.8, Ar-H), 3.84 (3H, s, CH<sub>3</sub>). *t*<sub>R</sub> (HPLC) 3.90 min.

**4-(2-(4-[2-(4-Methoxy-phenyl)-thiazol-4-yl]-pyrazol-1-yl)-ethyl)-morpholine, 136** (JCC-CRT-101)



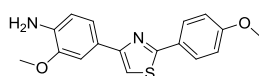
Light brown gum (16.6 mg, 45% yield, *ca.* 95% purity by <sup>1</sup>H-NMR),  $\delta_{\text{H}}$  (400 MHz, DMSO-*d*<sub>6</sub>) 8.20 (1H, s, thiazole-H), 7.91-7.87 (3H, m, 2 × Ar-H, pyrazole-H), 7.63 (1H, s, pyrazole-H), 7.07 (2H, d, *J* 8.9, Ar-H), 4.27 (2H, t, *J* 6.6, NNCH<sub>2</sub>), 3.83 (3H, s, CH<sub>3</sub>), 3.59-3.52 (4H, m, 2 × OCH<sub>2</sub>), 2.74 (2H, t, *J* 6.6, NNCH<sub>2</sub>CH<sub>2</sub>N), 2.44-2.39 (4H, m, 2 × NCH<sub>2</sub>CH<sub>2</sub>O). *t*<sub>R</sub> (HPLC) 2.21 min.

**4-(1-Isobutyl-1H-pyrazol-4-yl)-2-(4-methoxy-phenyl)-thiazole, 137** (JCC-CRT-102)



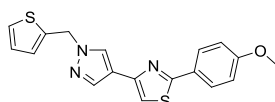
Light brown gum (18.2 mg, 58% yield, *ca.* 95% purity by  $^1\text{H-NMR}$ ),  $\delta_{\text{H}}$  (400 MHz, DMSO- $\text{d}_6$ ) 8.16 (1H, s, thiazole-H), 7.97-7.86 (3H, m, 2  $\times$  Ar-H, pyrazole-H), 7.63 (1H, s, pyrazole-H), 7.13-7.01 (2H, m, Ar-H), 3.95 (2H, d,  $J$  7.2,  $\text{CH}_2$ ), 3.82 (3H, s,  $\text{OCH}_3$ ), 2.20-2.09 (1H, m,  $\text{CH}(\text{CH}_3)_2$ ), 0.86 (6H, d,  $J$  6.7,  $\text{CH}(\text{CH}_3)_2$ ).  $t_{\text{R}}$  (HPLC) 3.89 min.

**2-Methoxy-4-[2-(4-methoxy-phenyl)-thiazol-4-yl]-phenylamine, 138** (JCC-CRT-103)



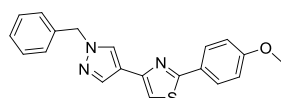
Brown solid (8.9 mg, 28% yield, *ca.* 85% purity by  $^1\text{H-NMR}$ ),  $\delta_{\text{H}}$  (400 MHz, DMSO- $\text{d}_6$ ) 7.98-7.91 (2H, m, Ar-H), 7.74 (1H, s, thiazole-H), 7.46-7.43 (1H, m, Ar-H), 7.40 (1H, dd,  $J$  8.1, 1.7, Ar-H), 7.12-7.03 (2H, m, Ar-H), 6.68 (1H, d,  $J$  8.0, Ar-H), 4.96 (2H, s,  $\text{NH}_2$ ), 3.86 (3H, s,  $\text{CH}_3$ ), 3.83 (3H, s,  $\text{CH}_3$ ).  $t_{\text{R}}$  (HPLC) 3.50 min.

**2-(4-Methoxy-phenyl)-4-(1-thiophen-2-ylmethyl-1H-pyrazol-4-yl)-thiazole, 139** (JCC-CRT-106)



Light brown solid (10.5 mg, 30% yield, *ca.* 95% purity by  $^1\text{H-NMR}$ ),  $\delta_{\text{H}}$  (400 MHz, DMSO- $\text{d}_6$ ) 8.26 (1H, s, thiazole-H), 7.97-7.88 (3H, m, Ar-H), 7.66 (1H, s, Ar-H), 7.49 (1H, dd,  $J$  5.1, 1.2, Ar-H), 7.21-7.13 (1H, m, Ar-H), 7.11-7.05 (2H, m, Ar-H), 7.05-6.98 (1H, m, Ar-H), 5.57 (2H, s,  $\text{CH}_2$ ), 3.83 (3H, s,  $\text{CH}_3$ ).  $t_{\text{R}}$  (HPLC) 3.80 min.

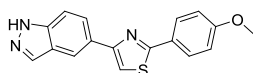
**4-(1-Benzyl-1H-pyrazol-4-yl)-2-(4-methoxy-phenyl)-thiazole, 140** (JCC-CRT-109)



Brown gum (17.4 mg, 50% yield, *ca.* 95% purity by  $^1\text{H-NMR}$ ),  $\delta_{\text{H}}$  (400 MHz, DMSO- $\text{d}_6$ ) 8.28 (1H, s, thiazole-H), 7.95 (1H, s, pyrazole-H), 7.94-7.88 (2H, m, Ar-H), 7.65 (1H, s, pyrazole-H), 7.41-7.33 (2H, m, Ar-H), 7.33-7.25 (3H, m, Ar-H), 7.10-7.03 (2H, m, Ar-H), 5.38 (2H, s,  $\text{CH}_2$ ), 3.83 (3H, s,  $\text{CH}_3$ ).  $t_{\text{R}}$  (HPLC) 3.90 min.



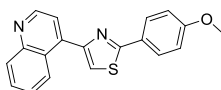
**5-[2-(4-Methoxy-phenyl)-thiazol-4-yl]-1H-indazole, 141** (JCC-CRT-113)



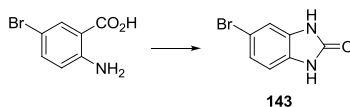
Off-white solid (9.1 mg, 30%, *ca.* 1:2 starting material/product),  $\delta_{\text{H}}$  (400 MHz, DMSO- $d_6$ ) 13.15 (1H, s, NH), 8.46 (1H, s, indazole-H), 8.16 (1H, s, thiazole-H), 8.06-7.95 (4H, m, Ar-H), 7.61 (1H, d, *J* 8.7, Ar-H), 7.12-7.08 (2H, m, Ar-H), 3.84 (3H, s, CH<sub>3</sub>).  $t_{\text{R}}$  (HPLC) 3.70 min.

One further compound was successfully synthesised, but the purification was not sufficient for assignment of the <sup>1</sup>H-NMR data. This compound was tested in the enzyme assays.

- 4-[2-(4-Methoxy-phenyl)-thiazol-4-yl]-quinoline, **142** (JCC-CRT-69)

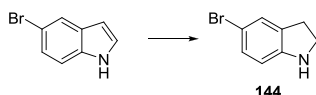


**5-Bromo-1,3-dihydro-benzoimidazol-2-one, 143** <sup>224</sup>



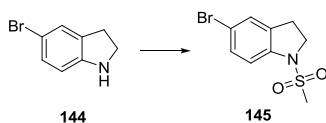
According to the method of Vernier,<sup>225</sup> Et<sub>3</sub>N (1.55 mL, 11.1 mmol) was added to a stirred suspension of 5-bromoanthranilic acid (2.00 g, 9.26 mmol) in PhMe (50 mL) to give a dark red solution. DPPA (2.00 mL, 9.26 mmol) was then added and the reaction mixture heated to 90 °C for 3 h before cooling to r.t. The reaction mixture was then partitioned between 1 M NaOH (50 mL) and EtOAc (100 mL). The aqueous layer was extracted with EtOAc (2 × 100 mL) and the combined organic layers washed with brine (100 mL), dried (MgSO<sub>4</sub>) and the solvent removed *in vacuo*. Recrystallisation from EtOAc afforded the title compound as a white powder (1.58 g, 80%), mp >250 °C;  $\delta_{\text{H}}$  (400 MHz, DMSO- $d_6$ ) 10.80 (2H, br s, 2 × NH), 7.14-7.00 (2H, m, Ar-H), 6.87 (1H, d, *J* 7.9, Ar-H); *m/z* (ES) 256 (78%), 254 (100), 229 (11), 227 (11), 215 (MH<sup>+</sup>, 10), 213 (MH<sup>+</sup>, 10). Found MH<sup>+</sup>, 212.9673. C<sub>7</sub>H<sub>6</sub>N<sub>2</sub>OBr requires 212.9663. Data is in agreement with the literature.<sup>224</sup>

### 5-Bromo-2,3-dihydro-1H-indole, **144**<sup>226</sup>



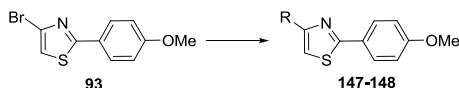
According to the method of Chandra,<sup>226</sup> 5-bromoindole (2.00 g, 10 mmol) was added to AcOH (20 mL). After stirring for 10 min, NaBH<sub>3</sub>CN (2.56 g, 41 mmol) was added in portions. The reaction was stirred for a further 1 h before slow addition to a solution of NaOH (14.0 g) in H<sub>2</sub>O (100 mL). This was extracted with Et<sub>2</sub>O (4 × 75 mL), the combined organic layers dried (MgSO<sub>4</sub>) and the solvent removed *in vacuo*. Column chromatography eluting with Et<sub>2</sub>O/petrol (1:3 → 3:2) afforded the title compound as a colourless oil that became a white semi-solid on storage at -20 °C (1.62 g, 80%), R<sub>f</sub> 0.20 (Et<sub>2</sub>O/petrol 1:3); δ<sub>H</sub> (400 MHz, CDCl<sub>3</sub>) 7.20-7.15 (1H, m, Ar-H), 7.07 (1H, dd, *J* 8.3, 1.9, Ar-H), 6.48 (1H, d, *J* 8.2, Ar-H), 3.60 (1H, br s, NH), 3.54 (2H, t, *J* 8.4, NCH<sub>2</sub>), 3.00 (2H, t, *J*, 8.4, ArCH<sub>2</sub>); *m/z* (CI) 217 (24%), 215 (25), 200 (MH<sup>+</sup>, 97) 199 (33), 198 (MH<sup>+</sup>, 100). Found MH<sup>+</sup>, 197.9915. C<sub>8</sub>H<sub>9</sub>NBr requires 197.9918. Data is in agreement with the literature.<sup>226</sup>

### 5-Bromo-1-methanesulfonyl-2,3-dihydro-1H-indole, **145**



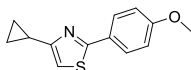
MsCl (470 μL, 6.1 mmol) was added dropwise to a stirred solution of Et<sub>3</sub>N (1.06 mL, 7.6 mmol) and dihydroindole **144** (1.00 g, 5.1 mmol) in CH<sub>2</sub>Cl<sub>2</sub> at 0 °C. The reaction was stirred at r.t. for 48 h before the addition of H<sub>2</sub>O (30 mL). The aqueous layer was extracted with CH<sub>2</sub>Cl<sub>2</sub> (3 × 25 mL) and the combined organic layers were washed with 1 M HCl (50 mL) and brine (50 mL) and dried (MgSO<sub>4</sub>). The solvent was removed *in vacuo* and purification by column chromatography eluting with Et<sub>2</sub>O/petrol (1:2 → 1:0) afforded the title compound as off-white rods (1.37 g, 99%), mp 139-140.5 °C; R<sub>f</sub> 0.14 (Et<sub>2</sub>O/petrol 1:1); ν<sub>max</sub> (neat)/cm<sup>-1</sup> 1467, 1321, 1146, 1104, 1031; δ<sub>H</sub> (400 MHz, CDCl<sub>3</sub>) 7.36-7.25 (3H, m, Ar-H), 3.97 (2H, t, *J* 8.5, NCH<sub>2</sub>), 3.14 (2H, t, *J* 8.5, ArCH<sub>2</sub>), 2.86 (3H, s, CH<sub>3</sub>); δ<sub>C</sub> (101 MHz, CDCl<sub>3</sub>) 141.3, 133.7, 131.0, 128.7, 116.5, 115.2, 50.7, 34.7, 27.8; *m/z* (CI) 296 (21%), 295 (MNH<sub>4</sub><sup>+</sup>, 100), 294 (20), 293 (MNH<sub>4</sub><sup>+</sup>, 98). Found MNH<sub>4</sub><sup>+</sup>, 292.9958. C<sub>9</sub>H<sub>14</sub>N<sub>2</sub>O<sub>2</sub>BrS requires 292.9959.

### Parallel Synthesis: General Procedure for Negishi Couplings



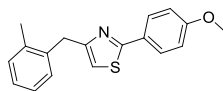
A solution of bromide **93** (27 mg, 100  $\mu\text{mol}$ ), alkyl zinc chloride (120  $\mu\text{mol}$ ) and  $\text{Pd}(\text{PPh}_3)_4$  (5.8 mg, 5  $\mu\text{mol}$ ) in THF (0.4 mL) was heated (70  $^\circ\text{C}$ , 16 h). Upon cooling, the reaction mixture was partitioned between  $\text{H}_2\text{O}$  (5 mL) and  $\text{CH}_2\text{Cl}_2$  (10 mL), the organic layer separated, the solvent removed *in vacuo* and the product purified by HPLC under acidic conditions.

#### 4-Cyclopropyl-2-(4-methoxy-phenyl)-thiazole, **147** (JCC-CRT-80)



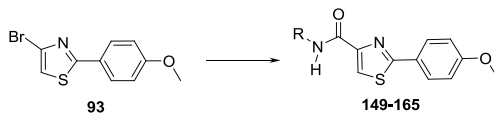
Brown gum (3.1 mg, 13% yield, *ca.* 75% purity by  $^1\text{H-NMR}$ ),  $\delta_{\text{H}}$  (400 MHz,  $\text{DMSO-d}_6$ ) 7.83-7.78 (2H, m, Ar-H), 7.20 (1H, s, thiazole-H), 7.04-7.00 (2H, m, Ar-H), 3.81 (3H, s,  $\text{OCH}_3$ ), 2.16-2.04 (1H, m, CH), 0.96-0.83 (4H, m,  $2 \times \text{CH}_2$ ).  $t_{\text{R}}$  (HPLC) 3.68 min.

#### 2-(4-Methoxy-phenyl)-4-(2-methyl-benzyl)-thiazole, **148** (JCC-CRT-81)



Light brown gum (1.5 mg, 5% yield, *ca.* 85% purity by  $^1\text{H-NMR}$ ),  $\delta_{\text{H}}$  (400 MHz,  $\text{DMSO-d}_6$ ) 7.85-7.80 (2H, m, Ar-H), 7.21-7.11 (4H, m, Ar-H), 7.07 (1H, s, thiazole-H), 7.05-7.01 (2H, m, Ar-H), 4.08 (2H, s,  $\text{CH}_2$ ), 3.81 (3H, s,  $\text{OCH}_3$ ), 2.33 (3H, s,  $\text{ArCH}_3$ ).  $t_{\text{R}}$  (HPLC) 3.72 min.

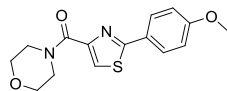
### Parallel Synthesis: General Procedure for Aminocarbonylation Reactions



A solution of bromide **93** (27 mg, 100  $\mu\text{mol}$ ), amine (200  $\mu\text{mol}$ ), DBU (45  $\mu\text{L}$ , 300  $\mu\text{mol}$ ),  $^t\text{Bu}_3\text{PHBF}_4$  (2.9 mg, 10  $\mu\text{mol}$ ), *trans*-di( $\mu$ -acetato)bis[*o*-(di-*o*-tolyl-phosphino)benzyl] dipalladium(II) (4.8 mg, 5  $\mu\text{mol}$ ), DMAP (24.4 mg, 200  $\mu\text{mol}$ ) and  $\text{Mo}(\text{CO})_6$  (26.4 mg, 100  $\mu\text{mol}$ ) in dioxane (1 mL) was heated (MW, 140  $^\circ\text{C}$ , 20 min). Upon cooling, the reaction mixture was partitioned between  $\text{H}_2\text{O}$  (5 mL) and  $\text{CH}_2\text{Cl}_2$  (10 mL), the organic layer

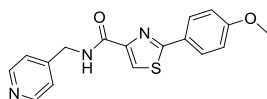
separated, the solvent removed *in vacuo* and the product purified by HPLC under acidic conditions.

**[2-(4-Methoxy-phenyl)-thiazol-4-yl]-morpholin-4-yl-methanone, 149** (JCC-CRT-83)



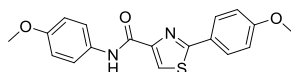
Off-white solid (8.6 mg, 28% yield, *ca.* 85% purity by  $^1\text{H-NMR}$ ),  $\delta_{\text{H}}$  (400 MHz, DMSO- $\text{d}_6$ ) 8.09 (1H, s, thiazole-H), 7.97-7.84 (2H, m, Ar-H), 7.14-7.01 (2H, m, Ar-H), 3.83 (3H, s,  $\text{CH}_3$ ), 3.85-3.60 (6H, m,  $3 \times \text{CH}_2$ ), 3.28 (2H, d,  $J$  12.2,  $\text{CH}_2$ ).  $t_{\text{R}}$  (HPLC) 2.97 min.

**2-(4-Methoxy-phenyl)-thiazole-4-carboxylic acid (pyridin-4-ylmethyl)-amide, 150** (JCC-CRT-84)



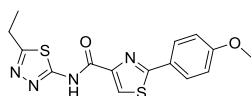
Off-white solid (8.7 mg, 27% yield, *ca.* 95% purity by  $^1\text{H-NMR}$ ),  $\delta_{\text{H}}$  (400 MHz, DMSO- $\text{d}_6$ ) 9.18 (1H, t,  $J$  6.2, NH), 8.50 (2H, d,  $J$  5.4, pyridine-H), 8.25 (1H, s, thiazole-H), 8.06-7.96 (2H, m, Ar-H), 7.32 (2H, d,  $J$  5.7, pyridine-H), 7.15-7.04 (2H, m, Ar-H), 4.52 (2H, d,  $J$  6.3,  $\text{CH}_2$ ), 3.84 (3H, s,  $\text{CH}_3$ ).  $t_{\text{R}}$  (HPLC) 2.10 min.

**2-(4-Methoxy-phenyl)-thiazole-4-carboxylic acid (4-methoxy-phenyl)-amide, 151** (JCC-CRT-85)



Dark brown gum (2.7 mg, 8% yield, *ca.* 1:1 starting material/product),  $\delta_{\text{H}}$  (400 MHz, DMSO- $\text{d}_6$ ) 10.10 (1H, s, NH), 8.33 (1H, s, thiazole-H), 8.13-8.05 (2H, m, Ar-H), 7.79-7.72 (2H, m, Ar-H), 7.12-7.08 (2H, m, Ar-H), 6.97-6.91 (2H, m, Ar-H), 3.85 (3H, s,  $\text{CH}_3$ ), 3.76 (3H, s,  $\text{CH}_3$ ).  $t_{\text{R}}$  (HPLC) 3.41 min.

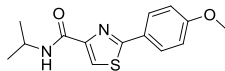
**2-(4-Methoxy-phenyl)-thiazole-4-carboxylic acid (5-ethyl-[1,3,4]thiadiazol-2-yl)-amide, 152** (JCC-CRT-114)



Light brown solid (8.2 mg, 24% yield, *ca.* 50% purity by  $^1\text{H-NMR}$ ),  $\delta_{\text{H}}$  (400 MHz, DMSO- $\text{d}_6$ ) 12.69 (1H, s, NH), 8.60 (1H, s, thiazole-H), 8.13 (2H, d,  $J$  8.8, Ar-H), 7.09 (2H, d,  $J$  8.8, Ar-

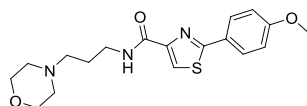
H), 3.85 (3H, s, OCH<sub>3</sub>), 3.04 (2H, q, *J* 7.5, CH<sub>2</sub>), 1.33 (3H, t, *J* 7.5, CH<sub>2</sub>CH<sub>3</sub>). t<sub>R</sub> (HPLC) 3.76 min.

**2-(4-Methoxy-phenyl)-thiazole-4-carboxylic acid isopropylamide, 153** (JCC-CRT-115)



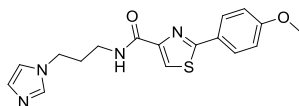
Brown solid (8.2 mg, 30% yield, *ca.* 80% purity by <sup>1</sup>H-NMR), δ<sub>H</sub> (400 MHz, DMSO-d<sub>6</sub>) 8.17 (1H, d, *J* 2.4, thiazole-H), 8.07-7.97 (2H, m, Ar-H), 7.15-7.04 (2H, m, Ar-H), 4.20-4.07 (1H, m, NCH), 3.84 (3H, s, OCH<sub>3</sub>), 1.21 (6H, d, *J* 6.7, 2 × C(CH<sub>3</sub>)<sub>2</sub>). t<sub>R</sub> (HPLC) 3.49 min.

**2-(4-Methoxy-phenyl)-thiazole-4-carboxylic acid (3-morpholin-4-yl-propyl)-amide, 154** (JCC-CRT-117)



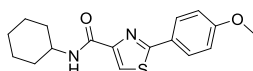
Light brown gum (15.4 mg, 43% yield, *ca.* 85% purity by <sup>1</sup>H-NMR), δ<sub>H</sub> (400 MHz, DMSO-d<sub>6</sub>) 8.56 (1H, s, NH), 8.17 (1H, s, thiazole-H), 7.98 (2H, d, *J* 8.9, Ar-H), 7.08 (2H, d, *J* 8.9, Ar-H), 3.84 (3H, s, CH<sub>3</sub>), 3.60-3.56 (4H, m, 2 × OCH<sub>2</sub>), 3.34 (2H, dd, *J* 13.1, 6.7, NHCH<sub>2</sub>), 2.41-2.32 (6H, m, N(CH<sub>2</sub>)<sub>3</sub>), 1.76-1.66 (2H, m, NHCH<sub>2</sub>CH<sub>2</sub>). t<sub>R</sub> (HPLC) 1.59 min.

**2-(4-Methoxy-phenyl)-thiazole-4-carboxylic acid (3-imidazol-1-yl-propyl)-amide, 155** (JCC-CRT-118)



Light yellow solid (6.4 mg, 19% yield, *ca.* 90% purity by <sup>1</sup>H-NMR), δ<sub>H</sub> (400 MHz, DMSO-d<sub>6</sub>) 8.58 (1H, s, NH), 8.19 (1H, s, thiazole-H), 8.04-7.95 (2H, m, Ar-H), 7.68 (1H, s, imidazole-H), 7.23 (1H, s, imidazole-H), 7.08 (2H, d, *J* 8.9, Ar-H), 6.89 (1H, s, imidazole-H), 4.02 (2H, t, *J* 6.9, imidazole-CH<sub>2</sub>), 3.84 (3H, s, CH<sub>3</sub>), 3.28 (2H, dd, *J* 13.1, 6.7, NHCH<sub>2</sub>), 2.04-1.93 (2H, m, NHCH<sub>2</sub>CH<sub>2</sub>). t<sub>R</sub> (HPLC) 1.60 min.

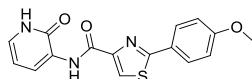
**2-(4-Methoxy-phenyl)-thiazole-4-carboxylic acid cyclohexylamide, 156** (JCC-CRT-119)



Pale orange solid (6.9 mg, 22% yield, *ca.* 80% purity by <sup>1</sup>H-NMR), δ<sub>H</sub> (400 MHz, DMSO-d<sub>6</sub>) 8.17 (1H, s, thiazole-H), 8.00 (2H, d, *J* 8.9, Ar-H), 7.07 (2H, d, *J* 8.9, Ar-H), 3.84 (3H, s,

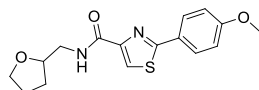
CH<sub>3</sub>), 3.81-3.72 (1H, m, NCH), 1.81 (2H, d, *J* 12.0, NHCHCH<sub>2</sub>), 1.73 (2H, d, *J* 12.7, NHCHCH<sub>2</sub>), 1.65-1.27 (6H, m, 3 × CH<sub>2</sub>). t<sub>R</sub> (HPLC) 4.05 min.

**2-(4-Methoxy-phenyl)-thiazole-4-carboxylic acid (2-oxo-1,2-dihydro-pyridin-3-yl)-amide, 157** (JCC-CRT-129)



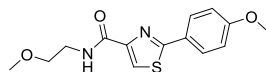
Pale brown solid (3.5 mg, 11% yield, *ca.* 85% purity by <sup>1</sup>H-NMR), δ<sub>H</sub> (400 MHz, DMSO-d<sub>6</sub>) 12.17 (1H, s, NH), 10.09 (1H, s, NH), 8.44 (1H, s, thiazole-H), 8.39 (1H, dd, *J* 7.2, 1.7, pyridone-H), 7.99-7.91 (2H, m, Ar-H), 7.20-7.11 (3H, m, 2 × Ar-H, pyridone-H), 6.31 (1H, t, *J* 6.9, pyridone-H), 3.85 (3H, s, CH<sub>3</sub>). t<sub>R</sub> (HPLC) 3.49 min.

**2-(4-Methoxy-phenyl)-thiazole-4-carboxylic acid (tetrahydro-furan-2-ylmethyl)-amide, 158** (JCC-CRT-130)



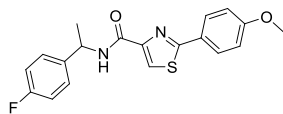
Orange solid (8.3 mg, 26% yield, *ca.* 80% purity by <sup>1</sup>H-NMR), δ<sub>H</sub> (400 MHz, DMSO-d<sub>6</sub>) 8.39 (1H, t, *J* 6.0, NH), 8.20 (1H, s, thiazole-H), 8.01-7.95 (2H, m, Ar-H), 7.11-7.06 (2H, m, Ar-H), 4.06-3.96 (1H, m, OCH), 3.84 (3H, s, CH<sub>3</sub>), 3.81-3.75 (1H, m, OCHH), 3.64 (1H, dd, *J* 14.5, 7.3, OCHH), 1.96-1.74 (3H, m, NCH<sub>2</sub>, OCHCH<sub>2</sub>), 1.67-1.54 (1H, m, OCHCH<sub>2</sub>), 1.28 (2H, m, OCH<sub>2</sub>CH<sub>2</sub>). t<sub>R</sub> (HPLC) 3.36 min.

**2-(4-Methoxy-phenyl)-thiazole-4-carboxylic acid (2-methoxy-ethyl)-amide, 159** (JCC-CRT-131)



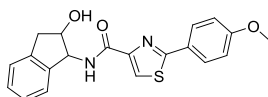
Orange solid (11.2 mg, 38% yield, *ca.* 70% purity by <sup>1</sup>H-NMR), δ<sub>H</sub> (400 MHz, DMSO-d<sub>6</sub>) 8.44 (1H, s, NH), 8.20 (1H, s, thiazole-H), 8.02-7.95 (2H, m, Ar-H), 7.12-7.06 (2H, m, Ar-H), 3.84 (3H, s, CH<sub>3</sub>), 3.53-3.39 (4H, m, CH<sub>2</sub>), 3.27 (3H, s, CH<sub>3</sub>). t<sub>R</sub> (HPLC) 3.21 min.

**2-(4-Methoxy-phenyl)-thiazole-4-carboxylic acid [1-(4-fluoro-phenyl)-ethyl]-amide, 160**  
(JCC-CRT-136)



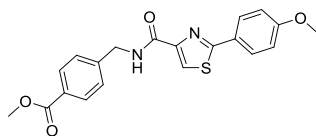
Orange gum (5.0 mg, 14% yield, *ca.* 60% purity by  $^1\text{H-NMR}$ ),  $\delta_{\text{H}}$  (400 MHz, DMSO- $d_6$ ) 8.80 (1H, d,  $J$  8.5, NH), 8.21 (1H, s, thiazole-H), 8.07-7.99 (2H, m, Ar-H), 7.41-7.22 (4H, m, Ar-H), 7.11-7.07 (2H, m, Ar-H), 5.21 (1H, p,  $J$  7.1, NCH), 3.84 (3H, s, OCH<sub>3</sub>), 1.54 (3H, d,  $J$  7.0, CHCH<sub>3</sub>).  $t_{\text{R}}$  (HPLC) 3.92 min.

**2-(4-Methoxy-phenyl)-thiazole-4-carboxylic acid (2-hydroxy-indan-1-yl)-amide, 161**  
(JCC-CRT-140)



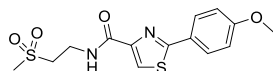
Brown solid (1.4 mg, 4% yield, *ca.* 65% purity by  $^1\text{H-NMR}$ ),  $\delta_{\text{H}}$  (400 MHz, DMSO- $d_6$ ) 8.80 (1H, d,  $J$  9.1, NH), 8.28 (1H, s, thiazole-H), 8.02 (2H, d,  $J$  8.9, Ar-H), 7.24-7.08 (4H, m, Ar-H), 7.07-7.03 (2H, m, Ar-H), 5.40 (1H, d,  $J$  6.0, OH), 5.30 (1H, t,  $J$  8.0, OCH), 4.62-4.50 (1H, m, NCH), 3.82 (3H, s, CH<sub>3</sub>), 3.18 (1H, dd,  $J$  15.4, 7.3, CHH), 2.76 (1H, dd,  $J$  15.4, 8.0, CHH).  $t_{\text{R}}$  (HPLC) 3.60 min.

**4-([2-(4-Methoxy-phenyl)-thiazole-4-carbonyl]-amino)-methyl)-benzoic acid methyl ester, 162**  
(JCC-CRT-142)



Brown gum (4.9 mg, 13% yield, *ca.* 95% purity by  $^1\text{H-NMR}$ ),  $\delta_{\text{H}}$  (400 MHz, DMSO- $d_6$ ) 9.20 (1H, t,  $J$  6.3, NH), 8.24 (1H, s, thiazole-H), 8.04-7.98 (2H, d,  $J$  8.9, Ar-H), 7.93 (2H, d,  $J$  8.3, Ar-H), 7.47 (2H, d,  $J$  8.3, Ar-H), 7.08 (2H, d,  $J$  8.9, Ar-H), 4.57 (2H, d,  $J$  6.3, CH<sub>2</sub>), 3.84 (6H, s, 2  $\times$  CH<sub>3</sub>).  $t_{\text{R}}$  (HPLC) 3.60 min.

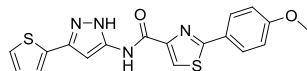
**2-(4-Methoxy-phenyl)-thiazole-4-carboxylic acid (2-methanesulfonyl-ethyl)-amide, 163**  
(JCC-CRT-143)



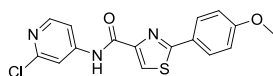
White solid (5.9 mg, 17% yield, *ca.* 95% purity by <sup>1</sup>H-NMR),  $\delta_{\text{H}}$  (400 MHz, DMSO-*d*<sub>6</sub>) 8.73 (1H, t, *J* 5.9, NH), 8.24 (1H, s, thiazole-H), 8.05-7.91 (2H, m, Ar-H), 7.17-7.01 (2H, m, Ar-H), 3.84 (3H, s, OCH<sub>3</sub>), 3.73 (2H, dd, *J* 13.1, 6.6, NCH<sub>2</sub>), 3.40 (2H, dd, *J* 16.3, 9.5, SO<sub>2</sub>CH<sub>2</sub>), 3.06 (3H, s, SO<sub>2</sub>CH<sub>3</sub>). *t*<sub>R</sub> (HPLC) 2.85 min.

Two further compounds were successfully synthesised, but the purification was not sufficient for assignment of the <sup>1</sup>H-NMR data. These compounds were tested in the enzyme assays.

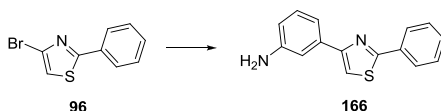
- 2-(4-Methoxy-phenyl)-thiazole-4-carboxylic acid (5-thiophen-2-yl-2*H*-pyrazol-3-yl)-amide, **164** (JCC-CRT-132)



- 2-(4-Methoxy-phenyl)-thiazole-4-carboxylic acid (2-chloro-pyridin-4-yl)-amide, **165** (JCC-CRT-139)



**3-(2-Phenyl-thiazol-4-yl)-phenylamine, 166**<sup>227</sup>

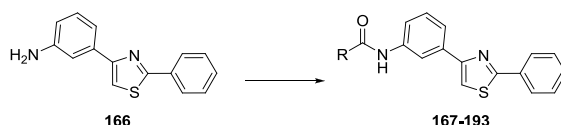


A solution of bromide **96** (240 mg, 1.00 mmol), 3-aminophenylboronic acid (164 mg, 1.20 mmol), K<sub>2</sub>CO<sub>3</sub> (346 mg, 2.50 mmol) and Pd(PPh<sub>3</sub>)<sub>4</sub> (35 mg, 0.030 mmol) in DME/H<sub>2</sub>O (4:1, 7.5 mL) was stirred at reflux for 14 h. The reaction mixture was partitioned between H<sub>2</sub>O (20 mL) and EtOAc (20 mL), the aqueous layer extracted with EtOAc (3 × 20 mL), the combined organic layers dried (MgSO<sub>4</sub>) and the solvent removed *in vacuo*. Column chromatography eluting with EtOAc/hexane (1:3 → 1:2) afforded the title compound as white rods (204 mg, 81%), mp 96-99 °C; *R*<sub>f</sub> 0.20 (EtOAc/hexane 1:3);  $\nu_{\text{max}}$  (neat)/cm<sup>-1</sup> 3332, 1606, 1585, 1471, 1458;  $\delta_{\text{H}}$  (400 MHz, CDCl<sub>3</sub>) 8.06-8.01 (2H, m, Ar-H), 7.48-7.41 (3H, m, Ar-H), 7.40 (1H, s, thiazole-H), 7.39-7.38 (1H, m, Ar-H), 7.36-7.32 (1H, m, Ar-H), 7.22 (1H, t, *J* 7.8, Ar-H), 6.67 (1H, ddd, *J* 7.8, 2.3, 0.7, Ar-H), 3.75 (2H, br s, NH<sub>2</sub>);  $\delta_{\text{C}}$  (101 MHz, CDCl<sub>3</sub>) 167.8, 156.5,



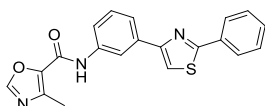
147.0, 135.6, 133.9, 130.1, 129.8, 129.1, 126.7, 116.9, 115.2, 113.4, 112.9;  $m/z$  (ES) 295 (7%), 294 (32), 254 (18), 253 ( $MH^+$ , 100). Found  $MH^+$ , 253.0804.  $C_{15}H_{13}N_2S$  requires 253.0799. Data is in agreement with the literature.<sup>227</sup>

*Parallel Synthesis: General Procedure for Aniline Acylations*



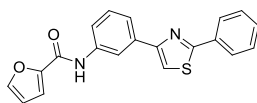
A solution of aniline **166** (20 mg, 80  $\mu$ mol), acid chloride (100  $\mu$ mol) and DIPEA (35  $\mu$ L, 200  $\mu$ mol) in  $CH_2Cl_2$  (0.5 mL) was shaken (24 h). The solvent was removed under a stream of  $N_2$  and the product purified by HPLC under acidic conditions.

**4-Methyl-oxazole-5-carboxylic acid [3-(2-phenyl-thiazol-4-yl)-phenyl]-amide, 167** (JCC-CRT-161)



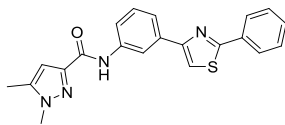
Pale orange solid (13.9 mg, 48% yield, *ca.* 98% purity by  $^1H$ -NMR),  $\delta_H$  (400 MHz,  $DMSO-d_6$ ) 10.41 (1H, s, NH), 8.56 (1H, s, oxazole-H), 8.48-8.45 (1H, m, Ar-H), 8.13 (1H, s, thiazole-H), 8.04 (2H, dd,  $J$  7.8, 1.7, Ar-H), 7.82-7.76 (2H, m, Ar-H), 7.58-7.49 (3H, m, Ar-H), 7.45 (1H, t,  $J$  7.9, Ar-H), 2.46 (3H, s,  $CH_3$ ).  $t_R$  (HPLC) 3.93 min.

**Furan-2-carboxylic acid [3-(2-phenyl-thiazol-4-yl)-phenyl]-amide, 168** (JCC-CRT-166)



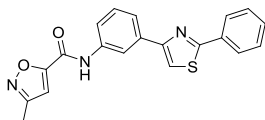
Off-white solid (7.0 mg, 25% yield, *ca.* 98% purity by  $^1H$ -NMR),  $\delta_H$  (400 MHz,  $DMSO-d_6$ ) 10.33 (1H, s, NH), 8.45 (1H, t,  $J$  1.7, Ar-H), 8.13 (1H, s, thiazole-H), 8.07-8.02 (2H, m, Ar-H, furan-H), 7.97-7.95 (1H, m, Ar-H), 7.84-7.80 (1H, m, Ar-H), 7.78-7.74 (1H, m, Ar-H), 7.58-7.50 (3H, m, Ar-H), 7.45 (1H, t,  $J$  7.9, Ar-H), 7.39 (1H, d,  $J$  3.3, furan-H), 6.73 (1H, dd,  $J$  3.5, 1.7, furan-H).  $t_R$  (HPLC) 3.88 min.

**1,5-Dimethyl-1*H*-pyrazole-3-carboxylic acid [3-(2-phenyl-thiazol-4-yl)-phenyl]-amide, 169** (JCC-CRT-167)



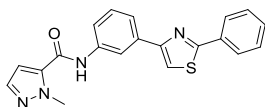
Pale yellow solid (5.9 mg, 20% yield, *ca.* 90% purity by <sup>1</sup>H-NMR),  $\delta_{\text{H}}$  (400 MHz, DMSO-*d*<sub>6</sub>) 10.03 (1H, s, NH), 8.53 (1H, t, *J* 1.7, Ar-H), 8.11 (1H, s, thiazole-H), 8.05 (2H, dd, *J* 7.7, 1.6, Ar-H), 7.87-7.83 (1H, m, Ar-H), 7.75-7.71 (1H, m, Ar-H), 7.58-7.50 (3H, m, Ar-H), 7.41 (1H, t, *J* 7.9, Ar-H), 6.59 (1H, s, pyrazole-H), 3.86 (3H, s, NCH<sub>3</sub>), 2.32 (3H, s, pyrazole-CH<sub>3</sub>). *t*<sub>R</sub> (HPLC) 3.99 min.

**3-Methyl-isoxazole-5-carboxylic acid [3-(2-phenyl-thiazol-4-yl)-phenyl]-amide, 170** (JCC-CRT-168)



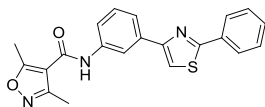
Pale yellow solid (15.6 mg, 54% yield, *ca.* 98% purity by <sup>1</sup>H-NMR),  $\delta_{\text{H}}$  (400 MHz, DMSO-*d*<sub>6</sub>) 10.83 (1H, s, NH), 8.48 (1H, t, *J* 1.6, Ar-H), 8.15 (1H, s, thiazole-H), 8.04 (2H, dd, *J* 7.7, 1.7, Ar-H), 7.84-7.79 (2H, m, Ar-H), 7.58-7.50 (3H, m, Ar-H), 7.48 (1H, t, *J* 8.0, Ar-H), 7.16 (1H, s, isoxazole-H), 2.36 (3H, s, CH<sub>3</sub>). *t*<sub>R</sub> (HPLC) 4.01 min.

**2-Methyl-2*H*-pyrazole-3-carboxylic acid [3-(2-phenyl-thiazol-4-yl)-phenyl]-amide, 171** (JCC-CRT-172)



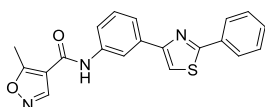
White solid (8.9 mg, 31% yield, *ca.* 95% purity by <sup>1</sup>H-NMR),  $\delta_{\text{H}}$  (400 MHz, DMSO-*d*<sub>6</sub>) 10.35 (1H, s, NH), 8.40 (1H, t, *J* 1.7, Ar-H), 8.15 (1H, s, thiazole-H), 8.04 (2H, dd, *J* 7.7, 1.6, Ar-H), 7.82-7.77 (2H, m, Ar-H), 7.58-7.50 (4H, m, 3 × Ar-H, pyrazole-H), 7.47 (1H, t, *J* 7.9, Ar-H), 7.13 (1H, d, *J* 2.1, pyrazole-H), 4.12 (3H, s, CH<sub>3</sub>). *t*<sub>R</sub> (HPLC) 3.97 min.

**3,5-Dimethyl-isoxazole-4-carboxylic acid [3-(2-phenyl-thiazol-4-yl)-phenyl]-amide, 172**  
(JCC-CRT-179)



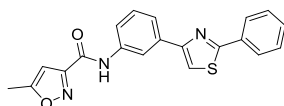
Off-white solid (18.7 mg, 62% yield, *ca.* 98% purity by  $^1\text{H-NMR}$ ),  $\delta_{\text{H}}$  (400 MHz, DMSO- $\text{d}_6$ ) 10.19 (1H, s, NH), 8.37 (1H, t,  $J$  1.6, Ar-H), 8.14 (1H, s, thiazole-H), 8.03 (2H, dd,  $J$  7.8, 1.6, Ar-H), 7.79-7.75 (1H, m,  $J$  7.8, Ar-H), 7.72-7.69 (1H, m, Ar-H), 7.58-7.50 (3H, m, Ar-H), 7.46 (1H, t,  $J$  7.9, Ar-H), 2.58 (3H, s,  $\text{CH}_3$ ), 2.36 (3H, s,  $\text{CH}_3$ ).  $t_{\text{R}}$  (HPLC) 3.94 min.

**5-Methyl-isoxazole-4-carboxylic acid [3-(2-phenyl-thiazol-4-yl)-phenyl]-amide, 173**  
(JCC-CRT-180)



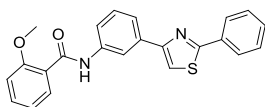
Pale orange solid (5.5 mg, 19% yield, *ca.* 90% purity by  $^1\text{H-NMR}$ ),  $\delta_{\text{H}}$  (400 MHz, DMSO- $\text{d}_6$ ) 10.20 (1H, s, NH), 9.13 (1H, s, isoxazole-H), 8.35 (1H, t,  $J$  1.7, Ar-H), 8.16 (1H, s, thiazole-H), 8.04 (2H, dd,  $J$  7.9, 1.6, Ar-H), 7.81-7.75 (2H, m, Ar-H), 7.59-7.50 (4H, m, Ar-H), 7.49-7.44 (1H, m, Ar-H), 2.71 (3H, s,  $\text{CH}_3$ ).  $t_{\text{R}}$  (HPLC) 3.98 min.

**5-Methyl-isoxazole-3-carboxylic acid [3-(2-phenyl-thiazol-4-yl)-phenyl]-amide, 174**  
(JCC-CRT-181)



White solid (16.1 mg, 56% yield, *ca.* 98% purity by  $^1\text{H-NMR}$ ),  $\delta_{\text{H}}$  (400 MHz, DMSO- $\text{d}_6$ ) 10.76 (1H, s, NH), 8.52 (1H, d,  $J$  1.7, Ar-H), 8.14 (1H, s, thiazole-H), 8.06-8.02 (2H, m, Ar-H), 7.81 (2H, dt,  $J$  6.8, 1.6, Ar-H), 7.58-7.50 (3H, m, Ar-H), 7.47 (1H, t,  $J$  7.9, Ar-H), 6.71 (1H, s, isoxazole-H), 2.52 (3H, s,  $\text{CH}_3$ ).  $t_{\text{R}}$  (HPLC) 4.13 min.

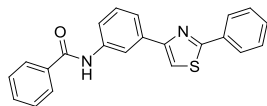
**2-Methoxy-N-[3-(2-phenyl-thiazol-4-yl)-phenyl]-benzamide, 175** (JCC-CRT-151)



Orange solid (9.7 mg, 31% yield, *ca.* 95% purity by  $^1\text{H-NMR}$ ),  $\delta_{\text{H}}$  (400 MHz, DMSO- $\text{d}_6$ ) 10.26 (1H, s, NH), 8.46 (1H, s, Ar-H), 8.13 (1H, s, thiazole-H), 8.04 (2H, dd,  $J$  7.6, 1.7, Ar-H), 7.80-7.73 (2H, m, Ar-H), 7.66 (1H, dd,  $J$  7.6, 1.6, Ar-H), 7.60-7.48 (4H, m, Ar-H), 7.44

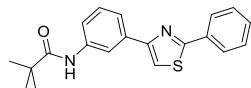
(1H, t, *J* 7.9, Ar-H), 7.20 (1H, d, *J* 8.3, Ar-H), 7.08 (1H, t, *J* 7.6, Ar-H), 3.92 (3H, s, CH<sub>3</sub>). t<sub>R</sub> (HPLC) 4.67 min.

***N*-[3-(2-Phenyl-thiazol-4-yl)-phenyl]-benzamide, 176** (JCC-CRT-152)



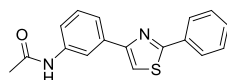
Pale orange solid (5.1 mg, 18% yield, *ca.* 98% purity by <sup>1</sup>H-NMR), δ<sub>H</sub> (400 MHz, DMSO-d<sub>6</sub>) 10.41 (1H, s, NH), 8.55-8.44 (1H, m, Ar-H), 8.14 (1H, s, thiazole-H), 8.08-7.97 (4H, m, Ar-H), 7.88-7.73 (2H, m, Ar-H), 7.67-7.51 (6H, m, Ar-H), 7.46 (1H, t, *J* 7.9, Ar-H). t<sub>R</sub> (HPLC) 4.21 min.

**2,2-Dimethyl-*N*-[3-(2-phenyl-thiazol-4-yl)-phenyl]-propionamide, 177** (JCC-CRT-153)



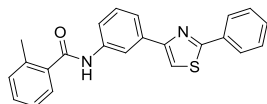
White solid (5.5 mg, 21% yield, *ca.* 95% purity by <sup>1</sup>H-NMR), δ<sub>H</sub> (400 MHz, DMSO-d<sub>6</sub>) 9.36 (1H, s, NH), 8.31 (1H, t, *J* 1.8, Ar-H), 8.10 (1H, s, thiazole-H), 8.06-8.01 (2H, m, Ar-H), 7.75-7.67 (2H, m, Ar-H), 7.59-7.51 (3H, m, Ar-H), 7.39 (1H, t, *J* 7.9, Ar-H), 1.26 (9H, s, C(CH<sub>3</sub>)<sub>3</sub>). t<sub>R</sub> (HPLC) 4.07 min.

***N*-[3-(2-Phenyl-thiazol-4-yl)-phenyl]-acetamide, 178** (JCC-CRT-154)



Off-white solid (9.2 mg, 39% yield, *ca.* 90% purity by <sup>1</sup>H-NMR), δ<sub>H</sub> (400 MHz, DMSO-d<sub>6</sub>) 10.09 (1H, s, NH), 8.24 (1H, s, Ar-H), 8.10 (1H, s, thiazole-H), 8.06-7.99 (2H, m, Ar-H), 7.71-7.63 (2H, m, Ar-H), 7.59-7.50 (3H, m, Ar-H), 7.39 (1H, t, *J* 7.9, Ar-H), 2.08 (3H, s, CH<sub>3</sub>). t<sub>R</sub> (HPLC) 3.72 min.

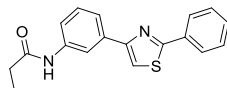
**2-Methyl-*N*-[3-(2-phenyl-thiazol-4-yl)-phenyl]-benzamide, 179** (JCC-CRT-155)



White solid (8.9 mg, 30% yield, *ca.* 95% purity by <sup>1</sup>H-NMR), δ<sub>H</sub> (400 MHz, DMSO-d<sub>6</sub>) 10.45 (1H, s, NH), 8.48 (1H, s, Ar-H), 8.11 (1H, s, thiazole-H), 8.03 (2H, dd, *J* 7.6, 1.7, Ar-H), 7.77

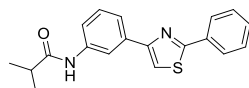
(2H, dd, *J* 15.0, 8.1, Ar-H), 7.58-7.48 (4H, m, Ar-H), 7.48-7.36 (2H, m, Ar-H), 7.32 (2H, d, *J* 7.4, Ar-H), 2.42 (3H, s, CH<sub>3</sub>). *t*<sub>R</sub> (HPLC) 4.22 min.

***N*-[3-(2-Phenyl-thiazol-4-yl)-phenyl]-propionamide, 180<sup>228</sup>** (JCC-CRT-156)



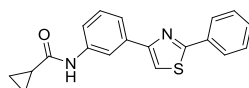
Off-white solid (9.2 mg, 37% yield, *ca.* 98% purity by <sup>1</sup>H-NMR),  $\delta_{\text{H}}$  (400 MHz, DMSO-*d*<sub>6</sub>) 10.02 (1H, s, NH), 8.28 (1H, s, Ar-H), 8.10 (1H, s, thiazole-H), 8.04-8.00 (2H, m, Ar-H), 7.67 (2H, dd, *J* 7.9, 1.6, Ar-H), 7.59-7.49 (3H, m, Ar-H), 7.39 (1H, t, *J* 7.9, Ar-H), 2.36 (2H, q, *J* 7.6, CH<sub>2</sub>), 1.11 (3H, t, *J* 7.5, CH<sub>3</sub>). *t*<sub>R</sub> (HPLC) 3.87 min.

***N*-[3-(2-Phenyl-thiazol-4-yl)-phenyl]-isobutyramide, 181<sup>228</sup>** (JCC-CRT-157)



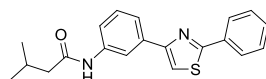
Off-white solid (6.6 mg, 25% yield, *ca.* 95% purity by <sup>1</sup>H-NMR),  $\delta_{\text{H}}$  (400 MHz, DMSO-*d*<sub>6</sub>) 9.99 (1H, s, NH), 8.31 (1H, t, *J* 1.6, Ar-H), 8.10 (1H, s, thiazole-H), 8.03 (2H, dd, *J* 7.7, 1.6, Ar-H), 7.72-7.65 (2H, m, Ar-H), 7.59-7.50 (3H, m, Ar-H), 7.39 (1H, t, *J* 7.9, Ar-H), 2.63 (1H, hept, *J* 6.9, COCH), 1.13 (6H, d, *J* 6.8, C(CH<sub>3</sub>)<sub>2</sub>). *t*<sub>R</sub> (HPLC) 3.94 min.

**Cyclopropanecarboxylic acid [3-(2-phenyl-thiazol-4-yl)-phenyl]-amide, 182** (JCC-CRT-158)



Pale orange solid (7.5 mg, 29% yield, *ca.* 95% purity by <sup>1</sup>H-NMR),  $\delta_{\text{H}}$  (400 MHz, DMSO-*d*<sub>6</sub>) 10.34 (1H, s, NH), 8.29 (1H, t, *J* 1.7, Ar-H), 8.09 (1H, s, thiazole-H), 8.06-7.99 (2H, m, Ar-H), 7.71-7.63 (2H, m, Ar-H), 7.59-7.49 (3H, m, Ar-H), 7.39 (1H, t, *J* 7.9, Ar-H), 1.92-1.74 (1H, m, COCH), 0.93-0.70 (4H, m, 2 × CH<sub>2</sub>). *t*<sub>R</sub> (HPLC) 3.94 min.

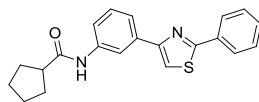
**3-Methyl-*N*-[3-(2-phenyl-thiazol-4-yl)-phenyl]-butyramide, 183<sup>228</sup>** (JCC-CRT-159)



Off-white solid (8.1 mg, 30% yield, *ca.* 95% purity by <sup>1</sup>H-NMR),  $\delta_{\text{H}}$  (400 MHz, DMSO-*d*<sub>6</sub>) 10.00 (1H, s, NH), 8.27 (1H, t, *J* 1.6, Ar-H), 8.09 (1H, s, thiazole-H), 8.05-7.98 (2H, m, Ar-H), 7.72-7.64 (2H, m, Ar-H), 7.59-7.49 (3H, m, Ar-H), 7.38 (1H, t, *J* 7.9, Ar-H), 2.22 (2H, d,

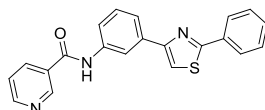
*J* 7.0, CH<sub>2</sub>), 2.16-2.05 (1H, m, CH(CH<sub>3</sub>)<sub>2</sub>), 0.96 (6H, d, *J* 6.7, CH(CH<sub>3</sub>)<sub>2</sub>). *t*<sub>R</sub> (HPLC) 4.17 min.

**Cyclopentanecarboxylic acid [3-(2-phenyl-thiazol-4-yl)-phenyl]-amide, 184** (JCC-CRT-160)



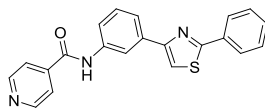
Off-white needles (11.4 mg, 41% yield, *ca.* 95% purity by <sup>1</sup>H-NMR),  $\delta_{\text{H}}$  (400 MHz, DMSO-d<sub>6</sub>) 10.00 (1H, s, NH), 8.31 (1H, t, *J* 1.7, Ar-H), 8.09 (1H, s, thiazole-H), 8.06-8.00 (2H, m, Ar-H), 7.68 (2H, dd, *J* 7.9, 1.8, Ar-H), 7.58-7.48 (3H, m, Ar-H), 7.38 (1H, t, *J* 7.9, Ar-H), 2.82 (1H, p, *J* 7.9, COCH), 1.99-1.82 (2H, m, CH<sub>2</sub>), 1.82-1.65 (4H, m, 2 × CH<sub>2</sub>), 1.65-1.50 (2H, m, CH<sub>2</sub>). *t*<sub>R</sub> (HPLC) 4.38 min.

***N*-[3-(2-Phenyl-thiazol-4-yl)-phenyl]-nicotinamide, 185** (JCC-CRT-162)



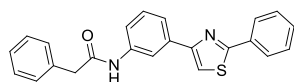
Off-white product (7.8 mg, 27% yield, *ca.* 98% purity by <sup>1</sup>H-NMR),  $\delta_{\text{H}}$  (400 MHz, DMSO-d<sub>6</sub>) 10.59 (1H, s, NH), 9.17-9.14 (1H, m, pyridine-H), 8.78 (1H, dd, *J* 4.8, 1.6, pyridine-H), 8.48 (1H, t, *J* 1.8, Ar-H), 8.38-8.31 (1H, m, pyridine-H), 8.15 (1H, s, thiazole-H), 8.08-8.01 (2H, m, Ar-H), 7.88-7.76 (2H, m, Ar-H, pyridine-H), 7.62-7.44 (5H, m, Ar-H). *t*<sub>R</sub> (HPLC) 3.84 min.

***N*-[3-(2-Phenyl-thiazol-4-yl)-phenyl]-isonicotinamide, 186** (JCC-CRT-163)



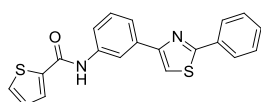
White solid (8.0 mg, 28% yield, *ca.* 98% purity by <sup>1</sup>H-NMR),  $\delta_{\text{H}}$  (400 MHz, DMSO-d<sub>6</sub>) 10.64 (1H, s, NH), 8.81 (2H, dd, *J* 4.4, 1.7, pyridine-H), 8.48 (1H, t, *J* 1.7, Ar-H), 8.16 (1H, s, thiazole-H), 8.07-8.01 (2H, m, Ar-H), 7.92 (2H, dd, *J* 4.4, 1.7, pyridine-H), 7.88-7.78 (2H, m, Ar-H), 7.58-7.52 (3H, m, Ar-H), 7.49 (1H, t, *J* 7.9, Ar-H). *t*<sub>R</sub> (HPLC) 3.92 min.

**2-Phenyl-N-[3-(2-phenyl-thiazol-4-yl)-phenyl]-acetamide, 187** (JCC-CRT-164)



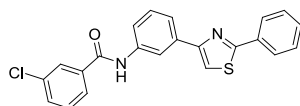
White solid (9.2 mg, 31% yield, *ca.* 98% purity by  $^1\text{H-NMR}$ ),  $\delta_{\text{H}}$  (400 MHz, DMSO- $d_6$ ) 10.32 (1H, s, NH), 8.30 (1H, t,  $J$  1.7, Ar-H), 8.10 (1H, s, thiazole-H), 8.06-7.98 (2H, m, Ar-H), 7.73-7.65 (2H, m, Ar-H), 7.61-7.48 (3H, m, Ar-H), 7.44-7.29 (5H, m, Ar-H), 7.29-7.20 (1H, m, Ar-H), 3.68 (2H, s, CH $_2$ ).  $t_{\text{R}}$  (HPLC) 4.21 min.

**Thiophene-2-carboxylic acid [3-(2-phenyl-thiazol-4-yl)-phenyl]-amide, 188<sup>228</sup>** (JCC-CRT-165)



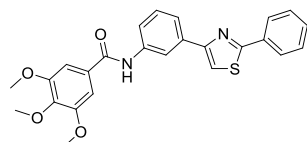
White solid (7.5 mg, 56% yield, *ca.* 98% purity by  $^1\text{H-NMR}$ ),  $\delta_{\text{H}}$  (400 MHz, DMSO- $d_6$ ) 10.38 (1H, s, NH), 8.42 (1H, t,  $J$  1.8, Ar-H), 8.15 (1H, s, thiazole-H), 8.09 (1H, dd,  $J$  3.7, 1.0, thiophene-H), 8.07-8.01 (2H, m, Ar-H), 7.88 (1H, dd,  $J$  5.0, 1.0, thiophene-H), 7.83-7.74 (2H, m, Ar-H), 7.60-7.51 (3H, m, Ar-H), 7.46 (1H, t,  $J$  7.9, Ar-H), 7.25 (1H, dd,  $J$  5.0, 3.7, thiophene-H).  $t_{\text{R}}$  (HPLC) 4.18 min.

**3-Chloro-N-[3-(2-phenyl-thiazol-4-yl)-phenyl]-benzamide, 189** (JCC-CRT-169)



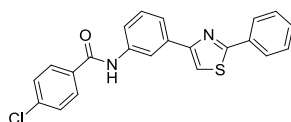
White solid (9.2 mg, 30% yield, *ca.* 98% purity by  $^1\text{H-NMR}$ ),  $\delta_{\text{H}}$  (400 MHz, DMSO- $d_6$ ) 10.49 (1H, s, NH), 8.47 (1H, t,  $J$  1.8, Ar-H), 8.14 (1H, s, thiazole-H), 8.09-8.01 (3H, m, Ar-H), 8.00-7.94 (1H, m, Ar-H), 7.89-7.82 (1H, m, Ar-H), 7.81-7.76 (1H, m, Ar-H), 7.68 (1H, ddd,  $J$  7.9, 2.0, 0.9, Ar-H), 7.62-7.50 (4H, m, Ar-H), 7.47 (1H, t,  $J$  7.9, Ar-H).  $t_{\text{R}}$  (HPLC) 4.95 min.

**3,4,5-Trimethoxy-N-[3-(2-phenyl-thiazol-4-yl)-phenyl]-benzamide, 190** (JCC-CRT-171)



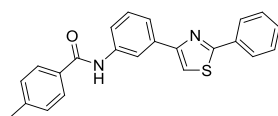
White needles (9.9 mg, 28% yield, *ca.* 98% purity by  $^1\text{H-NMR}$ ),  $\delta_{\text{H}}$  (400 MHz, DMSO- $d_6$ ) 10.28 (1H, s, NH), 8.42 (1H, t,  $J$  1.8, Ar-H), 8.15 (1H, s, thiazole-H), 8.07-8.02 (2H, m, Ar-H), 7.84-7.75 (2H, m, Ar-H), 7.59-7.50 (3H, m, Ar-H), 7.47 (1H, t,  $J$  7.9, Ar-H), 7.34 (2H, s, Ar-H), 3.89 (6H, s, 2  $\times$  CH $_3$ ), 3.75 (3H, s, CH $_3$ ).  $t_{\text{R}}$  (HPLC) 4.29 min.

#### 4-Chloro-*N*-[3-(2-phenyl-thiazol-4-yl)-phenyl]-benzamide, **191** (JCC-CRT-173)



White solid (2.3 mg, 7% yield, *ca.* 95% purity by  $^1\text{H-NMR}$ ),  $\delta_{\text{H}}$  (400 MHz,  $\text{DMSO-d}_6$ ) 10.46 (1H, s, NH), 8.46 (1H, t,  $J$  1.8, Ar-H), 8.14 (1H, s, thiazole-H), 8.09-8.01 (4H, m, Ar-H), 7.88-7.80 (1H, m, Ar-H), 7.80-7.74 (1H, m, Ar-H), 7.66-7.61 (2H, m, Ar-H), 7.59-7.52 (3H, m, Ar-H), 7.47 (1H, t,  $J$  7.9, Ar-H).  $t_{\text{R}}$  (HPLC) 4.70 min.

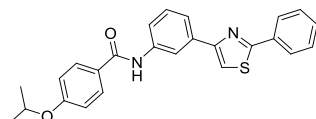
#### 4-Methyl-*N*-[3-(2-phenyl-thiazol-4-yl)-phenyl]-benzamide, **192** (JCC-CRT-174)



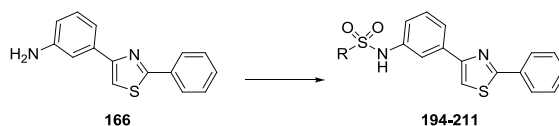
White solid (6.9 mg, 23% yield, *ca.* 95% purity by  $^1\text{H-NMR}$ ),  $\delta_{\text{H}}$  (400 MHz,  $\text{DMSO-d}_6$ ) 10.30 (1H, s, NH), 8.48 (1H, t,  $J$  1.8, Ar-H), 8.13 (1H, s, thiazole-H), 8.09-8.02 (2H, m, Ar-H), 7.93 (2H, d,  $J$  8.2, Ar-H), 7.89-7.82 (1H, m, Ar-H), 7.79-7.73 (1H, m, Ar-H), 7.59-7.49 (3H, m, Ar-H), 7.45 (1H, t,  $J$  7.9, Ar-H), 7.36 (2H, d,  $J$  8.2, Ar-H), 2.40 (3H, s,  $\text{CH}_3$ ).  $t_{\text{R}}$  (HPLC) 4.47 min.

One further compound was successfully synthesised, but the purification was not sufficient for assignment of the  $^1\text{H-NMR}$  data. This compound was tested in the enzyme assays.

- 4-Isopropoxy-*N*-[3-(2-phenyl-thiazol-4-yl)-phenyl]-benzamide, **193** (JCC-CRT-175)



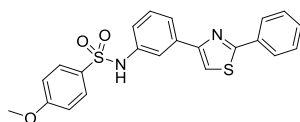
#### Parallel Synthesis: General Procedure for Sulfonamide Synthesis



A solution of aniline **166** (20 mg, 80  $\mu\text{mol}$ ), sulfonyl chloride (100  $\mu\text{mol}$ ) and DIPEA (35  $\mu\text{L}$ , 200  $\mu\text{mol}$ ) in  $\text{CH}_2\text{Cl}_2$  (0.5 mL) was shaken (24 h). The solvent was removed under a stream of  $\text{N}_2$  and the product purified by HPLC under acidic conditions.

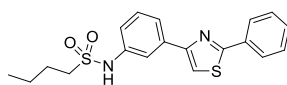


**4-Methoxy-N-[3-(2-phenyl-thiazol-4-yl)-phenyl]-benzenesulfonamide, 194** (JCC-CRT-184)



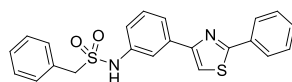
Pale orange solid (14.1 mg, 33% yield, *ca.* 85% purity by  $^1\text{H-NMR}$ ),  $\delta_{\text{H}}$  (400 MHz, DMSO- $d_6$ ) 10.29 (1H, s, NH), 8.08 (1H, s, thiazole-H), 8.03-7.97 (2H, m, Ar-H), 7.82 (1H, s, Ar-H), 7.75 (2H, d, *J* 8.9, Ar-H), 7.65 (1H, d, *J* 7.8, Ar-H), 7.59-7.52 (3H, m, Ar-H), 7.32 (1H, t, *J* 7.9, Ar-H), 7.12-7.04 (3H, m, Ar-H), 3.77 (3H, s, CH<sub>3</sub>).  $t_{\text{R}}$  (HPLC) 3.46 min.

**Butane-1-sulfonic acid [3-(2-phenyl-thiazol-4-yl)-phenyl]-amide, 195** (JCC-CRT-185)



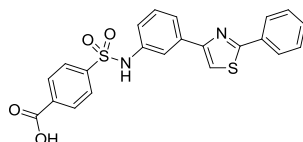
Pale orange solid (3.9 mg, 10% yield, *ca.* 95% purity by  $^1\text{H-NMR}$ ),  $\delta_{\text{H}}$  (400 MHz, DMSO- $d_6$ ) 9.90 (1H, s, NH), 8.14 (1H, s, thiazole-H), 8.02 (2H, dd, *J* 7.6, 1.7, Ar-H), 7.94 (1H, s, Ar-H), 7.74 (1H, d, *J* 7.9, Ar-H), 7.58-7.51 (3H, m, Ar-H), 7.42 (1H, t, *J* 7.9, Ar-H), 7.23 (1H, d, *J* 7.9, Ar-H), 3.17-3.08 (2H, m, SO<sub>2</sub>CH<sub>2</sub>), 1.73-1.61 (2H, m, SO<sub>2</sub>CH<sub>2</sub>CH<sub>2</sub>), 1.42-1.30 (2H, m, CH<sub>3</sub>CH<sub>2</sub>), 0.83 (3H, t, *J* 7.3, CH<sub>3</sub>).  $t_{\text{R}}$  (HPLC) 3.51 min.

**C-Phenyl-N-[3-(2-phenyl-thiazol-4-yl)-phenyl]-methanesulfonamide, 196** (JCC-CRT-190)



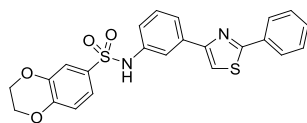
Pale orange solid (9.0 mg, 22% yield, *ca.* 85% purity by  $^1\text{H-NMR}$ ),  $\delta_{\text{H}}$  (400 MHz, DMSO- $d_6$ ) 9.97 (1H, s, NH), 8.13 (1H, s, thiazole-H), 8.03 (2H, dd, *J* 7.7, 1.6, Ar-H), 7.94-7.89 (1H, m, Ar-H), 7.74 (1H, d, *J* 7.9, Ar-H), 7.59-7.52 (3H, m, Ar-H), 7.43 (1H, t, *J* 7.9, Ar-H), 7.38-7.29 (5H, m, Ar-H), 7.21 (1H, dd, *J* 8.1, 1.5, Ar-H), 4.51 (2H, s, CH<sub>2</sub>).  $t_{\text{R}}$  (HPLC) 3.51 min.

**4-[3-(2-Phenyl-thiazol-4-yl)-phenylsulfamoyl]-benzoic acid, 197** (JCC-CRT-191)



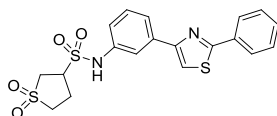
White solid (34.3 mg, 79% yield, *ca.* 75% purity by  $^1\text{H-NMR}$ ),  $\delta_{\text{H}}$  (400 MHz, DMSO- $d_6$ ) 10.44 (1H, s, NH), 8.49 (1H, t, *J* 1.6, Ar-H), 8.15 (1H, s, thiazole-H), 8.05 (2H, dd, *J* 7.9, 1.6, Ar-H), 7.99 (2H, d, *J* 8.3, Ar-H), 7.91-7.84 (1H, m, Ar-H), 7.81-7.73 (3H, m, Ar-H), 7.60-7.49 (3H, m, Ar-H), 7.46 (1H, t, *J* 7.9, Ar-H).  $t_{\text{R}}$  (HPLC) 2.68 min.

**2,3-Dihydro-benzo[1,4]dioxine-6-sulfonic acid [3-(2-phenyl-thiazol-4-yl)-phenyl]-amide, 198** (JCC-CRT-193)



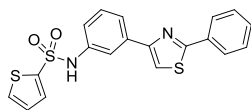
White solid (9.9 mg, 22% yield, *ca.* 95% purity by  $^1\text{H-NMR}$ ),  $\delta_{\text{H}}$  (400 MHz,  $\text{DMSO-d}_6$ ) 10.33 (1H, s, NH), 8.09 (1H, s, thiazole-H), 8.01 (2H, dd,  $J$  7.7, 1.6, Ar-H), 7.84 (1H, t,  $J$  1.8, Ar-H), 7.66 (1H, d,  $J$  7.9, Ar-H), 7.59-7.51 (3H, m, Ar-H), 7.34 (1H, t,  $J$  7.9, Ar-H), 7.31-7.26 (2H, m, Ar-H), 7.13-7.09 (1H, m, Ar-H), 7.00 (1H, d,  $J$  8.8, Ar-H), 4.29-4.22 (4H, m,  $J$  4.7,  $2 \times \text{CH}_2$ ).  $t_{\text{R}}$  (HPLC) 3.39 min.

**1,1-Dioxo-tetrahydro-1 $\lambda$ <sup>6</sup>-thiophene-3-sulfonic acid [3-(2-phenyl-thiazol-4-yl)-phenyl]-amide, 199** (JCC-CRT-194)



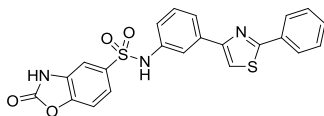
Off-white solid (8.4 mg, 19% yield, *ca.* 90% purity by  $^1\text{H-NMR}$ ),  $\delta_{\text{H}}$  (400 MHz,  $\text{DMSO-d}_6$ ) 10.28 (1H, s, NH), 8.18 (1H, s, thiazole-H), 8.02 (2H, dd,  $J$  7.8, 1.7, Ar-H), 7.93 (1H, t,  $J$  1.7, Ar-H), 7.81 (1H, d,  $J$  7.9, Ar-H), 7.58-7.51 (3H, m, Ar-H), 7.46 (1H, t,  $J$  7.9, Ar-H), 7.26 (1H, dd,  $J$  7.8, 1.5, Ar-H), 4.28-4.16 (1H, m,  $\text{SO}_2\text{CH}$ ), 4.11 (2H, d,  $J$  4.8,  $\text{SO}_2\text{CH}_2$ ), 3.53 (2H, dd,  $J$  13.9, 9.4,  $\text{SO}_2\text{CH}_2$ ), 1.14 (2H, d,  $J$  6.6,  $\text{SO}_2\text{CH}_2\text{CH}_2$ ).  $t_{\text{R}}$  (HPLC) 2.58 min.

**Thiophene-2-sulfonic acid [3-(2-phenyl-thiazol-4-yl)-phenyl]-amide, 200** (JCC-CRT-195)



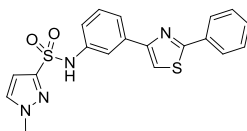
Orange gum (2.7 mg, 7% yield, *ca.* 90% purity by  $^1\text{H-NMR}$ ),  $\delta_{\text{H}}$  (400 MHz,  $\text{DMSO-d}_6$ ) 8.09 (1H, s, thiazole-H), 8.01 (2H, dd,  $J$  7.8, 1.5, Ar-H), 7.90-7.85 (2H, m, Ar-H), 7.69 (1H, d,  $J$  7.8, thiophene-H), 7.59-7.51 (4H, m, Ar-H), 7.35 (1H, t,  $J$  7.9, Ar-H), 7.15-7.10 (2H, m, thiophene-H).  $t_{\text{R}}$  (HPLC) 2.83 min.

**2-Oxo-2,3-dihydro-benzooxazole-5-sulfonic acid [3-(2-phenyl-thiazol-4-yl)-phenyl]-amide, 201** (JCC-CRT-197)



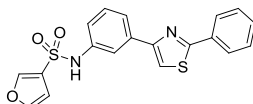
Light brown solid (1.5 mg, 3% yield, *ca.* 85% purity by  $^1\text{H-NMR}$ ),  $\delta_{\text{H}}$  (400 MHz, DMSO- $d_6$ ) 10.36 (1H, br s, NH), 8.08 (1H, s, thiazole-H), 7.99 (2H, dd,  $J$  7.9, 1.4, Ar-H), 7.82 (1H, t,  $J$  1.7, Ar-H), 7.64 (1H, d,  $J$  7.9, Ar-H), 7.59-7.49 (5H, m, Ar-H), 7.32 (1H, t,  $J$  7.9, Ar-H), 7.13-7.05 (2H, m, Ar-H).  $t_{\text{R}}$  (HPLC) 3.24 min.

**1-Methyl-1H-pyrazole-3-sulfonic acid [3-(2-phenyl-thiazol-4-yl)-phenyl]-amide, 202** (JCC-CRT-199)



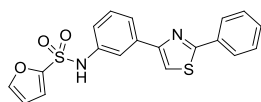
Off-white solid (4.8 mg, 12% yield, *ca.* 95% purity by  $^1\text{H-NMR}$ ),  $\delta_{\text{H}}$  (400 MHz, DMSO- $d_6$ ) 10.50 (1H, s, NH), 8.08 (1H, s, thiazole-H), 8.01 (2H, dd,  $J$  7.8, 1.5, Ar-H), 7.89 (1H, t,  $J$  1.8, Ar-H), 7.85 (1H, d,  $J$  2.3, Ar-H), 7.67 (1H, d,  $J$  7.9, Ar-H), 7.59-7.50 (3H, m, Ar-H), 7.34 (1H, t,  $J$  7.9, Ar-H), 7.15 (1H, m, pyrazole-H), 6.67 (1H, d,  $J$  2.3, pyrazole-H), 3.88 (3H, s,  $\text{CH}_3$ ).  $t_{\text{R}}$  (HPLC) 2.69 min.

**Furan-3-sulfonic acid [3-(2-phenyl-thiazol-4-yl)-phenyl]-amide, 203** (JCC-CRT-200)



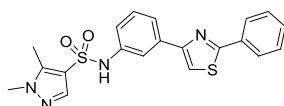
Orange gum (4.6 mg, 12% yield, *ca.* 85% purity by  $^1\text{H-NMR}$ ),  $\delta_{\text{H}}$  (400 MHz, DMSO- $d_6$ ) 10.34 (1H, s, NH), 8.37-8.34 (1H, m, furan-H), 8.13 (1H, s, thiazole-H), 8.02 (2H, dd,  $J$  7.7, 1.6, Ar-H), 7.88 (1H, t,  $J$  1.8, Ar-H), 7.84 (1H, t,  $J$  1.8, Ar-H), 7.73 (1H, d,  $J$  7.8, Ar-H), 7.58-7.52 (3H, m, Ar-H), 7.39 (1H, t,  $J$  7.9, Ar-H), 7.17 (1H, dd,  $J$  8.0, 1.3, furan-H), 6.74-6.66 (1H, m, furan-H).  $t_{\text{R}}$  (HPLC) 2.86 min.

**Furan-2-sulfonic acid [3-(2-phenyl-thiazol-4-yl)-phenyl]-amide, 204** (JCC-CRT-201)



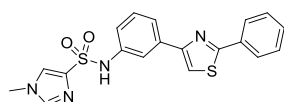
Pale orange solid (2.8 mg, 7% yield, *ca.* 85% purity by  $^1\text{H-NMR}$ ),  $\delta_{\text{H}}$  (400 MHz,  $\text{DMSO-d}_6$ ) 8.10 (1H, s, thiazole-H), 8.01 (2H, dd,  $J$  7.9, 1.6, Ar-H), 7.95 (1H, s, Ar-H), 7.83 (1H, s, Ar-H), 7.69 (1H, d,  $J$  7.8, Ar-H), 7.59-7.52 (4H, m, Ar-H, furan-H), 7.35 (1H, t,  $J$  7.9, Ar-H), 7.17 (1H, d,  $J$  3.4, Ar-H), 7.11 (1H, dd,  $J$  7.9, 1.6, furan-H), 6.63 (1H, dd,  $J$  3.5, 1.6, furan-H).  $t_{\text{R}}$  (HPLC) 2.63 min.

**1,5-Dimethyl-1H-pyrazole-4-sulfonic acid [3-(2-phenyl-thiazol-4-yl)-phenyl]-amide, 205** (JCC-CRT-203)



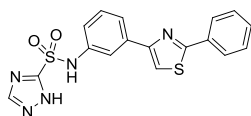
Pale orange gum (14.5 mg, 35% yield, *ca.* 75% purity by  $^1\text{H-NMR}$ ),  $\delta_{\text{H}}$  (400 MHz,  $\text{DMSO-d}_6$ ) 10.27 (1H, s, NH), 8.10 (1H, s, thiazole-H), 8.01 (2H, dd,  $J$  7.8, 1.6, Ar-H), 7.86 (1H, t,  $J$  1.8, Ar-H), 7.72 (1H, s, pyrazole-H), 7.67 (1H, d,  $J$  7.8, Ar-H), 7.58-7.50 (4H, m, Ar-H), 7.34 (1H, t,  $J$  7.9, Ar-H), 7.10 (1H, dd,  $J$  8.0, 1.4, Ar-H), 3.69 (3H, s,  $\text{NCH}_3$ ), 2.35 (3H, s, pyrazole- $\text{CH}_3$ ).  $t_{\text{R}}$  (HPLC) 3.24 min.

**1-Methyl-1H-imidazole-4-sulfonic acid [3-(2-phenyl-thiazol-4-yl)-phenyl]-amide, 206** (JCC-CRT-204)



Off-white solid (7.2 mg, 18% yield, *ca.* 95% purity by  $^1\text{H-NMR}$ ),  $\delta_{\text{H}}$  (400 MHz,  $\text{DMSO-d}_6$ ) 10.33 (1H, s, NH), 8.06 (1H, s, thiazole-H), 8.02 (2H, dd,  $J$  7.9, 1.6, Ar-H), 7.88 (1H, d,  $J$  1.0, imidazole-H), 7.86 (1H, t,  $J$  1.8, Ar-H), 7.75 (1H, d,  $J$  1.0, imidazole-H), 7.63 (1H, d,  $J$  7.8, Ar-H), 7.58-7.51 (3H, m, Ar-H), 7.31 (1H, t,  $J$  7.9, Ar-H), 7.16 (1H, dd,  $J$  8.1, 1.4, Ar-H), 3.64 (3H, s,  $\text{CH}_3$ ).  $t_{\text{R}}$  (HPLC) 2.99 min.

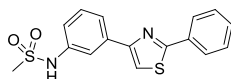
**2H-[1,2,4]Triazole-3-sulfonic acid [3-(2-phenyl-thiazol-4-yl)-phenyl]-amide, 207** (JCC-CRT-205)



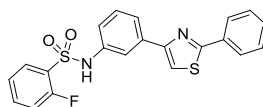
White solid (12.1 mg, 32% yield, *ca.* 90% purity by  $^1\text{H-NMR}$ ),  $\delta_{\text{H}}$  (400 MHz, DMSO- $d_6$ ) 8.69 (1H, s, triazole-H), 8.06 (1H, s, thiazole-H), 8.01 (2H, dd, *J* 7.7, 1.7, Ar-H), 7.90 (1H, t, *J* 1.8, Ar-H), 7.68 (1H, d, *J* 7.9, Ar-H), 7.58-7.52 (3H, m, Ar-H), 7.34 (1H, t, *J* 7.9, Ar-H), 7.21-7.16 (1H, m, Ar-H).  $t_{\text{R}}$  (HPLC) 2.48 min.

Four further compounds were successfully synthesised, but the purification was not sufficient for assignment of the  $^1\text{H-NMR}$  data. These compounds were tested in the enzyme assays.

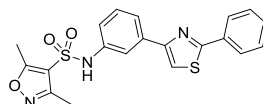
- *N*-[3-(2-Phenyl-thiazol-4-yl)-phenyl]-methanesulfonamide, **208** (JCC-CRT-183)



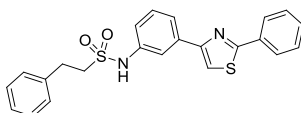
- 2-Fluoro-*N*-[3-(2-phenyl-thiazol-4-yl)-phenyl]-benzenesulfonamide, **209** (JCC-CRT-186)



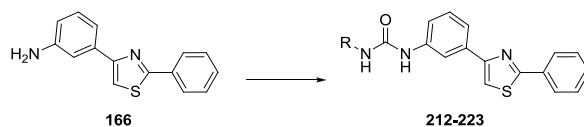
- 3,5-Dimethyl-isoxazole-4-sulfonic acid [3-(2-phenyl-thiazol-4-yl)-phenyl]-amide, **210** (JCC-CRT-189)



- 2-Phenyl-ethanesulfonic acid [3-(2-phenyl-thiazol-4-yl)-phenyl]-amide, **211** (JCC-CRT-192)

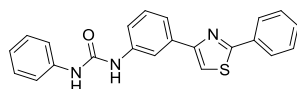


*Parallel Synthesis: General Procedure for Urea Synthesis*



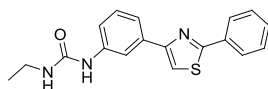
A solution of aniline **166** (20 mg, 80  $\mu\text{mol}$ ) and isocyanate (100  $\mu\text{mol}$ ) in  $\text{CH}_2\text{Cl}_2$  (0.5 mL) was shaken (24 h). The solvent was removed under a stream of  $\text{N}_2$  and the product purified by HPLC under acidic conditions.

**1-Phenyl-3-[3-(2-phenyl-thiazol-4-yl)-phenyl]-urea, 212** (JCC-CRT-206)



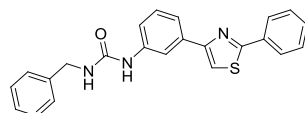
White solid (1.2 mg, 4% yield, *ca.* 90% purity by  $^1\text{H-NMR}$ ),  $\delta_{\text{H}}$  (400 MHz,  $\text{DMSO-d}_6$ ) 8.87 (1H, s, NH), 8.71 (1H, s, NH), 8.14 (1H, t,  $J$  1.7, Ar-H), 8.12 (1H, s, thiazole-H), 8.03 (2H, dd,  $J$  7.8, 1.6, Ar-H), 7.65-7.61 (1H, m, Ar-H), 7.58-7.46 (6H, m, Ar-H), 7.38 (1H, t,  $J$  7.9, Ar-H), 7.31-7.27 (2H, m, Ar-H), 6.98 (1H, t,  $J$  7.4, Ar-H).  $t_{\text{R}}$  (HPLC) 4.26 min.

**1-Ethyl-3-[3-(2-phenyl-thiazol-4-yl)-phenyl]-urea, 213** (JCC-CRT-207)



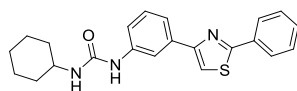
White solid (2.7 mg, 10% yield, *ca.* 98% purity by  $^1\text{H-NMR}$ ),  $\delta_{\text{H}}$  (400 MHz,  $\text{DMSO-d}_6$ ) 8.58 (1H, s, NH), 8.08-8.05 (2H, m, thiazole-H, Ar-H), 8.04-8.01 (2H, m, Ar-H), 7.57-7.51 (4H, m, Ar-H), 7.46-7.43 (1H, m, Ar-H), 7.31 (1H, t,  $J$  7.9, Ar-H), 6.11 (1H, t,  $J$  5.6, NH), 3.17-3.06 (2H, m,  $\text{CH}_2$ ), 1.07 (3H, t,  $J$  7.1,  $\text{CH}_3$ ).  $t_{\text{R}}$  (HPLC) 3.73 min.

**1-Benzyl-3-[3-(2-phenyl-thiazol-4-yl)-phenyl]-urea, 214** (JCC-CRT-208)



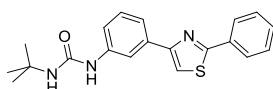
White solid (0.5 mg, 1.5% yield, *ca.* 90% purity by  $^1\text{H-NMR}$ ),  $\delta_{\text{H}}$  (400 MHz,  $\text{DMSO-d}_6$ ) 8.76 (1H, s, NH), 8.09 (1H, t,  $J$  1.8, Ar-H), 8.07 (1H, s, thiazole-H), 8.04-7.99 (2H, m, Ar-H), 7.58-7.50 (4H, m, Ar-H), 7.49-7.43 (1H, m, Ar-H), 7.37-7.30 (5H, m, Ar-H), 7.28-7.23 (1H, m, Ar-H), 6.66 (1H, t,  $J$  5.9, NH), 4.33 (2H, d,  $J$  6.0,  $\text{CH}_2$ ).  $t_{\text{R}}$  (HPLC) 4.05 min.

**1-Cyclohexyl-3-[3-(2-phenyl-thiazol-4-yl)-phenyl]-urea, 215** (JCC-CRT-209)



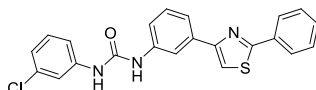
White solid (1.3 mg, 4% yield, *ca.* 90% purity by <sup>1</sup>H-NMR),  $\delta_{\text{H}}$  (400 MHz, DMSO-*d*<sub>6</sub>) 8.47 (1H, s, NH), 8.08-8.06 (2H, m, Ar-H, thiazole-H), 8.05-7.99 (2H, m, Ar-H), 7.58-7.49 (4H, m, Ar-H), 7.45-7.37 (1H, m, Ar-H), 7.31 (1H, t, *J* 7.9, Ar-H), 6.09 (1H, d, *J* 7.8, NH), 3.56-3.43 (1H, m, NCH), 1.82 (2H, d, *J* 12.2, CH<sub>2</sub>), 1.71-1.62 (2H, m, CH<sub>2</sub>), 1.60-1.51 (1H, m, CHH), 1.39-1.26 (2H, m, CH<sub>2</sub>), 1.26-1.11 (3H, m, CHH, CH<sub>2</sub>). *t*<sub>R</sub> (HPLC) 4.36 min.

**1-*tert*-Butyl-3-[3-(2-phenyl-thiazol-4-yl)-phenyl]-urea, 216** (JCC-CRT-210)



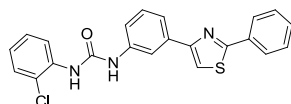
White solid (4.4 mg, 15% yield, *ca.* 90% purity by <sup>1</sup>H-NMR),  $\delta_{\text{H}}$  (400 MHz, DMSO-*d*<sub>6</sub>) 8.41 (1H, s, NH), 8.07 (1H, s, thiazole-H), 8.04-7.99 (3H, m, Ar-H), 7.57-7.49 (4H, m, Ar-H), 7.43-7.38 (1H, m, Ar-H), 7.30 (1H, t, *J* 7.9, Ar-H), 6.01 (1H, s, NH), 1.31 (9H, s, C(CH<sub>3</sub>)<sub>3</sub>). *t*<sub>R</sub> (HPLC) 4.08 min.

**1-(3-Chloro-phenyl)-3-[3-(2-phenyl-thiazol-4-yl)-phenyl]-urea, 217** (JCC-CRT-211)



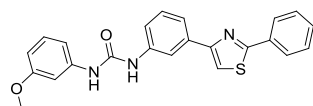
White solid (1.2 mg, 4% yield, *ca.* 95% purity by <sup>1</sup>H-NMR),  $\delta_{\text{H}}$  (400 MHz, DMSO-*d*<sub>6</sub>) 8.97 (2H, m, NH), 8.15 (1H, t, *J* 1.8, Ar-H), 8.13 (1H, s, thiazole-H), 8.03 (2H, dd, *J* 7.8, 1.6, Ar-H), 7.75-7.73 (1H, m, Ar-H), 7.68-7.63 (1H, m, Ar-H), 7.58-7.52 (3H, m, Ar-H), 7.52-7.48 (1H, m, Ar-H), 7.39 (1H, t, *J* 7.9, Ar-H), 7.32-7.28 (2H, m, Ar-H), 7.03 (1H, dt, *J* 6.6, 2.3, Ar-H). *t*<sub>R</sub> (HPLC) 4.93 min.

**1-(2-Chloro-phenyl)-3-[3-(2-phenyl-thiazol-4-yl)-phenyl]-urea, 218** (JCC-CRT-212)



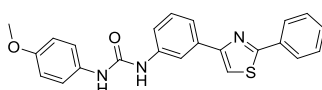
White solid (1.7 mg, 5% yield, *ca.* 95% purity by <sup>1</sup>H-NMR),  $\delta_{\text{H}}$  (400 MHz, DMSO-*d*<sub>6</sub>) 9.61 (1H, s, NH), 8.35 (1H, s, NH), 8.20 (1H, dd, *J* 8.3, 1.5, Ar-H), 8.14 (2H, m, thiazole-H, Ar-H), 8.06-8.00 (2H, m, Ar-H), 7.67-7.63 (1H, m, Ar-H), 7.59-7.52 (4H, m, Ar-H), 7.47 (1H, dd, *J* 8.0, 1.4, Ar-H), 7.41 (1H, t, *J* 7.9, Ar-H), 7.36-7.28 (1H, m, Ar-H), 7.09-7.00 (1H, m, Ar-H). *t*<sub>R</sub> (HPLC) 4.78 min.

**1-(3-Methoxy-phenyl)-3-[3-(2-phenyl-thiazol-4-yl)-phenyl]-urea, 219** (JCC-CRT-214)



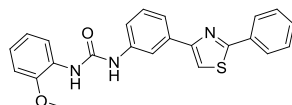
White solid (1.3 mg, 4% yield, *ca.* 90% purity by  $^1\text{H-NMR}$ ),  $\delta_{\text{H}}$  (400 MHz, DMSO- $d_6$ ) 8.86 (1H, s, NH), 8.73 (1H, s, NH), 8.12 (2H, m, thiazole-H, Ar-H), 8.03 (2H, dd,  $J$  7.9, 1.7, Ar-H), 7.66-7.61 (1H, m, Ar-H), 7.58-7.52 (4H, m, Ar-H), 7.52-7.48 (1H, m, Ar-H), 7.38 (1H, t,  $J$  7.9, Ar-H), 7.22-7.16 (2H, m, Ar-H), 6.96 (1H, dd,  $J$  7.9, 1.2, Ar-H), 6.56 (1H, dd,  $J$  8.3, 2.2, Ar-H), 3.82 (3H, s,  $\text{CH}_3$ ).  $t_{\text{R}}$  (HPLC) 4.20 min.

**1-(4-Methoxy-phenyl)-3-[3-(2-phenyl-thiazol-4-yl)-phenyl]-urea, 220** (JCC-CRT-215)



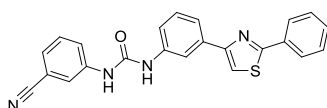
White solid (0.7 mg, 2% yield, *ca.* 90% purity by  $^1\text{H-NMR}$ ),  $\delta_{\text{H}}$  (400 MHz, DMSO- $d_6$ ) 8.80 (1H, s, NH), 8.53 (1H, s, NH), 8.15-8.12 (1H, m, Ar-H), 8.11 (1H, s, thiazole-H), 8.03 (2H, dd,  $J$  7.8, 1.6, Ar-H), 7.62 (1H, d,  $J$  7.8, Ar-H), 7.58-7.51 (3H, m, Ar-H), 7.51-7.47 (1H, m, Ar-H), 7.40-7.34 (3H, m, Ar-H), 6.88 (2H, d,  $J$  9.1, Ar-H), 3.72 (3H, s,  $\text{CH}_3$ ).  $t_{\text{R}}$  (HPLC) 4.14 min.

**1-(2-Methoxy-phenyl)-3-[3-(2-phenyl-thiazol-4-yl)-phenyl]-urea, 221** (JCC-CRT-216)



White solid (5.2 mg, 16% yield, *ca.* 95% purity by  $^1\text{H-NMR}$ ),  $\delta_{\text{H}}$  (400 MHz, DMSO- $d_6$ ) 9.50 (1H, s, NH), 8.28 (1H, s, NH), 8.17 (1H, dd,  $J$  7.8, 1.8, Ar-H), 8.13 (2H, m, thiazole-H, Ar-H), 8.03 (2H, dd,  $J$  7.7, 1.6, Ar-H), 7.63 (1H, d,  $J$  7.7, Ar-H), 7.59-7.49 (4H, m, Ar-H), 7.38 (1H, t,  $J$  7.9, Ar-H), 7.03 (1H, dd,  $J$  8.0, 1.5, Ar-H), 6.96 (1H, td,  $J$  7.7, 1.8, Ar-H), 6.91 (1H, td,  $J$  7.6, 1.5, Ar-H), 3.89 (3H, s,  $\text{CH}_3$ ).  $t_{\text{R}}$  (HPLC) 4.46 min.

**1-(3-Cyano-phenyl)-3-[3-(2-phenyl-thiazol-4-yl)-phenyl]-urea, 222** (JCC-CRT-218)



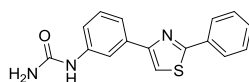
White solid (1.4 mg, 5% yield, *ca.* 90% purity by  $^1\text{H-NMR}$ ),  $\delta_{\text{H}}$  (400 MHz, DMSO- $d_6$ ) 9.10 (2H, m, NH), 8.16 (1H, t,  $J$  1.7, Ar-H), 8.14 (1H, s, thiazole-H), 8.03 (2H, dd,  $J$  7.8, 1.5, Ar-



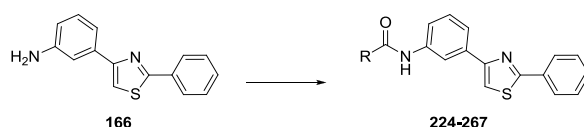
H), 8.02-7.99 (1H, m, Ar-H), 7.73-7.69 (1H, m, Ar-H), 7.69-7.64 (1H, m, Ar-H), 7.59-7.48 (5H, m, Ar-H), 7.46-7.37 (2H, m, Ar-H).  $t_R$  (HPLC) 4.17 min.

One further compound was successfully synthesised, but the purification was not sufficient for assignment of the  $^1\text{H-NMR}$  data. This compound was tested in the enzyme assays.

– [3-(2-Phenyl-thiazol-4-yl)-phenyl]-urea, **223** (JCC-CRT-217)

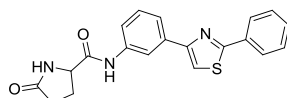


*Parallel Synthesis: General Procedure for HATU Amide Couplings*



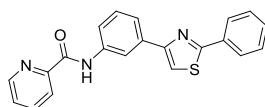
A solution of aniline **166** (20 mg, 80  $\mu\text{mol}$ ), carboxylic acid (88  $\mu\text{mol}$ ), DIPEA (35  $\mu\text{L}$ , 200  $\mu\text{mol}$ ) and HATU (34 mg, 88  $\mu\text{mol}$ ) in  $\text{CH}_2\text{Cl}_2$  (0.5 mL) was shaken (72 h). The solvent was removed under a stream of  $\text{N}_2$  and the product purified by HPLC under acidic conditions.

**5-Oxo-pyrrolidine-2-carboxylic acid [3-(2-phenyl-thiazol-4-yl)-phenyl]-amide, 224** (JCC-CRT-231)



Pale orange solid (16.6 mg, 57% yield, *ca.* 90% purity by  $^1\text{H-NMR}$ ),  $\delta_H$  (400 MHz,  $\text{DMSO-d}_6$ ) 10.21 (1H, s, NH), 8.32 (1H, t,  $J$  1.6, Ar-H), 8.13 (1H, s, thiazole-H), 8.03 (2H, dd,  $J$  7.8, 1.5, Ar-H), 7.93 (1H, s, NH), 7.75-7.68 (2H, m, Ar-H), 7.59-7.50 (3H, m, Ar-H), 7.42 (1H, t,  $J$  7.9, Ar-H), 4.23 (1H, dd,  $J$  8.6, 4.3, NCH), 2.41-1.99 (4H, m,  $2 \times \text{CH}_2$ ).  $t_R$  (HPLC) 4.17 min.

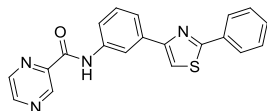
**Pyridine-2-carboxylic acid [3-(2-phenyl-thiazol-4-yl)-phenyl]-amide, 225** (JCC-CRT-232)



Pale orange solid (14.9 mg, 52% yield, *ca.* 98% purity by  $^1\text{H-NMR}$ ),  $\delta_H$  (400 MHz,  $\text{DMSO-d}_6$ ) 10.76 (1H, s, NH), 8.77 (1H, d,  $J$  4.4, pyridine-H), 8.63 (1H, t,  $J$  1.7, Ar-H), 8.21 (1H, d,  $J$  7.8, pyridine-H), 8.15 (1H, s, thiazole-H), 8.11 (1H, dd,  $J$  7.7, 1.7, Ar-H), 8.09-8.04 (2H, m, Ar-H,

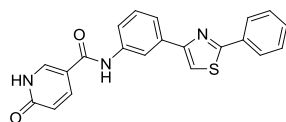
pyridine-H), 7.96 (1H, dd, *J* 8.0, 1.2, pyridine-H), 7.82-7.79 (1H, m, Ar-H), 7.70 (1H, ddd, *J* 7.6, 4.8, 1.2, Ar-H), 7.59-7.52 (3H, m, Ar-H), 7.48 (1H, t, *J* 7.9, Ar-H). *t*<sub>R</sub> (HPLC) 4.61 min.

**Pyrazine-2-carboxylic acid [3-(2-phenyl-thiazol-4-yl)-phenyl]-amide, 226** (JCC-CRT-234)



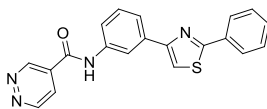
Off-white solid (11.9 mg, 41% yield, *ca.* 98% purity by <sup>1</sup>H-NMR),  $\delta_{\text{H}}$  (400 MHz, DMSO-*d*<sub>6</sub>) 10.86 (1H, s, NH), 9.34 (1H, d, *J* 1.5, pyrazine-H), 8.96 (1H, d, *J* 2.4, pyrazine-H), 8.84 (1H, dd, *J* 2.4, 1.5, pyrazine-H), 8.64 (1H, t, *J* 1.7, Ar-H), 8.15 (1H, s, thiazole-H), 8.07-8.04 (2H, m, Ar-H), 7.94 (1H, dd, *J* 8.0, 1.3, Ar-H), 7.84-7.80 (1H, m, Ar-H), 7.59-7.51 (3H, m, Ar-H), 7.49 (1H, t, *J* 7.9, Ar-H). *t*<sub>R</sub> (HPLC) 4.11 min.

**6-Hydroxy-*N*-[3-(2-phenyl-thiazol-4-yl)-phenyl]-nicotinamide, 227** (JCC-CRT-235)



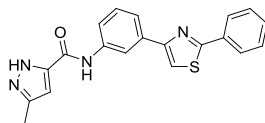
Orange solid (13.0 mg, 43% yield, *ca.* 95% purity by <sup>1</sup>H-NMR),  $\delta_{\text{H}}$  (400 MHz, DMSO-*d*<sub>6</sub>) 12.14 (1H, s, pyridone-NH), 10.12 (1H, s, NH), 8.38 (1H, t, *J* 1.7, Ar-H), 8.26 (1H, d, *J* 2.6, pyridone-H), 8.13 (1H, s, thiazole-H), 8.05-7.99 (3H, m, Ar-H, pyridone-H), 7.79 (1H, dd, *J* 8.1, 1.2, Ar-H), 7.75-7.71 (1H, m, Ar-H), 7.58-7.51 (3H, m, Ar-H), 7.44 (1H, t, *J* 7.9, Ar-H), 6.43 (1H, d, *J* 9.6, pyridone-H). *t*<sub>R</sub> (HPLC) 3.69 min.

**Pyridazine-4-carboxylic acid [3-(2-phenyl-thiazol-4-yl)-phenyl]-amide, 228** (JCC-CRT-237)



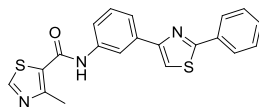
Pale orange solid (14.4 mg, 50% yield, *ca.* 98% purity by <sup>1</sup>H-NMR),  $\delta_{\text{H}}$  (400 MHz, DMSO-*d*<sub>6</sub>) 10.87 (1H, s, NH), 9.70 (1H, dd, *J* 2.1, 1.1, pyridazine-H), 9.52 (1H, dd, *J* 5.3, 1.1), 8.48 (1H, s, Ar-H), 8.19-8.16 (2H, m, pyridazine-H, thiazole-H), 8.04 (2H, dd, *J* 7.7, 1.7, Ar-H), 7.87-7.81 (2H, m, Ar-H), 7.58-7.48 (4H, m, Ar-H). *t*<sub>R</sub> (HPLC) 3.74 min.

**5-Methyl-2H-pyrazole-3-carboxylic acid [3-(2-phenyl-thiazol-4-yl)-phenyl]-amide, 229**  
(JCC-CRT-245)



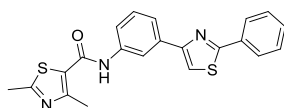
Off-white solid (12.3 mg, 43% yield, *ca.* 98% purity by  $^1\text{H-NMR}$ ),  $\delta_{\text{H}}$  (400 MHz, DMSO- $d_6$ ) 13.12 (1H, s, pyrazole-NH), 10.05 (1H, s, CONH), 8.54 (1H, s, Ar-H), 8.10 (1H, s, thiazole-H), 8.05 (2H, dd,  $J$  7.7, 1.6, Ar-H), 7.85 (1H, d,  $J$  8.5, Ar-H), 7.74 (1H, d,  $J$  7.7, Ar-H), 7.58-7.52 (3H, m, Ar-H), 7.42 (1H, t,  $J$  7.9, Ar-H), 6.54 (1H, s, pyrazole-H), 2.31 (3H, s,  $\text{CH}_3$ ).  $t_{\text{R}}$  (HPLC) 3.90 min.

**4-Methyl-thiazole-5-carboxylic acid [3-(2-phenyl-thiazol-4-yl)-phenyl]-amide, 230** (JCC-CRT-249)



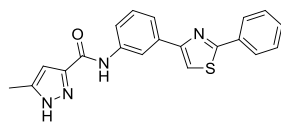
Off-white solid (18.5 mg, 61% yield, *ca.* 98% purity by  $^1\text{H-NMR}$ ),  $\delta_{\text{H}}$  (400 MHz, DMSO- $d_6$ ) 10.38 (1H, s, NH), 9.15 (1H, s, thiazole 2-H), 8.38 (1H, t,  $J$  1.6, Ar-H), 8.14 (1H, s, thiazole 5-H), 8.04 (2H, dd,  $J$  7.8, 1.7, Ar-H), 7.80-7.77 (1H, m, Ar-H), 7.73 (1H, dd,  $J$  8.0, 1.2, Ar-H), 7.58-7.51 (3H, m, Ar-H), 7.46 (1H, t,  $J$  7.9, Ar-H), 2.65 (3H, s,  $\text{CH}_3$ ).  $t_{\text{R}}$  (HPLC) 3.93 min.

**2,4-Dimethyl-thiazole-5-carboxylic acid [3-(2-phenyl-thiazol-4-yl)-phenyl]-amide, 231**  
(JCC-CRT-250)



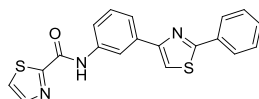
Off-white solid (13.0 mg, 41% yield, *ca.* 95% purity by  $^1\text{H-NMR}$ ),  $\delta_{\text{H}}$  (400 MHz, DMSO- $d_6$ ) 10.23 (1H, s, NH), 8.36 (1H, t,  $J$  1.7, Ar-H), 8.14 (1H, s, thiazole-H), 8.03 (2H, dd,  $J$  7.7, 1.7, Ar-H), 7.79-7.76 (1H, m, Ar-H), 7.71 (1H, dd,  $J$  8.2, 1.1, Ar-H), 7.58-7.51 (3H, m, Ar-H), 7.45 (1H, t,  $J$  7.9, Ar-H), 2.67 (3H, s,  $\text{CH}_3$ ), 2.57 (3H, s,  $\text{CH}_3$ ).  $t_{\text{R}}$  (HPLC) 4.07 min.

**5-Methyl-1H-pyrazole-3-carboxylic acid [3-(2-phenyl-thiazol-4-yl)-phenyl]-amide, 232**  
(JCC-CRT-251)



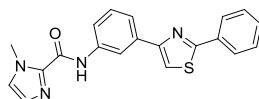
Off-white solid (8.8 mg, 31% yield, *ca.* 95% purity by  $^1\text{H-NMR}$ ),  $\delta_{\text{H}}$  (400 MHz, DMSO- $\text{d}_6$ ) 13.12 (1H, s, pyrazole-NH), 10.05 (1H, s, CONH), 8.54 (1H, s, Ar-H), 8.10 (1H, s, thiazole-H), 8.05 (2H, dd,  $J$  7.7, 1.6, Ar-H), 7.85 (1H, d,  $J$  8.4, Ar-H), 7.74 (1H, d,  $J$  7.7, Ar-H), 7.58-7.52 (3H, m, Ar-H), 7.42 (1H, t,  $J$  7.9, Ar-H), 6.54 (1H, s, pyrazole-H), 2.31 (3H, s,  $\text{CH}_3$ ).  $t_{\text{R}}$  (HPLC) 3.88 min.

**Thiazole-2-carboxylic acid [3-(2-phenyl-thiazol-4-yl)-phenyl]-amide, 233** (JCC-CRT-252)



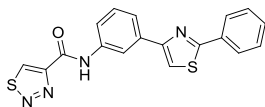
Pale orange solid (14.2 mg, 49% yield, *ca.* 90% purity by  $^1\text{H-NMR}$ ),  $\delta_{\text{H}}$  (400 MHz, DMSO- $\text{d}_6$ ) 9.95 (1H, s, NH), 8.53 (1H, s, Ar-H), 8.11 (1H, s, thiazole-H), 8.05 (2H, dd,  $J$  7.7, 1.6, Ar-H), 7.88 (2H, m, thiazole-H), 7.85 (1H, d,  $J$  1.0, Ar-H), 7.73 (1H, d,  $J$  7.8, Ar-H), 7.58-7.52 (3H, m, Ar-H), 7.42 (1H, t,  $J$  7.9, Ar-H).  $t_{\text{R}}$  (HPLC) 3.72 min.

**1-Methyl-1H-imidazole-2-carboxylic acid [3-(2-phenyl-thiazol-4-yl)-phenyl]-amide, 234**  
(JCC-CRT-256)



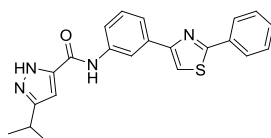
White solid (5.7 mg, 20% yield, *ca.* 98% purity by  $^1\text{H-NMR}$ ),  $\delta_{\text{H}}$  (400 MHz, DMSO- $\text{d}_6$ ) 10.42 (1H, s, NH), 8.54 (1H, t,  $J$  1.7, Ar-H), 8.11 (1H, s, thiazole-H), 8.05 (2H, dd,  $J$  7.8, 1.7, Ar-H), 7.85 (1H, dd,  $J$  8.1, 1.2, Ar-H), 7.76 (1H, d,  $J$  7.8, Ar-H), 7.58-7.52 (3H, m, Ar-H), 7.47 (1H, br s, imidazole-H), 7.44 (1H, t,  $J$  7.9, Ar-H), 7.11 (1H, d,  $J$  0.8, imidazole-H), 4.02 (3H, s,  $\text{CH}_3$ ).  $t_{\text{R}}$  (HPLC) 4.09 min.

**[1,2,3]Thiadiazole-4-carboxylic acid [3-(2-phenyl-thiazol-4-yl)-phenyl]-amide, 235** (JCC-CRT-257)



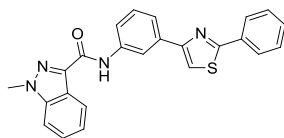
Off-white solid (3.8 mg, 13% yield, *ca.* 90% purity by  $^1\text{H-NMR}$ ),  $\delta_{\text{H}}$  (400 MHz,  $\text{DMSO-d}_6$ ) 11.08 (1H, s, NH), 9.87 (1H, s, thiadiazole-H), 8.61 (1H, s, Ar-H), 8.15 (1H, s, thiazole-H), 8.06 (2H, dd,  $J$  7.8, 1.6, Ar-H), 7.91 (1H, dd,  $J$  8.0, 1.2, Ar-H), 7.82 (1H, d,  $J$  7.8, Ar-H), 7.59-7.52 (3H, m, Ar-H), 7.49 (1H, t,  $J$  7.9, Ar-H).  $t_{\text{R}}$  (HPLC) 4.02 min.

**5-Isopropyl-2H-pyrazole-3-carboxylic acid [3-(2-phenyl-thiazol-4-yl)-phenyl]-amide, 236** (JCC-CRT-259)



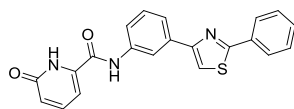
Off-white solid (7.7 mg, 25% yield, *ca.* 95% purity by  $^1\text{H-NMR}$ ),  $\delta_{\text{H}}$  (400 MHz,  $\text{DMSO-d}_6$ ) 13.12 (1H, s, pyrazole-NH), 10.04 (1H, s, CONH), 8.52 (1H, s, Ar-H), 8.11 (1H, s, thiazole-H), 8.05 (2H, dd,  $J$  7.6, 1.5, Ar-H), 7.85 (1H, dd,  $J$  8.1, 1.1, Ar-H), 7.74 (1H, d,  $J$  7.7, Ar-H), 7.58-7.52 (3H, m, Ar-H), 7.42 (1H, t,  $J$  7.9, Ar-H), 6.57 (1H, s, pyrazole-H), 3.03 (1H, sept,  $J$  6.9,  $\text{CH}(\text{CH}_3)_2$ ), 1.27 (6H, d,  $J$  6.9,  $\text{CH}(\text{CH}_3)_2$ ).  $t_{\text{R}}$  (HPLC) 4.20 min.

**1-Methyl-1H-indazole-3-carboxylic acid [3-(2-phenyl-thiazol-4-yl)-phenyl]-amide, 237** (JCC-CRT-260)



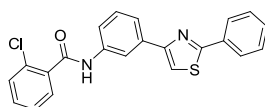
Off-white solid (6.1 mg, 19% yield, *ca.* 95% purity by  $^1\text{H-NMR}$ ),  $\delta_{\text{H}}$  (400 MHz,  $\text{DMSO-d}_6$ ) 10.45 (1H, s, NH), 8.62 (1H, s, Ar-H), 8.27 (1H, d,  $J$  8.0, Ar-H), 8.14 (1H, s, thiazole-H), 8.07 (2H, s, Ar-H), 7.95 (1H, d,  $J$  7.7, Ar-H), 7.84-7.75 (2H, m, Ar-H), 7.61-7.43 (5H, m, Ar-H), 7.35 (1H, s, Ar-H), 4.23 (3H, s,  $\text{CH}_3$ ).  $t_{\text{R}}$  (HPLC) 5.14 min.

**6-Hydroxy-pyridine-2-carboxylic acid [3-(2-phenyl-thiazol-4-yl)-phenyl]-amide, 238**  
(JCC-CRT-284)



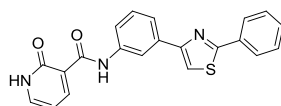
Orange solid (10.8 mg, 36% yield, *ca.* 95% purity by  $^1\text{H-NMR}$ ),  $\delta_{\text{H}}$  (400 MHz, DMSO- $\text{d}_6$ ) 11.33 (1H, s, pyridone-NH), 10.37 (1H, s, NH), 8.46 (1H, s, Ar-H), 8.17 (1H, s, thiazole-H), 8.05 (2H, dd,  $J$  7.8, 1.6, Ar-H), 7.85 (1H, dd,  $J$  8.1, 1.3, Ar-H), 7.83-7.78 (2H, m, pyridone-H, Ar-H), 7.59-7.52 (3H, m, Ar-H), 7.51-7.42 (2H, m, pyridone-H, Ar-H), 6.84 (1H, d,  $J$  8.4, pyridone-H).  $t_{\text{R}}$  (HPLC) 3.86 min.

**2-Chloro-*N*-[3-(2-phenyl-thiazol-4-yl)-phenyl]-benzamide, 239** (JCC-CRT-229)



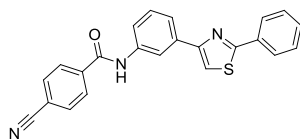
Off-white crystalline solid (17.4 mg, 56% yield, *ca.* 95% purity by  $^1\text{H-NMR}$ ),  $\delta_{\text{H}}$  (400 MHz, DMSO- $\text{d}_6$ ) 10.65 (1H, s, NH), 8.45 (1H, t,  $J$  1.7, Ar-H), 8.13 (1H, s, thiazole-H), 8.07-7.99 (2H, m, Ar-H), 7.77 (2H, dd,  $J$  8.0, 1.8, Ar-H), 7.66-7.42 (8H, m, Ar-H).  $t_{\text{R}}$  (HPLC) 3.58 min.

**2-Oxo-1,2-dihydro-pyridine-3-carboxylic acid [3-(2-phenyl-thiazol-4-yl)-phenyl]-amide, 240** (JCC-CRT-233)



Red solid (6.2 mg, 21% yield, *ca.* 80% purity by  $^1\text{H-NMR}$ ),  $\delta_{\text{H}}$  (400 MHz, DMSO- $\text{d}_6$ ) 12.46 (1H, s, pyridone-NH), 8.48 (1H, dd,  $J$  7.2, 2.2, pyridone-H), 8.33 (1H, s, Ar-H), 8.22 (1H, s, thiazole-H), 8.08-7.98 (2H, m, Ar-H), 7.85 (1H, dd,  $J$  6.2, 2.2, Ar-H), 7.81-7.72 (2H, m, pyridone-H, Ar-H), 7.57-7.51 (3H, m, Ar-H), 7.47 (1H, t,  $J$  7.9, Ar-H), 6.58 (1H, m, pyridone-H).  $t_{\text{R}}$  (HPLC) 3.44 min.

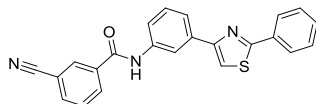
**4-Cyano-*N*-[3-(2-phenyl-thiazol-4-yl)-phenyl]-benzamide, 241** (JCC-CRT-236)



Pale orange solid (15.2 mg, 50% yield, *ca.* 95% purity by  $^1\text{H-NMR}$ ),  $\delta_{\text{H}}$  (400 MHz, DMSO- $\text{d}_6$ ) 10.65 (1H, s, NH), 8.51-8.43 (1H, m, Ar-H), 8.19-8.13 (3H, m,  $2 \times$  Ar-H, thiazole-H), 8.07-

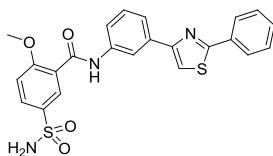
8.01 (4H, m, Ar-H), 7.88-7.83 (1H, m, Ar-H), 7.82-7.77 (1H, m, Ar-H), 7.57-7.51 (3H, m, Ar-H), 7.52-7.44 (1H, m, Ar-H).  $t_R$  (HPLC) 3.56 min.

**3-Cyano-*N*-[3-(2-phenyl-thiazol-4-yl)-phenyl]-benzamide, 242** (JCC-CRT-238)



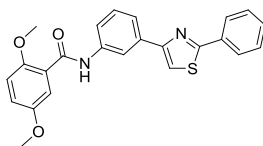
Off-white solid (11.3 mg, 37% yield, *ca.* 85% purity by  $^1\text{H-NMR}$ ),  $\delta_H$  (400 MHz, DMSO- $d_6$ ) 10.58 (1H, s, NH), 8.47 (2H, s, Ar-H), 8.33-8.28 (1H, m, Ar-H), 8.16 (1H, s, thiazole-H), 8.11-8.07 (1H, m, Ar-H), 8.07-8.01 (2H, m, Ar-H), 7.90-7.85 (1H, m, Ar-H), 7.82-7.74 (2H, m, Ar-H), 7.59-7.52 (3H, m, Ar-H), 7.52-7.45 (1H, m, Ar-H).  $t_R$  (HPLC) 3.58 min.

**2-Methoxy-*N*-[3-(2-phenyl-thiazol-4-yl)-phenyl]-5-sulfamoyl-benzamide, 243** (JCC-CRT-262)



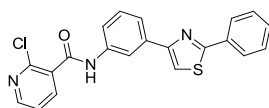
White solid (14.3 mg, 39% yield, *ca.* 80% purity by  $^1\text{H-NMR}$ ),  $\delta_H$  (400 MHz, DMSO- $d_6$ ) 10.40 (1H, s, CONH), 8.43 (1H, s, Ar-H), 8.15 (1H, s, thiazole-H), 8.07 (1H, d,  $J$  2.4, Ar-H), 8.06-8.02 (2H, m, Ar-H), 7.94 (1H, dd,  $J$  8.7, 2.4, Ar-H), 7.80-7.73 (2H, m, Ar-H), 7.59-7.49 (4H, m, Ar-H), 7.46 (1H, t,  $J$  7.9, Ar-H), 7.37 (2H, s,  $\text{SO}_2\text{NH}_2$ ), 3.98 (3H, s,  $\text{CH}_3$ ).  $t_R$  (HPLC) 3.39 min.

**2,5-Dimethoxy-*N*-[3-(2-phenyl-thiazol-4-yl)-phenyl]-benzamide, 244** (JCC-CRT-263)



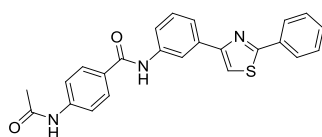
Pale yellow solid (7.9 mg, 24% yield, *ca.* 80% purity by  $^1\text{H-NMR}$ ),  $\delta_H$  (400 MHz, DMSO- $d_6$ ) 10.28 (1H, s, NH), 8.46 (1H, s, Ar-H), 8.14 (1H, s, thiazole-H), 8.06-8.00 (2H, m, Ar-H), 7.79-7.71 (2H, m, Ar-H), 7.53 (3H, dd,  $J$  12.7, 6.1, Ar-H), 7.45 (1H, t,  $J$  7.9, Ar-H), 7.25 (1H, d,  $J$  3.0, Ar-H), 7.14 (1H, d,  $J$  9.0, Ar-H), 7.09 (1H, dd,  $J$  9.0, 3.1, Ar-H), 3.89 (3H, s,  $\text{CH}_3$ ), 3.77 (3H, s,  $\text{CH}_3$ ).  $t_R$  (HPLC) 3.73 min.

**2-Chloro-*N*-[3-(2-phenyl-thiazol-4-yl)-phenyl]-nicotinamide, 245** (JCC-CRT-265)



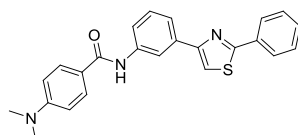
Pale yellow needles (16.4 mg, 52% yield, *ca.* 85% purity by  $^1\text{H-NMR}$ ),  $\delta_{\text{H}}$  (400 MHz, DMSO- $d_6$ ) 10.80 (1H, s, NH), 8.56 (1H, dd,  $J$  4.9, 1.9, pyridine-H), 8.42 (1H, s, Ar-H), 8.16 (1H, s, thiazole-H), 8.13 (1H, dd,  $J$  7.6, 1.9, pyridine-H), 8.05-8.01 (2H, m, Ar-H), 7.81-7.75 (2H, m, Ar-H), 7.59 (1H, dd,  $J$  7.6, 4.9, pyridine-H), 7.56-7.51 (3H, m, Ar-H), 7.48 (1H, t,  $J$  7.9, Ar-H).  $t_{\text{R}}$  (HPLC) 3.46 min.

**4-Acetylamino-*N*-[3-(2-phenyl-thiazol-4-yl)-phenyl]-benzamide, 246** (JCC-CRT-268)



Pale orange solid (12.1 mg, 37% yield, *ca.* 90% purity by  $^1\text{H-NMR}$ ),  $\delta_{\text{H}}$  (400 MHz, DMSO- $d_6$ ) 10.27 (1H, s, NH), 10.25 (1H, s, NH), 8.47 (1H, s, Ar-H), 8.13 (1H, s, thiazole-H), 8.06-8.03 (2H, m, Ar-H), 8.00-7.96 (2H, m, Ar-H), 7.87-7.82 (1H, m, Ar-H), 7.77-7.71 (3H, m, Ar-H), 7.56-7.51 (3H, m, Ar-H), 7.45 (1H, t,  $J$  8.0, Ar-H), 2.67 (3H, s,  $\text{CH}_3$ ).  $t_{\text{R}}$  (HPLC) 3.49 min.

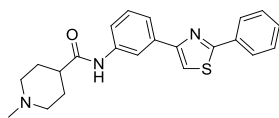
**4-Dimethylamino-*N*-[3-(2-phenyl-thiazol-4-yl)-phenyl]-benzamide, 247** (JCC-CRT-270)



Orange solid (9.3 mg, 29% yield, *ca.* 85% purity by  $^1\text{H-NMR}$ ),  $\delta_{\text{H}}$  (400 MHz, DMSO- $d_6$ ) 10.02 (1H, s, NH), 8.47 (1H, t,  $J$  1.7, Ar-H), 8.11 (1H, s, thiazole-H), 8.05 (2H, dd,  $J$  7.8, 1.6, Ar-H), 7.93 (2H, d,  $J$  9.0, Ar-H), 7.84 (1H, dd,  $J$  8.0, 1.2, Ar-H), 7.74-7.69 (1H, m, Ar-H), 7.57-7.51 (3H, m, Ar-H), 7.42 (1H, t,  $J$  7.9, Ar-H), 6.78 (2H, d,  $J$  9.0, Ar-H), 3.01 (6H, s,  $\text{N}(\text{CH}_3)_2$ ).  $t_{\text{R}}$  (HPLC) 3.64 min.

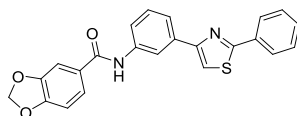


**1-Methyl-piperidine-4-carboxylic acid [3-(2-phenyl-thiazol-4-yl)-phenyl]-amide, 248**  
(JCC-CRT-271)



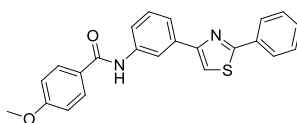
Off-white solid (7.6 mg, 25% yield, *ca.* 95% purity by  $^1\text{H-NMR}$ ),  $\delta_{\text{H}}$  (400 MHz, DMSO- $d_6$ ) 10.01 (1H, s, NH), 8.35-8.27 (1H, m, Ar-H), 8.10 (1H, s, thiazole-H), 8.03 (2H, dd,  $J$  7.8, 1.7, Ar-H), 7.70-7.64 (2H, m, Ar-H), 7.58-7.50 (3H, m, Ar-H), 7.38 (1H, t,  $J$  7.9, Ar-H), 2.83 (2H, d,  $J$  11.3,  $\text{NCH}_2$ ), 2.35-2.25 (1H, m, COCH), 2.16 (3H, s,  $\text{NCH}_3$ ), 1.92-1.81 (2H, m,  $\text{NCH}_2$ ), 1.81-1.73 (2H, m,  $\text{NCH}_2\text{CH}_2$ ), 1.73-1.61 (2H, m,  $\text{NCH}_2\text{CH}_2$ ).  $t_{\text{R}}$  (HPLC) 3.44 min.

**Benzo[1,3]dioxole-5-carboxylic acid [3-(2-phenyl-thiazol-4-yl)-phenyl]-amide, 249** (JCC-CRT-273)



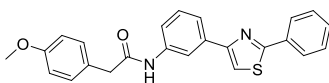
Pale orange solid (9.9 mg, 31% yield, *ca.* 95% purity by  $^1\text{H-NMR}$ ),  $\delta_{\text{H}}$  (400 MHz, DMSO- $d_6$ ) 10.22 (1H, s, NH), 8.46 (1H, t,  $J$  1.7, Ar-H), 8.13 (1H, s, thiazole-H), 8.05 (2H, dd,  $J$  7.8, 1.7, Ar-H), 7.83 (1H, dd,  $J$  8.1, 1.2, Ar-H), 7.75 (1H, d,  $J$  7.8, Ar-H), 7.64 (1H, dd,  $J$  8.2, 1.8, Ar-H), 7.57 (1H, d,  $J$  1.8, Ar-H), 7.56-7.51 (3H, m, Ar-H), 7.45 (1H, t,  $J$  7.9, Ar-H), 7.08 (1H, d,  $J$  8.2, Ar-H), 6.15 (2H, s,  $\text{CH}_2$ ).  $t_{\text{R}}$  (HPLC) 3.61 min.

**4-Methoxy-N-[3-(2-phenyl-thiazol-4-yl)-phenyl]-benzamide, 250** (JCC-CRT-274)



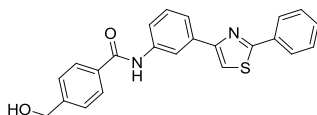
Pale yellow solid (5.0 mg, 16% yield, *ca.* 85% purity by  $^1\text{H-NMR}$ ),  $\delta_{\text{H}}$  (400 MHz, DMSO- $d_6$ ) 10.24 (1H, s, NH), 8.47 (1H, t,  $J$  1.8, Ar-H), 8.13 (1H, s, thiazole-H), 8.05-8.00 (4H, m, Ar-H), 7.87-7.82 (1H, m, Ar-H), 7.77-7.72 (1H, m, Ar-H), 7.56-7.52 (3H, m, Ar-H), 7.45 (1H, t,  $J$  7.9, Ar-H), 7.10-7.06 (2H, m, Ar-H), 3.85 (3H, s,  $\text{CH}_3$ ).  $t_{\text{R}}$  (HPLC) 3.61 min.

**2-(4-Methoxy-phenyl)-N-[3-(2-phenyl-thiazol-4-yl)-phenyl]-acetamide, 251** (JCC-CRT-275)



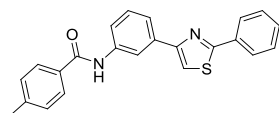
Off-white solid (9.6 mg, 30% yield, *ca.* 85% purity by  $^1\text{H-NMR}$ ),  $\delta_{\text{H}}$  (400 MHz, DMSO- $d_6$ ) 10.27 (1H, s, NH), 8.29 (1H, t,  $J$  1.7, Ar-H), 8.10 (1H, s, thiazole-H), 8.04-8.01 (2H, m, Ar-H), 7.71-7.65 (2H, m, Ar-H), 7.55-7.51 (3H, m, Ar-H), 7.39 (1H, t,  $J$  7.9, Ar-H), 7.28 (2H, d,  $J$  8.6, Ar-H), 6.92-6.88 (2H, m, Ar-H), 3.73 (3H, s,  $\text{CH}_3$ ), 3.60 (2H, s,  $\text{CH}_2$ ).  $t_{\text{R}}$  (HPLC) 3.59 min.

**4-Hydroxymethyl-N-[3-(2-phenyl-thiazol-4-yl)-phenyl]-benzamide, 252** (JCC-CRT-277)



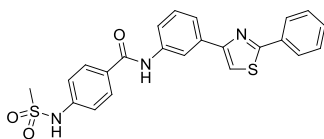
Pale brown solid (7.0 mg, 22%, *ca.* 90% purity by  $^1\text{H-NMR}$ ),  $\delta_{\text{H}}$  (400 MHz, DMSO- $d_6$ ) 10.34 (1H, s, NH), 8.48 (1H, t,  $J$  1.8, Ar-H), 8.13 (1H, s, thiazole-H), 8.08-8.03 (2H, m, Ar-H), 7.99 (2H, d,  $J$  8.3, Ar-H), 7.88-7.84 (1H, m, Ar-H), 7.79-7.74 (1H, m, Ar-H), 7.57-7.52 (3H, m, Ar-H), 7.50-7.43 (3H, m, Ar-H), 5.35 (1H, t,  $J$  5.8, OH), 4.60 (2H, d,  $J$  5.8,  $\text{CH}_2$ ).  $t_{\text{R}}$  (HPLC) 3.46 min.

**4-Methyl-N-[3-(2-phenyl-thiazol-4-yl)-phenyl]-benzamide, 253** (JCC-CRT-278)



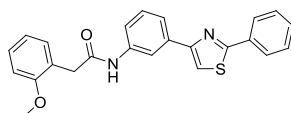
Off-white solid (2.3 mg, 8% yield, *ca.* 90% purity by  $^1\text{H-NMR}$ ),  $\delta_{\text{H}}$  (400 MHz, DMSO- $d_6$ ) 10.35 (1H, s, NH), 8.47 (1H, t,  $J$  1.8, Ar-H), 8.13 (1H, s, thiazole-H), 8.05 (2H, dd,  $J$  7.9, 1.7, Ar-H), 7.87-7.82 (2H, m, Ar-H), 7.82-7.79 (1H, m, Ar-H), 7.78-7.74 (1H, m, Ar-H), 7.57-7.51 (3H, m, Ar-H), 7.48-7.42 (3H, m, Ar-H), 2.42 (3H, s,  $\text{CH}_3$ ).  $t_{\text{R}}$  (HPLC) 4.47 min.

**4-Methanesulfonylamino-N-[3-(2-phenyl-thiazol-4-yl)-phenyl]-benzamide, 254** (JCC-CRT-280)



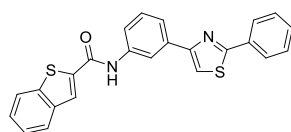
Off-white solid (3.3 mg, 9% yield, *ca.* 90% purity by  $^1\text{H-NMR}$ ),  $\delta_{\text{H}}$  (400 MHz, DMSO- $\text{d}_6$ ) 10.29 (1H, s, CONH), 10.21 (1H, s, SO $_2$ NH), 8.46 (1H, t, *J* 1.7, Ar-H), 8.13 (1H, s, thiazole-H), 8.05 (2H, dd, *J* 7.9, 1.7, Ar-H), 8.00 (2H, d, *J* 8.7, Ar-H), 7.85-7.82 (1H, m, Ar-H), 7.78-7.74 (1H, m, Ar-H), 7.58-7.52 (3H, m, Ar-H), 7.45 (1H, t, *J* 7.9, Ar-H), 7.32 (2H, d, *J* 8.7, Ar-H), 3.11 (3H, s, CH $_3$ ).  $t_{\text{R}}$  (HPLC) 3.77 min.

**2-(2-Methoxy-phenyl)-N-[3-(2-phenyl-thiazol-4-yl)-phenyl]-acetamide, 255** (JCC-CRT-285)



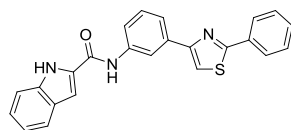
White solid (2.4 mg, 7% yield, *ca.* 90% purity by  $^1\text{H-NMR}$ ),  $\delta_{\text{H}}$  (400 MHz, DMSO- $\text{d}_6$ ) 10.20 (1H, s, NH), 8.33 (1H, s, Ar-H), 8.10 (1H, s, thiazole-H), 8.02 (2H, dd, *J* 7.8, 1.6, Ar-H), 7.67 (2H, dd, *J* 12.9, 8.6, Ar-H), 7.57-7.50 (3H, m, Ar-H), 7.39 (1H, t, *J* 7.9, Ar-H), 7.24 (2H, d, *J* 7.5, Ar-H), 6.99 (1H, d, *J* 7.9, Ar-H), 6.95-6.88 (1H, m, Ar-H), 3.78 (3H, s, CH $_3$ ), 3.67 (2H, s, CH $_2$ ).  $t_{\text{R}}$  (HPLC) 4.12 min.

**Benzo[*b*]thiophene-2-carboxylic acid [3-(2-phenyl-thiazol-4-yl)-phenyl]-amide, 256** (JCC-CRT-242)



Off-white solid (15.7 mg, 38% yield, *ca.* 90% purity by  $^1\text{H-NMR}$ ),  $\delta_{\text{H}}$  (400 MHz, DMSO- $\text{d}_6$ ) 10.68 (1H, s, NH), 8.48 (1H, t, *J* 1.8, Ar-H), 8.45 (1H, s, Ar-H), 8.17 (1H, s, thiazole-H), 8.11-8.01 (4H, m, Ar-H), 7.89-7.85 (1H, m, Ar-H), 7.81-7.78 (1H, m, Ar-H), 7.57-7.52 (3H, m, Ar-H), 7.52-7.46 (3H, m, Ar-H).  $t_{\text{R}}$  (HPLC) 3.76 min.

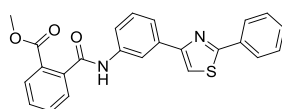
**1*H*-Indole-2-carboxylic acid [3-(2-phenyl-thiazol-4-yl)-phenyl]-amide, 257** (JCC-CRT-248)



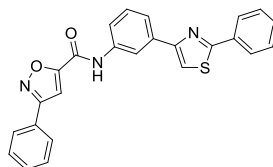
Pale orange solid (11.0 mg, 28% yield, *ca.* 90% purity by <sup>1</sup>H-NMR),  $\delta_{\text{H}}$  (400 MHz, DMSO-*d*<sub>6</sub>) 11.81 (1H, s, indole-NH), 10.39 (1H, s, CONH), 8.52 (1H, t, *J* 1.7, Ar-H), 8.15 (1H, s, thiazole-H), 8.06 (2H, dd, *J* 7.9, 1.6, Ar-H), 7.95-7.88 (1H, m, Ar-H), 7.79-7.72 (1H, m, Ar-H), 7.70 (1H, d, *J* 7.9, Ar-H), 7.58-7.47 (6H, m, Ar-H), 7.27-7.19 (1H, m, Ar-H), 7.12-7.04 (1H, m, Ar-H). *t*<sub>R</sub> (HPLC) 3.64 min.

Ten further compounds were successfully synthesised, but the purification was not sufficient for assignment of the <sup>1</sup>H-NMR data. These compounds were tested in the enzyme assays.

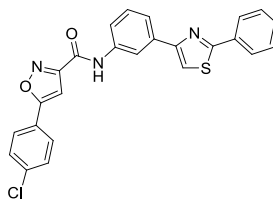
- *N*-[3-(2-Phenyl-thiazol-4-yl)-phenyl]-phthalamic acid methyl ester, **258** (JCC-CRT-228)



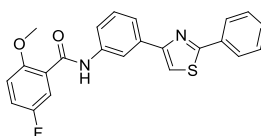
- 3-Phenyl-isoxazole-5-carboxylic acid [3-(2-phenyl-thiazol-4-yl)-phenyl]-amide, **259** (JCC-CRT-255)



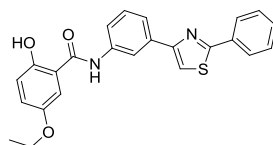
- 5-(4-Chloro-phenyl)-isoxazole-3-carboxylic acid [3-(2-phenyl-thiazol-4-yl)-phenyl]-amide, **260** (JCC-CRT-261)



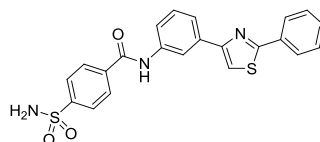
- 5-Fluoro-2-methoxy-*N*-[3-(2-phenyl-thiazol-4-yl)-phenyl]-benzamide, **261** (JCC-CRT-264)



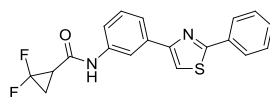
- 5-Ethoxy-2-hydroxy-*N*-[3-(2-phenyl-thiazol-4-yl)-phenyl]-benzamide, **262** (JCC-CRT-266)



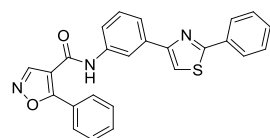
- *N*-[3-(2-Phenyl-thiazol-4-yl)-phenyl]-4-sulfamoyl-benzamide, **263** (JCC-CRT-269)



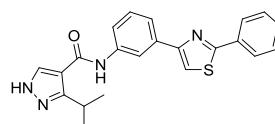
- 2,2-Difluoro-cyclopropanecarboxylic acid [3-(2-phenyl-thiazol-4-yl)-phenyl]-amide, **264** (JCC-CRT-272)



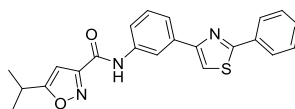
- 5-Phenyl-isoxazole-4-carboxylic acid [3-(2-phenyl-thiazol-4-yl)-phenyl]-amide, **265** (JCC-CRT-241)



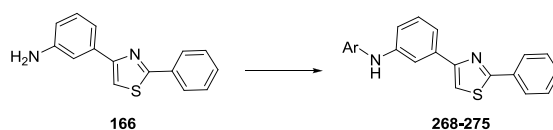
- 3-Isopropyl-1*H*-pyrazole-4-carboxylic acid [3-(2-phenyl-thiazol-4-yl)-phenyl]-amide, **266** (JCC-CRT-243)



- 5-Isopropyl-isoxazole-3-carboxylic acid [3-(2-phenyl-thiazol-4-yl)-phenyl]-amide, **267** (JCC-CRT-244)



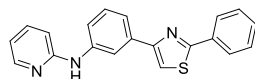
*Parallel Synthesis: General Procedure for Buchwald-Hartwig Couplings of Aniline 166*



A solution of aniline **166** (20 mg, 100  $\mu$ mol), aryl halide (100  $\mu$ mol), NaO<sup>t</sup>Bu (19.6 mg, 200  $\mu$ mol), Xantphos (5.8 mg, 10  $\mu$ mol) and Pd(dba)<sub>2</sub> (2.9 mg, 5  $\mu$ mol) in dioxane (1.5 mL) was

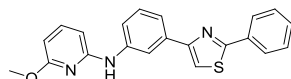
heated (MW, 150 °C, 15 min). Upon cooling, H<sub>2</sub>O (2 mL) was added and the aqueous layer extracted with CH<sub>2</sub>Cl<sub>2</sub> (5 mL), the solvent removed *in vacuo* and the product purified by HPLC under basic conditions.

**[3-(2-Phenyl-thiazol-4-yl)-phenyl]-pyridin-2-yl-amine, 268** (JCC-CRT-324)



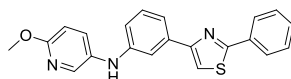
Orange gum (6.2 mg, 19% yield, *ca.* 90% purity by <sup>1</sup>H-NMR),  $\delta_{\text{H}}$  (400 MHz, DMSO-d<sub>6</sub>) 9.18 (1H, s, NH), 8.25 (1H, t, *J* 1.8, Ar-H), 8.19 (1H, dd, *J* 5.2, 1.5, pyridine-H), 8.07 (1H, s, thiazole-H), 8.04 (2H, dd, *J* 7.8, 1.5, Ar-H), 7.88 (1H, dd, *J* 8.3, 1.5, pyridine-H), 7.62-7.50 (5H, m), 7.36 (1H, t, *J* 7.9, Ar-H), 6.88 (1H, d, *J* 8.3, pyridine-H), 6.80-6.72 (1H, m, pyridine-H). *t<sub>R</sub>* (HPLC) 5.88 min.

**(6-Methoxy-pyridin-2-yl)-[3-(2-phenyl-thiazol-4-yl)-phenyl]-amine, 269** (JCC-CRT-331)



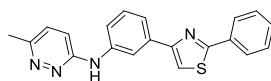
Red gum (20.4 mg, 57% yield, *ca.* 90% purity by <sup>1</sup>H-NMR),  $\delta_{\text{H}}$  (400 MHz, DMSO-d<sub>6</sub>) 9.20 (1H, s, NH), 8.57 (1H, t, *J* 1.8, Ar-H), 8.07 (1H, s, thiazole-H), 8.03-7.99 (2H, m, Ar-H), 7.65-7.60 (1H, m, pyridine-H), 7.58-7.47 (5H, m, Ar-H), 7.35 (1H, t, *J* 7.9, Ar-H), 6.44 (1H, d, *J* 7.8, pyridine-H), 6.17 (1H, d, *J* 7.8, pyridine-H), 3.92 (3H, s, CH<sub>3</sub>). *t<sub>R</sub>* (HPLC) 5.79 min.

**(6-Methoxy-pyridin-3-yl)-[3-(2-phenyl-thiazol-4-yl)-phenyl]-amine, 270** (JCC-CRT-332)



Red gum (17.6 mg, 49% yield, *ca.* 85% purity by <sup>1</sup>H-NMR),  $\delta_{\text{H}}$  (400 MHz, DMSO-d<sub>6</sub>) 8.13 (1H, s, Ar-H), 8.06 (1H, s, thiazole-H), 8.03 (1H, d, *J* 2.7, Ar-H), 8.02-7.98 (2H, m, Ar-H, NH), 7.65-7.62 (1H, m, pyridine-H), 7.58 (1H, dd, *J* 8.8, 2.9, Ar-H), 7.54-7.50 (3H, m, Ar-H), 7.43-7.39 (1H, m, Ar-H), 7.28 (1H, t, *J* 7.8, Ar-H), 6.92 (1H, dd, *J* 7.8, 1.7, pyridine-H), 6.81 (1H, d, *J* 7.8, pyridine-H), 3.83 (3H, s, OCH<sub>3</sub>). *t<sub>R</sub>* (HPLC) 5.12 min.

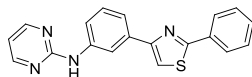
**(6-Methyl-pyridazin-3-yl)-[3-(2-phenyl-thiazol-4-yl)-phenyl]-amine, 271** (JCC-CRT-334)



Light brown solid (6.7 mg, 19% yield, *ca.* 90% purity by <sup>1</sup>H-NMR),  $\delta_{\text{H}}$  (400 MHz, DMSO-d<sub>6</sub>) 9.28 (1H, s, NH), 8.29 (1H, t, *J* 1.9, Ar-H), 8.09 (1H, s, thiazole-H), 8.05-8.02 (2H, m, Ar-H),

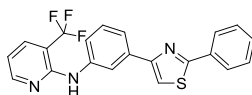
7.92 (1H, dd, *J* 8.2, 1.5, Ar-H), 7.60-7.52 (4H, m, Ar-H), 7.41 (1H, t, *J* 7.9, Ar-H), 7.35 (1H, d, *J* 9.1, pyridazine-H), 7.11 (1H, d, *J* 9.1, pyridazine-H), 2.48 (3H, s).  $t_R$  (HPLC) 3.29 min.

**[3-(2-Phenyl-thiazol-4-yl)-phenyl]-pyrimidin-2-yl-amine, 272** (JCC-CRT-338)



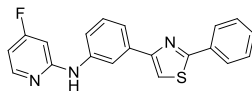
Off-white solid (7.6 mg, 23% yield, *ca.* 90% purity by  $^1\text{H-NMR}$ ),  $\delta_H$  (400 MHz, DMSO- $d_6$ ) 9.72 (1H, s, NH), 8.51 (2H, d, *J* 4.8, pyrimidine-H), 8.43 (1H, t, *J* 1.8, Ar-H), 8.06 (1H, s, thiazole-H), 8.04 (2H, dd, *J* 7.8, 1.6, Ar-H), 7.83 (1H, dd, *J* 8.2, 1.4, Ar-H), 7.65-7.59 (1H, m, Ar-H), 7.58-7.52 (3H, m, Ar-H), 7.38 (1H, t, *J* 7.9, Ar-H), 6.86 (1H, t, *J* 4.8, pyrimidine-H).  $t_R$  (HPLC) 4.70 min.

**[3-(2-Phenyl-thiazol-4-yl)-phenyl]-(3-trifluoromethyl-pyridin-2-yl)-amine, 273** (JCC-CRT-339)



Orange solid (3.6 mg, 9% yield, *ca.* 60% purity by  $^1\text{H-NMR}$ ),  $\delta_H$  (400 MHz, DMSO- $d_6$ ) 8.38-8.35 (1H, m, pyridine-H), 8.25 (1H, s, NH), 8.15 (1H, t, *J* 1.9, Ar-H), 8.13 (1H, s, thiazole-H), 8.03 (2H, dd, *J* 7.9, 1.7, Ar-H), 8.01-7.98 (1H, m, pyridine-H), 7.75-7.72 (1H, m, Ar-H), 7.57-7.52 (4H, m, Ar-H), 7.40 (1H, t, *J* 7.9, Ar-H), 6.97 (1H, dd, *J* 7.8, 5.0, pyridine-H).  $t_R$  (HPLC) 5.62 min.

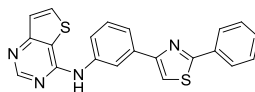
**(4-Fluoro-pyridin-2-yl)-[3-(2-phenyl-thiazol-4-yl)-phenyl]-amine, 274** (JCC-CRT-340)



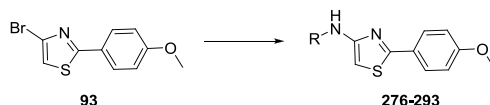
Off-white solid (12.5 mg, 36% yield, *ca.* 60% purity by  $^1\text{H-NMR}$ ),  $\delta_H$  (400 MHz, DMSO- $d_6$ ) 9.40 (1H, s, NH), 8.24-8.19 (2H, m, Ar-H, pyridine-H), 8.10 (1H, s, thiazole-H), 8.03 (2H, dd, *J* 7.8, 1.6, Ar-H), 7.84 (1H, dd, *J* 7.7, 1.7, Ar-H), 7.61-7.51 (4H, m, Ar-H), 7.39 (1H, t, *J* 7.9, Ar-H), 6.73-6.67 (1H, m, pyridine-H), 6.63 (1H, dd, *J* 11.8, 2.2, pyridine-H).  $t_R$  (HPLC) 4.83 min.

One further compound was successfully synthesised, but the purification was not sufficient for assignment of the  $^1\text{H-NMR}$  data. This compound was tested in the enzyme assays.

- [3-(2-Phenyl-thiazol-4-yl)-phenyl]-thieno[3,2-*d*]pyrimidin-4-yl-amine, **275** (JCC-CRT-341)

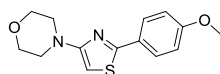


*Parallel Synthesis: General Procedure for Buchwald-Hartwig Couplings of Bromide 93*



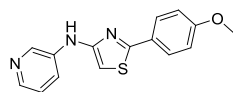
A solution of bromide **93** (27 mg, 100  $\mu\text{mol}$ ), amine (200  $\mu\text{mol}$ ),  $\text{NaO}^t\text{Bu}$  (19.6 mg, 200  $\mu\text{mol}$ ), Xantphos (5.8 mg, 10  $\mu\text{mol}$ ) and  $\text{Pd}_2(\text{dba})_3$  (4.6 mg, 5  $\mu\text{mol}$ ) in dioxane (1.0 mL) was heated (MW, 150  $^\circ\text{C}$ , 20 min). Upon cooling, the reaction mixture was partitioned between  $\text{H}_2\text{O}$  (2 mL) and  $\text{CH}_2\text{Cl}_2$  (5 mL), the organic layer separated, the solvent removed *in vacuo* and the product purified by HPLC under acidic conditions.

**4-[2-(4-Methoxy-phenyl)-thiazol-4-yl]-morpholine, 276** (JCC-CRT-346)



Red gum (2.2 mg, 8% yield, *ca.* 95% purity by  $^1\text{H-NMR}$ ),  $\delta_{\text{H}}$  (400 MHz,  $\text{DMSO-d}_6$ ) 7.81 (2H, d,  $J$  8.9, Ar-H), 7.02 (2H, d,  $J$  8.9, Ar-H), 6.25 (1H, s, thiazole-H), 3.81 (3H, s,  $\text{CH}_3$ ), 3.77-3.70 (4H, m,  $2 \times \text{OCH}_2$ ), 3.26-3.19 (4H, m,  $2 \times \text{NCH}_2$ ).  $t_{\text{R}}$  (HPLC) 3.31 min.

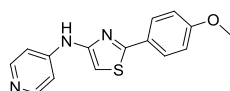
**[2-(4-Methoxy-phenyl)-thiazol-4-yl]-pyridin-3-yl-amine, 277** (JCC-CRT-351)



Dark orange gum (0.7 mg, 3% yield, *ca.* 75% purity by  $^1\text{H-NMR}$ ),  $\delta_{\text{H}}$  (400 MHz,  $\text{DMSO-d}_6$ ) 9.71 (1H, s, NH), 8.74 (1H, d,  $J$  2.6, pyridine-H), 8.17 (1H, dd,  $J$  5.1, 1.0, pyridine-H), 8.03 (1H, dd,  $J$  8.4, 1.6, pyridine-H), 7.92-7.86 (2H, m, Ar-H), 7.58 (1H, dd,  $J$  8.4, 5.1, pyridine-H), 7.11-7.04 (2H, m, Ar-H), 6.81 (1H, s, thiazole-H), 3.83 (3H, s,  $\text{CH}_3$ ).  $t_{\text{R}}$  (HPLC) 3.24 min.

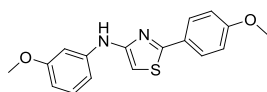


**[2-(4-Methoxy-phenyl)-thiazol-4-yl]-pyridin-4-yl-amine, 278** (JCC-CRT-352)



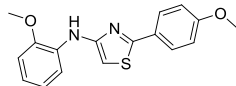
Dark orange gum (2.9 mg, 10% yield, *ca.* 98% purity by  $^1\text{H-NMR}$ ),  $\delta_{\text{H}}$  (400 MHz, DMSO- $\text{d}_6$ ) 10.85 (1H, s, NH), 8.35 (2H, d,  $J$  7.0, pyridine-H), 7.92 (2H, d,  $J$  8.8, Ar-H), 7.53 (2H, d,  $J$  7.0, pyridine-H), 7.15 (1H, s, thiazole-H), 7.08 (2H, d,  $J$  8.8, Ar-H), 3.84 (3H, s,  $\text{CH}_3$ ).  $t_{\text{R}}$  (HPLC) 3.23 min.

**(3-Methoxy-phenyl)-[2-(4-methoxy-phenyl)-thiazol-4-yl]-amine, 279** (JCC-CRT-357)



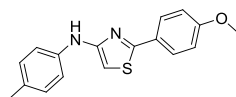
Brown gum (3.0 mg, 10% yield, *ca.* 60% purity by  $^1\text{H-NMR}$ ),  $\delta_{\text{H}}$  (400 MHz, DMSO- $\text{d}_6$ ) 8.99 (1H, s, NH), 7.91-7.81 (2H, m, Ar-H), 7.13 (1H, t,  $J$  8.2, Ar-H), 7.09-7.04 (2H, m, Ar-H), 6.91 (1H, t,  $J$  2.2, Ar-H), 6.83 (1H, dd,  $J$  8.2, 1.6, Ar-H), 6.62 (1H, s, thiazole-H), 6.39 (1H, dd,  $J$  8.2, 2.2, Ar-H), 3.82 (3H, s,  $\text{CH}_3$ ), 3.73 (3H, s,  $\text{CH}_3$ ).  $t_{\text{R}}$  (HPLC) 3.53 min.

**(2-Methoxy-phenyl)-[2-(4-methoxy-phenyl)-thiazol-4-yl]-amine, 280** (JCC-CRT-358)



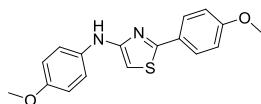
Brown solid (2.5 mg, 8% yield, *ca.* 85% purity by  $^1\text{H-NMR}$ ),  $\delta_{\text{H}}$  (400 MHz, DMSO- $\text{d}_6$ ) 7.89-7.82 (2H, m, Ar-H), 7.79 (1H, s, NH), 7.64 (1H, dd,  $J$  7.9, 1.6, Ar-H), 7.08-7.03 (2H, m, Ar-H), 6.99 (1H, dd,  $J$  7.9, 1.6, Ar-H), 6.93-6.80 (2H, m, Ar-H), 6.69 (1H, s, thiazole-H), 3.86 (3H, s,  $\text{CH}_3$ ), 3.82 (3H, s,  $\text{CH}_3$ ).  $t_{\text{R}}$  (HPLC) 3.69 min.

**[2-(4-Methoxy-phenyl)-thiazol-4-yl]-*p*-tolyl-amine, 281** (JCC-CRT-359)



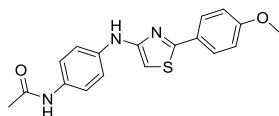
Brown solid (3.6 mg, 12% yield, *ca.* 95% purity by  $^1\text{H-NMR}$ ),  $\delta_{\text{H}}$  (400 MHz, DMSO- $\text{d}_6$ ) 8.86 (1H, s, NH), 7.88-7.81 (2H, m, Ar-H), 7.16 (2H, d,  $J$  8.5, Ar-H), 7.08-7.02 (4H, m, Ar-H), 6.53 (1H, s, thiazole-H), 3.82 (3H, s,  $\text{OCH}_3$ ), 2.22 (3H, s,  $\text{ArCH}_3$ ).  $t_{\text{R}}$  (HPLC) 3.66 min.

**(4-Methoxy-phenyl)-[2-(4-methoxy-phenyl)-thiazol-4-yl]-amine, 282** (JCC-CRT-367)



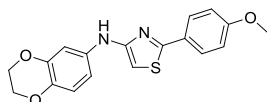
Brown solid (2.3 mg, 7% yield, *ca.* 90% purity by  $^1\text{H-NMR}$ ),  $\delta_{\text{H}}$  (400 MHz, DMSO- $d_6$ ) 8.71 (1H, s, NH), 7.90-7.80 (2H, m, Ar-H), 7.25-7.18 (2H, m, Ar-H), 7.05 (2H, d,  $J$  9.0, Ar-H), 6.86 (2H, d,  $J$  9.0, Ar-H), 6.42 (1H, s, thiazole-H), 3.82 (3H, s,  $\text{CH}_3$ ), 3.70 (3H, s,  $\text{CH}_3$ ).  $t_{\text{R}}$  (HPLC) 4.00 min.

***N*-(4-[2-(4-Methoxy-phenyl)-thiazol-4-ylamino]-phenyl)-acetamide, 283** (JCC-CRT-370)



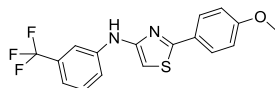
Brown solid (5.6 mg, 17% yield, *ca.* 85% purity by  $^1\text{H-NMR}$ ),  $\delta_{\text{H}}$  (400 MHz, DMSO- $d_6$ ) 9.75 (1H, s, CONH), 8.89 (1H, s, NH), 7.88-7.83 (2H, m, Ar-H), 7.44 (2H, d,  $J$  9.0, Ar-H), 7.20 (2H, d,  $J$  9.0, Ar-H), 7.09-7.04 (2H, m, Ar-H), 6.53 (1H, s, thiazole-H), 3.82 (3H, s,  $\text{OCH}_3$ ), 2.00 (3H, s,  $\text{COCH}_3$ ).  $t_{\text{R}}$  (HPLC) 4.66 min.

**(2,3-Dihydro-benzo[1,4]dioxin-6-yl)-[2-(4-methoxy-phenyl)-thiazol-4-yl]-amine, 284** (JCC-CRT-374)



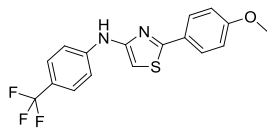
Brown solid (5.7 mg, 17% yield, *ca.* 75% purity by  $^1\text{H-NMR}$ ),  $\delta_{\text{H}}$  (400 MHz, DMSO- $d_6$ ) 8.72 (1H, s, NH), 7.86-7.80 (2H, m, Ar-H), 7.07-7.04 (2H, m, Ar-H), 6.84 (1H, d,  $J$  2.2, Ar-H), 6.75-6.71 (2H, m, Ar-H), 6.44 (1H, s, thiazole-H), 4.23-4.16 (4H, m,  $2 \times \text{CH}_2$ ), 3.82 (3H, s,  $\text{CH}_3$ ).  $t_{\text{R}}$  (HPLC) 3.66 min.

**[2-(4-Methoxy-phenyl)-thiazol-4-yl]-(3-trifluoromethyl-phenyl)-amine, 285** (JCC-CRT-376)



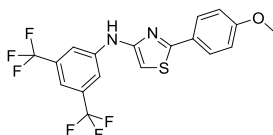
Dark red gum (11.1 mg, 32% yield, *ca.* 80% purity by  $^1\text{H-NMR}$ ),  $\delta_{\text{H}}$  (400 MHz, DMSO- $d_6$ ) 9.39 (1H, s, NH), 7.89-7.84 (2H, m, Ar-H), 7.68 (1H, s, ArH), 7.54 (1H, d,  $J$  9.9, ArH), 7.45 (1H, t,  $J$  7.9, ArH), 7.14-7.04 (3H, m, Ar-H), 6.72 (1H, s, thiazole-H), 3.82 (3H, s,  $\text{CH}_3$ ).  $t_{\text{R}}$  (HPLC) 3.86 min.

**[2-(4-Methoxy-phenyl)-thiazol-4-yl]-(4-trifluoromethyl-phenyl)-amine, 286** (JCC-CRT-377)



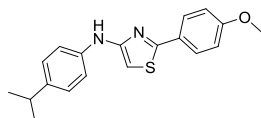
Light brown solid (4.3 mg, 12% yield, *ca.* 95% purity by  $^1\text{H-NMR}$ ),  $\delta_{\text{H}}$  (400 MHz, DMSO- $d_6$ ) 9.52 (1H, s, NH), 7.91-7.85 (2H, m, Ar-H), 7.56 (2H, d, *J* 8.7, Ar-H), 7.42 (2H, d, *J* 8.6, Ar-H), 7.11-7.03 (2H, m, Ar-H), 6.81 (1H, s, thiazole-H), 3.83 (3H, s,  $\text{CH}_3$ ).  $t_{\text{R}}$  (HPLC) 3.90 min.

**(3,5-Bis-trifluoromethyl-phenyl)-[2-(4-methoxy-phenyl)-thiazol-4-yl]-amine, 287** (JCC-CRT-378)



Dark orange solid (5.6 mg, 13% yield, *ca.* 95% purity by  $^1\text{H-NMR}$ ),  $\delta_{\text{H}}$  (400 MHz, DMSO- $d_6$ ) 9.81 (1H, s, NH), 7.95 (2H, s, Ar-H), 7.90-7.82 (2H, m, Ar-H), 7.39 (1H, s, Ar-H), 7.13-7.05 (2H, m, Ar-H), 6.82 (1H, s, thiazole-H), 3.83 (3H, s,  $\text{CH}_3$ ).  $t_{\text{R}}$  (HPLC) 4.22 min.

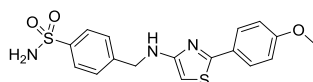
**(4-Isopropyl-phenyl)-[2-(4-methoxy-phenyl)-thiazol-4-yl]-amine, 288** (JCC-CRT-384)



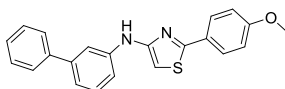
Brown solid (10.3 mg, 32% yield, *ca.* 95% purity by  $^1\text{H-NMR}$ ),  $\delta_{\text{H}}$  (400 MHz, DMSO- $d_6$ ) 8.87 (1H, s, NH), 7.89-7.82 (2H, m, Ar-H), 7.25-7.18 (2H, m, Ar-H), 7.15-7.11 (2H, m, Ar-H), 7.09-7.05 (2H, m, Ar-H), 6.55 (1H, s, thiazole-H), 3.84 (3H, s,  $\text{OCH}_3$ ), 2.82 (1H, hept, *J* 7.0,  $\text{CH}(\text{CH}_3)_2$ ), 1.19 (6H, d, *J* 7.0,  $\text{CH}(\text{CH}_3)_2$ ).  $t_{\text{R}}$  (HPLC) 3.89 min.

Five further compounds were successfully synthesised, but the purification was not sufficient for assignment of the  $^1\text{H-NMR}$  data. These compounds were tested in the enzyme assays.

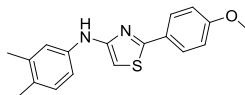
- 4-([2-(4-Methoxy-phenyl)-thiazol-4-ylamino]-methyl)-benzenesulfonamide, **289** (JCC-CRT-373)



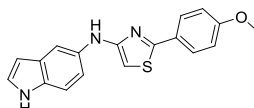
- Biphenyl-3-yl-[2-(4-methoxy-phenyl)-thiazol-4-yl]-amine, **290** (JCC-CRT-380)



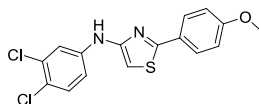
- (3,4-Dimethyl-phenyl)-[2-(4-methoxy-phenyl)-thiazol-4-yl]-amine, **291** (JCC-CRT-381)



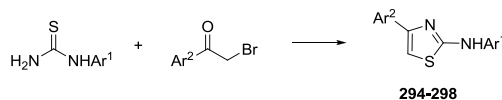
- (1*H*-Indol-5-yl)-[2-(4-methoxy-phenyl)-thiazol-4-yl]-amine, **292** (JCC-CRT-382)



- (3,4-Dichloro-phenyl)-[2-(4-methoxy-phenyl)-thiazol-4-yl]-amine, **293** (JCC-CRT-383)

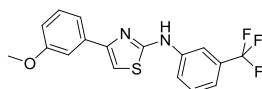


*Parallel Synthesis: General Procedure for Aminothiazole Synthesis*



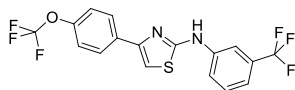
A solution of thiourea (100  $\mu\text{mol}$ ) and  $\alpha$ -bromo ketone (100  $\mu\text{mol}$ ) in EtOH (0.5 mL) was heated (MW, 160  $^{\circ}\text{C}$ , 10 min). Upon cooling, the product was purified by HPLC under acidic conditions.

- [4-(3-Methoxy-phenyl)-thiazol-2-yl]-[3-(trifluoromethyl-phenyl)-amine, 294** (JCC-CRT-307)



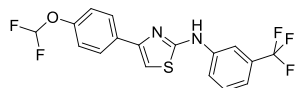
Orange gum (26.3 mg, 75% yield, *ca.* 98% purity by  $^1\text{H-NMR}$ ),  $\delta_{\text{H}}$  (400 MHz, DMSO- $\text{d}_6$ ) 10.68 (1H, s, NH), 8.53 (1H, s, thiazole-H), 7.74 (1H, d, *J* 8.3, Ar-H), 7.57 (1H, t, *J* 8.0, Ar-H), 7.52-7.49 (2H, m, Ar-H), 7.47 (1H, s, Ar-H), 7.35 (1H, t, *J* 8.0, Ar-H), 7.30 (1H, d, *J* 7.7, Ar-H), 6.92-6.87 (1H, m, Ar-H), 3.82 (3H, s,  $\text{CH}_3$ ).  $t_{\text{R}}$  (HPLC) 4.34 min.

**[4-(4-Trifluoromethoxy-phenyl)-thiazol-2-yl]-(3-trifluoromethyl-phenyl)-amine, 295**  
(JCC-CRT-308)



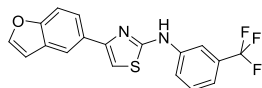
Orange gum (26.4 mg, 65% yield, *ca.* 90% purity by <sup>1</sup>H-NMR),  $\delta_{\text{H}}$  (400 MHz, DMSO-d<sub>6</sub>) 10.70 (1H, s, NH), 8.28 (1H, s, thiazole-H), 8.05-8.00 (2H, m, Ar-H), 7.91 (1H, d, *J* 9.4, Ar-H), 7.57 (1H, t, *J* 8.0, Ar-H), 7.52 (1H, s, Ar-H), 7.44 (2H, d, *J* 8.1, Ar-H), 7.30 (1H, d, *J* 7.8, Ar-H).  $t_{\text{R}}$  (HPLC) 4.98 min.

**[4-(4-Difluoromethoxy-phenyl)-thiazol-2-yl]-(3-trifluoromethyl-phenyl)-amine, 296**  
(JCC-CRT-309)



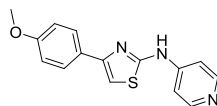
Orange gum (37.6 mg, 98% yield, *ca.* 90% purity by <sup>1</sup>H-NMR),  $\delta_{\text{H}}$  (400 MHz, DMSO-d<sub>6</sub>) 10.68 (1H, s, NH), 8.34 (1H, s, thiazole-H), 7.99-7.94 (2H, m, Ar-H), 7.88 (1H, d, *J* 9.5, Ar-H), 7.57 (1H, t, *J* 8.0, Ar-H), 7.43 (1H, s, Ar-H), 7.30 (1H, t, *J* 74.1, OCHF<sub>2</sub>), 7.29 (1H, d, *J* 7.6, Ar-H), 7.26 (2H, d, *J* 8.7, Ar-H).  $t_{\text{R}}$  (HPLC) 4.00 min.

**(4-Benzofuran-5-yl-thiazol-2-yl)-(3-trifluoromethyl-phenyl)-amine, 297** (JCC-CRT-313)



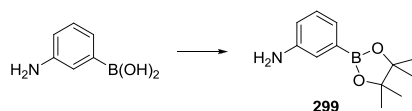
Orange gum (10.7 mg, 30% yield, *ca.* 90% purity by <sup>1</sup>H-NMR),  $\delta_{\text{H}}$  (400 MHz, DMSO-d<sub>6</sub>) 10.66 (1H, s, NH), 8.35 (1H, s, thiazole-H), 8.20 (1H, d, *J* 1.5, Ar-H), 8.03 (1H, d, *J* 2.1, Ar-H), 7.95-7.88 (2H, m, Ar-H), 7.66 (1H, d, *J* 8.7, Ar-H), 7.59 (1H, t, *J* 8.0, Ar-H), 7.41 (1H, s, Ar-H), 7.30 (1H, d, *J* 7.7, Ar-H), 7.01-7.00 (1H, m, Ar-H).  $t_{\text{R}}$  (HPLC) 4.36 min.

**[4-(4-Methoxy-phenyl)-thiazol-2-yl]-pyridin-4-yl-amine, 298** (JCC-CRT-315)



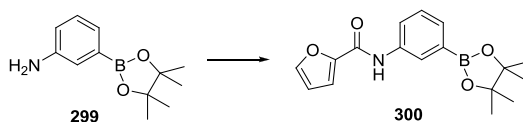
Pale yellow gum (11.3 mg, 40% yield, *ca.* 98% purity by <sup>1</sup>H-NMR),  $\delta_{\text{H}}$  (400 MHz, DMSO-d<sub>6</sub>) 8.42 (2H, d, *J* 6.3, pyridine-H), 8.14 (1H, s, NH), 7.88 (2H, d, *J* 8.8, Ar-H), 7.70 (2H, d, *J* 6.3, pyridine-H), 7.35 (1H, s, thiazole-H), 7.01 (2H, d, *J* 8.8, Ar-H), 3.80 (3H, s, CH<sub>3</sub>).  $t_{\text{R}}$  (HPLC) 1.79 min.

### 3-(4,4,5,5-Tetramethyl-[1,3,2]dioxaborolan-2-yl)-phenylamine, **299** <sup>229</sup>



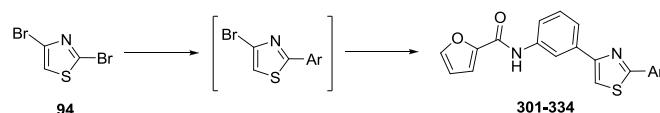
A suspension of 3-aminobenzenboronic acid monohydrate (2.30 g, 14.8 mmol), pinacol (2.11 g, 17.8 mmol) and  $\text{MgSO}_4$  (3.57 g, 29.7 mmol) in  $\text{CH}_2\text{Cl}_2$  (15 mL) was stirred at r.t. for 20 h, before being filtered and the solvent removed *in vacuo*. Column chromatography eluting with EtOAc/petrol (1:3) afforded the title compound as a white amorphous solid (3.24 g, 100%), mp 90-92 °C;  $R_f$  0.30 (EtOAc/petrol 1:3);  $\delta_{\text{H}}$  (400 MHz,  $\text{DMSO-d}_6$ ) 7.23-7.12 (3H, m, Ar-H), 6.78 (1H, ddd,  $J$  7.6, 2.4, 1.1, Ar-H), 3.62 (2H, br s,  $\text{NH}_2$ ), 1.33 (12H, s,  $4 \times \text{CH}_3$ );  $m/z$  (CI) 439 (100%), 438 (68), 220 ( $\text{MH}^+$ , 77), 219 ( $\text{MH}^+$ , 85). Found  $\text{MH}^+$ , 220.1501.  $\text{C}_{12}\text{H}_{19}\text{BNO}_2$  requires 220.1509. Data is in agreement with the literature.<sup>229</sup>

### Furan-2-carboxylic acid [3-(4,4,5,5-tetramethyl-[1,3,2]dioxaborolan-2-yl)-phenyl]-amide, **300**



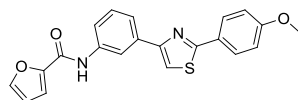
2-Furoyl chloride (0.90 mL, 9.13 mmol) was added dropwise to a stirred solution of pinacol boronate **299** (2.00 g, 9.13 mmol) and  $\text{Et}_3\text{N}$  (2.55 mL, 18.3 mmol) in THF (40 mL) at 0 °C. The resulting white suspension was stirred for 3 h, filtered and the solvent removed *in vacuo*. Column chromatography eluting with EtOAc/petrol (1:3  $\rightarrow$  1:1) afforded the title compound as a white solid (2.83 g, 99%),  $\nu_{\text{max}}$  (neat)/ $\text{cm}^{-1}$  1665, 1583, 1539, 1352;  $\delta_{\text{H}}$  (400 MHz,  $\text{CDCl}_3$ ) 8.11 (1H, br s, NH), 8.06 (1H, d,  $J$  8.1, furan 5-H), 7.75 (1H, s, Ar-H), 7.55 (1H, d,  $J$  7.3, Ar-H), 7.46 (1H, s, Ar-H), 7.37 (1H, t,  $J$  7.7, Ar-H), 7.20 (1H, d,  $J$  3.4, furan 3-H), 6.52 (1H, dd,  $J$  3.4, 1.7, furan 4-H), 1.32 (12H, s,  $4 \times \text{CH}_3$ );  $\delta_{\text{C}}$  (101 MHz,  $\text{CDCl}_3$ ) 156.2, 148.0, 144.4, 137.1, 130.9, 128.9, 125.9, 123.1, 115.4, 112.8, 84.2, 77.4, 25.1;  $m/z$  (CI) 331 ( $\text{MNH}_4^+$ , 87%), 330 ( $\text{MNH}_4^+$ , 22), 314 ( $\text{MH}^+$ , 100), 313 ( $\text{MH}^+$ , 48), 274 (29). Found  $\text{MH}^+$ , 314.1563.  $\text{C}_{17}\text{H}_{21}\text{BNO}_4$  requires 314.1564.

*Parallel Synthesis: General Procedure for One-Pot, Consecutive Suzuki Couplings*



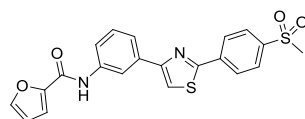
A solution of 2,4-dibromothiazole **94** (24 mg, 100  $\mu\text{mol}$ ), boronic acid (100  $\mu\text{mol}$ ),  $\text{K}_2\text{CO}_3$  (41.5 mg, 300  $\mu\text{mol}$ ) and  $\text{Pd}(\text{PPh}_3)_4$  (3.5 mg, 3  $\mu\text{mol}$ ) in DME/ $\text{H}_2\text{O}$  (4:1, 1 mL) was heated (MW, 140  $^\circ\text{C}$ , 15 min). Upon cooling, boronic ester **300** (35 mg, 150  $\mu\text{mol}$ ) and  $\text{Pd}(\text{PPh}_3)_4$  (3.5 mg, 3  $\mu\text{mol}$ ) were added and the reaction mixture heated (MW, 160  $^\circ\text{C}$ , 20 min). Upon cooling,  $\text{H}_2\text{O}$  (5 mL) was added and the aqueous layer extracted with  $\text{CH}_2\text{Cl}_2$  (10 mL), the solvent removed *in vacuo* and the product purified by HPLC under acidic conditions.

**Furan-2-carboxylic acid (3-[2-(4-methoxy-phenyl)-thiazol-4-yl]-phenyl)-amide, 301**  
(JCC-CRT-398B)



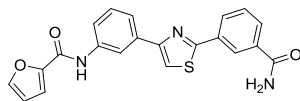
Brown solid (11.3 mg, 30% yield, *ca.* 85% purity by  $^1\text{H-NMR}$ ),  $\delta_{\text{H}}$  (400 MHz,  $\text{DMSO-d}_6$ ) 10.32 (1H, s, NH), 8.44-8.41 (1H, m, Ar-H), 8.02 (1H, s, thiazole-H), 7.99 (1H, s, furan-H), 7.97-7.95 (2H, m, Ar-H), 7.83-7.79 (1H, m, Ar-H), 7.76-7.72 (1H, m, Ar-H), 7.43 (1H, t,  $J$  8.0, Ar-H), 7.41-7.39 (1H, m, furan-H), 7.10 (2H, d,  $J$  8.8, Ar-H), 6.72 (1H, dd,  $J$  3.5, 1.8, furan-H), 3.84 (3H, s,  $\text{CH}_3$ ).  $t_{\text{R}}$  (HPLC) 3.99 min.

**Furan-2-carboxylic acid (3-[2-(4-methanesulfonyl-phenyl)-thiazol-4-yl]-phenyl)-amide, 302**  
(JCC-CRT-402)



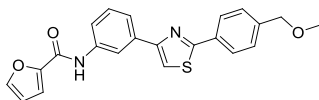
White solid (10.7 mg, 25% yield, *ca.* 85% purity by  $^1\text{H-NMR}$ ),  $\delta_{\text{H}}$  (400 MHz,  $\text{DMSO-d}_6$ ) 10.34 (1H, s, NH), 8.46 (1H, t,  $J$  1.8, Ar-H), 8.32-8.26 (3H, m,  $2 \times$  Ar-H, thiazole-H), 8.13-8.07 (2H, m, Ar-H, furan-H), 7.97-7.95 (1H, m, Ar-H), 7.86-7.81 (1H, m, Ar-H), 7.80-7.76 (1H, m, Ar-H), 7.46 (1H, t,  $J$  7.9, Ar-H), 7.41-7.38 (1H, m, furan-H), 6.73 (1H, dd,  $J$  3.5, 1.7, furan-H), 3.30 (3H, s,  $\text{CH}_3$ ).  $t_{\text{R}}$  (HPLC) 3.39 min.

**Furan-2-carboxylic acid (3-[2-(3-carbamoyl-phenyl)-thiazol-4-yl]-phenyl)-amide, 303**  
(JCC-CRT-403)



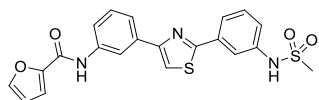
Off-white solid (8.8 mg, 23% yield, *ca.* 85% purity by  $^1\text{H-NMR}$ ),  $\delta_{\text{H}}$  (400 MHz, DMSO- $\text{d}_6$ ) 10.35 (1H, s, NH), 8.50 (1H, t,  $J$  1.7, Ar-H), 8.43 (1H, t,  $J$  1.8, Ar-H), 8.23-8.15 (3H, m, thiazole-H, 2  $\times$  Ar-H), 8.03-7.99 (1H, m, furan-H), 7.97-7.95 (1H, m, Ar-H), 7.87-7.83 (1H, m, Ar-H), 7.80-7.76 (1H, m, Ar-H), 7.46 (1H, t,  $J$  7.9, Ar-H), 7.42-7.39 (1H, m, furan-H), 6.72 (1H, dd,  $J$  3.4, 1.9, furan-H).  $t_{\text{R}}$  (HPLC) 3.36 min.

**Furan-2-carboxylic acid (3-[2-(4-methoxymethyl-phenyl)-thiazol-4-yl]-phenyl)-amide, 304**  
(JCC-CRT-404)



Off-white solid (14.7 mg, 38% yield, *ca.* 90% purity by  $^1\text{H-NMR}$ ),  $\delta_{\text{H}}$  (400 MHz, DMSO- $\text{d}_6$ ) 10.32 (1H, s, NH), 8.44 (1H, t,  $J$  1.8, Ar-H), 8.11 (1H, s, thiazole-H), 8.05-8.00 (2H, m, Ar-H), 7.96-7.95 (1H, m, furan-H), 7.85-7.80 (1H, m, Ar-H), 7.77-7.74 (1H, m, Ar-H), 7.49 (2H, d,  $J$  8.1, Ar-H), 7.44 (1H, t,  $J$  7.9, Ar-H), 7.40 (1H, d,  $J$  3.4, furan-H), 6.72 (1H, dd,  $J$  3.4, 1.7, furan-H), 4.49 (2H, s,  $\text{CH}_2$ ), 3.34 (3H, s,  $\text{CH}_3$ ).  $t_{\text{R}}$  (HPLC) 3.89 min.

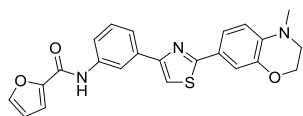
**Furan-2-carboxylic acid (3-[2-(3-methanesulfonylamino-phenyl)-thiazol-4-yl]-phenyl)-amide, 305**  
(JCC-CRT-406)



Orange solid (18.6 mg, 42% yield, *ca.* 90% purity by  $^1\text{H-NMR}$ ),  $\delta_{\text{H}}$  (400 MHz, DMSO- $\text{d}_6$ ) 10.33 (1H, s, NH), 8.42 (1H, t,  $J$  1.8, Ar-H), 8.13 (1H, s, thiazole-H), 7.97-7.95 (1H, m, Ar-H), 7.90 (1H, t,  $J$  1.9, furan-H), 7.80 (1H, dd,  $J$  8.2, 1.2, Ar-H), 7.78-7.73 (2H, m, Ar-H), 7.46 (1H, t,  $J$  7.9, Ar-H), 7.40-7.35 (3H, m, 2  $\times$  Ar-H, furan-H), 6.72 (1H, dd,  $J$  3.5, 1.9, furan-H), 3.06 (3H, s,  $\text{CH}_3$ ).  $t_{\text{R}}$  (HPLC) 3.04 min.

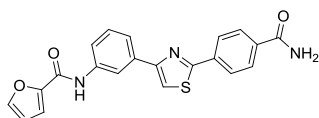


**Furan-2-carboxylic acid (3-[2-(4-methyl-3,4-dihydro-2H-benzo[1,4]oxazin-7-yl)-thiazol-4-yl]-phenyl)-amide, 306 (JCC-CRT-407)**



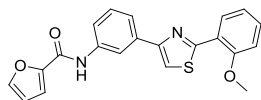
Orange gum (6.2 mg, 15% yield, *ca.* 70% purity by <sup>1</sup>H-NMR),  $\delta_{\text{H}}$  (400 MHz, DMSO-*d*<sub>6</sub>) 10.29 (1H, s, NH), 8.40 (1H, t, *J* 1.8, Ar-H), 7.97-7.95 (1H, m, furan-H), 7.91 (1H, s, thiazole-H), 7.83-7.79 (1H, m, Ar-H), 7.74-7.69 (1H, m, Ar-H), 7.47-7.41 (2H, m, Ar-H), 7.40-7.38 (1H, m, furan-H), 7.33 (1H, d, *J* 2.0, Ar-H), 6.78 (1H, d, *J* 8.4, Ar-H), 6.72 (1H, dd, *J* 3.5, 1.7, furan-H), 4.30-4.24 (2H, m, OCH<sub>2</sub>), 3.39-3.33 (2H, m, NCH<sub>2</sub>), 2.93 (3H, s, CH<sub>3</sub>). *t*<sub>R</sub> (HPLC) 3.95 min.

**Furan-2-carboxylic acid (3-[2-(4-carbamoyl-phenyl)-thiazol-4-yl]-phenyl)-amide, 307 (JCC-CRT-408)**



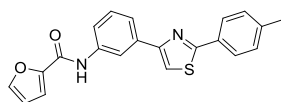
White solid (8.0 mg, 21% yield, *ca.* 60% purity by <sup>1</sup>H-NMR),  $\delta_{\text{H}}$  (400 MHz, DMSO-*d*<sub>6</sub>) 10.33 (1H, s, NH), 8.45 (1H, t, *J* 1.8, Ar-H), 8.20 (1H, s, thiazole-H), 8.12 (2H, d, *J* 8.4, Ar-H), 8.04 (2H, d, *J* 8.4, Ar-H), 7.97-7.95 (1H, m, furan-H), 7.87-7.82 (1H, m, Ar-H), 7.79-7.75 (1H, m, Ar-H), 7.46 (1H, t, *J* 7.9, Ar-H), 7.40 (1H, dd, *J* 4.2, 1.0, furan-H), 6.73 (1H, dd, *J* 3.5, 1.9, furan-H). *t*<sub>R</sub> (HPLC) 3.35 min.

**Furan-2-carboxylic acid (3-[2-(2-methoxy-phenyl)-thiazol-4-yl]-phenyl)-amide, 308 (JCC-CRT-409)**



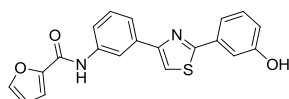
Light brown solid (10.7 mg, 28% yield, *ca.* 85% purity by <sup>1</sup>H-NMR),  $\delta_{\text{H}}$  (400 MHz, DMSO-*d*<sub>6</sub>) 10.32 (1H, s, NH), 8.52-8.41 (2H, m, Ar-H), 8.13 (1H, s, thiazole-H), 7.96 (1H, s, furan-H), 7.80 (2H, dd, *J* 16.0, 7.8, Ar-H), 7.51 (1H, t, *J* 7.8, Ar-H), 7.44 (1H, t, *J* 7.9, Ar-H), 7.40 (1H, d, *J* 2.7, furan-H), 7.28 (1H, d, *J* 8.3, Ar-H), 7.17 (1H, t, *J* 7.5, Ar-H), 6.77-6.66 (1H, m, furan-H), 4.05 (3H, s, CH<sub>3</sub>). *t*<sub>R</sub> (HPLC) 3.98 min.

**Furan-2-carboxylic acid [3-(2-*p*-tolyl-thiazol-4-yl)-phenyl]-amide, 309** (JCC-CRT-410)



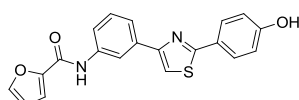
Light brown solid (13.7 mg, 38% yield, *ca.* 90% purity by  $^1\text{H-NMR}$ ),  $\delta_{\text{H}}$  (400 MHz, DMSO- $\text{d}_6$ ) 10.33 (1H, s, NH), 8.43 (1H, s, Ar-H), 8.08 (1H, s, thiazole-H), 7.99-7.90 (3H, m,  $2 \times$  Ar-H, furan-H), 7.82 (1H, d,  $J$  8.1, Ar-H), 7.75 (1H, d,  $J$  7.6, Ar-H), 7.44 (1H, t,  $J$  8.0, Ar-H), 7.40 (1H, d,  $J$  3.1, furan-H), 7.36 (2H, d,  $J$  7.8, Ar-H), 6.73 (1H, s, furan-H), 2.38 (3H, s,  $\text{CH}_3$ ).  $t_{\text{R}}$  (HPLC) 4.15 min.

**Furan-2-carboxylic acid (3-[2-(3-hydroxy-phenyl)-thiazol-4-yl]-phenyl)-amide, 310** (JCC-CRT-411)



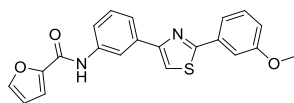
Off-white solid (13.8 mg, 38% yield, *ca.* 85% purity by  $^1\text{H-NMR}$ ),  $\delta_{\text{H}}$  (400 MHz, DMSO- $\text{d}_6$ ) 10.34 (1H, s, NH), 9.86 (1H, s, OH), 8.45 (1H, s, Ar-H), 8.10 (1H, s, thiazole-H), 7.96 (1H, s, furan-H), 7.80 (1H, d,  $J$  8.1, Ar-H), 7.74 (1H, d,  $J$  7.6, Ar-H), 7.49-7.42 (3H, m, Ar-H), 7.40 (1H, d,  $J$  2.9, furan-H), 7.34 (1H, t,  $J$  7.7, Ar-H), 6.91 (1H, d,  $J$  7.8, Ar-H), 6.73 (1H, d,  $J$  1.5, furan-H).  $t_{\text{R}}$  (HPLC) 3.53 min.

**Furan-2-carboxylic acid (3-[2-(4-hydroxy-phenyl)-thiazol-4-yl]-phenyl)-amide, 311** (JCC-CRT-412)



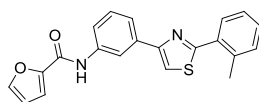
Light brown solid (7.9 mg, 22% yield, *ca.* 85% purity by  $^1\text{H-NMR}$ ),  $\delta_{\text{H}}$  (400 MHz, DMSO- $\text{d}_6$ ) 10.31 (1H, s, NH), 10.04 (1H, s, OH), 8.42 (1H, s, Ar-H), 7.97 (2H, m, thiazole-H, furan-H), 7.87 (2H, d,  $J$  7.8, Ar-H), 7.80 (1H, d,  $J$  8.1, Ar-H), 7.73 (1H, d,  $J$  7.7, Ar-H), 7.43 (1H, t,  $J$  8.1, Ar-H), 7.39 (1H, d,  $J$  2.7, furan-H), 6.91 (2H, d,  $J$  7.8, Ar-H), 6.72 (1H, s, furan-H).  $t_{\text{R}}$  (HPLC) 3.33 min.

**Furan-2-carboxylic acid (3-[2-(3-methoxy-phenyl)-thiazol-4-yl]-phenyl)-amide, 312** (JCC-CRT-413)



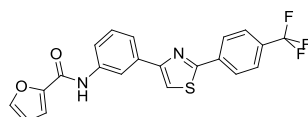
Off-white solid (14.8 mg, 39% yield, *ca.* 85% purity by  $^1\text{H-NMR}$ ),  $\delta_{\text{H}}$  (400 MHz, DMSO- $\text{d}_6$ ) 10.33 (1H, s, NH), 8.43 (1H, s, Ar-H), 8.13 (1H, s, thiazole-H), 7.96 (1H, s, furan-H), 7.83 (1H, d,  $J$  8.2, Ar-H), 7.76 (1H, d,  $J$  7.5, Ar-H), 7.60 (1H, d,  $J$  7.6, Ar-H), 7.56 (1H, s, Ar-H), 7.46 (2H, q,  $J$  8.1, Ar-H), 7.40 (1H, d,  $J$  3.1, furan-H), 7.11 (1H, d,  $J$  8.2, Ar-H), 6.72 (1H, s, furan-H), 3.87 (3H, s,  $\text{CH}_3$ ).  $t_{\text{R}}$  (HPLC) 4.00 min.

**Furan-2-carboxylic acid [3-(2-*o*-tolyl-thiazol-4-yl)-phenyl]-amide, 313** (JCC-CRT-414)



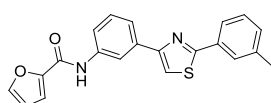
Light brown solid (13.7 mg, 38% yield, *ca.* 85% purity by  $^1\text{H-NMR}$ ),  $\delta_{\text{H}}$  (400 MHz, DMSO- $\text{d}_6$ ) 10.32 (1H, s, NH), 8.44 (1H, s, Ar-H), 8.18 (1H, s, thiazole-H), 7.96 (1H, s, furan-H), 7.82 (2H, t,  $J$  9.2, Ar-H), 7.75 (1H, d,  $J$  7.7, Ar-H), 7.48-7.34 (5H, m,  $4 \times$  Ar-H, furan-H), 6.72 (1H, s, furan-H), 2.65 (3H, s,  $\text{CH}_3$ ).  $t_{\text{R}}$  (HPLC) 4.08 min.

**Furan-2-carboxylic acid (3-[2-(4-trifluoromethyl-phenyl)-thiazol-4-yl]-phenyl)-amide, 314** (JCC-CRT-415)



Off-white solid (11.4 mg, 28% yield, *ca.* 95% purity by  $^1\text{H-NMR}$ ),  $\delta_{\text{H}}$  (400 MHz, DMSO- $\text{d}_6$ ) 10.36 (1H, s, NH), 8.47 (1H, s, Ar-H), 8.30-8.21 (3H, m, thiazole-H,  $2 \times$  Ar-H), 7.97 (1H, s, furan-H), 7.92 (2H, d,  $J$  8.0, Ar-H), 7.83 (1H, d,  $J$  8.0, Ar-H), 7.77 (1H, d,  $J$  7.6, Ar-H), 7.46 (1H, t,  $J$  7.9, Ar-H), 7.40 (1H, d,  $J$  2.8, furan-H), 6.76-6.70 (1H, m, furan-H).  $t_{\text{R}}$  (HPLC) 4.18 min.

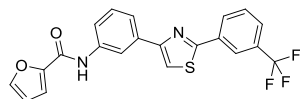
**Furan-2-carboxylic acid [3-(2-*m*-tolyl-thiazol-4-yl)-phenyl]-amide, 315** (JCC-CRT-416)



White solid (10.8 mg, 30% yield, *ca.* 95% purity by  $^1\text{H-NMR}$ ),  $\delta_{\text{H}}$  (400 MHz, DMSO- $\text{d}_6$ ) 10.33 (1H, s, NH), 8.42 (1H, s, Ar-H), 8.12 (1H, s, thiazole-H), 7.96 (1H, s, furan-H), 7.90-

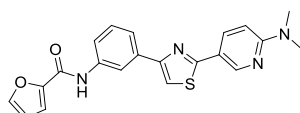
7.80 (3H, m, Ar-H), 7.76 (1H, d, *J* 7.6, Ar-H), 7.48-7.37 (3H, m, 2 × Ar-H, furan-H), 7.34 (1H, d, *J* 7.4, Ar-H), 6.73 (1H, s, furan-H), 2.42 (3H, s, CH<sub>3</sub>). t<sub>R</sub> (HPLC) 4.15 min.

**Furan-2-carboxylic acid (3-[2-(3-trifluoromethyl-phenyl)-thiazol-4-yl]-phenyl)-amide, 316 (JCC-CRT-417)**



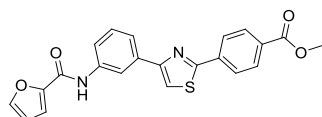
Pale brown solid (2.5 mg, 6% yield, *ca.* 85% purity by <sup>1</sup>H-NMR), δ<sub>H</sub> (400 MHz, DMSO-d<sub>6</sub>) 10.34 (1H, s, NH), 8.43 (1H, s, Ar-H), 8.33 (2H, s, Ar-H), 8.24 (1H, s, thiazole-H), 7.97 (1H, s, furan-H), 7.91 (1H, d, *J* 7.7, Ar-H), 7.88-7.75 (3H, m, Ar-H), 7.46 (1H, t, *J* 7.8, Ar-H), 7.39 (1H, d, *J* 3.2, furan-H), 6.73 (1H, s, furan-H). t<sub>R</sub> (HPLC) 4.19 min.

**Furan-2-carboxylic acid (3-[2-(6-dimethylamino-pyridin-3-yl)-thiazol-4-yl]-phenyl)-amide, 317 (JCC-CRT-421)**



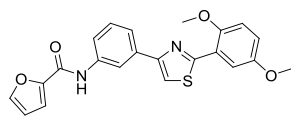
Yellow solid (11.2 mg, 29% yield, *ca.* 85% purity by <sup>1</sup>H-NMR), δ<sub>H</sub> (400 MHz, DMSO-d<sub>6</sub>) 10.31 (1H, s, NH), 8.79-8.69 (1H, m, pyridine-H), 8.40 (1H, s, Ar-H), 8.08 (1H, d, *J* 9.1, pyridine-H), 7.95 (2H, m, thiazole-H, furan-H), 7.81 (1H, d, *J* 8.0, Ar-H), 7.77-7.70 (1H, m, Ar-H), 7.43 (1H, t, *J* 8.1, Ar-H), 7.39 (1H, d, *J* 2.8, furan-H), 6.77 (1H, d, *J* 9.1, pyridine-H), 6.74-6.71 (1H, m, furan-H), 3.12 (3H, s, CH<sub>3</sub>), 3.10 (3H, s, CH<sub>3</sub>). t<sub>R</sub> (HPLC) 3.99 min.

**4-(4-(3-[(Furan-2-carbonyl)-amino]-phenyl)-thiazol-2-yl)-benzoic acid methyl ester, 318 (JCC-CRT-424)**



White solid (8.8 mg, 22% yield, *ca.* 85% purity by <sup>1</sup>H-NMR), δ<sub>H</sub> (400 MHz, DMSO-d<sub>6</sub>) 10.34 (1H, s, NH), 8.45 (1H, t, *J* 1.8, Ar-H), 8.24 (1H, s, thiazole-H), 8.21-8.16 (2H, m, Ar-H), 8.14-8.10 (2H, m, Ar-H), 7.98-7.95 (1H, m, furan-H), 7.86-7.81 (1H, m, Ar-H), 7.80-7.75 (1H, m, Ar-H), 7.46 (1H, t, *J* 7.9, Ar-H), 7.41-7.38 (1H, m, furan-H), 6.73 (1H, dd, *J* 3.5, 1.7, furan-H), 3.90 (3H, s, CH<sub>3</sub>). t<sub>R</sub> (HPLC) 4.05 min.

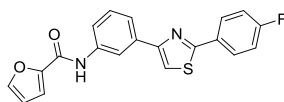
**Furan-2-carboxylic acid (3-[2-(2,5-dimethoxy-phenyl)-thiazol-4-yl]-phenyl)-amide, 319**  
(JCC-CRT-430)



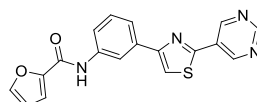
Brown solid (11.1 mg, 27% yield, *ca.* 80% purity by  $^1\text{H-NMR}$ ),  $\delta_{\text{H}}$  (400 MHz, DMSO- $d_6$ ) 10.31 (1H, s, NH), 8.45 (1H, t,  $J$  1.8, Ar-H), 8.12 (1H, s, thiazole-H), 7.98 (1H, d,  $J$  3.2, furan-H), 7.96 (1H, dd,  $J$  3.3, 2.4, Ar-H), 7.85-7.80 (1H, m, Ar-H), 7.80-7.76 (1H, m, Ar-H), 7.44 (1H, t,  $J$  7.9, Ar-H), 7.41-7.38 (1H, m, furan-H), 7.22 (1H, d,  $J$  9.1, Ar-H), 7.10 (1H, dd,  $J$  9.1, 3.2, Ar-H), 6.72 (1H, dd,  $J$  3.5, 1.6, furan-H), 3.99 (3H, s,  $\text{CH}_3$ ), 3.83 (3H, s,  $\text{CH}_3$ ).  $t_{\text{R}}$  (HPLC) 3.92 min.

Fifteen further compounds were successfully synthesised, but the purification was not sufficient for assignment of the  $^1\text{H-NMR}$  data. These compounds were tested in the enzyme assays.

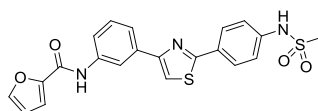
- Furan-2-carboxylic acid (3-[2-(4-fluoro-phenyl)-thiazol-4-yl]-phenyl)-amide, **320** (JCC-CRT-398A)



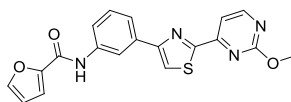
- Furan-2-carboxylic acid [3-(2-pyrimidin-5-yl-thiazol-4-yl)-phenyl]-amide, **321** (JCC-CRT-398C)



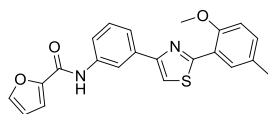
- Furan-2-carboxylic acid (3-[2-(4-methanesulfonylamino-phenyl)-thiazol-4-yl]-phenyl)-amide, **322** (JCC-CRT-405)



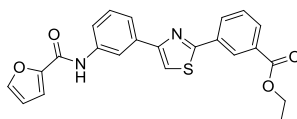
- Furan-2-carboxylic acid (3-[2-(2-methoxy-pyrimidin-4-yl)-thiazol-4-yl]-phenyl)-amide, **323** (JCC-CRT-418)



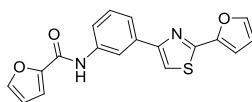
- Furan-2-carboxylic acid (3-[2-(2-methoxy-5-methyl-phenyl)-thiazol-4-yl]-phenyl)-amide, **324** (JCC-CRT-419)



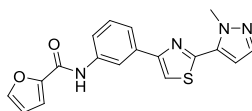
- 3-(4-(3-[(Furan-2-carbonyl)-amino]-phenyl)-thiazol-2-yl)-benzoic acid ethyl ester, **325** (JCC-CRT-423)



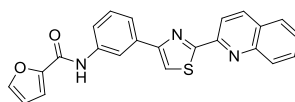
- Furan-2-carboxylic acid [3-(2-furan-2-yl-thiazol-4-yl)-phenyl]-amide, **326** (JCC-CRT-427)



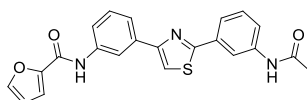
- Furan-2-carboxylic acid (3-[2-(2-methyl-2*H*-pyrazol-3-yl)-thiazol-4-yl]-phenyl)-amide, **327** (JCC-CRT-428)



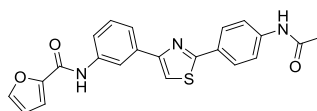
- Furan-2-carboxylic acid [3-(2-quinolin-2-yl-thiazol-4-yl)-phenyl]-amide, **328** (JCC-CRT-429)



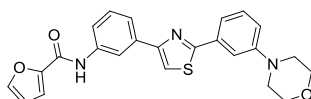
- Furan-2-carboxylic acid (3-[2-(3-acetylamino-phenyl)-thiazol-4-yl]-phenyl)-amide, **329** (JCC-CRT-431)



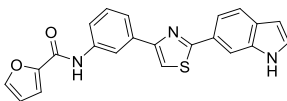
- Furan-2-carboxylic acid (3-[2-(4-acetylamino-phenyl)-thiazol-4-yl]-phenyl)-amide, **330** (JCC-CRT-432)



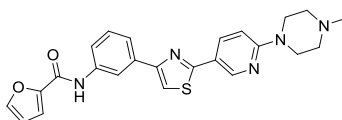
- Furan-2-carboxylic acid (3-[2-(3-morpholin-4-yl-phenyl)-thiazol-4-yl]-phenyl)-amide, **331** (JCC-CRT-437)



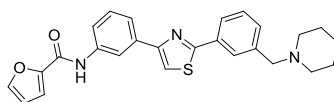
- Furan-2-carboxylic acid (3-[2-(1*H*-indol-6-yl)-thiazol-4-yl]-phenyl)-amide, **332** (JCC-CRT-438)



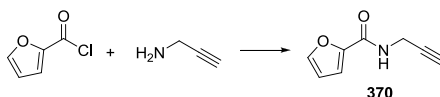
- Furan-2-carboxylic acid (3-(2-[6-(4-methyl-piperazin-1-yl)-pyridin-3-yl]-thiazol-4-yl)-phenyl)-amide, **333** (JCC-CRT-439)



- Furan-2-carboxylic acid (3-[2-(3-piperidin-1-ylmethyl-phenyl)-thiazol-4-yl]-phenyl)-amide, **334** (JCC-CRT-440)

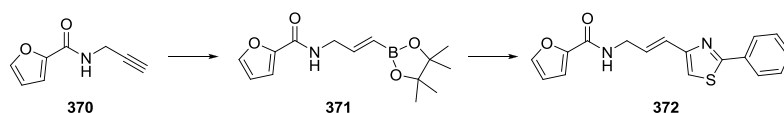


### ***N*-Propargyl-furan-2-carboxamide, **370****<sup>230</sup>



Furoyl chloride (1.00 mL, 10.2 mmol) was added dropwise to a stirred solution of propargylamine (720  $\mu$ L, 11.2 mmol) and Et<sub>3</sub>N (1.70 mL, 12.2 mmol) in CH<sub>2</sub>Cl<sub>2</sub> (40 mL) at 0 °C, and the reaction mixture was allowed to warm to r.t. and stirred for 5 h. The reaction mixture was then sequentially washed with 1 M HCl (50 mL) and sat. aq. NaHCO<sub>3</sub> (50 mL), dried (Na<sub>2</sub>SO<sub>4</sub>) and the solvent removed *in vacuo* to give the title compound as colourless rods (1.39 g, 92%), mp 90-91.5 °C;  $\nu_{\max}$  (neat)/cm<sup>-1</sup> 3295, 2360, 1647, 1592, 1519, 1470;  $\delta_{\text{H}}$  (400 MHz, CDCl<sub>3</sub>) 7.45-7.39 (1H, m, furan 5-H), 7.13-7.09 (1H, m, furan 3-H), 6.54 (1H, br s, NH), 6.47 (1H, dd, *J* 3.4, 1.9, furan 4-H), 4.20 (2H, dd, *J* 5.5, 2.6, CH<sub>2</sub>), 2.25 (1H, t, *J* 2.6, C $\equiv$ CH);  $\delta_{\text{C}}$  (101 MHz, CDCl<sub>3</sub>) 157.9, 147.4, 144.2, 114.8, 112.2, 79.3, 71.8, 28.9; *m/z* (ES) 154 (20%), 150 (MH<sup>+</sup>, 100). Found MH<sup>+</sup>, 150.0549. C<sub>8</sub>H<sub>8</sub>NO<sub>2</sub> requires 150.0555. Data is in agreement with the literature.<sup>230</sup>

### Furan-2-carboxylic acid [(E)-3-(2-phenyl-thiazol-4-yl)-allyl]-amide, **372**

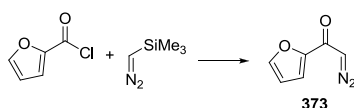


According to the method of Pietruszka,<sup>231</sup> to a stirred solution of  $\text{BH}_3\cdot\text{SMe}_2$  (290  $\mu\text{L}$ , 3.0 mmol) in THF (3 mL) at 0 °C was added cyclohexene (0.61 mL, 6.0 mmol) dropwise, and the reaction mixture warmed to r.t. and stirred for 2 h to form a white precipitate. *N*-propargyl-furan-2-carboxamide **370** (447 mg, 3.0 mmol) was then added at 0 °C, and the reaction mixture stirred for a further 1.5 h at r.t. to become a clear yellow solution. A solution of trimethylamine-*N*-oxide (451 mg, 6.0 mmol) in  $\text{CH}_2\text{Cl}_2$  (3 mL) was then added, and the reaction mixture stirred for 2 h before the addition of pinacol (355 mg, 3.0 mmol), whereupon the reaction was stirred overnight. The solvent was removed *in vacuo* to give a yellow oil, and partial purification by column chromatography eluting with EtOAc/hexane (1:3  $\rightarrow$  2:3) afforded crude boronate **371** as a pale yellow oil (683 mg), which was used directly in the next reaction.

A portion of the crude boronate **371** (171 mg, 0.62 mmol) was added to a stirred solution of 4-bromo-2-phenylthiazole (**96**) (50 mg, 0.21 mmol) and  $\text{K}_2\text{CO}_3$  (73 mg, 0.53 mmol) in degassed DME/ $\text{H}_2\text{O}$  (4:1, 3 mL), followed by  $\text{Pd}(\text{PPh}_3)_4$  (7.3 mg, 0.006 mmol) and the reaction mixture stirred at reflux for 24 h. Upon cooling, EtOAc (10 mL) and  $\text{H}_2\text{O}$  (10 mL) were added, and the aqueous layer extracted with EtOAc (3  $\times$  10 mL). The combined organic layers were dried ( $\text{Na}_2\text{SO}_4$ ) and the solvent removed *in vacuo* to give a brown oil. Partial purification by column chromatography eluting with EtOAc/hexane (1:4  $\rightarrow$  1:1) gave the title compound as a colourless oil (51 mg, 62% over 2 steps, >80% purity by  $^1\text{H-NMR}$  with pinacol as the major contaminant),  $R_f$  0.4 (EtOAc/hexane 1:1);  $\nu_{\text{max}}$  (neat)/ $\text{cm}^{-1}$  1647, 1593, 1522, 1476, 1294;  $\delta_{\text{H}}$  (400 MHz,  $\text{CDCl}_3$ ) 7.96-7.92 (2H, m, Ar 2-H, 6-H), 7.42-7.38 (4H, m, Ar 3-H, 4-H, 5-H, furan 5-H), 7.12 (1H, d,  $J$  3.3, furan 3-H), 7.03 (1H, s, thiazole-H), 6.72 (1H, dt,  $J$  15.5, 6.0,  $\text{CH}_2\text{C}(\text{H})=\text{C}$ ), 6.60 (1H, dt,  $J$  15.5, 1.0,  $\text{CH}_2\text{C}(\text{H})=\text{CH}$ ), 6.56 (1H, br s, NH), 6.47 (1H, dd,  $J$  3.5, 1.7, furan 4-H), 4.23 (2H, td,  $J$  6.0, 1.0,  $\text{CH}_2\text{C}(\text{H})=\text{C}$ );  $\delta_{\text{C}}$  (101 MHz,  $\text{CDCl}_3$ ) 168.3, 158.4, 154.2, 148.1, 144.1, 133.7, 130.3, 129.1, 128.7, 126.8, 125.3, 115.3, 114.5, 112.3, 40.9;  $m/z$  (ES) 643 (38%), 492 (27), 470 (34), 333 (59), 311 ( $\text{MH}^+$ , 100). Found  $\text{MH}^+$ , 311.0851.  $\text{C}_{17}\text{H}_{15}\text{N}_2\text{O}_2\text{S}$  requires 311.0854.

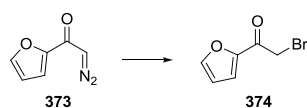


## 2-Diazoacetylfuran, **373**<sup>232</sup>



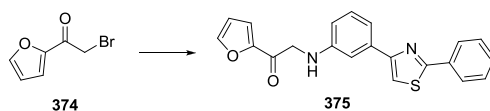
Trimethylsilyldiazomethane (2 M in hexanes, 1.53 mL, 3.1 mmol) was added dropwise to a stirred solution of 2-furoyl chloride (200  $\mu$ L, 2.0 mmol) and Et<sub>3</sub>N (0.43 mL, 3.1 mmol) in CH<sub>2</sub>Cl<sub>2</sub> at 0 °C, and the reaction mixture allowed to warm to r.t. and stirred for 24 h. Sat. aq. NaHCO<sub>3</sub> (40 mL) was added, and the aqueous layer extracted with CH<sub>2</sub>Cl<sub>2</sub> (3  $\times$  30 mL). The combined organic layers were washed with brine (40 mL), dried (Na<sub>2</sub>SO<sub>4</sub>) and the solvent removed *in vacuo* to give a yellow oil. Column chromatography eluting with EtOAc/hexane (1:3) afforded the title compound as a yellow oil which became a pale yellow solid on storage at -20 °C (202 mg, 73%), R<sub>f</sub> 0.33 (EtOAc/hexane 1:3);  $\delta_{\text{H}}$  (400 MHz, CDCl<sub>3</sub>) 7.48-7.46 (1H, m, furan 5-H), 7.13-7.11 (1H, m, furan 3-H), 6.52 (1H, dd, *J* 3.5, 1.8, furan 4-H), 5.86 (1H, s, CHN<sub>2</sub>); *m/z* (CI) 154 (37%), 137 (MH<sup>+</sup>, 44), 106 (100). Found MH<sup>+</sup>, 137.0350. C<sub>6</sub>H<sub>5</sub>N<sub>2</sub>O<sub>2</sub> requires 137.0351. Data is in agreement with the literature.<sup>232</sup>

## 2-Bromo-1-furan-2-yl-ethanone, **374**<sup>233</sup>



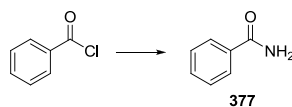
According to the method of Pallavicini,<sup>234</sup> HBr (2 M in H<sub>2</sub>O, 1 mL) was added dropwise to a stirred yellow solution of diazoketone **373** (89 mg, 0.65 mmol) in Et<sub>2</sub>O at 0 °C, causing effervescence and loss of the yellow colour. The reaction mixture was stirred for 30 min at 0 °C and 1 h at r.t. before being partitioned between Et<sub>2</sub>O (20 mL) and sat. aq. NaHCO<sub>3</sub> (40 mL). The aqueous layer was extracted with Et<sub>2</sub>O (3  $\times$  20 mL), the combined organic layers dried (MgSO<sub>4</sub>) and the solvent removed *in vacuo*. Column chromatography eluting with EtOAc/hexane (1:4  $\rightarrow$  1:3) afforded the title compound as a colourless oil (110 mg, 94%), R<sub>f</sub> 0.36 (Et<sub>2</sub>O/petrol 1:3);  $\delta_{\text{H}}$  (400 MHz, CDCl<sub>3</sub>) 7.61 (1H, d, *J* 1.5, furan 5-H), 7.30 (1H, d, *J* 3.8, furan 3-H), 6.56 (1H, dd, *J* 3.8, 1.5, furan 4-H), 4.28 (2H, s, CH<sub>2</sub>);  $\delta_{\text{C}}$  (101 MHz, CDCl<sub>3</sub>) 180.5, 150.5, 147.5, 119.3, 113.0, 30.2; *m/z* (CI) 208 (MNH<sub>4</sub><sup>+</sup>, 100%), 206 (MNH<sub>4</sub><sup>+</sup>, 100), 190 (MH<sup>+</sup>, 32), 188 (MH<sup>+</sup>, 32), 95 (72). Found MH<sup>+</sup>, 205.9814. C<sub>6</sub>H<sub>9</sub>NO<sub>2</sub>Br requires 205.9817. Data is in agreement with the literature.<sup>233</sup>

### 1-Furan-2-yl-2-[3-(2-phenyl-thiazol-4-yl)-phenylamino]-ethanone, **375**



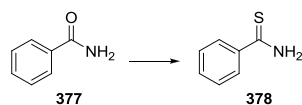
A mixture of bromoketone **374** (29 mg, 0.16 mmol), aniline **166** (37 mg, 0.15 mmol) and  $\text{NaHCO}_3$  (15 mg, 0.18 mmol) in DMF (1 mL) was stirred at r.t. for 3 d. EtOAc (10 mL) was added and extracted with 50% brine ( $3 \times 20$  mL). The organic layer was dried ( $\text{MgSO}_4$ ) and the solvent removed *in vacuo* and purification by column chromatography eluting with EtOAc/hexane (1:3  $\rightarrow$  1:1) afforded the title compound as a colourless oil (31 mg, 59%),  $R_f$  0.28 (EtOAc/hexane 1:3);  $\nu_{\text{max}}$  (neat)/ $\text{cm}^{-1}$  1761, 1681, 1607, 1572, 1467;  $\delta_{\text{H}}$  (400 MHz,  $\text{CDCl}_3$ ) 8.06-8.00 (2H, m Ar-H), 7.64-7.59 (1H, m, furan 5-H), 7.48-7.39 (6H, m,  $4 \times$  Ar-H, thiazole-H, NH), 7.36 (1H, d,  $J$  7.7, Ar-H), 7.33 (1H, d,  $J$  3.6, furan 3-H), 7.27 (1H, t,  $J$  6.5, Ar-H), 6.75 (1H, dd,  $J$  8.0, 1.7, Ar-H), 6.57 (1H, dd,  $J$  3.6, 1.6, furan 4-H), 4.58 (2H, s,  $\text{CH}_2$ );  $\delta_{\text{C}}$  (101 MHz,  $\text{CDCl}_3$ ) 184.5, 167.9, 156.5, 151.3, 147.0, 146.9, 135.7, 133.9, 130.2, 129.9, 129.1, 126.9, 117.9, 117.2, 113.9, 113.1, 112.8, 112.1, 50.7;  $m/z$  (ES) 399 (12%), 383 (30), 362 (28), 361 ( $\text{MH}^+$ , 100). Found  $\text{MH}^+$ , 361.1006.  $\text{C}_{21}\text{H}_{17}\text{N}_2\text{O}_2\text{S}$  requires 361.1011.

### Benzamide, **377**<sup>235</sup>



According to the method of Reuman,<sup>236</sup> benzoyl chloride (20.0 mL, 174 mmol) was added slowly to a stirred solution of  $\text{NH}_3$  (*ca.* 14 M in  $\text{H}_2\text{O}$ , 49.6 mL, 694 mmol) in  $\text{H}_2\text{O}$  (250 mL), and the reaction mixture stirred at r.t. for 18 h. The resulting white precipitate was collected by filtration and dried *in vacuo* to give the title compound as colourless plates (17.2 g, 82%), mp 133-134.5  $^\circ\text{C}$ ;  $\delta_{\text{H}}$  (400 MHz,  $\text{CDCl}_3$ ) 7.83-7.76 (2H, m, Ar-H), 7.54-7.48 (1H, m, Ar-H), 7.46-7.39 (2H, m, Ar-H), 6.16 (2H, br s,  $\text{NH}_2$ ).  $m/z$  (ES) 268 (48%), 163 (100), 122 ( $\text{MH}^+$ , 88), 118 (43). Found  $\text{MH}^+$ , 122.0604.  $\text{C}_7\text{H}_8\text{NO}$  requires 122.0606. Data is in agreement with the literature.<sup>235</sup>

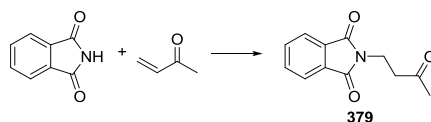
### Thiobenzamide, **378**<sup>237</sup>



Adapted from the method of Colabufo,<sup>238</sup> a suspension of benzamide (2.72 g, 22.5 mmol) and Lawesson's reagent (10.0 g, 24.7 mmol) in THF (250 mL) was stirred at reflux for 5 h to give

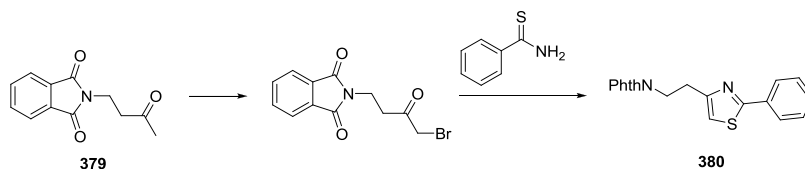
a clear, deep yellow solution. The solvent was removed *in vacuo*, and the residue was taken up in EtOAc (100 mL) and washed with 1 M HCl (2 × 100 mL). The aqueous layers were basified with Na<sub>2</sub>CO<sub>3</sub> and extracted with EtOAc (3 × 100 mL). The organic layers before and after the acid wash were found to both contain the product by TLC, so were combined, dried (Na<sub>2</sub>SO<sub>4</sub>) and the solvent removed *in vacuo* to give a yellow solid. Column chromatography eluting with EtOAc/hexane (1:3 → 1:1) afforded the title compound as yellow needles (2.55 g, 83%), mp 123-125 °C; R<sub>f</sub> 0.51 (EtOAc/hexane 1:1); δ<sub>H</sub> (400 MHz, CDCl<sub>3</sub>) 7.89-7.82 (2H, m, Ar-H), 7.68 (1H, br s, NH), 7.50 (1H, t, *J* 7.4, Ar-H), 7.39 (2H, t, *J* 7.7, Ar-H), 7.19 (1H, br s, NH). *m/z* (ES) 138 (MH<sup>+</sup>, 100%), 121 (41). Found MH<sup>+</sup>, 138.0372. C<sub>7</sub>H<sub>8</sub>NS requires 138.0377. Data is in agreement with the literature.<sup>237</sup>

#### 4-Phthalimido-2-butanone, **379**<sup>239</sup>



According to the method of Timmerman,<sup>239</sup> NaOEt (410 mg, 6.0 mmol) was added to a stirred suspension of phthalimide (17.7 g, 120 mmol) and 1-buten-3-one (10.0 mL, 120 mmol) in EtOH/EtOAc (1:4, 150 mL), and the reaction mixture was stirred at reflux for 4.5 h to give an almost clear solution. The solvent was removed *in vacuo* and the residue recrystallised from 96% EtOH to give the title compound as a white crystalline powder (24.7 g, 95%), mp 112.5-115 °C; δ<sub>H</sub> (400 MHz, CDCl<sub>3</sub>) 7.83-7.79 (2H, m, Ar 3-H, 6-H), 7.70-7.67 (2H, m, Ar 4-H, 5-H), 3.96-3.90 (2H, m, NCH<sub>2</sub>), 2.88-2.82 (2H, m, COCH<sub>2</sub>), 2.16 (3H, s, CH<sub>3</sub>); *m/z* (ES) 309 (13%), 282 (17), 281 (MH<sup>+</sup>, 100), 240 (14), 218 (37). Found MH<sup>+</sup>, 218.0819. C<sub>12</sub>H<sub>12</sub>NO<sub>3</sub> requires 218.0817. Data is in agreement with the literature.<sup>239</sup>

#### 2-[2-(2-Phenyl-thiazol-4-yl)-ethyl]-isoindole-1,3-dione, **380**<sup>240</sup>

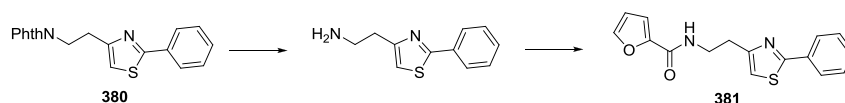


Bromine (0.71 mL, 13.8 mmol) was added to a stirred solution of ketone **379** (3.00 g, 13.8 mmol) in MeOH (20 mL) at 0 °C, and the reaction mixture stirred at r.t. for 5 h to give a yellow precipitate. Sat. aq. NaHCO<sub>3</sub> (40 mL) was added and extracted with EtOAc (3 × 50 mL). The combined organic layers were washed with sat. aq. Na<sub>2</sub>S<sub>2</sub>O<sub>3</sub> (20 mL), dried (Na<sub>2</sub>SO<sub>4</sub>) and the solvent removed *in vacuo*. Partial purification by column chromatography

eluting with EtOAc/hexane (1:3 → 1:1) afforded the crude bromoketone as a white solid (4.04 g), which was used directly in the subsequent thiazole formation.

A solution of bromoketone (2.86 g, 9.67 mmol) and thiobenzamide (1.33 g, 9.67 mmol) in EtOH (35 mL) was heated to reflux for 5 h, cooled and the solvent removed *in vacuo*. The residue was partitioned between EtOAc (50 mL) and sat. aq. NaHCO<sub>3</sub> (50 mL), the aqueous layer was extracted with EtOAc (3 × 50 mL), the combined organic layers dried (MgSO<sub>4</sub>) and the solvent removed *in vacuo*. Column chromatography eluting with EtOAc/hexane (1:5 → 1:2) afforded the title compound as a white solid (1.07 g, 33% over 2 steps), mp 118-120 °C;  $\delta_{\text{H}}$  (400 MHz, CDCl<sub>3</sub>) 7.80-7.77 (2H, m, phthalimide 3-H, 6-H), 7.76-7.72 (2H, m, phthalimide 4-H, 5-H), 7.68-7.63 (2H, m, Ar-H), 7.34-7.29 (3H, m, Ar-H), 6.96 (1H, s, thiazole-H), 4.08 (2H, t, *J* 7.0, NCH<sub>2</sub>), 3.20 (2H, t, *J* 7.0, NCH<sub>2</sub>CH<sub>2</sub>); *m/z* (CI) 336 (40%), 335 (MH<sup>+</sup>, 100), 189 (22). Found MH<sup>+</sup>, 335.0861. C<sub>19</sub>H<sub>15</sub>N<sub>2</sub>O<sub>2</sub>S requires 335.0854. Data is in agreement with the literature.<sup>240</sup>

### Furan-2-carboxylic acid [2-(2-phenyl-thiazol-4-yl)-ethyl]-amide, **381**

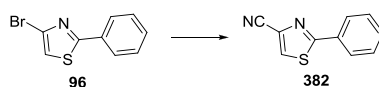


A solution of thiazole **380** (288 mg, 0.86 mmol) and hydrazine hydrate (70  $\mu$ L, 1.72 mmol) in MeOH (15 mL) was heated to reflux for 6 h. After cooling, addition of EtOAc (10 mL) resulted in precipitation of the phthalazinedione by-product as a white solid, which was removed by filtration, washing with EtOAc. The solvent was removed *in vacuo* and the residue partitioned between CH<sub>2</sub>Cl<sub>2</sub> (50 mL) and 1 M HCl (50 mL). The aqueous layer was basified with Na<sub>2</sub>CO<sub>3</sub> and extracted with CH<sub>2</sub>Cl<sub>2</sub> (3 × 50 mL). The combined organic layers were dried (MgSO<sub>4</sub>) and the solvent removed *in vacuo* to give the crude amine as a colourless oil (91 mg, 52%), which was used directly in the subsequent reaction.

To a solution of this amine (69 mg, 0.34 mmol) and Et<sub>3</sub>N (142  $\mu$ L, 1.02 mmol) in CH<sub>2</sub>Cl<sub>2</sub> (2 mL) at 0 °C was added 2-furoyl chloride (37  $\mu$ L, 0.37 mmol), and the reaction stirred at r.t. for 5 h. EtOAc (15 mL) was added and extracted with sat. aq. NaHCO<sub>3</sub> (15 mL) and 1 M HCl (15 mL). The organic layer was dried (MgSO<sub>4</sub>), the solvent removed *in vacuo* and purification by column chromatography eluting with EtOAc/hexane (1:1) afforded the title compound as a white semi-solid (55 mg, 54%), *R<sub>f</sub>* (EtOAc/hexane 1:1);  $\nu_{\text{max}}$  (neat)/cm<sup>-1</sup> 3308, 1647, 1594, 1515, 1475;  $\delta_{\text{H}}$  (400 MHz, CDCl<sub>3</sub>) 8.01-7.95 (2H, m, Ar-H), 7.66 (1H, br s, NH), 7.45-7.39

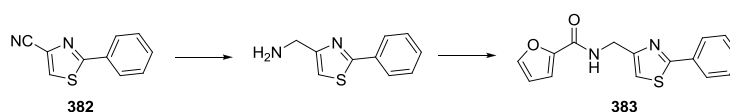
(4H, m, furan 5-H, 3 × Ar-H), 7.09 (1H, d, *J* 3.4, furan 3-H), 6.98 (1H, s, thiazole-H), 6.46 (1H, dd, *J* 3.5, 1.7, furan 4-H), 3.79 (2H, m, NCH<sub>2</sub>), 3.06 (2H, t, *J* 6.2, NCH<sub>2</sub>CH<sub>2</sub>); δ<sub>C</sub> (101 MHz, CDCl<sub>3</sub>) 168.5, 158.6, 155.6, 148.6, 143.8, 133.7, 130.3, 129.1, 126.6, 114.6, 114.0, 112.3, 38.8, 31.0; *m/z* (ES) 620 (15%), 619 (38), 362 (14), 321 (46), 299 (MH<sup>+</sup>, 100). Found MH<sup>+</sup>, 299.0853. C<sub>16</sub>H<sub>15</sub>N<sub>2</sub>O<sub>2</sub>S requires 299.0854.

### 2-Phenyl-thiazole-4-carbonitrile <sup>241</sup>



A mixture of 4-bromothiophene **96** (360 mg, 1.5 mmol), Zn(CN)<sub>2</sub> (264 mg, 2.25 mmol) and Pd(dppf)Cl<sub>2</sub> (33 mg, 0.045 mmol) in DMF (5 mL) was heated in a microwave reactor at 220 °C for 10 min. The reaction mixture was then filtered through Celite<sup>®</sup> and partitioned between EtOAc (20 mL) and H<sub>2</sub>O (20 mL). The aqueous layer was extracted with EtOAc (3 × 20 mL) and the combined organic layers dried (MgSO<sub>4</sub>) and the solvent removed *in vacuo*. Column chromatography eluting with EtOAc/hexane (0:1 → 1:4) afforded the title compound as a white solid (110 mg, 39%), mp 97-99 °C; δ<sub>H</sub> (400 MHz, CDCl<sub>3</sub>) 7.95 (1H, s, thiazole-H), 7.95-7.91 (2H, m, Ar-H), 7.49-7.43 (3H, m, Ar-H); δ<sub>C</sub> (101 MHz, CDCl<sub>3</sub>) 170.1, 132.0, 131.6, 130.1, 129.4, 127.7, 127.1, 114.3; *m/z* (CI) 204 (23%), 188 (28), 187 (MH<sup>+</sup>, 100), 186 (29). Found MH<sup>+</sup>, 187.0325. C<sub>10</sub>H<sub>7</sub>N<sub>2</sub>S requires 187.0330. Data is in agreement with the literature.<sup>241</sup>

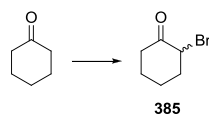
### Furan-2-carboxylic acid (2-phenyl-thiazol-4-ylmethyl)-amide, **383**



To a solution of nitrile **382** (99 mg, 0.53 mmol) in THF (6 mL) was added LiAlH<sub>4</sub> (1 M in Et<sub>2</sub>O, 1.60 mL, 1.60 mmol). The reaction mixture was heated to reflux for 45 min, before being allowed to cool and carefully quenched with H<sub>2</sub>O (0.5 mL). 2 M NaOH (10 mL), H<sub>2</sub>O (2 mL) and EtOAc (20 mL) were added and the reaction mixture stirred vigorously for 30 min before being filtered through Celite<sup>®</sup>, washing with EtOAc. The organic layer was washed with brine (20 mL), dried (MgSO<sub>4</sub>) and the solvent removed *in vacuo* to give the crude amine as a colourless oil (100 mg), which was used without purification. δ<sub>H</sub> (400 MHz, CDCl<sub>3</sub>) 7.93-7.86 (2H, m, Ar-H), 7.42-7.35 (3H, m, Ar-H), 7.05 (1H, s, thiazole-H), 3.99 (2H, s, CH<sub>2</sub>), 2.64 (2H, br s, NH<sub>2</sub>).

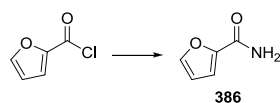
To a solution of this amine (50 mg, 0.27 mmol) and Et<sub>3</sub>N (74  $\mu$ L, 0.53 mmol) in CH<sub>2</sub>Cl<sub>2</sub> (1.5 mL) at 0 °C was added 2-furoyl chloride (29  $\mu$ L, 0.29 mmol), and the reaction stirred at r.t. for 24 h. EtOAc (15 mL) was added and the organic layer extracted with 1 M HCl (15 mL) and sat. aq. NaHCO<sub>3</sub> (15 mL) before being dried (MgSO<sub>4</sub>) and the solvent removed *in vacuo*. Column chromatography eluting with EtOAc/hexane (1:2  $\rightarrow$  1:1) afforded the title compound as an orange gum (74 mg, 99% over 2 steps).  $R_f$  0.27 (EtOAc/hexane 1:1);  $\nu_{\max}$  (neat)/cm<sup>-1</sup> 3304, 1655, 1593, 1523, 1475;  $\delta_H$  (400 MHz, CDCl<sub>3</sub>) 7.93-7.89 (2H, m, Ar-H), 7.42-7.38 (4H, m, 3  $\times$  Ar-H, furan 5-H), 7.17 (1H, s, thiazole-H), 7.11 (1H, br s, NH), 7.11 (1H, d,  $J$  3.4, furan 3-H), 6.45 (1H, dd,  $J$  3.5, 1.7, furan 4-H), 4.73 (2H, d,  $J$  5.8, CH<sub>2</sub>);  $\delta_C$  (101 MHz, CDCl<sub>3</sub>) 168.9, 158.4, 153.7, 148.0, 144.2, 133.5, 130.4, 129.1, 126.7, 115.7, 114.6, 112.3, 39.4;  $m/z$  (ES) 348 (52%), 307 (53), 285 (MH<sup>+</sup>, 100). Found MH<sup>+</sup>, 285.0700. C<sub>15</sub>H<sub>13</sub>N<sub>2</sub>O<sub>2</sub>S requires 285.0698.

### 2-Bromocyclohexanone, 385<sup>242</sup>



Adapted from the method of Easter,<sup>243</sup> bromine (1.48 mL, 29.0 mmol) was added slowly to a stirred solution of cyclohexanone (3.00 mL, 29.0 mmol) in MeOH (20 mL) at -10 °C, and the reaction mixture was allowed to warm to r.t. and stirred for 6 h. H<sub>2</sub>O (20 mL) was then added and the reaction mixture left stirring overnight to give a light brown solution. Brine (20 mL) and EtOAc (40 mL) were added, the aqueous layer extracted with EtOAc (3  $\times$  40 mL), the combined organic layers dried (Na<sub>2</sub>SO<sub>4</sub>) and the solvent removed *in vacuo* to give a brown oil. Column chromatography eluting with EtOAc/hexane (1:4  $\rightarrow$  1:3) afforded the title compound as a colourless oil (3.92 g, 77%),  $R_f$  0.45 (EtOAc/hexane 1:3);  $\delta_H$  (400 MHz, CDCl<sub>3</sub>) 4.44-4.39 (1H, m, CHBr), 3.01-2.91 (1H, m, CH<sub>2</sub>CO), 2.36-2.26 (2H, m, CH<sub>2</sub>), 2.25-2.16 (1H, m, CH<sub>2</sub>CO), 2.07-1.88 (2H, m, CH<sub>2</sub>), 1.85-1.66 (2H, m, CH<sub>2</sub>). Data is in agreement with the literature.<sup>242</sup>

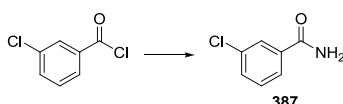
### Furan-2-carboxylic acid amide, 386<sup>244</sup>



According to the method of Reuman,<sup>236</sup> 2-furoyl chloride (1.00 mL, 10.2 mmol) was added slowly to a stirred solution of NH<sub>3</sub> (*ca.* 14 M in H<sub>2</sub>O, 2.4 mL, 40.6 mmol) in H<sub>2</sub>O (6 mL), and

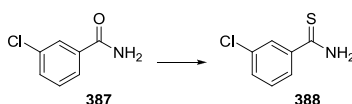
the reaction mixture stirred at r.t. for 1.5 h. The resulting white precipitate was collected by filtration and dried *in vacuo* overnight to give the title compound as colourless rods (855 mg, 76%), mp 135-137 °C;  $\delta_{\text{H}}$  (400 MHz,  $\text{CDCl}_3$ ) 7.46-7.43 (1H, m, furan 5-H), 7.14 (1H, d,  $J$  3.4, furan 3-H), 6.49 (1H, dd,  $J$  3.4, 1.7, furan 4-H), 6.27 (1H, br s, NH), 6.08 (1H, br s, NH).  $m/z$  (ES) 223 (22%), 129 (100), 112 ( $\text{MH}^+$ , 74). Found  $\text{MH}^+$ , 112.0394.  $\text{C}_5\text{H}_6\text{NO}_2$  requires 112.0399. Data is in agreement with the literature.<sup>244</sup>

### 3-Chlorobenzamide, 387<sup>245,246</sup>



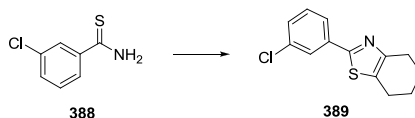
According to the method of Reuman,<sup>236</sup> 3-chlorobenzoyl chloride (10.0 mL, 78.1 mmol) was added slowly to a stirred solution of  $\text{NH}_3$  (*ca.* 14 M in  $\text{H}_2\text{O}$ , 22.3 mL, 312 mmol) in  $\text{H}_2\text{O}$  (120 mL), and the reaction mixture stirred at r.t. for 5 h. The resulting white precipitate was collected by filtration and dried *in vacuo* overnight to give the title compound as colourless plates (12.2 g, 97%), mp 139.5-140 °C;  $\delta_{\text{H}}$  (400 MHz,  $\text{CDCl}_3$ ) 7.79 (1H, t,  $J$  1.9, Ar-H), 7.68-7.63 (1H, m, Ar-H), 7.49 (1H, ddd,  $J$  8.2, 1.9, 1.0, Ar-H), 7.37 (1H, t,  $J$  7.9, Ar-H), 6.07 (1H, br s, NH), 5.94 (1H, br s, NH).  $m/z$  (ES) 199 (34%), 197 (100), 156 ( $\text{MH}^+$ , 45). Found  $\text{MH}^+$ , 156.0213.  $\text{C}_7\text{H}_7\text{NOCl}$  requires 156.0216. Data is in agreement with the literature.<sup>245,246</sup>

### 3-Chloro-thiobenzamide, 388<sup>240</sup>



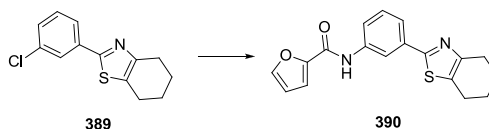
Adapted from the method of Colabufo,<sup>238</sup> a suspension of 3-chlorobenzamide (3.50 g, 22.5 mmol) and Lawesson's reagent (10.0 g, 24.7 mmol) in THF (250 mL) was stirred at reflux for 5 h to give a clear, deep yellow solution. The solvent was removed *in vacuo*, and the residue was partitioned between EtOAc (50 mL) and sat. aq.  $\text{NaHCO}_3$  (50 mL). The aqueous layers were extracted with EtOAc ( $3 \times 50$  mL), the organic layers combined, dried ( $\text{Na}_2\text{SO}_4$ ) and the solvent removed *in vacuo* to give a yellow solid. Column chromatography eluting with EtOAc/hexane (1:3  $\rightarrow$  1:2) afforded the title compound as yellow rods (3.33 g, 86%), mp 120-120.5 °C;  $R_f$  0.61 (EtOAc/hexane 1:1);  $\delta_{\text{H}}$  (400 MHz,  $\text{CDCl}_3$ ) 7.89-7.82 (2H, m, Ar-H), 7.68 (1H, br s, NH), 7.50 (1H, t,  $J$  7.4, Ar-H), 7.39 (2H, t,  $J$  7.7, Ar-H), 7.19 (1H, br s, NH).  $m/z$  (ES) 138 ( $\text{MH}^+$ , 100%), 121 (41). Found  $\text{MH}^+$ , 138.0372.  $\text{C}_7\text{H}_8\text{NS}$  requires 138.0377. Data is in agreement with the literature.<sup>240</sup>

## 2-(3-Chloro-phenyl)-4,5,6,7-tetrahydro-benzothiazole, **389**



A solution of thiobenzamide **388** (795 mg, 4.64 mmol) and bromide **385** (820 mg, 4.64 mmol) in EtOH (15 mL) was heated at reflux for 6.5 h, cooled and the solvent removed *in vacuo*. The residue was dissolved in a small volume of acetone and poured into Et<sub>2</sub>O to give a white precipitate. Column chromatography eluting with hexane afforded the title compound as a white solid (696 mg, 60%), mp 78-80 °C; *R<sub>f</sub>* 0.70 (EtOAc/hexane 1:3);  $\nu_{\max}$  (neat)/cm<sup>-1</sup> 3005, 2949, 2375, 2201, 1801, 1603;  $\delta_{\text{H}}$  (400 MHz, CDCl<sub>3</sub>) 8.42 (1H, dt, *J* 6.9, 1.7, Ar-H), 8.08-8.05 (1H, m, Ar-H), 7.57-7.49 (2H, m, Ar-H), 3.21 (2H, t, *J* 4.7, NCCH<sub>2</sub>), 2.85 (2H, t *J* 4.6, SCCH<sub>2</sub>), 1.98-1.88 (4H, m, 2 × CH<sub>2</sub>);  $\delta_{\text{C}}$  (101 MHz, CDCl<sub>3</sub>) 166.2, 146.1, 136.1, 133.8, 132.1, 131.6, 127.9, 126.7, 117.4, 24.4, 23.7, 22.4, 21.3; *m/z* (CI) 252 (59%), 251 (40), 250 (MH<sup>+</sup>, 100). Found MH<sup>+</sup>, 250.0458. C<sub>13</sub>H<sub>13</sub>NSCl requires 250.0457.

## Furan-2-carboxylic acid [3-(4,5,6,7-tetrahydro-benzothiazol-2-yl)-phenyl]-amide, **390**

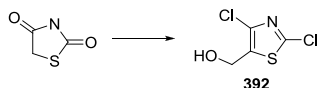


According to the method of Fors,<sup>168</sup> a solution of Pd(OAc)<sub>2</sub> (1.1 mg, 1 mol%), BrettPhos (5.9 mg, 2.2 mol%) in degassed <sup>t</sup>BuOH (1 mL) containing H<sub>2</sub>O (4 mol%) was heated to 110 °C for 2 min, before being cooled to r.t. This activated catalyst solution was then added to chloride **389** (125 mg, 0.50 mmol), amide **386** (83 mg, 0.75 mmol) and finely ground K<sub>3</sub>PO<sub>4</sub> (173 mg, 0.75 mmol). The resulting suspension was stirred at 110 °C for 14 h before being cooled to r.t. and partitioned between EtOAc (10 mL) and H<sub>2</sub>O (10 mL). The aqueous layer was extracted with EtOAc (10 mL), the combined organic layers dried (MgSO<sub>4</sub>) and the solvent removed *in vacuo*. Column chromatography eluting with EtOAc/hexane (1:4 → 1:1) afforded the title compound as a white amorphous solid (140 mg, 86%), mp 124-125 °C; *R<sub>f</sub>* 0.38 (EtOAc/hexane 1:1);  $\nu_{\max}$  (neat)/cm<sup>-1</sup> 3275, 2933, 1662, 1608, 1594, 1580, 1543, 1494, 1473;  $\delta_{\text{H}}$  (400 MHz, CDCl<sub>3</sub>) 8.32 (1H, s, NH), 8.01 (1H, t, *J* 1.6, Ar-H), 7.86 (1H, dd, *J* 8.1, 1.4, Ar-H), 7.57 (1H, d, *J* 7.9, Ar-H), 7.42 (1H, d, *J* 0.7, furan 5-H), 7.32 (1H, t, *J* 7.9, Ar-H), 7.18 (1H, d, *J* 3.5, furan 3-H), 6.48 (1H, dd, *J* 3.5, 1.7, furan 4-H), 2.76 (4H, dt, *J* 9.8, 4.4, thiazole-CH<sub>2</sub>), 1.88-1.77 (4H, m, 2 × CH<sub>2</sub>);  $\delta_{\text{C}}$  (101 MHz, CDCl<sub>3</sub>) 163.9, 156.3, 151.5, 147.7, 144.5, 138.2, 134.8, 129.7, 129.7, 122.2, 121.0, 117.3, 115.4, 112.6, 26.9, 23.7, 23.4, 23.0; *m/z* (ES)



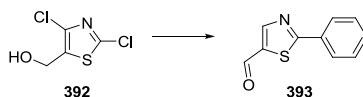
388 (8%), 347 (22), 327 (8), 326 (21), 325 (MH<sup>+</sup>, 100). Found MH<sup>+</sup>, 325.0999. C<sub>18</sub>H<sub>17</sub>N<sub>2</sub>O<sub>2</sub>S requires 325.1011;

**(2,4-Dichloro-thiazol-5-yl)-methanol, 392**<sup>169</sup>



According to the method of Kerdesky,<sup>169</sup> to a stirred suspension of 2,4-thiazolidinedione (3.00 g, 90% purity, 25.9 mmol) in POCl<sub>3</sub> (10.7 mL, 116.4 mmol) was added dropwise DMF (2.04 mL, 26.4 mmol) and the reaction mixture stirred at 85 °C for 1 h, then at reflux for 8 h. After cooling to r.t., the mixture was poured onto ice and extracted with EtOAc (2 × 100 mL). The combined organic layers were washed with NaHCO<sub>3</sub> (100 mL), dried (MgSO<sub>4</sub>) and the solvent removed *in vacuo*. Partial purification by column chromatography eluting with EtOAc/hexane (0:1 → 1:19) afforded the slightly crude intermediate aldehyde as a white solid (2.32 g). To a solution of a portion of this material (2.00 g) in MeOH (20 mL) at 0 °C was added portionwise NaBH<sub>4</sub> (416 mg, 11 mmol). The reaction was allowed to warm to r.t. and stirred for 4 h to give a green solution. The solvent was removed *in vacuo* and the residue partitioned between CH<sub>2</sub>Cl<sub>2</sub> (20 mL) and sat aq. NH<sub>4</sub>Cl (20 mL). The aqueous layer was extracted with CH<sub>2</sub>Cl<sub>2</sub> (3 × 20 mL), the combined organic layers dried (MgSO<sub>4</sub>) and the solvent removed *in vacuo*. Column chromatography eluting with EtOAc/hexane (1:3) afforded the title compound as a pale green amorphous solid (1.41 g, 30% over 2 steps), mp 50-51 °C; R<sub>f</sub> 0.11 (EtOAc/hexane 1:9); δ<sub>H</sub> (400 MHz, CDCl<sub>3</sub>) 4.75 (2H, d, *J* 5.9, CH<sub>2</sub>O), 2.90 (1H, t, *J* 5.9, OH); δ<sub>C</sub> (101 MHz, CDCl<sub>3</sub>) 151.2, 133.8, 133.4, 56.9; *m/z* (CI) 203 (MNH<sub>4</sub><sup>+</sup>, 32%), 201 (MNH<sub>4</sub><sup>+</sup>, 40), 186 (MH<sup>+</sup>, 80), 184 (MH<sup>+</sup>, 100). Found MH<sup>+</sup>, 183.9391. C<sub>4</sub>H<sub>4</sub>NOSCl<sub>2</sub> requires 183.9391. Data is in agreement with the literature.<sup>169</sup>

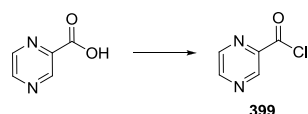
**2-Phenyl-thiazole-5-carbaldehyde, 393**<sup>247</sup>



A stirred solution of dichlorothiazole **392** (100 mg, 0.54 mmol), phenylboronic acid (79 mg, 0.65 mmol), K<sub>2</sub>CO<sub>3</sub> (187 mg, 1.35 mmol) and Pd(PPh<sub>3</sub>)<sub>4</sub> (15 mg, 0.022 mmol) in DME/H<sub>2</sub>O (3 mL, 4:1) was heated to 100 °C for 14 h. The reaction mixture was partitioned between H<sub>2</sub>O (20 mL) and EtOAc (20 mL), and the aqueous layer was extracted with EtOAc (2 × 20 mL). The combined organic layers were dried (MgSO<sub>4</sub>) and the solvent removed *in vacuo*. Column

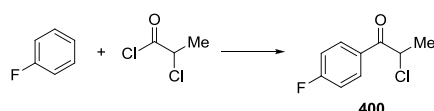
chromatography eluting with EtOAc/hexane (0:1 → 1:4) afforded the title compound as an off-white amorphous solid (77 mg, 75%), mp 93-95 °C;  $R_f$  0.43 (EtOAc/hexane 1:3);  $\nu_{\max}$  (neat)/ $\text{cm}^{-1}$  3056, 2835, 1673, 1653, 1508, 1452;  $\delta_{\text{H}}$  (400 MHz,  $\text{CDCl}_3$ ) 10.00 (1H, s, CHO), 8.39 (1H, s, thiazole-H), 8.00-7.95 (2H, m, Ar-H), 7.49-7.40 (3H, m, Ar-H);  $\delta_{\text{C}}$  (101 MHz,  $\text{CDCl}_3$ ) 182.3, 175.7, 152.5, 139.0, 132.7, 132.0, 129.4, 127.4;  $m/z$  (ES) 231 (7%), 224 (9), 196 (7), 191 (21), 190 ( $\text{MH}^+$ , 100). Found  $\text{MH}^+$ , 190.0323.  $\text{C}_{10}\text{H}_8\text{NOS}$  requires 190.0320. Data is in agreement with the literature.<sup>247</sup>

### Pyrazine-2-carbonyl chloride, **399**<sup>248</sup>



To a stirred suspension of pyrazine-2-carboxylic acid (1.50 g, 12.1 mmol) and oxalyl chloride (3.07 mL, 36.3 mmol) in  $\text{CH}_2\text{Cl}_2$  (100 mL) was added DMF (3 drops), causing vigorous effervescence at the surface of the suspended particles. After 5.5 h at r.t., the solvent was removed *in vacuo* to give the title compound as a purple powder, which was stored under Ar at -20 °C and used without purification in subsequent steps.  $\delta_{\text{H}}$  (400 MHz,  $\text{CDCl}_3$ ) 9.30 (1H, d,  $J$  1.3, pyrazine 3-H), 8.86 (1H, d,  $J$  2.4, pyrazine 5-H), 8.81-8.79 (1H, m, pyrazine 6-H);  $\delta_{\text{C}}$  (101 MHz,  $\text{CDCl}_3$ ) 169.1, 149.4, 146.0, 145.0, 144.6. Data is in agreement with the literature.<sup>248</sup>

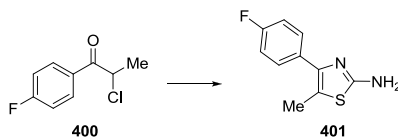
### 2-Chloro-1-(4-fluorophenyl)propan-1-one, **400**<sup>249</sup>



According to the method of Burpitt,<sup>249</sup> to a stirred suspension of  $\text{AlCl}_3$  (4.12 g, 30.9 mmol) in  $\text{CH}_2\text{Cl}_2$  (18 mL) was added dropwise a solution of 2-chloropropanoyl chloride (3.00 mL, 30.9 mmol) in  $\text{CH}_2\text{Cl}_2$  (6 mL) and the reaction mixture stirred for 10 min. A solution of fluorobenzene (2.90 mL, 30.9 mmol) in  $\text{CH}_2\text{Cl}_2$  (6 mL) was then added dropwise to give a clear orange solution, which was stirred at r.t. for 2.5 h. The reaction mixture was then cautiously poured onto HCl/ice (100 mL), stirred for 15 min and extracted with  $\text{CH}_2\text{Cl}_2$  (3 × 75 mL). The combined organic layers were washed with 2 M NaOH (2 × 50 mL),  $\text{H}_2\text{O}$  (50 mL) and brine (100 mL), dried ( $\text{MgSO}_4$ ) and the solvent removed *in vacuo* to give the title compound as a pale yellow oil which solidified on storage at -20 °C to an off-white solid (5.42 g, 94%),  $\delta_{\text{H}}$  (400 MHz,  $\text{CDCl}_3$ ) 8.07-8.00 (2H, m, Ar-H), 7.18-7.11 (2H, m, Ar-H), 5.17

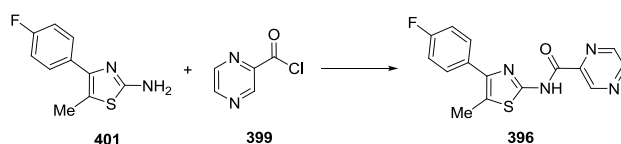
(1H, q, *J* 7.0, CHCl), 1.72 (3H, d, *J* 7.0, CH<sub>3</sub>); *m/z* (CI) 206 (36%), 204 (MH<sup>+</sup>, 100), 123 (100), 52 (57). Found MH<sup>+</sup>, 204.0586. C<sub>9</sub>H<sub>12</sub>NOCIF requires 204.0591. Data is in agreement with the literature.<sup>249</sup>

#### 4-(4-Fluoro-phenyl)-5-methyl-thiazol-2-ylamine, **401**<sup>250</sup>



A mixture of chloroketone **400** (3.00 g, 16.1 mmol) and thiourea (2.45 g, 32.2 mmol) in EtOH (60 mL) was heated to reflux for 2 h to give a pale yellow solution. The solvent was removed *in vacuo* and the residue partitioned between EtOAc (50 mL) and 50% sat. aq. NaHCO<sub>3</sub> (100 mL). The aqueous layer was extracted with EtOAc (3 × 50 mL), the combined organic layers washed with brine (100 mL), dried (MgSO<sub>4</sub>) and the solvent removed *in vacuo*. Column chromatography eluting with EtOAc/hexane (1:3 → 1:1) afforded the title compound as pale yellow plates (3.32 g, 99%), mp 133.5-134 °C, *R<sub>f</sub>* 0.24 (EtOAc/hexane 1:3); δ<sub>H</sub> (400 MHz, CDCl<sub>3</sub>) 7.53-7.47 (2H, m, Ar-H), 7.09-7.02 (2H, m, Ar-H), 4.87 (2H, br s, NH<sub>2</sub>), 2.35 (3H, s, CH<sub>3</sub>); *m/z* (CI) 209 (MH<sup>+</sup>, 100%), 210 (27), 52 (40). Found MH<sup>+</sup>, 209.0543. C<sub>10</sub>H<sub>10</sub>FN<sub>2</sub>S requires 209.0549. Data is in agreement with the literature.<sup>250,251</sup>

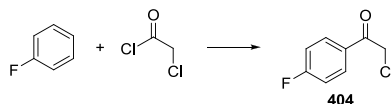
#### Pyrazine-2-carboxylic acid [4-(4-fluoro-phenyl)-5-methyl-thiazol-2-yl]-amide, **396**



To a stirred solution of aminothiazole **401** (200 mg, 0.96 mmol) and DMAP (118 mg, 0.96 mmol) in CH<sub>2</sub>Cl<sub>2</sub> (10 mL) was added acid chloride **399** (161 mg, 1.15 mmol) and the reaction stirred at r.t. for 16 h. The reaction mixture was partitioned between EtOAc (100 mL) and 50% sat. aq. NaHCO<sub>3</sub> (100 mL). The aqueous layer was extracted with EtOAc (2 × 100 mL), the combined organic layers were dried (MgSO<sub>4</sub>) and the solvent removed *in vacuo* to give a yellow solid. Recrystallisation from EtOAc gave the title compound as yellow crystals (224 mg, 74%), mp >250 °C; ν<sub>max</sub> (neat)/cm<sup>-1</sup> 3297, 3127, 1757, 1612, 1517, 1500, 1318, 1258; δ<sub>H</sub> (400 MHz, DMSO-*d*<sub>6</sub>) 12.44 (1H, s, NH), 9.31 (1H, d, *J* 1.5, pyrazine 3-H), 8.95 (1H, d, *J* 2.4, pyrazine 5-H), 8.83 (1H, dd, *J* 2.4, 1.5, pyrazine 6-H), 7.76-7.70 (2H, m, Ar-H), 7.34-7.27 (2H, m, Ar-H), 2.52 (3H, s, CH<sub>3</sub>); Sufficient concentration in solution could not be achieved

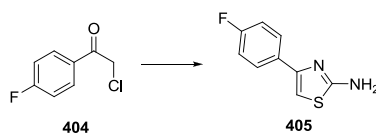
for a fully-resolved  $^{13}\text{C}$  spectrum;  $\delta_{\text{F}}$  (377 MHz,  $\text{DMSO-}d_6$ ) -114.52;  $m/z$  (ES) 315 ( $\text{MH}^+$ , 100%), 282 (65), 240 (36), 160 (35). Found 315.0724.  $\text{C}_{15}\text{H}_{12}\text{N}_4\text{OSF}$  requires 315.0716.

### 2-Chloro-1-(4-fluoro-phenyl)-ethanone, **404**<sup>252</sup>



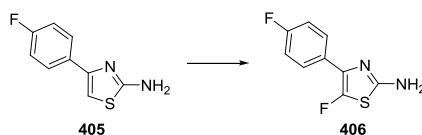
According to the method of Burpitt,<sup>249</sup> to a stirred suspension of  $\text{AlCl}_3$  (4.12 g, 30.9 mmol) in  $\text{CH}_2\text{Cl}_2$  (18 mL) was added dropwise a solution of chloroacetyl chloride (2.46 mL, 30.9 mmol) in  $\text{CH}_2\text{Cl}_2$  (6 mL) and the reaction mixture stirred for 10 min. A solution of fluorobenzene (2.90 mL, 30.9 mmol) in  $\text{CH}_2\text{Cl}_2$  (6 mL) was then added dropwise to give a clear orange solution, which was stirred at r.t. for 3 h. The reaction mixture was then cautiously poured onto  $\text{HCl/ice}$  (100 mL), stirred for 15 min and extracted with  $\text{CH}_2\text{Cl}_2$  ( $3 \times 75$  mL). The combined organic layers were washed with 2 M  $\text{NaOH}$  ( $2 \times 50$  mL),  $\text{H}_2\text{O}$  (50 mL) and brine (100 mL), dried ( $\text{MgSO}_4$ ) and the solvent removed *in vacuo* to give the title compound as a white solid (4.80 g, 90%), mp 46-47.5 °C,  $\delta_{\text{H}}$  (400 MHz,  $\text{CDCl}_3$ ) 8.02-7.95 (2H, m, Ar-H), 7.24-7.18 (2H, m, Ar-H), 4.64 (2H, s,  $\text{CH}_2\text{Cl}$ );  $m/z$  (CI) 192 ( $\text{MH}^+$ , 20%), 190 ( $\text{MH}^+$ , 62), 123 (44), 52 (100). Found  $\text{MH}^+$ , 190.0437.  $\text{C}_8\text{H}_{10}\text{NOCIF}$  requires 190.0435. Data is in agreement with the literature.<sup>252</sup>

### 4-(4-Fluoro-phenyl)-thiazol-2-ylamine, **405**<sup>253</sup>



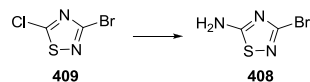
A mixture of chloroketone **404** (2.78 g, 16.1 mmol) and thiourea (2.45 g, 32.2 mmol) in  $\text{EtOH}$  (60 mL) was heated to reflux for 2 h to give a pale yellow solution. The solvent was removed and the residue partitioned between  $\text{EtOAc}$  (50 mL), 50% sat. aq.  $\text{NaHCO}_3$  (100 mL). The aqueous layer was extracted with  $\text{EtOAc}$  ( $3 \times 50$  mL), the combined organic layers washed with brine (100 mL), dried ( $\text{MgSO}_4$ ) and the solvent removed *in vacuo* to give an orange solid. Column chromatography eluting with  $\text{EtOAc/hexane}$  (1:3  $\rightarrow$  1:1) afforded the title compound as colourless rods (2.96 g, 95%), mp 111-114 °C;  $R_f$  0.32 ( $\text{EtOAc/hexane}$  1:3);  $\delta_{\text{H}}$  (400 MHz,  $\text{CDCl}_3$ ) 7.76-7.69 (2H, m, Ar-H), 7.08-7.00 (2H, m, Ar-H), 6.63 (1H, s, thiazole-H), 5.08 (2H, br s,  $\text{NH}_2$ );  $m/z$  (CI) 197 (19%), 196 (32), 195 ( $\text{MH}^+$ , 100), 194 (20). Found  $\text{MH}^+$ , 195.0393.  $\text{C}_9\text{H}_8\text{N}_2\text{SF}$  requires 195.0392. Data is in agreement with the literature.<sup>253</sup>

### 5-Fluoro-4-(4-fluoro-phenyl)-thiazol-2-ylamine, **406**



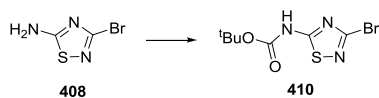
Selectfluor<sup>®</sup> (1-chloromethyl-4-fluoro-1,4-diazoniabicyclo[2.2.2]octane bis(tetrafluoro-borate, 401 mg, 1.13 mmol) was added in one portion to a stirred solution of aminothiazole **405** (200 mg, 1.03 mmol) in MeCN (5 mL) at 0 °C and the resulting orange solution allowed to warm to r.t. over 14 h. The reaction mixture was partitioned between EtOAc (20 mL) and H<sub>2</sub>O (10 mL), the aqueous layer extracted with EtOAc (20 mL), the combined organic layers dried (MgSO<sub>4</sub>) and the solvent removed *in vacuo*. Column chromatography eluting with EtOAc/hexane (1:3 → 2:3) afforded the title compound as off-white amorphous crystals (122 mg, 56%), mp 126-128 °C, R<sub>f</sub> 0.32 (EtOAc/hexane 1:3);  $\nu_{\max}$  (neat)/cm<sup>-1</sup> 3459, 3284, 3122, 1636, 1605, 1587, 1541, 1505;  $\delta_{\text{H}}$  (400 MHz, CDCl<sub>3</sub>) 7.76-7.70 (2H, m, Ar-H), 7.10-7.03 (2H, m, Ar-H), 4.99 (2H, br s, NH<sub>2</sub>);  $\delta_{\text{C}}$  (101 MHz, CDCl<sub>3</sub>) 162.0 (dd, *J* 248.6, 2.3), 155.3 (d, *J* 10.6), 147.8 (dd, *J* 297.0, 1.9), 129.0 (d, *J* 3.5), 128.7 (dd, *J* 8.0, 6.2), 128.4 (dd, *J* 5.7, 3.4) 115.5 (d, *J* 21.6);  $\delta_{\text{F}}$  (376 MHz, CDCl<sub>3</sub>) -113.7, -154.3; *m/z* (CI) 215 (13%), 214 (20), 213 (MH<sup>+</sup>, 100), 212 (13), 195 (8). Found MH<sup>+</sup>, 213.0306. C<sub>9</sub>H<sub>7</sub>N<sub>2</sub>SF<sub>2</sub> requires 213.0298.

### 3-Bromo-[1,2,4]thiadiazol-5-ylamine, **408**<sup>172</sup>



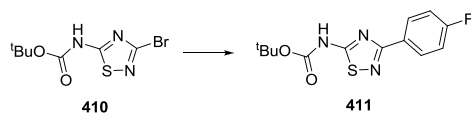
According to the method of Wehn,<sup>172</sup> a mixture of 3-bromo-5-chloro-[1,2,4]thiadiazole (2.00 g, 10.0 mmol) and ethanolic ammonia (2 M, 10.0 mL, 20.1 mmol) was heated in a sealed tube at 70 °C for 6 h, forming a white precipitate. After cooling to 0 °C, the reaction mixture was taken up in EtOAc (25 mL) and washed with H<sub>2</sub>O (25 mL) and brine (25 mL). The organic layer was dried (MgSO<sub>4</sub>) and the solvent removed *in vacuo* to give the title compound as a white solid (1.51 g, 84%), mp >250 °C;  $\delta_{\text{H}}$  (400 MHz, DMSO-*d*<sub>6</sub>) 8.48 (2H, br s, NH<sub>2</sub>); *m/z* (CI) 182 (MH<sup>+</sup>, 100%), 180 (MH<sup>+</sup>, 100), 119 (33), 52 (28). Found MH<sup>+</sup>, 179.9235. C<sub>2</sub>H<sub>3</sub>N<sub>3</sub>BrS requires 179.9231. Data is in agreement with the literature.<sup>172</sup>

### (3-Bromo-[1,2,4]thiadiazol-5-yl)-carbamic acid *tert*-butyl ester, **410**<sup>172</sup>



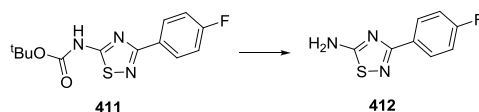
According to the method of Wehn,<sup>172</sup> a solution of amine **408** (1.50 g, 8.34 mmol), di-*tert*-butyl dicarbonate (2.55 g, 11.7 mmol) and DMAP (102 mg, 0.83 mmol) in THF (20 mL) was stirred at 70 °C for 40 h. The solvent was removed *in vacuo* and purification by column chromatography eluting with EtOAc/hexane (0:1 → 1:3) afforded the title compound as colourless amorphous crystals (2.15 g, 92%), mp 92-94 °C;  $\delta_{\text{H}}$  (400 MHz, CDCl<sub>3</sub>) 10.66 (1H, s, NH), 1.55 (9H, s, C(CH<sub>3</sub>)<sub>3</sub>);  $m/z$  (CI) 282 (MH<sup>+</sup>, 100%), 280 (MH<sup>+</sup>, 100), 219 (5), 217 (5). Found MH<sup>+</sup>, 279.9761. C<sub>7</sub>H<sub>11</sub>N<sub>3</sub>O<sub>2</sub>BrS requires 279.9755. Data is in agreement with the literature.<sup>172</sup>

### (3-(4-Fluoro-phenyl)-[1,2,4]thiadiazol-5-yl)-carbamic acid *tert*-butyl ester, **411**



According to the method of Wehn,<sup>172</sup> a mixture of bromide **410** (560 mg, 2.0 mmol), 4-fluorophenylboronic acid (364 mg, 2.6 mmol), CsF (638 mg, 4.2 mmol) and PdCl<sub>2</sub>[P<sup>t</sup>Bu<sub>2</sub>(*p*-NMe<sub>2</sub>-C<sub>6</sub>H<sub>4</sub>)<sub>2</sub>] (71 mg, 0.10 mmol) in degassed dioxane/H<sub>2</sub>O (6.6 mL, 10:1) was stirred at 80 °C for 24 h to give a red solution. The reaction mixture was diluted with EtOAc (100 mL), washed with H<sub>2</sub>O (2 × 20 mL) and brine (20 mL), the organic layer dried (MgSO<sub>4</sub>) and the solvent removed *in vacuo*. Column chromatography eluting with EtOAc/hexane (1:10 → 1:2) followed by trituration with hexane afforded the title compound as white amorphous crystals (465 mg, 79%), mp 161-164 °C;  $\nu_{\text{max}}$  (neat)/cm<sup>-1</sup> 3204, 2985, 1713, 1549, 1243, 1153, 1129;  $\delta_{\text{H}}$  (400 MHz, CDCl<sub>3</sub>) 11.01 (1H, s, NH), 8.17 (2H, dd, *J* 8.3, 5.6, Ar-H), 7.11 (2H, t, *J* 8.6, Ar-H), 1.26 (9H, s, C(CH<sub>3</sub>)<sub>3</sub>);  $\delta_{\text{C}}$  (101 MHz, CDCl<sub>3</sub>) 178.7, 166.8, 164.3 (d, *J* 250.4), 153.0, 130.3 (d, *J* 8.4), 129.18, 115.8 (d, *J* 21.5), 84.2, 27.9;  $m/z$  (ES) 297 (13%), 296 (MH<sup>+</sup>, 96), 281 (30), 240 (100). Found MH<sup>+</sup>, 296.0864. C<sub>13</sub>H<sub>15</sub>N<sub>3</sub>O<sub>2</sub>SF requires 296.0869.

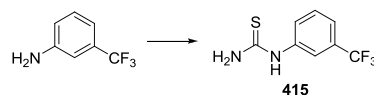
### 3-(4-Fluoro-phenyl)-[1,2,4]thiadiazol-5-ylamine, **412**



According to the method of Wehn,<sup>172</sup> a mixture of carbamate **411** (150 mg, 0.51 mmol), TFA (1.5 mL) and anisole (0.1 mL) in CH<sub>2</sub>Cl<sub>2</sub> (3 mL) was stirred at r.t. for 4.5 h. The solvent was

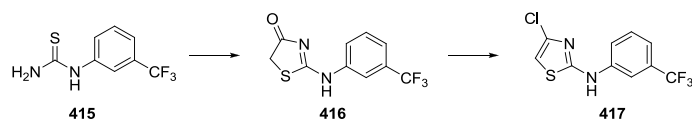
removed and the residue partitioned between sat. aq. NaHCO<sub>3</sub> (5 mL) and CH<sub>2</sub>Cl<sub>2</sub> (20 mL). The aqueous layer was extracted with CH<sub>2</sub>Cl<sub>2</sub> (2 × 20 mL), the combined organic layers dried (MgSO<sub>4</sub>) and the solvent removed *in vacuo*. Column chromatography eluting with EtOAc/hexane (1:3 → 1:1) afforded the title compound as a white amorphous solid (95 mg, 96%), mp 153-155 °C;  $\nu_{\max}$  (neat)/cm<sup>-1</sup> 3286, 3125, 1643, 1600, 1548, 1459;  $\delta_{\text{H}}$  (400 MHz, MeOD) 8.14-8.08 (2H, m, Ar-H), 7.17-7.10 (2H, m, Ar-H);  $\delta_{\text{C}}$  (101 MHz, MeOD) 185.9, 169.9, 165.4 (d, *J* 248.8), 131.2 (d, *J* 8.7), 131.1 (d, *J* 2.9), 116.4 (d, *J* 22.4);  $\delta_{\text{F}}$  (377 MHz, MeOD) -113.1; *m/z* (ES) 237 (47%), 198 (8), 197 (11), 196 (MH<sup>+</sup>, 100). Found MH<sup>+</sup>, 196.0340. C<sub>8</sub>H<sub>7</sub>N<sub>3</sub>SF requires 196.0345.

**(3-Trifluoromethyl-phenyl)-thiourea, 415**<sup>176</sup>



According to the method of Rasmussen,<sup>176</sup> benzoyl chloride (12.08 mL, 104 mmol) was added slowly to a solution of ammonium thiocyanate (9.14 g, 120 mmol) in acetone (90 mL). The reaction mixture was stirred at reflux for 15 min, before the heating was stopped to allow rapid addition of 3-trifluoromethylaniline (10.0 mL, 80.06 mmol) in acetone (10 mL). The reaction mixture was heated to reflux for a further 30 min before being cooled to r.t. and poured onto a large excess of ice with vigorous stirring to cause precipitation of a yellow solid, which was collected under vacuum. This crude benzoylthiourea was added in one portion to a stirred solution of 5% NaOH (160 mL) at 80 °C. The reaction mixture was stirred for 25 min before being cooled to r.t. and poured into ice-cold 1 M HCl (200 mL) to give a white precipitate. The pH was adjusted to *ca.* 9 with Na<sub>2</sub>CO<sub>3</sub> to remove benzoic acid, and the white solid filtered under vacuum to give the title compound as amorphous colourless crystals (17.46 g, 99%), mp 105-107 °C,  $\delta_{\text{H}}$  (400 MHz, DMSO-*d*<sub>6</sub>) 8.05-7.94 (1H, m, Ar 2-H), 7.68 (1H, d, *J* 8.0, Ar 4-H), 7.54 (1H, t, *J* 7.9, Ar 5-H), 7.43 (1H, d, *J* 7.8, Ar 6-H);  $\delta_{\text{F}}$  (377 MHz, DMSO-*d*<sub>6</sub>) -61.4; *m/z* (CI) 222 (23%), 221 (MH<sup>+</sup>, 100). Found MH<sup>+</sup>, 221.0355. C<sub>8</sub>H<sub>8</sub>N<sub>2</sub>SF<sub>3</sub> requires 221.0360. Data is in agreement with the literature.<sup>176</sup>

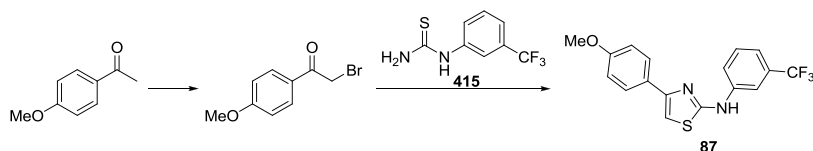
### (4-Chloro-thiazol-2-yl)-(3-trifluoromethyl-phenyl)-amine, **417**



According to the method of Mahboobi,<sup>177</sup> ethyl bromoacetate (2.31 mL, 20.8 mmol) was added to a stirred solution of thiourea **415** (3.52 g, 16.0 mmol) in EtOH (60 mL) at 50 °C. The reaction mixture was stirred for 18 h, before being cooled whereupon the solvent was removed *in vacuo*. Partial purification by column chromatography eluting with EtOAc/petrol (1:4 → 1:1) afforded the intermediate thiazolone **416** as an off-white solid (1.352 g), which was used directly in the subsequent chlorination.

A portion of thiazolone **416** (520 mg, 2.0 mmol) was added to a stirred solution of POCl<sub>3</sub> (1.12 mL, 12.0 mmol), dimethylaniline (250 μL, 2.0 mmol) and TBAB (1.61 g, 5.0 mmol) in MeCN (20 mL). The reaction mixture was stirred at reflux for 4 h, before being cooled and the solvent removed *in vacuo*. The residue was partitioned between EtOAc (20 mL) and H<sub>2</sub>O (20 mL), the aqueous layers extracted with EtOAc (3 × 20 mL), the combined organic layers dried (MgSO<sub>4</sub>) and the solvent removed *in vacuo*. Column chromatography eluting with EtOAc/petrol (1:5 → 1:3) afforded the title compound as off-white needles (208 mg, 12% over 2 steps), mp 140-143 °C; R<sub>f</sub> 0.51 (EtOAc/petrol 1:3); ν<sub>max</sub> (neat)/cm<sup>-1</sup> 1603, 1557, 1464, 1421; δ<sub>H</sub> (400 MHz, DMSO-d<sub>6</sub>) 8.03 (1H, s, Ar 2-H), 7.77 (1H, d, *J* 8.1, Ar 4-H), 7.55 (1H, t, *J* 8.0, Ar 5-H), 7.30 (1H, d, *J* 7.6, Ar 6-H), 6.94 (1H, s, thiazole-H); δ<sub>C</sub> (101 MHz, DMSO-d<sub>6</sub>) 162.7, 141.0, 132.9, 130.3, 129.8 (q, *J* 31.5), 124.2 (q, *J* 272.2), 120.6, 118.0, 112.9, 103.2; δ<sub>F</sub> (377 MHz, DMSO-d<sub>6</sub>) -61.40; *m/z* (CI) 280 (50%), 279 (MH<sup>+</sup>, 100). Found MH<sup>+</sup>, 278.9966. C<sub>10</sub>H<sub>7</sub>N<sub>2</sub>SClF<sub>3</sub> requires 278.9971.

### [4-(4-Methoxy-phenyl)-thiazol-2-yl]-(3-trifluoromethyl-phenyl)-amine, **87**

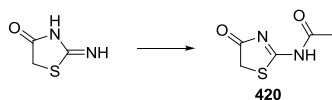


Bromine (0.68 mL, 13.3 mmol) was added dropwise to a solution of 4-methoxyacetophenone (2.00 g, 13.3 mmol) in Et<sub>2</sub>O (20 mL). The resulting suspension was stirred at r.t. for 16 h before being poured into 30 mL sat. aq. NaHCO<sub>3</sub>. The organic layer was washed with sat. aq. NaHCO<sub>3</sub> (30 mL) and H<sub>2</sub>O (30 mL), dried (MgSO<sub>4</sub>) and the solvent removed *in vacuo* to give the crude bromide intermediate as a white solid. This was added to a solution of thiourea **415**



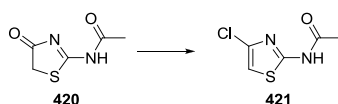
(2.93 g, 13.3 mmol) in EtOH (30 mL) and the reaction mixture stirred at reflux for 2.5 h. The solvent was removed *in vacuo* and the residue recrystallised from EtOH to give the title compound as yellow needles (2.90 g, 63% over 2 steps), mp 171-172 °C;  $\nu_{\max}$  (neat)/cm<sup>-1</sup> 1611, 1583, 1565, 1532, 1511;  $\delta_{\text{H}}$  (400 MHz, DMSO-d<sub>6</sub>) 8.40 (1H, s, Ar 2-H), 7.90-7.83 (3H, m, Ar 4-H, 3'-H, 5'-H), 7.57 (1H, t, *J* 8.0, Ar 5-H), 7.29 (1H, d, *J* 7.7, Ar 6-H), 7.26 (1H, s, thiazole-H), 7.00 (2H, d, *J* 8.8, Ar 2'-H, 6'-H), 3.79 (3H, s, CH<sub>3</sub>);  $\delta_{\text{C}}$  (101 MHz, DMSO-d<sub>6</sub>) 162.8, 159.4, 150.1, 142.2, 130.6, 130.1 (q, *J* 31.7), 127.6, 127.4, 124.8 (q, *J* 271.4) 117.6, 114.5, 114.3, 113.1, 102.2, 55.6;  $\delta_{\text{F}}$  (377 MHz, DMSO-d<sub>6</sub>) -61.41; *m/z* (CI) 353 (20%), 352 (50), 351 (MH<sup>+</sup>, 100), 350 (17). Found MH<sup>+</sup>, 351.0772. C<sub>17</sub>H<sub>14</sub>N<sub>2</sub>OSF<sub>3</sub> requires 351.0779.

***N*-(4-Oxo-4,5-dihydro-thiazol-2-yl)-acetamide, 420**<sup>254</sup>

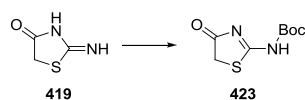


According to the method of Novartis,<sup>188</sup> a stirred suspension of pseudothiohydantoin (3.89 g, 33.5 mmol) in Ac<sub>2</sub>O (4.11 mL, 43.5 mmol) and pyridine (35 mL) was heated to reflux for 1.5 h, cooled to r.t. and filtered, washing with Et<sub>2</sub>O, to give the title compound as light brown needles (3.48 g, 66%), mp > 250 °C;  $\delta_{\text{H}}$  (400 MHz, DMSO-d<sub>6</sub>) 3.83 (2H, s, CH<sub>2</sub>) 2.17 (3H, s, CH<sub>3</sub>); *m/z* (CI) 176 (68%), 159 (MH<sup>+</sup>, 100). Found MH<sup>+</sup>, 159.0230. C<sub>5</sub>H<sub>7</sub>N<sub>2</sub>O<sub>2</sub>S requires 159.0228. Data is in agreement with the literature.<sup>254</sup>

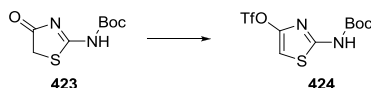
***N*-(4-Chloro-thiazol-2-yl)-acetamide, 421**<sup>188</sup>



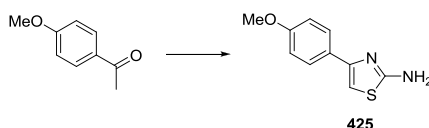
According to the method of Novartis,<sup>188</sup> a suspension of acetamide **420** (1.74 g, 11.0 mmol) in POCl<sub>3</sub> (20 mL) was heated to reflux for 20 min before being cooled to r.t. whereupon the reaction mixture was poured carefully onto ice/H<sub>2</sub>O, washing with EtOH. The resulting solution was neutralised with solid Na<sub>2</sub>CO<sub>3</sub> and extracted with EtOAc (3 × 20 mL). The combined organic layers were dried (MgSO<sub>4</sub>) and the solvent removed *in vacuo* to give the title compound as an orange amorphous solid (1.82 g, 94%), mp 149-151 °C;  $\delta_{\text{H}}$  (400 MHz, CDCl<sub>3</sub>) 6.72 (1H, s, thiazole-H), 2.32 (3H, s, CH<sub>3</sub>);  $\delta_{\text{C}}$  (101 MHz, CDCl<sub>3</sub>) 169.1, 159.7, 134.2, 107.9, 23.6; *m/z* (CI) 196 (22%), 194 (43), 179 (55), 177 (MH<sup>+</sup>, 100). Found MH<sup>+</sup>, 176.9888. C<sub>5</sub>H<sub>6</sub>N<sub>2</sub>OCl requires 250.0457. Data is in agreement with the literature.<sup>188</sup>

**(4-Oxo-4,5-dihydro-thiazol-2-yl)-carbamic acid *tert*-butyl ester, 423**<sup>189</sup>

According to the method of Reiter,<sup>189</sup> a stirred suspension of pseudothiohydantoin (5.82 g, 50.0 mmol) and di-*tert*-butyl dicarbonate (21.8 g, 100 mmol) in THF (200 mL) was heated at 65 °C for 60 h, before being allowed to cool to r.t. and filtered. The solvent was removed *in vacuo* to give a white powder, which was suspended in hexane and filtered to give the title compound as a white powder (4.85 g, 45%), mp >250 °C;  $\delta_{\text{H}}$  (400 MHz, CDCl<sub>3</sub>) 3.75 (2H, s, CH<sub>2</sub>), 1.53 (9H, s, C(CH<sub>3</sub>)<sub>3</sub>);  $\delta_{\text{C}}$  (101 MHz, CDCl<sub>3</sub>) 183.7, 182.9, 153.8, 84.6, 36.5, 28.1;  $m/z$  (CI) 217 (MH<sup>+</sup>, 100%), 134 (53), 117 (66). Found MH<sup>+</sup>, 217.0655. C<sub>8</sub>H<sub>13</sub>N<sub>2</sub>O<sub>3</sub>S requires 217.0647.

**Trifluoro-methanesulfonic acid 2-*tert*-butoxycarbonylamino-thiazol-4-yl ester, 424**<sup>189</sup>

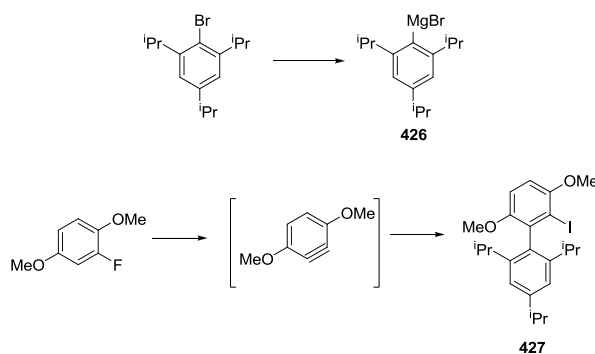
According to the method of Reiter,<sup>189</sup> to a stirred solution of thiazolone **423** (1.08 g, 5.00 mmol) and 2,6-lutidine (1.75 mL, 15.0 mmol) in CH<sub>2</sub>Cl<sub>2</sub> (50 mL) at 0 °C was added dropwise Tf<sub>2</sub>O (1.68 mL, 10.0 mmol). The reaction mixture stirred at this temperature for 1 h before being poured into sat. aq. NH<sub>4</sub>Cl (100 mL). The organic layer was washed with sat. aq. NaHCO<sub>3</sub> (100 mL), dried (MgSO<sub>4</sub>) and the solvent removed *in vacuo* to give a red oil. Column chromatography eluting with EtOAc/hexane (0:1 → 1:4) afforded the title compound as amorphous crystals (1.65 g, 95%), mp 94-96 °C, R<sub>f</sub> 0.60 (EtOAc/hexane 1:3);  $\delta_{\text{H}}$  (400 MHz, CDCl<sub>3</sub>) 8.81 (1H, s, NH), 6.60 (1H, s, thiazole-H), 1.52 (9H, s, C(CH<sub>3</sub>)<sub>3</sub>);  $\delta_{\text{C}}$  (101 MHz, CDCl<sub>3</sub>) 159.2, 152.4, 146.7, 118.8 (q,  $J$  321), 99.3, 83.9, 28.2;  $\delta_{\text{F}}$  (377 MHz, CDCl<sub>3</sub>) -72.6;  $m/z$  (CI) 367 (28%), 366 (MNH<sub>4</sub><sup>+</sup>, 100), 349 (MH<sup>+</sup>, 39), 310 (43). Found MH<sup>+</sup>, 349.0144. C<sub>9</sub>H<sub>12</sub>N<sub>2</sub>O<sub>5</sub>S<sub>2</sub>F<sub>3</sub> requires 349.0140.

**4-(4-Methoxy-phenyl)-thiazol-2-ylamine, 425**<sup>255</sup>

To a stirred solution of 4-methoxyacetophenone (10.0 g, 66.6 mmol) in Et<sub>2</sub>O (100 mL) was added slowly bromine (3.41 mL, 66.6 mmol), and the reaction mixture stirred at r.t. for 20 h. Further bromine (1.70 mL, 33.3 mmol) was added and the reaction stirred for an additional 1

h before being poured into sat. aq. NaHCO<sub>3</sub> (150 mL). The organic layer was washed with sat. aq. NaHCO<sub>3</sub> (100 mL) and H<sub>2</sub>O (100 mL), dried (MgSO<sub>4</sub>) and the solvent removed *in vacuo* to give a white solid, which was dissolved in EtOH (250 mL). To this solution was added thiourea (10.14 g, 133 mmol), and the mixture was heated to reflux for 2 h. The solvent was removed and the residue taken up in EtOAc (300 mL), which was washed with H<sub>2</sub>O (2 × 100 mL) and brine (100 mL). The organic layer was dried (MgSO<sub>4</sub>), the solvent removed *in vacuo* and the residue recrystallised from EtOAc to give the title compound as yellow rods (6.51 g, 47% over 2 steps), mp 217-219 °C; δ<sub>H</sub> (400 MHz, DMSO-*d*<sub>6</sub>) 7.74-7.70 (2H, m, Ar-H), 7.01 (2H, s, NH<sub>2</sub>), 6.94-6.89 (2H, m, Ar-H), 6.80 (1H, s, thiazole-H), 3.76 (3H, s, CH<sub>3</sub>); δ<sub>C</sub> (101 MHz, DMSO-*d*<sub>6</sub>) 168.1, 158.5, 149.7, 127.9, 126.8, 113.8, 99.3, 55.1; *m/z* (CI) 209 (10%), 208 (22), 207 (MH<sup>+</sup>, 100). Found MH<sup>+</sup>, 207.0591. C<sub>10</sub>H<sub>11</sub>N<sub>2</sub>OS requires 207.0592. Data is in agreement with the literature.<sup>255</sup>

### 2-Iodo-2',4',6'-triisopropyl-3,6-dimethoxy-biphenyl, **427**<sup>192</sup>

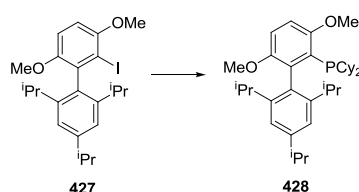


According to the method of Fors,<sup>192</sup> to a stirred suspension of Mg turnings (746 mg, 30.7 mmol) in THF (60 mL) was added 2-bromo-1,3,5-triisopropylbenzene (6.14 mL, 25.6 mmol). The reaction mixture was heated to reflux and 1,2-dibromoethane (20 μL, 0.2 μmol) was added. The reaction mixture was stirred at reflux for 1 h before being cooled to r.t. to give a solution of Grignard reagent **426**.

<sup>n</sup>BuLi (2.5 M in hexanes, 10.2 mL, 25.6 mmol) was added dropwise to a stirred solution of 1,4-dimethoxy-2-fluorobenzene (3.41 mL, 25.6 mmol) in THF (150 mL) at -78 °C. The reaction was stirred for 30 min at this temperature, before Grignard reagent **426** was introduced dropwise by cannula. The reaction mixture was stirred for a further 1 h at -78 °C and then for 1.5 h at r.t. before being cooled to 0 °C. A solution of iodine (7.79 g, 30.7 mmol) in THF (30 mL) was added dropwise, and the resulting dark red solution was stirred at r.t. for 1 h. The solvent was removed *in vacuo* and the residue partitioned between CH<sub>2</sub>Cl<sub>2</sub> (100 mL) and sat. aq. Na<sub>2</sub>SO<sub>3</sub> (100 mL). The aqueous layer was extracted with CH<sub>2</sub>Cl<sub>2</sub> (50 mL), and the

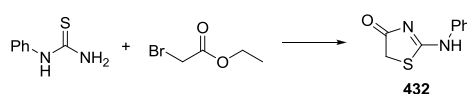
combined organic layers washed with brine (100 mL), dried (MgSO<sub>4</sub>) and the solvent removed *in vacuo* to give a light brown solid. Recrystallisation from EtOAc gave the title compound as white plates (3.03 g, 25%), mp 206.5-208 °C;  $\delta_{\text{H}}$  (400 MHz, CDCl<sub>3</sub>) 7.02 (2H, s, Ar-H), 6.87 (1H, d, *J* 8.9, Ar-H), 6.79 (1H, d, *J* 8.9, Ar-H), 3.87 (3H, s, OCH<sub>3</sub>), 3.64 (3H, s, OCH<sub>3</sub>), 2.93 (1H, hept, *J* 6.9, CH(CH<sub>3</sub>)<sub>2</sub>), 2.34 (2H, hept, *J* 6.9, 2 × CH(CH<sub>3</sub>)<sub>2</sub>), 1.29 (6H, d, *J* 6.9, CH(CH<sub>3</sub>)<sub>2</sub>), 1.16 (6H, d, *J* 6.9, CH(CH<sub>3</sub>)<sub>2</sub>), 0.98 (6H, d, *J* 6.9, CH(CH<sub>3</sub>)<sub>2</sub>); *m/z* (CI) 485 (45%), 484 (MNH<sub>4</sub><sup>+</sup>, 100), 437 (23), 436 (82). Found MNH<sub>4</sub><sup>+</sup>, 484.1723. C<sub>23</sub>H<sub>35</sub>NO<sub>2</sub>I requires 484.1713. Data is in agreement with the literature.<sup>192</sup>

### Dicyclohexyl-(2',4',6'-triisopropyl-3,6-dimethoxy-biphenyl-2-yl)-phosphane, **428**<sup>192</sup>



According to the method of Fors,<sup>192</sup> to a stirred solution of biphenyl iodide **427** (1.00 g, 2.15 mmol) in THF (10 mL) at -78 °C was added <sup>n</sup>BuLi (2.5 M in hexane, 944  $\mu$ L, 2.36 mmol) dropwise over 10 min. The reaction mixture was stirred at -78 °C for 30 min before chlorodicyclohexylphosphine (499  $\mu$ L, 2.26 mmol) was added dropwise over 10 min. The reaction mixture was stirred for a further 1 h at -78 °C and for 1.5 h at r.t. before being filtered through a plug of Celite<sup>®</sup> layered over a plug of silica, washing with EtOAc. The solvent was removed *in vacuo* and the resulting white solid recrystallised from acetone to give the title compound as white amorphous crystals (914 mg, 79%), mp 188-190 °C;  $\delta_{\text{H}}$  (400 MHz, CDCl<sub>3</sub>) 6.94 (2H, s, Ar-H), 6.83 (1H, d, *J* 8.9, Ar-H), 6.76 (1H, d, *J* 8.9, Ar-H), 3.80 (3H, s, OCH<sub>3</sub>), 3.54 (3H, s, OCH<sub>3</sub>), 2.91 (1H, hept, *J* 6.9, CH(CH<sub>3</sub>)<sub>2</sub>), 2.40 (2H, hept, *J* 6.9, 2 × CH(CH<sub>3</sub>)<sub>2</sub>), 2.23-2.12 (2H, m, 2 × PCH), 1.84-1.75 (2H, m, Cy-H), 1.72-1.55 (6H, m, Cy-H), 1.42-0.87 (12H, m, Cy-H), 1.29 (6H, d, *J* 6.9, CH(CH<sub>3</sub>)<sub>2</sub>), 1.18 (6H, d, *J* 6.9, CH(CH<sub>3</sub>)<sub>2</sub>), 0.91 (6H, d, *J* 6.9, CH(CH<sub>3</sub>)<sub>2</sub>); *m/z* (ES) 553 (3%), 539 (8), 538 (32), 537 (MH<sup>+</sup>, 100). Found MH<sup>+</sup>, 537.3854. C<sub>35</sub>H<sub>54</sub>O<sub>2</sub>P requires 537.3861. Data is in agreement with the literature.<sup>192</sup>

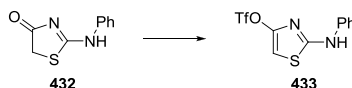
### 2-Phenylamino-thiazol-4-one, **432**<sup>256</sup>



A mixture of phenylthiourea (80%, 7.42 g, 39.0 mmol) and ethyl bromoacetate (4.33 mL, 39.0 mmol) in EtOH (120 mL) was stirred at 50 °C for 1 h to give an orange solution. Upon

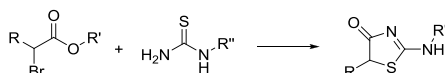
cooling, the solvent was removed *in vacuo* and the residue partitioned between CH<sub>2</sub>Cl<sub>2</sub> (200 mL) and sat. aq. NaHCO<sub>3</sub> (100 mL). The aqueous layer was extracted with CH<sub>2</sub>Cl<sub>2</sub> (100 mL), the combined organic layers dried (MgSO<sub>4</sub>) and the solvent removed *in vacuo* to give an orange solid. Column chromatography eluting with EtOAc/hexane (1:2 → 1:0) afforded the title compound as pale orange plates (5.93 g, 79%), mp 186-188 °C; R<sub>f</sub> 0.4 (EtOAc/hexane 1:1); δ<sub>H</sub> (400 MHz, DMSO-*d*<sub>6</sub>) (mixture of tautomers) 11.74 (0.5H, s, NH), 11.16 (0.5H, s, NH), 7.70 (1H, d, *J* 7.2, Ar-H), 7.37 (2H, d, *J* 6.4, Ar-H), 7.15 (1H, t, *J* 7.2, Ar-H), 7.00 (1H, d, *J* 6.4, Ar-H), 4.01 (1H, s, CHH), 3.96 (1H, s, CHH); *m/z* (CI) 210 (24%), 194 (25), 193 (MH<sup>+</sup>, 100), 102 (43), 85 (30). Found MH<sup>+</sup>, 193.0435. C<sub>9</sub>H<sub>9</sub>N<sub>2</sub>OS requires 193.0436. Data is in agreement with the literature.<sup>256</sup>

### Trifluoro-methanesulfonic acid 2-phenylamino-thiazol-4-yl ester, **433**



To a stirred solution of aminothiazolone **432** (1.92 g, 10.0 mmol) and Et<sub>3</sub>N (4.18 mL, 30.0 mmol) in CH<sub>2</sub>Cl<sub>2</sub> (150 mL) at 0 °C was added dropwise Tf<sub>2</sub>O (2.52 mL, 15.0 mmol). The reaction mixture was stirred for 30 min before dropwise addition of further Tf<sub>2</sub>O (0.84 mL, 5.0 mmol) and stirring for an additional 30 min. The reaction mixture was then poured into sat. aq. NH<sub>4</sub>Cl (100 mL), the organic layer was washed with sat. aq. NaHCO<sub>3</sub> (100 mL), dried (MgSO<sub>4</sub>) and the solvent removed *in vacuo* to give a red oil. Column chromatography eluting with EtOAc/hexane (1:10 → 1:4) afforded the title compound as off-white cubes (2.62 g, 85%), mp 58-61 °C, R<sub>f</sub> 0.54 (EtOAc/hexane 1:3); ν<sub>max</sub> (neat)/cm<sup>-1</sup> 1603, 1530, 1495, 1210, 1134; δ<sub>H</sub> (400 MHz, CDCl<sub>3</sub>) 7.96 (1H, s, NH), 7.38 (2H, t, *J* 7.7, Ar-H), 7.31 (2H, d, *J* 7.7, Ar-H), 7.15 (1H, t, *J* 7.2, Ar-H), 6.29 (1H, s, thiazole-H); δ<sub>C</sub> (101 MHz, CDCl<sub>3</sub>) 164.0, 146.8, 139.0, 129.9, 124.9, 119.8, 118.8 (q, *J* 321.2), 93.1; δ<sub>F</sub> (377 MHz, CDCl<sub>3</sub>) -72.6; *m/z* (ES) 367 (28%), 366 (12), 326 (14), 325 (MH<sup>+</sup>, 100), 245 (38). Found MH<sup>+</sup>, 324.9930. C<sub>10</sub>H<sub>8</sub>N<sub>2</sub>O<sub>3</sub>S<sub>2</sub>F<sub>3</sub> requires 324.9928.

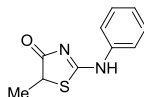
### General procedure for aminothiazolone synthesis



To a stirred suspension of the 1-substituted thiourea (1.0 eq.) and NaOAc (1.5 eq.) in EtOH (*ca.* 0.3 M) was added the bromoacetate (1.05 eq.) and the reaction mixture heated at reflux until completion (1-5 h). The solvent was removed *in vacuo*, the residue dissolved in EtOAc,

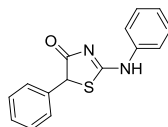
the organic layer washed with sat. aq. NaHCO<sub>3</sub>, dried (MgSO<sub>4</sub>) and the solvent removed *in vacuo*. The crude product was purified by column chromatography or recrystallisation.

### 5-Methyl-2-phenylamino-thiazol-4-one, 437<sup>256</sup>



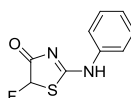
According to the general procedure, a suspension of phenylthiourea (2.00 g, 80% grade, 10.5 mmol), methyl 2-bromopropionate (1.23 mL, 11.1 mmol) and NaOAc (1.30 g, 15.8 mmol) in EtOH (30 mL) was heated at reflux for 4 h. Column chromatography eluting with EtOAc/hexane (1:2 → 1:1) gave the title compound as a white powder (1.91 g, 88%), mp 137-139 °C,  $\delta_{\text{H}}$  (400 MHz, CDCl<sub>3</sub>) 11.84 (1H, br s, NH), 7.35 (2H, t, *J* 7.7, Ar-H), 7.29 (2H, d, *J* 7.4, Ar-H), 7.19 (1H, t, *J* 7.2, Ar-H), 4.08 (1H, q, *J* 7.3, CHCH<sub>3</sub>), 1.59 (3H, d, *J* 7.3, CH<sub>3</sub>);  $\delta_{\text{C}}$  (101 MHz, CDCl<sub>3</sub>) 183.0, 169.6, 141.8, 129.4, 126.3, 122.8, 46.5, 19.0; *m/z* (ES) 270 (19%), 248 (4), 224 (2), 207 (MH<sup>+</sup>, 100). Found MH<sup>+</sup>, 207.0588. C<sub>10</sub>H<sub>11</sub>N<sub>2</sub>OS requires 207.0590. Data is in agreement with the literature.<sup>192</sup>

### 5-Phenyl-2-phenylamino-thiazol-4-one, 438<sup>256</sup>



According to the general procedure, a suspension of phenylthiourea (2.00 g, 80% grade, 10.5 mmol), 2-bromo phenylacetic acid (2.38 g, 11.1 mmol) and NaOAc (1.30 g, 15.8 mmol) in EtOH (150 mL) was heated at reflux for 2.5 h. Recrystallisation (EtOAc) gave the title compound as colourless plates (2.39 g, 85%), mp 192-193 °C,  $\delta_{\text{H}}$  (400 MHz, CDCl<sub>3</sub>) 11.59 (1H, br s, NH), 7.76 (1H, d, *J* 8.0, Ar-H), 7.45-7.30 (7H, m, Ar-H), 7.18 (1H, q, *J* 7.6, Ar-H), 7.09 (1H, d, *J* 7.7, Ar-H), 5.56 (1H, s, SCH). *m/z* (ES) 332 (22%), 270 (15), 269 (MH<sup>+</sup>, 100), 224 (12), 196 (10). Found MH<sup>+</sup>, 269.0753. C<sub>15</sub>H<sub>13</sub>N<sub>2</sub>OS requires 269.0749. Data is in agreement with the literature.<sup>192</sup>

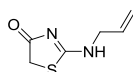
### 5-Fluoro-2-phenylamino-thiazol-4-one, 439



According to the general procedure, a suspension of phenylthiourea (2.00 g, 80% grade, 10.5 mmol), ethyl bromofluoroacetate (1.31 mL, 11.1 mmol) and NaOAc (1.30 g, 15.8 mmol) in

EtOH (30 mL) was heated at reflux for 3 h, before addition of further ethyl bromofluoroacetate (0.31 mL, 0.24 mmol) and heating for an additional 1 h. Column chromatography eluting with EtOAc/hexane (0:1 → 2:1) followed by recrystallisation (EtOAc) gave the title compound as a pale orange powder (1.15 g, 52%), mp 163-164 °C;  $\nu_{\max}$  (neat)/cm<sup>-1</sup> 3277, 3213, 2994, 1698, 1633, 1570, 1490, 1448;  $\delta_{\text{H}}$  (400 MHz, DMSO-d<sub>6</sub>) (mixture of tautomers) 11.95 (1H, br s, NH), 7.70 (1H, d, *J* 7.9, Ar-H), 7.43 and 7.40 (1H, 2 × t, *J* 7.8, Ar-H), 7.26-7.18 (1H, m, Ar-H), 7.01 (1H, d, *J* 7.7, Ar-H), 6.73 and 6.70 (1H, 2 × d, *J* 56.6, CHF).  $\delta_{\text{C}}$  (101 MHz, DMSO-d<sub>6</sub>) (mixture of tautomers) 183.6, 183.4, 174.2, 138.0, 129.5, 129.2, 125.8, 125.5, 121.5, 121.1, 96.7 (d, *J* 222), 93.5 (d, *J* 222).  $\delta_{\text{F}}$  (377 MHz, DMSO-d<sub>6</sub>) (mixture of tautomers) -157.6 (br s), -160.2 (d, *J* 56.6); *m/z* (ES) 252 (32%), 224 (4), 211 (MH<sup>+</sup>, 100), 196 (8). Found MH<sup>+</sup>, 211.0351. C<sub>9</sub>H<sub>8</sub>N<sub>2</sub>OFS requires 211.0341.

## 2-Allylamino-thiazol-4-one, 440



According to the general procedure, a suspension of 1-allyl-2-thiourea (500 mg, 4.30 mmol), ethyl bromoacetate (0.50 mL, 4.52 mmol) and NaOAc (529 mg, 6.45 mmol) in EtOH (12 mL) was heated at reflux for 1 h. Column chromatography eluting with EtOAc/hexane (1:2 → 1:1) gave the title compound as a colourless oil (405 mg, 60%),  $\nu_{\max}$  (neat)/cm<sup>-1</sup> 3290, 1713, 1607, 1422, 1384, 1335;  $\delta_{\text{H}}$  (400 MHz, CDCl<sub>3</sub>) 7.82 (1H, br s, NH), 5.77 (1H, ddd, *J* 22.6, 10.7, 5.6, NHCH<sub>2</sub>CH), 5.19-5.09 (2H, m, C=CH<sub>2</sub>), 4.28 (2H, d, *J* 5.7, NHCH<sub>2</sub>), 3.84 (2H, s, SCH<sub>2</sub>);  $\delta_{\text{C}}$  (101 MHz, CDCl<sub>3</sub>) 171.3, 160.0, 130.7, 118.0, 44.1, 34.0; *m/z* (ES) 159 (5%), 158 (8), 157 (MH<sup>+</sup>, 100). Found MH<sup>+</sup>, 157.0430. C<sub>6</sub>H<sub>9</sub>N<sub>2</sub>OS requires 157.0436.

## 13 Biochemistry – Materials and Methods

### Recombinant DNA Techniques

#### *Transformation of Bacterial Cells (Electroporation)*

Plasmid DNA (1 µg) was added to competent *E. coli* DH5α or BL21 cells and the mixture electroporated at 2.2 kV using a BioRad Gene Pulser. Following addition of LB (1 mL), the resulting suspension was centrifuged (13 krpm) and 800 µL of the supernatant removed. Following resuspension of the pellet, the mixture was spread onto antibiotic-supplemented agar plates and incubated at 37 °C for 14-24 h.

#### *Enzymatic Digestion of DNA*

A mixture of DNA (0.5 µg), the chosen restriction enzymes (total of 1 µL) and the appropriate 10 × restriction buffer (1 µL) was made up to 10 µL using sterile water and incubated at 37 °C for 30 min. For larger volume digests, the quantity of restriction enzyme and subsequent incubation time was proportionately increased. For mini-prep DNA digests, 5 µL DNA was used along with loading buffer supplemented with RNase A (10 µg/mL).

#### *Agarose Gel Electrophoresis*

A suspension of 1% (w/v) agarose in TAE buffer was heated to solution, and upon partial cooling ethidium bromide (1 µg/mL) was added before the gel was allowed to set. The samples were added in 5 × TAE loading buffer and electrophoresed at 80 mA for 45-60 min. Visualisation was performed using UV-C for non-preparative samples or UV-A for preparative samples.

#### *Gene Clean DNA Purification*

The excised agarose gel bands were incubated with an approximately equal volume of 6 M NaI at 65 °C for 5 min. The resulting solution was mixed with glass-milk beads (5 µL) on ice for 5 min prior to brief centrifugation (13 krpm, 1 s). The pellet was washed with gene clean solution (3 × 500 µL) and resuspended in water (20 µL). Further incubation at 65 °C for 2 min was followed by a final centrifugation as before to give the desired DNA solution.



### *Jetsorb Purification*

The excised agarose gel bands were incubated with Jetsorb Buffer 1 (300  $\mu$ L) and Jetsorb beads (10  $\mu$ L) at 65 °C for 15 min. The resulting suspension was briefly centrifuged at (13 krpm, 1 s) and the pellet washed with Jetsorb Buffer 1 (300  $\mu$ L), Jetsorb Buffer 2 (2  $\times$  300  $\mu$ L) and resuspended in water (20  $\mu$ L). Further incubation at 65 °C for 5 min was followed by a final centrifugation as before to give the desired DNA solution.

### *DNA Ligation*

A mixture of purified DNA (16  $\mu$ L), the chosen DNA ligase (1  $\mu$ L) and the appropriate 10  $\times$  ligation buffer (2  $\mu$ L) was made up to 20  $\mu$ L using sterile water and incubated at 37 °C for a minimum of 3 h, prior to gene clean purification.

### *PCR Reaction*

A mixture of the DNA template (1  $\mu$ L), the 5'- and 3'-primers (each 1  $\mu$ L), the mutation-bearing oligonucleotide (1  $\mu$ L) and standard PCR components (see Section 15.1) was made up to 50  $\mu$ L with sterile water. PCR was run under conditions dictated by the properties of the oligonucleotides used (typical conditions: 15 s, 98 °C; 15 s, 52 °C; 25 cycles), and the resulting mixtures were separated by agarose gel electrophoresis.

### *DNA Sequencing*

DNA sequencing was performed commercially by Cogenics.

## **Preparation of Plasmid DNA**

### *Small Scale Preparation of Plasmid DNA (Mini-Prep)*

A single colony was removed from the culture plate and added to antibiotic-supplemented LB (2 mL) before incubation at 37 °C for 8-12 h in a shaker. A portion (1.5 mL) was centrifuged at 13 krpm for 20 s and the resulting pellet resuspended in Solution I (100  $\mu$ L). The cells were then lysed by addition of Solution II (200  $\mu$ L) and the mixture neutralised by addition of Solution III (150  $\mu$ L). Following centrifugation at 13 krpm for 5 min, the DNA was precipitated from the supernatant using NaOAc, pH 5.2 (50  $\mu$ L) and ethanol (1 mL).

Following centrifugation at 13 krpm for 5 min, the resultant pellet was suspended in sterile water (50  $\mu$ L).

#### *Large Scale Preparation of Plasmid DNA (Maxi-Prep)*

The 2 mL culture obtained in the above procedure following incubation was added to antibiotic-supplemented LB (200 mL) and further incubated at 37 °C for 16 h in a shaker. Centrifugation of the resulting suspension at 5 krpm for 5 min at 4 °C was followed by resuspension in Solution I (100  $\mu$ L). Subsequent addition of Solution II (200  $\mu$ L) and Solution III (150  $\mu$ L) as above was followed by further centrifugation at 9 krpm for 5 min at 4 °C. Addition of <sup>1</sup>PrOH (45 mL) was followed by further centrifugation (9 krpm, 5 min, 4 °C) and the resulting DNA pellet was resuspended in sterile water (3 mL) and ice-cold 5 M LiCl (4 mL). Following incubation on ice for 5 min, centrifugation at 13 krpm for 5 min removed any contaminating RNA. Addition of cold ethanol (14 mL) to the supernatant again precipitated the DNA and, following centrifugation at 13 krpm for 5 min at 4 °C, the pellet was resuspended in sterile water (600  $\mu$ L). Incubation of this solution with RNase A (10  $\mu$ L) at 37 °C for 15 min destroyed any remaining RNA, and contaminating protein was denatured by the addition of 1:1 (v/v) phenol/chloroform. Following centrifugation at 13 krpm for 5 min, the aqueous layer from this mixture was removed and further extracted with chloroform to remove any remaining phenol. Finally, addition of 3 M NaOAc, pH 5.2 (50  $\mu$ L) and ethanol (1 mL) precipitated the purified DNA, and following centrifugation at 13 krpm for 5 min, the pellet was resuspended in an appropriate quantity of sterile water to give a concentration of *ca.* 1  $\mu$ g/ $\mu$ L, as determined by UV absorbance (260 nm).

### **Protein Analysis**

#### *SDS-Polyacrylamide Gel Electrophoresis*

10% SDS-PAGE gels were prepared using standard techniques (see Section 15.1 for gel constituents), and the protein samples loaded in SDS loading buffer. Electrophoresis was performed using SDS running buffer at 200V for *ca.* 1 h. Visualisation of the protein bands was performed by incubation with either Coomassie blue staining solution for *ca.* 1-2 h, (before being incubated in destaining solution overnight) or Instant Blue<sup>TM</sup> staining solution for 10-20 min.

## **Protein Purification**

### *Purification via GST-Tag Chelation*

Antibiotic-supplemented LB (100-3000 mL) was added to a small culture (10-100 mL, prepared as above) and the suspension incubated at 37 °C for 1 h in a shaker. Addition of 1 M IPTG (0.1% total volume) induced protein expression, and the culture was incubated at 18 or 37 °C for 4-16 h in a shaker. Centrifugation of the culture at 5 krpm for 5 min at 4 °C was followed by resuspension of the cell pellet in NETN (10 mL). Sonication of this suspension to lyse the cells (18W, 2 × 30 s, 0 °C) was followed by centrifugation at 9 krpm for 5 min at 4 °C. The supernatant was added to glutathione-sepharose beads (250 µL, pre-equilibrated by washing with NETN) and the resulting suspension mixed by inversion for 1 h at 4 °C. Centrifugation at 2 krpm for 1 min at 4 °C gave the pellet of beads, which was washed with NETN (3 × 10 mL) and resuspended (NETN, 1 mL) prior to a final centrifugation at 13 krpm, for 1 s. The volume of NETN was reduced to approximately 150 µL and an equal volume of 80% glycerol was added. The resulting mixture was kept on ice for 30 min, with frequent mixing by inversion, before storage at -20 °C.

### *Purification via 2-stage Chromatography*

Antibiotic-supplemented LB (100-3000 mL) was added to a small culture (10-100 mL, prepared as above) and the suspension incubated at 37 °C for 1 h in a shaker. Addition of 1 M IPTG (0.1% total volume) induced protein expression, and the culture was incubated at 18 or 37 °C for 4-16 h in a shaker. Centrifugation of the culture at 5 krpm for 5 min at 4 °C was followed by resuspension of the cell pellet in Buffer A (10 mL). Sonication of this suspension to lyse the cells (18W, 2 × 30 s, 0 °C) was followed by centrifugation at 9 krpm for 5 min at 4 °C. The supernatant was syringe-filtered (0.45 µm) and added to Sepharose SP Fast Flow beads (3 mL), pre-equilibrated by washing with Buffer A (15 mL). The suspension was mixed by inversion (1 h, 4 °C) and then loaded into a column. The protein was eluted with Buffer A plus an increasing linear gradient of NaCl (0-0.5 M). Fractions found in an assay to contain high levels of cdc25 were concentrated using a centrifugal filter (Amicon<sup>®</sup> Ultra-4, 10,000 NMWL, Millipore). The retentate was then loaded onto a packed gel filtration column (Sephadex G-50) and eluted with Buffer B. Fractions found in a fluorimetric assay to contain high levels of cdc25 were concentrated as before.

## Phosphatase Assays

### *OMFP Fluorimetric Assay*

The phosphatase activities of *cdc25A*, B and C, VHR, PTP1B, MKP-5 and AP were measured in Microfluor black 96-well plates in a buffer with final concentration of 400  $\mu$ M OMFP, 100 mM Tris pH 8.0, 150 mM NaCl, 1 mM EDTA, 0.1% BME, 5% DMSO. The enzyme concentrations for *cdc25A*, B and C, VHR, PTP1B and MKP-5 were 50-125 ng/well, and the inhibitors were tested at concentrations up to 100  $\mu$ M following 15 min pre-incubation with the enzyme. The fluorescence reading was measured using a Cary Eclipse fluorimeter (excitation 471 nm, emission 530 nm) over a period of 20-60 min at 25 °C.

The phosphatase activity of MKP-3 (as a stoichiometric complex with ERK2) was measured in clear 96-well plates in a buffer with final concentration of 20 mM PNPP, 50 mM imidazole pH 7.5 and 10 mM DTT. The enzyme concentration was 5  $\mu$ g/well, and the inhibitors were tested at concentrations up to 100  $\mu$ M. The colourimetric reading was measured at 405 nm over a period of 60 min at 25 °C.

### 13.1 *Preparation of Constructs*

*N-GST-cat.cdc25A-pGEX-KG* was created by sub-cloning the *cdc25A* catalytic fragment from *cat.cdc25A-pRSETA*<sup>119</sup> into *pGEX-KG* using BamHI and EcoRI.

*cat.cdc25A(F432A)-pET21a* was created by two-step site-directed mutagenesis of *N-GST-cat.cdc25A-pGEX-KG* and sub-cloning the fragment into pET21a using BamHI and HindIII.

- 5' end created from pGEX 5' primer (5'-CAGCAAGTATATAGCATGGC-3') and mutagenic 3' primer (5'-GGGACCTCTCTCACTCGAGGCCTCGCAGTGAAAC-3')
- 3' end created from pGEX 3' primer (5'-GAGGTTTTACCGTCATCAACC-3') and mutagenic 5' primer (5'-GTTTCACTGCGAGGCCTCGAGTGAGAGAGGTCCC-3')

*cat.cdc25A(R439A)-pET21a* was created by two-step site-directed mutagenesis of *N-GST-cat.cdc25A-pGEX-KG* and sub-cloning the fragment into pET21a using BamHI and HindIII.

- 5' end created from pGEX 5' primer (5'-CAGCAAGTATATAGCATGGC-3') and mutagenic 3' primer (5'-CACATACCGGCACATGGCCGGCCCTCTCTCAGA-3')

- 3' end created from pGEX 3' primer (5'-CACATACCGGCACATGGCCGGCCCTCTCTCAGA-3') and mutagenic 5' primer (5'-TCTGAGAGAGGGCCGGCCATGTGCCGGTATGTG-3')

*cat.cdc25A(R439D)-pET21a* was created by two-step site-directed mutagenesis of *N-GST-cat.cdc25A-pGEX-KG* and sub-cloning the fragment into pET21a using BamHI and HindIII.

- 5' end created from pGEX 5' primer (5'-CAGCAAGTATATAGCATGGC-3') and mutagenic 3' primer (5'-CACATACCGGCACATGTCCGGACCTCTCTCAGA-3')
- 3' end created from pGEX 3' primer (5'-CACATACCGGCACATGGCCGGCCCTCTCTCAGA-3') and mutagenic 5' primer (5'-TCTGAGAGAGGTCCGGACATGTGCCGGTATGTG-3')

*cat.cdc25A-pET21a* was created by sub-cloning the *cdc25A* catalytic fragment from *N-GST-cat.cdc25A-pGEX-KG* into pET21a using BamHI and HindIII.

*cat.cdc25B-pET21a* was created by sub-cloning the *cdc25B* catalytic fragment from *cat.cdc25B-pGEM-T<sup>119</sup>* into pET21a using BamHI and XhoI.

*cat.cdc25C-pGEM-T* was created by truncation of *cdc25C-pOTB7<sup>119</sup>* using PCR primers 5'-GGATCCATGTCTACGGA ACTCTTCTCATCC-3' and 5'-CTCGAGTCATGGGCTCATGTCCTTCACC-3' and ligation of the fragment into *pGEM-T*.

*cat.cdc25C-pET21a* was created by sub-cloning the *cdc25C* catalytic fragment from *cat.cdc25C-pGEM-T* into *pET21a* using BamHI and XhoI.

## 14 References

- (1) Alberts, B.; Bray, D.; Lewis, J.; Raff, M.; Roberts, K.; Watson, J. D. *Molecular Biology of the Cell*; Garland Science: London, 2002.
- (2) Boutros, R.; Lobjois, V.; Ducommun, B. *Nat. Rev. Cancer*. **2007**, *7*, 495-507.
- (3) Russell, P.; Nurse, P. *Cell* **1986**, *45*, 145.
- (4) De Bondt, H. L.; Rosenblatt, J.; Jancarik, J.; Jones, H. D.; Morgan, D. O.; Kim, S. H. *Nature* **1993**, *363*, 595-602.
- (5) Donzelli, M.; Draetta, G. F. *EMBO reports* **2003**, *4*, 671-677.
- (6) Rudolph, J. *Nat. Rev. Cancer* **2007**, *7*, 202-211.
- (7) Boutros, R.; Dozier, C.; Ducommun, B. *Curr. Op. Cell. Biol.* **2006**, *18*, 185-191.
- (8) Jinno, S.; Suto, K.; Nagata, A.; Igarashi, M.; Kanaoka, Y.; Nojima, H.; Okayama, H. *EMBO J.* **1994**, *13*, 1549-1556.
- (9) Hoffmann, I.; Draetta, G.; Karsenti, E. *EMBO J.* **1994**, *13*, 4302-4310.
- (10) Garner-Hamrick, P. A.; Fisher, C. *Int. J. Cancer* **1998**, *76*, 720-728.
- (11) Turowski, P.; Franckhauser, C.; Morris, M. C.; Vaglio, P.; Fernandez, A.; Lamb, N. *J. Mol. Biol. Cell* **2003**, *14*, 2984-2998.
- (12) Mailand, N.; Podtelejnikov, A. V.; Groth, A.; Mann, M.; Bartek, J.; Lukas, J. *EMBO J.* **2002**, *21*, 5911-5920.
- (13) Ferguson, A. M.; White, L. S.; Donovan, P. J.; Piwnica-Worms, H. *Mol. Cell Biol.* **2005**, *25*, 2853-2860.
- (14) Karlsson-Rosenthal, C.; Millar, J. B. A. *Trends Cell Biol.* **2006**, *16*, 285-292.
- (15) Van Vugt, M. A.; Bras, A.; Medema, R. H. *Mol. Cell* **2004**, *15*, 799-811.
- (16) Ray, D.; Terao, Y.; Nimbalkar, D.; Hirai, H.; Osmundson, E. C.; Zou, X.; Franks, R.; Christov, K.; Kiyokawa, H. *Cancer Res.* **2007**, *67*, 6605-6611.
- (17) Galaktionov, K.; Jesus, C.; Beach, D. *Genes Dev.* **1995**, *9*, 1046-1058.
- (18) Galaktionov, K.; Chen, X. C.; Beach, D. *Nature* **1996**, *382*, 511-517.
- (19) Ray, D.; Kiyokawa, H. *Cancer Res.* **2008**, *68*, 1251-1253.
- (20) Kristjansdottir, K.; Rudolph, J. *Chem. Biol.* **2004**, *11*, 1043-1051.
- (21) de Sousa Abreu, R.; Penalva, L. O.; Marcotte, E. M.; Vogel, C. *Mol. Biosyst.* **2009**, *5*, 1512-1526.
- (22) Eckstein, J. W. *Inv. New Drugs* **2000**, *18*, 149-156.

- (23) Cazales, M.; Boutros, R.; Brezak, M.-C.; Chaumeron, S.; Prevost, G.; Ducommun, B. *Mol. Cancer Ther.* **2007**, *6*, 318-325.
- (24) Jeffrey, K. L.; Camps, M.; Rommel, C.; Mackay, C. R. *Nat. Rev. Drug. Discov.* **2007**, *6*, 391-403.
- (25) Barr, A. J.; Knapp, S. *Trends Pharmacol. Sci.* **2006**, *27*, 525.
- (26) Lazo, J. S.; Nemoto, K.; Pestell, K. E.; Cooley, K.; Southwick, E. C.; Mitchell, D. A.; Furey, W.; Gussio, R.; Zaharevitz, D. W.; Joo, B.; Wipf, P. *Mol. Pharmacol.* **2002**, *61*, 720-728.
- (27) Contour-Galcerá, M.-O.; Sidhu, A.; Prevost, G.; Bigg, D.; Ducommun, B. *Pharmacol. Therapeut.* **2007**, *115*, 1-12.
- (28) Wipf, P.; Aslan, D. C.; Southwick, E. C.; Lazo, J. S. *Bioorg. Med. Chem. Lett.* **2001**, *11*, 313-317.
- (29) Sohn, J.; Kiburz, B.; Li, Z.; Deng, L.; Safi, A.; Pirrung, M. C.; Rudolph, J. *J. Med. Chem.* **2003**, *46*, 2580-2588.
- (30) Kar, S.; Lefterov, I. M.; Wang, M.; Lazo, J. S.; Scott, C. N.; Wilcox, C. S.; Carr, B. I. *Biochemistry* **2003**, *42*, 10490-10497.
- (31) Brisson, M.; Nguyen, T.; Vogt, A.; Yalowich, J.; Giorgianni, A.; Tobi, D.; Bahar, I.; Stephenson, C. R. J.; Wipf, P.; Lazo, J. S. *Mol. Pharmacol.* **2004**, *66*, 824-833.
- (32) Ham, S. W.; Lee, S. B. *Kor. Chem. Soc.* **2004**, *25*, 1755-1756.
- (33) Huang, W. G.; Jiang, Y. Y.; Li, Q.; Li, J.; Li, J. Y.; Lu, W.; Cai, J. C. *Tetrahedron* **2005**, *61*, 1863-1870.
- (34) Cao, S.; Foster, C.; Brisson, M.; Lazo, J. S.; Kingston, D. G. I. *Bioorg. Med. Chem.* **2005**, *13*, 999-1003.
- (35) Peyregne, V. P.; Kar, S.; Ham, S. W.; Wang, M.; Wang, Z.; Carr, B. I. *Mol. Cancer Ther.* **2005**, *4*, 595-602.
- (36) Brezak, M.-C.; Quaranta, M.; Contour-Galcerá, M.-O.; Lavergne, O.; Mondesert, O.; Auvray, P.; Kasprzyk, P. G.; Prevost, G. P.; Ducommun, B. *Mol. Cancer Ther.* **2005**, *4*, 1378-1387.
- (37) Shimbashi, A.; Tsuchiya, A.; Imoto, M.; Nishiyama, S. *Bioorg. Med. Chem. Lett.* **2005**, *15*, 61-65.
- (38) Lavergne, O.; Fernandes, A.-C.; Brehu, L.; Sidhu, A.; Brezak, M.-C.; Prevost, G.; Ducommun, B.; Contour-Galcerá, M.-O. *Bioorg. Med. Chem. Lett.* **2006**, *16*, 171-175.

- (39) Huang, W.; Li, J.; Zhang, W.; Zhou, Y.; Xie, C.; Luo, Y.; Li, Y.; Wang, J.; Li, J.; Lu, W. *Bioorg. Med. Chem. Lett.* **2006**, *16*, 1905-1908.
- (40) Cossy, J.; Belotti, D.; Brisson, M.; Skoko, J. J.; Wipf, P.; Lazo, J. S. *Bioorg. Med. Chem.* **2006**, *14*, 6283-6287.
- (41) Brisson, M.; Foster, C.; Wipf, P.; Joo, B.; Tomko, R. J., Jr.; Nguyen, T.; Lazo, J. S. *Mol. Pharmacol.* **2007**, *71*, 184-192.
- (42) Park, H.; Carr, B. I.; Li, M.; Ham, S. W. *Bioorg. Med. Chem. Lett.* **2007**, *17*, 2351-2354.
- (43) Brezak, M.-C.; Valette, A.; Quaranta, M.; Contour-Galcera, M.-O.; Jullien, D.; Lavergne, O.; Frongia, C.; Bigg, D.; Kasprzyk, P. G.; Prevost, G. P.; Ducommun, B. *Int. J. Cancer* **2009**, *124*, 1449-1456.
- (44) Nussbaum, F.; Ebbinghaus, A.; Mayer-Bartschmid, A.; Zitzmann, W.; Wiese, W.; Stadler, M.; Anlauf, S. EP 2130831, 2009.
- (45) Liberatore, A.-M.; Pons, D.; Bigg, D.; Prevost, G.; Marie-Christine, B.-P. WO 2009034258, 2009.
- (46) Kar, S.; Wang, M.; Ham, S. W.; Carr, B. I. *Biochem. Pharmacol.* **2006**, *72*, 1217-1227.
- (47) Kim, H. R.; No, J.; Seo, M. J.; Song, B. G.; Son, B. S.; Kim, J. K.; Kim, K.-R.; Cheon, H. G.; Lee, G. H. WO 2006101307, 2006.
- (48) Kolb, S.; Mondésert, O.; Goddard, M.-L.; Jullien, D.; Villoutreix, Bruno O.; Ducommun, B.; Garbay, C.; Braud, E. *ChemMedChem* **2009**, *4*, 633-648.
- (49) Kim, K.-R.; Kwon, J.-L.; Kim, J.-S.; No, Z.; Kim, H. R.; Cheon, H. G. *Eur. J. Pharmacol.* **2005**, *528*, 37-42.
- (50) Johnston, P. A.; Foster, C.; Tierno, M. B.; Shun, T. Y.; Shinde, S. N.; Paquette, W. D.; Brummond, K. M.; Wipf, P.; Lazo, J. S. *Assay Drug Dev. Technol.* **2009**, *7*, 250-265.
- (51) Bolton, J. L.; Trush, M. A.; Penning, T. M.; Dryhurst, G.; Monks, T. J. *Chem. Res. Toxicol.* **2000**, *13*, 135-160.
- (52) Rice, R. L.; Rusnak, J. M.; Yokokawa, F.; Yokokawa, S.; Messner, D. J.; Boynton, A. L.; Wipf, P.; Lazo, J. S. *Biochemistry* **1997**, *36*, 15965-15974.
- (53) Peng, H.; Zalkow, L. H.; Abraham, R. T.; Powis, G. J. *Med. Chem.* **1998**, *41*, 4677-4680.
- (54) Blanchard, J. L.; Epstein, D.; Boisclair, M. D.; Rudolph, J.; Pal, K. *Bioorg. Med. Chem. Lett.* **1999**, *9*, 2537-2538.



- (55) Ducruet, A. P.; Rice, R. L.; Tamura, K.; Yokokawa, F.; Yokokawa, S.; Wipf, P.; Lazo, J. S. *Bioorg. Med. Chem.* **2000**, *8*, 1451-1466.
- (56) Takahashi, M.; Dodo, K.; Sugimoto, Y.; Aoyagi, Y.; Yamada, Y.; Hashimoto, Y.; Shirai, R. *Bioorg. Med. Chem. Lett.* **2000**, *10*, 2571-2574.
- (57) Sodeoka, M.; Sampe, R.; Kojima, S.; Baba, Y.; Usui, T.; Ueda, K.; Osada, H. *J. Med. Chem.* **2001**, *44*, 3216-3222.
- (58) Brohm, D.; Metzger, S.; Bhargava, A.; Muller, O.; Lieb, F.; Waldmann, H. *Angew. Chem. Int. Ed.* **2002**, *41*, 307-311.
- (59) Brohm, D.; Phillippe, N.; Metzger, S.; Bhargava, A.; Muller, O.; Lieb, F.; Waldmann, H. *J. Am. Chem. Soc.* **2002**, *124*, 13171-13178.
- (60) Shimazawa, R.; Gochomori, M.; Shirai, R. *Bioorg. Med. Chem. Lett.* **2004**, *14*, 4339-4342.
- (61) Shimazawa, R.; Suzuki, T.; Dodo, K.; Shirai, R. *Bioorg. Med. Chem. Lett.* **2004**, *14*, 3291-3294.
- (62) Baurle, S.; Blume, T.; Gunther, J.; Henschel, D.; Hillig, R. C.; Husemann, M.; Mengel, A.; Parchmann, C.; Schmid, E.; Skuballa, W. *Bioorg. Med. Chem. Lett.* **2004**, *14*, 1673-1677.
- (63) Erdogan-Orhan, I.; Sener, B.; De Rosa, S.; Perez-Baz, J.; Lozach, O.; Leost, M.; Rakhilin, S.; Meijer, L. *Nat. Prod. Res.* **2004**, *18*, 1 - 9.
- (64) Cao, S.; Foster, C.; Lazo, J. S.; Kingston, D. G. I. *Bioorg. Med. Chem.* **2005**, *13*, 5830-5834.
- (65) Aoyagi, Y.; Masuko, N.; Ohkubo, S.; Kitade, M.; Nagai, K.; Okazaki, S.; Wierzba, K.; Terada, T.; Sugimoto, Y.; Yamada, Y. *Cancer Sci.* **2005**, *96*, 614-619.
- (66) Cao, S.; Foster, C.; Lazo, J. S.; Kingston, D. G. I. *Bioorg. Med. Chem.* **2005**, *13*, 5094-5098.
- (67) Shin, D.-S.; Kim, J.-H.; Lee, S.-K.; Han, D. C.; Son, K.-H.; Kim, H.-M.; Cheon, H.-G.; Kim, K.-R.; Sung, N.-D.; Lee, S. J.; Kang, S. K.; Kwon, B.-M. *Bioorg. Med. Chem.* **2006**, *14*, 2498-2506.
- (68) Brondel, N.; Renoux, B.; Gesson, J.-P. *Tetrahedron Lett.* **2006**, *47*, 9305-9308.
- (69) Brault, L.; Denance, M.; Banaszak, E.; El Maadidi, S.; Battaglia, E.; Bagrel, D.; Samadi, M. *Eur. J. Med. Chem.* **2007**, *42*, 243-247.
- (70) Erbe, D. V.; Wang, S.; Zhang, Y.-L.; Harding, K.; Kung, L.; Tam, M.; Stolz, L.; Xing, Y.; Furey, S.; Qadri, A.; Klaman, L. D.; Tobin, J. F. *Mol. Pharmacol.* **2005**, *67*, 69-77.

- (71) Rudolph, J. *Biochemistry* **2007**, *46*, 3595-3604.
- (72) Fauman, E. B.; Cogswell, J. P.; Lovejoy, B.; Rocque, W. J.; Holmes, W.; Montana, V. G.; Piwnica-Worms, H.; Rink, M. J.; Saper, M. A. *Cell* **1998**, *93*, 617-625.
- (73) Reynolds, R. A.; Yem, A. W.; Wolfe, C. L.; Deibel, M. R.; Chidester, C. G.; Watenpaugh, K. D. *J. Mol. Biol.* **1999**, *293*, 559-568.
- (74) Sohn, J.; Rudolph, J. *Biochemistry* **2003**, *42*, 10060-10070.
- (75) Buhrman, G.; Parker, B.; Sohn, J.; Rudolph, J.; Mattos, C. *Biochemistry* **2005**, *44*, 5307-5316.
- (76) Chen, W.; Wilborn, M.; Rudolph, J. *Biochemistry* **2000**, *39*, 10781-10789.
- (77) Rudolph, J. *Anal. Biochem.* **2001**, *289*, 43-51.
- (78) McCain, D. F.; Catrina, I. E.; Hengge, A. C.; Zhang, Z.-Y. *J. Biol. Chem.* **2002**, *277*, 11190-11200.
- (79) Sohn, J.; Parks, J. M.; Buhrman, G.; Brown, P.; Kristjansdottir, K.; Safi, A.; Edelsbrunner, H.; Yang, W.; Rudolph, J. *Biochemistry* **2005**, *44*, 16563-16573.
- (80) Sohn, J.; Kristjansdottir, K.; Safi, A.; Parker, B.; Kiburz, B.; Rudolph, J. *Proc. Nat. Acad. Sci. USA* **2004**, *101*, 16437-16441.
- (81) Sohn, J.; Rudolph, J. *J. Mol. Biol.* **2006**, *362*, 1060-1071.
- (82) Sohn, J.; Buhrman, G.; Rudolph, J. *Biochemistry* **2007**, *46*, 807-818.
- (83) Wilborn, M.; Free, S.; Ban, A.; Rudolph, J. *Biochemistry* **2001**, *40*, 14200-14206.
- (84) Rudolph, J. *Mol. Pharm.* **2004**, *66*, 780-782.
- (85) Koh, J. T. *Chem. Biol.* **2002**, *9*, 17-23.
- (86) Walsh, D. P.; Chang, Y.-T. *Chem. Rev.* **2006**, *106*, 2476-2530.
- (87) Gaffney, P. In *Chemical Biology*; Larijani, B., Woscholski, R., Rosser, C. A., Eds.; John Wiley and Sons: 2006.
- (88) Koch, A.; Hauf, S. *Eur. J. Cell Biol.*, *89*, 184-193.
- (89) Bishop, A. C.; Zhang, X.-Y.; Lone, A. M. *Methods* **2007**, *42*, 278-288.
- (90) Gunasekera, S. P.; McCarthy, P. J.; Kelly-Borges, M. *J. Am. Chem. Soc.* **1996**, *118*, 8759-8760.
- (91) Dodo, K.; Takahashi, M.; Yamada, Y.; Sugimoto, Y.; Hashimoto, Y.; Shirai, R. *Bioorg. Med. Chem. Lett.* **2000**, *10*, 615-617.
- (92) Lima, L. M.; Barreiro, E. J. *Curr. Med. Chem.* **2005**, *12*, 23-49.
- (93) Leung, C.; Grzyb, J.; Lee, J.; Meyer, N.; Hum, G.; Jia, C.; Liu, S.; Taylor, S. D. *Bioorg. Med. Chem.* **2002**, *10*, 2309-2323.
- (94) Berkowitz, D. B.; Bose, M. *J. Fluorine Chem.* **2001**, *112*, 13-33.

- (95) Baeza, A.; Nájera, C.; Retamosa, M. d. G.; Sansano, J. *Synthesis* **2005**, 2787-2797.
- (96) Shindo, M.; Sato, Y.; Yoshikawa, T.; Koretsune, R.; Shishido, K. *J. Org. Chem.* **2004**, *69*, 3912-3916.
- (97) Gottlin, E. B.; Xu, X.; Epstein, D. M.; Burke, S. P.; Eckstein, J. W.; Ballou, D. P.; Dixon, J. E. *J. Biol. Chem.* **1996**, *271*, 27445-27449.
- (98) <http://www.sigmaplot.com>.
- (99) Lavecchia, A.; Cosconati, S.; Limongelli, V.; Novellino, E. *ChemMedChem* **2006**, *1*, 540-550.
- (100) Arantes, G. M. *Proteins* **2010**, *78*, 3017-3032.
- (101) Orito, K.; Horibata, A.; Nakamura, T.; Ushito, H.; Nagasaki, H.; Yuguchi, M.; Yamashita, S.; Tokuda, M. *J. Am. Chem. Soc.* **2004**, *126*, 14342-14343.
- (102) Karplus, S.; Lifson, S. *Biopolymers* **1971**, *10*, 1973-1982.
- (103) Lieberknecht, A.; Griesser, H. *Tetrahedron Lett.* **1987**, *28*, 4275-4278.
- (104) Jin, S.; Wessig, P.; Liebscher, J. *J. Org. Chem.* **2001**, *66*, 3984-3997.
- (105) Cavelier, F.; Verducci, J. *Tetrahedron Lett.* **1995**, *36*, 4425-4428.
- (106) Gallina, C.; Liberatori, A. *Tetrahedron* **1974**, *30*, 667-673.
- (107) Gonzalez, J. F.; de la Cuesta, E.; Avendano, C. *Synth. Commun.* **2004**, *34*, 1589 - 1597.
- (108) Chary, K. V. R.; Govil, G. *NMR in Biological Systems*; Springer, 2008.
- (109) Bondos, S. E.; Bicknell, A. *Anal. Biochem.* **2003**, *316*, 223-31.
- (110) Ducat, T., Declerck, N., Gostan, T., Kochoyan, M. and Demene, H. *J. Biomol. NMR* **2006**, *34*, 137-151.
- (111) Baldwin, R. L. *Biophys. J.* **1996**, *71*, 2056-2063.
- (112) Scrivens, P. J.; Alaoui-Jamali, M. A.; Giannini, G.; Wang, T.; Loignon, M.; Batist, G.; Sandor, V. A. *Mol. Cancer Ther.* **2003**, *2*, 1053-1059.
- (113) Golovanov, A. P.; Hautbergue, G. M.; Wilson, S. A.; Lian, L. Y. *J. Am. Chem. Soc.* **2004**, *126*, 8933-8939.
- (114) Matthews, S. J.; Leatherbarrow, R. J. *J. Biomol. NMR* **1993**, *3*, 597-600.
- (115) Lane, A. N.; Arumugam, S. *J. Magn. Reson.* **2005**, *173*, 339-343.
- (116) Sambrook, J.; Fritsch, E. F.; Maniatis, T. *Molecular Cloning: A Laboratory Manual*; Cold Spring Harbour Laboratory Press: New York, 1989; Vol. 3.
- (117) Mossakoska, D. E.; Smith, R. A. G. *Methods in Molecular Biology*; Humana Press Inc.: Totowa, 1997; Vol. 60.
- (118) <http://www3.imperial.ac.uk/xraycrystallography/crystn>.

- (119) Mann Group, unpublished results.
- (120) Park, H.; Bahn, Y. J.; Jung, S.-K.; Jeong, D. G.; Lee, S.-H.; Seo, I.; Yoon, T.-S.; Kim, S. J.; Ryu, S. E. *J. Med. Chem.* **2008**, *51*, 5533-5541.
- (121) Montes, M.; Braud, E.; Miteva, M. A.; Goddard, M.-L.; Mondesert, O.; Kolb, S.; Brun, M.-P.; Ducommun, B.; Garbay, C.; Villoutreix, B. O. *J. Chem. Inf. Model.* **2008**, *48*, 157-165.
- (122) Cresset BioMolecular Discovery Ltd. **2008**.
- (123) Cheeseright, T.; Mackey, M.; Rose, S.; Vinter, A. *J. Chem. Inf. Model.* **2006**, *46*, 665-76.
- (124) Cheeseright, T. J.; Holm, M.; Lehmann, F.; Luik, S.; Gottert, M.; Melville, J. L.; Laufer, S. *J. Med. Chem.* **2009**.
- (125) Tresadern, G.; Bemporad, D.; Howe, T. *J. Mol. Graph. Model.* **2009**, *27*, 860-70.
- (126) Bellenie, B. R.; Barton, N. P.; Emmons, A. J.; Heer, J. P.; Salvagno, C. *Bioorg. Med. Chem. Lett.* **2009**, *19*, 990-4.
- (127) Taylor, N. R.; Borhani, D.; Epstein, D.; Rudolph, J.; Ritter, K.; Fujimori, T.; Robinson, S.; Eckstein, J.; Haupt, A.; Walker, N.; Dixon, R. W.; Choquette, D.; Blanchard, J.; Kluge, A.; Pal, K.; Bockovich, N.; Come, J.; Hediger, M. *WIPO*, WO 2001016300, 2001.
- (128) Stuiblé, M.; Zhao, L.; Aubry, I.; Schmidt-Arras, D.; Böhmer, F.-D.; Li, C.-J.; Tremblay, M. L. *ChemBioChem* **2007**, *8*, 179-186.
- (129) Low, C. M. R.; Vinter, J. G. *J. Med. Chem.* **2008**, *51*, 565-573.
- (130) Cheeseright, T. J.; Mackey, M. D.; Melville, J. L.; Vinter, J. G. *J. Chem. Inf. Model.* **2008**, *48*, 2108-17.
- (131) Coleman, J. E. *Annu. Rev. Biophysics* **1992**, *21*, 441-483.
- (132) Zhang, S.; Zhang, Z.-Y. *Drug Discov. Today* **2007**, *12*, 373-381.
- (133) Patterson, K. I.; Brummer, T.; O'Brien, P. M.; Daly, R. J. *Biochem. J.* **2009**, *418*, 475-489.
- (134) Cerignoli, F.; Rahmouni, S.; Ronai, Z. e.; Mustelin, T. *Cell Cycle* **2006**, *5*, 2210-2215.
- (135) Rahmouni, S.; Cerignoli, F.; Alonso, A.; Tsutji, T.; Henkens, R.; Zhu, C.; Louisdit-Sully, C.; Moutschen, M.; Jiang, W.; Mustelin, T. *Nat. Cell. Biol.* **2006**, *8*, 524-531.

- (136) Arnoldussen, Y. J.; Lorenzo, P. I.; Pretorius, M. E.; Waehre, H.; Risberg, B.; Maelandsmo, G. M.; Danielsen, H. E.; Saatcioglu, F. *Cancer Res.* **2008**, *68*, 9255-9264.
- (137) Henkens, R.; Delvenne, P.; Arafa, M.; Moutschen, M.; Zeddou, M.; Tautz, L.; Boniver, J.; Mustelin, T.; Rahmouni, S. *BMC Cancer* **2008**, *8*, 147.
- (138) Lazo, J. S.; Nunes, R.; Skoko, J. J.; de Oliveira, P. E. Q.; Vogt, A.; Wipf, P. *Bioorg. Med. Chem.* **2006**, *14*, 5643-5650.
- (139) Lazo, J. S.; Skoko, J. J.; Werner, S.; Mitasev, B.; Bakan, A.; Koizumi, F.; Yellow-Duke, A.; Bahar, I.; Brummond, K. M. *J. Pharmacol. Exp. Ther.* **2007**, *322*, 940.
- (140) Vogt, A.; McDonald, P. R.; Tamewitz, A.; Sikorski, R. P.; Wipf, P.; Skoko, J. J.; Lazo, J. S. *Mol. Cancer Ther.* **2008**, *7*, 330-340.
- (141) Vogt, A.; Tamewitz, A.; Skoko, J.; Sikorski, R. P.; Giuliano, K. A.; Lazo, J. S. *J. Biol. Chem.* **2005**, *280*, 19078.
- (142) Lee, M.; Oh, W. K.; Kim, B. Y.; Ahn, S. C.; Kang, D. O.; Sohn, C. B.; Osada, H.; Ahn, J. S. *Planta Med.* **2002**, *68*, 1063.
- (143) Bae, E.; Oh, H.; Oh, W. K.; Kim, M. S.; Kim, B. S.; Kim, B. Y.; Sohn, C. B.; Osada, H.; Ahn, J. S. *Planta Med.* **2004**, *70*, 869.
- (144) Shi, Z.; Tabassum, S.; Jiang, W.; Zhang, J.; Mathur, S.; Wu, J.; Shi, Y. *ChemBioChem* **2007**, *8*, 2092-2099.
- (145) Park, H.; Jung, S.-K.; Jeong, Dae G.; Ryu, Seong E.; Kim, Seung J. *ChemMedChem* **2008**, *3*, 877-880.
- (146) Wu, S.; Vossius, S.; Rahmouni, S.; Miletic, A. V.; Vang, T.; Vazquez-Rodriguez, J.; Cerignoli, F.; Arimura, Y.; Williams, S.; Hayes, T.; Moutschen, M.; Vasile, S.; Pellecchia, M.; Mustelin, T.; Tautz, L. *J. Med. Chem.* **2009**, *52*, 6716-6723.
- (147) Jeong, D. G.; Yoon, T.-S.; Kim, J. H.; Shim, M. Y.; Jung, S.-K.; Son, J. H.; Ryu, S. E.; Kim, S. J. *J. Mol. Biol.* **2006**, *360*, 946-955.
- (148) Vogt, A.; Lazo, J. S. *Methods* **2007**, *42*, 268-277.
- (149) Strotman, N. A.; Chobanian, H. R.; He, J.; Guo, Y.; Dormer, P. G.; Jones, C. M.; Steves, J. E. *J. Org. Chem.* **2010**, *75*, 1733-1739.
- (150) Amb, C. M.; Rasmussen, S. C. *J. Org. Chem.* **2006**, *71*, 4696-4699.
- (151) Cancer Research Technology chemicals database, July 2009.
- (152) StarDrop, v 4.0, Optibrium Ltd, Cambridge, U.K., 2009.  
<http://www.optibrium.com/stardrop.php>.
- (153) T.T. Tanimoto, 1957, IBM Internal Report 17th Nov.

- (154) Lipinski, C. A.; Lombardo, F.; Dominy, B. W.; Feeney, P. J. *Adv. Drug Deliv. Rev.* **2001**, *46*, 3-26.
- (155) Ishiyama, T.; Murata, M.; Miyaura, N. *J. Org. Chem.* **1995**, *60*, 7508-7510.
- (156) Kleeberg, C.; Dang, L.; Lin, Z.; Marder, T. *Angew. Chem. Int. Ed.* **2009**, *48*, 5350-5354.
- (157) Schnurch, M.; Hammerle, J.; Mihovilovic, M. D.; Stanetty, P. *Synthesis* **2010**, 837-843.
- (158) Amatore, C.; Jutand, A.; Negri, S.; Fauvarque, J.-F. *J. Organomet. Chem.* **1990**, *390*, 389-398.
- (159) Herrmann, W. A.; Böhm, V. P. W.; Reisinger, C.-P. *J. Organomet. Chem.* **1999**, *576*, 23-41.
- (160) Gillespie, J.; Jamieson, C.; Maclean, J. K. F.; Moir, E. M.; Rankovic, Z. WO2009/147167A1, 2009.
- (161) Guari, Y.; van Es, D. S.; Reek, J. N. H.; Kamer, P. C. J.; van Leeuwen, P. W. N. M. *Tetrahedron Lett.* **1999**, *40*, 3789-3790.
- (162) Littke, A. F.; Dai, C.; Fu, G. C. *J. Am. Chem. Soc.* **2000**, *122*, 4020-4028.
- (163) Old, D. W.; Wolfe, J. P.; Buchwald, S. L. *J. Am. Chem. Soc.* **1998**, *120*, 9722-9723.
- (164) Hopkins, A. L.; Groom, C. R.; Alex, A. *Drug Discov. Today* **2004**, *9*, 430-431.
- (165) Leeson, P. D.; Springthorpe, B. *Nat. Rev. Drug. Discov.* **2007**, *6*, 881-890.
- (166) Brighty, K. E.; Lowe III, J. A.; McGuirk, P. R. US5037834 A1, 1991.
- (167) Bach, T.; Heuser, S. *J. Org. Chem.* **2002**, *67*, 5789-5795.
- (168) Fors, B. P.; Dooleweerd, K.; Zeng, Q.; Buchwald, S. L. *Tetrahedron* **2009**, *65*, 6576-6583.
- (169) Kerdesky, F. A. J.; Seif, L. S. *Synth. Commun.* **1995**, *25*, 2639 - 2645.
- (170) Kalgutkar, A. S.; Driscoll, J.; Zhao, S. X.; Walker, G. S.; Shepard, R. M.; Soglia, J. R.; Atherton, J.; Yu, L.; Mutlib, A. E.; Munchhof, M. J.; Reiter, L. A.; Jones, C. S.; Doty, J. L.; Trevena, K. A.; Shaffer, C. L.; Ripp, S. L. *Chem. Res. Toxicol.* **2007**, *20*, 1954-1965.
- (171) Obach, R. S.; Kalgutkar, A. S.; Ryder, T. F.; Walker, G. S. *Chem. Res. Toxicol.* **2008**, *21*, 1890-1899.
- (172) Wehn, P. M.; Harrington, P. E.; Eksterowicz, J. E. *Org. Lett.* **2009**, *11*, 5666-5669.
- (173) Hooper, M. W.; Utsunomiya, M.; Hartwig, J. F. *J. Org. Chem.* **2003**, *68*, 2861-2873.
- (174) Liu, Y.; Bai, Y.; Zhang, J.; Li, Y.; Jiao, J.; Qi, X. *Eur. J. Org. Chem.* **2007**, *2007*, 6084-6088.

- (175) Lee, S.; Jorgensen, M.; Hartwig, J. F. *Org. Lett.* **2001**, *3*, 2729-2732.
- (176) Rasmussen, C. R.; Villani Jr, F. J.; Weaner, L. E.; Reynolds, B. E.; Hood, A. R.; Hecker, L. R.; Nortey, S. O.; Hanslin, A.; Costanzo, M. J.; Powell, E. T.; Molinari, A. J. *Synthesis* **1988**, *1988*, 456-459.
- (177) Mahboobi, S.; Sellmer, A.; Hoche, H.; Eichhorn, E.; Bar, T.; Schmidt, M.; Maier, T.; Stadlwieser, J. F.; Beckers, T. L. *J. Med. Chem.* **2006**, *49*, 5769-5776.
- (178) Monguchi, D.; Fujiwara, T.; Furukawa, H.; Mori, A. *Org. Lett.* **2009**, *11*, 1607-1610.
- (179) Daugulis, O.; Do, H.-Q.; Shabashov, D. *Acc. Chem. Res.* **2009**, *42*, 1074-1086.
- (180) Beletskaya, I. P.; Cheprakov, A. V. *Coord. Chem. Rev.* **2004**, *248*, 2337-2364.
- (181) Hamada, T.; Ye, X.; Stahl, S. S. *J. Am. Chem. Soc.* **2008**, *130*, 833-835.
- (182) Bordwell, F. G.; Drucker, G. E.; Andersen, N. H.; Denniston, A. D. *J. Am. Chem. Soc.* **2002**, *108*, 7310-7313.
- (183) Bordwell, F. G. *Acc. Chem. Res.* **1988**, *21*, 463.
- (184) Fukuzawa, S.-i.; Shimizu, E.; Atsumi, Y.; Haga, M.; Ogata, K. *Tetrahedron Lett.* **2009**, *50*, 2374-2376.
- (185) Yin, J.; Zhao, M. M.; Huffman, M. A.; McNamara, J. M. *Org. Lett.* **2002**, *4*, 3481-3484.
- (186) Shen, Q.; Ogata, T.; Hartwig, J. F. *J. Am. Chem. Soc.* **2008**, *130*, 6586-6596.
- (187) Takahashi *Chem. Abstr.* **1952**, 112.
- (188) Caravatti, G.; Fairhurst, R. A.; Furet, P.; Guagnano, V.; Imbach, P. US 2009/163469 A1, 2009.
- (189) Reiter, L. A.; Linde, R. G. US2008/076771, 2008.
- (190) Högermeier, J.; Reissig, H.-U. *Adv. Synth. Catal.* **2009**, *351*, 2747-2763.
- (191) Grimm, J. B.; Wilson, K. J.; Witter, D. J. *J. Org. Chem.* **2009**, *74*, 6390-6393.
- (192) Fors, B. P.; Watson, D. A.; Biscoe, M. R.; Buchwald, S. L. *J. Am. Chem. Soc.* **2008**, *130*, 13552-13554.
- (193) Fors, B. P.; Krattiger, P.; Strieter, E.; Buchwald, S. L. *Org. Lett.* **2008**, *10*, 3505-3508.
- (194) Maiti, D.; Fors, B. P.; Henderson, J. L.; Nakamura, Y.; Buchwald, S. L. *Chem. Sci.*, doi. 10.1039/C0SC00330A.
- (195) Dvorak, C. A.; Rudolph, D. A.; Ma, S.; Carruthers, N. I. *J. Org. Chem.* **2005**, *70*, 4188-4190.

- (196) Zhang, C.; Huang, J.; Trudell, M. L.; Nolan, S. P. *J. Org. Chem.* **1999**, *64*, 3804-3805.
- (197) Guram, A. S.; King, A. O.; Allen, J. G.; Wang, X.; Schenkel, L. B.; Chan, J.; Bunel, E. E.; Faul, M. M.; Larsen, R. D.; Martinelli, M. J.; Reider, P. J. *Org. Lett.* **2006**, *8*, 1787-1789.
- (198) Ohe, T.; Miyaura, N.; Suzuki, A. *Synlett* **1990**, 221-223.
- (199) Ohe, T.; Miyaura, N.; Suzuki, A. *J. Org. Chem.* **1993**, *58*, 2201.
- (200) Wang, B.; Sun, H.-X.; Sun, Z.-H. *Eur. J. Org. Chem.* **2009**, *2009*, 3688-3692.
- (201) Coan, K. E. D.; Shoichet, B. K. *J. Am. Chem. Soc.* **2008**, *130*, 9606-9612.
- (202) Ferreira, R. S.; Bryant, C.; Ang, K. K. H.; McKerrow, J. H.; Shoichet, B. K.; Renslo, A. R. *J. Med. Chem.* **2009**, *52*, 5005-5008.
- (203) Okamura, W. H.; Zhu, G.-D.; Hill, D. K.; Thomas, R. J.; Ringe, K.; Borchardt, D. B.; Norman, A. W.; Mueller, L. J. *J. Org. Chem.* **2002**, *67*, 1637-1650.
- (204) Duraisamy, M.; Walborsky, H. M. *J. Am. Chem. Soc.* **1983**, *105*, 3270-3273.
- (205) Sangshetti, J. N.; Nagawade, R. R.; Shinde, D. B. *Bioorg. Med. Chem. Lett.* **2009**, *19*, 3564-3567.
- (206) Cox, G. G.; Miller, D. J.; Moody, C. J.; Sie, E.-R. H. B.; Kulagowski, J. J. *Tetrahedron* **1994**, *50*, 3195-3212.
- (207) Baeza, A.; Nájera, C.; Retamosa, M. d. G.; Sansano, J. M. *Synthesis* **2005**, *2005*, 2787-2797.
- (208) Kenner, G. W.; Rimmer, J.; Smith, K. M.; Unsworth, J. F. *J. Chem. Soc., Perkin Trans. 1* **1977**, 332-340.
- (209) Kalikhman, I. D.; Bannikova, O. B.; Volkova, L. I.; Sultangareev, R. G.; Lopyrev, V. A. *Russ. Chem. Bull.* **1981**, *30*, 1001-1005.
- (210) Bose, D. S.; Chary, M. V. *Synthesis* **2010**, 643-650.
- (211) Jainta, M.; Nieger, M.; Bräse, S. *Eur. J. Org. Chem.* **2008**, 5418-5424.
- (212) Nitecki, D. E.; Halpern, B.; Westley, J. W. *J. Org. Chem.* **1968**, *33*, 864-866.
- (213) Armstrong, A.; Baxter, C. A.; Lamont, S. G.; Pape, A. R.; Wincewicz, R. *Org. Lett.* **2006**, *9*, 351-353.
- (214) Yoo, D.; Oh, J. S.; Lee, D. W.; Kim, Y. G. *J. Org. Chem.* **2003**, *68*, 2979-2982.
- (215) Stocksdale, M. G.; Ramurthy, S.; Miller, M. J. *J. Org. Chem.* **1998**, *63*, 1221-1225.
- (216) Shawe, T. T.; Liebeskind, L. S. *Tetrahedron* **1991**, *47*, 5643-5666.
- (217) Rathelot, P.; Azas, N.; El-Kashef, H.; Delmas, F.; Di Giorgio, C.; Timon-David, P.; Maldonado, J.; Vanelle, P. *Eur. J. Med. Chem.* **2002**, *37*, 671-679.



- (218) De Luca, L.; Giacomelli, G.; Masala, S.; Porcheddu, A. *Synlett* **2004**, 2004, 2299-2302.
- (219) Shin, C.-g.; Sato, Y.; Hayakawa, M.; Kondo, M.; Yoshimura, J. *Heterocycles* **1981**, 16, 1573-1578.
- (220) Le Flohic, A.; Meyer, C.; Cossy, J. *Tetrahedron* **2006**, 62, 9017-9037.
- (221) Bey, E.; Marchais-Oberwinkler, S.; Werth, R.; Negri, M.; Al-Soud, Y. A.; Kruchten, P.; Oster, A.; Frotscher, M.; Birk, B.; Hartmann, R. W. *J. Med. Chem.* **2008**, 51, 6725-6739.
- (222) Patil, V. *J. Ind. Chem. Soc.* **1979**, 56, 1243-1245.
- (223) Ishizuka, N.; Nagata, K.; Yamamori, T.; Sakai, K. JP2001233767, 2001.
- (224) Branco, P. S.; Prabhakar, S.; Lobo, A. M.; Williams, D. J. *Tetrahedron* **1992**, 48, 6335-6360.
- (225) Vernier, J.-M.; Maderna, A.; Koh, Y.; Hong, Z. WO 2008/89459A1, 2008.
- (226) Chandra, T.; Brown, K. L. *Tetrahedron Lett.* **2005**, 46, 2071-2074.
- (227) Zhang, M. Q.; Haemers, A.; Vanden Berghe, D.; Pattyn, S. R.; Bollaert, W.; Levshin, I. *J. Heterocycl. Chem.* **1991**, 28, 673-683.
- (228) Goldfarb, D. S. US2009163545, 2009.
- (229) Vogels, C. M.; Wellwood, H. L.; Biradha, K.; Zaworotko, M. J.; Westcott, S. A. *Can. J. Chem.* **1999**, 77, 1196-1207.
- (230) Hashmi, A. S. K.; Weyrauch, J. P.; Frey, W.; Bats, J. W. *Org. Lett.* **2004**, 6, 4391-4394.
- (231) Pietruszka, J.; Witt, A.; Frey, W. *Eur. J. Org. Chem.* **2003**, 2003, 3219-3229.
- (232) Fu, N.; Allen, A. D.; Chan, W.; Kobayashi, S.; Tidwell, T. T.; Tahmessebi, D.; Aguilar, A.; Cabrera, E. P.; Godoy, J. *Can. J. Chem.* **2008**, 86, 333-341.
- (233) Ostrowski, T.; Golankiewicz, B.; De Clercq, E.; Andrei, G.; Snoeck, R. *Eur. J. Med. Chem.* **2009**, 44, 3313-3317.
- (234) Pallavicini, M.; Bolchi, C.; Binda, M.; Cilia, A.; Clementi, F.; Ferrara, R.; Fumagalli, L.; Gotti, C.; Moretti, M.; Pedretti, A.; Vistoli, G.; Valoti, E. *Bioorg. Med. Chem. Lett.* **2009**, 19, 854-859.
- (235) Theo, Z.; Jean-Valère, N.; Hansjörg, G. *Angew. Chem. Int. Ed.* **2009**, 48, 559-563.
- (236) Reuman, M.; Hu, Z.; Kuo, G.-H.; Li, X.; Russell, R. K.; Shen, L.; Youells, S.; Zhang, Y. *Org. Process Res. Dev.* **2007**, 11, 1010-1014.
- (237) Pathak, U.; Pandey, L. K.; Tank, R. *J. Org. Chem.* **2008**, 73, 2890-2893.

- (238) Colabufo, N. A.; Berardi, F.; Perrone, M. G.; Cantore, M.; Contino, M.; Inglese, C.; Niso, M.; Perrone, R. *ChemMedChem* **2009**, *4*, 188-195.
- (239) Eriks, J. C.; Van der Goot, H.; Sterk, G. J.; Timmerman, H. *J. Med. Chem.* **1992**, *35*, 3239-3246.
- (240) Walczynski, K.; Timmerman, H.; Zuiderveld, O. P.; Zhang, M. Q.; Glinka, R. *Farmaco* **1999**, *54*, 533-541.
- (241) Hall, G. E.; Walker, J. J. *Chem. Soc. C* **1966**, 1357-1360.
- (242) Kavala, V.; Naik, S.; Patel, B. K. *J. Org. Chem.* **2005**, *70*, 4267-4271.
- (243) Easter, J. A.; Stolle, W. T. *J. Labelled Cpd Radiopharm.* **2001**, *44*, 797-810.
- (244) Ali, M. A.; Punniyamurthy, T. *Adv. Synth. Catal.*, *352*, 288-292.
- (245) Kuang, L.; Zhou, J.; Chen, S.; Ding, K. *Synthesis* **2007**, *2007*, 3129-3134.
- (246) Herbst, R. M.; Wilson, K. R. *J. Org. Chem.* **1957**, *22*, 1142-1145.
- (247) Daly, K.; Heron, N.; Hird, A.; Ioannidis, S.; Janetka, J. W.; Lyne, P.; Scott, J.; Toader, D.; Vasbinder, M.; Yu, D.; Yu, Y. WO2006/106326 A1, 2006.
- (248) Solomons, I. A.; Spoerri, P. E. *J. Am. Chem. Soc.* **1953**, *75*, 679-681.
- (249) Burpitt, B. E.; Crawford, L. P.; Davies, B. J.; Mistry, J.; Mitchell, M. B.; Pancholi, K. D.; Coates, W. J. *J. Heterocycl. Chem.* **1988**, *25*, 1689-1695.
- (250) Deprez, P.; Jary, H.; Temal, T. WO 2006/117211 A2, 2006.
- (251) Joshi, K. C.; Bahel, S. C. *J. Ind. Chem. Soc.* **1962**, *39*, 121-128.
- (252) Kamigata, N.; Udodaira, K.; Yoshikawa, M.; Shimizu, T. *J. Organomet. Chem.* **1998**, *552*, 39-43.
- (253) Potewar, T. M.; Ingale, S. A.; Srinivasan, K. V. *Tetrahedron* **2008**, *64*, 5019-5022.
- (254) Ramsh, S.; Basova, Y.; Ginak, A.; Smorygo, N.; Rodin, A. *Chem. Heterocycl. Compd.* **1982**, *18*, 24-28.
- (255) Gaikwad, S. A.; Patil, A. A.; Deshmukh, M. B. *Phosphorus Sulfur* **2010**, *185*, 103 - 109.
- (256) Caille, S.; Bercot, E. A.; Cui, S.; Faul, M. M. *J. Org. Chem.* **2008**, *73*, 2003-2006.

## 15 Appendix

### 15.1 Solution Constitutions

Assay Buffer	100 mM Tris pH 8, 150 mM NaCl, 1 mM EDTA, 0.1% BME
Buffer A	25 mM Tris pH 7.5, 2 mM DTT, 1 mM EDTA
Buffer B	25 mM Tris pH 7.5, 2 mM DTT, 1 mM EDTA, 200 mM NaCl
Coomassie destaining solution	10% (v/v) AcOH, 10% (v/v) MeOH
Coomassie staining solution	0.25% (w/v) Coomassie blue dye, 10% (v/v) AcOH, 10% (v/v) MeOH
Gene clean solution	10mM Tris HCl, 50 mM NaCl, 2.5 mM EDTA, 50% v/v EtOH, pH 7.5
KOD DNA polymerase	2.5 U $\mu\text{L}^{-1}$ KOD, 50 mM Tris-HCl, 50 mM KCl, 1 mM DTT, 0.1 mM EDTA, 50% (v/v) glycerol, 0.1% (v/v) NP40, 0.1% (v/v) Tween, pH 8.0
KOD buffer 1	1.2 M Tris-HCl, 100 mM KCl, 60 mM $(\text{NH}_4)_2\text{SO}_4$ , 1% (v/v) Triton X-100, 0.01% (w/v) BSA, pH 8.0
KOD buffer 2	1.2 M Tris-HCl, 100 mM KCl, 60 mM $(\text{NH}_4)_2\text{SO}_4$ , 1% (v/v) Triton X-100, 0.01% (w/v) BSA, pH 8.8
LB	1% (w/v) bactotryptone, 1% (w/v) NaCl, 0.5% (w/v) bacto yeast extract, pH 7.0
M9 micronutrients (per 100 mL)	conc. HCl (8 mL), $\text{FeCl}_2 \cdot 4\text{H}_2\text{O}$ (5 g), $\text{CaCl}_2 \cdot 2\text{H}_2\text{O}$ (184 mg), $\text{H}_3\text{BO}_3$ (64 mg), $\text{MnCl}_2 \cdot 4\text{H}_2\text{O}$ (40 mg), $\text{CoCl}_2 \cdot 6\text{H}_2\text{O}$ (18 mg), $\text{CuCl}_2 \cdot 2\text{H}_2\text{O}$ (4 mg), $\text{ZnCl}_2$ (340 mg), $\text{Na}_2\text{MoO}_4 \cdot 2\text{H}_2\text{O}$ (605 mg)
M9 minimal medium (per litre)	$\text{Na}_2\text{HPO}_4$ (12.8 g), $\text{KH}_2\text{PO}_4$ (3.0 g), NaCl (0.5 g), $\text{NH}_4\text{Cl}$ (1.0 g), glucose (2.0 g), $\text{MgSO}_4 \cdot 7\text{H}_2\text{O}$ (0.494 g), $\text{CaCl}_2 \cdot \text{H}_2\text{O}$ (0.015 g), thiamine (0.01 g), $\text{FeSO}_4 \cdot 7\text{H}_2\text{O}$ (0.01 g), pH 7.4
M9 vitamins (per litre)	biotin (1.1 mg), folic acid (1.1 mg), para-aminobenzoic acid (110 mg), riboflavin (110 mg), pantothenic acid (220 mg), pyridoxine HCl (220 mg), thiamine HCl (220 mg), niacinamide (220 mg), ethanol (500 mL)
NETN	0.5% (v/v) NP40, 20 mM Tris-HCl, 250 mM NaCl, 1 mM EDTA
KOD PCR components	KOD buffer 1 (5 $\mu\text{L}$ ), 25 mM $\text{MgCl}_2$ (4 $\mu\text{L}$ ), 2 mM dNTPs (5 $\mu\text{L}$ ), KOD DNA polymerase (0.5 $\mu\text{L}$ )
Taq PCR components	Taq buffer (5 $\mu\text{L}$ ), 25 mM $\text{MgCl}_2$ (4 $\mu\text{L}$ ), 100 mM dNTP (2 $\mu\text{L}$ ), Taq DNA polymerase (2 $\mu\text{L}$ )
5 $\times$ SDS loading buffer	0.16 M Tris-HCl, pH 6.8, 24% (v/v) glycerol, 5% SDS, 12.5% (v/v) BME, 0.1% (w/v) bromophenol blue

SDS-PAGE stacking gel	0.1% (v/v) SDS, 5% (v/v) acrylamide, 0.1 M Tris-HCl, pH 6.8
SDS-PAGE resolving gel	0.2% (v/v) SDS, 10% (v/v) acrylamide, 0.4 M Tris-HCl, pH 8.8
SDS running buffer	7.8 mM Tris-HCl, 80 mM glycine, 10% (v/v) MeOH, 10% (w/v) SDS
Solution I	50 mM glucose, 25 mM Tris-HCl, 10 mM EDTA, pH 8
Solution II	0.2 M NaOH, 1% SDS solution
Solution III	3 M KOAc, 5 M glacial acetic acid
TAE	40 mM Tris-acetate, 1 mM EDTA, pH 8.0
TAE loading buffer	TAE + 0.04% (w/v) bromophenol blue, 2.5% (w/v) ficoll
Taq buffer	100 mM Tris-HCl, 500 mM KCl, 0.8% (v/v) NP40, pH 8.8

## 15.2 Parallel Synthesis – Attempted Reactions

*Suzuki coupling (boronic acids or esters)*

### Successful reactions:

4-pyridyl	4-acetaminophenyl
2-trifluoromethylphenyl	4- <i>N</i> -Tosyl-aminophenyl
4-(1-pyrazolylmethyl)-phenyl	2-methoxy-3-hydroxy-4-chlorophenyl
3-acetamidophenyl	2-pyrrolyl ( <i>N</i> -Boc)
4-(SO <sub>2</sub> NEt)-phenyl	4-amino-2-fluorophenyl
4-pyridyl (2-methyl)	2-( <i>N</i> -mesyl)-aminophenyl
2-mesylphenyl	3-pyridyl (5-fluoro)
3-mesylphenyl	3-isopropoxy- 4-methoxyphenyl
3- (1-piperidinylmethyl)phenyl	4-SO <sub>2</sub> N(cyclopropyl)-phenyl
5-indolyl	5-(2-aminopyrimidinyl)
3-fluoro-4-methylphenyl	5-(2-dimethylamino)pyridyl
4-SO <sub>2</sub> N(benzyl)phenyl	3-(1-phenyl)pyrazolyl
3-methoxy-5-fluorophenyl	3-(CO <sub>2</sub> Et) phenyl
3-morpholino-phenyl	4-quinolyl
4-indazolyl	4-(2-dimethylaminoethoxy)phenyl
2-hydroxy-4-fluorophenyl	3-(5-phenyl)pyrazolyl
5-(2-methoxy)-pyrimidyl	4-( <i>N</i> -mesyl)aminophenyl
2-furyl	3-nitrophenyl
3-carboxyphenyl	4-(1-(2-morpholinoethyl)-)pyrazolyl
4-(1-isobutyl)-pyrazolyl	4-amino-3-methoxyphenyl
4-(1-benzyl)-pyrazolyl	4-(1-(thiophen-2-ylmethyl)-pyrazolyl
5-indazolyl	

### Unsuccessful reactions:

4-pyrazolyl (3,5-dimethyl, <i>N</i> -Boc)	5-indolyl ( <i>N</i> -benzenesulfonyl)
2- <i>N</i> -Boc-aminophenyl	5-Indolyl ( <i>N</i> -Tosyl)
<i>trans</i> -styryl	4-pyridyl (2,3-dichloro)
7-benzomorpholine ( <i>N</i> -methyl)	2-benzothiophene
2-methoxy-5-isopropylphenyl	2-isopropoxy-5-fluorophenyl
2-trifluoromethoxyphenyl	3-pyridyl (2-chloro-4-methyl)
3-pyridyl (2,6-difluoro)	4-phenoxyphenyl
4-isoxazolyl	4-(4-methoxybenzyloxy)-phenyl
4-ethoxy(2-piperidinyl)phenyl	3-pyridyl (5-CO <sub>2</sub> Et)
3-pyridyl (4- <i>N</i> -methylpiperazine)	4-pyridyl (3-morpholine)
3-fluoro-4-(CO <sub>2</sub> NHNH <sub>2</sub> )phenyl	5-cyano-benzothiophene
3-methoxy-4-( <i>N</i> -Boc)aminophenyl	3-indolyl ( <i>N</i> -benzenesulfonyl)
5-(2-cyano)pyrimidinyl	4-( <i>N</i> -succinic acid)phenyl
8-quinolyl	5-benzimidazolyl
4-(CONH <sub>2</sub> )phenyl	5-pyrimidyl
4-(aminomethyl)-phenyl	4-(3,5-dimethyl)-pyrazolyl
2-aminophenyl	3-pyridyl (4-methoxy)

## Aminocarbonylation (amines)

### Successful reactions:

morpholine	4-(aminomethyl)pyridine
4-anisidine	isopropylamine
2-amino-5-ethyl-1,3,4-thiadiazole	4-(3-aminopropyl)morpholine
1-(3-aminopropyl)-imidazole	cyclohexylamine
3-(2-thienyl)-1H-pyrazol-5-amine	3-amino-2-pyridinol
tetrahydrofurfurylamine	2-methoxyethylamine
4-amino-2-chloropyridine	R-1-(4-fluorophenyl)ethylamine
(1R,2R)-(-)- <i>trans</i> -1-amino-2-indanol	2-aminoethylmethylsulfone
methyl 4-(aminomethyl)benzoate	

### Unsuccessful reactions:

4-trifluoromethyl aniline	2-aminoimidazole hemisulfate
4-amino-5-imidazole carboxamide	5-aminosalicylic acid
3-amino-5-methylisoxazole	2-amino-5-(4-methoxyphenyl)-1,3,4-thiadiazole
aminopyrazine	3-amino-1-benzofuran-2-carbonitrile
3-amino-2-pyrazinecarboxylic acid	3-(trifluoromethyl)-1H-pyrazol-5-amine
3-aminopyridine-2-carboxylic acid methyl ester	D- <i>p</i> -hydroxyphenylglycine methylester
2-aminobenzimidazole	2-amino-4- <i>tert</i> -butylthiazole
trifluoromethoxyphenylethylamine	5-amino-1H-[1,2,4]-triazole-3-carboxylic acid methyl ester

## Aniline Amides (acid chlorides)

### Successful reactions:

<i>o</i> -anisoyl chloride	benzoyl chloride
trimethylacetyl chloride	acetyl chloride
<i>o</i> -toluyl chloride	propionyl chloride
isobutyryl chloride	cyclopropane carbonyl chloride
isovaleryl chloride	cyclopentane carbonyl chloride
4-methyloxazole-5-carbonyl chloride	nicotinoyl chloride
isonicotinoyl chloride	phenylacetyl chloride
2-thiophene carbonyl chloride	2-furoyl chloride
1,5-dimethyl-1H-pyrazole-3-carbonyl chloride	3-methylisoxazole-5-carbonyl chloride
3-chlorobenzoyl chloride	3,4,5-trimethoxybenzoyl chloride
2-methyl-2H-pyrazole-3-carbonyl chloride	4-chlorobenzoyl chloride
<i>p</i> -toluoyl chloride	4-isopropoxybenzoyl chloride
5-methyl-isoxazole-3-carbonyl chloride	3,5-dimethylisoxazole-4-carbonyl chloride
5-methyl-4-isoxazole carbonyl chloride	

### Unsuccessful reactions:

1-methyl-1H-imidazole-5-carbonyl chloride	2,3-dihydro-1,4-benzodioxine-5-carbonyl chloride
2-methyl-1,3-thiazole-4-carbonyl chloride	4-isopropylbenzoyl chloride
2,5-dimethyloxazole-4-carbonyl chloride	

## *Aniline amides (carboxylic acids)*

### **Successful reactions:**

2-chlorobenzoic acid  
(S)-(-)-2-pyrrolidine-5-carboxylic acid  
2-hydroxynicotinic acid  
6-hydroxynicotinic acid  
4-pyridazinecarboxylic acid  
5-phenyl-4-isoxazolecarboxylic acid  
3-isopropylpyrazole-4-carboxylic acid  
3-methylpyrazole-5-carboxylic acid  
indole-2-carboxylic acid  
2,4-dimethylthiazole-5-carboxylic acid  
1-methyl-1H-imidazole-2-carboxylic acid  
1-methylindazole-3-carboxylic acid  
2-methoxy-5-sulfamoylbenzoic acid  
5-fluoro-2-methoxybenzoic acid  
5-ethoxysalicylic acid  
4-acetamidobenzoic acid  
4-dimethylaminobenzoic acid  
2,2-difluorocyclopropanecarboxylic acid  
4-methoxybenzoic acid  
4-toluic acid  
4-[(methylsulfonyl)amino]benzoic acid  
6-hydroxypyridine-2-carboxylic acid  
mono-methyl phthalate  
picolinic acid  
2-pyrazinecarboxylic acid  
4-cyanobenzoic acid  
3-cyanobenzoic acid  
thianaphthene-2-carboxylic acid  
5-isopropylisoxazole-3-carboxylic acid  
4-methyl-5-thiazole carboxylic acid  
5-methyl-1H-pyrazole-3-carboxylic acid  
3-phenylisoxazole-5-carboxylic acid  
[1,2,3]thiadiazole-4-carboxylic acid  
3-isopropylpyrazole-5-carboxylic acid  
5-(4-chlorophenyl)-isoxazole-3-carboxylic acid  
2,5-dimethoxybenzoic acid  
2-chloronicotinic acid  
4-carboxybenzenesulfonamide  
1-methylpiperidine-4-carboxylic acid hydrochloride  
piperonylic acid  
4-methoxyphenylacetic acid  
4-hydroxymethylbenzoic acid  
2-methoxyphenylacetic acid  
2-thiazolecarboxylic acid

### **Unsuccessful reactions:**

4-imidazoleacetic acid hydrochloride  
1,3-dimethyl-1H-pyrazole-5-carboxylic acid  
2-cyanobenzoic acid  
2-pyrrolidin-1-yl-propionic acid hydrochloride  
2,6-dimethylbenzoic acid  
1-methyl-1H-imidazole-4-carboxylic acid  
3-hydroxypicolinic acid  
salicylic acid  
3-methylsalicylic acid  
4-methanesulfonylmethylbenzoic acid  
3-morpholin-4-yl-propionic acid  
indan-2-carboxylic acid  
5-isopropylisoxazole-4-carboxylic acid  
3-hydroxybenzoic acid  
4-pyrazolecarboxylic acid  
1-piperidinepropionic acid

## *Sulfonamides (sulfonyl chlorides)*

### **Successful reactions:**

methanesulfonyl chloride  
1-butan sulfonyl chloride  
3,5-dimethylisoxazole-4-sulfonyl chloride  
phenylmethanesulfonyl chloride  
2-phenylethanesulfonyl chloride  
tetrahydrothiophene-3-sulfonyl chloride 1,1-dioxide  
2-oxo-2,3-dihydro-1,3-benzoxazole-6-sulfonyl chloride  
furan-3-sulfonyl chloride  
1,5-dimethyl-1H-pyrazole-4-sulfonyl chloride  
4-methoxybenzenesulfonyl chloride  
2-fluorobenzenesulfonyl chloride  
4-(chlorosulfonyl)benzoic acid  
2,3-dihydro-1,4-benzodioxine-6-sulfonyl chloride  
thiophene-2-sulfonyl chloride  
1-methyl-1H-pyrazole-3-sulfonyl chloride  
furan-2-sulfonyl chloride  
1-methylimidazole-4-sulfonyl chloride  
2H-[1,2,4]-triazole-3-sulfonyl chloride

### **Unsuccessful reactions:**

pyridine-3-sulfonyl chloride hydrochloride  
5-methyl-4-isoxazolesulfonyl chloride  
3-chlorobenzenesulfonyl chloride  
methyl-3-(chlorosulfonyl)-2,2-dimethylpropanoate  
4-chlorosulfonylpyrazole

## *Ureas (isocyanates)*

### **Successful reactions:**

phenylisocyanate  
benzylisocyanate  
*tert*-butylisocyanate  
2-chlorophenylisocyanate  
3-methoxyphenylisocyanate  
2-methoxyphenylisocyanate

ethylisocyanate  
cyclohexylisocyanate  
3-chlorophenylisocyanate  
3-cyanophenylisocyanate  
4-methoxyphenylisocyanate  
trimethylsilylisocyanate

### **Unsuccessful reactions:**

4-chlorophenylisocyanate

## *Buchwald-Hartwig couplings (halides)*

### **Successful reactions:**

2-bromopyridine  
3-bromo-6-methoxypyridine  
2-bromopyrimidine  
2-chloro-4-fluoropyridine

2-bromo-6-methoxypyridine  
3-chloro-6-methylpyridazine  
2-chloro-3-trifluoromethylpyridine  
4-chlorothiopyrimidine

### **Unsuccessful reactions:**

5-bromo-2-cyanopyrimidine  
3-bromo-5-cyanopyridine  
2-bromo-6-(CO<sub>2</sub>Me)-pyridine  
7-bromoindole  
2-bromo-4-methylanisole

3-bromo-5-(CO<sub>2</sub>Me)-1-methylpyrrole  
4-bromo-1-methylpyrazole  
4-bromo-2-methoxythiazole  
2-bromo-5-(CO<sub>2</sub>Et)-thiophene

## *Buchwald-Hartwig couplings (amines)*

### **Successful reactions:**

morpholine  
4-aminopyridine  
2-anisidine  
4-anisidine  
3-trifluoroaniline  
3,5-di-(trifluoro)aniline  
*N*-(3-aminophenyl)-methanesulfonamide  
3,4-dimethylaniline  
3,4-dichloroaniline

3-aminopyridine  
3-anisidine  
4-toluidine  
4-aminoacetanilide  
4-trifluoroaniline  
4-isopropylaniline  
3-aminobiphenyl  
5-aminoindole  
6-amino-1,4-benzodioxane

### **Unsuccessful reactions:**

4-piperidinecarboxamide  
*N*-(3-aminopropyl)-2-pyrrolidinone  
2-aminomethylpyridine  
furfurylamine  
4-aminophenol  
*N*-methylbenzylamine  
4-amino-5-imidazolecarboxamide  
*N,N*-dimethyl-4-phenylene diamine  
anthranilic acid  
2-methoxybenzylamine  
3-cyclopropyl-1H-pyrazole-5-amine

benzylamine  
4-methoxybenzylamine  
2-(2-aminoethyl)-1-methylpyrrolidine  
4-(3-aminopropyl)morpholine  
2-oxopiperazine  
3-aminobenzoic acid  
5-amino-3-methylisoxazole  
tryptamine  
2-(2-furyl)-1H-pyrazole-5-amine  
6-aminoindazole



*One-pot consecutive Suzuki couplings (boronic acids or esters)*

**Successful reactions:**

4-methoxyphenyl	4-(methanesulfonyl)phenyl
3-aminocarbonylphenyl	4-(methoxymethyl)phenyl
3-(methanesulfonylamino)phenyl	7-(4-methyl-3,4-dihydro-2H-1,4-benzoxazinyl)
4-aminocarbonylphenyl	2-methoxyphenyl
4-tolyl	3-hydroxyphenyl
4-hydroxyphenyl	3-methoxyphenyl
2-tolyl	4-trifluorophenyl
3-tolyl	3-trifluorophenyl
5-(2- <i>N,N</i> -dimethylaminopyridinyl)	4-(methoxycarbonyl)phenyl
2,5-dimethoxyphenyl	4-fluorophenyl
5-pyrimidinyl	4-(methanesulfonylamino)phenyl
5-(2-methoxypyrimidyl)	2-methoxy-5-methylphenyl
3-(ethoxycarbonyl)phenyl	2-furyl
5-(1-methylpyrazolyl)	3-quinolinyl
3-acetamidophenyl	4-acetamidophenyl
4-morpholinophenyl	5-indolyl
5-(2- <i>N</i> -methylpiperazinyl-pyridinyl)	3-(piperidin-1-ylmethyl)phenyl

**Unsuccessful reactions:**

benzyl	4-(hydroxymethyl)phenyl
3-thienyl	5-(2,4-dimethoxypyrimidinyl)
4-carboxylphenyl	4-pyrazolyl
3,5-dimethylisoxazolyl	5-(2-cyanopyrimidinyl)
4-indazolyl	3-(4-methoxypyridinyl)
4-(SO <sub>2</sub> N-cyclopropyl)phenyl	5-(2-aminopyrimidinyl)

### 15.3 Full In Vitro Phosphatase Assay Results for Synthesised Compounds

The table below gives abbreviated initial assay data for all the compounds both synthesised and tested in this project, shown in the order tested. The standard error for each activity or IC<sub>50</sub> measurement is omitted for clarity and brevity.

ID	Cdc25A			VHR		
	Activity (%) 50 $\mu$ M	Activity (%) 10 $\mu$ M	IC <sub>50</sub> ( $\mu$ M)	Activity (%) 50 $\mu$ M	Activity (%) 10 $\mu$ M	IC <sub>50</sub> ( $\mu$ M)
JCC-CRT-161	33	100		24	106	
JCC-CRT-166	25	101		43	125	
JCC-CRT-167	-3	91	<b>11.0</b>	6	93	<b>10.5</b>
JCC-CRT-168	59	100		83	118	
JCC-CRT-172	54	111		43	118	
JCC-CRT-179	48	107		46	129	
JCC-CRT-180	25	85	<b>10.8</b>	32	114	<b>16.2</b>
JCC-CRT-181	90	110		97	145	
JCC-CRT-231	104	109		102	136	
JCC-CRT-232	39	111	<b>16.8</b>	22	117	<b>17.8</b>
JCC-CRT-234	54	98		27	127	<b>100</b>
JCC-CRT-235	14	110	<b>21.0</b>	38	122	<b>23.1</b>
JCC-CRT-237	127	109		117	126	
JCC-CRT-245	22	108	<b>23.1</b>	19	122	<b>16.7</b>
JCC-CRT-249	76	128		52	101	
JCC-CRT-250	67	130		95	128	
JCC-CRT-251	20	113	<b>13.3</b>	-9	72	<b>15.4</b>
JCC-CRT-252	100	137		51	117	
JCC-CRT-256	100	132		86	132	
JCC-CRT-257	26	111	<b>28.1</b>	50	128	
JCC-CRT-259	12	100	<b>15.0</b>	13	103	<b>21.9</b>
JCC-CRT-260	14	112	<b>12.4</b>	2	92	<b>16.1</b>
JCC-CRT-284	-11	42	<b>1.17</b>	-13	27	<b>2.60</b>
JCC-CRT-10	68	127		92	92	
JCC-CRT-13	56	126		54	99	
JCC-CRT-16	65	100		44	51	<b>25.1</b>
JCC-CRT-17	76	89		-11	-16	<b>16.7</b>
JCC-CRT-22	18	104	<b>31.5</b>	5	55	<b>39.0</b>
JCC-CRT-23	76	107		6	35	<b>25.1</b>
JCC-CRT-24	36	69	<b>25.6</b>	15	52	<b>12.6</b>
JCC-CRT-27	70	133		99	119	
JCC-CRT-29	39	103	<b>22.5</b>	-2	62	<b>20.5</b>
JCC-CRT-30	75	128		4	58	<b>26.6</b>
JCC-CRT-31	89	123		107	84	
JCC-CRT-32	62	96		14	62	<b>16.6</b>
JCC-CRT-34	23	109	<b>100</b>	84	88	
JCC-CRT-35	86	151		75	103	
JCC-CRT-36	119	129		212	138	
JCC-CRT-51	80	135		34	99	<b>75</b>
JCC-CRT-54	124	127		131	125	
JCC-CRT-55	97	115		87	82	
JCC-CRT-56	46	97		-14	18	<b>15.7</b>
JCC-CRT-57	46	103	<b>75</b>	52	75	<b>9.65</b>
JCC-CRT-59	37	109	<b>16.7</b>	69	149	
JCC-CRT-60	70	106		95	116	
JCC-CRT-62	50	61	<b>24.4</b>	58	102	
JCC-CRT-63	74	123		86	114	
JCC-CRT-65	86	99		92	108	
JCC-CRT-67	87	105		98	88	
JCC-CRT-68	112	112		109	142	

JCC-CRT-69	81	112		69	94	
JCC-CRT-71	135	145		188	108	
JCC-CRT-72	62	123		65	73	
JCC-CRT-73	64	86		-3	36	<b>15.6</b>
JCC-CRT-74	94	119		85	100	
JCC-CRT-75	57	128		14	70	<b>15.6</b>
JCC-CRT-77	21	111	<b>24.9</b>	84	84	
JCC-CRT-92	38	130	<b>40.4</b>	57	112	
JCC-CRT-95	89	122		91	117	
JCC-CRT-97	91	116		62	126	
JCC-CRT-99	50	95	<b>14.5</b>	69	102	
JCC-CRT-100	71	132		72	92	
JCC-CRT-101	155	146		180	109	
JCC-CRT-102	84	139		66	99	
JCC-CRT-103	80	143		5	110	<b>13.3</b>
JCC-CRT-106	46	129	<b>100</b>	7	61	<b>10.7</b>
JCC-CRT-109	97	140		-7	41	<b>18.9</b>
JCC-CRT-113	40	101	<b>48.0</b>	27	104	<b>8.85</b>
JCC-CRT-80	105	136		64	92	
JCC-CRT-81	111	141		71	128	
JCC-CRT-307				62	135	
JCC-CRT-308				-11	79	<b>39.6</b>
JCC-CRT-309				-11	114	<b>36.4</b>
JCC-CRT-313				1	91	<b>45.1</b>
JCC-CRT-315				9	123	<b>100</b>
JCC-CRT-83	194	143		135	151	
JCC-CRT-84	109	119		103	137	
JCC-CRT-85	110	122		41	124	<b>75</b>
JCC-CRT-114	44	105	<b>50.8</b>	44	111	<b>17.0</b>
JCC-CRT-115	121	172		127	121	
JCC-CRT-117	88	135		109	124	
JCC-CRT-118	106	167		101	158	
JCC-CRT-119	62	139		80	107	
JCC-CRT-129	50	161	<b>18.1</b>	45	134	<b>5.29</b>
JCC-CRT-130	61	104		96	107	
JCC-CRT-131	117	178		87	94	
JCC-CRT-132	45	98		12	77	
JCC-CRT-136	61	132		23	72	<b>39.4</b>
JCC-CRT-139	39	133		63	122	
JCC-CRT-140	101	155		101	98	
JCC-CRT-142	66	109		26	125	<b>33.9</b>
JCC-CRT-143	134	217		135	125	
JCC-CRT-151	89	126		91	111	
JCC-CRT-152	106	152		33	51	<b>22.0</b>
JCC-CRT-153	33	112	<b>25.1</b>	41	84	<b>16.0</b>
JCC-CRT-154	227	264		107	101	
JCC-CRT-155	77	127		74	69	
JCC-CRT-156	172	293		19	70	<b>75</b>
JCC-CRT-157	38	87	<b>75</b>	71	115	
JCC-CRT-158	56	95		6	114	<b>42.2</b>
JCC-CRT-159	62	86		83	107	
JCC-CRT-160	64	91		132	129	
JCC-CRT-162	41	84	<b>26.6</b>	108	135	
JCC-CRT-163	107	164		168	229	
JCC-CRT-164	31	19	<b>46.9</b>	54	76	<b>17.7</b>
JCC-CRT-165	61	89		105	109	
JCC-CRT-169	27	17	<b>39.5</b>	130	153	
JCC-CRT-171	74	116		141	172	
JCC-CRT-173	52	62	<b>26.6</b>	121	126	
JCC-CRT-174	64	87		128	153	

JCC-CRT-175	75	84		129	157	
JCC-CRT-228	100	170		167	193	
JCC-CRT-229	61	62		71	68	
JCC-CRT-233	80	92		19	67	<b>5.26</b>
JCC-CRT-236	75	62		59	49	<b>14.7</b>
JCC-CRT-238	55	83		43	74	
JCC-CRT-255	85	80		90	128	
JCC-CRT-261	74	84		88	151	
JCC-CRT-262	36	78	<b>21.6</b>	40	91	<b>30.8</b>
JCC-CRT-263	92	91		124	135	
JCC-CRT-264	81	90		111	107	
JCC-CRT-265	93	113		35	95	<b>46.7</b>
JCC-CRT-266	79	72		83	83	
JCC-CRT-268	99	144		121	150	
JCC-CRT-269	38	145		85	176	
JCC-CRT-270	82	101		54	112	
JCC-CRT-271	166	170		209	195	
JCC-CRT-272	75	107		-12	127	
JCC-CRT-273	53	64		78	89	
JCC-CRT-274	61	78		88	131	
JCC-CRT-275	28	32	<b>51.4</b>	43	57	<b>20.2</b>
JCC-CRT-277	98	132		131	190	
JCC-CRT-278	46	76	<b>46.5</b>	85	114	
JCC-CRT-280	40	75	<b>9.44</b>	104	135	
JCC-CRT-285	53	62		92	122	
JCC-CRT-206	19	58	<b>23.7</b>	61	103	
JCC-CRT-207	36	91	<b>20.0</b>	26	134	<b>12.6</b>
JCC-CRT-208	37	57	<b>14.9</b>	26	121	<b>8.50</b>
JCC-CRT-209	47	58		82	130	
JCC-CRT-210	52	89		18	56	<b>22.5</b>
JCC-CRT-211	27	47	<b>26.1</b>	15	86	<b>9.23</b>
JCC-CRT-212	37	57	<b>32.1</b>	65	98	
JCC-CRT-214	26	55	<b>28.6</b>	71	109	
JCC-CRT-215	25	85	<b>47.9</b>	43	111	<b>7.03</b>
JCC-CRT-216	35	43	<b>45.1</b>	57	108	
JCC-CRT-217	125	86		135	155	
JCC-CRT-218	36	41	<b>18.2</b>	42	74	<b>5.59</b>
JCC-CRT-183	10	105		39	124	
JCC-CRT-184	31	57	<b>100</b>	37	44	<b>22.8</b>
JCC-CRT-185	21	47	<b>150</b>	48	56	<b>42.2</b>
JCC-CRT-186	23	68		6	10	
JCC-CRT-189	25	70		38	84	
JCC-CRT-190	50	72		65	52	<b>39.8</b>
JCC-CRT-191	23	67	<b>150</b>	196	167	
JCC-CRT-192	-1	11		54	65	
JCC-CRT-193	-5	10	<b>100</b>	16	24	<b>9.29</b>
JCC-CRT-194	52	75		14	90	<b>75</b>
JCC-CRT-195	12	29	<b>47.2</b>	-6	6	<b>13.3</b>
JCC-CRT-197	-7	10	<b>3.21</b>	16	21	<b>11.7</b>
JCC-CRT-199	23	127	<b>34.4</b>	91	112	
JCC-CRT-200	-8	22	<b>26.5</b>	7	48	<b>17.5</b>
JCC-CRT-201	-5	95	<b>75</b>	-10	40	<b>13.1</b>
JCC-CRT-203	7	80	<b>58.4</b>	9	77	<b>22.4</b>
JCC-CRT-204	49	100		91	120	
JCC-CRT-205	39	57	<b>300</b>	75	118	
JCC-CRT-241	-3	3		26	82	
JCC-CRT-242	8	23	<b>75</b>	56	67	
JCC-CRT-243	53	137		18	102	
JCC-CRT-244	89	81		78	78	
JCC-CRT-248	18	42	<b>30.3</b>	2	21	<b>10.3</b>

JCC-CRT-324	18	48	<b>75</b>	10	30	<b>25.8</b>
JCC-CRT-331	43	77	<b>200</b>	21	32	<b>38.9</b>
JCC-CRT-332	51	85		22	61	<b>53.8</b>
JCC-CRT-334	33	132	<b>29.7</b>	24	54	<b>20.6</b>
JCC-CRT-338	20	83	<b>50</b>	-12	38	<b>50</b>
JCC-CRT-339	29	114	<b>100</b>	54	110	
JCC-CRT-340	38	79	<b>47.1</b>	61	51	<b>50</b>
JCC-CRT-341	15	115		-3	84	
JCC-CRT-346	12	90	<b>100</b>	10	85	<b>26.8</b>
JCC-CRT-351	14	53	<b>33.4</b>	15	71	<b>7.13</b>
JCC-CRT-352	30	184	<b>200</b>	89	130	
JCC-CRT-357	27	83	<b>60</b>	53	111	
JCC-CRT-358	76	90		39	80	<b>45.0</b>
JCC-CRT-359	79	124		87	98	
JCC-CRT-367	79	86		28	84	<b>26.9</b>
JCC-CRT-370	104	119		41	91	<b>13.3</b>
JCC-CRT-373	96	124		34	112	<b>14.6</b>
JCC-CRT-374	126	127		25	89	<b>30.9</b>
JCC-CRT-376	62	107	<b>50.6</b>	57	79	
JCC-CRT-377	89	153		13	116	<b>27.5</b>
JCC-CRT-378	63	100	<b>21.0</b>	84	81	
JCC-CRT-380	128	132		17	94	<b>21.8</b>
JCC-CRT-381	95	107		10	64	<b>30.9</b>
JCC-CRT-382	128	129		9	75	<b>20.5</b>
JCC-CRT-383	101	102		-5	73	<b>25.1</b>
JCC-CRT-384	122	156		110	113	
JCC-CRT-398A	69	103		57	49	<b>29.1</b>
JCC-CRT-398B	96	109		32	75	<b>27.1</b>
JCC-CRT-398C	92	98		67	84	
JCC-CRT-402	91	137		36	113	<b>22.2</b>
JCC-CRT-403	67	142		36	87	<b>27.6</b>
JCC-CRT-404	120	171		40	98	<b>50.3</b>
JCC-CRT-405	61	119		12	77	<b>28.7</b>
JCC-CRT-406	67	170		-8	97	<b>16.2</b>
JCC-CRT-407	73	131		15	52	<b>18.8</b>
JCC-CRT-408	71	145		27	123	<b>12.6</b>
JCC-CRT-409	82	115		32	36	<b>19.7</b>
JCC-CRT-410	80	137		52	94	
JCC-CRT-411	16	155	<b>41.7</b>	17	100	<b>28.3</b>
JCC-CRT-412	5	146	<b>39.4</b>	10	112	<b>27.2</b>
JCC-CRT-413	61	105	<b>100</b>	32	10	<b>29.1</b>
JCC-CRT-414	138	166		24	59	<b>39.6</b>
JCC-CRT-415	70	131		58	33	<b>34.7</b>
JCC-CRT-416	110	179		13	42	<b>28.3</b>
JCC-CRT-417	109	160		109	84	
JCC-CRT-418	159	209		7	141	<b>32.1</b>
JCC-CRT-419	113	149		41	66	<b>23.6</b>
JCC-CRT-421	218	231		126	182	
JCC-CRT-423	130	161		29	51	<b>25.5</b>
JCC-CRT-424	154	174		45	92	<b>14.2</b>
JCC-CRT-427	116	159		2	110	<b>20.6</b>
JCC-CRT-428	165	177		0	36	<b>13.6</b>
JCC-CRT-429	145	185		49	50	<b>12.9</b>
JCC-CRT-430	166	231		29	81	<b>13.8</b>
JCC-CRT-431	86	97		59	69	
JCC-CRT-432	127	140		78	147	
JCC-CRT-437	85	97		6	52	<b>16.1</b>
JCC-CRT-438	64	85		-6	24	<b>10.1</b>
JCC-CRT-439	229	195		148	138	
JCC-CRT-440	170	179		126	131	